



# **Modelling drying and autogenous shrinkage of high strength concrete with and without mineral and chemical admixtures**

**Rahima Noordien  
213073838**

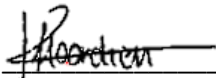
*“A thesis submitted to the Faculty of Engineering, Cape Peninsula University of Technology, Cape Town, in fulfilment of the requirements for the MEng Degree in Civil Engineering”*

**Cape Town  
22 October 2020**

---

## Declaration

I declare that this research thesis is my own unaided work. It is being submitted for the MEng Degree at Cape Peninsula University of Technology, Cape Town. It has not been submitted before for any degree or examination in any other University.

A handwritten signature in black ink, appearing to read 'H. Gordon', written over a horizontal line.

(Signature)

Signed in Cape Town this 22<sup>nd</sup> day of October 2020

---

---

## Abstract

Parameters of some well known concrete shrinkage prediction models have not been updated to account for modern high performance concrete data. Consequently, their predictions are not accurate for high strength concrete with chemical admixtures and high mineral admixtures content.

This study considered modifying three well known shrinkage models, the RILEM B4, MC 2010 and WITS models, to predict drying and autogenous (RILEM B4 and MC 2010 only) shrinkage for high strength concrete. Experimental data for concrete shrinkage specimens that met the criteria of rapid hardening or rapid development of early age strength, a water-to-cementitious material ratio  $\leq 0.42$  or 28<sup>th</sup> day compressive strength  $\geq 60$  MPa was extracted from the 2018 version NU database (Northwestern University, 2018), a technical report (Al-Manaseer and Fayyaz, 2011) and the Concrete Institute of South Africa database. This gave reliable data for 220 drying and 342 autogenous shrinkage experiments. These data were used to (i) assess accuracies of the original versions of the selected models in predicting shrinkage of high strength concrete (using only data within the covariate ranges on which each model was developed), (ii) update model parameters to improve the accuracy of high strength concrete shrinkage predictions using data subsets (from the 562 experiments) for comparable experiments and (iii) propose composite models constructed as logistic dose curves (combining two or more individual functions) to fit high strength concrete drying shrinkage data that had an early age peak before reaching the final shrinkage value. Excel Solver<sup>®</sup> was used to update model parameters.

Shrinkage residuals of both original and modified models were used to rank the models for the complete HSC datasets, the data subsets and for individual shrinkage time periods (0 to 99, 100 to 199, 200 to 499 and  $\geq 500$  days). Ranking was done using the statistical indicators Root Mean Square Error, adjusted Coefficient of Determination, Akaike's Information Criterion and overall coefficient of variation. High strength concrete drying shrinkage predictions of the original models were best overall for the WITS, then the RILEM B4 and MC 2010 models. After parameter modification they were best for overall for the WITS, then the MC 2010 and RILEM B4 models. For high strength concrete autogenous shrinkage prediction, the RILEM B4 model performed better than the MC 2010 overall (original and modified versions). The proposed composite models outranked the existing models in overall performance and per shrinkage term for the high strength concrete data subsets with an early age peak. Prediction errors for the original models were high for drying shrinkage experiments, of the order  $-235\%$  to  $+100\%$  for short-term shrinkage (0 to 99 days) and  $-257\%$  to  $+74\%$  for medium- and long-term shrinkage ( $\geq 100$  days). For the modified models, residuals were generally much smaller for the medium- and long-term shrinkage, with errors ranging from  $-57\%$  to  $+48\%$ . For some data subsets the model parameters could not be improved, due to the large variations in the actual shrinkage data. For autogenous shrinkage experiments, original model prediction errors ranged from  $-2943\%$  to  $+81\%$  for short-term shrinkage and  $-321\%$  to  $35\%$  for medium- and long-term shrinkage. The modified model prediction errors ranged from  $-381\%$  to  $99\%$  for short-term and  $-98\%$  and  $+29\%$  for medium- and long-term shrinkage.

Comparisons were also made across the different geographical regions from which the experiments originated, because of their different test specifications and cement classifications. The original RILEM B4 and MC 2010 models predicted worse for North American concretes than for European concretes, but the RILEM B4 model was the more accurate for concretes from both these regions and from East Asia. Surprisingly the MC 2010 achieved the lowest overall coefficient of variation ( $<40\%$ ) for Southern African concretes.

---

## Acknowledgements

For my beloved grandfather who inspired me to pursue my tertiary education in engineering and the built environment. He was a Master Builder, jack of all trades, a true craftsman, the best story-teller and an inspiration to many. A lesson learnt from him: always finish what you've started.

My sincere gratitude (firstly to my Creator) and appreciation to all that have assisted me (in many forms) in completing this thesis. Thanks to my supervisor, Mr Andrew Sutherland, who pursued this with me until the end through all adversities. Thanks Dr Kumar Pallav for the extra guidance and advice. Thanks to my work colleagues, managers, friends and family for their support and encouragement. A special thanks to my parents and husband for their unwavering support and reassurance. Lastly, thanks to NRF for the financial assistance.

---

---

# Table of Contents

	<b>Page</b>
Declaration .....	ii
Abstract.....	iii
Acknowledgements.....	iv
Table of Contents .....	v
List of Figures.....	viii
List of Tables.....	xxi
Nomenclature.....	xxvi
Terms and concepts .....	xxviii
Chapter 1 Introduction .....	1
1.1 Background and Motivation .....	1
1.2 Research problem.....	2
1.3 Research Questions .....	2
1.4 Aims, objectives and outcomes .....	2
1.5 Significance .....	3
1.6 Delineation .....	3
1.7 Assumptions .....	4
1.8 Methodology .....	4
1.9 Organisation of thesis.....	5
Chapter 2 Literature review and theory .....	6
2.1 HSC & concrete mix constituents .....	6
2.1.1 Portland cement and supplementary cement materials .....	6
2.1.2 Aggregates .....	9
2.1.3 Chemical admixtures.....	10
2.2 Moisture movement in concrete.....	12
2.2.1 Capillary absorption .....	13
2.2.2 Permeation.....	13
2.2.3 Diffusion .....	14
2.3 Types of concrete shrinkage.....	14
2.3.1 Plastic shrinkage.....	15
2.3.2 Autogenous shrinkage .....	16
2.3.3 Drying shrinkage.....	17
2.3.4 Thermal shrinkage.....	19
2.3.5 Carbonation shrinkage .....	20
2.4 Intrinsic & extrinsic influence on shrinkage in hardened HSC.....	20
2.4.1 Influence of water content and w/c .....	21
2.4.2 Influence of supplementary cementitious materials.....	22
2.4.3 Influence of aggregate type and origin.....	24
2.4.4 Influence of chemical admixture content and type.....	26
2.4.5 Influence of curing, temperature and relative humidity .....	29
2.5 Estimating shrinkage and development of shrinkage database.....	30
2.6 Prediction model criteria .....	31
2.7 Shrinkage prediction models - performance studies .....	33
2.7.1 American and Canadian models .....	33

---

---

2.7.2	European models .....	34
2.7.3	South African models .....	37
2.7.4	Comparison between the models .....	37
2.8	Non-linear solution software .....	40
2.9	Statistical methods to evaluate models. ....	40
2.9.1	Root mean square error (RMSE) .....	41
2.9.2	Coefficient of determination ( $R^2$ ) .....	41
2.9.3	Akaike's information criterion (AIC) .....	42
2.9.4	CEB mean deviation ( $M_{CEB}$ ) .....	43
2.9.5	CEB coefficient of variation ( $V_{CEB}$ ) .....	43
2.9.6	Bažant and Baweja's coefficient of variation ( $\bar{\omega}_j$ ) .....	44
2.10	Conclusion .....	45
Chapter 3	Research methodology .....	46
3.1	Research approach .....	46
3.2	Data preparation .....	46
3.2.1	Shrinkage database preparation .....	46
3.2.2	Experiment selection and grouping .....	48
3.2.3	Missing covariate data analysis .....	51
3.2.4	Derived datasets and subsets .....	52
3.2.5	Experimental shrinkage profile analysis .....	56
3.3	Existing model evaluation and modification .....	57
3.3.1	Fitting of selected models to experimental data .....	57
3.3.2	Update of existing model parameters .....	57
3.3.3	Composite model development .....	57
3.4	Analysis and presentation of results .....	60
3.5	Methodology conclusion .....	61
Chapter 4	Results .....	62
4.1	Applicable shrinkage experiments per dataset .....	62
4.2	Original and modified shrinkage results for HSC .....	63
4.2.1	Updated RILEM B4 model – drying shrinkage .....	63
4.2.2	Updated RILEM B4 model – autogenous shrinkage .....	67
4.2.3	Updated MC 2010 model – drying shrinkage .....	70
4.2.4	Updated MC 2010 model – autogenous shrinkage .....	73
4.2.5	Updated WITS model – drying shrinkage .....	75
4.3	Proposed composite model .....	79
4.3.1	Model parameters .....	79
4.3.2	Proposed composite model for data Subset S2-08 .....	80
4.3.3	Proposed model for Subset S2-09 .....	81
4.3.4	Proposed model for Subset S2-10 .....	83
4.3.5	Proposed model for Subset S2-12 .....	84
4.4	Validation of modified shrinkage functions .....	85
4.4.1	Dataset 1-HSC results .....	85
4.4.2	Dataset 2-HSC results .....	88
4.5	Ranking model results .....	90
4.5.1	Model performance for drying shrinkage per subset .....	90

---

---

4.5.2	Model performances for time ranges 0 to 99, 100 to 199, 200 to 499 and 500 days or more (drying shrinkage).....	91
4.5.3	Model performance for autogenous shrinkage per subset .....	94
4.5.4	Model performances for time ranges 0 to 99, 100 to 199, 200 to 499 and 500 days or more (autogenous shrinkage).....	95
4.6	Shrinkage prediction performance for the RILEM B4, MC 2010 and WITS models within their covariate limits.....	96
4.6.1	RILEM B4 predictions for Dataset 3 .....	97
4.6.2	MC 2010 predictions for Dataset 4 .....	97
4.6.3	WITS model predictions for Dataset 5 .....	97
4.7	Results conclusion .....	98
Chapter 5	Discussion.....	99
5.1	Predictions for experiments falling within model applicable covariate range.....	99
5.2	Original and modified model predictions for HSC without admixtures (drying $\epsilon$ ) .....	102
5.3	Original and modified model predictions for HSC with mineral admixtures (drying $\epsilon$ ).....	104
5.4	Original and modified model predictions for HSC with mineral and chemical admixtures (drying $\epsilon$ ).....	106
5.5	Original and modified model predictions for HSC with mineral and chemical admixtures (autogenous $\epsilon$ ).....	109
5.6	Overall model performance - original and modified models .....	111
5.7	Original vs. modified model overall ranking.....	116
5.8	Conclusions .....	117
Chapter 6	Conclusions and recommendations .....	119
6.1	Conclusions .....	119
6.2	Recommendations.....	121
References	.....	123
Appendices	.....	129
Appendix A.	MC 2010, RILEM B4 and WITS model formulae .....	129
Appendix B.	Statistical results per data subset of Dataset 1-HSC & Dataset 2-HSC.....	136
Appendix C.	Statistical results per shrinkage range of data subsets in Dataset 1-HSC & Dataset 2-HSC.....	142
Appendix D.	Statistical results for each experiment in Dataset 3, 4 and 5.....	160
Appendix E.	Original and modified shrinkage predictions of RILEM B4, MC 2010 and WITS model for Dataset 1-HSC .....	171
Appendix F.	Original and modified shrinkage predictions of RILEM B4 and MC 2010 for Dataset 2-HSC.....	220

---

---

## List of Figures

	<b>Page</b>
<b>Body</b>	
Figure 2.1	Diagrammatic presentation of ITZ location and its mineral composition (Mehta & Monteiro, 2006). ..... 10
Figure 2.2	Different locations of water in hydrated cement matrix (Mehta & Monteiro, 2006). ..... 12
Figure 2.3	Conceptual illustration of autogenous shrinkage (Pease, 2005). ..... 16
Figure 2.4	Conceptual illustration of drying shrinkage (Mehta & Monteiro, 2006). ..... 17
Figure 2.5	Comparator – to measure change in length of concrete specimen (Tam, Tam & Ng, 2012). ..... 19
Figure 2.6	Drying and basic (autogenous) shrinkage over time for NSC and HSC (CEB-FIP, 2013). .... 20
Figure 2.7	Drying shrinkage results (microstrain $\times 10^{-6}$ ) over time (days) for varying w/c ratios (Tam <i>et al</i> , 2012). ..... 22
Figure 2.8	Drying shrinkage results (microstrain) over time (days) of concrete mix with 0% and 10% FA and SF (Gupta <i>et al</i> , 2006). ..... 23
Figure 2.9	Drying shrinkage results (microstrain) over time (days) for varying FA dosages, excluding SRA influence (Al-Manaseer & Fayyaz, 2011). ..... 24
Figure 2.10	Drying shrinkage results (microstrain) over time (days) of concrete mix with granite and sandstone coarse aggregate (Gupta <i>et al</i> , 2006) ..... 25
Figure 2.11	Drying shrinkage (microstrain) over time (days) for varying SP dosages (Tam <i>et al</i> , 2012). ..... 27
Figure 2.12	Drying shrinkage results (microstrain) over time (days) for varying FA dosages, including SRA influence (Al-Manaseer & Fayyaz, 2011). ..... 28
Figure 2.13	Drying shrinkage results (microstrain) over time (days) for varying SRA dosages (Al-Manaseer & Fayyaz, 2011). ..... 28
Figure 2.14	Development of shrinkage prediction models between 1970 and 2020 (Bažant and Baweja, 1995(a); CEB, 1999; ACI Gardner and Lockman, 2001; Committee 209, 2008; CEB-FIP, 2012 and RILEM TC-242-MDC, 2015) ..... 33
Figure 3.1	Percentage of (a) drying and (b) autogenous shrinkage experiments per data source. .. 48
Figure 3.2	Schematic diagram of datasets extracted from the complete compiled database used in this study. .... 53
Figure 3.3	Schematic of data subsets derived from Dataset 1-HSC and Dataset 2-HSC. .... 54
Figure 3.4	Fitted functions for different data segments. .... 58
Figure 3.5	Composite power law-exponential function $F1$ and linear function $f_d$ . .... 59
Figure 3.6	Final composite logistic dose function $[\epsilon_{dst}]$ . .... 59
Figure 4.1	Percentage of applicable drying shrinkage experiments per dataset from the compiled database used in this study. .... 62
Figure 4.2	Percentage of applicable autogenous shrinkage experiments per dataset from the compiled database used in this study. .... 62
Figure 4.3	RILEM B4 model predicted and actual drying shrinkage (microstrain) for Dataset 1-HSC, Subset S1-03, Experiment #0264 (without admixtures) ..... 66
Figure 4.4	RILEM B4 model predicted and actual drying shrinkage (microstrain) for Dataset 1-HSC, Subset S2-02, Experiment #0249 (with mineral admixtures). ..... 67

---



---

Figure 4.5	RILEM B4 model predicted and actual drying shrinkage (microstrain) for Dataset 1-HSC, Subset S2-08, Experiment no. 6 (with mineral and chemical admixtures).	67
Figure 4.6	RILEM B4 model predicted and actual autogenous shrinkage (microstrain) for Dataset 2-HSC, Subset S2-02a, Experiment A_007_09 (with chemical admixtures).	69
Figure 4.7	RILEM B4 model predicted and actual autogenous shrinkage (microstrain) for Dataset 2-HSC, Subset S2-09a, Experiment A_031_06 (with chemical admixtures).	69
Figure 4.8	MC 2010 predicted and actual drying shrinkage (microstrain) for Dataset 1-HSC, Subset S1-03, Experiment #0261 (without admixtures).	72
Figure 4.9	MC 2010 predicted and actual drying shrinkage (microstrain) for Dataset 1-HSC, Subset S2-02, Experiment #0240 (with mineral admixtures).	72
Figure 4.10	MC 2010 predicted and actual drying shrinkage (microstrain) for Dataset 1-HSC, Subset S2-08, Experiment no. 6 (with mineral and chemical admixtures).	73
Figure 4.11	MC 2010 predicted and actual autogenous shrinkage (microstrain) for Dataset 2-HSC, Subset S2-02a, Experiment A_007_09 (with chemical admixtures).	75
Figure 4.12	MC 2010 predicted and actual autogenous shrinkage (microstrain) for Dataset 2-HSC, Subset S2-09a, Experiment A_031_06 (with chemical admixtures).	75
Figure 4.13	WITS model predicted and actual drying shrinkage (microstrain) for Dataset 1-HSC, Subset S1-03, Experiment #0261 (without admixtures).	78
Figure 4.14	WITS model predicted and actual drying shrinkage (microstrain) for Dataset 1-HSC, Subset S2-02, Experiment #0249 (with mineral admixtures).	78
Figure 4.15	WITS model predicted and actual drying shrinkage (microstrain) for Dataset 1-HSC, Subset S2-08, Experiment no. 6 (with mineral & chemical admixtures).	79
Figure 4.16	Proposed composite model predicted and actual drying shrinkage (microstrain) for Experiment no. 6 of data Subset S2-08 (0.6% SP, 25-30 % FA and 5% M).	81
Figure 4.17	Proposed composite model predicted and actual drying shrinkage (microstrain) for Experiment 10 of data Subset S2-08 (0.6% SP, 25-30 % FA and 5% M).	81
Figure 4.18	Proposed composite model predicted and actual drying shrinkage (microstrain) for Experiment 31 of data Subset S2-09 (< 1% SP; < 0.5% P; 5% M).	82
Figure 4.19	Proposed composite model predicted and actual drying shrinkage (microstrain) for Experiment 33 of data Subset S2-09 (< 1% SP; < 0.5% P; 5% M).	82
Figure 4.20	Proposed composite model predicted and actual drying shrinkage (microstrain) for Experiment 5 of data Subset S2-10 (> 1% SP).	83
Figure 4.21	Proposed composite model predicted and actual drying shrinkage (microstrain) for Experiment 9 of data Subset S2-10 (> 1% SP).	84
Figure 4.22	Proposed composite model predicted and actual drying shrinkage (microstrain) for Experiment 17 of data Subset S2-12 (< 1% SP, < 0.5% P).	85
Figure 4.23	Proposed composite model predicted and actual drying shrinkage (microstrain) for Experiment 25 of data Subset S2-12 (< 1% SP, < 0.5% P).	85
Figure 4.24	Modified model prediction and actual drying shrinkage (microstrain) for Experiment #0258.	86
Figure 4.25	Modified model prediction and actual drying shrinkage (microstrain) for Experiment #0011.	86
Figure 4.26	Modified model prediction and actual drying shrinkage (microstrain) for Experiment #0105.	87
Figure 4.27	Modified model prediction and actual drying shrinkage (microstrain) for Experiment #0231.	87
Figure 4.28	Modified model prediction and actual drying shrinkage (microstrain) for Experiment 14.	87

---

---

Figure 4.29	Modified model prediction and actual drying shrinkage (microstrain) for Experiment 20. ....	88
Figure 4.30	Modified model prediction and actual autogenous shrinkage (microstrain) for Experiment A_068_16. ....	88
Figure 4.31	Modified model prediction and actual autogenous shrinkage (microstrain) for ExperimentA_086_19. ....	89
Figure 4.32	Modified model prediction and actual autogenous shrinkage (microstrain) for Experiment A_086_25. ....	89
Figure 4.33	Modified model prediction and actual autogenous shrinkage (microstrain) for Experiment A_086_35. ....	89
Figure 4.34	RILEM B4 overall mean C.o.V for drying (left) and autogenous (right) shrinkage - Dataset 3. ....	97
Figure 4.35	MC 2010 overall mean C.o.V for drying (left) and autogenous (right) shrinkage - Dataset 4. ....	97
Figure 4.36	WITS model overall mean C.o.V for drying shrinkage - Dataset 5. ....	98
Figure 5.1	Drying shrinkage - overall C.o.V <sub>all</sub> values for the RILEM B4, MC 2010 and WITS models for experiments grouped by geographical region. ....	100
Figure 5.2	Autogenous shrinkage - overall C.o.V <sub>all</sub> values for the RILEM B4 and MC 2010 models for experiments grouped by geographical region. ....	100
Figure 5.3	Drying shrinkage - overall C.o.V <sub>all</sub> values for the RILEM B4, MC 2010 and WITS models for NSC (< 60 MPa) and HSC (≥ 60 MPa) experiments. ....	101
Figure 5.4	Autogenous shrinkage - overall C.o.V <sub>all</sub> values for the RILEM B4 and MC 2010 models for NSC (< 60 MPa) and HSC (≥ 60 MPa) experiments. ....	101
Figure 5.5	Graphical representation of overall ranking of original and modified model predictions for drying shrinkage data subsets without admixture. ....	102
Figure 5.6	Modified RILEM B4 model: residual (error) distribution for Experiment #0011 (Dataset 1-HSC). (blue bars indicate residual distribution, + indicates scaled normal values for experimental bins, red line indicates scaled theoretical normal distribution -3 to 3 standard deviations). ....	103
Figure 5.7	Graphical representation of overall ranking of original and modified model predictions for drying shrinkage - data subsets with mineral admixtures. ....	104
Figure 5.8	Modified WITS model: residual (error) distribution for Experiment #0258 (Dataset 1-HSC). (blue bars indicate residual distribution, + indicates scaled normal values for experimental bins, red line indicates scaled theoretical normal distribution -3 to 3 standard deviations). ....	105
Figure 5.9	Graphical representation of overall ranking of original and modified model predictions and actual drying shrinkage – data subsets with mineral and chemical admixtures. ....	106
Figure 5.10	Graphical representation of overall ranking of proposed composite and modified model predictions for drying shrinkage - data subsets with mineral and chemical admixtures. ....	107
Figure 5.11	Modified WITS model: residual (error) distribution for Experiment 14 (Dataset 1-HSC). (blue bars indicate residual distribution, + indicates scaled normal values for experimental bins, red line indicates scaled theoretical normal distribution -3 to 3 standard deviations). ....	108
Figure 5.12	Graphical representation of overall ranking of original and modified model predictions for autogenous shrinkage of subsets – data subsets with mineral and chemical admixtures. ....	109

---

---

Figure 5.13	Modified MC 2010 model: residual ( error) distribution for validation Experiment A_086_19 (Dataset 2-HSC). (blue bars indicate residual distribution, + indicates scaled normal values for experimental bins, red line indicates scaled theoretical normal distribution -3 to 3 standard deviations).....	110
Figure 5.14	Original and modified RILEM B4 model: actual vs. predicted shrinkage for Dataset 1-HSC.....	111
Figure 5.15	Original and modified MC 2010 model: actual vs. predicted shrinkage for Dataset 1-HSC.....	111
Figure 5.16	Original and modified WITS model: actual vs. predicted shrinkage for Dataset 1-HSC..	112
Figure 5.17	Original and modified RILEM B4 model: actual vs. predicted shrinkage for Dataset 2-HSC.....	112
Figure 5.18	Original and modified MC 2010 model: actual vs. predicted shrinkage for Dataset 2-HSC.....	112
Figure 5.19	Original and modified RILEM B4 model error % over time for entire Dataset 1-HSC.....	113
Figure 5.20	Original and modified MC 2010 model error % over time for entire Dataset 1-HSC. ....	113
Figure 5.21	Original and modified WITS model error % over time for entire Dataset 1-HSC.....	114
Figure 5.22	Original and modified RILEM B4 model error % over time for entire Dataset 2-HSC.....	114
Figure 5.23	Original and modified MC 2010 model error % over time for entire Dataset 2-HSC. ....	114
Figure 5.24	Original and modified model C.o.V <sub>all</sub> for data subsets without admixtures, with mineral admixtures and with both mineral and chemical admixtures – drying shrinkage.....	115
Figure 5.25	Original and modified model C.o.V <sub>all</sub> for data subsets with mineral and chemical admixtures – autogenous shrinkage. ....	115

## Appendices

Figure A.1	Summary of the MC 2010 model formulae(CEB-FIP, 2012) .....	129
Figure A.2	Summary of the RILEM B4 model formulae (RILEM TC-242-MDC, 2015) .....	130
Figure A.3	Summary of the WITS model formulae (Gaylard, 2011) .....	133
Figure E.1	RILEM B4 model predicted and actual drying shrinkage (microstrain) for Dataset 1-HSC, Subset S1-01, experiment #0158 .....	171
Figure E.2	MC 2010 model predicted and actual drying shrinkage (microstrain) for Dataset 1-HSC, Subset S1-01, experiment #0158 .....	171
Figure E.3	WITS model predicted and actual drying shrinkage (microstrain) for Dataset 1-HSC, Subset S1-01, experiment #0158 .....	171
Figure E.4	RILEM B4 model predicted and actual drying shrinkage (microstrain) for Dataset 1-HSC, Subset S1-01, experiment #0219 .....	172
Figure E.5	MC 2010 model predicted and actual drying shrinkage (microstrain) for Dataset 1-HSC, Subset S1-01, experiment #0219 .....	172
Figure E.6	WITS model predicted and actual drying shrinkage (microstrain) for Dataset 1-HSC, Subset S1-01, experiment #0219 .....	172
Figure E.7	RILEM B4 model predicted and actual drying shrinkage (microstrain) for Dataset 1-HSC, Subset S1-02, experiment #0108 .....	173
Figure E.8	MC 2010 model predicted and actual drying shrinkage (microstrain) for Dataset 1-HSC, Subset S1-02, experiment #0108 .....	173
Figure E.9	WITS model predicted and actual drying shrinkage (microstrain) for Dataset 1-HSC, Subset S1-02, experiment #0108 .....	173

---

---

Figure E.10	RILEM B4 model predicted and actual drying shrinkage (microstrain) for Dataset 1-HSC, Subset S1-02, experiment #0217 .....	174
Figure E.11	MC 2010 model predicted and actual drying shrinkage (microstrain) for Dataset 1-HSC, Subset S1-02, experiment #0217 .....	174
Figure E.12	WITS model predicted and actual drying shrinkage (microstrain) for Dataset 1-HSC, Subset S1-02, experiment #0217 .....	174
Figure E.13	RILEM B4 model predicted and actual drying shrinkage (microstrain) for Dataset 1-HSC, Subset S1-03, experiment #0261 .....	175
Figure E.14	MC 2010 model predicted and actual drying shrinkage (microstrain) for Dataset 1-HSC, Subset S1-03, experiment #0261 .....	175
Figure E.15	WITS model predicted and actual drying shrinkage (microstrain) for Dataset 1-HSC, Subset S1-03, experiment #0261 .....	175
Figure E.16	RILEM B4 model predicted and actual drying shrinkage (microstrain) for Dataset 1-HSC, Subset S1-03, experiment #0264 .....	176
Figure E.17	MC 2010 model predicted and actual drying shrinkage (microstrain) for Dataset 1-HSC, Subset S1-03, experiment #0264 .....	176
Figure E.18	WITS model predicted and actual drying shrinkage (microstrain) for Dataset 1-HSC, Subset S1-03, experiment #0264 .....	176
Figure E.19	RILEM B4 model predicted and actual drying shrinkage (microstrain) for Dataset 1-HSC, Subset S1-04, experiment #0079 .....	177
Figure E.20	MC 2010 model predicted and actual drying shrinkage (microstrain) for Dataset 1-HSC, Subset S1-04, experiment #0079 .....	177
Figure E.21	WITS model predicted and actual drying shrinkage (microstrain) for Dataset 1-HSC, Subset S1-04, experiment #0079 .....	177
Figure E.22	RILEM B4 model predicted and actual drying shrinkage (microstrain) for Dataset 1-HSC, Subset S1-04, experiment #0081 .....	178
Figure E.23	MC 2010 model predicted and actual drying shrinkage (microstrain) for Dataset 1-HSC, Subset S1-04, experiment #0081 .....	178
Figure E.24	WITS model predicted and actual drying shrinkage (microstrain) for Dataset 1-HSC, Subset S1-04, experiment #0081 .....	178
Figure E.25	RILEM B4 model predicted and actual drying shrinkage (microstrain) for Dataset 1-HSC, Subset S1-04, experiment #0083 .....	179
Figure E.26	MC 2010 model predicted and actual drying shrinkage (microstrain) for Dataset 1-HSC, Subset S1-04, experiment #0083 .....	179
Figure E.27	WITS model predicted and actual drying shrinkage (microstrain) for Dataset 1-HSC, Subset S1-04, experiment #0083 .....	179
Figure E.28	RILEM B4 model predicted and actual drying shrinkage (microstrain) for Dataset 1-HSC, Subset S1-04, experiment #0221 .....	180
Figure E.29	MC 2010 model predicted and actual drying shrinkage (microstrain) for Dataset 1-HSC, Subset S1-04, experiment #0221 .....	180
Figure E.30	WITS model predicted and actual drying shrinkage (microstrain) for Dataset 1-HSC, Subset S1-04, experiment #0221 .....	180
Figure E.31	RILEM B4 model predicted and actual drying shrinkage (microstrain) for Dataset 1-HSC, Subset S1-04, experiment #0225 .....	181
Figure E.32	MC 2010 model predicted and actual drying shrinkage (microstrain) for Dataset 1-HSC, Subset S1-04, experiment #0225 .....	181

---

---

Figure E.33	WITS model predicted and actual drying shrinkage (microstrain) for Dataset 1-HSC, Subset S1-04, experiment #0225 .....	181
Figure E.34	RILEM B4 model predicted and actual drying shrinkage (microstrain) for Dataset 1-HSC, Subset S1-05, experiment #0015 .....	182
Figure E.35	MC 2010 model predicted and actual drying shrinkage (microstrain) for Dataset 1-HSC, Subset S1-05, experiment #0015 .....	182
Figure E.36	WITS model predicted and actual drying shrinkage (microstrain) for Dataset 1-HSC, Subset S1-05, experiment #0015 .....	182
Figure E.37	RILEM B4 model predicted and actual drying shrinkage (microstrain) for Dataset 1-HSC, Subset S1-05, experiment #0031 .....	183
Figure E.38	MC 2010 model predicted and actual drying shrinkage (microstrain) for Dataset 1-HSC, Subset S1-05, experiment #0031 .....	183
Figure E.39	WITS model predicted and actual drying shrinkage (microstrain) for Dataset 1-HSC, Subset S1-05, experiment #0031 .....	183
Figure E.40	RILEM B4 model predicted and actual drying shrinkage (microstrain) for Dataset 1-HSC, Subset S1-05, experiment #0033 .....	184
Figure E.41	MC 2010 model predicted and actual drying shrinkage (microstrain) for Dataset 1-HSC, Subset S1-05, experiment #0033 .....	184
Figure E.42	WITS model predicted and actual drying shrinkage (microstrain) for Dataset 1-HSC, Subset S1-05, experiment #0033 .....	184
Figure E.43	RILEM B4 model predicted and actual drying shrinkage (microstrain) for Dataset 1-HSC, Subset S2-01, experiment #0228 .....	185
Figure E.44	MC 2010 model predicted and actual drying shrinkage (microstrain) for Dataset 1-HSC, Subset S2-01, experiment #0228 .....	185
Figure E.45	WITS model predicted and actual drying shrinkage (microstrain) for Dataset 1-HSC, Subset S2-01, experiment #0228 .....	185
Figure E.46	RILEM B4 model predicted and actual drying shrinkage (microstrain) for Dataset 1-HSC, Subset S2-01, experiment #0237 .....	186
Figure E.47	MC 2010 model predicted and actual drying shrinkage (microstrain) for Dataset 1-HSC, Subset S2-01, experiment #0237 .....	186
Figure E.48	WITS model predicted and actual drying shrinkage (microstrain) for Dataset 1-HSC, Subset S2-01, experiment #0237 .....	186
Figure E.49	RILEM B4 model predicted and actual drying shrinkage (microstrain) for Dataset 1-HSC, Subset S2-01, experiment #0246 .....	187
Figure E.50	MC 2010 model predicted and actual drying shrinkage (microstrain) for Dataset 1-HSC, Subset S2-01, experiment #0246 .....	187
Figure E.51	WITS model predicted and actual drying shrinkage (microstrain) for Dataset 1-HSC, Subset S2-01, experiment #0246 .....	187
Figure E.52	RILEM B4 model predicted and actual drying shrinkage (microstrain) for Dataset 1-HSC, Subset S2-02, experiment #0240 .....	188
Figure E.53	MC 2010 model predicted and actual drying shrinkage (microstrain) for Dataset 1-HSC, Subset S2-02, experiment #0240 .....	188
Figure E.54	WITS model predicted and actual drying shrinkage (microstrain) for Dataset 1-HSC, Subset S2-02, experiment #0240 .....	188
Figure E.55	RILEM B4 model predicted and actual drying shrinkage (microstrain) for Dataset 1-HSC, Subset S2-02, experiment #0249 .....	189

---

---

Figure E.56	MC 2010 model predicted and actual drying shrinkage (microstrain) for Dataset 1-HSC, Subset S2-02, experiment #0249 .....	189
Figure E.57	WITS model predicted and actual drying shrinkage (microstrain) for Dataset 1-HSC, Subset S2-02, experiment #0249 .....	189
Figure E.58	RILEM B4 model predicted and actual drying shrinkage (microstrain) for Dataset 1-HSC, Subset S2-03, experiment #0234 .....	190
Figure E.59	MC 2010 model predicted and actual drying shrinkage (microstrain) for Dataset 1-HSC, Subset S2-03, experiment #0234 .....	190
Figure E.60	WITS model predicted and actual drying shrinkage (microstrain) for Dataset 1-HSC, Subset S2-03, experiment #0234 .....	190
Figure E.61	RILEM B4 model predicted and actual drying shrinkage (microstrain) for Dataset 1-HSC, Subset S2-03, experiment #0252 .....	191
Figure E.62	MC 2010 model predicted and actual drying shrinkage (microstrain) for Dataset 1-HSC, Subset S2-03, experiment #0252 .....	191
Figure E.63	WITS model predicted and actual drying shrinkage (microstrain) for Dataset 1-HSC, Subset S2-03, experiment #0252 .....	191
Figure E.64	RILEM B4 model predicted and actual drying shrinkage (microstrain) for Dataset 1-HSC, Subset S2-04, experiment A_007_13 .....	192
Figure E.65	MC 2010 model predicted and actual drying shrinkage (microstrain) for Dataset 1-HSC, Subset S2-04, experiment A_007_13 .....	192
Figure E.66	WITS model predicted and actual drying shrinkage (microstrain) for Dataset 1-HSC, Subset S2-04, experiment A_007_13 .....	192
Figure E.67	RILEM B4 model predicted and actual drying shrinkage (microstrain) for Dataset 1-HSC, Subset S2-04, experiment A_007_16 .....	193
Figure E.68	MC 2010 model predicted and actual drying shrinkage (microstrain) for Dataset 1-HSC, Subset S2-04, experiment A_007_16 .....	193
Figure E.69	WITS model predicted and actual drying shrinkage (microstrain) for Dataset 1-HSC, Subset S2-04, experiment A_007_16 .....	193
Figure E.70	RILEM B4 model predicted and actual drying shrinkage (microstrain) for Dataset 1-HSC, Subset S2-05, experiment #0109 .....	194
Figure E.71	MC 2010 model predicted and actual drying shrinkage (microstrain) for Dataset 1-HSC, Subset S2-05, experiment #0109 .....	194
Figure E.72	WITS model predicted and actual drying shrinkage (microstrain) for Dataset 1-HSC, Subset S2-05, experiment #0109 .....	194
Figure E.73	RILEM B4 model predicted and actual drying shrinkage (microstrain) for Dataset 1-HSC, Subset S2-05, experiment #0255 .....	195
Figure E.74	MC 2010 model predicted and actual drying shrinkage (microstrain) for Dataset 1-HSC, Subset S2-05, experiment #0255 .....	195
Figure E.75	WITS model predicted and actual drying shrinkage (microstrain) for Dataset 1-HSC, Subset S2-05, experiment #0255 .....	195
Figure E.76	RILEM B4 model predicted and actual drying shrinkage (microstrain) for Dataset 1-HSC, Subset S2-06, experiment A_070_34 .....	196
Figure E.77	MC 2010 model predicted and actual drying shrinkage (microstrain) for Dataset 1-HSC, Subset S2-06, experiment A_070_34 .....	196
Figure E.78	WITS model predicted and actual drying shrinkage (microstrain) for Dataset 1-HSC, Subset S2-06, experiment A_070_34 .....	196

---

---

Figure E.79	RILEM B4 model predicted and actual drying shrinkage (microstrain) for Dataset 1-HSC, Subset S2-06, experiment A_070_38.....	197
Figure E.80	MC 2010 model predicted and actual drying shrinkage (microstrain) for Dataset 1-HSC, Subset S2-06, experiment A_070_38.....	197
Figure E.81	WITS model predicted and actual drying shrinkage (microstrain) for Dataset 1-HSC, Subset S2-06, experiment A_070_38.....	197
Figure E.82	RILEM B4 model predicted and actual drying shrinkage (microstrain) for Dataset 1-HSC, Subset S2-06, experiment A_070_39.....	198
Figure E.83	MC 2010 model predicted and actual drying shrinkage (microstrain) for Dataset 1-HSC, Subset S2-06, experiment A_070_39.....	198
Figure E.84	WITS model predicted and actual drying shrinkage (microstrain) for Dataset 1-HSC, Subset S2-06, experiment A_070_39.....	198
Figure E.85	RILEM B4 model predicted and actual drying shrinkage (microstrain) for Dataset 1-HSC, Subset S2-07, experiment A_007_14.....	199
Figure E.86	MC 2010 model predicted and actual drying shrinkage (microstrain) for Dataset 1-HSC, Subset S2-07, experiment A_007_14.....	199
Figure E.87	WITS model predicted and actual drying shrinkage (microstrain) for Dataset 1-HSC, Subset S2-07, experiment A_007_14.....	199
Figure E.88	RILEM B4 model predicted and actual drying shrinkage (microstrain) for Dataset 1-HSC, Subset S2-07, experiment A_007_15.....	200
Figure E.89	MC 2010 model predicted and actual drying shrinkage (microstrain) for Dataset 1-HSC, Subset S2-07, experiment A_007_15.....	200
Figure E.90	WITS model predicted and actual drying shrinkage (microstrain) for Dataset 1-HSC, Subset S2-07, experiment A_007_15.....	200
Figure E.91	RILEM B4 model predicted and actual drying shrinkage (microstrain) for Dataset 1-HSC, Subset S2-08, experiment no. 6.....	201
Figure E.92	MC 2010 model predicted and actual drying shrinkage (microstrain) for Dataset 1-HSC, Subset S2-08, experiment no. 6.....	201
Figure E.93	WITS model predicted and actual drying shrinkage (microstrain) for Dataset 1-HSC, Subset S2-08, experiment no. 6.....	201
Figure E.94	RILEM B4 model predicted and actual drying shrinkage (microstrain) for Dataset 1-HSC, Subset S2-08, experiment no. 10.....	202
Figure E.95	MC 2010 model predicted and actual drying shrinkage (microstrain) for Dataset 1-HSC, Subset S2-08, experiment no. 10.....	202
Figure E.96	WITS model predicted and actual drying shrinkage (microstrain) for Dataset 1-HSC, Subset S2-08, experiment no. 10.....	202
Figure E.97	RILEM B4 model predicted and actual drying shrinkage (microstrain) for Dataset 1-HSC, Subset S2-09, experiment no. 31.....	203
Figure E.98	MC 2010 model predicted and actual drying shrinkage (microstrain) for Dataset 1-HSC, Subset S2-09, experiment no. 31.....	203
Figure E.99	WITS model predicted and actual drying shrinkage (microstrain) for Dataset 1-HSC, Subset S2-09, experiment no. 31.....	203
Figure E.100	RILEM B4 model predicted and actual drying shrinkage (microstrain) for Dataset 1-HSC, Subset S2-09, experiment no. 33.....	204
Figure E.101	MC 2010 model predicted and actual drying shrinkage (microstrain) for Dataset 1-HSC, Subset S2-09, experiment no. 33.....	204

---

---

Figure E.102	WITS model predicted and actual drying shrinkage (microstrain) for Dataset 1-HSC, Subset S2-09, experiment no. 33 .....	204
Figure E.103	RILEM B4 model predicted and actual drying shrinkage (microstrain) for Dataset 1-HSC, Subset S2-10, experiment no. 5 .....	205
Figure E.104	MC 2010 model predicted and actual drying shrinkage (microstrain) for Dataset 1-HSC, Subset S2-10, experiment no. 5 .....	205
Figure E.105	WITS model predicted and actual drying shrinkage (microstrain) for Dataset 1-HSC, Subset S2-10, experiment no. 5 .....	205
Figure E.106	RILEM B4 model predicted and actual drying shrinkage (microstrain) for Dataset 1-HSC, Subset S2-10, experiment no. 9 .....	206
Figure E.107	MC 2010 model predicted and actual drying shrinkage (microstrain) for Dataset 1-HSC, Subset S2-10, experiment no. 9 .....	206
Figure E.108	WITS model predicted and actual drying shrinkage (microstrain) for Dataset 1-HSC, Subset S2-10, experiment no. 9 .....	206
Figure E.109	RILEM B4 model predicted and actual drying shrinkage (microstrain) for Dataset 1-HSC, Subset S2-11, experiment no. 7 .....	207
Figure E.110	MC 2010 model predicted and actual drying shrinkage (microstrain) for Dataset 1-HSC, Subset S2-11, experiment no. 7 .....	207
Figure E.111	WITS model predicted and actual drying shrinkage (microstrain) for Dataset 1-HSC, Subset S2-11, experiment no. 7 .....	207
Figure E.112	RILEM B4 model predicted and actual drying shrinkage (microstrain) for Dataset 1-HSC, Subset S2-11, experiment no. 13 .....	208
Figure E.113	MC 2010 model predicted and actual drying shrinkage (microstrain) for Dataset 1-HSC, Subset S2-11, experiment no. 13 .....	208
Figure E.114	WITS model predicted and actual drying shrinkage (microstrain) for Dataset 1-HSC, Subset S2-11, experiment no. 13 .....	208
Figure E.115	RILEM B4 model predicted and actual drying shrinkage (microstrain) for Dataset 1-HSC, Subset S2-11, experiment no. 15 .....	209
Figure E.116	MC 2010 model predicted and actual drying shrinkage (microstrain) for Dataset 1-HSC, Subset S2-11, experiment no. 15 .....	209
Figure E.117	WITS model predicted and actual drying shrinkage (microstrain) for Dataset 1-HSC, Subset S2-11, experiment no. 15 .....	209
Figure E.118	RILEM B4 model predicted and actual drying shrinkage (microstrain) for Dataset 1-HSC, Subset S2-11, experiment no. 16 .....	210
Figure E.119	MC 2010 model predicted and actual drying shrinkage (microstrain) for Dataset 1-HSC, Subset S2-11, experiment no. 16 .....	210
Figure E.120	WITS model predicted and actual drying shrinkage (microstrain) for Dataset 1-HSC, Subset S2-11, experiment no. 16 .....	210
Figure E.121	RILEM B4 model predicted and actual drying shrinkage (microstrain) for Dataset 1-HSC, Subset S2-12, experiment no. 17 .....	211
Figure E.122	MC 2010 model predicted and actual drying shrinkage (microstrain) for Dataset 1-HSC, Subset S2-12, experiment no. 17 .....	211
Figure E.123	WITS model predicted and actual drying shrinkage (microstrain) for Dataset 1-HSC, Subset S2-12, experiment no. 17 .....	211
Figure E.124	RILEM B4 model predicted and actual drying shrinkage (microstrain) for Dataset 1-HSC, Subset S2-12, experiment no. 25 .....	212

---



---

Figure E.125	MC 2010 model predicted and actual drying shrinkage (microstrain) for Dataset 1-HSC, Subset S2-12, experiment no. 25 .....	212
Figure E.126	WITS model predicted and actual drying shrinkage (microstrain) for Dataset 1-HSC, Subset S2-12, experiment no. 25 .....	212
Figure E.127	RILEM B4 model predicted and actual drying shrinkage (microstrain) for Dataset 1-HSC, Subset S2-13, experiment no. 19 .....	213
Figure E.128	MC 2010 model predicted and actual drying shrinkage (microstrain) for Dataset 1-HSC, Subset S2-13, experiment no. 19 .....	213
Figure E.129	WITS model predicted and actual drying shrinkage (microstrain) for Dataset 1-HSC, Subset S2-13, experiment no. 19 .....	213
Figure E.130	RILEM B4 model predicted and actual drying shrinkage (microstrain) for Dataset 1-HSC, Subset S2-13, experiment no. 21 .....	214
Figure E.131	MC 2010 model predicted and actual drying shrinkage (microstrain) for Dataset 1-HSC, Subset S2-13, experiment no. 21 .....	214
Figure E.132	WITS model predicted and actual drying shrinkage (microstrain) for Dataset 1-HSC, Subset S2-13, experiment no. 21 .....	214
Figure E.133	RILEM B4 model predicted and actual drying shrinkage (microstrain) for Dataset 1-HSC, Subset S2-13, experiment no. 22 .....	215
Figure E.134	MC 2010 model predicted and actual drying shrinkage (microstrain) for Dataset 1-HSC, Subset S2-13, experiment no. 22 .....	215
Figure E.135	WITS model predicted and actual drying shrinkage (microstrain) for Dataset 1-HSC, Subset S2-13, experiment no. 22 .....	215
Figure E.136	RILEM B4 model predicted and actual drying shrinkage (microstrain) for Dataset 1-HSC, Subset S2-14, experiment no. 27 .....	216
Figure E.137	MC 2010 model predicted and actual drying shrinkage (microstrain) for Dataset 1-HSC, Subset S2-14, experiment no. 27 .....	216
Figure E.138	WITS model predicted and actual drying shrinkage (microstrain) for Dataset 1-HSC, Subset S2-14, experiment no. 27 .....	216
Figure E.139	RILEM B4 model predicted and actual drying shrinkage (microstrain) for Dataset 1-HSC, Subset S2-14, experiment no. 28 .....	217
Figure E.140	MC 2010 model predicted and actual drying shrinkage (microstrain) for Dataset 1-HSC, Subset S2-14, experiment no. 28 .....	217
Figure E.141	WITS model predicted and actual drying shrinkage (microstrain) for Dataset 1-HSC, Subset S2-14, experiment no. 28 .....	217
Figure E.142	RILEM B4 model predicted and actual drying shrinkage (microstrain) for Dataset 1-HSC, Subset S2-14, experiment no. 29 .....	218
Figure E.143	MC 2010 model predicted and actual drying shrinkage (microstrain) for Dataset 1-HSC, Subset S2-14, experiment no. 29 .....	218
Figure E.144	WITS model predicted and actual drying shrinkage (microstrain) for Dataset 1-HSC, Subset S2-14, experiment no. 29 .....	218
Figure E.145	RILEM B4 model predicted and actual drying shrinkage (microstrain) for Dataset 1-HSC, Subset S2-14, experiment no. 30 .....	219
Figure E.146	MC 2010 model predicted and actual drying shrinkage (microstrain) for Dataset 1-HSC, Subset S2-14, experiment no. 30 .....	219
Figure E.147	WITS model predicted and actual drying shrinkage (microstrain) for Dataset 1-HSC, Subset S2-14, experiment no. 30 .....	219

---

---

Figure F.1	RILEM B4 model predicted and actual drying shrinkage (microstrain) for Dataset 2-HSC, Subset S2-01a, experiment A_072_04 .....	220
Figure F.2	MC 2010 model predicted and actual drying shrinkage (microstrain) for Dataset 2-HSC, Subset S2-01a, experiment A_072_04 .....	220
Figure F.3	RILEM B4 model predicted and actual drying shrinkage (microstrain) for Dataset 2-HSC, Subset S2-01a, experiment A_072_05 .....	220
Figure F.4	MC 2010 model predicted and actual drying shrinkage (microstrain) for Dataset 2-HSC, Subset S2-01a, experiment A_072_05 .....	221
Figure F.5	RILEM B4 model predicted and actual drying shrinkage (microstrain) for Dataset 2-HSC, Subset S2-02a, experiment A_007_09 .....	221
Figure F.6	MC 2010 model predicted and actual drying shrinkage (microstrain) for Dataset 2-HSC, Subset S2-02a, experiment A_007_09 .....	221
Figure F.7	RILEM B4 model predicted and actual drying shrinkage (microstrain) for Dataset 2-HSC, Subset S2-02a, experiment A_007_12 .....	222
Figure F.8	MC 2010 model predicted and actual drying shrinkage (microstrain) for Dataset 2-HSC, Subset S2-02a, experiment A_007_12 .....	222
Figure F.9	RILEM B4 model predicted and actual drying shrinkage (microstrain) for Dataset 2-HSC, Subset S2-03a, experiment A_072_06 .....	222
Figure F.10	MC 2010 model predicted and actual drying shrinkage (microstrain) for Dataset 2-HSC, Subset S2-03a, experiment A_072_06 .....	223
Figure F.11	RILEM B4 model predicted and actual drying shrinkage (microstrain) for Dataset 2-HSC, Subset S2-03a, experiment A_086_18 .....	223
Figure F.12	MC 2010 model predicted and actual drying shrinkage (microstrain) for Dataset 2-HSC, Subset S2-03a, experiment A_086_18 .....	223
Figure F.13	RILEM B4 model predicted and actual drying shrinkage (microstrain) for Dataset 2-HSC, Subset S2-03a, experiment A_086_20 .....	224
Figure F.14	MC 2010 model predicted and actual drying shrinkage (microstrain) for Dataset 2-HSC, Subset S2-03a, experiment A_086_20 .....	224
Figure F.15	RILEM B4 model predicted and actual drying shrinkage (microstrain) for Dataset 2-HSC, Subset S2-04a, experiment A_068_01 .....	224
Figure F.16	MC 2010 model predicted and actual drying shrinkage (microstrain) for Dataset 2-HSC, Subset S2-04a, experiment A_068_01 .....	225
Figure F.17	RILEM B4 model predicted and actual drying shrinkage (microstrain) for Dataset 2-HSC, Subset S2-04a, experiment A_068_19 .....	225
Figure F.18	MC 2010 model predicted and actual drying shrinkage (microstrain) for Dataset 2-HSC, Subset S2-04a, experiment A_068_19 .....	225
Figure F.19	RILEM B4 model predicted and actual drying shrinkage (microstrain) for Dataset 2-HSC, Subset S2-05a, experiment A_022_03 .....	226
Figure F.20	MC 2010 model predicted and actual drying shrinkage (microstrain) for Dataset 2-HSC, Subset S2-05a, experiment A_022_03 .....	226
Figure F.21	RILEM B4 model predicted and actual drying shrinkage (microstrain) for Dataset 2-HSC, Subset S2-05a, experiment A_022_05 .....	226
Figure F.22	MC 2010 model predicted and actual drying shrinkage (microstrain) for Dataset 2-HSC, Subset S2-05a, experiment A_022_05 .....	227
Figure F.23	RILEM B4 model predicted and actual drying shrinkage (microstrain) for Dataset 2-HSC, Subset S2-06a, experiment A_086_41 .....	227

---

---

Figure F.24	MC 2010 model predicted and actual drying shrinkage (microstrain) for Dataset 2-HSC, Subset S2-06a, experiment A_086_41 .....	227
Figure F.25	RILEM B4 model predicted and actual drying shrinkage (microstrain) for Dataset 2-HSC, Subset S2-06a, experiment A_086_42 .....	228
Figure F.26	MC 2010 model predicted and actual drying shrinkage (microstrain) for Dataset 2-HSC, Subset S2-06a, experiment A_086_42 .....	228
Figure F.27	RILEM B4 model predicted and actual drying shrinkage (microstrain) for Dataset 2-HSC, Subset S2-07a, experiment A_086_36 .....	228
Figure F.28	MC 2010 model predicted and actual drying shrinkage (microstrain) for Dataset 2-HSC, Subset S2-07a, experiment A_086_36 .....	229
Figure F.29	RILEM B4 model predicted and actual drying shrinkage (microstrain) for Dataset 2-HSC, Subset S2-07a, experiment A_086_37 .....	229
Figure F.30	MC 2010 model predicted and actual drying shrinkage (microstrain) for Dataset 2-HSC, Subset S2-07a, experiment A_086_37 .....	229
Figure F.31	RILEM B4 model predicted and actual drying shrinkage (microstrain) for Dataset 2-HSC, Subset S2-08a, experiment A_086_26 .....	230
Figure F.32	MC 2010 model predicted and actual drying shrinkage (microstrain) for Dataset 2-HSC, Subset S2-08a, experiment A_086_26 .....	230
Figure F.33	RILEM B4 model predicted and actual drying shrinkage (microstrain) for Dataset 2-HSC, Subset S2-08a, experiment A_086_30 .....	230
Figure F.34	MC 2010 model predicted and actual drying shrinkage (microstrain) for Dataset 2-HSC, Subset S2-08a, experiment A_086_30 .....	231
Figure F.35	RILEM B4 model predicted and actual drying shrinkage (microstrain) for Dataset 2-HSC, Subset S2-08a, experiment A_086_31 .....	231
Figure F.36	MC 2010 model predicted and actual drying shrinkage (microstrain) for Dataset 2-HSC, Subset S2-08a, experiment A_086_31 .....	231
Figure F.37	RILEM B4 model predicted and actual drying shrinkage (microstrain) for Dataset 2-HSC, Subset S2-09a, experiment A_031_04 .....	232
Figure F.38	MC 2010 model predicted and actual drying shrinkage (microstrain) for Dataset 2-HSC, Subset S2-09a, experiment A_031_04 .....	232
Figure F.39	RILEM B4 model predicted and actual drying shrinkage (microstrain) for Dataset 2-HSC, Subset S2-09a, experiment A_031_06 .....	232
Figure F.40	MC 2010 model predicted and actual drying shrinkage (microstrain) for Dataset 2-HSC, Subset S2-09a, experiment A_031_06 .....	233
Figure F.41	RILEM B4 model predicted and actual drying shrinkage (microstrain) for Dataset 2-HSC, Subset S2-09a, experiment A_046_02 .....	233
Figure F.42	MC 2010 model predicted and actual drying shrinkage (microstrain) for Dataset 2-HSC, Subset S2-09a, experiment A_046_02 .....	233
Figure F.43	RILEM B4 model predicted and actual drying shrinkage (microstrain) for Dataset 2-HSC, Subset S2-09a, experiment A_046_07 .....	234
Figure F.44	MC 2010 model predicted and actual drying shrinkage (microstrain) for Dataset 2-HSC, Subset S2-09a, experiment A_046_07 .....	234
Figure F.45	RILEM B4 model predicted and actual drying shrinkage (microstrain) for Dataset 2-HSC, Subset S2-10a, experiment A_086_07 .....	234
Figure F.46	MC 2010 model predicted and actual drying shrinkage (microstrain) for Dataset 2-HSC, Subset S2-10a, experiment A_086_07 .....	235

---

---

Figure F.47	RILEM B4 model predicted and actual drying shrinkage (microstrain) for Dataset 2-HSC, Subset S2-10a, experiment A_086_09 .....	235
Figure F.48	MC 2010 model predicted and actual drying shrinkage (microstrain) for Dataset 2-HSC, Subset S2-10a, experiment A_086_09 .....	235
Figure F.49	RILEM B4 model predicted and actual drying shrinkage (microstrain) for Dataset 2-HSC, Subset S2-10a, experiment A_086_11 .....	236
Figure F.50	MC 2010 model predicted and actual drying shrinkage (microstrain) for Dataset 2-HSC, Subset S2-10a, experiment A_086_11 .....	236
Figure F.51	RILEM B4 model predicted and actual drying shrinkage (microstrain) for Dataset 2-HSC, Subset S2-11a, experiment A_086_13 .....	236
Figure F.52	MC 2010 model predicted and actual drying shrinkage (microstrain) for Dataset 2-HSC, Subset S2-11a, experiment A_086_13 .....	237
Figure F.53	RILEM B4 model predicted and actual drying shrinkage (microstrain) for Dataset 2-HSC, Subset S2-11a, experiment A_086_14 .....	237
Figure F.54	MC 2010 model predicted and actual drying shrinkage (microstrain) for Dataset 2-HSC, Subset S2-11a, experiment A_086_14 .....	237
Figure F.55	RILEM B4 model predicted and actual drying shrinkage (microstrain) for Dataset 2-HSC, Subset S2-12a, experiment A_007_06 .....	238
Figure F.56	MC 2010 model predicted and actual drying shrinkage (microstrain) for Dataset 2-HSC, Subset S2-12a, experiment A_007_06 .....	238
Figure F.57	RILEM B4 model predicted and actual drying shrinkage (microstrain) for Dataset 2-HSC, Subset S2-12a, experiment A_007_07 .....	238
Figure F.58	MC 2010 model predicted and actual drying shrinkage (microstrain) for Dataset 2-HSC, Subset S2-12a, experiment A_007_07 .....	239

---

---

## List of Tables

<b>Body</b>	<b>Page</b>
Table 2.1	European common cement and sulphate resisting cement types (SANS 50197-1, 2013) . 8
Table 2.2	American Portland cement and blended hydraulic cement types (ASTM C150 and ASTM C595) ..... 8
Table 2.3	Typical chemical admixtures used and their purpose according to Setareh & Darvas (2007), Al-Manaseer & Fayyaz (2011), Mehta & Monteiro (2006) and Pease (2005). .... 11
Table 2.4	ASTM C157 - Required equipment and facilities. .... 19
Table 2.5	HSC mix proportions of experiments conducted by Lee <i>et al</i> (2017) ..... 21
Table 2.6	HSC mix proportions of experiments with varying w/c ratios by Tam <i>et al</i> (2012) ..... 22
Table 2.7	HSC mix proportions of experiments conducted by Lee <i>et al</i> (2017). .... 23
Table 2.8	HSC mix proportions of experiments conducted by Guðmundsson (2013). .... 26
Table 2.9	HSC mix proportions of experiments conducted by (Tam <i>et al</i> , 2012). .... 26
Table 2.10	Covariate data required for selected shrinkage prediction models (Adapted from Gaylard, 2011; RILEM TC-242-MDC, 2015 and CEB-FIP, 2012). .... 38
Table 2.11	Applicable data ranges for covariates of selected shrinkage prediction models (Adapted from Gaylard, 2011; RILEM TC-242-MDC, 2015 and CEB-FIP, 2012). .... 39
Table 3.1	Different presentation of covariate data between NU Database, RSA Database and Technical report (Al-Manaseer & Fayyaz, 2011). .... 47
Table 3.2	Total number of shrinkage experiments per data source. .... 47
Table 3.3	Number of shrinkage experiments for Dataset 1 and Dataset 2. .... 48
Table 3.4	Data extracted from the original data sources. .... 49
Table 3.5	Data extracted from the original data sources (continuation). .... 50
Table 3.6	Averaged percentage of 28 <sup>th</sup> day compressive strength to estimate the 2 and 7 day compressive strengths. .... 50
Table 3.7	Percentage of missing covariate data per Dataset 1 and Dataset 2. .... 51
Table 3.8	Number of shrinkage experiments for Datasets 1-HSC and 2-HSC, Datasets 3, 4 and 5. . 54
Table 3.9	Data subsets derived from Dataset 1-HSC. .... 55
Table 3.10	Data subsets derived from Dataset 1-HSC. .... 55
Table 3.11	Data subsets derived from Dataset 2-HSC. .... 56
Table 4.1	RILEM B4 model original coefficients for cement type – drying shrinkage ..... 63
Table 4.2	RILEM B4 model updated coefficients for cement type – drying shrinkage ..... 64
Table 4.3	RILEM B4 model original coefficients for aggregate and admixture combination – drying shrinkage ..... 64
Table 4.4	RILEM B4 model updated coefficients for aggregate and admixture combination – drying shrinkage. .... 65
Table 4.5	RILEM B4 model updated coefficients for aggregate and admixture combination – drying shrinkage (continuation). .... 66
Table 4.6	RILEM B4 original model coefficients for cement type and admixture combination – autogenous shrinkage. .... 68
Table 4.7	RILEM B4 updated model coefficients for cement type – autogenous shrinkage. .... 68
Table 4.8	MC 2010 original model coefficients for cement type and most influential constant (exponent 2) – drying shrinkage ..... 70

---

---

Table 4.9	MC 2010 updated model coefficients for cement type coefficient and most influential model constant (exponent 2) – drying shrinkage. ....	70
Table 4.10	MC 2010 updated model coefficients for cement type coefficient and most influential model constant (exponent 2) – drying shrinkage (continuation). ....	71
Table 4.11	MC 2010 original model coefficient for cement type and constant in exponent in $\beta_{as}(t)$ – autogenous shrinkage. ....	73
Table 4.12	CEB-FIB MC 2010 updated model coefficient for cement type coefficient and constant in exponent in $\beta_{as}(t)$ – autogenous shrinkage.....	74
Table 4.13	WITS model original factors for aggregate type– drying shrinkage.....	76
Table 4.14	WITS model updated factors for aggregate type and admixture combination– drying shrinkage. ....	76
Table 4.15	WITS model updated factors for aggregate type and admixture combination– drying shrinkage (continuation). ....	77
Table 4.16	Composite model initial and fitted $t_x$ values. ....	79
Table 4.17	Composite model fitted curvature smoothness parameter ( $m, q$ ) for data subsets S2-08, S2-09, S2-10 and S2-12.....	80
Table 4.18	Ranking of the RILEM B4, MC 2010 and WITS models for data subset S1-03 (Dataset 1-HSC). ....	90
Table 4.19	Ranking of the RILEM B4, MC 2010 and WITS models for data subset S2-02 (Dataset 1-HSC). ....	91
Table 4.20	Ranking of the RILEM B4, MC 2010 and WITS models for data subset S2-08 (Dataset 1-HSC ). ....	91
Table 4.21	Ranking of the RILEM B4, MC 2010 and WITS models for data subset S1-03 (Dataset 1-HSC) over the time range 0 to 99 days.....	92
Table 4.22	Ranking of the RILEM B4, MC 2010 and WITS models for data subset S2-02 (Dataset 1-HSC) over the time ranges 0 to 99, 100 to 199 and 200 to 499 days.....	92
Table 4.23	Ranking of the RILEM B4, MC 2010, WITS and composite models for data subset S2-08 (Dataset 1-HSC) over the time ranges 0 to 99, 100 to 199 and 200 to 499 days and 500 days or more. ....	93
Table 4.24	Ranking of the RILEM B4 and MC 2010 models for data subset S2-02a (Dataset 2-HSC).94	
Table 4.25	Ranking of the RILEM B4 and MC 2010 models for data subset S2-09a (Dataset 2-HSC).94	
Table 4.26	Ranking of the RILEM B4 and MC 2010 models for data subset S2-02a (Dataset 2-HSC) over the time ranges 0 to 99 and 100 to 199 days. ....	95
Table 4.27	Ranking of the RILEM B4 and MC 2010 models for data subset S2-09a (Dataset 2-HSC) over the time ranges 0 to 99 days.....	95
Table 4.28	Ranking of the RILEM B4 and MC 2010 models for data subset S2-09a (Dataset 2-HSC) over the time ranges 100 to 199 and 200 to 499 days. ....	96
Table 5.1	Subsets without admixtures: error ranges (%) of original and modified models for short- and medium-term drying shrinkage.....	103
Table 5.2	Subsets with mineral admixtures: error ranges (%) of original and modified models for short- and medium-term drying shrinkage.....	105
Table 5.3	Subsets with mineral and chemical admixtures: error ranges (%) of original and modified models for short-, medium- and long-term drying shrinkage. ....	107
Table 5.4	Subsets S2-08, S2-09, S2-10 and S2-12: error ranges (%) for modified and proposed composite shrinkage models for short-, medium and long-term periods - drying shrinkage. ....	108

---

---

Table 5.5	Subsets S2-01a to S2-12a with mineral and chemical admixtures: error ranges (%) of original and modified models for short-, medium- and long-term periods - autogenous shrinkage. ....	110
Table 5.6	Summary of averaged statistical indicators RMSE, $R^2_{adj}$ , $AIC_c$ and $C.o.V_{all}$ for original and modified versions of the RILEM B4, MC 2010 and WITS models - Dataset 1-HSC.....	116
Table 5.7	Summary of averaged statistical indicators RMSE, $R^2_{adj}$ , $AIC_c$ and $C.o.V_{all}$ calculated for original and modified versions of the RILEM B4 and MC 2010 models - Dataset 2-HSC.....	117

## Appendices

Table A.1	Cement type dependant RILEM B4 model parameters for drying shrinkage (RILEM TC-242-MDC, 2015).....	131
Table A.2	Cement type dependant RILEM B4 model parameters for autogenous shrinkage (RILEM TC-242-MDC, 2015). ....	131
Table A.3	Aggregate type dependant RILEM B4 model parameters for drying shrinkage (RILEM TC-242-MDC, 2015). ....	131
Table A.4	Admixture combination type dependant RILEM B4 model parameters for drying and autogenous shrinkage (RILEM TC-242-MDC, 2015). ....	132
Table A.5	Cement, stone and sand types considered by the WITS model (Gaylard, 2011; Gaylard <i>et al</i> , 2013). ....	134
Table A.6	Cement and sand types considered by the WITS model continuation (Gaylard, 2011; Gaylard <i>et al</i> , 2013). ....	135
Table B.1	Statistical indicator results of original model for data subsets without admixtures and with mineral admixtures of Dataset 1-HSC. ....	136
Table B.2	Statistical indicator results of original model for data subsets without admixtures and with mineral admixtures of Dataset 1-HSC. ....	137
Table B.3	Statistical indicator results of modified models for data subsets without admixtures and with mineral admixtures of Dataset 1-HSC. ....	138
Table B.4	Statistical indicator results of modified models for data subsets with mineral and chemical admixtures of Dataset 1-HSC. ....	139
Table B.5	Statistical indicator results of original models for data subsets with mineral and chemical admixtures of Dataset 2-HSC. ....	140
Table B.6	Statistical indicator results of modified models for data subsets with mineral and chemical admixtures of Dataset 2-HSC. ....	141
Table C.1	$R^2_{adj}$ results of original models per shrinkage range for data subsets without and with mineral admixtures of Dataset 1-HSC. ....	142
Table C.2	$R^2_{adj}$ results of original models per shrinkage range for data subsets with mineral and chemical admixtures of Dataset 1-HSC. ....	143
Table C.3	$R^2_{adj}$ results of modified models per shrinkage range for data subsets without and with mineral admixtures of Dataset 1-HSC. ....	144
Table C.4	$R^2_{adj}$ results of modified models per shrinkage range for data subsets with mineral and chemical admixtures of Dataset 1-HSC. ....	145
Table C.5	RMSE results of original models per shrinkage range for data subsets without and with mineral admixtures of Dataset 1-HSC. ....	146
Table C.6	RMSE results of original models per shrinkage range for data subsets with mineral and chemical admixtures of Dataset 1-HSC. ....	147

---

---

Table C.7	RMSE results of modified models per shrinkage range for data subsets without and with mineral admixtures of Dataset 1-HSC. ....	148
Table C.8	RMSE results of modified models per shrinkage range for data subsets with mineral and chemical admixtures of Dataset 1-HSC. ....	149
Table C.9	C.o.V results of original models per shrinkage range for data subsets without and with mineral admixtures of Dataset 1-HSC. ....	150
Table C.10	C.o.V results of original models per shrinkage range for data subsets with mineral and chemical admixtures of Dataset 1-HSC. ....	151
Table C.11	C.o.V results of modified models per shrinkage range for data subsets without and with mineral admixtures of Dataset 1-HSC. ....	152
Table C.12	C.o.V results of modified models per shrinkage range for data subsets with mineral and chemical admixtures of Dataset 1-HSC. ....	153
Table C.13	$R^2_{adj}$ results of original models per shrinkage range for data subsets with mineral and chemical admixtures of Dataset 2-HSC. ....	154
Table C.14	$R^2_{adj}$ results of modified models per shrinkage range for data subsets with mineral and chemical admixtures of Dataset 2-HSC. ....	155
Table C.15	RMSE results of original models per shrinkage range for data subsets with mineral and chemical admixtures of Dataset 2-HSC. ....	156
Table C.16	RMSE results of modified models per shrinkage range for data subsets with mineral and chemical admixtures of Dataset 2-HSC. ....	157
Table C.17	C.o.V results of original models per shrinkage range for data subsets with mineral and chemical admixtures of Dataset 2-HSC. ....	158
Table C.18	C.o.V results of modified models per shrinkage range for data subsets with mineral and chemical admixtures of Dataset 2-HSC. ....	159
Table D.1	RMSE and C.o.V values for each experiment and per shrinkage range for Dataset 3 (drying shrinkage) – RILEM B4 model. ....	160
Table D.2	RMSE and C.o.V values for each experiment and per shrinkage range for Dataset 3 (drying shrinkage) – RILEM B4 model (continuation 1). ....	161
Table D.3	RMSE and C.o.V values for each experiment and per shrinkage range for Dataset 3 (autogenous shrinkage) – RILEM B4 model. ....	162
Table D.4	RMSE and C.o.V values for each experiment and per shrinkage range for Dataset 4 (drying shrinkage) – MC 2010 model. ....	163
Table D.5	RMSE and C.o.V values for each experiment and per shrinkage range for Dataset 4 (drying shrinkage) – MC 2010 model (continuation 1). ....	164
Table D.6	RMSE and C.o.V values for each experiment and per shrinkage range for Dataset 4 (drying shrinkage) – MC 2010 model (continuation 2). ....	165
Table D.7	RMSE and C.o.V values for each experiment and per shrinkage range for Dataset 4 (autogenous shrinkage) – MC 2010 model. ....	165
Table D.8	RMSE and C.o.V values for each experiment and per shrinkage range for Dataset 4 (autogenous shrinkage) – MC 2010 model (Continuation 1). ....	166
Table D.9	RMSE and C.o.V values for each experiment and per shrinkage range for Dataset 4 (autogenous shrinkage) – MC 2010 model (Continuation 2). ....	167
Table D.10	RMSE and C.o.V values for each experiment and per shrinkage range for Dataset 4 (autogenous shrinkage) – MC 2010 model (Continuation 3). ....	168
Table D.11	RMSE and C.o.V values for each experiment and per shrinkage range for Dataset 5 – WITS model. ....	169

---



---

Table D.12	RMSE and C.o.V values for each experiment and per shrinkage range for Dataset 5 – WITS model (continuation). .....	170
------------	--	-----

---

# Nomenclature

## Constants

$A$	Cross-sectional area ( $mm^2$ )
$a/c$	Aggregate-to-cement ratio
$a/cm$	Aggregate-to-cement ratio by weight
AEA	Air entrainment agent ( $\%/cm$ ; $\%/c$ or $kg/m^3$ )
$c$	Cement content of concrete ( $\%$ or $kg/m^3$ )
$C_i$	Concentration of substance ( $mol/m^3$ )
$cm$	Cementitious material content of concrete ( $\%$ or $kg/m^3$ )
$D$	Coefficient of diffusion
$E_{28}$	Elastic modulus at 28 days ( $GPa$ )
FA	Fly ash ( $\%/cm$ ; $\%/c$ or $kg/m^3$ )
$f_{cm28}$	28 <sup>th</sup> day standard cylinder compressive strength ( $MPa$ )
GGBS	Ground granulated blast furnace slag ( $\%/cm$ ; $\%/c$ or $kg/m^3$ )
GGCS	Ground granulated Corex slag ( $\%/cm$ ; $\%/c$ or $kg/m^3$ )
GGFS	Ground granulated Ferro-manganese slag ( $\%/cm$ ; $\%/c$ or $kg/m^3$ )
$h$	MC 2010 notional size of member model parameter for drying shrinkage
$\Delta_{hw}$	Hydraulic grade
$k$	Number of free parameters per model plus 1
$k_{\epsilon a}$	RILEM B4 model aggregate type dependant parameter for drying shrinkage
$k_{ta}$	RILEM B4 model aggregate type dependant parameter for drying shrinkage
$K_w$	Water permeability coefficient ( $m/s$ )
$L$	Length ( $mm$ )
$m$	Curvature smoothness constant
M	Metakaolin ( $\%/cm$ ; $\%/c$ or $kg/m^3$ )
$n$	Number of data points
$n_d$	Number of time intervals in decades
$n_i$	Number of data points per time interval
$N$	Number of intervals/datasets in a database
$r$	Radius or size of the capillary pore ( $nm$ )
$r_a$	RILEM B4 model cement type dependant parameter for autogenous shrinkage
$r_{\epsilon a}$	RILEM B4 model cement type dependant parameter for autogenous shrinkage
$r_{\epsilon w}$	RILEM B4 model cement type dependant parameter for autogenous shrinkage
$r_t$	RILEM B4 model cement type dependant parameter for autogenous shrinkage
$p$	Number of model parameters
P	Plasticiser ( $\%/cm$ ; $\%/c$ or $kg/m^3$ )
$P_{\epsilon a}$	RILEM B4 model cement type dependant parameter for drying shrinkage
$P_{\epsilon w}$	RILEM B4 model cement type dependant parameter for drying shrinkage

---

$P_t$	RILEM B4 model cement type dependant parameter for drying shrinkage
$\Delta P$	Capillary pressure ( <i>nmHg</i> )
$q$	Curvature smoothness constant determines the slope of the transition part of the growth curve
$Q$	Volume of fluid over time ( $m^3/s$ )
RD	Relative density ( $kg/m^3$ )
RE	Retarder ( $\%/cm$ ; $\%/c$ or $kg/m^3$ )
RH	Relative humidity (%)
SF	Silica fume ( $\%/cm$ ; $\%/c$ or $kg/m^3$ )
SP	Superplasticiser ( $\%/cm$ ; $\%/c$ or $kg/m^3$ )
SRA	Shrinkage reducing admixture ( $\%/cm$ ; $\%/c$ or $kg/m^3$ )
SRA-E	Eclipse <sup>®</sup> shrinkage reducing admixture ( $\%/cm$ ; $\%/c$ or $kg/m^3$ )
SRA-T	Tetraguard AS20 <sup>®</sup> shrinkage reducing admixture ( $\%/cm$ ; $\%/c$ or $kg/m^3$ )
$T$	Temperature ( $^{\circ}C$ )
$t$	Time / age of concrete ( <i>days</i> )
$t_0$	Age at first drying of concrete ( <i>days</i> )
$t_{dry}$	Age at first drying of concrete ( <i>days</i> )
$t_x$	Inflection point
V/S	Volume-to-surface area ratio
w	Water content of concrete ( $kg/m^3$ )
w/c	Water-to-cement ratio
w/cm	Water-to-cementitious material ratio
$x$	Location/ distance ( <i>mm</i> )

## Greek letters

$\alpha$	WITS model parameter = -2245.19
$\alpha_{as1}$	MC 2010 model cement type and strength class dependant parameter for autogenous shrinkage
$\alpha_{ds1}$	MC 2010 model cement type and strength class dependant parameter for drying shrinkage
$\beta_{ds}(t)$	Drying shrinkage model time function: rate of shrinkage development with time
$\beta_{as}(t)$	Autogenous shrinkage model time function: rate of shrinkage development with time
$\sigma$	Surface tension
$\theta$	Angle of contact between the liquid and capillary wall
$\epsilon_{cem}$	RILEM B4 model cement type dependant parameter for drying shrinkage
$\epsilon_{as,cem}$	RILEM B4 model cement type dependant parameter for autogenous shrinkage
$\epsilon$	Shrinkage
$\epsilon_{as}(t)$	Standard mean autogenous shrinkage

---

$\varepsilon_{ds}(t-t_0)$	Standard mean drying shrinkage strain
$\ln(\beta)$	WITS model parameter = 9.76
$\ln(\gamma)$	WITS model parameter = 3.04
$\tau_{cem}$	RILEM B4 model cement type dependant parameter for drying shrinkage
$\bar{\omega}_{all}$	Bažant and Baweja overall coefficient of variation
$y_i$	Observed/measured value
$\bar{y}_i$	Average observed/measured value
$\hat{y}_i$	Predicted value

## Terms and concepts

ACI	American Concrete Institute
AIC	Akaike's information criterion
AIC <sub>c</sub>	Corrected Akaike's information criterion
ASTM	American Society for Testing and Materials
BS	British Standard
CEB-FIB	Comité Européen du Béton - Fédération Internationale du Béton
CO <sub>2</sub>	Carbon dioxide
C.o.V	Coefficient of variation
C.o.V <sub>all</sub>	Overall coefficient of variation
C-S-H	Calcium-Silicate-Hydrate
EN	European standard
ER <sub>i</sub>	Evidence ratio
HRWR	High-range water-reducer
HSC	High strength concrete
ITZ	Interfacial transition zone
LRWR	Low-range water-reducer
MC 2010	Model Code 2010
M <sub>CEB</sub>	CEB mean deviation
ML	Maximum likelihood estimate
MS	Microsoft
NCSS	Statistical software
NSC	Normal strength concrete
NU	Northwestern University
R	CEB Model Code definition: Rapid hardening cement type
R <sup>2</sup>	Coefficient of determination
R <sup>2</sup> <sub>adj</sub>	Adjusted coefficient of determination

---

RILEM	Réunion Internationale des Laboratoires et Experts des Matériaux, systèmes de construction et ouvrages (English translation: International Union of Laboratories and Experts in Construction Materials, Systems, and Structures)
RMSE	Root Mean Square Error
RS	CEB Model Code definition: Rapid hardening and early high strength cement type RILEM B4 definition: Rapid hardening cement type
RSA	Republic of South Africa
RSS	Residual sum of squares
SANS	South African National Standards
$S_j$	Standard deviation per dataset
SL	Slow hardening cement type
Slump	Consistency measurement of fresh concrete in mm
TSS	Total sum of squares
USA	United States of America
$V_{CEB}$	CEB overall coefficient of variation
$w_{ij}$	Bažant and Baweja weights applied to the $i^{th}$ time interval
WITS	University of the Witwatersrand

---

# Chapter 1 Introduction

Concrete is a building material that is commonly used worldwide because of its resource availability and adaptable properties (such as durability, workability and strength) to meet the requirements of architects, engineers and contractors (Aïctin & Mindess, 2011). Constant advancements in the concrete industry have led to the manufacture of concrete with specialised properties, such as High Strength Concrete (HSC) (Pomeroy & Marsh, 2014).

## 1.1 Background and Motivation

The prediction of shrinkage in HSC is important when dealing with heavily loaded and large concrete structures such as dam walls and bridges. The pre-stressed force in long span bridges can be compromised due to shrinkage and creep, which reduces the structure's serviceability (Sagara & Pane, 2015). Shrinkage prediction models are used during the design stage of concrete structures and established prediction models are either based on the concrete composition or the design compressive strength (Rasoolinejad, Rahimi-Aghdam & Bažant, 2019). The physical process of shrinkage at nanoscopic level is yet to be fully understood, so predictions are largely empirical (Wedner, Hubler & Bažant, 2015(b)). Over the years shrinkage deformation for various concrete compositions have been recorded in laboratories, and from these experiments databases were compiled and used to develop shrinkage prediction models. The majority of globally recognised and recommended shrinkage prediction models were developed primarily using Normal Strength Concrete (NSC) data. More recently published models are the RILEM B4 model (Wedner, Hubler & Bažant, 2014), referred to from here on as RILEM B4, and CEB-FIB Model Code 2010 model (CEB-FIB, 2012), referred to from here on as the MC 2010 model. The RILEM B4 model was calibrated on the largest database, the NU database, which includes creep and shrinkage data of modern concretes (Fanourakis, 2017). The MC 2010 model was calibrated on 168 long-term experiments from the 1998 version RILEM database (CEB-FIB, 2013).

### *Predicting HSC drying shrinkage*

Shrinkage in concrete is a progressive deformation defined as a volumetric decrease of an unloaded and unrestrained or restrained specimen. Drying shrinkage, specifically, occurs in hardened concrete due to the loss of internal moisture through the surfaces of the concrete specimen. This causes the formation of cracks which have a long-term deleterious effect on hardened concrete. The drying shrinkage in HSC is generally low. However, in ACI Committee 363 (1997) it was noted that HSC has greater early-age shrinkage, up until about the 180<sup>th</sup> day, compared to NSC.

Alexander and Beushausen (2009) explain that autogenous shrinkage, which takes place in the early ages, is higher in HSC than in ordinary concrete, thus HSC is more susceptible to early-age cracking. Accurate total shrinkage (autogenous plus drying shrinkage) prediction is important in the design of sustainable concrete infrastructure as it enables calculation of the long-term serviceability (ACI Committee 209, 2008). Many existing prediction models cannot be used to predict HSC shrinkage as they were not calibrated using strength and shrinkage data for modern concrete compositions (Mazloom, 2008; Pan & Meng, 2016). Bažant and Baweja (2000) state, "The updating of model parameters is particularly important for high-strength concretes and other special concretes containing various admixtures, superplasticizers, water-reducing agents and pozzolanic materials".

Compared to ordinary concrete mixes, HSC requires carefully proportioned amounts of concrete constituents to achieve the required strength and durability. A low water-to-cementitious material ratio ( $w/cm$ ) is an indication of HSC. This effectively decreases the mixture workability, so admixtures are introduced to the concrete mixture to increase the workability and manipulate other physical properties, such as setting-time and shrinkage. These modern concretes are more complex than traditional concretes due to the large amounts of chemical and mineral admixtures. The admixtures cause different reactions in the HSC micro-structure to those occurring in NSC, and these resulting reactions may reduce or increase the shrinkage effect in hardened concrete. Modern concretes with low  $w/cm$  are impossible to achieve without the inclusion of chemical admixtures and are prone to increased early-age shrinkage and cracking (Ebrahim, 2017; Al-Manaseer & Fayyaz, 2011).

Factors in the shrinkage prediction models that determine the shrinkage magnitude and rate are referred to as covariates. They are the variables in the empirical equations used to determine shrinkage strain. The values of these variables are determined by experimental conditions, methodology, test specimen composition, specimen size and applied loads. Prediction models cannot cater for all the possible covariates (Gaylard, Ballim & Fatti, 2013). Covariates therefore differ between the various prediction models. Covariates commonly found in the prediction models are:

- Experimental conditions and methods (temperature, relative humidity, curing type and period).
- Test specimen geometry (size and shape of the test specimen).
- Test specimen composition type and amount (water, cement, aggregate, sand, admixtures and additives).
- Test specimen physical properties (compressive strength, elastic modulus).

## **1.2 Research problem**

Many of the well known and accepted concrete shrinkage prediction models, such as the MC 2010 model, have not been updated to accommodate the modern high-performance concrete shrinkage data that is now available. Consequently, when used to make shrinkage predictions for HSC with chemical admixtures and high mineral admixtures content, the models are inaccurate.

## **1.3 Research Questions**

How do the drying and autogenous shrinkage prediction accuracies of some established, well known shrinkage models compare for both NSC and HSC? Can the selected models be modified (adapted) to predict drying and autogenous shrinkage of HSC with mineral and chemical admixtures (superplasticiser, plasticiser, shrinkage reducing agent, silica fume, fly ash, metakaolin and slag) with acceptable accuracy, based on available published experimental data?

## **1.4 Aims, objectives and outcomes**

The aim of this study was twofold (i) to evaluate and compare the shrinkage prediction accuracies of the RILEM B4, MC 2010 and WITS shrinkage models for NSC and HSC, and to modify (adapt) these models to predict drying and autogenous shrinkage (with acceptable accuracy) of HSC without and with admixtures, based on the latest available published HSC shrinkage data and (ii) propose a composite drying shrinkage prediction model that can accommodate the shrinkage peak between days 85 and 120 exhibited by a group of HSCs with chemical admixtures. To achieve this, the objectives of the study were to:

- Extract and collate a subset of reliable HSC drying and autogenous shrinkage data from a larger set of published South African and international data.
- Using this HSC shrinkage data subset (i) re-evaluate model parameters and adapt the RILEM B4, MC 2010 and the WITS models to enable their use in predicting shrinkage of HSC and (ii) develop a composite equation able to model the early age shrinkage peak shown by some HSC with mineral and chemical admixtures.
- Compare the performances (prediction accuracies) of the selected and proposed models and recommend appropriate use for each of them.

The study established:

- A focused subset of data for re-calibration (modification) and evaluation of shrinkage prediction models, for HSC.
- The accuracies of shrinkage predictions for HSC (with and without admixtures) of the modified RILEM B4, MC 2010 and WITS models, and so their suitability for use in this application.
- Composite empirical prediction models that accommodate the early age shrinkage peak seen in some HSC containing mineral and chemical admixtures.

## 1.5 Significance

Understanding shrinkage and being able to predict it at the design stage of concrete structures is important. The significance of this study therefore is to show that the functional form of existing concrete models is suitable, and that model parameter modification (based on available data) is feasible, to enable their use in shrinkage prediction of modern HSC. The study compared the models' performances, showing where each is most appropriate for HSC, and how prediction accuracy varies for data originating from different geographical regions. The study shows as well that empirical composite models can be developed to cater for HSC that exhibits specific characteristics, such as the early age shrinkage peak seen in some of the data considered here.

## 1.6 Delineation

This research study considered only:

- Drying and autogenous shrinkage.
- The RILEM B4, MC 2010 and the WITS shrinkage prediction models.
- Data extracted from the 2018 version NU database (Northwestern University, 2018), Akthem Al-Manaseer and Abdullah Fayyaz's published experimental data (Al-Manaseer & Fayyaz, 2011) and the Concrete Institute of South Africa database. The criteria for inclusion of data were that the concrete for any experiment had cement type of either rapid hardening or rapid development of early age strength (class according to SANS 50197-1 (2013)), a w/cm ratio  $\leq 0.42$  or a compressive strength  $\geq 60$  MPa.
- From the extracted data, a reduced dataset for model re-calibration, which . The reduced set of data included only experiments that showed an increase in drying or autogenous shrinkage from zero and had known or unambiguous covariate data, at least 4 data points, a duration greater than the minimum drying time (60 days) and sufficient information to determine the cement class according to SANS 50197-1 (2013). Ambiguous data is, for example, the specification of coarse aggregate type as stone or gravel but with no geological information provided.



Creep was not considered at all in this study, and the CEB statistical indicators were not used to assess the accuracies (performances) to rank the shrinkage models. Existing model parameters were updated based on cement type, w/cm, aggregate type and admixture type/combination. The proposed composite models were derived using limited drying shrinkage subsets, referred to in this study as S2-08, S2-09, S2-10 and S2-12, from Dataset 1-HSC.

## 1.7 Assumptions

The following assumptions were made in this research study:

- Concretes used in experiments for which no curing method information was given (including the absence of any notes in the original source of the data stating unusual or non-standard curing methods) were assumed water or moist cured, as this is the norm in drying shrinkage testing.
- Missing curing temperature for any experiment was assumed to be the same or within  $\pm 2$  °C from the controlled temperature after curing. This assumption was made based on other experiments forming part of the data subset and that there was no note to the contrary in the original data source.

## 1.8 Methodology

A subset of secondary experimental HSC drying and autogenous shrinkage data was extracted from the published 2018 version NU database (Northwestern University, 2018), Akthem Al-Manaseer and Abdullah Fayyaz's published experimental data (Al-Manaseer & Fayyaz, 2011) and the Concrete Institute of South Africa shrinkage database. This HSC subset included data from 562 (220 drying shrinkage and 342 autogenous shrinkage) of the original 2192 experiments. From these 562 experiments 3 further (separate) groups of data were derived, each including only experiments whose covariate values lay within the valid ranges (i.e. ranges for which they were derived) of the RILEM B4, MC 2010 and WITS models, to be used to evaluate the prediction performances of the original versions of these models.

With the assistance of an independent statistician consultant (Van Schalkwyk, 2019-2020) who used the NCSS 2019 statistical analysis software package, values for missing covariate data in the HSC data subset were estimated and added. Subsets of data which grouped comparable experiments were then derived from the 562 experiments and used to modify the existing RILEM B4, MC 2010 and WITS model parameters, focussing on SANS 50917-1 (2013) cement type, w/cm ratio, coarse aggregate type and admixture content. A limited number of these subsets, for concretes with mineral and chemical admixtures, showed shrinkage profiles with an early age peak (between 85 and 120 days) and included long-term ( $\geq 500$  days) data. These were used to derive an empirical composite function that could model the early age shrinkage peak and follow the "final" shrinkage closely.

The existing model parameters were modified using Solver<sup>®</sup>, a desktop or online Excel add-in which can be used to optimise complex non-linear problems (find the "best" solution) by changing multiple input values to the equation defining the problem. The most influential parameters in each of the selected models were identified and modified individually for each subset, using non-linear regression. In each analysis the Root Mean Square Error (RMSE) value was minimised, to attain updated model parameters that represented the SANS 50917-1 (2013) cement type, w/cm ratio, coarse aggregate type or varying admixture content for HSC. The proposed composite function for the experimental data that showed the shrinkage peak was developed as a logistic-dose growth curve. Multiple model constants were

determined by dividing the data into separate sections (on the time scale) appropriate to the experimental profile, using Excel Solver® to fit functions to these separate parts of the curve and then combining these into the final composite function.

The differences between the predicted and experimental shrinkage values (residuals) of the existing (original and modified) and proposed composite models were evaluated statistically for grouped data subsets, without and with admixtures. The statistical indicators used to evaluate and rank the models for all data in a subset were Adjusted Coefficient of Determination ( $R^2_{adj}$ ), RMSE and Akaike's Information Criterion (AIC). The statistical indicators used to evaluate and rank the models over different shrinkage time intervals (0 to 99, 100 to 199, 200 to 499 and  $\geq 500$  days) were  $R^2_{adj}$ , RMSE and Overall Coefficient of Variation (C.o.V<sub>all</sub>).

## **1.9 Organisation of thesis**

Chapter 2 provides a review of literature relevant to the topic, from background knowledge on concrete constituents to what the topic is essentially about, prediction of shrinkage in HSC and methods to evaluate the prediction models.

Chapter 3 encompasses the methodology used to extract and formulate the data sets and subsets used in this study to modify the existing model parameters and develop a composite model. This chapter also covers how the existing models were analysed and compared.

The achieved results are presented in Chapter 4, showcasing the compiled datasets extracted from the published data and results obtained (shrinkage predictions and modified model parameters) from the existing and proposed prediction models. The statistical indicators and ranking of models is shown here as well. Derived results are discussed in Chapter 5 in terms of model performances and rankings for concretes without admixtures, with mineral admixtures and with mineral and chemical admixtures. The performances of the original and modified models over all experiments used in this study are compared and discussed as well.

Lastly, Chapter 6 concludes the thesis with a summary of what was done in this study. Successful or failed outcomes are described along with recommendations for future studies.

---

## Chapter 2 Literature review and theory

The literature reviewed here covers four areas related to this work. Firstly, the materials used in concrete, including intrinsic and extrinsic interactions that result in shrinkage. Types of concrete shrinkage and the requirements for deriving shrinkage prediction models are then reviewed. The challenges of predicting drying shrinkage for HSC are addressed as well. Lastly, statistics relevant to non-linear regression and selecting the best model from a group are presented.

### 2.1 HSC & concrete mix constituents

HSC is recognised as an advanced or high performance concrete in which the water-to-cement (w/c) ratio is reduced to achieve greater compressive strength, whilst maintaining a workable consistency. The definition of HSC varies between countries depending on availability of required resources and manufacturing facilities. In Europe, HSC is defined as a concrete reaching a compressive strength equal to or greater than 60 MPa at the 28<sup>th</sup> day after placement (Alexander & Beushausen, 2009). As greater strengths in concrete have become more easily achievable, the ACI Committee 363 (1997) has revised the design compressive strength of HSC from 40 MPa to 55 MPa or greater.

The compositions of HSC and NSC differ in both quality and ratios of the constituents. To achieve higher compressive strength, HSC has a higher cement and admixture content than NSC. HSC usually has a w/c ratio less than 0.4, which results in a rather stiff paste if a chemical admixture (superplasticiser, SP) is not incorporated to improve the concrete workability (Alexander & Beushausen, 2009).

The cost of HSC is significantly more than that of NSC, but HSC is necessary when smaller concrete structural elements or cross-sections are required (Domone, 2010). Factors that establish and affect the strength of concrete are (Fulton, 1986; Al-Manaseer & Fayyaz, 2011; ACI Committee 363, 1997):

- Availability of local materials
- w/c ratio
- Shape and size of aggregates (gradation of aggregates)
- Complementary use of cementitious material (cm) and admixtures
- Early-age relative temperature and humidity of the concrete structure
- Compaction method
- Curing
- Reinforcement

#### 2.1.1 Portland cement and supplementary cement materials

The main constituents of Portland cement are silicates, aluminates, oxides of lime and iron. Hydration is a process which takes place when water is added to cement to form a binding gel known as Calcium-Silicate-Hydrate (C-S-H). This hydrated cement paste is the basis of concrete, as it binds the aggregate which provides the required strength when the cement hardens (Mehta & Monteiro, 2006).

To manipulate the strength, workability, particle cohesiveness and permeability of concrete, mineral admixtures are used as cement extenders and are generally industrial by-products. Mineral admixtures are divided into two categories, cementitious and pozzolanic additives. When in contact with water, the cementitious additives possess cementing properties, but mineral admixtures on their own have little to

no cementing properties. However, when pozzolanic material is mixed with calcium hydroxide, usually lime, a cm is formed (Gonen & Yazicioglu, 2006). The w/c ratio is also generally lower for blended cements with mineral admixtures, to prevent excessive bleeding of water and self-desiccation of the cement microstructure (Grieve, 2009).

Some recognised mineral admixtures according to Aïtcin & Mindess (2011) are:

- Fly ash (FA) is a pozzolan derived from burning anthracite or bituminous coal and lignite fuel in power plants. Early age strength is reduced with the use of FA. According to SANS 50197-1 (2013) between 6 and 35% FA is the standard amount to substitute Portland cement.
- Silica fume (SF) is considerably finer than Portland cement and is therefore highly reactive. It is a by-product of the silicon and ferrosilicon industries, used in high strength concrete (HSC) to decrease cement matrix porosity to achieve early age high strength. According to SANS 50197-1 (2013) between 6 and 10% is the standard amount to replace Portland cement. Greater substitution will reduce the concrete workability.
- Ground granulated blast furnace slag (GGBFS) is a cementitious additive derived from the pig iron manufacturing process and has a similar chemical composition to Portland cement. According to SANS 50197-1 (2013) 35 to 95% GGBFS is the standard amount to substitute Portland cement.
- Metakaolin is an example of calcined clay and is derived by dehydrating kaolin clay. It is a highly reactive pozzolanic material. According to SANS 50197-1 (2013) between 6 and 35% calcined clay is the standard amount to substitute Portland cement.
- Natural pozzolans, such as volcanic ash which has high vitreous silica content and is a slow reacting pozzolan at room temperature. According to SANS 50197-1 (2013) 6 to 35% natural pozzolanic material is the standard amount to substitute Portland cement.
- Limestone, which is crushed sedimentary rock. According to SANS 50197-1 (2013), between 6 and 35% limestone is the standard amount to substitute Portland cement.

Incorporating filler material in the concrete composition alters and densifies the cement matrix to restrict the loss of water from the structure, and assists in increasing compressive strength due to the reduced number and size of capillary pores in the concrete microstructure. Nucleation is a pozzolanic behaviour used as an organising agent of fine material or cement matrix to speed up the rate of hydration (Aïtcin & Mindess, 2011; Grieve, 2009). Partially substituting cement with pozzolanic material effectively reduces the thermal heat given off during hydration as it does not take part in this process. (Grieve, 2009). Thermal cracking is often seen in HSC due to the increased amount cement content (Mehta & Monteiro, 2006).

According to Gupta, Aggarwal & Aggarwal (2006) pozzolanic materials like SF and FA typically increase the drying shrinkage due to several factors. With adequate curing, pozzolans generally increase pore refinement. Use of pozzolans results in an increase in the relative paste volume due to two mechanisms. Pozzolans have a lower specific gravity than Portland cement and in practice more slowly reacting pozzolans such as SF and FA are frequently added in order to attain specified strength at 28 days. Additionally, pozzolans such as FA and SF do not contribute significantly to early age strength. Pastes containing pozzolans generally also have a lower stiffness at earlier ages, making them more susceptible to increased shrinkage.

A research study conducted by Lam, Wong and Poon (1998) investigated the effect of FA and SF in HSC on concrete compressive fracture behaviour. Their test results indicated that 15 to 25% FA and 5% SF increased the compressive strength of HSC by 7% compared to NSC. Incorporating industrial by-products

---

for more sustainable concrete production is the new trend in the concrete industry, as the manufacturing of Portland cement contributes heavily to CO<sub>2</sub> gas emissions into the atmosphere (Aïtcin & Mindess, 2011).

The varying proportions of Portland cement and supplementary cementitious materials (cm) result in different types of cements, categorised for different functions. The two most world-wide recognised cement type standards are the American and European standards. South Africa uses an adapted version of the European standard (Grieve, 2009). World-recognised standards are usually adapted for national use as there are local factors that affect the quality of cement. It is important to have control measures in place to achieve cement properties within the standard limits (Fulton, 1986). Tables 2.1 and 2.2 list the European and American cement categories, respectively.

Table 2.1 European common cement and sulphate resisting cement types (SANS 50197-1, 2013)

Cement types	Description
CEM I	Portland cement with ≤ 5% of additional minor constituents
CEM II	Portland – SF cement
	Portland – pozzolana cement
	Portland – fly ash
	Portland – burnt shale cement
	Portland – limestone cement
	Portland – composite cement
CEM III	Blast furnace cement
CEM IV	Pozzolanic cement
CEM V	Composite cement
CEM I – SR	Sulphate resisting Portland cement
CEM III – SR	Sulphate resisting blast furnace cement
CEM IV – SR	Sulphate resisting pozzolanic cement

Table 2.2 American Portland cement and blended hydraulic cement types (ASTM C150, 2012 and ASTM C595, 2016)

Cement types	Description
Type I	Normal Portland cement
Type II	Moderate sulphate resistance
Type II (MH)	Moderate heat of hydration & moderate sulphate resistance
Type III	High early strength
Type IV	Low heat hydration
Type V	High sulphate resistance
Type IL	Portland – limestone cement
Type IS	Portland – slag cement
Type IP	Portland – pozzolana cement
Type IT	Ternary blended cement

### 2.1.2 Aggregates

Typical concretes contain approximately 40% aggregates. South Africa makes use of several aggregate types which originate from three major rock groups, namely igneous, metamorphic and sedimentary rock. Examples of these aggregate types are: andesite, basalt, dolerite, granite, quartzite, sandstone, greywacke and tillite. Dolerite, dolomite and andesite are the most favourable fine and coarse aggregate type used in South Africa (Grieve, 2009). Construction rubble, manufacturing by-products and recycled material such as concrete, tires and glass are also used as aggregate. However, the use of these unnatural aggregates is rare due to large variations in the resulting concrete (Aïtcin & Mindess, 2011).

Aggregate attributes such as shape, size, texture, chemical composition, mineral composition and microstructure determine the quality of the aggregate in terms of its crushing strength, elastic modulus, abrasion resistance and soundness. Unsuitable aggregates may be incompatible with certain cement types or environmental conditions and could have a detrimental effect on the hardened concrete properties. The concrete durability and strength can be affected in the following ways (Grieve, 2009; Aïtcin & Mindess, 2011):

- Poor distribution of different aggregate sizes affects workability and durability of concrete.
- Volume changing (chalk or clayey material) induces cracking in concrete.
- Long and flat shaped aggregates decrease concrete strength.
- Large quantities of common salt substances weaken the concrete through efflorescence and can cause reinforcement corrosion.
- Large quantities of reactive silica substances react with alkaline cement and result in swelling.
- Large quantities of sulphate react with the cement and cause concrete cracking.
- Lightweight or porous aggregates produce concrete of lower compressive strength and elastic modulus.
- Decreasing the maximum size of aggregate effectively increases the concrete compressive strength.

HSC is obtained by decreasing the w/c ratio and increasing the cm content, creating a more compact and stronger cement matrix. However, some low w/c ratio concretes also have low compressive strengths. This happens when the aggregate crushing strength is lower than the cement matrix strength (Aïtcin & Mindess, 2011; Beushausen & Dehn, 2009). HSC in tension with partial substitution of light weight aggregates is an example of such a concrete. In such concretes cracks usually form in the aggregates which render the concrete weaker (CEB-FIP, 2012). It is therefore important to use “strong” aggregates of good quality in manufacturing HSC. Aïtcin & Mindess (2011) also stated that there are many other influencing factors that can decrease the compressive strength of concrete.

In addition, with the increase in cm content in HSC, the interfacial transition zone (ITZ) becomes compact compared to NSC where the ITZ is more porous. The ITZ describes the bonding zone between aggregate and cement paste matrix and is usually seen as the weakest zone of the concrete microstructure (Aïtcin & Mindess, 2011; Mehta & Monteiro, 2006). In NSC calcium hydroxide forms on the aggregates when cement hydration takes place, and cracks usually form between the ITZ and aggregates due to this phenomenon. In HSC, the mineral admixtures react with and reduce the content of calcium hydroxide. Fractures or cracks can then occur in the aggregates of weak strength rather than in the cement matrix (Beushausen & Dehn, 2009). Figure 2.1 illustrates the location of the ITZ and the arrangement of C-S-H, calcium hydroxide crystals and trisulphate hydrate needle-like crystals (ettringite) in the cement matrix.

---

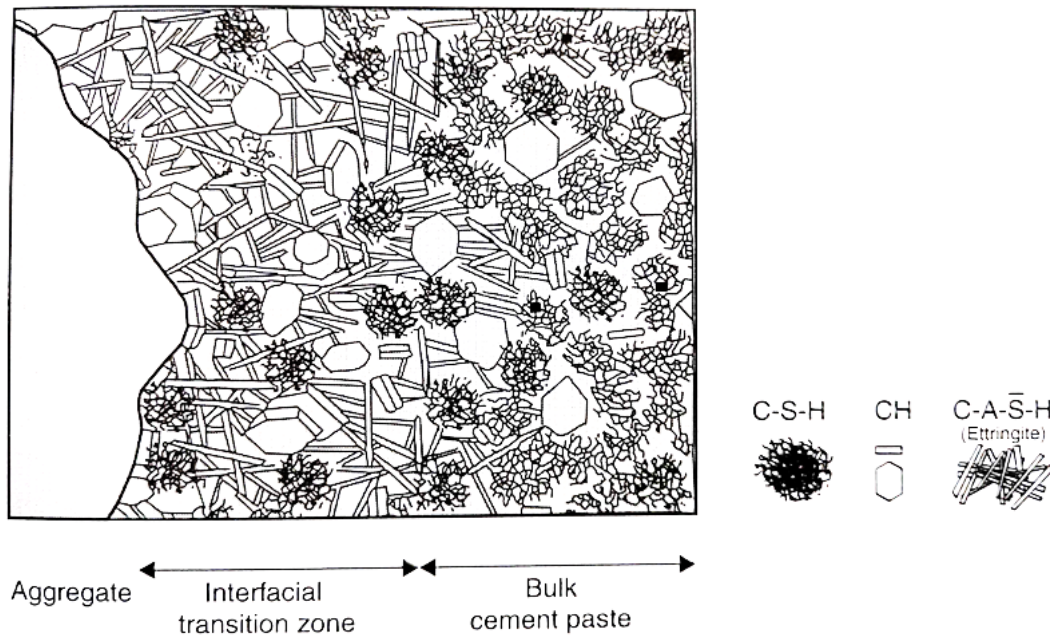


Figure 2.1 Diagrammatic presentation of ITZ location and its mineral composition (Mehta & Monteiro, 2006).

Since shrinkage only takes place in the cement matrix, increasing the aggregate content and decreasing the cement matrix volume in concrete will effectively decrease the shrinkage experienced in the structure. The aggregate confines the shrinkage in the cement matrix, therefore it is recommended to use the optimum content that will maintain the necessary rheological properties of fresh concrete (Aïtcin & Mindess, 2011).

Partial substitution of saturated lightweight coarse and fine aggregate (especially expanded slate) in concrete will promote internal curing to reduce autogenous shrinkage. The porosity of the lightweight coarse aggregate ranges between 5 and 6%, whilst for fine aggregate, the porosity ranges from 10 to 20%. Therefore, the fine lightweight aggregate holds more water when saturated. Compared to the coarse aggregate, the fine aggregate is more dispersed in the cement matrix and has greater contact with and influence on the cement matrix. With the partial substitution of coarse aggregate, the concrete properties such as elastic modulus and concrete strength may reduce. Conversely, substituting fine aggregates results in only minor changes of the elastic modulus and actually increases the compressive strength of the concrete (Aïtcin & Mindess, 2011).

### 2.1.3 Chemical admixtures

With the growing demand for more complex concrete requirements, admixtures are used to manipulate the workability, strength and durability of concrete mixes. Great compressive strength is achieved through better arrangement of the concrete particles to increase the compaction. This creates a more impervious solid concrete mix which is one of the main influential parameters that affects shrinkage. The chemical admixtures are available as surface-active agents, soluble-salts and polymers. The required admixture can be added at different stages within the concrete life. It can be added to the concrete in its fresh green state or when it has already hardened, whichever state is required to adapt the concrete for its purpose, such as (Pomeroy & Marsh, 2014):

- Increase particle dispersion.
- Air entrainment.
- Increase the compressive strength.
- Increase or decrease the hydration rate.
- Decrease the water requirements.
- Increase the cohesion of fresh state concrete.
- Improve particle properties for material or reinforcement protection such as permeability.

Table 2.3 lists the most commonly used mineral and chemical admixtures and their manipulative properties.

Table 2.3 Typical chemical admixtures used and their purpose according to Setareh & Darvas (2007), Al-Manaseer & Fayyaz (2011), Mehta & Monteiro (2006) and Pease (2005).

Admixture	Properties
Plasticiser (P) and superplasticiser (SP)	Also known as a water-reducer, this admixture subdues the surface tension (of water within the concrete pores) and internal tensile forces, to facilitate low w/c concretes and early high strength. Also used to reduce the amount of cement content and effectively reduce the amount of heat given off during the hydration phase. A side-effect of over dosage of plasticiser is possible entrainment of large air voids which increases the setting time. Superplasticisers (SPs) were developed in the 1970s to drastically reduce the amount of water used whilst maintaining a workable consistency. Large amounts of SP can be used without major concrete bleeding and reduction in setting time.
Shrinkage reducing admixture (SRA)	SRA is much like a plasticiser and is generally used to decrease water ingress, which results in a decrease of drying and autogenous shrinkage. This is done to ultimately improve the aesthetics and durability of concrete.
Air-entrainment	Arrangement of air bubbles within the cement paste to increase the freeze-thaw resistance. Air-entrainment agents are commonly used for lightweight and mass concrete as the entrained air increases workability in concretes with less cement and water as well as lightweight and rough-edged aggregates.
Setting-retarders	Setting-retarders are used to delay the setting time and increase the workability of concrete. This facilitates the placement of concrete in hot environmental conditions as well as controlling the placement of large concrete structures. This is done to attain proper concrete finishes and to avoid discontinuity and cracking in structures.
Accelerators	Used to decrease the curing time and accelerate the cement hydration process in order to reach early acceptable compressive strength in a shorter time. This benefits construction projects with time constraints to open to the public, facilitates quick remedies/rehabilitation and early removal of form work to speed up production and reduce cost.



Aïtcin & Mindess (2011) pointed out that polycarboxylate SPs require more in-depth study as they are the key to the idea of sustainable concrete. High performance concrete, such as HSC, or even self-levelling concrete, cannot exist without the inclusion of a SP. One of the major downfalls in the use of plasticisers is their incompatibility with cm resulting in less robust concrete.

Producing Portland cement with identical clinker and composition is practically impossible. Some cement therefore reacts differently with SPs and may be incompatible. The cement particle shapes and forms also vary within a batch of Portland cement and some might be incompatible when reacting with SP molecules. Incompatibility and a lack of robustness can be identified by the inability to maintain concrete slump and by observing a large deviation from the usual reaction when a small change is made (perhaps an increase in the dosage of the SP or cement) (Aïtcin & Mindess, 2011). Precision in the amounts of different admixtures used together in a concrete mix is very important to maintain compatibility and suitability. Over-dosage of one admixture might have more deleterious effects than intended benefits for the concrete (Pomeroy & Marsh, 2014; Hassan, Cabrera & Maliene, 2000).

## 2.2 Moisture movement in concrete

The movement of water or chemicals in the cement matrix of a concrete structure plays a major role in the development of cracks and the deterioration of the durability and life span performance of concrete. Engineers and designers therefore adapt the concrete composition of stone, cement and water to prevent the migration of moisture into and within concrete (Domone, 2010). The prediction of moisture movement in concrete is challenging as concrete constituents and environmental conditions vary. To achieve more accurate measurements of moisture movement, laboratory tests should be conducted on the specific concrete mix (CEB-FIP, 2012).

The porous cement matrix promotes the presence of water along with dissolved chemicals and gases in capillary voids, voids close to the structure's surface and C-S-H interlayer cavities. Figure 2.2 illustrates the different areas in which water is found within the cement microstructure. As mentioned previously, moisture can also be found in porous aggregates (Aïtcin & Mindess, 2011). The movement mechanisms of water in the cement matrix are capillary absorption, permeation and diffusion (CEB-FIP, 2012).

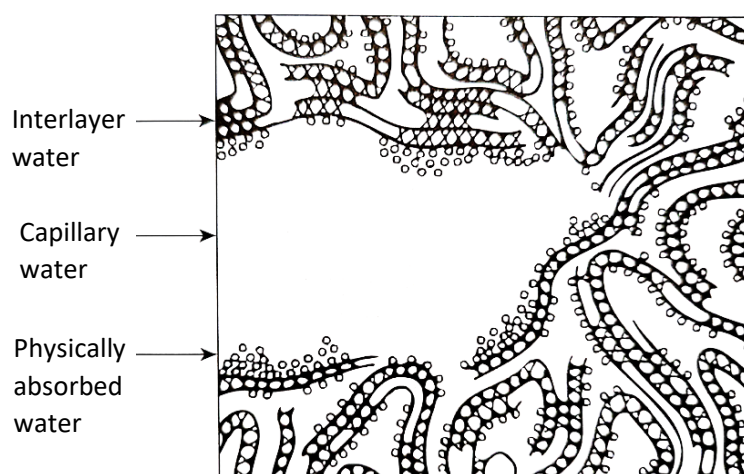


Figure 2.2 Different locations of water in hydrated cement matrix (Mehta & Monteiro, 2006).

### 2.2.1 Capillary absorption

The capillary absorption mechanism is more significant at the surface of the concrete structure and relies on capillary pore radii and degree of saturation. Capillary action is the movement of a liquid within the concrete pores without the assistance of an external head/force. The rate at which external water from the structure's surface is absorbed and moves through the interconnected macro-pores is called sorptivity. This mechanism is influenced by a) aggregate spread and arrangement and b) concrete mix composition (Ballim, Alexander and Beushausen, 2009). The capillary stresses are proportional to the surface tension and inversely proportional to the meniscus curvature of the liquid. When the liquid quantity decreases, so will the meniscus curvature and effectively the capillary stress will increase, which causes both fresh and hardened concrete to shrink. Equilibrium of vapour pressure and water pressure is found at the meniscus (Wittmann, 1968). This is explained by the Laplace law, Equation 2.1 (Aïtcin & Mindess, 2011).

$$\Delta P = \frac{2\sigma \cos \theta}{r} \quad (2.1)$$

where  $\Delta P$  = capillary pressure,  $\sigma$  = surface tension,  $\theta$  = angle of contact between the liquid and capillary wall and  $r$  = radius or size of the capillary pore.

Equation 2.1 also indicates the relationship of the size of the capillary pore to the magnitude of the capillary pressure. Small capillary pores result in greater tensile stresses than do large pores. According to Aïtcin & Mindess (2011), moisture in capillary pores greater than 50 nm (also known as macropores) is classified as "free water" and does not bring about volume change in the structure. On the other hand, Alexander and Beushausen (2009) indicate that free water contributes to early age concrete deformation.

Moisture in capillary pores between 5 and 50 nm (micropores) can cause concrete drying shrinkage. The cavity size in the C-S-H is approximately 1 nm and can contribute to drying shrinkage too as the hydrogen-bonded water molecules move in and out of the C-S-H layers. Cement extenders such as FA, SF and GGBFS are added to reduce the porosity and increase the density of the cement matrix to restrict movement of moisture in the C-S-H layers and capillary pores or voids (Alexander & Beushausen, 2009; Aïtcin & Mindess, 2011; Mehta & Monteiro, 2006). The capillary absorption mechanism is influenced by the degree of saturation. Surface tension is only applicable in the range of 5 to 50% relative humidity (RH) and capillary tension is only significant between 50 and 100% RH (Kovler & Zhutovsky, 2006; Wittmann, 1968, 1982). Interlayer movement contributes to shrinkage within concrete below 11% RH (Mehta & Monteiro, 2006).

### 2.2.2 Permeation

Permeability is a property of concrete that determines the ease with which liquids and gas can move through the porous cement matrix under a pressure head (CEB-FIP, 2012). Permeation through a concrete is dependent on a) the concrete microstructure b) saturation level of the concrete and c) properties of the permeating fluid (Ballim *et al*, 2009). The surface tension within the liquid and adhesion between the concrete pore surfaces pushes the liquid between the concrete pores from an area of high water content to an area of low water content (Kovler & Zhutovsky, 2006). The fluid or gases can only move along interconnecting capillary pores or voids. The w/c ratio and the degree of hydration govern the formation and connection of capillary pores. HSC generally has low permeability due to the dense and compact microstructure. However, if there is insufficient hydration, the permeability will be higher. Therefore,

sufficient curing is required for proper cement hydration. Internal cracks promote the permeation of water and gases through the concrete structure as well (CEB-FIP, 2012). The permeability of the concrete for water can be generally defined by Darcy's Law, Equation 2.2 (CEB-FIP, 2012).

$$Q = K_w \frac{A}{L} \Delta h_w t \quad (2.2)$$

where  $Q$  = the volume of fluid over time,  $\Delta h_w$  = hydraulic grade,  $A$  = cross-sectional area,  $t$  = time,  $L$  = length over pressure drop and  $K_w$  = water permeability coefficient in m/s.

### 2.2.3 Diffusion

Fick's second law, Equation 2.3, defines diffusion of varying concentrations (CEB-FIP, 2012).

$$\frac{\partial c}{\partial t} = D \frac{\partial^2 C_i}{\partial x^2} \quad (2.3)$$

where  $C_i$  = concentration of substance,  $x$  = location,  $t$  = time and  $D$  = coefficient of diffusion.

According to Kim and Lee (1999) diffusion of chloride ions is the movement of deleterious salts facilitated by moisture within the concrete. The chloride ions move from a higher ion concentration to a lower ion concentration within a solution. Thus, the concrete structure must be saturated for this mechanism to activate. If the chloride comes into contact with reinforcement, expansion of the steel will take place causing cracks to start from within. See Equation 2.4 for Fick's second law for the diffusion of free ions.

$$\frac{\partial C_{free}}{\partial t} = D_{eff} \frac{\partial^2 C_{free}}{\partial x^2} \quad (2.4)$$

Diffusion of ions is found in concrete structures exposed to sea water or saturated soil containing chloride ions. In a concrete structure (for example a concrete tower on a coastal shore) exposed to wet-drying cycles, the depth of the back and forth movement of the seawater ingress from the structure's surface is called the convection zone. Once the seawater penetrates past this zone and travels further into the structure towards the steel reinforcement, corrosion occurs which weakens the structure. This is the diffusion zone (Ballim *et al*, 2009).

## 2.3 Types of concrete shrinkage

Shrinkage in concrete is a progressive deformation which can be defined as a volumetric decrease or increase on an unloaded and unrestrained structure due to extreme relative temperatures and movement or loss of internal water through cement hydration or evaporation. These phenomena result in cracking which affects the durability of the concrete structure as the movement or loss of water induces tensile stresses inside capillary pores, which exceed the tensile strength of the concrete.

Various internal restraints create tensile stresses and as a result different types of shrinkage occur within the concrete. The five known types of shrinkage that concrete experiences are:

- Plastic shrinkage
- Autogenous shrinkage
- Drying shrinkage
- Thermal shrinkage
- Carbonation shrinkage

The magnitude of the shrinkage strain is affected simultaneously by various factors, but the interrelationships between these factors are difficult to understand. Examples of these factors are (Pomeroy & Marsh, 2014; Mehta & Monteiro, 2006):

- Environmental conditions - surrounding humidity, temperature and rainfall.
- State of the concrete - degree of saturation.
- Shape and size of the structure.
- Concrete mix composition, material properties and material pairing.

### **2.3.1 Plastic shrinkage**

Plastic shrinkage occurs during the beginning phase or in the first few moments after casting and placing of wet concrete. The influential parameters that effect the evaporation of moisture from the freshly placed concrete are the relative temperature, humidity and wind. The mechanistic expulsion of water from capillaries within is associated with concrete bleeding. If this is followed by evaporation, shrinkage occurs. The initiation of the early deterioration or cracking within the first few hours after placement is caused by the plastic settlement of the concrete and is accelerated by plastic shrinkage (Boshoff & Combrink, 2013). Concrete bleeding is a form of protection against cracking, but once the water has evaporated, cracks occur. In concretes with a high w/c ratio, there is excessive bleeding, but on the other hand concretes with low w/c ratio have less water and therefore less bleeding. This renders low w/c ratio concretes more susceptible to plastic shrinkage (Aïtcin & Mindess, 2011).

To mitigate the cause of the plastic shrinkage, correct pouring/placing of the concrete and appropriate curing is required. Aïtcin & Mindess (2011) recommend:

- Fog curing to create a saturated external environment to decrease evaporation.
- Impermeable coverings applied over the concrete structure during its curing period to restrict the movement of the water. Examples are: a) aliphatic alcohols, b) curing membranes.
- Temporary umbrellas to provide shade and reduce evaporation.
- Windbreaks to mitigate evaporation.
- SRAs to lower the tensile forces created in the capillary pores.
- Synthetic fibres to increase the strength of the plastic concrete and reduce crack formation.

Curing membranes have the disadvantage of inhibiting the ingress of water when it is required for concrete of low w/c ratio. External water absorption is necessary to mitigate autogenous shrinkage. In the case of high w/c concretes, the curing membrane also restricts the excess water from escaping the structure, unless the membrane has a slit to allow for evaporation (Aïtcin & Mindess, 2011).

### 2.3.2 Autogenous shrinkage

Autogenous shrinkage (also known as basic shrinkage) is significantly seen at the start of the drying phase of hardened concrete, when the cement hydration process begins or after setting. Rasoolinejad *et al* (2019), however, indicated that autogenous shrinkage is an ongoing phenomena which occurs beyond the early age of concrete. Some historic autogenous shrinkage experiments did not reach final shrinkage after many years. A possible reason could be that the core of a thicker specimen remains moist for longer, resulting in on-going autogenous shrinkage taking place at the specimen core (Hubler, Wedner & Bažant, 2015). During this chemical reaction between the mixed water and cement (hydration) heat is given off, concrete strength increases and the volume subsequently decreases. The volume of the hydrated cement accounts for approximately 90 to 92% of the original volume of materials before hydration.

Another phenomenon which causes autogenous shrinkage and early-age cracks is known as self-desiccation (Kim & Lee, 1999; Aïtcin & Mindess, 2011). Self-desiccation, as explained by Domone (2010) is when the moisture content of a specimen reduces from within through mechanical expulsion of water from the capillary pores caused by the hydration and decrease in humidity. The mechanical expulsion results in the development of local tensile stresses in the cement matrix. See Figure 2.3 for a conceptual illustration of autogenous shrinkage.

Self-desiccation can be reduced by saturating the structure to remove the menisci in pores which cause the tensile stresses, so autogenous shrinkage cannot take place in 100% saturated concrete structures. This can be achieved through external and internal curing. Insufficient curing leads to the formation of internal and surface cracks due to autogenous shrinkage. External curing penetrates 50 to 100 mm into the concrete structure, ensuring that surface cracking, which leads to water ingress and the deterioration of the steel reinforcement, does not occur. Utilising an impermeable covering over the concrete structure is an example of an external method of mitigating autogenous shrinkage. Water curing for a week is highly recommended, especially for HSC which experiences greater autogenous shrinkage. Including admixtures or additives in the concrete composition is another avenue to reduce autogenous shrinkage, as they reduce the tensile forces in the capillary pores, or promote early-age swelling or material expansion which neutralises the effects of shrinkage (Aïtcin & Mindess, 2011).

Kim & Lee (1999) state that HSC with low w/c ratios is more affected by self-desiccation than NSC with high w/c ratios. Much research has been done on surrounding temperature and RH effects on the initiation and progression of self-desiccation, as they are key influential parameters. Due to the gradual decrease in heat caused by the hydration process, thermal shrinkage occurs as well.

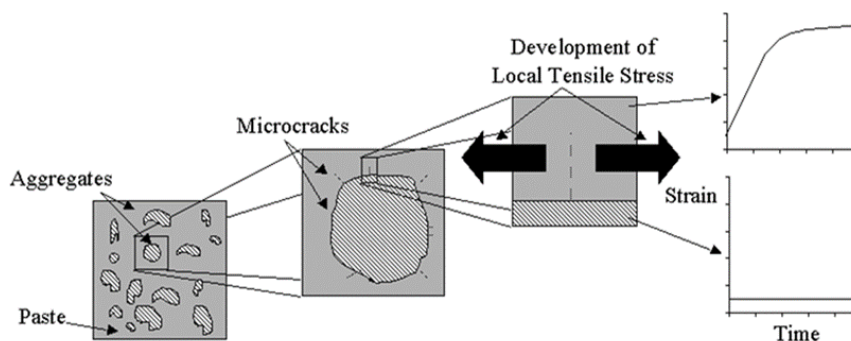


Figure 2.3 Conceptual illustration of autogenous shrinkage (Pease, 2005).

### 2.3.3 Drying shrinkage

Drying shrinkage occurs in hardened concrete when the excess moisture found in macro-pores and capillary pores is lost to evaporation as the concrete dries over the its life span. Generally, therefore, concretes with greater initial water content experience greater drying shrinkage compared to concretes with less water content (Fulton, 1986). The RH and temperature both play an important role in the development of drying shrinkage. During the first stage of drying, maximum shrinkage strain occurs and there is a period of alternating hydration and drying, also known as wet-drying cycles. The specimen will recover (regain volume) to a certain point and then shrink again. Concrete is known as a rigid construction material, but it has elastic recovery properties. Surface cracks result from the concrete recovering a little less over time which causes permanent deformation. Permanent deformation, also known as irreversible shrinkage, occurs when the shrinkage is beyond the maximum point of recovery (Domone, 2010). This is shown in Figure 2.4 which also illustrates that the rate of shrinkage decreases over time and reaches a plateau, known as the final or ultimate shrinkage.

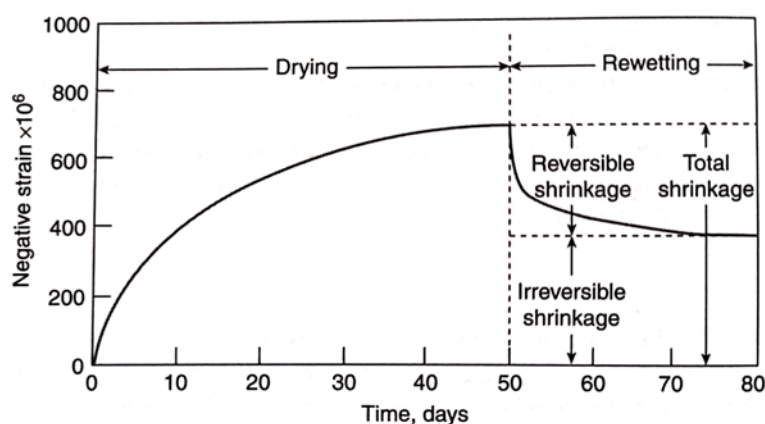


Figure 2.4 Conceptual illustration of drying shrinkage (Mehta & Monteiro, 2006).

RH and temperature are significant external influences on the rate of shrinkage. With increasing humidity, drying shrinkage decreases as there is less moisture movement. According to Mehta and Monteiro (2006), 100% RH produced zero drying shrinkage, 80% RH increased final shrinkage by 200 microstrain and at 45% RH, final drying shrinkage was 400 microstrain.

At a constant RH, the concrete size and dimensions play a role in the rate of drying shrinkage. Moisture loss takes place only from the surface of the exposed structure, so the moisture travel distance to the surface is affected by the cross-section of the structure (Domone, 2010).

The concrete microstructure comprises the hydrated cement matrix, ITZ and aggregates. As already mentioned, tensile stresses are experienced in capillary pores due to the movement or loss of water. However, the resulting cracks and total deformation is significantly influenced by the aggregate skeleton of the concrete structure. A greater quantity of aggregates in the overall volume of the concrete structure reduces the drying shrinkage experienced as the aggregates provide internal restraint against the tensile stresses. When predicting drying shrinkage, the elastic modulus of the aggregate (usually taken as the elastic modulus of concrete) should be a factor used to represent this internal restraint. An aggregate with a higher elastic modulus will result in lower drying shrinkage. Common aggregates, listed from the higher to lower elastic modulus are quartz, limestone, granite, basalt, gravel and sandstone. The fineness and variations in Portland cement compositions have a negligible effect on the drying shrinkage if there is

sufficient aggregate restraint. However, the compatibility of the aggregate type with the cm should be considered too, as incompatible reactions could lead to micro-cracks forming in the ITZ (Mehta & Monteiro, 2006).

According to Mehta & Monteiro (2006) when the w/c ratio is reduced and cement content is increased, the aggregate volumetric content will decrease in the structure. This will then decrease the concrete elastic modulus and increase the drying shrinkage experienced in concrete (if the w/c ratio remains constant). In addition, Alexander and Beushausen (2009) indicated that concrete with a w/c ratio of 0.26 (a low w/c ratio) produced ultimate shrinkage around 1600 microstrain, whilst concrete with a w/c ratio of 0.45 produced ultimate shrinkage greater than 2400 microstrain. Alexander and Beushausen (2009) and Aïtcin & Mindess (2011) explain that the magnitude of the drying shrinkage of concretes with low w/c ratios (<0.4) is far less than that of concretes with high w/c ratios. This is the result of the compact microstructure of the cement matrix, which restricts the movement of the water in and out of the structure. The increased number of micro-pores in low w/c ratio concretes would theoretically increase the tensile stress and increase drying shrinkage, but the more compact and stiff cement matrix also acts as a restraint against the tensile stress. Therefore, it can be said that a concrete with the lowest w/c ratio and stiffest aggregate will have the lowest drying shrinkage.

Mehta & Monteiro (2006) stated that admixtures that create smaller pores (micro-pores of 3 to 20 nm) and better distribute and arrange them will increase drying shrinkage. Examples given of such admixtures are water-reducers (SPs), setting accelerators such as calcium chloride, pozzolanic material and ground granulated blast-furnace slag (GGBS). This statement partially agrees with Alexander and Beushausen (2009), who state the increased refinement and arrangement of micro-pores increases tensile stress and drying shrinkage, but does not comment on the restriction of moisture movement a denser cement matrix offers, which effectively decreases the drying shrinkage. Al-Manseer *et al* (2011) reported that for the concrete mixtures used in their study, the Oakland Bay Bridge project, the majority of the shrinkage took place within the first 100 days.

### *Drying shrinkage test standards*

SANS 6085 (2006) is an accelerated drying shrinkage test method which measures only the initial shrinkage of concrete. After 7 days of curing in a water bath, the SANS method requires the concrete prism specimens to dry in a storage room at a controlled temperature of  $52.5 \pm 2.5$  °C and RH of  $20 \pm 5\%$  for 7 days. Afterwards, the specimens are cooled down in a storage room at a controlled temperature of  $23.5 \pm 1.5$ °C. Equation 2.5 gives the calculation of the drying shrinkage as a percentage, using measurements made in a comparator, an example of which is shown in **Error! Reference source not found.**  $L_1$  is the specimen length (mm) after curing,  $L_2$  is the specimen length (mm) after drying and cooling and  $L_0$  is the initial specimen length (mm) between inner edges of the comparator anvils.

$$\frac{L_1 - L_2}{L_0} \times 100 \quad (2.5)$$

As stated by Al-Manaseer and Fayyaz (2011) after 7 days of curing in a water bath, ASTM C157 (2008) requires the concrete prism specimens to be stored in a room temperature controlled at  $23 \pm 1.7$ °C and RH at  $50 \pm 4\%$ . Specimen shrinkage readings are recorded by means of a comparator at different times. Cylindrical concrete specimens are tested for elastic modulus and compressive strength at the 28<sup>th</sup>, 56<sup>th</sup>, 90<sup>th</sup> and the 180<sup>th</sup> day of curing and storage.



Figure 2.5 Comparator – to measure change in length of concrete specimen (Tam, Tam & Ng, 2012).

Other equipment used to create, store and measure the test specimens for the ASTM C157 (2008) test method are listed in Table 2.4.

Table 2.4 ASTM C157 (2008) - Required equipment and facilities.

Equipment / Facility	Description
Specimen moulds	75 x 75 x 285mm prism moulds and 100 x 200mm cylinder moulds.
Tampering rod	The utensil is used to compact concrete into moulds.
Drying room and controls	Storage space for test specimens stored on racks with free air circulation around the specimens.
Assmann psychrometer	Used to measure the temperature within the drying room as well as the relative density of the specimen.
Atmometer	Used daily to measure the evaporation.
Length comparator	Used to measure the length of the specimens at certain intervals.

#### 2.3.4 Thermal shrinkage

In general, materials expand when heated and contract when cooled. Thermal shrinkage in concrete structures is caused by the heat energy given off during the cement hydration process. Heat is lost easily at the exposed surface of the structure compared to the structure's core, where it is retained. Cracks occur under extreme thermal gradient conditions (drastic fluctuation in temperatures) in the structure. Temperatures will vary within a concrete structure due to varying cross-sections exposed to the surrounding environment. The amount of heat given off depends on how much cement is available for hydration, while the cement fineness determines the rate of hydration. Small structures can release heat easily compared to large structures. HSC structures are additionally susceptible to thermal shrinkage and cracking due to their high cement content. It is important therefore in HS and large concrete structures to control thermal gradients through careful selection of compatible materials and proper proportioning. Materials used to curtail the heat gradients in concrete are (Aïtcin & Mindess, 2011; Mehta & Monteiro, 2006):

- Mineral admixtures such as FA to substitute up to half of the cement content.



- Cement that produces a low heat during the hydration process.
- Chilled aggregates.
- Ice chips added at time of mixing.

### 2.3.5 Carbonation shrinkage

Carbonation shrinkage does not result from the loss of moisture. Rather, moisture initiates a reaction in which carbon dioxide from the atmosphere and water within the concrete combine to produce carbonic acid. The carbonic acid then reacts with calcium hydroxide found within calcium carbonate crystals in the pores of the concrete and this decreases permeability. The reaction starts at the surface of the concrete and slowly moves towards the center. Carbonation shrinkage causes warping and many fine surface cracks, especially in structures with small cross-sections exposed to relative humidities of 50 to 80%. Carbonation cannot take place when the concrete pores are either fully saturated or completely dried out. Moisture is required to initiate the reaction (Domone, 2010; Mehta & Monteiro, 2006).

According to Mehta and Monteiro (2006) carbonation shrinkage can be greater than drying shrinkage when the RH is greater than about 40%. In addition, approximately one third of the shrinkage magnitude recorded in drying shrinkage experiments can be the result of carbonation shrinkage, as test conditions require 50% RH, generally in an atmosphere containing carbon dioxide. According to ACI Committee 224 (2001) carbonation shrinkage is of greater significance when small test specimens are used for long duration drying shrinkage experiments. Due to their increased surface-to-volume ratio, carbon dioxide can penetrate the test specimen more easily and cause greater shrinkage.

## 2.4 Intrinsic & extrinsic influence on shrinkage in hardened HSC

Intrinsic factors that affect the magnitude of shrinkage are the type and ratio of the materials used in the concrete mix. Much research has been conducted on the effects of concrete constituents (saturation, cement, aggregate, cm, admixture types and ratios) on HSC over the years. Extrinsic factors that affect the magnitude of shrinkage are RH, curing type and temperature. These intrinsic and extrinsic factors influence shrinkage in HSC and NSC differently, as seen in Figure 2.6.

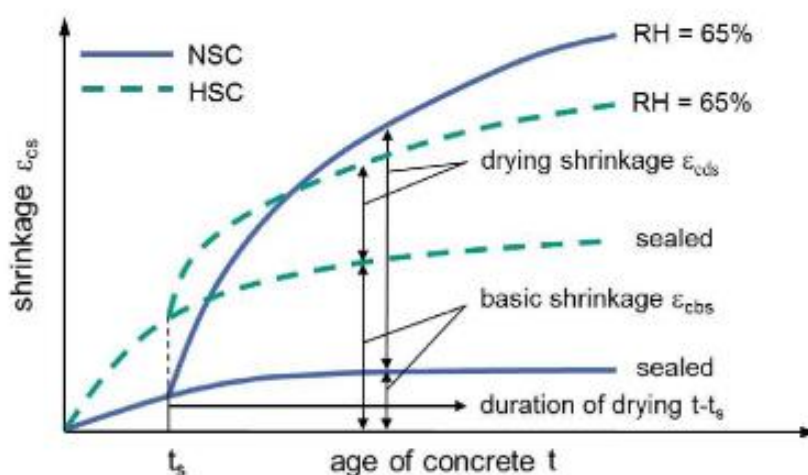


Figure 2.6 Drying and basic (autogenous) shrinkage over time for NSC and HSC (CEB-FIP, 2013).

### 2.4.1 Influence of water content and w/c

Drying shrinkage is greater in NSC than in HSC due to the higher w/c ratios. Autogenous shrinkage on the other hand is much greater in HSC than in NSC. The low w/c ratio in HSC considerably decreases pore humidity which results in a more rapid internal uptake of water in the concrete, which accelerates self-desiccation (Gupta *et al*, 2006; Bažant and Baweja, 2000).

#### Case study A

Lee, Lim, Yoo and Lim (2017) conducted laboratory experiments on the influence of the w/c ratio on the shrinkage of HSC. To increase the compressive strength of concrete, the w/c ratio is reduced, therefore there is a greater relative amount of cement. These experiments tested concrete with compressive strengths of 78, 98 and 125 MPa. Table 2.5 shows the controlled concrete constituents used in the experiments. 100 × 100 × 400 mm concrete specimens were tested for total shrinkage (autogenous and drying shrinkage) using the C157 test standard. After placement the specimens were exposed to a temperature of 23 ± 1 °C and RH of 60 ± 3%. Shrinkage recordings were taken over 60 days.

Table 2.5 HSC mix proportions of experiments conducted by Lee *et al* (2017)

Test No.	w/c	w (kg/m <sup>3</sup> )	c (kg/m <sup>3</sup> )	Cement type	SF (%)	Fine aggregate (RD)	Coarse aggregate (RD)	f <sub>cm28</sub> (MPa)
1	0.29	171	580	Type I	0	2.6	2.7	78
2	0.25	162	598	Type I	5	2.6	2.7	98
3	0.16	155	824	Type I	15	2.6	2.7	125

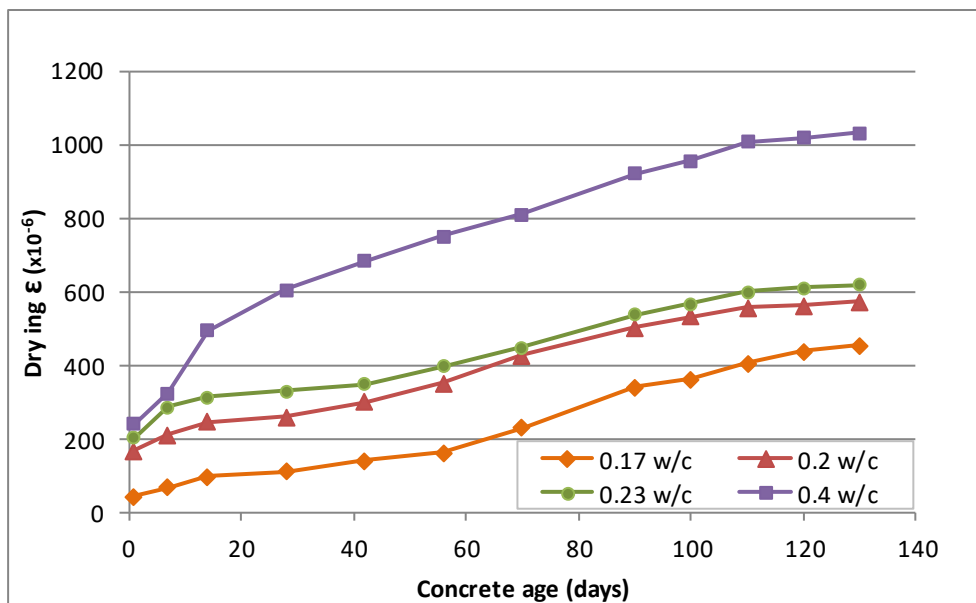
The results showed that the initial shrinkage (< 30 days) was much higher for the specimens with lower w/c ratios and was suggested to be the autogenous shrinkage. The 125 MPa concrete specimen had 250% greater total shrinkage at 60 days compared to the 98 MPa specimen and this was again attributed to the greater autogenous shrinkage found in higher strength concretes. The increase in SF content reduced the capillary pore size which resulted in greater self-desiccation in the 98 and 125 MPa specimens compared to the 78 MPa specimen.

#### Case study B

A study conducted by Tam *et al* (2012) also proved that drying shrinkage for high w/c ratio concrete is greater than for low w/c ratio concrete. The test specimen of 0.4 w/c ratio produced maximum shrinkage of 1033 microstrain and the test specimen of 0.17 w/c ratio produced maximum shrinkage of 454 microstrain. The experiment tested concretes with compressive strengths ranging between 90 and 145 MPa, with constituents as shown in Table 2.6. 75 × 75 × 250 mm prisms were tested for drying shrinkage. After 28 days of curing in a 27 °C water bath, the specimens were exposed to a temperature of 25 ± 2 °C and humidity of 50 ± 5 %. Shrinkage recordings were taken over a 130-day timespan. Figure 2.7 shows the measured drying shrinkage results for this study.

Table 2.6 HSC mix proportions of experiments with varying w/c ratios by Tam *et al* (2012)

Test No.	w/cm	w (kg/m <sup>3</sup> )	c (kg/m <sup>3</sup> )	Cement type	SF (%)	Quartz sand (kg/m <sup>3</sup> )	Crushed quartz (RD)	SP (%)
1	0.17	unknown	unknown	OPC	25	1090	226	2.5
2	0.20	202	761	OPC	25	1090	226	2.5
3	0.23	unknown	unknown	OPC	25	1090	226	2.5
4	0.40	unknown	unknown	OPC	25	1090	226	2.5

Figure 2.7 Drying shrinkage results (microstrain  $\times 10^{-6}$ ) over time (days) for varying w/c ratios (Tam *et al*, 2012).

The test specimens underwent water curing for 28 days yet shrinkage occurred from day 1, indicating that internal autogenous shrinkage took place, as the external water did not penetrate through the entire specimen which was therefore not 100% saturated. The general pattern in the rate of shrinkage for this study was that the initial shrinkage (between days 1 and 14) was rapid. From day 14 to day 100 the shrinkage rate increased gradually and after day 100 it decreased gradually (Tam *et al*, 2012).

## 2.4.2 Influence of supplementary cementitious materials

### Case study A

In addition to testing the influence of the w/c ratio on HSC, Lee *et al* (2017) also tested the influence of FA on the shrinkage experienced by 120 MPa HSC. Table 2.7 gives the controlled constituents used in the concretes for these experiments.  $100 \times 100 \times 400$  mm specimens were tested for total shrinkage (autogenous plus drying shrinkage) using the C157 test standard. After placement the specimens were exposed to temperature of  $23 \pm 1^\circ\text{C}$  and humidity of  $60 \pm 3\%$ .

Table 2.7 HSC mix proportions of experiments conducted by Lee *et al* (2017).

Test No.	w/c	w (kg/m <sup>3</sup> )	c (kg/m <sup>3</sup> )	Cement type	SF (%)	FA (%)	SP (%)	Fine aggregate (RD)	Coarse aggregate (RD)
Control	0.16	155	824	Type I	15	0	0.8	2.6	2.7
1	0.16	155	727	Type I	15	10	1.1	2.6	2.7
2	0.16	155	630	Type I	15	20	1.9	2.6	2.7

The results showed that drying shrinkage reduced with increasing FA. With a substitution of 10% FA drying shrinkage reduced by 15% and with a 20% substitution by 23%, at 60 days. This reduction in shrinkage was attributed to pore refinement that hindered the movement of capillary water (Lee *et al*, 2017).

### Case study B

Gupta *et al* (2006) investigated how shrinkage is influenced by the addition of fly ash and SF in HSC. 75 × 75 × 280 mm concrete beams were tested for drying shrinkage. The specimens were cured for 7 days in a water bath, after which initial readings were taken. They were then left to air dry. Shrinkage recordings were taken on 3 more occasions, with the last readings taken on the 90<sup>th</sup> day. Figure 2.8 shows the drying shrinkage results for this study.

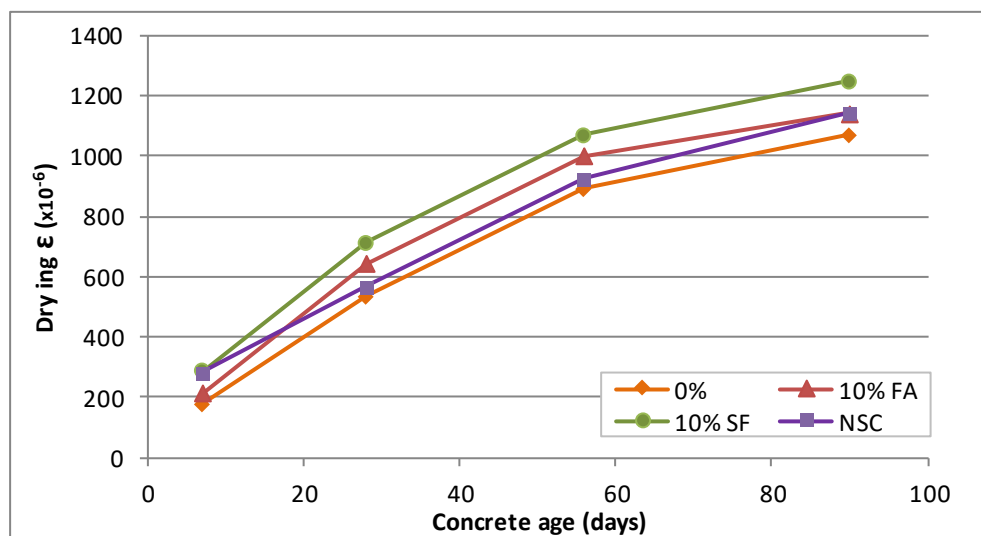


Figure 2.8 Drying shrinkage results (microstrain) over time (days) of concrete mix with 0% and 10% FA and SF (Gupta *et al*, 2006).

The results indicated that HSC with added FA or SF experienced greater shrinkage than HSC without FA or SF. The specimens with 10% SF generally had the greatest shrinkage of all the concrete mixes, including NSC. The HSC without the inclusion of any mineral admixture experienced the lowest shrinkage of the mixes, including the NSC.

### Case study C

The Oakland Bay Bridge Research Project led by Al-Manaseer and Fayyaz (2011) investigated the effect of different ratios of chemical and mineral admixtures on the drying shrinkage of HSC. The effects of varying

dosages of FA on drying shrinkage were investigated and the addition of SF and metakaolin were compared with each other.

Thirty-four (34) different concrete mixes were tested in this study. For each concrete mix, three  $75 \times 75 \times 285$  mm concrete prisms and twelve  $100 \times 200$  mm concrete cylinders were created. The first shrinkage readings were taken after specimens were left to cure for a day in a moist cure room under plastic covering. After this the demolded specimens were placed in a water bath for 6 days and then exposed to a temperature of  $23 \pm 1.7$  °C and humidity of  $50 \pm 4\%$ . Experimental shrinkage data were recorded for up to 9 years. Shrinkage of four cylindrical samples made using the same concrete mix as used for an in-service structure, the Skyway Structure of the San Francisco-Oakland Bay Bridge, were measured for 7 years (Al-Manaseer & Fayyaz, 2011).

With a constant w/c ratio of 0.33, 0.6% high-range water-reducer (HRWR), 5% SF or 5% metakaolin, samples with dosages of FA of 20, 25 and 30% were tested. Figure 2.9 shows shrinkage results for the varying FA dosages. In reference to Figure 2.9, Al-Manaseer and Fayyaz (2011) indicated that as the FA content increased in a concrete mix including 5% SF and 0.6% HRWR, the drying shrinkage increased. On the other hand, in a concrete mix including 5% metakaolin and 0.6% HRWR, an increase in FA decreased the drying shrinkage. The optimum paired ratio for mineral admixtures was found to be 25% FA and 5% SF which reduced shrinkage up to 36%. With the inclusion of the metakaolin, up to 20% of the drying shrinkage was reduced.

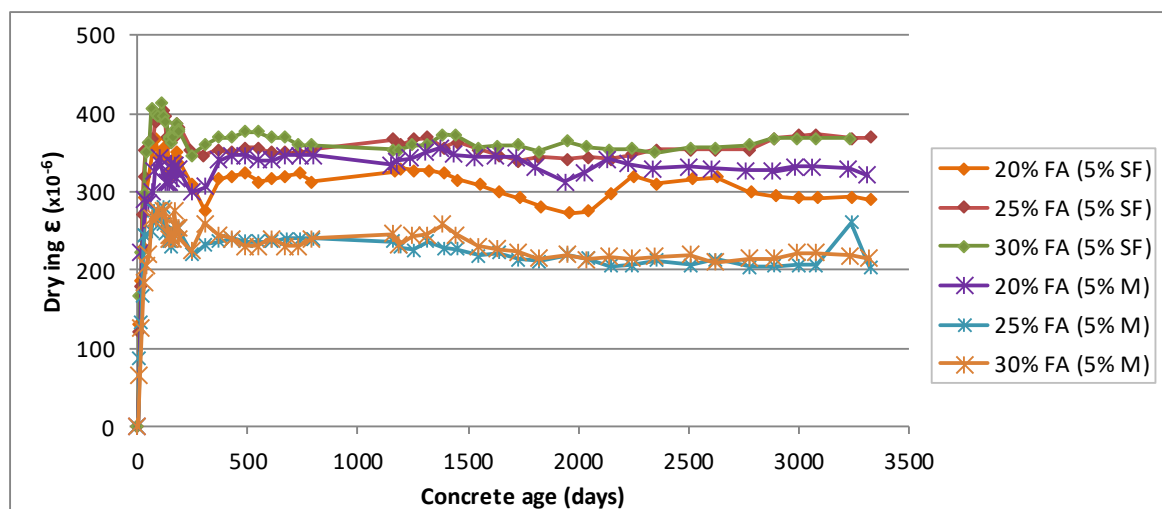


Figure 2.9 Drying shrinkage results (microstrain) over time (days) for varying FA dosages, excluding SRA influence (Al-Manaseer & Fayyaz, 2011).

### 2.4.3 Influence of aggregate type and origin

SANS 10100-1 (2000) indicates that use of aggregates from certain regions in South Africa, such as the Beaufort group - part of the Karoo supergroup - results in high shrinkage in concrete.

#### Case study A

In addition to investigating the effect of FA and SF, Gupta *et al* (2006) also looked at the effect of aggregate on drying shrinkage. They experimented with two types of fine sand and coarse aggregate, namely

Yamuna sand, Badarpur sand, 12.5 mm Granite and 12.5 mm Sandstone. Each coarse aggregate was paired with both sand types. The drying shrinkage results they obtained are presented in Figure 2.10.

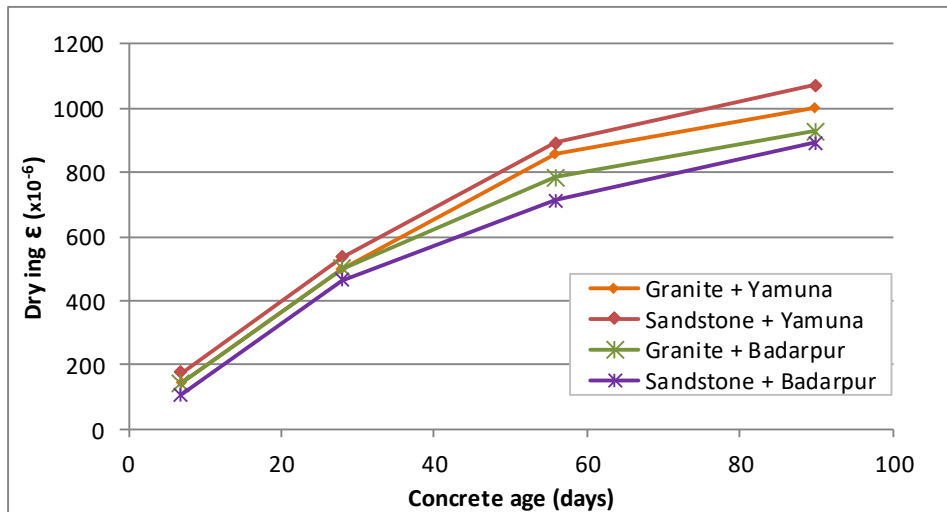


Figure 2.10 Drying shrinkage results (microstrain) over time (days) of concrete mix with granite and sandstone coarse aggregate (Gupta *et al*, 2006)

In reference to Figure 2.10, Gupta *et al* (2006) concluded that the concrete mix with the granite coarse aggregate had less drying shrinkage compared to the concrete mix with sandstone aggregate by only 7% at 90 days. The concrete mix with the Badarpur sand showed 10% less shrinkage than the concrete mix with Yamuna sand.

### Case study B

Guðmundsson (2013) investigated how drying shrinkage is influenced by the porosity and elastic modulus of aggregate in HSC. Table 2.8 gives the constituents of the four different concrete mix designs. 75 × 75 × 250 mm concrete prisms were tested for drying shrinkage. After placement, the prisms were left to harden for 23.5 hours. Once demolded, the prisms were placed in a lime water bath for 30 minutes, after which initial readings were taken. The specimens were then either water or air cured for 28 days. Shrinkage recordings were taken over 60 days. Three experiments were done per concrete mix. Each experiment tested a porous basalt rock type, but from different quarries in Iceland. These 3 selected basalt aggregates had different densities and their porosities ranged between 5 and 17%.

The results for concrete mixes with design strengths of 40, 60 and 70 MPa all showed that with increasing aggregate porosity drying shrinkage increased. Concrete using the aggregate from quarry 2, which had the highest porosity, showed the highest shrinkage. Another shrinkage experiment was done using the more porous aggregate from Iceland and less porous granite. The results of these tests showed similar shrinkage behaviour for the 9.1% porosity basalt and 1.2% porosity granite aggregates (Guðmundsson, 2013).

Table 2.8 HSC mix proportions of experiments conducted by Guðmundsson (2013).

Design strength (MPa)	Aggregate quarry	Aggregate porosity (%)	w/c	c (kg/m <sup>3</sup> )	Air (%)	Fine aggregate (%)	Coarse aggregate (%)	Slump (mm)	Density (kg/m <sup>3</sup> )
40	1	7 – 12	0.37	444	7.1	45	77	210	2272
	2	17	0.37	440	8.0	46	58	130	2228
	3	5 – 7	0.37	450	6.0	45	60	190	2372
60	1	7 – 12	0.31	505	4.7	49	75	80	2409
	2	17	0.31	498	6.2	47	58	100	2272
	3	5 – 7	0.31	506	4.7	45	60	90	2443
70	1	7 – 12	0.29	540	4.0	48	78	60	2473
	2	17	0.29	526	6.6	47	58	170	2309
	3	5 – 7	0.29	540	3.8	47	60	160	2517

#### 2.4.4 Influence of chemical admixture content and type

Gupta *et al* (2006) indicate that HSC mixes containing HRWR or SPs have a greater initial rate of shrinkage, but lower ultimate shrinkage, than NSC. With commercial products it is always best to conduct tests using different pairings/combinations of admixtures, as they may contain unknown materials which can cause unexpected reactions (Mehta & Monteiro, 2006).

##### Case study A

Tam *et al* (2012) conducted a laboratory experiment on the influence of SP on the shrinkage of HSC. Table 2.9 gives the constituents of the four different concrete mix designs. In their study a polycarboxylic polyether type polymer SP for extremely stiff concretes was used. With a constant w/c ratio of 0.2, four different dosages of the SP were tested, namely 2%, 2.5%, 3% and 3.5%.

Table 2.9 HSC mix proportions of experiments conducted by (Tam *et al*, 2012).

Test No.	w/c	w (kg/m <sup>3</sup> )	c (kg/m <sup>3</sup> )	Cement type	SF (%)	Quartz sand (kg/m <sup>3</sup> )	Crushed quartz (RD)	SP (%)
1	0.20	202	761	OPC	25	1090	226	2.0
2	0.20	202	761	OPC	25	1090	226	2.5
3	0.20	202	761	OPC	25	1090	226	3.0
4	0.20	202	761	OPC	25	1090	226	3.5

See Figure 2.11 for the shrinkage results for the varying plasticiser dosages. The results showed that with increasing plasticiser dosage the drying shrinkage rate and magnitude increased. The test specimens with 2% SP had an ultimate shrinkage of 501 microstrain, while those with 3.5% SP had an ultimate shrinkage of 1148 microstrain.

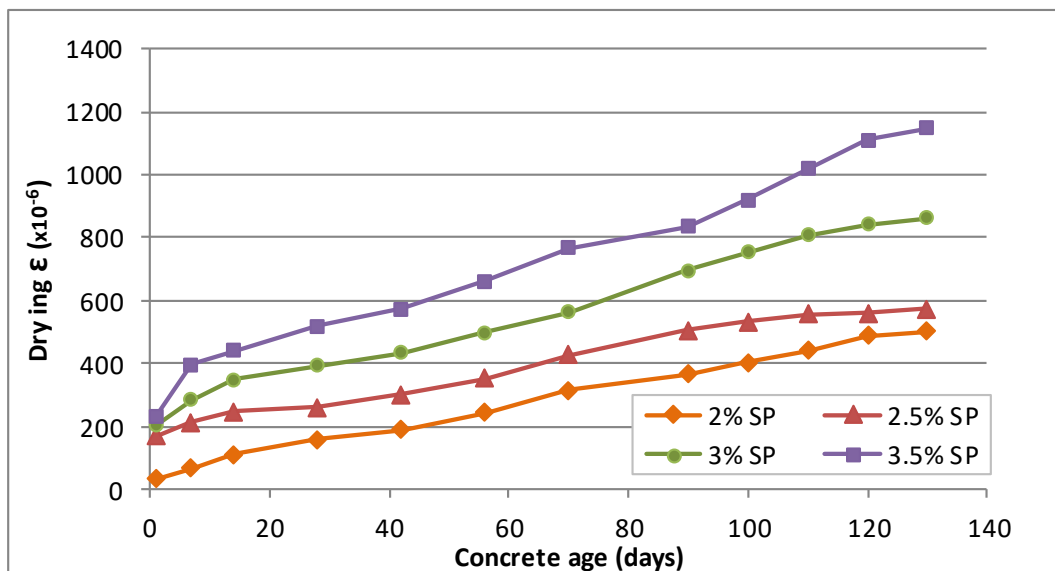


Figure 2.11 Drying shrinkage (microstrain) over time (days) for varying SP dosages (Tam *et al*, 2012).

### Case study B

The Oakland Bay Bridge Research Project investigated the effect of different ratios of SRAs on the drying shrinkage of HSC. The experimental results indicated that the type and amount of admixture used are factors that affect the drying shrinkage. Bažant and Baweja (2000) agree that admixtures and mineral admixtures added to concrete will increase its strength and significantly influence the shrinkage.

The SRA used in this study had polyoxyalkylene alkyl ether as its main component. Rajabipour *et al* (2008) state that commercially available SRA products do not all have the same composition, but all do have the same purpose, to reduce surface and capillary tension in the concrete pores. The research study by Pease (2005) evaluated the effect of SRA in concrete with low w/c ratios and found that the surface tension within the capillary pores of concrete was reduced by up to 54%. The dosage rate was 15%. It was noted that beyond this concentration the SRA had no additional effect on the surface tension. In addition, expansion was observed when a high concentration of SRA was used.

With a constant w/c ratio of 0.33, 0.6% HRWR, 5% SF or 5% metakaolin and 0.5% SRA, the different dosages of FA tested were 20%, 25% and 30%. Figure 2.12 shows the shrinkage results for these varying FA dosages.

In reference to Figure 2.12, Al-Manaseer and Fayyaz (2011) compared the drying shrinkage with the results shown in Figure 2.9 and indicated that the addition of 0.5% SRA decreased the ultimate shrinkage magnitude by 36% for the concrete mix with 5% SF and 0.6% HRWR. For the concrete mix with 5% metakaolin and 0.6% HRWR, the addition of the SRA reduced the final drying shrinkage magnitude by 10%. With a constant w/c ratio of 0.33, 0.6% HRWR, 25% FA and 5% SF, different dosages of SRA were tested. These were 0%, 0.5%, 1%, 1.5%, 2% and 2.5%.



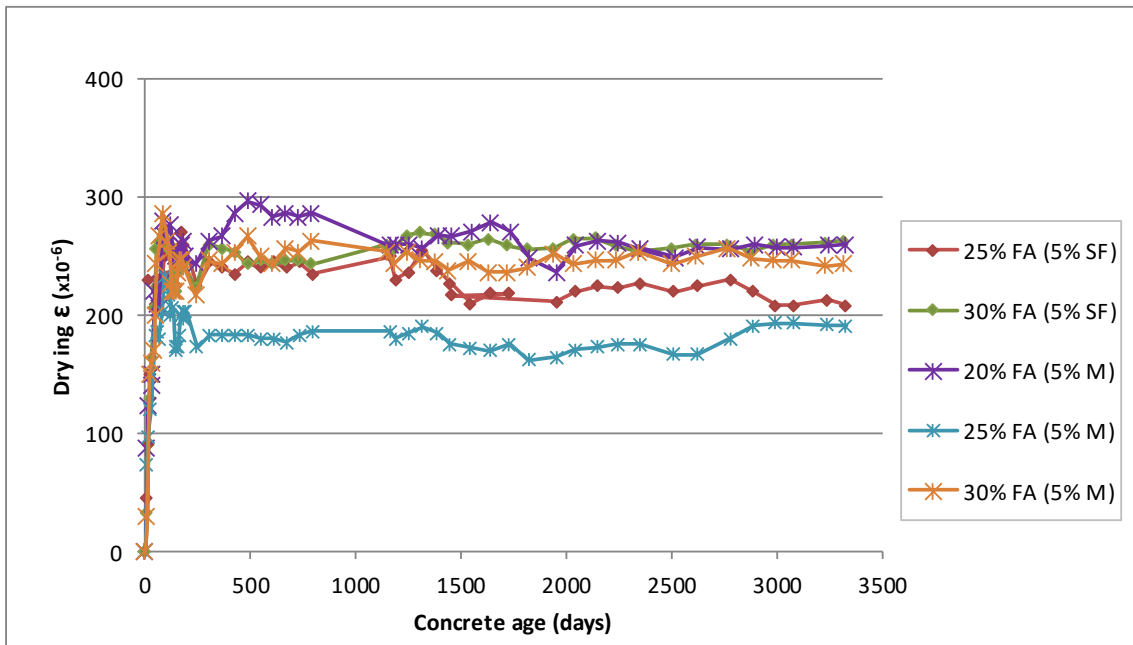


Figure 2.12 Drying shrinkage results (microstrain) over time (days) for varying FA dosages, including SRA influence (Al-Manaseer & Fayyaz, 2011).

Figure 2.13 presents the measured shrinkages for the varying SRA dosages. Al-Manaseer and Fayyaz (2011) observed a decrease in drying shrinkage when SRA was added. At an SRA concentration of 1.5%, ultimate drying shrinkage was reduced by approximately 57%. However, SRA dosages greater than 1,5% did not reduce the drying shrinkage any further.

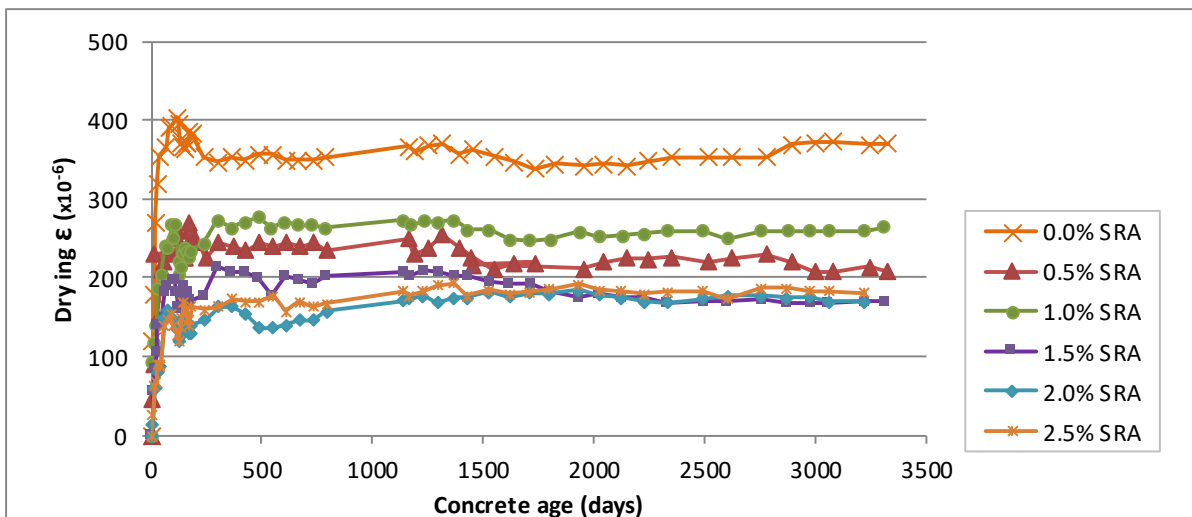


Figure 2.13 Drying shrinkage results (microstrain) over time (days) for varying SRA dosages (Al-Manaseer & Fayyaz, 2011).

The Oakland Bay Bridge study looked at two different chemical admixture brands, Master Builder and WR Grace. Three types of chemical admixtures per brand were tested, namely SRA, HRWR and low-range water reducing (LRWR) admixtures. Increments of 0.5% of SRA, 0.4 to 0.6% HRWR and 0 to 0.2% LRWR were used to replace the total weight of the cement. Three types of mineral admixtures were part of the

experiment as well, namely FA (class F), SF and metakaolin. 20 to 30% of FA, 0 to 5% of SF and 0 to 5% metakaolin were used to replace the total weight of cement. With the same admixture ratios for both brands, WR Grace performed 11% better than Master Builder in terms of reducing shrinkage. With regard to the compressive strength however, Master Builder performed 1% better than WR Grace (Al-Manaseer & Fayyaz, 2011). For the chemical admixtures, pairing SRA with 0.4% HRWR and 0.2% LRWR performed only 1% better than pairing SRA with 0.6% HRWR in terms of reducing the drying shrinkage (Al-Manaseer & Fayyaz, 2011).

### *Case study C*

The study conducted by Saliba, Rozière, Grondin and Loukili (2011) determined that the addition of 1%/cm SRA was more effective in reducing drying shrinkage at concrete age 7 days than it was at age 70 days. The SRA was also more effective at the higher w/cm ratios. A maximum reduction in shrinkage of 56% and 31% was seen at day 7 for concretes with a w/cm of 0.65 and 0.43, respectively.

### **2.4.5 Influence of curing, temperature and relative humidity**

The relative temperature fluctuates more in HSC or High Performance Concrete (HPC) with a low w/c ratio than concretes with a high w/c ratio as the hydration of the cement gives off large amounts of heat. Early-age autogenous shrinkage is greater when the low w/c ratio concrete specimen is subjected to high curing temperatures. This relationship was proved by test specimens reaching maximum autogenous shrinkage much quicker as the curing temperature increased from 20 to 40°C (Chu, Kwon, Amin, & Kim, 2012).

The magnitude of the final drying shrinkage lessens with increasing ambient RH. A low ambient RH promotes permeation of internal water through the concrete's interconnected pores, from high to low water concentration areas, effectively increasing the drying rate of the concrete. 100% ambient RH will result in the concrete specimen taking up moisture and swelling (Alexander & Beushausen, 2009).

### *Case study A*

Bouziadi, Boulekbache and Hamrat (2016) conducted a laboratory experiment on the influence of curing temperature on the total (autogenous and drying) shrinkage of HSC. In this study curing temperatures of 20, 35 and 50 °C were used. In order to prevent evaporation from the 100 × 100 × 400 mm concrete prisms they were sealed with wet burlap. Specimens were exposed to a temperature of 20 ± 2 °C and humidity of 90 ± 5% for 24 hours. Once demolded, the prism ends were coated with asphalt to restrict the movement of water from the exposed surfaces. Thereafter the specimens were stored in a steam oven where they were exposed to a constant humidity of 90 ± 5% at varying temperatures. Shrinkage recordings were taken over 180 days. The shrinkage results showed the following:

- The total shrinkages of the concrete samples exposed to a curing temperature of 20 °C were less than those of the samples exposed to temperatures of 35 and 50 °C. The highest shrinkage occurred in the concrete cured at 50 °C.
- Early-age shrinkage was influenced more than long-term shrinkage by varying curing temperature.
- There was no real proportional relationship between shrinkage and change in curing temperatures. This was explained to be a result of the hydration process, as different cement blends react differently at different temperatures.

---

## 2.5 Estimating shrinkage and development of shrinkage database

According to ISO 16311-1 (2014) the maintenance plan of concrete structures requires an assessment of the predicted deterioration. From this assessment, a prevention plan is executed to maintain the structural safety, serviceability and appearance.

There are different methods to assess the time-dependent shrinkage deterioration. These methods include mathematical modelling by means of finite element analysis and statistical modelling, which uses regression analysis based on existing shrinkage data. For more realistic predictions, theoretical considerations that account for the concrete shrinkage process are usually incorporated into the mathematical modelling equations. For example, diffusion theory, solidification theory and micro pre-stress theory support the models' empirical forms according to RILEM TC-242-MDC (2015). Another method of predicting the shrinkage deterioration is mechanistic modelling that predicts the cracks caused by shrinkage. ACI Committee 209 (2008) indicated that not incorporating the mechanistic behaviour of shrinkage, but only the concrete composition, in the development of a model might produce inaccurate results. On the other hand, there is mechanistic shrinkage behaviour that is unknown or not clear, such as the relationship between simultaneous drying and autogenous shrinkage. Therefore, large databases are still required for model development and calibration (Wedner *et al*, 2015(b)).

According to Goel, Kumar and Paul (2007), examples of mathematical models are the effective modulus method, double power law, double power logarithmic law and the age-adjusted method. These mathematical methods were used to predict shrinkage and creep when there was insufficient data for empirical modelling.

More recent shrinkage models were statistically derived from collated databanks of extensive experimental data. The compilation of a large database of experimental data was initiated by Bažant and Panula for the development of the BP model in 1978 (Wedner, Hubler & Bažant, 2015(a)). The database initially included only European and American experimental data (Wedner *et al*, 2015(a); ACI Committee 209, 2008). Expansion of this database was first carried out by a joint committee of CEB and ACI and later continued by the RILEM Committee TC107 to produce the RILEM-ACI 209 database in 1992 which comprised approximately 15000 data points (Bažant & Baweja, 1995(b)). Further additions to the database were done in 2008 and 2010 at Northwestern University (NU). The most recent database was first presented in 2013 and is known as the NU Database. It includes shrinkage and creep data of more modern concrete mixtures with different admixtures, recorded over longer time periods than the previous data. The NU database also includes results from more comprehensive concrete composition ratios, specimen shapes and testing conditions. The preceding database, the RILEM database, does not include autogenous shrinkage and modern HPC experimental data, mineralogical data or aggregate type (Wedner *et al*, 2015(a)).

The NU Database contains 1800 shrinkage curves of which about 1050 include data on concretes with admixtures. Compared with the former RILEM database, the NU database has extensive recordings of concrete composition and ratios, especially on admixtures and aggregate details, test conditions and specimen sizes and shapes. There is large variation between all the recorded experiments due to all the different concrete mix compositions, material types and constituent quantities. Consequently, using the entire database to verify or calibrate a model function is impossible (Wedner *et al*, 2015(a)). The NU database covers total shrinkage, drying and autogenous shrinkage experiments, but there are few corresponding drying and autogenous shrinkage experiments (for the same concrete mixes exposed to

the same environmental conditions and duration of testing) that can be used to further assess the relationship between drying and autogenous shrinkage (Hubler *et al*, 2015).

Mucambe (2010) highlights the importance of using local data when evaluating concrete produced in South African, because of different geographical conditions. Concrete classification systems and mixing standards also differ from country to country, so it was recommended to conduct local short-term experiments to calibrate the prediction models (ACI Committee 209, 2008; Bažant and Baweja, 2000). Mucambe (2010) stated that through partnership between universities in South Africa a shrinkage and creep database was compiled to calibrate existing models, taking South African conditions into consideration. Additional South African concrete shrinkage investigations are possible through this database, which comprises 291 country-wide drying shrinkage experiments obtained from 25 laboratories. However, due to missing data, the database includes reliable results from only 245 of these experiments. This dataset is also limited in that it includes only drying shrinkage data from experiments conducted in South Africa. It contains no autogenous shrinkage data (Gaylard, 2011).

### *Database and dataset development challenges*

The challenges in compiling a database or selecting datasets were stated in ACI Committee 209 (2008) and verified by Wedner *et al* (2015(a)) and Hubler *et al* (2015), who indicated that these challenges are still applicable. The obstacles are:

- Deciding whether datasets should be included or excluded, per researcher. Although the criteria for dataset selection should not be biased, only some of any particular researcher's work was included making it hard to pair experiments from different researchers.
- Missing data leads to uncertainties in datasets.
- Inconsistency in certain variables. For example, data for similar concrete compositions were measured for different shape and size test specimens.
- The cement type for datasets from different countries does not follow the same classification system, making it hard to group datasets from these different countries.
- The majority of the recorded experiments were conducted over a short duration which makes long-term or multi-decade predictions difficult. Small inaccuracies in the short term recordings could lead to large inaccuracies seen in long-term shrinkage predictions.
- The test specimens are small in size and might not accurately simulate the shrinkage that takes place in real-life structures.
- The recorded information may contain errors.

## **2.6 Prediction model criteria**

The modification of existing and development of new shrinkage prediction models is ongoing and progressive, to adapt to the continuous advancements in concrete technology. Thus the American Concrete Institute (ACI) Committee has published set model presentation and development standards and requirements, which are found in the Guide for Modeling and Calculating the Shrinkage and Creep in Hardened Concrete (ACI Committee 209, 2008).

The first consideration when selecting a model is to ensure the mathematical shape of the model fits the rate of shrinkage (shrinkage against time plot). It is also recommended that the shrinkage curve should be

compared to individual real shrinkage measurements when evaluating a prediction model (ACI Committee 209, 2008).

The principal requirement of a prediction model is that it should be accessible to and understood by engineers with minimal knowledge of concrete shrinkage and creep (ACI Committee 209, 2008). There is no requirement for specific data, such as the concrete's mechanical properties or a mix's constituent proportions, to be used or specified for the prediction of shrinkage. However, the following information and practices provided by ACI Committee 209 (2008) are minimum requirements for inclusion in shrinkage and creep prediction models:

- Description of the concrete constituents and mechanical properties.
- Ambient RH.
- Age of concrete specimen when loads are applied. This is only required when testing for creep in concrete.
- Duration of the drying period.
- Duration of applied loading to the concrete specimen.
- The concrete specimen size.
- Provision within the model to get long-term results through the measurement of shrinkage and creep.
- User-friendly mathematical expressions that are not significantly influenced (too sensitive) by small changes in input parameters.
- The prediction should have a limit in the length of time.
- Be able to determine the magnitude of shrinkage at a specific time.

A model development challenge acknowledged by ACI committee 209 (2008) was model complexity or simplicity. Too complex models defeat the principle rule of being user friendly, as specialised knowledge on shrinkage might be required by the user or engineer. However, RILEM TC-242-MDC (2015) stated that it would not be worthwhile to conduct extensive statistical recalibration on simple material models when designing for highly shrinkage sensitive structures such as bridges.

Another model development challenge mentioned was the determination of acceptable prediction accuracy. To achieve close to 100% accurate results, a model would need to be based on concrete of similar composition and test conditions which would then render the model bias in prediction. These challenges are, however, not necessarily limitations to the development of models according to ACI committee 209 (2008).

According to the ACI committee 209 (2008) only experimental measurements that fall within the covariate ranges for which a model was developed should be used to test the model's accuracy. Within these limitations a model should not produce large variations in predictions for small changes in the input parameters, and the shape of the predicted shrinkage curve should correctly follow that of the experimental shrinkage curve. The ACI committee 209 (2008) recommended the following:

- The effect of specimen shape and size should be incorporated in the model.
- Concrete specimens with mineral and chemical admixtures should be accounted for in the model.
- The RH be allowed for.

## 2.7 Shrinkage prediction models - performance studies

Engineering societies across the world recommend their in-house drying shrinkage models, which are all unique in their model time function and parameters they consider, and so produce different results for the same input data (Wedner, Hubler & Bažant, 2014). Updated versions of the recommended models are usually published by the engineering societies after the extension of shrinkage databases to keep up with advances in concrete technology. Figure 2.14 depicts the development of American (red), Canadian (green) and European (purple and orange) shrinkage prediction models over the last fifty years. Many accuracy compliancy studies for different concrete mixtures have been conducted using these listed models, showing large deviations from the experimental data. These large variations could be due to the differences in raw material properties between geographical regions (Kataoka, Machado and Bittencourt, 2011).

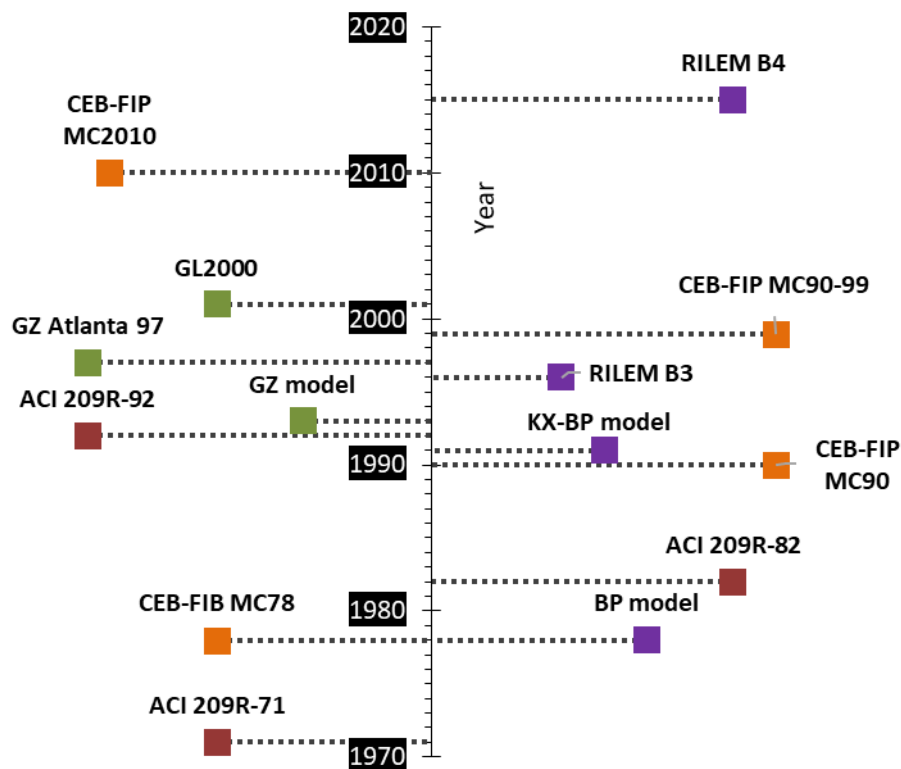


Figure 2.14 Development of shrinkage prediction models between 1970 and 2020 (Bažant and Baweja, 1995(a); CEB, 1999; ACI Gardner and Lockman, 2001; Committee 209, 2008; CEB-FIP, 2012 and RILEM TC-242-MDC, 2015)

### 2.7.1 American and Canadian models

The American Concrete Institute (ACI) (ACI Committee 209, 2008) state that the first recommended model was developed by Branson and Christianson and termed the ACI 209R-71 model, for the precast-prestressing industry. This was followed by the ACI 209R-82 model which incorporated minor changes, and the latest recommended model, the ACI 209R-92, which has not been updated or recalibrated since its introduction.

The advantage of the ACI 209R-92 model according to ACI committee 209 (2008) is that it is not complex and does not require advanced background knowledge. Disadvantages for the simplest form of the model

are that specimen size is not accommodated which limits prediction accuracy, and it is empirically based, so does not account for shrinkage or creep mechanisms. Gardner and Lockman (2001) compared the ACI 209R-92 model's prediction results with the RILEM shrinkage databank and concluded that the model underestimates high shrinkage values and overestimates low shrinkage values, indicating its limited ability to predict drying shrinkage. The model has not been modified/updated using data from the newer RILEM and NU databases (ACI Committee 209, 2008). This model is therefore not generally used for shrinkage and creep analyses for complex concrete structures. Equation 2.6 gives the drying shrinkage model time function  $\beta_{ds}(t)$  for the ACI 209R-92 model. A three parameter function is used. The parameter  $\alpha$  affects the final calculated shrinkage,  $\tau$  affects the rate of shrinkage and  $\gamma$  influences the shape or curvature of the growth function (Gaylard, 2011; ACI Committee 209, 2008).

$$\beta_{ds}(t) = \alpha \left( \frac{t^\gamma}{\tau + t^\gamma} \right) \quad (2.6)$$

Two Canadian researchers, Gardner and Lockman (2001) developed the GL2000 model in the year 2001. This is a modified version of the GZ Atlanta 97 model developed by Gardner and Zhao (ACI Committee 209, 2008). The GL2000 model was derived and calibrated using a subset of the RILEM database, for NSC only (Gaylard *et al*, 2013). This model follows the ACI guidelines and includes the compressive strength at the 28<sup>th</sup> day, so does not depend on covariate data that is still to be established at the time of design. See Equation 2.7 for the GL2000 model time function for drying shrinkage  $\beta_{ds}(t)$ , with parameters  $\alpha$  which influences the final shrinkage,  $\tau$  which determines the rate of shrinkage and  $\gamma$  which affects the shape or curvature of the growth function (Gaylard, 2011 and Gardner and Lockman, 2001).

$$\beta_{ds}(t) = \alpha \left( \frac{t}{\tau + t} \right)^\gamma \quad (2.7)$$

### 2.7.2 European models

According to CEB (1999) the Comité Européen du Béton - Fédération Internationale du Béton (CEB-FIB) released their first recommended model, termed CEB-FIB MC78, in 1978 and the second version, developed by Muller and Hillsdorf and termed CEB-FIB MC90, in 1990. This later model was updated in 1999 with the RILEM database to include HSC and autogenous shrinkage, and it is now known as the CEB-FIB MC90-99 model. The modifications to the model were to increase the overall accuracy of predictions of the time-dependent mean cross-section behaviour of a concrete structure (Hassoun & Al-Manaseer, 2008). The CEB-FIB MC90-99 model is extremely sensitive to the RH covariate value. The drying duration could have a direct impact on the shrinkage results and should therefore be ignored when dealing with shrinkage and creep compliance according to ACI committee 209 (2008). The CEB-FIB models were adapted in the Eurocode 2 drying shrinkage model, another widely accepted and used European standard (Holowaty, 2015).

The MC 2010 (short for CEB-FIB Model Code 2010) was published in 2012 and superseded all previous model versions. This model accommodates modern concretes such as high strength and fibre reinforced concretes (ACI Committee 209, 2008; Walraven & Bigaj-van Vliet, 2011) and was developed and calibrated to 168 long-term experiments from the RILEM database. A good range of covariate parameters was one of the main selection criteria for experimental data used to optimise this CEB-FIB model, rather than a large number of experiments. The time function of the shrinkage model is also consistent with diffusion

theory, as the cross-sectional area of test specimens primarily influences the rate of shrinkage (CEB-FIP, 2013). The MC 2010 model makes use of the same model function as the GL2000 (see Equation 2.7). The autogenous shrinkage time function  $\beta_{as}(t)$  is given in Equation 2.8. The parameter  $\tau$  influences the rate of shrinkage (CEB-FIP, 2012). Appendix A gives a complete listing of the MC 2010 model formulae.

$$\beta_{as}(t) = 1 - e^{-\tau\sqrt{t}} \quad (2.8)$$

According to Gaylard *et al* (2013) shrinkage predictions for Australian and New Zealand concretes are overestimated whilst those for North American concretes are underestimated by this model, as the concrete used in the European experiments for which the model was optimised may contain lower cement content. CEB-FIP (2013) indicated that getting correlation between results from North American (USA) and European shrinkage experiments is hard, as the USA concretes show greater final shrinkage than the European concretes for similar experiments. Predictions for non-European concretes can be incorrect by approximately 20%. A possible reason for this difference in final shrinkage magnitude could be the difference in cement classification and concrete composition (CEB-FIP, 2013). CEB-FIP (2012) indicated some limitations of the model and recommended conducting laboratory experiments to verify shrinkage instead. These limitations are:

- Predicting for low strength, normal hardening concrete with significant amounts of mineral admixtures or cement extenders.
- Predicting for cement types other than CEM I or CEM III. For CEM II with mineral admixtures, experiments should be conducted instead.
- Predicting for HSC when tensile strength growth is central to the success of the structure, as the effect of the concrete's strength on drying shrinkage is assumed to be negligible by the model.

CEB-FIP (2012) stated that poor predictions of shrinkage using the MC 2010 model are the result of errors in the model, and variations in concrete constituents and environmental exposure. It was recommended to determine the prediction error and implement modifications to increase the accuracy of the model.

According to studies conducted by CEB-FIP (2013), the coefficient of variation for autogenous shrinkage of HSC and NSC was recorded as 43.3% and 29%, respectively. The reason for the large C.o.V for HSC is the large scatter seen in the particular datasets that were used. It was also mentioned that the prediction accuracy between the CEB-FIP MC90 (applicable for NSC only) and the MC 2010 did not differ. A C.o.V of 33% was determined. CEB-FIP (2013) made the following suggestions to optimise the MC 2010 model predictions:

- Recalibrate the autogenous parameters based on experiments analysing the internal RH and exposure to different environments (curing, temperature, ambient humidity).
- Recalibrate the compressive strength parameter with concrete mix composition effects from the type of cement and admixtures, for example.

RILEM - Réunion Internationale des Laboratoires et Experts des Matériaux, systèmes de construction et ouvrages, an academic society, produced the BP, BP-KX and B3 models, which are the forerunners of the latest B4 model. The B3 model developed by Bažant and Baweja (1995(a)) is a hyperbolic tangent curve. The B4 model was developed by the RILEM technical committee TC-242-MDC and is an updated version of the B3 model. The B3 model mathematical form and theoretical equations were maintained, namely



“the solidification theory, theory of micro-prestress relaxation in the nano-structure, activation energy concepts, moisture diffusion theory and damage models for micro-cracking” (RILEM TC-242-MDC, 2015). The main difference between the B3 and B4 models is the incorporation of autogenous shrinkage. Autogenous shrinkage in HSC with a low w/c ratio is much larger and more significant, and the activation energy theory that is incorporated covers the temperature spike due to the increased hydration and self-desiccation. The autogenous shrinkage model is still quite conservative as the physical phenomena are not yet fully understood (Hubler *et al*, 2015). Other differences between the B3 and B4 models are that the shrinkage model parameters were revised by using newer information from the NU database to take modern concrete or HPC compositions into consideration, and the range of applicability of the B4 model for each covariate was extended beyond that of the B3 model. The B4 model now includes admixture parameters for combinations of chemical and mineral admixtures - retarding agents, SP (HRWR), air entraining agents, plasticisers (WR), fly ash and SF.

See Equation 2.9 and Equation 2.10 for the RILEM B4 time functions for drying shrinkage  $\beta_{ds}(t)$  and autogenous shrinkage  $\beta_{as}(t)$ , respectively. A two parameter function is used for the drying shrinkage, whereas a three parameter function is used for autogenous shrinkage. The parameter  $\alpha$  influences the final shrinkage,  $\tau$  is the rate of shrinkage and  $\gamma$  influences the shape or curvature of the growth function (Gaylard, 2011; RILEM TC-242-MDC, 2015). Appendix A lists all the elements of the RILEM B4 model.

$$\beta_{ds}(t) = \alpha \tanh \sqrt{\frac{t}{\tau}} \quad (2.9)$$

$$\beta_{as}(t) = \alpha \left[ 1 + \left( \frac{\tau}{t} \right)^\gamma \right]^\gamma \quad (2.10)$$

The cement type classification used in the B4 model is an adapted version of the CEB Model Code method. ‘R’ does not denote rapid hardening, but normal cement type. ‘RS’ is not rapid hardening and early high strength, only rapid hardening. ‘SL’ remains slow hardening cement type (RILEM TC-242-MDC, 2015).

A statistical comparison was done (Hubler *et al*, 2015) between an optimised RILEM B4 model and optimised versions of other established shrinkage models. Final parameter optimisation was done for the mean concrete composition of different selected datasets exhibiting various shrinkage behaviours, taken from the 2018 version NU database (Northwestern University, 2018). The model parameters were optimised by minimising the C.o.V of residuals and the coefficient of determination ( $R^2$ ). Further optimization was done on subsets of similar cement, admixture and aggregate types, at similar temperatures. Once the model fits were optimised statistically, individual visual inspections were done. The RILEM B4 model showed the best overall results with an average C.o.V of residuals of 10%. The calibrated models were statistically compared for experiments with and without admixtures. The RILEM B4 model achieved the smallest C.o.V of around 30% for both experimental datasets, with and without admixtures. The other models that were calibrated to these datasets ranked (from lowest to highest C.o.V) as GL2000, ACI 209R-92 and the MC 2010 (Hubler *et al*, 2015).

The datasets to optimise (calibrate) the shrinkage models were adjusted to combat the uncertainty seen between shrinkage profiles with large discrepancies and variation. Horizontal multiplicative factors, which

influenced the rate of shrinkage and vertical multiplicative factors, which influenced the final shrinkage, were statistically derived within 5% and 95% confidence limits (Hubler *et al*, 2015).

### 2.7.3 South African models

SANS 10100-1 (2000) refers to total shrinkage found in pre- and post-tensioning concrete systems for RH 35 to 80% and is specifically for South African conditions. This standard provides structural guidance for different structural elements to mitigate the deleterious effect of shrinkage. SANS adopted the BS 8110 method published in 1985. This method calculates drying shrinkage of concrete with normal weight aggregate and with no water-reducing admixtures. This method is presented as a nomograph and only considers the RH, V/S and the area of the concrete reinforcement/rebar to determine the magnitude of shrinkage. Two scales are available, to determine short-term (at 6 months) and long term drying shrinkage (at 30 years). The biggest attraction of this model is its simplicity, as the magnitude of shrinkage or swelling is determined from a graph. However, inaccuracies are potentially high and it should be used only as a rough guide (Alexander & Beushausen, 2009).

The WITS model was proposed and developed by Gaylard (2011) and is based on the RSA drying shrinkage database. This model was derived purely on statistical considerations and differs to the models previously described as it was developed using a non-linear hierarchical method for the prediction of drying shrinkage. The model is biased in that it was developed and calibrated using only data from South African experimental shrinkage research, conducted over 30 years. However, the WITS model provides a larger option range than other models in terms of selecting coefficients for various and more profound covariates, such as the types of cement, aggregate and sand. Parameter coefficients were derived statistically by optimising the model function through minimisation of the variation of predictions from the measured results of carefully selected data subsets (Gaylard, 2011; Gaylard *et al*, 2013). Equation 2.11 gives the three parameter function used for drying shrinkage  $\varepsilon_{ds}(t)$  in the WITS model. Parameter  $\alpha$  determines the final shrinkage,  $\tau$  the rate of shrinkage and  $\gamma$  the shape or curvature of the growth function (Gaylard, 2011). Complete details of the WITS model including the various cement types, stone types and sand types considered in the WITS model are given in Appendix A.

$$\varepsilon_{ds}(t) = \alpha(1 - e^{-\tau \cdot t})^\gamma \quad (2.11)$$

Using the RSA database as reference, the accuracy of the WITS model in predicting drying shrinkage was compared using several statistical methods to other well established concrete shrinkage prediction models. The WITS model outperformed all of these existing models, which was perhaps to be expected as the RSA database was used to derive the WITS model. The ACI 209R-92 fared second best, the RILEM B3 third, SANS 10100-1 fourth, CEB-FIB MC90-99 fifth and the GL2000 model fared worst of the other models that were evaluated. For long-term shrinkage (731 to 1095 days) the SANS 10100-1 model gave more accurate predictions than the WITS model (Gaylard, 2011; Gaylard *et al*, 2013).

### 2.7.4 Comparison between the models

The models mentioned previously are all valid for hardened concrete, moist cured for at least one day. For easy comparison between the selected prediction models, Table 2.10 and Table 2.11 summarise the covariates required and the applicable data ranges for each of these covariates, for each of the models.

Table 2.10 Covariate data required for selected shrinkage prediction models (Adapted from Gaylard, 2011; RILEM TC-242-MDC, 2015 and CEB-FIP, 2012).

Covariates	Model					
	ACI 209R - 92	GL2000	MC 2010	RILEM B4	WITS	SANS 10100
	Concrete raw material and composition					
Cement type		✓	✓	✓	✓	
Cement content	✓		✓		✓	
Water content				✓	✓	✓
Air content	✓					
Stone type					✓	
Stone content					✓	
Sand type					✓	
Sand / total aggregate mass ratio	✓					
Aggregate / binder mass ratio					✓	
	Testing conditions					
Specimen shape				✓		
Volume to surface area ratio	✓	✓	✓	✓	✓	
Cross-sectional area to exposed perimeter						✓
Humidity	✓	✓	✓	✓		
Curing method				✓		
Age at first drying	✓			✓		
Temperature					✓	
	Concrete properties					
28 <sup>th</sup> day strength		✓	✓	✓		
28 <sup>th</sup> day elastic modulus				✓		
Slump	✓					

Table 2.11 Applicable data ranges for covariates of selected shrinkage prediction models (Adapted from Gaylard, 2011; RILEM TC-242-MDC, 2015 and CEB-FIP, 2012).

Covariates	Model					
	ACI 209R - 92	GL2000	MC 2010	RILEM B4	WITS	SANS 10100
Concrete raw material and composition						
Cement type	Type I & II	Type I, II & III	CEM I, II* & III	Type I, II & III	CEM II, II, III & V	
Cement content	279 – 446 kg/m <sup>3</sup>			200 – 1500 kg/m <sup>3</sup>	112 – 536 kg/m <sup>3</sup>	
Water content					160 – 225 kg/m <sup>3</sup>	150 – 230 kg/m <sup>3</sup>
Water /cement mass				0.22 – 0.87 (w/c)		
Stone type					See Appendix A	
Stone content					900 – 1400 kg/m <sup>3</sup>	
Sand type					See Appendix A	
Aggregate/ binder mass or aggregate/ cement mass				1.0 – 13.2 (a/c)	3.18 – 8.74 (a/b)	
Testing conditions						
Volume to surface area ratio	$12 \cdot \exp(-0.004728V/S) \geq 0.2$			12 - 120	16.5 – 75.0	
Humidity	40 – 100%	20 – 100%	40 – 100%	40 – 100%	43 – 72%	20 – 100%
Curing method	Moist: $\geq 1$ day or steam: 1–3 days	Moist: $\geq 1$ day or steam	Moist cured: $\leq 14$ days	Moist / steam / fog cured: $\geq 1$ day		
Temperature	21.2 - 25.2°C		5 – 30 °C	-25 – 75 °C	21 - 25°C	
Temperature @ curing			Normal	20 – 30 °C		
Concrete properties						
28 <sup>th</sup> day compressive strength		16 – 82 MPa	15 – 130 MPa	15 – 70 MPa		

\* For the MC 2010, CEM II with only SF, FA and Slag additives should be considered. CEM II with pozzolanic material do not qualify.

Many studies have been conducted to compare the performance of existing shrinkage models for particular types of concrete or new concretes with specialised properties. In some cases existing model parameters were updated to better match these particular concretes. Examples of particular specialised concretes are infra-lightweight and self-compacting concrete.

In their study Abdalhmied, Ashour and Sheehan (2019) compared the drying shrinkage prediction performances of the ACI 209R, BSEN-92, B3 and GL2000 models for self-compacting concretes with  $w/cm$  0.44 and 0.33, using the statistical indicators standard deviation, coefficient of variation and mean absolute error. The ACI 209R-92 model predicted best for the self-compacting concretes they used.

Labbé and Lopez (2020) compared MC 2010 and ACI 209R model shrinkage predictions for normal, light and infra-lightweight concretes. The coarse and fine aggregate of normal weight concrete was substituted with a lightweight aggregate (recycled expanded glass and expanded clay were used separately) to obtain the lightweight concrete. Model parameters were calibrated to fit the measured lightweight concrete shrinkages better by deriving correction factors for this particular type of concrete, using nonlinear programming options in MATLAB. The re-calibrated ACI 209R model performed better than the MC 2010 model and its time function fitted their particular experimental data better.

## **2.8 Non-linear solution software**

There are a variety of software programs that can be used to develop non-linear models based on measured data. However, each of these different programs have their own particular characteristics which need to be understood when using them, in order to minimise errors in the results. According to John (1998) and Frontline Systems (2000-2020), Solver<sup>®</sup>, a desktop or online Excel add-in, is more user-friendly than other specialist software programs. Solver<sup>®</sup> can optimise a complex problem (find the “best” solution) by changing multiple input values which define the problem or model, within constraints imposed on these values and an output value, such as minimising RMSE. Solver<sup>®</sup> does this iteratively using linear or non-linear equations and inequalities. There is no unique answer for the iterative solution of non-linear equations (non-linear regression). The non-linear regression procedure needs to be given starting values to begin the iteration and the answers Solver<sup>®</sup> finds can depend on these. The “best” or optimum solution may be a local rather than a global optimum. To be reasonably sure of a global solution it is necessary to run Solver<sup>®</sup> several times with different starting values and check all the results converge to a similar solution.

## **2.9 Statistical methods to evaluate models.**

Competing prediction models require analytical investigation to rank and select the best model of a group with regard to goodness-of-fit. This is done by comparing the differences between measured data and predictions, also known as the residuals, using various statistical indicators. In estimating the goodness-of-fit of different prediction models the number of parameters in each can also be taken into account for a fairer comparison. Very complex models can be justified by exceptional fits to the data (Myung, 2000).

Some statistical techniques used to evaluate prediction models are the residual method, root mean square error, coefficient of determination, coefficient of variation, mean square error, mean deviation and Akaike’s information criterion (ACI Committee 209, 2008; Al-Manaseer & Prado, 2015; Myung, 2000; Gaylard, 2011). These model evaluation methods have set criteria that enable evaluation of the relative performance of models in any selected group of models applied to the same dataset.

The well-known issue of bias in recorded shrinkage data can be solved by conducting statistical analyses on groups of data for different time intervals, to mitigate the effect of many data points for short-term shrinkage, but few for long-term shrinkage and vice-versa (Gardner, 2004). Each time interval or data group should have sufficient data points to enable a statistically meaningful result. Groups for which there are unavoidably insufficient data should be excluded from the statistical analysis (Al-Manaseer & Prado, 2015).

According to Al-Manaseer and Prado (2015) when evaluating the residuals of different prediction models, for the same experimental data, the best performing models should show the smallest “even” distribution between overestimation and underestimation from the actual shrinkage. In other words, residuals should ideally be randomly distributed about zero.

### 2.9.1 Root mean square error (RMSE)

The RMSE can be defined as the standard deviation of residuals of the fit standard error of the regression and is an unbiased goodness-of-fit indicator. It requires the residual sum of squares (RSS), also known as the sum of squared residuals and incorporates the degrees of freedom ( $n - p$ ) which represents the model complexity or simplicity.  $n$  is the number of data points and  $p$  the number of model parameters (Myung, 2000). When the RMSE is averaged for a group of shrinkage experiments, this average can be normalised by the average shrinkage magnitude of the specific group, which is similar to calculating the coefficient of variation (C.o.V) (Gaylard, 2011; Gardner, 2004). RMSE is minimised when estimating model parameters and is calculated using Equation 2.12 and Equation 2.13 (Myung, 2000):

$$RSS = \sum_{i=1}^n (y_i - \hat{y}_i)^2 \quad (2.12)$$

$$RMSE = \sqrt{\frac{RSS}{(n - p)}} \quad (2.13)$$

where  $y_i$  are the measured values and  $\hat{y}_i$  the predicted values.

### 2.9.2 Coefficient of determination ( $R^2$ )

The coefficient of determination,  $R^2$ , describes a model's goodness-of-fit. This statistical measure shows how similar a predicted regression line is to the real data points, and indicates this as a value between 0 and 1. If the goodness of fit equals to 1 the model function exactly matches the data points without any scatter. If the goodness-of-fit equals to 0, the model function intersects the mean of all Y-values as a horizontal line. Values of  $R^2$  between 0 and 1 indicate the percentage of variance that is predictable (Gaylard, 2011) Negative values of  $R^2$  indicate very poor data fits.  $R^2$  is given by Equation 2.14.

$$R^2 = 1 - \frac{RSS}{TSS} \quad (2.14)$$

where TSS, the total sum of squares, is the sum of the squared differences between measured ( $y_i$ ) values and their average value ( $\bar{y}_i$ ), as shown in Equation 2.15.

$$TSS = \sum_{i=1}^n (y_i - \bar{y}_i) \quad (2.15)$$

$R^2$  can be adjusted to take the number parameters into consideration, as shown in Equation 2.16 (Burnham & Anderson, 2002). To create an unbiased calculation,  $(n - 1)$  is used (Bažant and Baweja, 1995(b)).

$$R^2_{adj.} = 1 - \frac{(n-1)RSS}{(n-p)TSS} \quad (2.16)$$

### 2.9.3 Akaike's information criterion (AIC)

AIC is a penalised maximum likelihood estimate (ML) and includes two components, negative log likelihood or the lack of fit component and a penalty component. The AIC takes the number of parameters, or model complexity, into consideration and in any group of models, favours the models with the fewest parameters. To compare models, parameter estimation for all of them must always be done using the same set of data (measured values). The AIC value for each proposed model is calculated using either its ML or the least squares regression statistic RSS if model errors follow a normal distribution with constant variance, as shown in Equation 2.17 and Equation 2.18. AIC values as such do not identify the best fit or most suitable model, but for a given set of data determine a trade-off between variance and bias for the fitted parameters of each model. The model with the lowest calculated AIC value is ranked as the best model in the group (Bozdogan, 2000; Burnham & Anderson, 2002; Burnham, Anderson & Huyvaert, 2011; McArdle, Navakatikyan & Davison, 2019). AIC values are calculated as:

$$AIC = -2\ln(ML) + 2k \quad (2.17)$$

or

$$AIC = n \ln\left(\frac{RSS}{n}\right) + 2k \quad (2.18)$$

where  $k$  is the number of free parameters per model plus 1 ( $p+1$ ) and  $n$  is the number of data points.

When the ratio  $n/k < 40$  (representing a small sample size), it has been recommended that a corrected AIC value ( $AIC_c$ ) be used, which tends towards AIC anyway as  $n$  gets large.  $AIC_c$  is given in Equation 2.19 (Burnham & Anderson, 2002):

$$AIC_c = AIC + 2k\left(\frac{k+1}{n-k-1}\right) \quad (2.19)$$

In order to rank the models in a group, the differences ( $\Delta_i$ ) between their  $AIC_c$  values are used, where:

$$\Delta_i = AIC_{Ci} - AIC_{cmin} \quad (2.20)$$

$AIC_{cmin}$  is the smallest of the  $AIC_c$  values of the proposed models. The “best” model has  $\Delta_i = 0$  and all other  $\Delta_i$  are positive. Models with  $\Delta_i$  of 0 to 2 are similar to the best performing model,  $\Delta_i$  of up to 7 are plausible and should be considered. Models with  $\Delta_i$  greater than 10 can be discarded (Burnham & Anderson, 2002).

Two further quantities that can be calculated from  $\Delta_i$  are the evidence ratio ( $ER_i$ ) which is used to indicate how much more likely the best model is than model  $i$  or to compare any two models in the set, and  $w_i$  (a value between 0 and 1) which gives the probability that model  $i$  is the best approximating model for the given data. The sum of the  $w_i$  values for all models in the group must equal 1.  $ER_i$  and  $w_i$  are calculated as (Burnham & Anderson, 2002):

$$ER_i = \frac{e\left(-\frac{\Delta_{best}}{2}\right)}{e\left(\frac{\Delta_i}{2}\right)} \quad (2.21)$$

$$w_i = \frac{e\left(-\frac{\Delta_i}{2}\right)}{\sum_{r=1}^R e\left(-\frac{\Delta_r}{2}\right)} \quad (2.22)$$

#### 2.9.4 CEB mean deviation ( $M_{CEB}$ )

The mean deviation measures the scatter of the data and is used to indicate over- and underestimation of predicted results in relation to average experimental data. A CEB mean deviation ( $M_{CEB}$ ) value closer to 1 implies a more accurate model. This measure was designed particularly for shrinkage prediction models, but ACI Committee 209 (2008) indicates that it is inadequate to decisively differentiate between prediction models (Al-Manaseer & Prado, 2015; ACI Committee 209, 2008; Gaylard, 2011). As shown in Equation 2.23, the CEB mean deviation ( $M_{CEB}$ ) model is calculated as:

$$M_{CEB} = \frac{\sum_{i=1}^N M_i}{N} \quad (2.23)$$

where  $N$  is the number of intervals and  $M_i$  is the sum of the ratio of predicted ( $\hat{y}_{ij}$ ) to experimental ( $y_{ij}$ ) values of shrinkage strain for the  $j^{\text{th}}$  point in the  $i^{\text{th}}$  interval, as seen in Equation 2.24.  $n$  is the number of data points per interval.

$$M_i = \frac{1}{n} \sum_{j=1}^n \frac{\hat{y}_{ij}}{y_{ij}} \quad (2.24)$$

#### 2.9.5 CEB coefficient of variation ( $V_{CEB}$ )

The CEB coefficient of variation ( $V_{CEB}$ ) is a measure of the relative variability between grouped data. Lower values of this coefficient indicate more accurate models. To determine  $V_{CEB}$  the shrinkage data are divided into specific intervals of drying time in days, for example 0 to 10, 11 to 100, 101 to 365, 366 to 730, 731 to 1095 and >1095 days. The CEB coefficient of variation was designed particularly to compare the performance of shrinkage prediction models. Gaylard (2011), however, points out that a disadvantage of the CEB coefficient of variation statistical measure is that the experimental shrinkage values are not equally weighted as are the set drying time intervals. This results in the overall  $V_{CEB}$  being over-estimated



for short drying time data, as large values are calculated for individual coefficients of variation ( $V_i$ ) for short drying times.

$V_{CEB}$  is a square root of the sum of the squares of the individual coefficients of variation ( $V_i$ ) divided by the number of intervals ( $N$ ), as shown in Equation 2.25.

$$V_{CEB} = \sqrt{\frac{1}{N} \sum_{i=1}^N V_i^2} \quad (2.25)$$

The  $V_i$  values are calculated as shown in Equation 2.26 and Equation 2.27, in which ( $\bar{y}_i$ ) is the mean shrinkage strain of data set  $i$ ,  $n$  is the number of data points within an interval, ( $\hat{y}_{ij}$ ) is the predicted shrinkage strain at time  $j$  in interval  $i$  and ( $y_{ij}$ ) is the observed shrinkage strain at time ' $j$ ' in interval ' $i$ '.

$$V_i = \frac{1}{\bar{y}_i} \sqrt{\frac{1}{n-1} \sum_{j=1}^n (\hat{y}_{ij} - y_{ij})^2} \quad (2.26)$$

$$\bar{y}_i = \frac{1}{n} \sum_{j=1}^n (y_{ij}) \quad (2.27)$$

### 2.9.6 Bažant and Baweja's coefficient of variation ( $\bar{\omega}_j$ )

Similar to the CEB coefficient of variation, the Bažant and Baweja (1995(b)) coefficient of variation is determined per interval, but for each decade of a logarithmic time scale. Firstly, the standard deviation ( $S_j$ ) per dataset is divided by the mean shrinkage strain ( $\bar{y}_j$ ) of the dataset. This requires the difference between the predicted and observed shrinkage strains for data point  $j$  in interval  $i$  ( $\Delta_{ij}$ ). For each time interval, different weights ( $w_{ij}$ ) are applied to the data points to mitigate the bias introduced due to the time intervals having differing numbers of data points (Labbé & Lopez, 2020; Gaylard, 2011). Equation 2.28 to Equation 2.31 give the formulae to determine  $\bar{\omega}_j$  per dataset and the overall coefficient of variation  $\bar{\omega}_{all}$  as defined by Bažant and Baweja (1995(b)).

$$\bar{\omega}_j = \frac{S_j}{\bar{y}_j} = \frac{1}{\bar{y}_j} \sqrt{\frac{1}{1-n} \sum_{i=1}^n (w_{ij} \Delta_{ij})^2} \quad (2.28)$$

$$\bar{y}_j = \frac{1}{n} \sum_{i=1}^n (w_{ij} y_{ij}) \quad (2.29)$$

$$w_{ij} = \frac{n}{n_d n_1} \quad (2.30)$$

$$\bar{\omega}_{all} = \sqrt{\frac{1}{N} \sum_{i=1}^N \bar{\omega}_j^2} \quad (2.31)$$

---

where  $n$  is the number of data points per dataset,  $N$  is the number of datasets in a database,  $n_d$  is the time intervals in decades and  $n_t$  is data points per time interval.

The overall coefficient of variation of Bažant and Baweja (1995(b)) is superior to the other statistical performance evaluation measures according to Gaylard (2011), as it provides a weighting for each dataset in addition to the weights per shrinkage data interval. Comparison of the values of global coefficient of variation (C.o.V) can be used to assess the time functions of “competing” shrinkage predicting models, with the smallest C.o.V suggesting the most suitable and correct function. The best calibrated model is the one with the lowest deviation from 1 (Hubler *et al*, 2015).

## 2.10 Conclusion

High performance concrete used today has complex cement matrices and includes advanced chemical and mineral admixtures. These admixtures play a role in the rate and magnitude of both drying and autogenous shrinkage in HSC. Accurate shrinkage predictions assist in the design of durable and safe concrete structures. However, it is clear from literature that with the exception of the RILEM B4 model, commonly used existing drying shrinkage prediction models still do not include admixture combinations as a model covariate. The RILEM B4 model is limited to the prescribed admixture combinations and the MC 2010 model does not cater for concretes with high content of mineral admixtures (RILEM TC-242-MDC, 2015; CEB-FIP, 2012). The WITS model was derived from an RSA drying shrinkage database, with the aim of more accurately predicting drying shrinkage for locally produced concretes. It was statistically compared with several other existing models, including the current SANS 10100-1 model, and outperformed each one based on the South African database (Gaylard, 2011).

Bažant, a pioneer in the development and assessment of concrete shrinkage prediction models, indicated that modification and calibration of the established shrinkage models is required, especially for modern HSC (Bažant and Baweja, 2000). The most recently published and most extensive concrete shrinkage database is the NU database. The NU database includes extensive information on the concrete composition and ratios, especially admixtures and aggregate details, test conditions and specimen geometry. However, many challenges are still encountered in attempting to combine experimental data from different countries to compile a dataset, as, for example, different drying shrinkage testing standards are followed in different countries.

Non-linear regression can be used to modify and evaluate the prediction models. The MS Excel add-in tool, Solver<sup>®</sup>, provides a user friendly and quick means of optimising model coefficients to determine the best-fit to a specific dataset. The accuracy of newly developed and modified models can be evaluated using graphical and statistical methods, which enables them to be easily compared and ranked. Graphical assessment can be used to assess model time functions to see which one best fits individual shrinkage curves. Statistical measures mentioned in this literature review that are used to gauge the goodness-of-fit of the non-linear shrinkage prediction functions are RMSE,  $R^2_{adj}$ , AIC, CEB mean deviation, CEB coefficient of variation and Bažant and Baweja’s coefficient of variation. Each of these indicators uses the difference between predicted and actual shrinkage values in some way.

---

## Chapter 3 Research methodology

The aim of this research was to evaluate the prediction accuracy of existing concrete shrinkage models (RILEM B4, MC 2010 and WITS model) for HSC with and without admixtures. According to the literature on the RILEM B4 and the MC 2010 models, they can be used to predict shrinkage of HSC (concrete with a compressive strength greater than 60 MPa in this study). However, chemical and mineral admixtures found in HSC are only partially accounted for in these prediction models and this affects the accuracy of predictions. For example, the MC 2010 does not cater for concretes with high pozzolanic material such as metakaolin (CEB-FIP, 2012). The RILEM B4 model does not have admixture combination multiplicative factors for shrinkage reducing admixtures (SRA) and metakaolin (RILEM TC-242-MDC, 2015). The WITS model does not indicate the range of compressive strengths for which it was developed and calibrated, nor were any data for concretes with SRA included in its calibration. This study attempted to determine the applicability of the RILEM B4, MC 2010 and WITS models in predicting shrinkage of HSC with and without admixtures, using applicable subsets of the 2018 version NU database (Northwestern University, 2018), data from the report of Al-Manaseer and Fayyaz (2011) and the Concrete Institute of South African shrinkage database. A composite shrinkage prediction model was also derived specifically for non-hyperbolic shrinkage profiles.

Details are given on the compilation of the HSC specific datasets extracted from the published databases, software programmes and models used to (a) model shrinkage (b) calibrate existing model parameters (non-linear regression analysis) (c) conduct an applicability analyses and (d) statistically rank the models.

### 3.1 Research approach

A correlation-based approach was used for the time functions of shrinkage and their relationships to model covariates, focusing on aggregate type, cement extenders and chemical admixture content for HSC. Statistical validation and comparison was used to assess the relative performances of the selected shrinkage models.

An extensive database of secondary experimental HSC data was compiled and used to evaluate and modify the selected shrinkage models and to develop a new composite HSC-focused shrinkage model. Model parameters were modified/updated using MS Excel Solver<sup>®</sup> to conduct non-linear regression analyses (Walsh & Diamond, 1994; Frontline Systems, 2000-2020). The model parameters were analysed based on SANS 50917-1 (2013) cement type, w/cm ratio, coarse aggregate type and admixture content.

The quality of predictions using the existing models (original and modified) and the proposed composite model predictions of the strain-time experimental data were evaluated graphically and statistically. The statistical indicators used to evaluate and rank the models were the  $R^2_{adj}$ , RMSE and AIC and C.o.V<sub>all</sub>.

### 3.2 Data preparation

#### 3.2.1 Shrinkage database preparation

The HSC focused database used in this study was compiled from selected experiments from the 2018 version NU database (Northwestern University, 2018), a technical report published by Al-Manaseer and

Fayyaz (2011) and the South African database compiled by the University of Witwatersrand and the University of Cape Town (Mucambe, 2010).

Collating the experimental shrinkage data from different sources and countries posed several challenges due to the different cement classifications and presentation of covariate data methods of the three databases. Misrepresented or missing covariate data required for the prediction models under evaluation were either calculated, reasonably assumed or statistically estimated (imputed). In Table 3.1, the following differences were seen:

Table 3.1 Different presentation of covariate data between NU Database, RSA Database and Technical report (Al-Manaseer & Fayyaz, 2011).

NU database	RSA database	Technical report (Al-Manaseer & Fayyaz, 2011)
w/c	w/cm	w/cm
a/c	a/cm	a/cm
-	coarse aggregate type and content	coarse aggregate type and content
-	fine aggregate type & content	-
chemical admixture content as %/c	chemical admixture content as %/cm	chemical admixture content as %/cm
ASTM and EN cement type classification	SANS cement type classification	ASTM cement type classification

The three shrinkage data sources together include information and results for a total of 2192 experiments. These experiments included drying, autogenous and total (drying + autogenous) shrinkage, as shown in Table 3.2. Some experiments had no information on the type of shrinkage that was tested for or was assumed by the original database authors. Figure 3.1 illustrates the percentage of drying and autogenous shrinkage experiments each data source contributed.

Table 3.2 Total number of shrinkage experiments per data source.

Data source	Drying shrinkage experiments	Autogenous shrinkage experiments	Total shrinkage experiments	Unknown
NU database	177 (of which 69 are uncertain)	418 (of which 28 are uncertain)	1046	228
RSA database	291	0	0	0
Technical report (Al-Manaseer & Fayyaz, 2011)	32	0	0	0

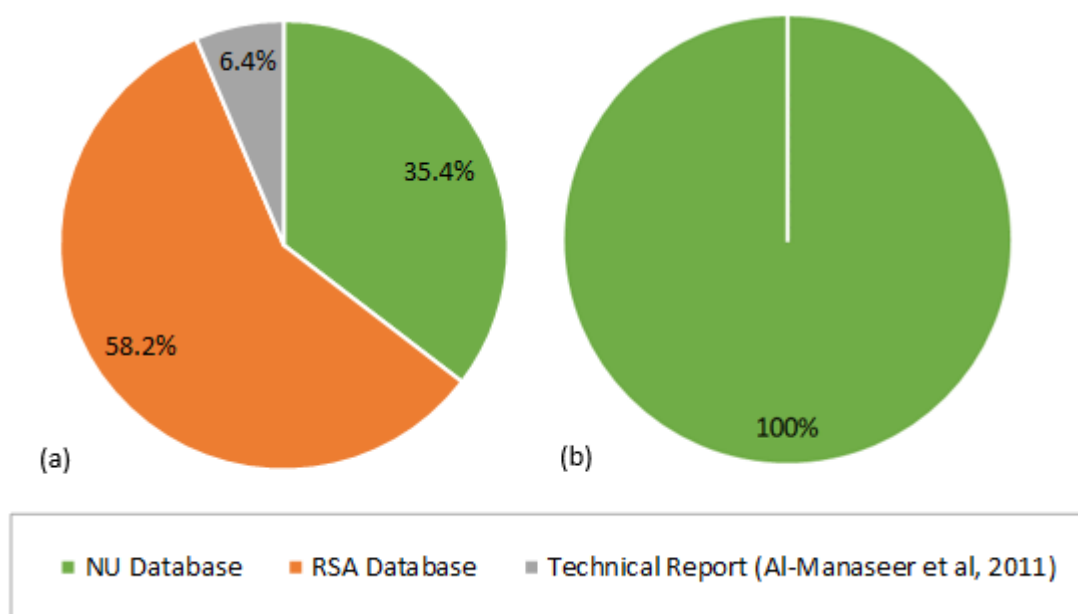


Figure 3.1 Percentage of (a) drying and (b) autogenous shrinkage experiments per data source.

### 3.2.2 Experiment selection and grouping

In choosing the subset of shrinkage experiments to use in this work for HSC, only known drying and autogenous shrinkage experiments were considered. Of these, only the experiments that met specific criteria listed were selected to be part of the data subset used in this study. These criteria were:

- rapid hardening cement type
- rapid development of early age strength
- w/cm ratio  $\leq 0.42$  (excluding normal hardening and slow hardening cement types)
- compressive strength  $\geq 60$  MPa

After applying these selection criteria, a total of 562 (220 drying shrinkage and 342 autogenous shrinkage) of the original 2192 experiments were left. This reduced database, for use in this study, was regrouped into Dataset 1 (drying shrinkage data) and Dataset 2 (autogenous shrinkage data), as shown in Table 3.3. Table 3.4 and Table 3.5 list the data extracted from the original database.

Table 3.3 Number of shrinkage experiments for Dataset 1 and Dataset 2.

Data source	Dataset 1 Drying $\epsilon$ experiments	Dataset 2 Autogenous $\epsilon$ experiments
NU-ITI database	91	342
RSA database	97	0
Technical report (Al-Manaseer & Fayyaz, 2011)	32	0
TOTAL SUM	220	342

Table 3.4 Data extracted from the original data sources.

Data	Data range or no. of categories		
	NU Database	Technical report	South African database
Last name of the experiment/ article author & reference of the source of data	66	1	10
Geographical region of the recorded experiment	21	1	1
Year of experiment or publication	1958 - 2011	2011	1990 - 2004
Type of shrinkage	autogenous & drying	drying	drying
Water-to-cement (w/c) or water-to-cementitious material (w/cm)	0.17 – 0.86 w/c	0.33 – 0.34 w/cm	0.3 – 0.68 w/cm
a/c or a/cm	1.11 – 7.96 a/c	4.76 – 5.28 a/cm	2.14 – 6.85 a/cm
Water content	107 – 393 kg/m <sup>3</sup> *	123 – 142 kg/m <sup>3</sup>	153 – 225 kg/m <sup>3</sup>
Cement content	250 – 915 kg/m <sup>3</sup>	243 – 293 kg/m <sup>3</sup>	135 – 700 kg/m <sup>3</sup>
Stone content	-	1039 kg/m <sup>3</sup>	900 – 1400 kg/m <sup>3</sup>
Sand content	-	838 – 928 kg/m <sup>3</sup>	323 – 1024 kg/m <sup>3</sup>
Cement classification	R = rapid hardening RS = rapid hardening and early strength	-	N = ordinary early strength R = high early strength
Specified cement type	OPC, Type I - III, CEM I - III, white Portland cement	Type II	12 types
Fine aggregate type	-	1 type	17 types
Coarse aggregate type	7 types	1 type	9 types
Silica fume (SF) content	1.14 – 25 %/cm **	5 %/cm	5 – 10 %/cm
Fly ash content	9 – 30 %/cm **	20 – 30 %/cm	13 – 30 %/cm
GGBS, GGCS and GGFS (slag) content	-	-	13 – 51 %/cm
Filler content	14 – 41 %/cm **	-	-
limestone powder content	23 – 25 %/cm **	-	13 %/cm
Metakaoline content	5 – 20 %/cm **	5 %/cm	-
Volcanic Ash content	0.09 – 0.39 %/cm **	-	-
Expansive additive content	0.224 – 7 %/cm **	-	-
Superplasticiser (SP)/ high-range water-reducer (HRWR) content	0.05 – 9.5 %/cm **	0.4 – 0.6 %/cm	0.1 – 0.8 %/cm
Plasticiser/ WR/ low-range water-reducer (LRWR)	0.005 – 1.6 %/cm **	0.2 %/cm	0.4 %/cm

\* data was calculated

\*\* converted from %/c → %/cm

Table 3.5 Data extracted from the original data sources (continuation).

Data	Data range or no. of categories		
	NU Database	Technical report	South African database
SRA content	0.5 – 8.6 %/cm **	0.5 – 2.5 %/cm	-
Retarder content (RE)	0.003 – 1 %/cm **	-	-
Air entraining agent content	0.005 – 1 %/cm **	-	-
Compressive strength of concrete at 28 <sup>th</sup> day after placement	15.5 – 197 MPa	52.4 – 73.3 MPa	34 – 78.5 MPa
Specimen geometry	38 types	2 types	5 types
Volume-to-surface area ratio (V/S)	4.7 – 89	20 – 30*	16.6 – 25.5
Age at drying	0 – 365 days	7 days	7 – 49 days
Temperature	15 – 130 °C	23 °C	21 – 25 °C
Curing Temperature	20 – 30 °C	-	-
Relative humidity (RH)	40 – 100 %	50 %	43 – 72 %
Curing method	4 types	1 types	-

\* data was calculated

\*\* converted from %/c → %/cm

All the selected experiments were then classified according to South African cement type, strength class and strength development specifications, SANS 50197-1 (2013), to facilitate their grouping. This method of cement classification required the composition of the cementitious material (cm) per experiment, which was available, unlike the American standard that requires the chemical composition of the cement, which was not available. The strength class and strength development specification required the early (2<sup>nd</sup>/7<sup>th</sup> day) compressive strength, standard 28<sup>th</sup> day compressive strength, initial setting time and volume change stability (soundness) or expansion of the cement (in mm). However, due to the lack of some early compressive strength data, a percentage of the 28<sup>th</sup> day compressive strength was used to determine the missing data. The percentages used were derived from published literature and experiments to predict compressive strength development in HSC and low w/cm concrete (Abdel-Jawad, 2006; Choi, Tareen, Kim, Park & Park, 2018). To determine a more realistic early compressive strength, it was assumed that the curing temperature (not given) was the same or within  $\pm 2^\circ\text{C}$  of the controlled temperature after curing. This assumption was based on the fact that there were no notes of any out of the ordinary curing temperatures for these experiments, and on other experiments for which the information was given. Table 3.6 gives the percentages of 28<sup>th</sup> day strength used for early age strength in this study.

Table 3.6 Averaged percentage of 28<sup>th</sup> day compressive strength to estimate the 2 and 7 day compressive strengths.

Curing temperature		18 °C	20 °C	23 °C	31 °C
Concrete with no admixtures	$f_{cm2}$	40 %	46 %	55 %	45 %
	$f_{cm7}$	76 %	70 %	63 %	80 %
Concrete with admixtures	$f_{cm2}$	-	50 %	62 %	70 %
	$f_{cm7}$	-	74 %	83 %	80 %

### 3.2.3 Missing covariate data analysis

As a consequence of experimental shrinkage data being acquired by different researchers in different laboratories, but not to any universally agreed test standard, not all the data required by each prediction model was captured or available. For example, some test programs may have been biased towards specific covariates and so did not recorded data for other covariates, considered now to be important (Wedner *et al*, 2015(b)). Generally, these incomplete experimental records are discarded. However, evaluating more experimental data renders the prediction models statistically more significant (Seijo-Pardo Alonso-Betanzos, Bennett, Bolón-Canedo, Josse, Saeed, & Guyon, 2019). Table 3.7 gives the percentage of missing covariate data in Dataset 1 and Dataset 2 used in this work.

Table 3.7 Percentage of missing covariate data per Dataset 1 and Dataset 2.

Covariate	Dataset 1 Drying $\epsilon$ experiments	Dataset 2 Autogenous $\epsilon$ experiments
Water content	2 %	18 %
Cement content	2 %	18 %
Coarse aggregate content	41 %	Not required
Coarse aggregate type	37 %	64 %
Fine aggregate type	43 %	Not required
$f_{cm28}$	11 %	41 %
Specimen geometry	4 %	5 %
V/S	6 %	7 %
$t_{dry}/t_0$	0 %	2 %
Temperature	0 %	24 %
RH	1 %	19 %
Curing method	8 %	95 %

An assumption was made that all experiments for which no curing method was stated were water cured, as this is the normal method in drying shrinkage testing. No notes to the contrary were recorded in the original sources of the data.

For the rest of the missing data, values were estimated (imputed). This was done through multiple regression and multivariate logistic regression analysis on the continuous and the discrete variables, respectively (variables pertaining to the covariate data of Dataset 1 and Dataset 2) using the NCSS 2019 statistical analysis software package, with the assistance of an independent statistician consultant (Van Schalkwyk, 2019-2020). Firstly, a preliminary descriptive analysis was done per covariate group, namely the water content, cement content,  $f_{cm28}$ ,  $E_{28}$ , V/S, coarse aggregate type and content, fine aggregate type, start of drying time, RH and temperature, to determine any outliers and misrepresented values. The normality of the data distribution and extent of missing data per covariate group was also determined.



---

The descriptive analyses considered the statistical indicators of mean, median, standard deviation, standard error, range and minimum and maximum value. Due to the large variation between the minimum and maximum values of the covariate groups, the geometric and harmonic mean was calculated at a 95% confidence level.

The different normality tests conducted were Shapiro-Wilk, Anderson-Darling, Martinez-Iglewicz, Kolmogorov-Smirnov, D'Agostino Skewness, D'Agostino Kurtosis and D'Agostino Omnibus. In instances where the normality tests were rejected, the data were transformed to achieve a normal distribution to avoid the very large values having an inordinate effect on the estimates of the missing values.

After the descriptive analyses were completed, a correlation matrix showing how many observations any two variables have in common was compiled. This was used to decide which multiple regression models to fit to the data. A stepwise regression analysis was also done to determine the best predictors for a variable. Multiple imputations were done by calculating the multiple regression equations for a variable with missing values with those variables that had complete data, and these functions were then used to estimate the missing data. A similar process was followed with the discrete data using multivariate logistic regression. It was not possible to obtain estimates for experiments missing both independent and dependent variables of interest.

The regression analysis considered at least two independent variables to derive estimates for the variable of interest. The estimated values for the missing covariate data were accepted based on the values of  $R^2_{adj}$ , coefficient of variation and RMSE, whether the regression had a normal distribution and whether the independent variables considered had any physical correlation to the dependent variable of interest. The estimated values were also checked to ensure they made physical sense - for example estimated values of more than 100% for RH were not accepted. Appendix BB (CPUT Library Repository, 2020(b)) gives the estimated values and details from the NCSS reports on the missing data analyses.

### **3.2.4 Derived datasets and subsets**

From the initially compiled database seven (7) smaller datasets, shown in Figure 3.2, were extracted to achieve the objectives of this study. As mentioned before Datasets 1 and 2, which include all the experiments for drying shrinkage and autogenous shrinkage, respectively, underwent a missing data analysis to determine weighted or estimated values for the missing covariate data. This resulted in Dataset 1-HSC and Dataset 2-HSC which are reduced versions of Dataset 1 and Dataset 2, respectively. These datasets exclude any experiments for which it was not possible to attain weighted values for the missing covariate data, and include only experiments with  $w/cm \leq 0.42$  and a 28<sup>th</sup> day compressive strength  $\geq 60$  MPa. The purpose of Datasets 1-HSC and 2-HSC was to assess the drying and autogenous shrinkage profiles of the selected experiments and to prepare for further grouping of data to modify the existing models and develop the new composite model.

Three additional datasets, Dataset 3, Dataset 4 and Dataset 5 were extracted from the initial combined database to evaluate the RILEM B4, MC 2010 and WITS models, respectively. In compiling each of these datasets the full dataset was filtered to extract only experiments that fell within applicable ranges of each model's covariate data, which are listed in Table 2.10. Table 3.8 gives the number of drying and autogenous shrinkage experiments per dataset.

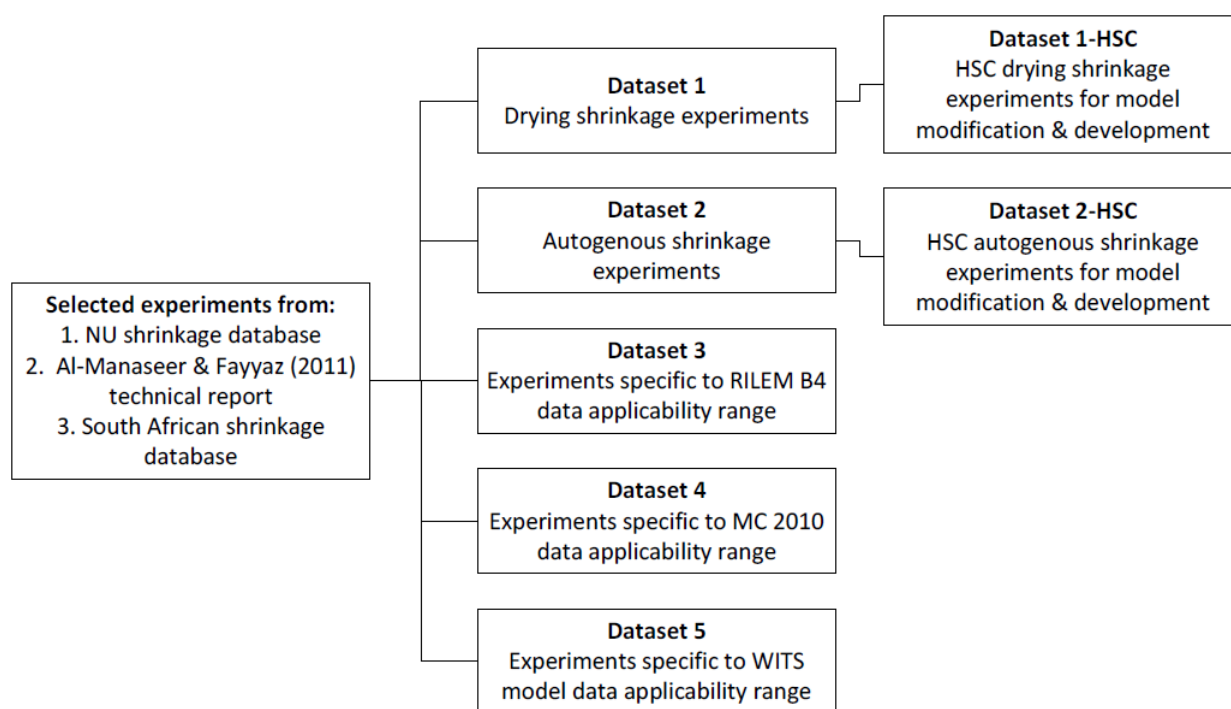


Figure 3.2 Schematic diagram of datasets extracted from the complete compiled database used in this study.

Shrinkage experiments that were not used in the modification of existing models and development of the new model were:

- Short term experiments that had not reached final (ultimate) shrinkage
- Experiments with 4 or fewer data points.
- Experiments that did not extend to the minimum drying time (60 days according the ASTM C157, 2008).
- Experiments with ambiguous or unknown covariate data (e.g. coarse aggregate used was recorded as 'stone' or 'gravel', not as a specific type of rock material)
- Experiments with insufficient information to determine the cement class according to SANS 50197-1 (2013).
- Experiments that exhibited swelling in the recorded data.
- Experiments that did not show an increase in shrinkage from the start of the specimen drying as their data would diverge from the existing prediction models.

The RSA database was the only data source that contributed to Dataset 5 as it had the fine aggregate recorded which is required for the WITS model.

Subsets were formed within Datasets 1-HSC and 2-HSC. Subset 1 includes only experiments for concretes that did not contain any mineral or chemical admixtures. Subset 2 includes only experiments for concretes that did contain mineral and chemical admixtures. For modification of the existing models based on shrinkage and high strength dependant covariates, the subsets were filtered further according to the SANS 50197-1 (2013) aggregate type, cement classification and w/cm ratio, and lastly the inclusion or not of chemical admixtures, as shown in Figure 3.3.

Table 3.8 Number of shrinkage experiments for Datasets 1-HSC and 2-HSC, Datasets 3, 4 and 5.

Data source	Dataset 1-HSC	Dataset 2-HSC	Dataset 3	Dataset 4	Dataset 5
NU database	11 drying $\epsilon$	73 autogenous $\epsilon$	23 drying $\epsilon$ 31 autogenous $\epsilon$	67 drying $\epsilon$ 152 autogenous $\epsilon$	-
RSA database	34 drying $\epsilon$	-	38 drying $\epsilon$	13 drying $\epsilon$	66 drying $\epsilon$
Technical report (Al-Manaseer & Fayyaz, 2011)	26 drying $\epsilon$	-	8 drying $\epsilon$	5 drying $\epsilon$	-
TOTAL SUM	71 drying $\epsilon$	73 autogenous $\epsilon$	69 drying $\epsilon$ 31 autogenous $\epsilon$	85 drying $\epsilon$ 152 autogenous $\epsilon$	66 drying $\epsilon$

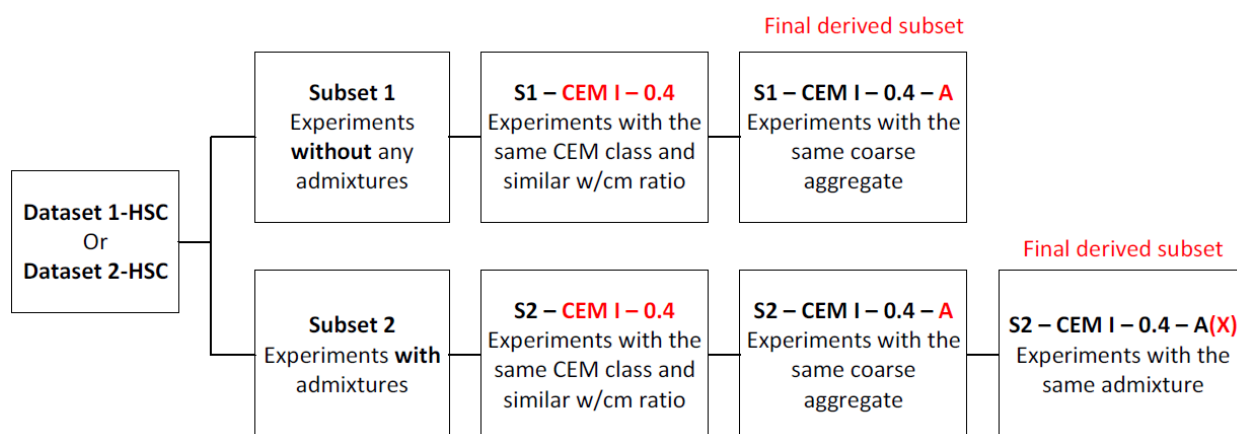


Figure 3.3 Schematic of data subsets derived from Dataset 1-HSC and Dataset 2-HSC.

As no experiments are precisely the same, within each of these final subsets experiments with similar covariate values were grouped. According to Mucambe (2010), who also analysed existing drying shrinkage models, differences between the following covariates are considered negligible if they fall within the indicated ranges:

- $RH \pm 3\%$  from average
- Temperature  $\pm 2\text{ }^\circ\text{C}$  from average
- $V/S \pm 2\text{ mm}$  from average
- $w/cm \pm 0.02$  from average

10 % of the experiments from each of Dataset 1-HSC and Dataset 2-HSC were used to evaluate the modified and proposed models in this study.

Four (4) data subsets without admixtures, three (3) data subsets with mineral admixtures only and eleven (11) data subsets with chemical admixtures for comparable experiments were derived from Dataset 1-

HSC, while from Dataset 2-HSC 12 subsets for concretes with chemical admixtures were extracted. Table 3.9 and

list these subsets for Datasets 1-HSC and 2-HSC, respectively. [Appendix AA](#) (CPUT Library Repository, 2020(a)) gives the covariate data for all the derived subsets.

Table 3.9 Data subsets derived from Dataset 1-HSC.

Sub-set no.	Description	No. of experiments
Without mineral or chemical admixtures		
S1-01	CEM I – 0.41 ( $\pm 0.02$ ) w/cm – Granite	2
S1-02	CEM I – 0.41 ( $\pm 0.02$ ) w/cm – Quartzite	2
S1-03	CEM I – 0.41 ( $\pm 0.02$ ) w/cm – Sandstone	2
S1-04	CEM I – 0.41 ( $\pm 0.02$ ) w/cm – Andesite	6
S1-05	CEM I – 0.41 ( $\pm 0.02$ ) w/cm – Dolerite	4
With mineral & without chemical admixtures		
S2-01	CEM II (A-S) – 0.40 ( $\pm 0.02$ ) w/cm – Andesite	3
S2-02	CEM II (B-S) – 0.4 ( $\pm 0.02$ ) w/cm – Andesite	3
S2-03	CEM III A – 0.4 ( $\pm 0.02$ ) w/cm – Andesite	2
With mineral & chemical admixtures		
S2-04	CEM I – 0.28 ( $\pm 0.02$ ) w/cm – Quartzite ( $>1$ % SP)	2
S2-05	CEM I – 0.40 ( $\pm 0.02$ ) w/cm – Sandstone ( $<1$ % SP)	3
S2-06	CEM II (A-D) – 0.36 ( $\pm 0.02$ ) w/cm – Sandstone ( $>1$ % SP)	3
S2-07	CEM II (A-Q) – 0.29 ( $\pm 0.02$ ) w/cm – Quartzite ( $>1$ % SP)	2
S2-08	CEM II (B-M) – 0.33 ( $\pm 0.02$ ) w/cm – Granite ( $<1$ % SP; 5 % Metakaolin)	2
S2-09	CEM II (B-M) – 0.33 ( $\pm 0.02$ ) w/cm – Granite ( $<1$ % SP; $<0.5$ % Plasticiser; 5 % Metakaolin)	2
S2-10	CEM II (B-M) – 0.33 ( $\pm 0.02$ ) w/cm – Granite ( $>1$ % SP)	2
S2-11	CEM II (B-M) – 0.33 ( $\pm 0.02$ ) w/cm – Granite ( $<1$ % SP; 0.5 – 2.5 % Eclipse SRA)	5
S2-12	CEM II (B-M) – 0.33 ( $\pm 0.02$ ) w/cm – Granite ( $<1$ % SP; $<0.5$ % Plasticiser)	2
S2-13	CEM II (B-M)-0.33 ( $\pm 0.02$ ) w/cm – Granite ( $<1$ % SP; $<0.5$ % Plasticiser; 1 – 2.5 % Eclipse SRA)	4
S2-14	CEM II (B-M)-0.33 ( $\pm 0.02$ ) w/cm – Granite ( $<1$ % SP; $<0.5$ % Plasticiser; 1 – 2.5 % Tetraguard SRA)	4

Table 3.10 Data subsets derived from Dataset 2-HSC.

Sub-set	Description	No. of experiments
With chemical admixtures		
S2-01a	CEM I - 0.27 ( $\pm 0.02$ ) w/cm – Granite (1 % SP)	2
S2-02a	CEM I - 0.27 ( $\pm 0.02$ ) w/cm – Quartzite (3 % SP)	2
S2-03a	CEM I - 0.31 ( $\pm 0.02$ ) w/cm – Granite (1 % SP)	4
S2-04a	CEM I - 0.31 ( $\pm 0.02$ ) w/cm – Granite (<0.5 % Plasticiser)	3
S2-05a	CEM I - 0.35 ( $\pm 0.02$ ) w/cm – Granite (3 % SP; 1% RE)	2
S2-06a	CEM II (A-D) - 0.23 ( $\pm 0.02$ ) w/cm – Quartzite (2 % SP)	2
S2-07a	CEM II (A-D) - 0.28 ( $\pm 0.02$ ) w/cm – Granite (2 % SP)	3
S2-08a	CEM II (A-D) - 0.28 ( $\pm 0.02$ ) w/cm – Quartzite (1 % SP)	4
S2-09a	CEM II (A-D) - 0.34 ( $\pm 0.02$ ) w/cm – Granite (2 % SP)	4
S2-10a	CEM II (A-D) - 0.34 ( $\pm 0.02$ ) w/cm – Quartzite (1 % SP)	3
S2-11a	CEM II (A-D) - 0.34 ( $\pm 0.02$ ) w/cm – Quartzite (1 % SP; <0.5% AEA)	2
S2-12a	CEM II (A-D) – 0.29 ( $\pm 0.02$ ) w/cm – Quartzite (3 % SP)	2

### 3.2.5 Experimental shrinkage profile analysis

An analysis of the shrinkage profiles for the experiments of Datasets 1-HSC and 2-HSC was conducted to get an indication of the type of function required to fit the data for a new shrinkage model in terms of the following criteria:

- The concrete age (day) at which shrinkage strain “plateaued”, signifying the final shrinkage.
- The magnitude of the final shrinkage in microstrains.
- The duration of the experiment.
- Number of shrinkage data points for the ranges 0 to 99 days, 100 to 499 days and  $\geq 500$  days.

These shrinkage duration ranges were chosen based on when the shrinkage profiles under evaluation reached a final shrinkage value. It was generally seen that occurred anywhere between day 100 and day 499 (day 499 was the latest start of final shrinkage in the experiments under consideration). In this study then, short- and medium-term shrinkage was taken to occur over the time period 0 to 499 days and long-term shrinkage was considered to be the observed shrinkage from day 500 onwards.

---

### 3.3 Existing model evaluation and modification

#### 3.3.1 Fitting of selected models to experimental data

The selected shrinkage models were fit to the experimental data using Solver<sup>®</sup>, an Excel add-in tool for non-linear regression analysis. Prior to the more detailed regression analyses, each of the selected models were verified using examples from literature (ACI Committee 209, 2008; RILEM TC-242-MDC, 2015). The models were also tested by varying a single parameter and checking the change in magnitude of the predicted shrinkage.

#### 3.3.2 Update of existing model parameters

A simple localised sensitivity analysis was done for each of the selected models in which one model parameter was varied (up and down) at a time. This was used to assess their significance on the calculated shrinkage to enable a decision as to which factors to update/recalibrate for the selected HSC data. Parameters that were highly sensitive to small changes were not modified. Only the cement type, aggregate and admixture model parameters were considered for modification. The RILEM B4 and WITS models had all 3 concrete composition parameters, and the MC 2010 model had only the cement parameter to modify. Therefore, a three-step modification process was conducted on the RILEM B4 and WITS models, whereas the MC 2010 was a two-step process. For the RILEM B4 and WITS models, first the cement parameters were updated for subsets sharing the same cement class and average w/cm. Then the aggregate parameters were updated for subsets sharing the same cement class and aggregate type. Lastly, the admixture parameter was updated for each subset. For the MC 2010 model, a single parameter was updated, taking into account the type of aggregate and admixture per subset.

The covariate parameters of the models considered in this study were updated using Excel Solver<sup>®</sup>, by minimising the Residual Sum of Squares (RSS) value per data subset. For the subsets with varying chemical admixtures, the relevant covariate parameters were modified individually per experiment by minimising the RSS (hence RMSE) value for each experiment. The resulting updated parameters were then plotted as a function of chemical admixture. Smooth, best-fit mathematical functions were then fitted through these points and these replaced the corresponding parameters in each model. This was done to link the effect of varying chemical admixture to the models' parameters.

#### 3.3.3 Composite model development

After plotting and scrutinising the individual drying shrinkage profiles it was noticed that some concrete mixes exhibited an early, fairly sharp peak in shrinkage between about days 85 and 117, before the shrinkage plateaued at a lower value. The mathematical forms of the existing models considered here, the RILEM B4, MC 2010 and WITS models, are not able to predict this sharp early peak and rapid decrease to the "final" shrinkage value. For this reason, a more flexible model function to accommodate the peak was proposed. Subsets S2-08, S2-09, S2-10 and S2-12 had this peak in their shrinkage behaviour, and they have long-term shrinkage data ( $\geq 500$  days). A composite model (combining two or more individual functions) was constructed as a logistic dose curve. The form of this function is given in Equation 3.1. Several different possible functions for  $F_1$  and  $F_2$  were fitted to the averaged shrinkage data of the subsets listed previously to see which would fit the data best (Gadagkar & Call, 2015; Hill, 1910).

$$\varepsilon_{ds}(t) = F_1 + \frac{F_2 - F_1}{\left[1 + \left(\frac{t}{t_x}\right)^m\right]^q} \quad (3.1)$$

where  $F_1$  and  $F_2$  are the functions to be combined,  $t_x$  is the “inflection point” (or critical value)  $F_1$  and  $F_2$  intersect,  $m$  determines the smoothness of the intersection and the product of  $m$  and  $q$  determines the slope of the transition part of the curve.

An equation of the form of Equation 3.1 was chosen to attempt to model the concrete shrinkage data which showed the peak, as it can be used to combine just two curves, or nested/repeated to combine multiple curves. With reference to Figure 3.4 the experimental data could be split into 4 groups, each represented by a different function denoted by  $f_a$ ,  $f_b$ ,  $f_c$  and  $f_d$ . Different combinations of these four functions can then be used, in the form of Equation 3.1, to produce a final composite function.

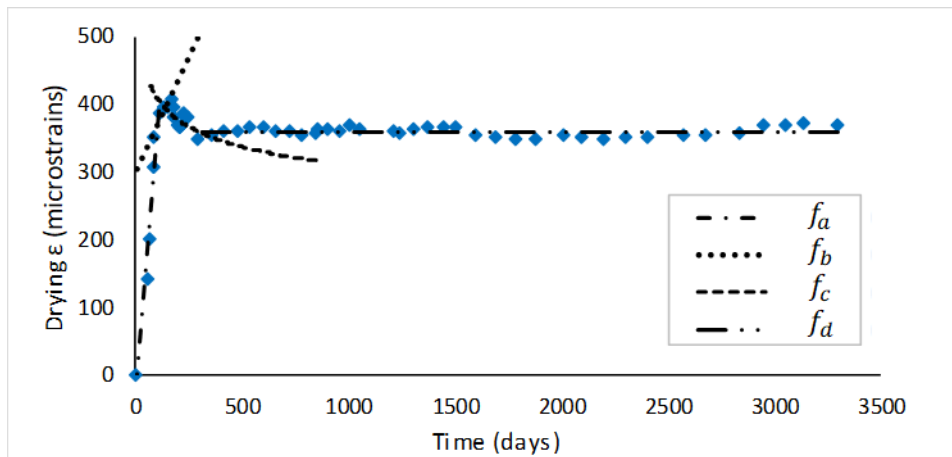


Figure 3.4 Fitted functions for different data segments.

For example,  $f_a$  and  $f_b$  could be combined to give  $F_1$  and  $f_c$  and  $f_d$  could be combined to give  $F_2$ . Then  $F_1$  and  $F_2$  could be combined to give the final composite function. Equally,  $f_a$  and  $f_b$  could be combined to give  $F_1$  which could then be combined with  $f_c$ , to give  $F_3$ . Finally,  $F_3$  and  $f_d$  could be used to get the final function. Other approaches can also be used, for example as done here and described next, to combine the  $f_b$  and  $f_c$  parts of the curve.

For the shrinkage data considered here that showed a peak, three approaches were tried. In reference to Figure 3.4, the  $f_b$  and  $f_c$  parts of the curve were fitted to a logistic-exponential curve, Equation 3.2, given by Kochel (2003) and a general bi-linear curve, Equation 3.3, given by Buchwald (2007). However, these functions could not produce good fits for this part of the shrinkage profiles and were abandoned.

$$f_{b+c} = \frac{Ae^{-kt}}{1 + e^{(a+bt)}} \quad (3.2)$$

$$f_{b+c} = a_1(t - t^*) + z \ln\left(1 - e^{(a_2 - a_1)(t - t^*)/z}\right) + y \quad (3.3)$$

The approach then adopted was to fit power law functions to the data for  $f_a$  and  $f_b$ , fit an exponential function to the data for  $f_c$  and a straight line to the data for  $f_d$ . First  $f_a$  and  $f_b$  were used to give  $f_{a+b}$ , which was then combined with  $f_c$  to give  $F_1$  as shown in Equation 3.4. To get the final composite function for  $\varepsilon_{ds}(t)$  representing all the data,  $F_1$  was combined with  $f_d$  (Figure 3.5) to give Equation 3.5. Figure 3.6 shows a plot of Equation 3.5 and the average shrinkage data for the subset of experiments with this characteristic.

$$F_1 = f_{a+b} + \frac{f_c - f_{a+b}}{\left[1 + \left(\frac{t}{t_{x1}}\right)^{m1}\right]^{q1}} \tag{3.4}$$

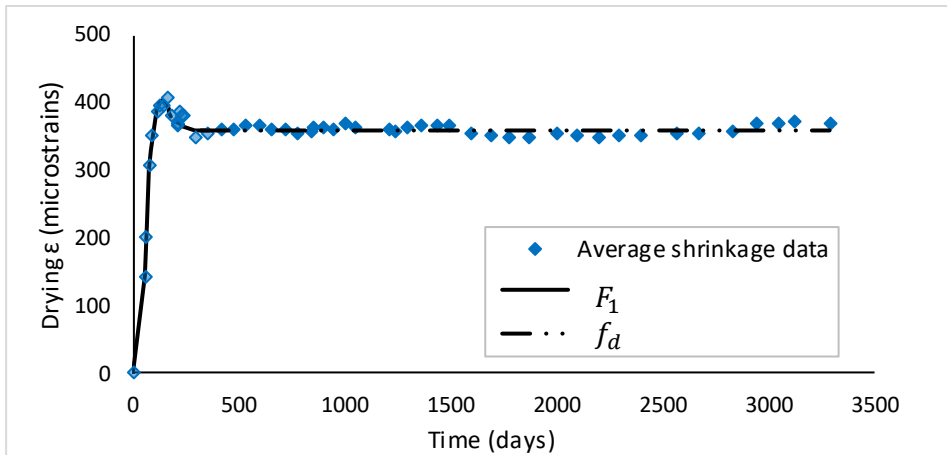


Figure 3.5 Composite power law-exponential function  $F_1$  and linear function  $f_d$ .

$$\varepsilon_{ds}(t) = F_1 + \frac{f_d - F_1}{\left[1 + \left(\frac{t}{t_{x2}}\right)^{m2}\right]^{q2}} \tag{3.5}$$

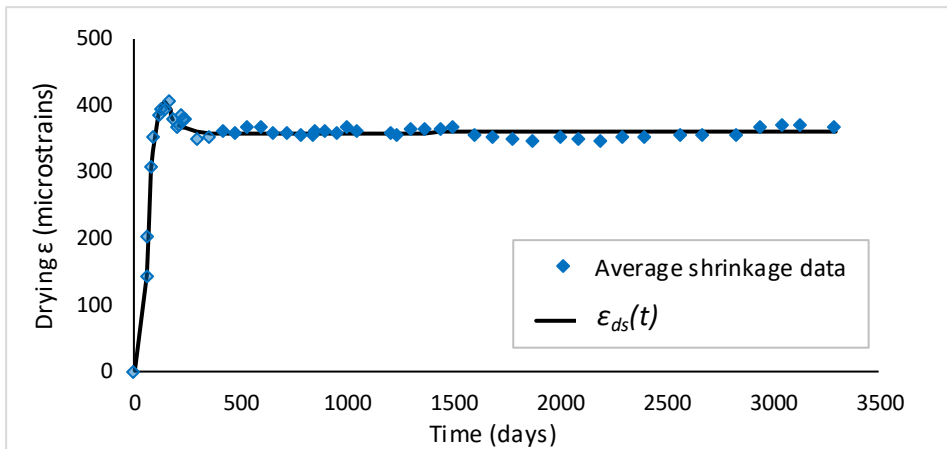


Figure 3.6 Final composite logistic dose function  $[\varepsilon_{ds}(t)]$ .



### 3.4 Analysis and presentation of results

Statistical measures were used to evaluate the proposed and existing (original and modified) prediction models, based on Dataset 1-HSC and Dataset 2-HSC. For each experiment RMSE,  $R^2_{adj}$  and the C.o.V of the errors were determined for different shrinkage time ranges considered (0 to 99, 100 to 199, 200 to 499 and 500 days or more). In this study the C.o.V for each shrinkage time range (interval) was calculated using the equation given by Gardner (2004), given in Equation 3.6, in which the mean RMSE per time interval 'i' is divided by the mean actual shrinkage  $\bar{y}_i$  (in microstrain) for the same interval 'i'. The overall C.o.V<sub>all</sub>, was calculated using the equation given by Bažant and Baweja (1995(b)), Equation 3.7. In this equation N is the number of datasets. According to Hubler *et al* (2015) the lowest C.o.V determines the model function most suited for the overall data under evaluation.

$$C.o.V_i = \frac{meanRMSE_i}{\bar{y}_i} \quad (3.6)$$

$$C.o.V_{all} = \left[ \frac{1}{N} \sum_{j=1}^{N_i} (C.o.V_i)^2 \right]^{0.5} \quad (3.7)$$

AICs were calculated to compare prediction performances and rank the different models for any given dataset. Statistical indicator values were averaged for data subsets without admixtures, with mineral admixtures and with chemical admixtures.

Errors (as a percentage) were calculated for each experiment using in Equation 3.8. Errors within  $\pm 20\%$  are deemed acceptable and within  $\pm 15\%$  excellent according to Gardner and Lockman (2001). According to Al-Manaseer and Prado (2015) the best model functions will have a random distribution of shrinkage prediction errors about a mean of zero. To summarise the model error performance over all experiments of data subsets without admixtures, with mineral admixtures and with mineral and chemical admixtures, tables indicating the overall maximum error percentage for each shrinkage term were derived. Plots of actual shrinkage versus predicted shrinkage values were used to broadly compare the performances of the original and modified models, by including plus and minus 20 % error lines.

$$Error(\%) = \frac{actual - predicted}{actual} \times 100 \quad (3.8)$$

The modified models were validated on 10 % of the total experimental data from Dataset 1-HSC and Dataset 2-HSC. For each experiment, the modified models were ranked according to their RMSE,  $R^2_{adj}$  and AIC<sub>c</sub> values. Error distribution plots, with a theoretical normal distribution overlay, were plotted for each validating experiment along with the standard deviation and skewness.

The results obtained from the relevant existing models for Datasets 3, 4 and 5 were evaluated individually and not compared with each other, as the datasets differ. For every experiment RMSE and C.o.V were determined. The C.o.V was calculated for the different shrinkage time ranges (0 to 99, 100 to 199, 200 to 499 and 500 days or more). The statistical results for each dataset were grouped into the categories, country or region where experiments were done and compressive strength (<60 MPa and  $\geq 60$  MPa). Within these groups, the overall C.o.V values were discussed.

### 3.5 Methodology conclusion

From the total of 562 (220 drying shrinkage and 342 autogenous shrinkage) experiments extracted from the published NU and RSA databases and the technical report by Al-Manaseer and Fayyaz (2011), seven (7) datasets were extracted to achieve the objectives of this study. HSC specific datasets (Datasets 1-HSC for drying shrinkage and Dataset 2-HSC for autogenous shrinkage experiments) were used to calibrate existing model parameters (RILEM B4, MC 2010 and the WITS models) through a non-linear regression analysis using Solver<sup>®</sup>, an Excel add-in tool. The existing models were not able to predict drying shrinkage profiles with a sharp early peak and rapid decrease to the “final” shrinkage value. For this reason, a more flexible model function to accommodate the peak was proposed. Subsets S2-08, S2-09, S2-10 and S2-12 from Dataset 1-HSC had this peak in their shrinkage behavior and a composite model (combining two or more functions) was constructed as a logistic dose curve. Statistical measures were used to evaluate the proposed and existing (original and modified) prediction models, based on Dataset 1-HSC and Dataset 2-HSC. Statistical indicators used to compare the prediction performances and rank the different models for any given subset and for the different shrinkage time ranges considered, were RMSE,  $R^2_{adj}$ ,  $AIC_c$  and C.o.V. Errors (differences between experimental and predicted shrinkage values) were calculated for each experiment. Errors within  $\pm 20\%$  are deemed acceptable and within  $\pm 15\%$  excellent according to Gardner and Lockman (2001).

Dataset 3, Dataset 4 and Dataset 5 were extracted from the initial combined database (of 562 experiments) to evaluate the RILEM B4, MC 2010 and WITS models, respectively. In compiling each of these datasets the full dataset was filtered to extract only experiments that fell within applicable ranges of each model’s covariate data. The overall C.o.Vs for each dataset were grouped into the categories, country or region where experiments were done, and compressive strength (<60 MPa and  $\geq 60$  MPa) and within these groups, compared and discussed.

## Chapter 4 Results

This chapter presents all the results obtained in this study following the methodology described in Chapter 3. Drying and autogenous shrinkage predictions were made using the RILEM B4, MC 2010 and WITS models. The model coefficients for cement type, w/cm ratio, aggregate type and chemical admixture content and type were updated to better predict for the HSC datasets used in this study (named Datasets 1-HSC and 2-HSC). Datasets 3, 4 and 5 included covariate data only in the ranges applicable for the RILEM B4, MC 2010 and the WITS models, respectively, and were used to test each model's performance (accuracy of shrinkage predictions) within these limits.

### 4.1 Applicable shrinkage experiments per dataset

Figure 4.1 and Figure 4.2 show the proportion of drying shrinkage and autogenous shrinkage experiments, respectively for each dataset (seen in Figure 3.2), extracted from the compiled database of 562 experiments used in this study.

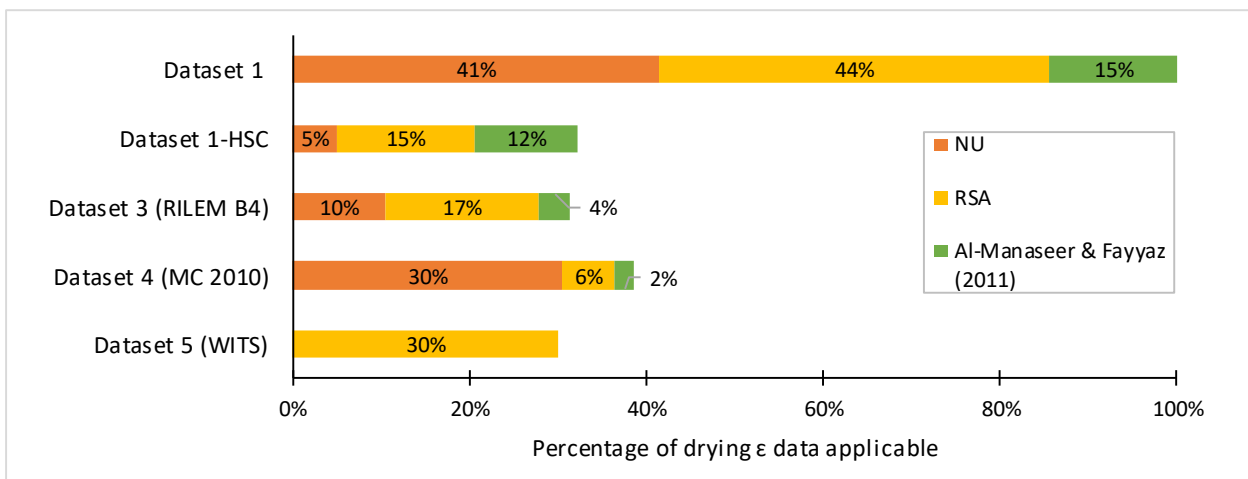


Figure 4.1 Percentage of applicable drying shrinkage experiments per dataset from the compiled database used in this study.

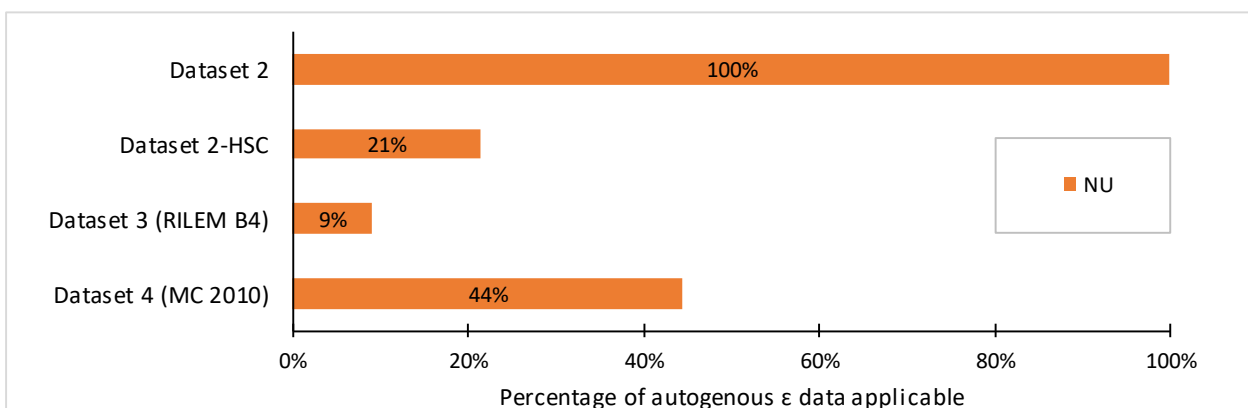


Figure 4.2 Percentage of applicable autogenous shrinkage experiments per dataset from the compiled database used in this study.

## 4.2 Original and modified shrinkage results for HSC

All original and modified shrinkage predictions for Dataset 1-HSC (drying shrinkage) and Dataset 2-HSC (autogenous shrinkage) of the RILEM B4, MC 2010 and WITS model can be found in Appendices E and F. The modified models, with updated model coefficients, are presented here.

The admixtures considered in this study are abbreviated as:

- Superplasticiser (SP)
- Plasticiser (P)
- Eclipse<sup>®</sup> shrinkage reducing admixture (SRA-E)
- Tetraguard AS20<sup>®</sup> shrinkage reducing admixture (SRA-T)
- Retarder (RE)
- Metakaolin (M)
- Silica fume (SF)
- Fly ash (FA)
- Air entraining agent (AEA)

### 4.2.1 Updated RILEM B4 model – drying shrinkage

The RILEM B4 model has cement type ( $P_{\epsilon\alpha}$ ,  $P_{\epsilon w}$ ,  $P_t$  and  $\epsilon_{cem}$ ), aggregate type ( $k_{\epsilon a}$  and  $k_{t a}$ ) and admixture combination type ( $\times \tau_{cem}$ ) dependant coefficients, so a three-phased process was conducted to modify it for drying shrinkage. First, the cement parameters for cement type 'R' were updated according to the SANS 50197-1 (2013) cement type and w/cm ratio, for each subset. The aggregate type coefficients in this model accommodate all the aggregate types occurring in the data used in this study, except for Andesite. All relevant aggregate type coefficients were, however, updated to incorporate the relationship between low w/cm concrete and coarse aggregate. Lastly, the admixture combination coefficients were updated for each subset. The existing RILEM B4 model covered some of the admixture combinations considered in this study, but were updated anyway to give better predictions for data subsets used in this study. For the subsets with varying SRA content, an equation was derived to replace the coefficient for the model's admixture combination. Table 4.1 gives the original model coefficients for cement type used to initially predict the drying shrinkage for Dataset 1-HSC. Table 4.2 gives the updated coefficients for varying w/cm ratios, for drying shrinkage.

Table 4.1 RILEM B4 model original coefficients for cement type – drying shrinkage

RILEM B4 Cement type	Original cement type model coefficients		
	$P_{\epsilon\alpha}$	$P_{\epsilon w}$	$P_{\epsilon c}$
R (Rapid hardening)	-0.8	1.1	0.11

Table 4.2 RILEM B4 model updated coefficients for cement type – drying shrinkage

Cement type & w/cm	Updated cement type model coefficients		
	$P_{\epsilon\alpha}$	$P_{\epsilon w}$	$P_{\epsilon c}$
CEM I 0.41 w/cm	-0.82	3.32	0.54
CEM I 0.28 w/cm	-2.65	-0.63	-1.13
CEM II (A-S) 0.40 w/cm	-0.46	1.07	0.06
CEM II (B-S) 0.40 w/cm	-0.40	1.06	0.21
CEM II (A-D) 0.36 w/cm	-0.80	1.10	0.11
CEM II (B-M) 0.33 w/cm	-1.12	0.72	0.25
CEM II (A-Q) 0.29 w/cm	-6.89	6.04	-0.04
CEM III A 0.40 w/cm	-0.65	1.09	0.22

For each cement type and w/cm group, the model coefficients for aggregate type and admixture combination were updated. Table 4.3 lists the original values for these coefficients while Table 4.4 and Table 4.5 gives the updated coefficients.

Table 4.3 RILEM B4 model original coefficients for aggregate and admixture combination – drying shrinkage

RILEM B4 Aggregate	Original aggregate type model coefficients	
	$k_{\epsilon\alpha}$	$k_{ta}$
Diabase / dolerite	0.76	0.06
Quartzite	0.71	0.59
Sandstone	1.60	2.30
Granite	1.05	4.00
RILEM B4 Admixture combination	Original admixture combination & cement type model coefficients	
	$\times \tau_{cem}$	$\epsilon_{cem}^{**}$
$\leq 5\% \text{ SP}; > 8\% \text{ SF}$	3.00	0.00036

\*\*The cement type coefficient ( $\epsilon_{cem}$ ) was used to update the model for an admixture combination as the admixture type coefficient ( $\times \tau_{cem}$ ) only influences the rate of shrinkage, whereas  $\epsilon_{cem}$  influences the final shrinkage. Both were required to modify the model for the subsets with varying SRA content.

Table 4.4 RILEM B4 model updated coefficients for aggregate and admixture combination – drying shrinkage.

Subset description		Aggregate type		Admixture combination model coefficient	
		$k_{ea}$	$k_{ta}$	$\times T_{cem}$	$\epsilon_{cem}$
Without mineral or chemical admixtures					
S1-01	CEM I 0.41 w/cm Granite	1.37	4.00*	-	-
S1-02	CEM I 0.41 w/cm Quartzite	0.72	0.59*	-	-
S1-03	CEM I 0.41 w/cm Sandstone	1.06	2.30*	-	-
S1-04	CEM I 0.41 w/cm Andesite	0.82	1.20	-	-
S1-05	CEM I 0.41 w/cm Dolerite	0.52	0.44	-	-
With mineral & without chemical admixtures					
S2-01	CEM II (A-S), 0.40 w/cm Andesite	0.97	0.84	-	-
S2-02	CEM II (B-S), 0.4 w/cm Andesite	1.02	1.12	-	-
S2-03	CEM III A 0.4 w/cm Andesite	0.91	0.52	-	-
With mineral & with chemical admixtures					
S2-04	CEM I, 0.28 w/cm Quartzite, > 1 % SP	0.71*	0.59*	1.00	-
S2-05	CEM I, 0.40 w/cm Sandstone, < 1 % SP	0.86	1.88	0.29	-
S2-06	CEM II (A-D), 0.36 w/cm Sandstone, > 1 % SP	0.72	0.24	0.79	-
S2-07	CEM II (A-Q), 0.29 w/cm Quartzite, > 1 % SP	0.71*	0.54	0.92	-
S2-08	CEM II (B-M) 0.33 w/cm Granite, < 1 % SP; 5% M	1.06	4.00*	0.075	0.00024
S2-09	CEM II (B-M), 0.33 w/cm Granite, < 1 % SP; < 0.5% P; 5 % M	1.06	4.00*	0.059	0.00036*
S2-10	CEM II (B-M), 0.33 w/cm Granite, > 1 % SP	1.06	4.00*	0.062	0.00036*
S2-11	CEM II (B-M), 0.33 w/cm Granite, < 1% SP, 0.5-2.5 % SRA-E	1.06	4.00*	0.062	$\epsilon_{cem} = 0.0003e^{-0.238x}$ (4.1) ( $x$ =SRA-E content)
S2-12	CEM II (B-M), 0.33 w/cm Granite, < 1 % SP, < 0.5% P	1.06	4.00*	0.16	0.00045

\* indicates that the original model coefficient was used.

Table 4.5 RILEM B4 model updated coefficients for aggregate and admixture combination – drying shrinkage (continuation).

Subset description		Aggregate type		Admixture combination model coefficient	
		$k_{\epsilon a}$	$k_{t a}$	$\times T_{cem}$	$\epsilon_{cem}$
With mineral & with chemical admixtures					
S2-13	CEM II (B-M), 0.33 w/cm Granite, < 1% SP, < 0.5% P;1- 2.5% SRA-E	1.06	4.00*	0.16	$\epsilon_{cem} = 0.0003x^{-0.46}$ (4.2) ( $x$ =SRA-E content)
S2-14	CEM II (B-M), 0.33 w/cm Granite, < 1% SP, < 0.5% P 1 – 2.5% SRA-T	1.06	4.00*	1.76	$\epsilon_{cem} = -0.0007\ln(x) + 0.0003$ (4.3) ( $x$ =SRA-T content)

\* indicates that the original model coefficient was used.

Figure 4.3, Figure 4.4 and Figure 4.5 show plots of drying shrinkage for the measured values, original model prediction and the modified RILEM B4 model prediction, for Subsets S1-03 (without admixtures), S2-02 (with mineral admixtures) and S2-08 (with mineral and chemical admixtures), respectively. The rest of the RILEM B4 model prediction plots for Dataset 1-HSC can be found in Appendix E.

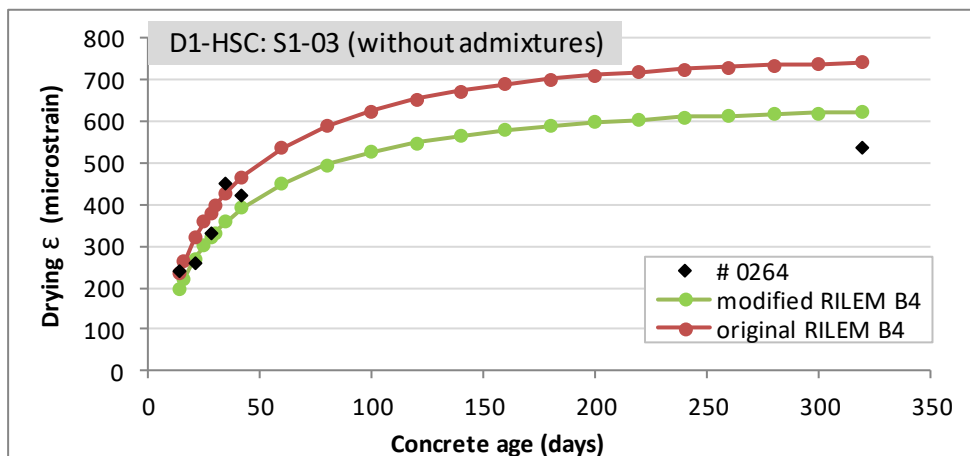


Figure 4.3 RILEM B4 model predicted and actual drying shrinkage (microstrain) for Dataset 1-HSC, Subset S1-03, Experiment #0264 (without admixtures).

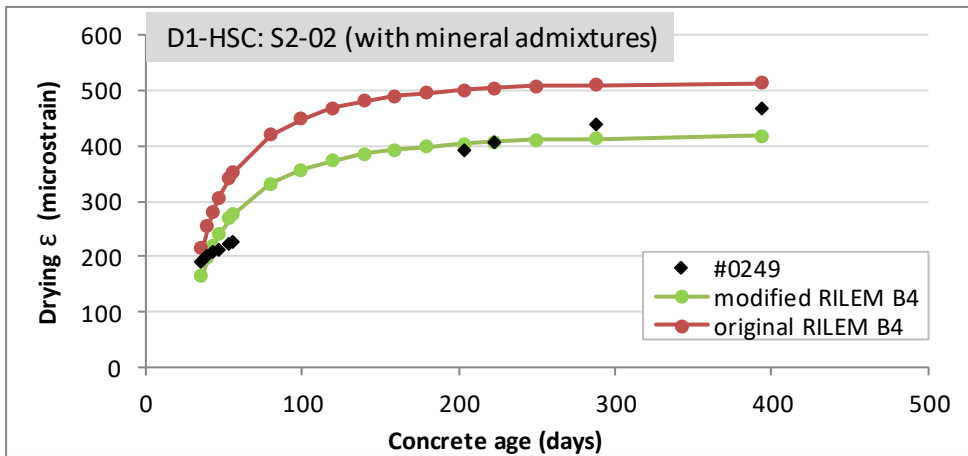


Figure 4.4 RILEM B4 model predicted and actual drying shrinkage (microstrain) for Dataset 1-HSC, Subset S2-02, Experiment #0249 (with mineral admixtures).

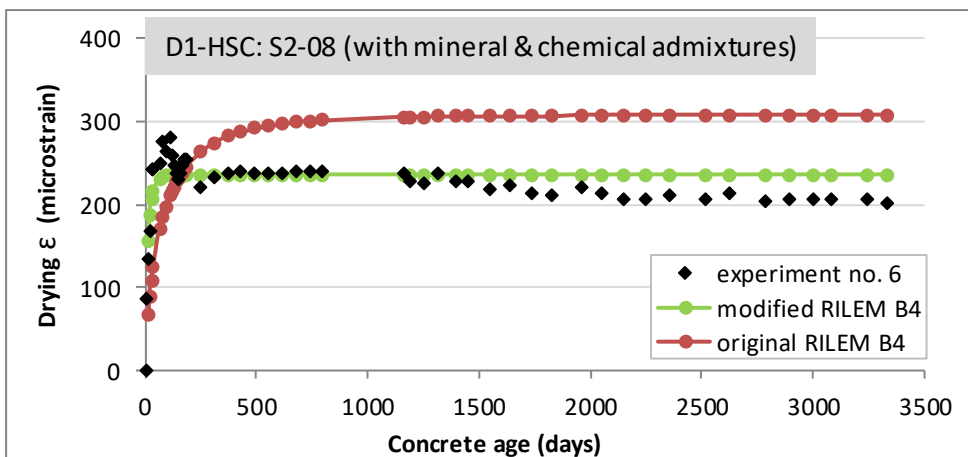


Figure 4.5 RILEM B4 model predicted and actual drying shrinkage (microstrain) for Dataset 1-HSC, Subset S2-08, Experiment no. 6 (with mineral and chemical admixtures).

#### 4.2.2 Updated RILEM B4 model – autogenous shrinkage

The RILEM B4 model includes coefficients for cement type ( $r_{\epsilon_a}$ ,  $r_{\epsilon_w}$  and  $r_t$ ) and admixture combination ( $\times \epsilon_{as,cm}$ ,  $\times r_{ew}$  and  $\times r_a$ ), so a two-phased process was conducted to modify it for autogenous shrinkage. First, the cement parameters for cement type 'R' (rapid hardening) were updated according to the SANS 50197-1 (2013) cement type, w/cm ratio and aggregate type, for each subset. Then the coefficients for admixture combination were updated for each subset. The original RILEM B4 model covers some of the admixture combinations used in this study. It was found though that updating was unnecessary for Subsets S2-01a and S2-09a as the original model already fitted these data optimally.

Table 4.6 gives the original RILEM B4 model coefficients for cement type and admixture combination, used to initially predict the autogenous shrinkage for Dataset 2-HSC. Table 4.7 lists the RILEM B4 updated model coefficients for varying w/cm ratios, for autogenous shrinkage.



Table 4.6 RILEM B4 original model coefficients for cement type and admixture combination – autogenous shrinkage.

RILEM B4 Cement type	Original cement type model coefficients		
	$r_{\epsilon\alpha}$	$r_{\epsilon w}$	$r_t$
R (Rapid hardening)	-0.75	-3.50	-4.50
RILEM B4 Admixture type combination	Original admixture type model coefficients		
	$\times \epsilon_{as, cem}$	$\times r_{\epsilon w}$	$\times r_a$
$\leq 5$ SP; $\leq 8$ SF	2.80	0.29	0.21
$\leq 5$ SP; $> 8$ SF	0.96	0.26	0.71
$\leq 2$ P	0.38	0.00	1.90

Table 4.7 RILEM B4 updated model coefficients for cement type – autogenous shrinkage.

Subset description		Updated cement type model coefficients			Updated admixture type model coefficients		
		$r_{\epsilon\alpha}$	$r_{\epsilon w}$	$r_t$	$\times \epsilon_{as, cem}$	$\times r_{\epsilon w}$	$\times r_a$
S2-02a	CEM I, 0.27 w/cm Quartzite, 3 % SP	-2.58	0.83	-4.50*	0.96	1.00	1.61
S2-03a	CEM I, 0.31 w/cm Granite, 1 % SP	-1.19	-1.24	-4.85	2.80*	0.29*	0.21*
S2-04a	CEM I, 0.31 w/cm Granite, < 0.5 % P	-2.41	-1.68	-11.66	0.38*	0.00*	1.90*
S2-05a	CEM I, 0.35 w/cm Granite, 3 % SP, 1% RE	0.23	-2.71	-5.47	0.39	1.00	0.79
S2-06a	CEM II (A-D) - 0.23 w/cm Quartzite, 2 % SP	-0.75	-0.91	-7.31	0.96*	0.26*	0.71*
S2-07a	CEM II (A-D), 0.28 w/cm Granite, 2 % SP	-1.43	-1.27	-19.06	0.96*	0.26*	0.71*
S2-08a	CEM II (A-D) - 0.28 w/cm Quartzite, 1 % SP	-3.89	5.85	-12.13	0.96*	0.26*	0.71*
S2-10a	CEM II (A-D) - 0.34 w/cm Quartzite, 1 % SP	-0.82	-0.92	-16.28	0.96*	0.26*	0.71*
S2-11a	CEM II (A-D), 0.34 w/cm Quartzite, 1 % SP, < 0.5% AEA	-0.75*	-3.76	-5.34	1.37	1.00	0.24
S2-12a	CEM II (A-D) 0.29 w/cm Quartzite, 3 % SP	0.96	-4.38	-12.02	0.43	1.00	1.87

\* indicates that the original model coefficient was used.

Figure 4.6 and Figure 4.7 show plots of autogenous shrinkage for the measured values, original model prediction and the modified RILEM B4 model prediction, for Subset S2-02a and Subset S2-09a, respectively, both subsets containing chemical admixtures. The original RILEM B4 model already fitted S2-09a optimally, therefore a modified RILEM B4 is not shown in Figure 4.7. The rest of the RILEM B4 model prediction plots for Dataset 2-HSC can be found in Appendix F.

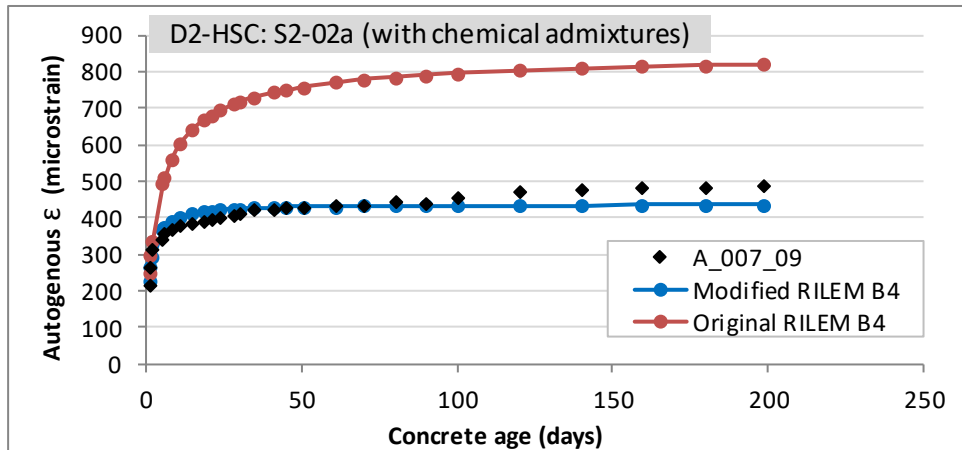


Figure 4.6 RILEM B4 model predicted and actual autogenous shrinkage (microstrain) for Dataset 2-HSC, Subset S2-02a, Experiment A\_007\_09 (with chemical admixtures).

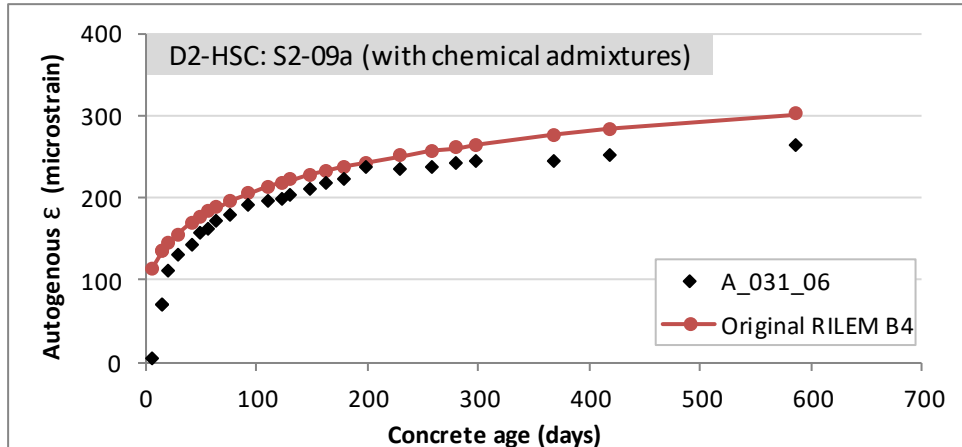


Figure 4.7 RILEM B4 model predicted and actual autogenous shrinkage (microstrain) for Dataset 2-HSC, Subset S2-09a, Experiment A\_031\_06 (with chemical admixtures).

### 4.2.3 Updated MC 2010 model – drying shrinkage

The MC 2010 for drying shrinkage only has two coefficients for cement type. Both of these coefficients influenced the final shrinkage, but only the one which has the greatest influence, ( $\alpha_{ds1}$ ) was updated. One other model parameter which had a significant influence on the rate of shrinkage was also modified, for a two phase modification process. This parameter is part of the model time function  $\beta_{ds}(t - t_0)$  given in Equation 4.4. To modify the model, firstly the parameters for cement type and strength class usually used for HSC (42.5N, 52.5N and 52.5R) were updated according to SANS 50197-1 (2013) cement and aggregate type, for each subset. Then the most influential parameter, being the exponent 2 of  $h_0$  in Equation 4.4, was updated for the admixture combinations of each subset.

$$\beta_{ds}(t - t_0) = \left( \frac{t - t_0}{0.035h_0^2 + (t - t_0)} \right)^{0.5} \quad (4.4)$$

Table 4.8 gives the original MC 2010 model coefficients for cement type and the exponent 2, part of  $\beta_{ds}(t - t_0)$ , used to initially predict the drying shrinkage for Dataset 1-HSC. Table 4.9 and Table 4.10 list the MC 2010 updated model coefficients at different w/cm ratios for the cement type and the exponent 2, part of  $\beta_{ds}(t - t_0)$ , for drying shrinkage.

Table 4.8 MC 2010 original model coefficients for cement type and most influential constant (exponent 2) – drying shrinkage

CEB-FIB MC 2010 cement type & strength class	Original coefficient and model constant	
	$\alpha_{ds1}$	part of $\beta_{ds}(t - t_0)$
42.5R, 52.5N, 52.5R	6	2

Table 4.9 MC 2010 updated model coefficients for cement type coefficient and most influential model constant (exponent 2) – drying shrinkage.

Subset description		Updated cement type coefficient	Updated model constant
		$\alpha_{ds1}$	part of $\beta_{ds}(t - t_0)$
Without mineral or chemical admixtures			
S1-01	CEM I, 0.41 w/cm Granite	5.96	1.74
S1-02	CEM I, 0.41 w/cm Quartzite	4.33	0.77
S1-03	CEM I, 0.41 w/cm Sandstone	6.60	1.95
S1-04	CEM I, 0.41 w/cm Andesite	6.79	1.79
S1-05	CEM I, 0.41 w/cm Dolerite	5.95	1.75

Table 4.10 MC 2010 updated model coefficients for cement type coefficient and most influential model constant (exponent 2) – drying shrinkage (continuation).

Subset description		Updated cement type coefficient	Updated model constant
		$\alpha_{ds1}$	part of $\beta_{ds}(t - t_0)$
With mineral & without chemical admixtures			
S2-01	CEM II (A-S), 0.40 w/cm Andesite	4.77	1.75
S2-02	CEM II (B-S), 0.4 w/cm Andesite	4.39	1.84
S2-03	CEM III A, 0.4 w/cm Andesite	4.16	1.61
With mineral & with chemical admixtures			
S2-04	CEM I, 0.28 w/cm Quartzite, > 1% SP	10.24	1.30
S2-05	CEM I, 0.40 w/cm Sandstone, < 1% SP	5.12	1.69
S2-06	CEM II (A-D), 0.36 w/cm Sandstone, > 1% SP	5.04	1.47
S2-07	CEM II (A-Q) 0.29 w/cm Quartzite, > 1% SP	9.39	1.08
S2-08	CEM II (B-M) 0.33 w/cm Granite, < 1% SP, 5% M	1.58	1.29
S2-09	CEM II (B-M) 0.33 w/cm Granite, < 1% SP, < 0.5% P, 5% M	3.77	1.24
S2-10	CEM II (B-M) 0.33 w/cm Granite, > 1% SP	3.63	1.37
S2-11	CEM II (B-M) 0.33 w/cm Granite, < 1% SP, 0.5-2.5% SRA-E	$\alpha_{ds1} = -0.79 \ln(x) + 2.52$ (4.5)  ( $x$ =SRA-E content)	1.76
S2-12	CEM II (B-M) 0.33 w/cm Granite, < 1% SP, < 0.5% P	4.36	1.41
S2-13	CEM II (B-M) 0.33 w/cm Granite, < 1% SP, < 0.5% P 1- 2.5% SRA-E	$\alpha_{ds1} = -1.63 \ln(x) + 2.73$ (4.6)  ( $x$ =SRA-E content)	1.80
S2-14	CEM II (B-M) 0.33 w/cm Granite, < 1% SP, < 0.5% P 1 – 2.5% SRA-T	$\alpha_{ds1} = -0.96 \ln(x) + 2.32$ (4.7)  ( $x$ =SRA-T content)	1.85

Figure 4.8, Figure 4.9 and Figure 4.10 show plots of drying shrinkage for the measured values, original model prediction and the modified MC 2010 model prediction, for Subsets S1-03 (without admixtures), S2-02 (with mineral admixtures) and S2-08 (with mineral & chemical admixtures), respectively. The rest of the MC 2010 model prediction plots for Dataset 1-HSC can be found in Appendix E.

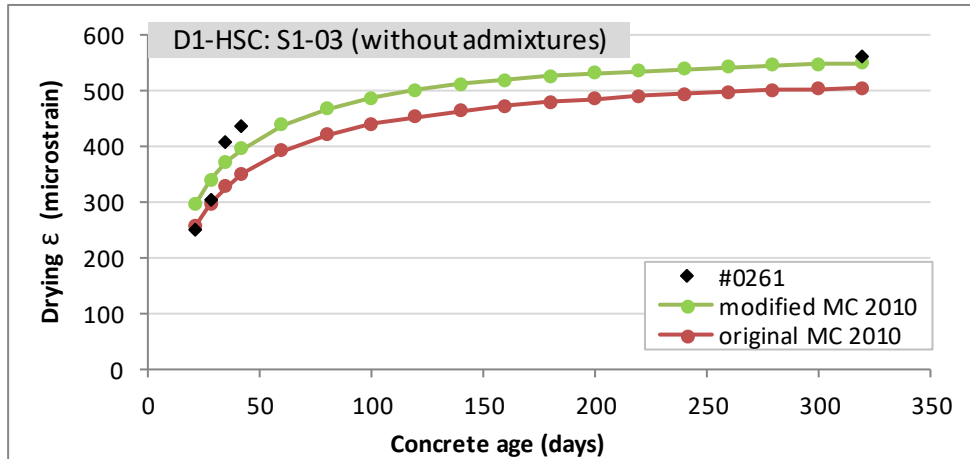


Figure 4.8 MC 2010 predicted and actual drying shrinkage (microstrain) for Dataset 1-HSC, Subset S1-03, Experiment #0261 (without admixtures).

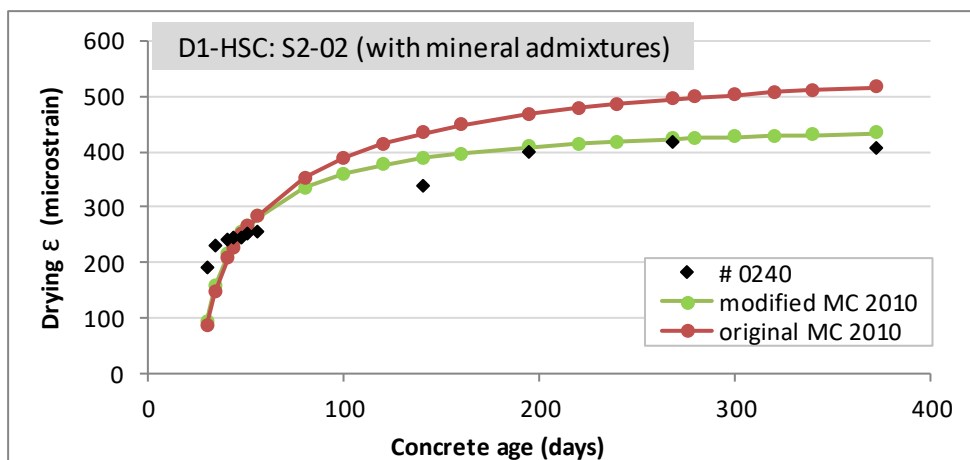


Figure 4.9 MC 2010 predicted and actual drying shrinkage (microstrain) for Dataset 1-HSC, Subset S2-02, Experiment #0240 (with mineral admixtures).

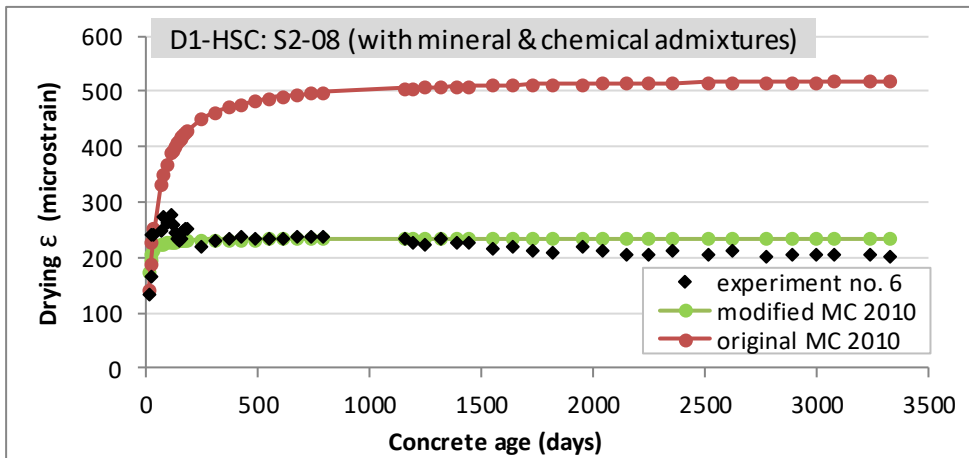


Figure 4.10 MC 2010 predicted and actual drying shrinkage (microstrain) for Dataset 1-HSC, Subset S2-08, Experiment no. 6 (with mineral and chemical admixtures)

#### 4.2.4 Updated MC 2010 model – autogenous shrinkage

For autogenous shrinkage, the MC 2010 model has only one coefficient ( $\alpha_{as1}$ ) for cement type, which influences the final shrinkage, and one model parameter which influences the rate of shrinkage. This second parameter is the constant in the exponent in model time function  $\beta_{as}(t)$  for autogenous shrinkage as seen in Equation 4.8. In modifying the model,  $\alpha_{as}$  was first updated for cement type and strength class usually used for HSC (42.5N, 52.5N and 52.5R) according to SANS 50197-1 (2013), for each subset. Then the constant in the exponent, being -0.2 in Equation 4.8, was updated for different w/cm ratios and admixture combinations for each subset.

$$\beta_{as}(t) = 1 - \exp(-0.2 \times \sqrt{t}) \tag{4.8}$$

Table 4.11 gives the original MC 2010 model coefficients for cement type and -0.2, part of  $\beta_{as}(t)$ , used to initially predict autogenous shrinkage for Dataset 2-HSC. Table 4.12 lists the MC 2010 updated model coefficients for cement type and -0.2, part of  $\beta_{as}(t)$ , for drying shrinkage, for different w/cm ratios and admixture combinations.

Table 4.11 MC 2010 original model coefficient for cement type and constant in exponent in  $\beta_{as}(t)$  – autogenous shrinkage.

CEB-FIB MC 2010 cement type & strength class	Original coefficient & model constant	
	$\alpha_{as}$	Constant in exponent in $\beta_{as}(t)$
42.5R, 52.5N, 52.5R	600	-0.2

Table 4.12 MC 2010 updated model coefficient for cement type coefficient and constant in exponent in  $\beta_{as}(t)$  – autogenous shrinkage.

Subset description		Updated cement type coefficient	Updated model constant
		$\alpha_{as}$	Constant in exponent in $\beta_{as}(t)$
S2-01a	CEM I - 0.27 w/cm Granite, 1% SP	228.29	-0.38
S2-02a	CEM I - 0.27 w/cm Quartzite, 3% SP	422.09	-0.88
S2-03a	CEM I - 0.31 w/cm Granite, 1% SP	455.1	-0.05
S2-04a	CEM I - 0.31 w/cm Granite, < 0.5% P	593.77	-0.37
S2-05a	CEM I - 0.35 w/cm Granite, 3% SP; 1% RE	440.12	-0.02
S2-06a	CEM II (A-D) - 0.23 w/cm Quartzite, 2% SP	540.36	-0.14
S2-07a	CEM II (A-D) - 0.28 w/cm Granite, 2% SP	693.46	-0.06
S2-08a	CEM II (A-D) - 0.28 w/cm Quartzite, 1% SP	534.00	-0.05
S2-09a	CEM II (A-D) - 0.34 w/cm Granite, 2% SP	203.04	-0.24
S2-10a	CEM II (A-D) - 0.34 w/cm Quartzite, 1% SP	389.94	-0.05
S2-11a	CEM II (A-D) - 0.34 w/cm Quartzite, 1% SP, < 0.5% AEA	315.14	-0.06
S2-12a	CEM II (A-D) - 0.29 w/cm Quartzite, 3% SP	231.09	-0.48

Figure 4.11 and Figure 4.12 show plots of autogenous shrinkage for the measured values, original model prediction and the modified MC 2010 model prediction, for Subsets S2-02 and S2-09, respectively, both containing chemical admixtures. The rest of the MC 2010 model prediction plots for Dataset 2-HSC can be found in Appendix F.

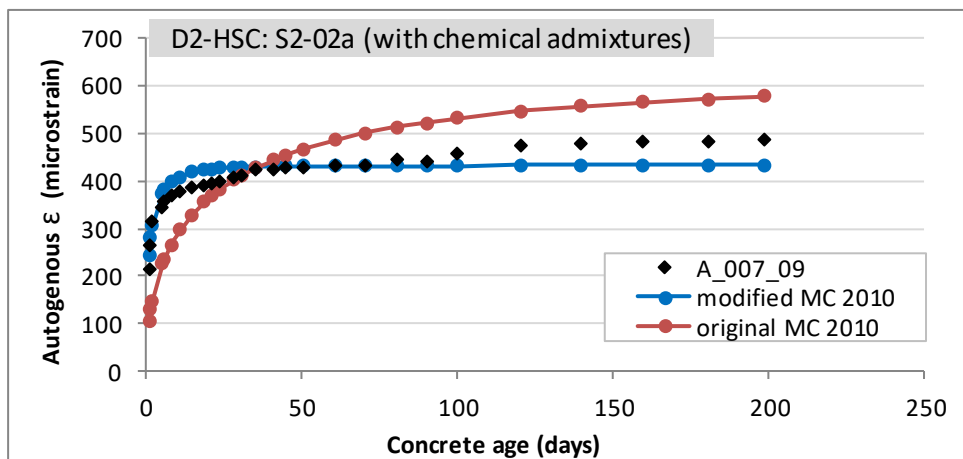


Figure 4.11 MC 2010 predicted and actual autogenous shrinkage (microstrain) for Dataset 2-HSC, Subset S2-02a, Experiment A\_007\_09 (with chemical admixtures).

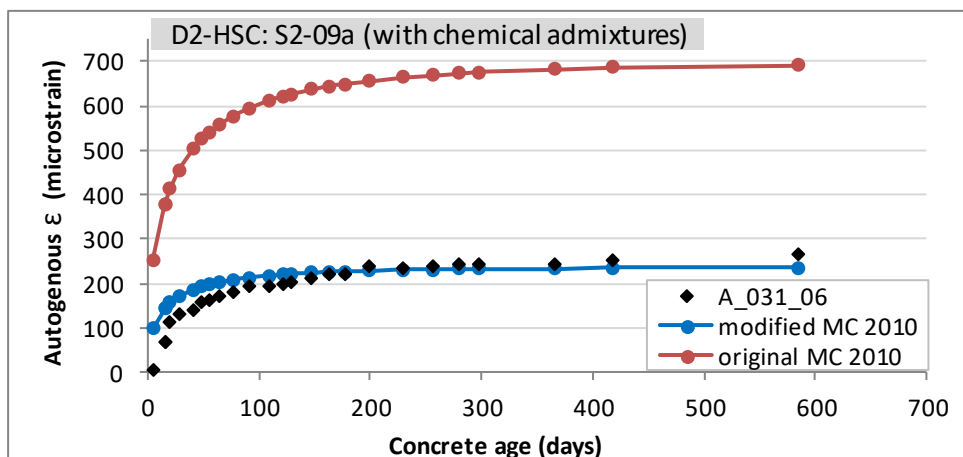


Figure 4.12 MC 2010 predicted and actual autogenous shrinkage (microstrain) for Dataset 2-HSC, Subset S2-09a, Experiment A\_031\_06 (with chemical admixtures).

#### 4.2.5 Updated WITS model – drying shrinkage

The WITS model uses factors for cement and aggregate type that are added to the model parameters  $\alpha$ ,  $\ln(\beta)$  and  $\ln(\gamma)$ . In this model the coefficients for cement type are already based on the SANS 50197-1 (2013) cement type classification method and consider all types except CEM II (A-D) paired with Sandstone, CEM II (A-Q) and CEM II (B-M). The original cement type model coefficients for cement types CEM I, CEM II and CEM III were all zero except for CEM VA. For the unaccounted for cement types, the coefficients were kept zero as this produced the best results.

The model's existing coefficients accommodated all the aggregate types occurring in the data evaluated in this study. Note though that sandstone coarse aggregate uses the greywacke aggregate coefficient as they can be classified similarly. All relevant aggregate type coefficients were, however, updated for the WITS model to incorporate the relationship between low w/cm concrete and coarse aggregate. Lastly, admixture combination coefficients were derived for each subset by conducting regression analysis for additional factors to be added to all three model parameters  $\alpha$ ,  $\ln(\beta)$  and  $\ln(\gamma)$ . For the subsets with varying SRA content, an equation was derived in place of a single factor. Predictions using the original



WITS model for the drying shrinkage Subsets S2-05 and S2-09 could not be improved upon, and so no modifications were made to the factors for these data subsets. For each cement type and w/cm group, the factors for aggregate type and admixture combination were updated. These, along with the original values are listed in Table 4.13, Table 4.14 and Table 4.15. The factors are added to the value (seen in brackets in Table 4.14, Table 4.14 and Table 4.15 ) under  $\alpha$ ,  $\ln(\beta)$  and  $\ln(\gamma)$ .

Table 4.13 WITS model original factors for aggregate type– drying shrinkage.

WITS Aggregate type	Original aggregate type model coefficients		
	$\alpha$ (-2245.19)	$\ln(\beta)$ (9.76)	$\ln(\gamma)$ (3.04)
Granite	-43.02	0.33	0.34
Andesite	0.00	0.00	0.00
Dolerite	0.00	0.00	0.00
Greywacke/ Sandstone	0.00	0.00	0.00
Quartzite	302.21	0.00	0.01

Table 4.14 WITS model updated factors for aggregate type and admixture combination– drying shrinkage.

Subset description		Aggregate type coefficients			Admixture combination coefficients		
		$\alpha$ (-2245.19)	$\ln(\beta)$ (9.76)	$\ln(\gamma)$ (3.04)	$\alpha$ (-2245.19)	$\ln(\beta)$ (9.76)	$\ln(\gamma)$ (3.04)
Without mineral or chemical admixtures							
S1-01	CEM I, 0.41 w/cm Granite	1.59	-2.79	-1.42	-	-	-
S1-02	CEM I, 0.41 w/cm Quartzite	763.59	-16.36	-2.56	-	-	-
S1-03	CEM I, 0.41 w/cm Sandstone	84.52	-0.79	-0.59	-	-	-
S1-04	CEM I, 0.41 w/cm Andesite	34.50	-2.12	-1.25	-	-	-
S1-05	CEM I, 0.41 w/cm Dolerite	27.07	0.00	-0.07	-	-	-

Table 4.15 WITS model updated factors for aggregate type and admixture combination– drying shrinkage (continuation).

Subset description		Aggregate type coefficients			Admixture combination coefficients		
		$\alpha$ (-2245.19)	$\ln(\beta)$ (9.76)	$\ln(\gamma)$ (3.04)	$\alpha$ (-2245.19)	$\ln(\beta)$ (9.76)	$\ln(\gamma)$ (3.04)
With mineral & without chemical admixtures							
S2-01	CEM II (A-S), 0.40 w/cm, Andesite	43.56	-3.01	-1.60	-	-	-
S2-02	CEM II (B-S), 0.4 w/cm, Andesite	218.27	-4.39	-1.45	-	-	-
S2-03	CEM III A, 0.4 w/cm Andesite	198.50	-5.46	-1.86	-	-	-
With mineral & with chemical admixtures							
S2-04	CEM I - 0.28 w/cm Quartzite, > 1% SP	302.21	0.00	0.01	46.045	-1.48	-0.85
S2-06	CEM II (A-D), 0.36 w/cm, Sandstone, > 1% SP	-53.96	0.00	0.00	188.46	0.085	-0.678
S2-07	CEM II (A-Q) - 0.29 w/cm, Quartzite, > 1% SP	306.41	9.16	-31.16	3.918	-11.848	29.153
S2-08	CEM II (B-M), 0.33 w/cm, Granite, < 1% SP; 5% M	-34.54	-0.065	-0.461	-49.58	0.741	0.000
S2-10	CEM II (B-M), 0.33 w/cm, Granite > 1% SP	-34.54	-0.065	-0.461	82.783	0.643	0.000
S2-11	CEM II (B-M), 0.33 w/cm, Granite < 1% SP, 0.5-2.5% SRA-E	-34.54	-0.065	-0.461	Eqn. 4.9	0.00	0.00
S2-12	CEM II (B-M) 0.33 w/cm, Granite < 1% SP, < 0.5% P	-34.54	-0.065	-0.461	126.603	0.000	0.000
S2-13	CEM II (B-M) 0.33 w/cm, Granite < 1% SP, < 0.5% P, 1- 2.5% SRA-E	-34.54	-0.065	-0.461	Eqn. 4.10	-0.472	0.000
S2-14	CEM II (B-M) 0.33 w/cm, Granite < 1% SP, < 0.5% P, 1 – 2.5% SRA-T	-34.54	-0.065	-0.461	Eqn. 4.11	-0.509	0.000

$$y = -72.35 \ln x - 72.691 \quad (x = \text{SRA-E content}) \quad (4.9)$$

$$y = -116.9 \ln(x) + 20.272 \quad (x = \text{SRA-E content}) \quad (4.10)$$

$$y = -52.82 \ln(x) - 27.32 \quad (x = \text{SRA-T content}) \quad (4.11)$$

Figure 4.13, Figure 4.14 and Figure 4.15 show plots of drying shrinkage for the measured values, original model prediction and the modified WITS model prediction, for Subsets S1-03 (without admixtures), S2-02 (with mineral admixtures) and S2-08 (with mineral & chemical admixtures), respectively. The rest of the WITS model prediction plots for Dataset 1-HSC can be found in Appendix E.

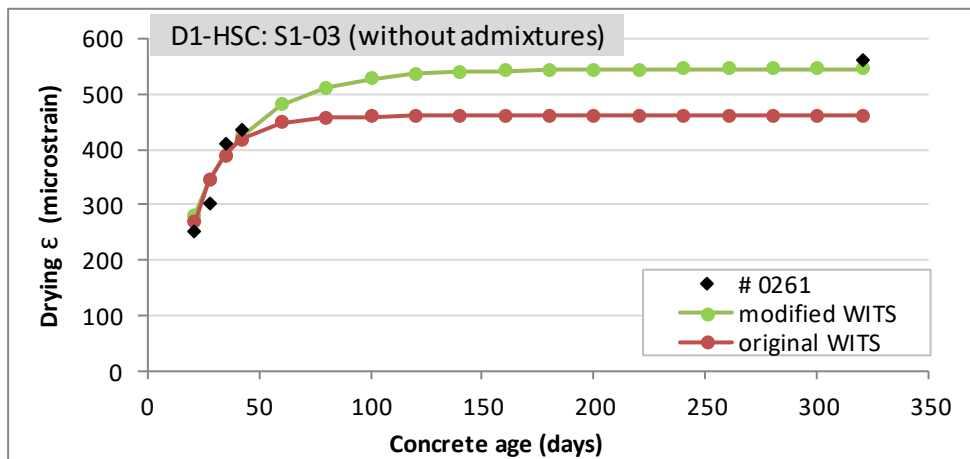


Figure 4.13 WITS model predicted and actual drying shrinkage (microstrain) for Dataset 1-HSC, Subset S1-03, Experiment #0261 (without admixtures).

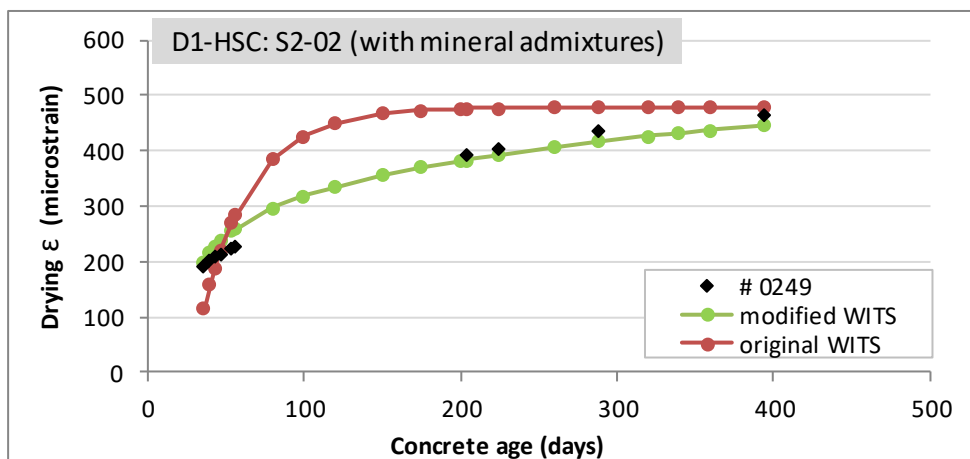


Figure 4.14 WITS model predicted and actual drying shrinkage (microstrain) for Dataset 1-HSC, Subset S2-02, Experiment #0249 (with mineral admixtures).

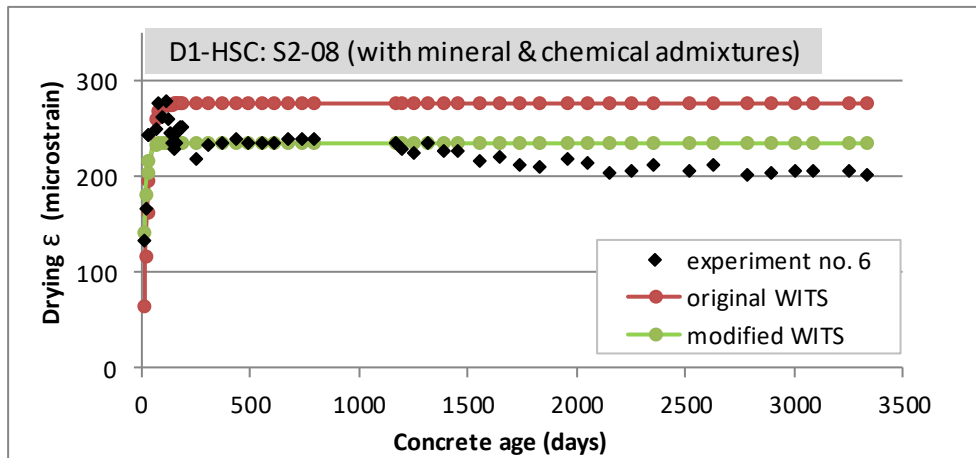


Figure 4.15 WITS model predicted and actual drying shrinkage (microstrain) for Dataset 1-HSC, Subset S2-08, Experiment no. 6 (with mineral & chemical admixtures).

### 4.3 Proposed composite model

A new empirical, composite model was proposed, based on the average of the experimental shrinkage data of Subsets S2-08, S2-09, S2-10 and S2-12, of the logistic dose form shown in Equation 3.1 (repeated below). The data were divided into the time ranges 0 to 130, 131 to 300 and > 300 days and selected functions were fitted individually to the experimental shrinkage data in these ranges before being combined to give the final composite equation, of the same form. The three time ranges were selected based on the shrinkage profiles of the specific subsets used for this proposed composite model. They split the shrinkage profiles into (i) a portion of steady increase in shrinkage from zero to the peak (ii) a portion where shrinkage decreased from the peak to the start of the final “plateau” value and (iii) the final values where shrinkage had essentially plateaued.

#### 4.3.1 Model parameters

$$\varepsilon_{ds}(t) = F_1 + \frac{F_2 - F_1}{\left[1 + \left(\frac{t}{t_x}\right)^m\right]^q} \quad (3.1)$$

Referring to Equation 3.4 and Equation 3.5 initial values for  $t_{x1}$  and  $t_{x2}$  were estimated from plots of the actual shrinkage profiles of Subsets S2-08, S2-09, S2-10 and S2-12 and starting values of  $m_1$ ,  $m_2$ ,  $q_1$  and  $q_2$  (curvature and smoothness parameters) were taken as 1. Solver® was used to fit Equation 3.4 and Equation 3.5 to the experimental shrinkage data to give the composite models. Table 4.16 gives the initial and fitted  $t_x$  values and Table 4.17 the fitted  $m$  and  $n$  values for each data subset.

Table 4.16 Composite model initial and fitted  $t_x$  values.

Converging parameter	Initial value	Fitted value
$t_{x1}$	115	130
$t_{x2}$	350	300

Table 4.17 Composite model fitted curvature smoothness parameter ( $m, q$ ) for data Subsets S2-08, S2-09, S2-10 and S2-12

Subset	$m_1$	$q_1$	$m_2$	$q_2$
S2-08	-4	0.17	-12	0.2
S2-09	-4	0.17	-12	0.2
S2-10	-36	0.02	-12	0.2
S2-12	-50	0.03	-12	0.2

#### 4.3.2 Proposed composite model for data Subset S2-08

Functions for the three segments of the average shrinkage data for Subset S2-08 are given in Equation 4.12, Equation 4.13 and Equation 4.14 where  $t$  is the concrete age in days and  $f_x$  is the shrinkage in microstrains.

$$f_{a+b} = 14.34t^{0.732} \quad (\text{for } 0 > t < 130) \quad (4.12)$$

$$f_c = 261.29t^{-0.015} \quad (\text{for } 130 > t < 300) \quad (4.13)$$

$$f_d = -0.012t + 245.1 \quad (\text{for } t > 300) \quad (4.14)$$

Combining  $f_{a+b}$  and  $f_c$  resulted in the function  $F_1$  given in Equation 4.15.

$$F_1 = f_c + \frac{f_{a+b} - f_c}{\left[1 + \left(\frac{t}{130}\right)^{-4}\right]^{0.17}} \quad (\text{for } 0 > t < 300) \quad (4.15)$$

The final proposed composite model for data Subset S2-08 is then obtained as the combination of  $F_1$  and  $f_d$ , Equation 4.16.

$$\varepsilon_{ds}(t) = f_d + \frac{F_1 - f_d}{\left[1 + \left(\frac{t}{300}\right)^{-12}\right]^{0.2}} \quad (4.16)$$

Figure 4.16 and Figure 4.17 show shrinkage profile plots for Equation 4.16 and the experimental values from experiments 6 and 10 of data Subset S2-08 (0.6% SP, 25-30 % FA and 5% M), respectively.

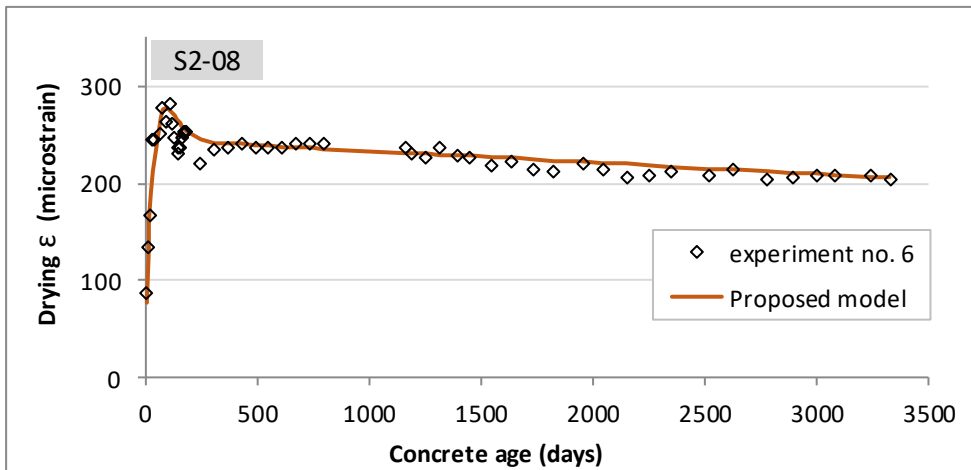


Figure 4.16 Proposed composite model predicted and actual drying shrinkage (microstrain) for Experiment no. 6 of data Subset S2-08 (0.6% SP, 25-30 % FA and 5% M).

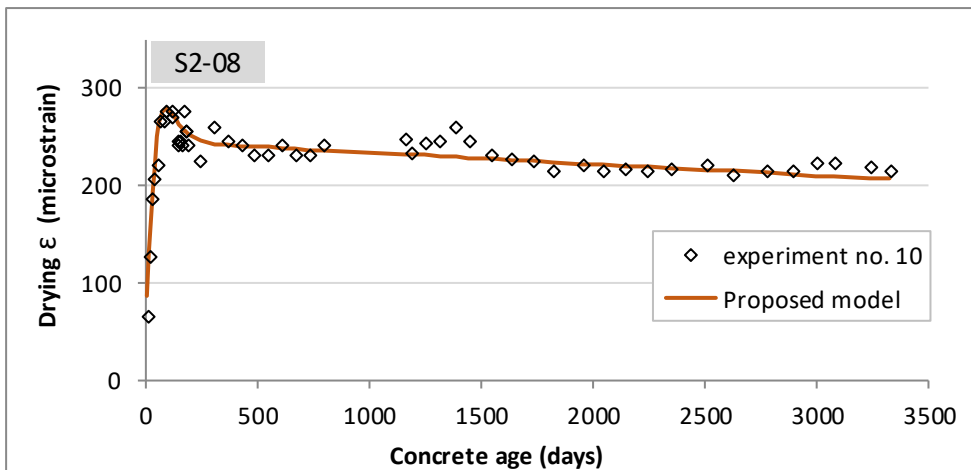


Figure 4.17 Proposed composite model predicted and actual drying shrinkage (microstrain) for Experiment 10 of data Subset S2-08 (0.6% SP, 25-30 % FA and 5% M).

### 4.3.3 Proposed model for Subset S2-09

Functions for the three segments of the average shrinkage data for Subset S2-09 are given in Equation 4.17, Equation 4.18 and Equation 4.19 where  $t$  is the concrete age in days and  $f_x$  is the shrinkage in microstrains.

$$f_{a+b} = 14.34t^{0.732} \quad (\text{for } 0 > t < 130) \quad (4.17)$$

$$f_c = 381.59t^{-0.007} \quad (\text{for } 130 > t < 300) \quad (4.18)$$

$$f_d = -0.005t + 368.65 \quad (\text{for } t > 300) \quad (4.19)$$

Combining  $f_{a+b}$  and  $f_c$  resulted in the function  $F_1$  given in Equation 4.20.

$$F_1 = f_c + \frac{f_{a+b} - f_c}{\left[1 + \left(\frac{t}{130}\right)^{-4}\right]^{0.17}} \quad (\text{for } 0 > t < 300) \quad (4.20)$$

The final proposed composite model for data Subset S2-09 is then obtained as the combination of  $F_1$  and  $f_d$ , Equation 4.21.

$$\varepsilon_{ds}(t) = f_d + \frac{F_1 - f_d}{\left[1 + \left(\frac{t}{300}\right)^{-12}\right]^{0.2}} \quad (4.21)$$

Figure 4. and Figure 4. show shrinkage profile plots for Equation 4.21 and the experimental values from Experiments 31 and 33 of data Subset S2-09 (< 1% SP; < 0.5% P; 5% M), respectively.

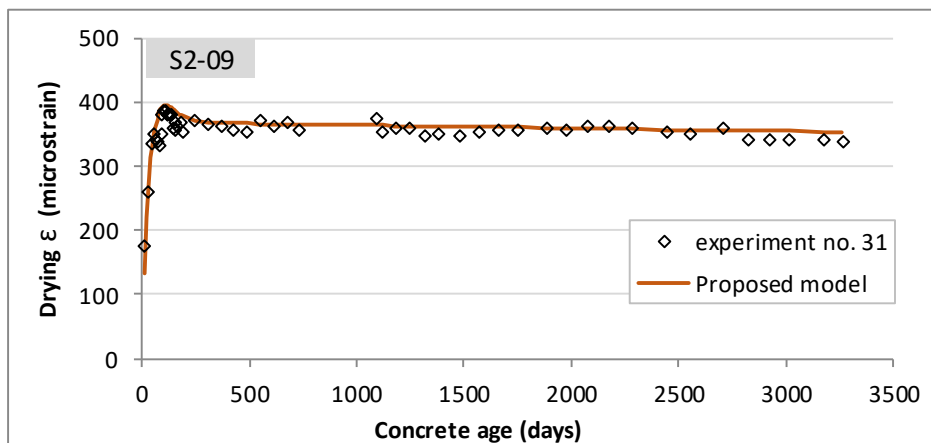


Figure 4.18 Proposed composite model predicted and actual drying shrinkage (microstrain) for Experiment 31 of data Subset S2-09 (< 1% SP; < 0.5% P; 5% M).

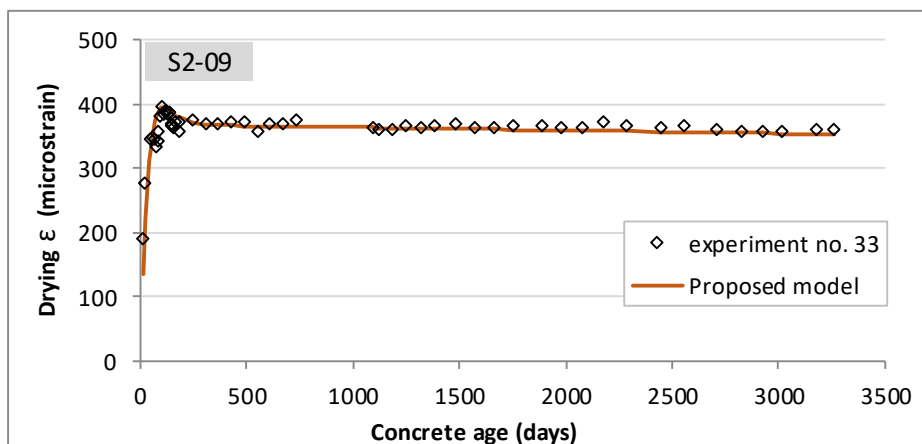


Figure 4.19 Proposed composite model predicted and actual drying shrinkage (microstrain) for Experiment 33 of data Subset S2-09 (< 1% SP; < 0.5% P; 5% M).

#### 4.3.4 Proposed model for Subset S2-10

Functions for the three segments of the average shrinkage data for Subset S2-10 are given in Equation 4.22, Equation 4.23 and Equation 4.24 where  $t$  is the concrete age in days and  $f_x$  is the shrinkage in microstrains.

$$f_{a+b} = 29.68t^{0.618} \quad (\text{for } 0 > t < 130) \quad (4.22)$$

$$f_c = 520.19t^{-0.065} \quad (\text{for } 130 > t < 300) \quad (4.23)$$

$$f_d = 0.0004t + 358.18 \quad (\text{for } t > 300) \quad (4.24)$$

Combining  $f_{a+b}$  and  $f_c$  resulted in the function  $F_1$  given in Equation 4.25.

$$F_1 = f_c + \frac{f_{a+b} - f_c}{\left[1 + \left(\frac{t}{130}\right)^{-36}\right]^{0.02}} \quad (\text{for } 0 > t < 300) \quad (4.25)$$

The final proposed composite model for data Subset S2-09 is then obtained as the combination of  $F_1$  and  $f_d$ , Equation 4.26.

$$\varepsilon_{ds}(t) = f_d + \frac{F_1 - f_d}{\left[1 + \left(\frac{t}{300}\right)^{-12}\right]^{0.2}} \quad (4.26)$$

Figure 4.20 and Figure 4. show shrinkage profile plots for Equation 4.26 and the experimental values from Experiments 5 and 9 of data Subset S2-10 (> 1% SP), respectively.

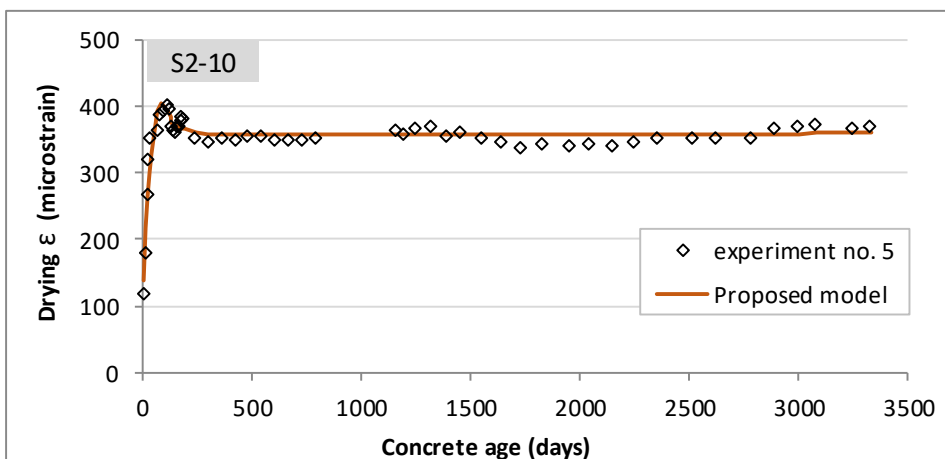


Figure 4.20 Proposed composite model predicted and actual drying shrinkage (microstrain) for Experiment 5 of data Subset S2-10 (> 1% SP).



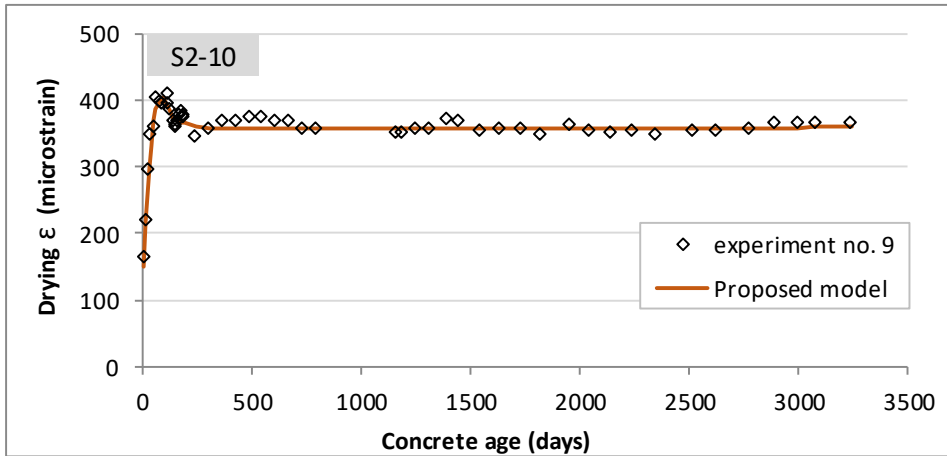


Figure 4.21 Proposed composite model predicted and actual drying shrinkage (microstrain) for Experiment 9 of data Subset S2-10 (> 1% SP).

#### 4.3.5 Proposed model for Subset S2-12

Functions for the three segments of the average shrinkage data for Subset S2-10 are given in Equation 4.27, Equation 4.28 and Equation 4.29 where  $t$  is the concrete age in days and  $f_x$  is the shrinkage in microstrains.

$$f_{a+b} = 135t^{0.265} \quad (\text{for } 0 > t < 130) \quad (4.27)$$

$$f_c = 612.5t^{-0.078} \quad (\text{for } 130 > t < 300) \quad (4.28)$$

$$f_d = -0.0051t + 408.41 \quad (\text{for } t > 300) \quad (4.29)$$

Combining  $f_{a+b}$  and  $f_c$  resulted in the function  $F_1$  given in Equation 4.30.

$$F_1 = f_c + \frac{f_{a+b} - f_c}{\left[1 + \left(\frac{t}{130}\right)^{-50}\right]^{0.03}} \quad (\text{for } 0 > t < 300) \quad (4.30)$$

The final proposed composite model for data Subset S2-09 is then obtained as the combination of  $F_1$  and  $f_d$ , Equation 4.31.

$$\varepsilon_{ds}(t) = f_d + \frac{F_1 - f_d}{\left[1 + \left(\frac{t}{300}\right)^{-12}\right]^{0.2}} \quad (4.31)$$

Figure 4.22 and Figure 4.23 show shrinkage profile plots for Equation 4.31 and the experimental values from Experiments 17 and 25 of data Subset S2-12 (< 1% SP, < 0.5% P), respectively.

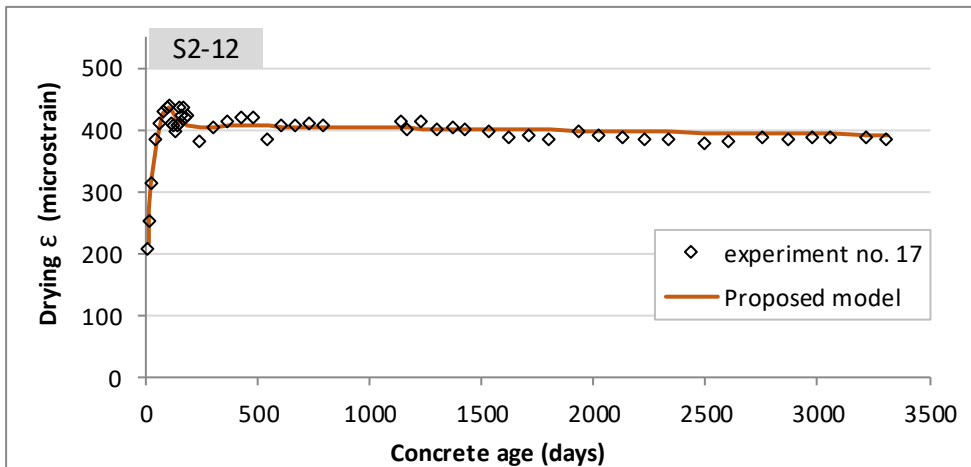


Figure 4.22 Proposed composite model predicted and actual drying shrinkage (microstrain) for Experiment 17 of data Subset S2-12 (< 1% SP, < 0.5% P).

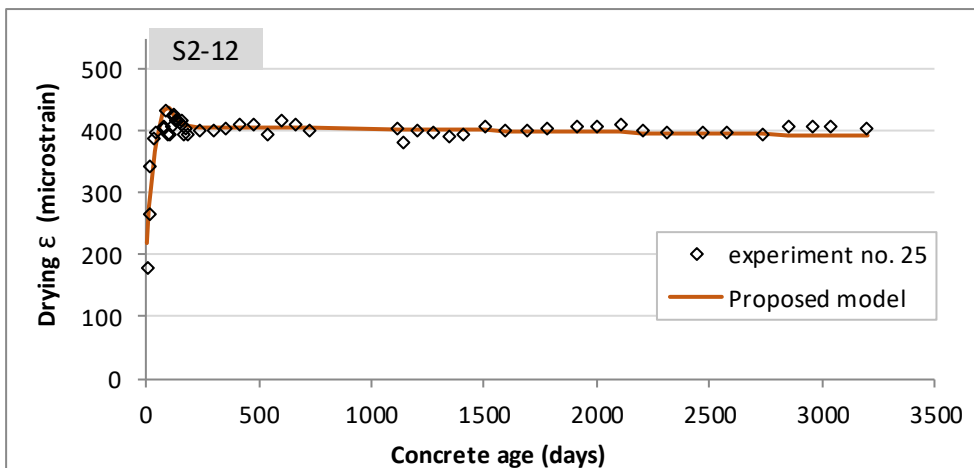


Figure 4.23 Proposed composite model predicted and actual drying shrinkage (microstrain) for Experiment 25 of data Subset S2-12 (< 1% SP, < 0.5% P).

## 4.4 Validation of modified shrinkage functions

Data from six (6) experiments in Dataset 1-HSC and four (4) experiments in Dataset 2-HSC, none of which were used in modifying any of the models, were used to validate the modified models. These six experiments were randomly selected from data subsets that included four (4) or more experiments, to ensure sufficient data remained for meaningful model calibration.

### 4.4.1 Dataset 1-HSC results

Figure 4. to Figure 4.29 show plots of the experimental and predicted drying shrinkage strains for the six listed experiments to follow. In some experiments, such as those seen in Figure 4. to Figure 4.27 curing occurred for relatively long periods. As drying shrinkage starts after curing, and occurs in drying conditions, the drying shrinkage predictions in these cases start only at the end of the curing time. Actual experimental shrinkage values, however, include also the measurements taken during the curing process. This explains the apparent “time shift” in the plots.

For drying shrinkage, data from the following experiments were used to validate the existing models:

Experiment number	Cement type	w/cm	Aggregate type	Additive
#0258	CEM I	0.40	sandstone	-
#0011	CEM I	0.41	dolerite	-
#0105	CEM I	0.41	andesite	-
#0231	CEM I	0.40	andesite	35% slag
14	CEM II	0.33	granite	0.6% SP, 1.5% SRA-E, 25% FA & 5% SF
20	CEM I	0.33	granite	0.4% SP, 0.2% P, 1.5% SRA-E, 25% FA & 5% SF

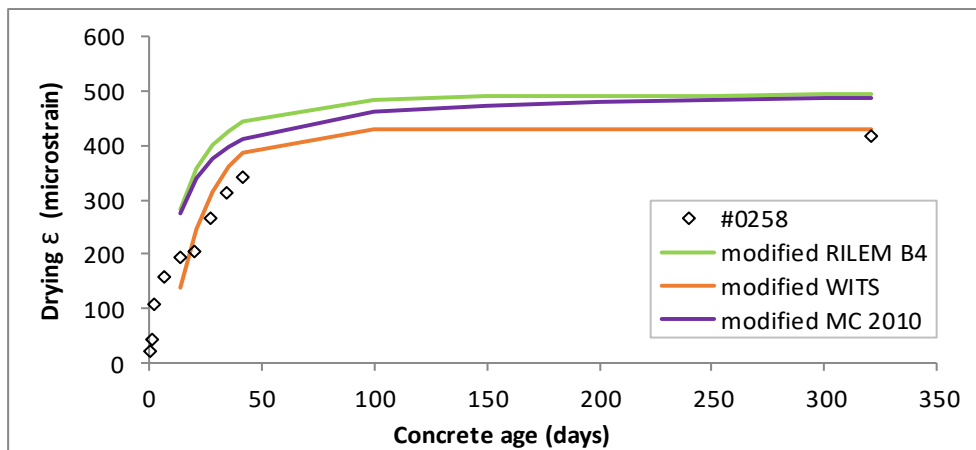


Figure 4.24 Modified model prediction and actual drying shrinkage (microstrain) for Experiment #0258.

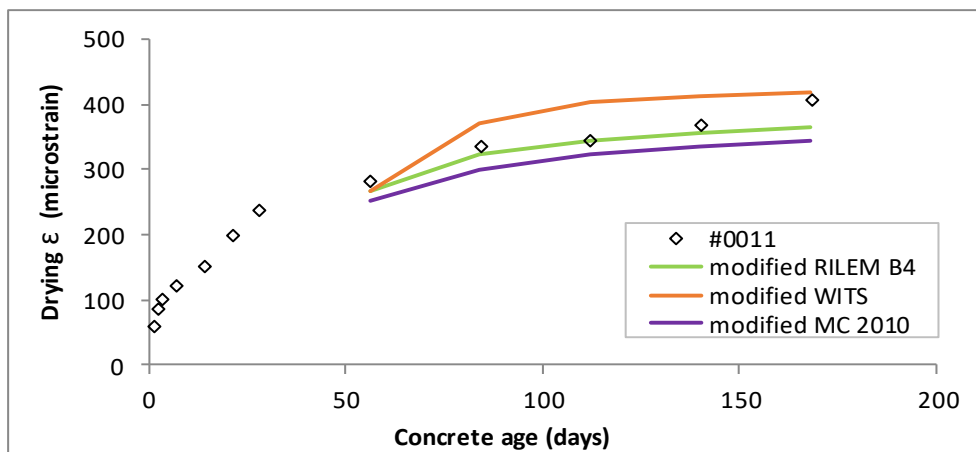


Figure 4.25 Modified model prediction and actual drying shrinkage (microstrain) for Experiment #0011.

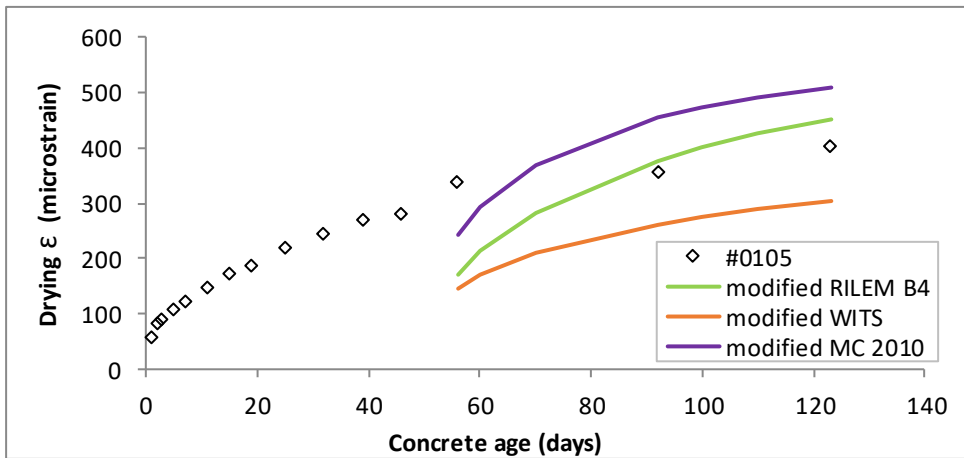


Figure 4.26 Modified model prediction and actual drying shrinkage (microstrain) for Experiment #0105.

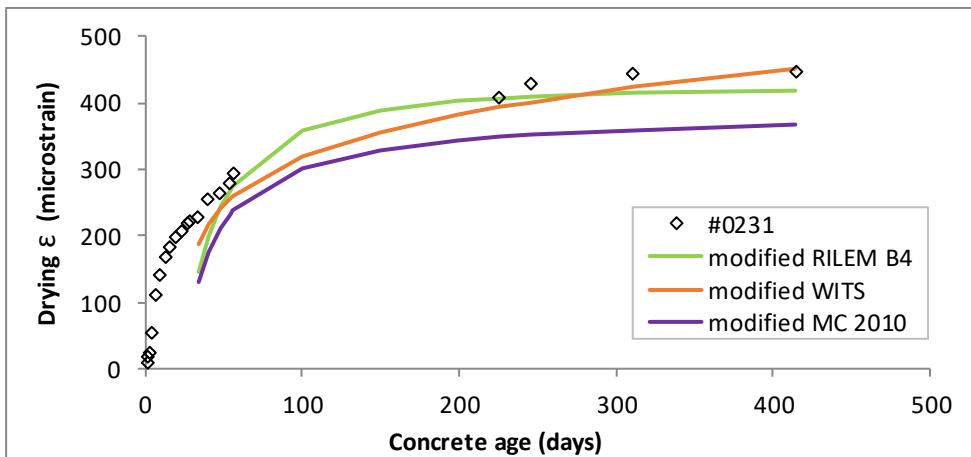


Figure 4.27 Modified model prediction and actual drying shrinkage (microstrain) for Experiment #0231.

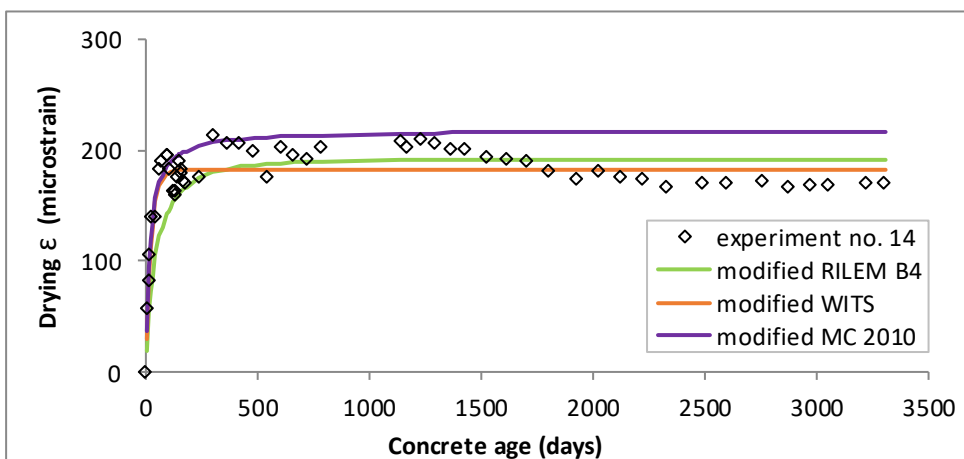


Figure 4.28 Modified model prediction and actual drying shrinkage (microstrain) for Experiment 14.

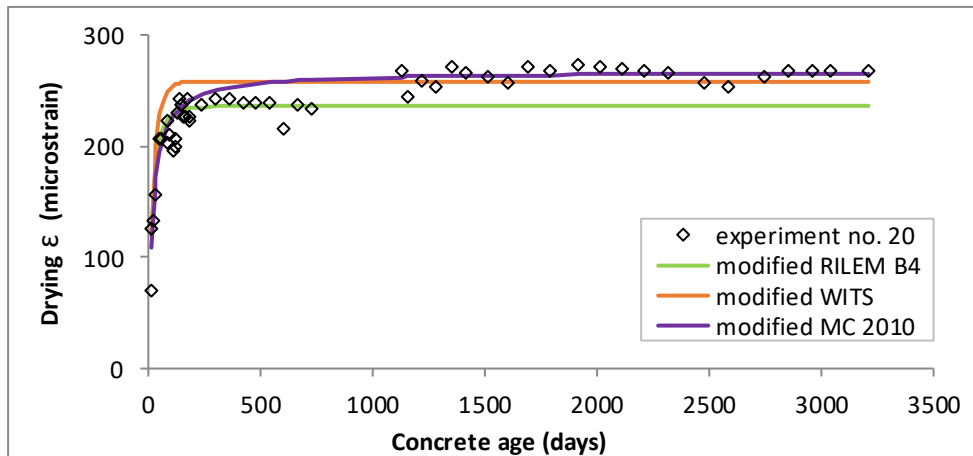


Figure 4.29 Modified model prediction and actual drying shrinkage (microstrain) for Experiment 20.

#### 4.4.2 Dataset 2-HSC results

For autogenous shrinkage, data from the following experiments were used to validate the existing models:

Experiment number	Cement type	w/cm	Aggregate type	Additive
A-068_16	CEM I	0.31	granite	< 0.5% P
A_086_19	CEM I	0.31	granite	1% SP
A_086_25	CEM II	0.28	quartzite	1% SP
A_086_35	CEM II	0.28	granite	2% SP

Figure 4.30 to Figure 4.33 show plots of the experimental and predicted drying shrinkage strains for the four experiments listed previously.

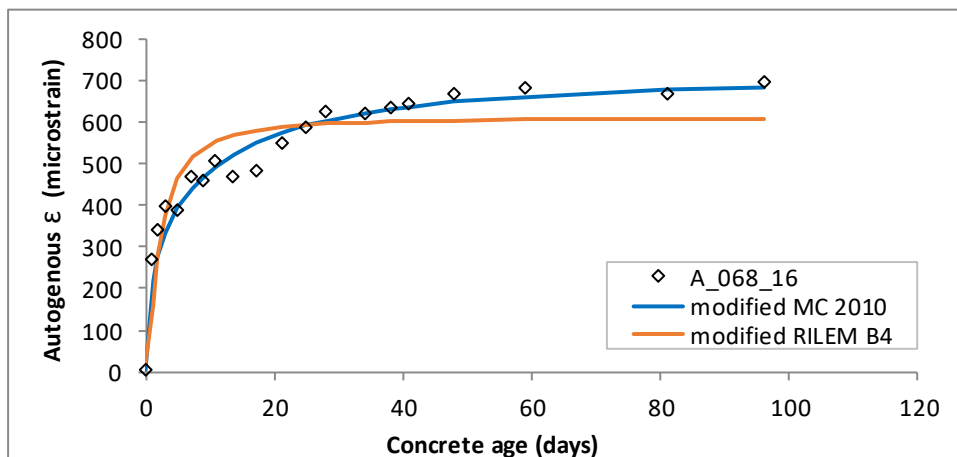


Figure 4.30 Modified model prediction and actual autogenous shrinkage (microstrain) for Experiment A\_068\_16.

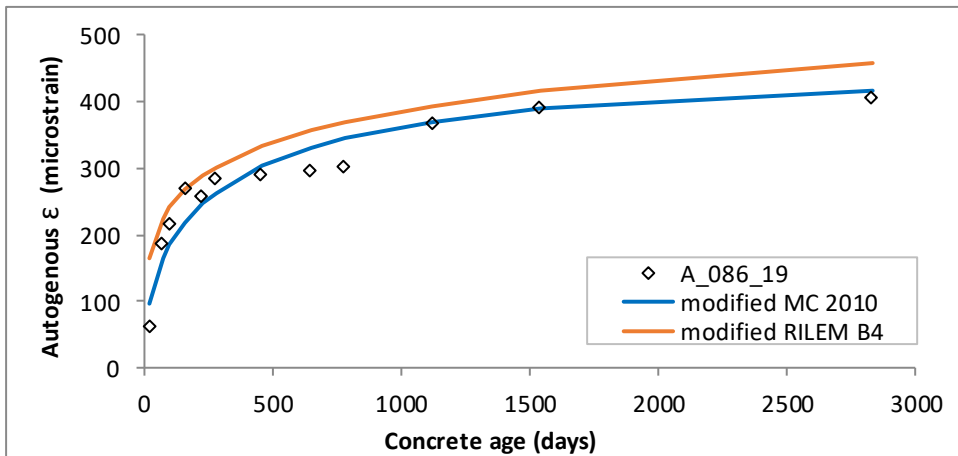


Figure 4.31 Modified model prediction and actual autogenous shrinkage (microstrain) for Experiment A\_086\_19.

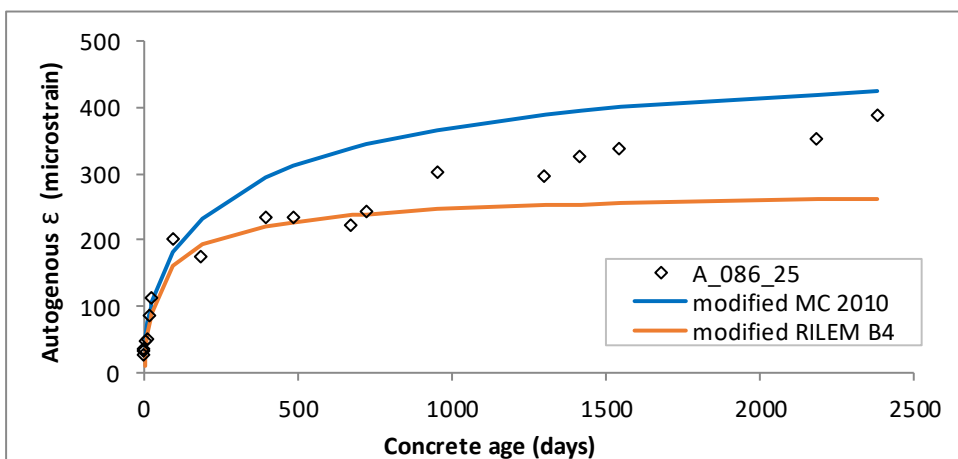


Figure 4.32 Modified model prediction and actual autogenous shrinkage (microstrain) for Experiment A\_086\_25.

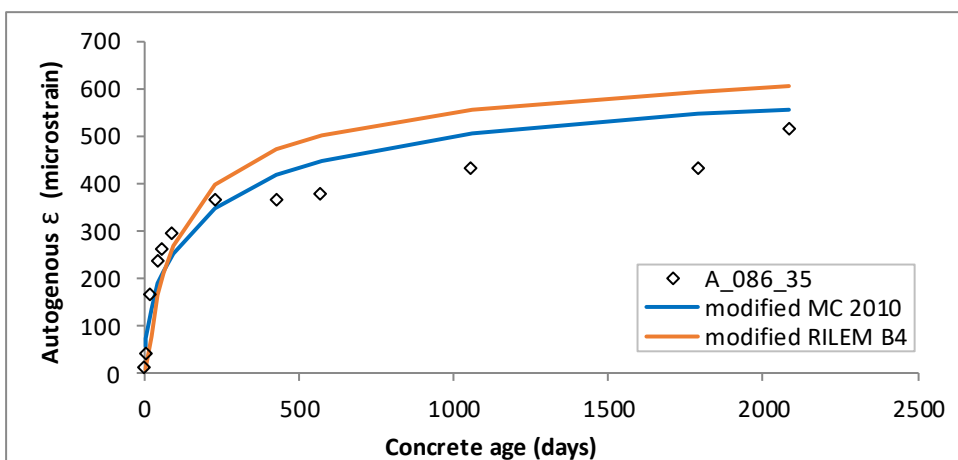


Figure 4.33 Modified model prediction and actual autogenous shrinkage (microstrain) for Experiment A\_086\_35.

## 4.5 Ranking model results

The performances of the original and modified versions of the existing shrinkage prediction models, as well as the proposed composite models, were ranked using the statistical indicators RMSE,  $R^2_{adj}$  and AIC for each experiment in the different data subsets. These rankings are based on each model's performance over the entire experiment duration. Examples of these rankings are given in Table 4.18 to Table 4.20, Table 4.24 and Table 4.25. All the calculated statistical indicators for each experiment are tabulated in Appendix C.

The performances of the models over each of the shrinkage time ranges (0 to 99, 100 to 199, 200 to 499 and 500 days or more) were also ranked, using the statistical indicators RMSE,  $R^2_{adj}$  and C.o.V, for each experiment in the different data subsets. Examples of these rankings are given in Table 4.21 to Table 4.23, Table 4.26 to Table 4.28. All the calculated statistical indicators, per shrinkage time range, for each experiment are tabulated in Appendix D.

### 4.5.1 Model performance for drying shrinkage per subset

Table 4.18, Table 4.19 and Table 4.20 give some example rankings of the original and modified RILEM B4, MC 2010 and WITS models for drying shrinkage data Subsets S1-03 (without admixture), S2-02 (with mineral admixtures) and S2-08 (with chemical admixtures). The rankings for the new composite model are included for S2-08 as well. Model rankings for all the data subsets are given in Appendix HH (CPUT Library Repository, 2020(b)).

Table 4.18 Ranking of the RILEM B4, MC 2010 and WITS models for data Subset S1-03 (Dataset 1-HSC).

S1-03	ORIGINAL MODEL			S1-03	MODIFIED MODEL		
	RILEM B4	MC 2010	WITS		RILEM B4	MC 2010	WITS
RMSE	118.55	84.75	74.54	RMSE	61.01	53.71	43.70
Rank <sub>RMSE</sub>	3	2	1	Rank <sub>RMSE</sub>	3	2	1
$R^2$	0.23	0.72	0.79	$R^2$	0.79	0.89	0.92
$R^2_{adj}$	0.00	0.49	0.61	$R^2_{adj}$	0.73	0.80	0.86
Rank <sub>R<sup>2</sup><sub>adj</sub></sub>	3	2	1	Rank <sub>R<sup>2</sup><sub>adj</sub></sub>	3	2	1
AIC <sub>c</sub>	72.3	96.2	94.8	AIC <sub>c</sub>	66.2	91.2	90.1
$\Delta_{aic}$	0.0	23.9	22.5	$\Delta_{aic}$	0.0	25.0	23.9
$e^{(-0.5\Delta_i)}$	1.0	0.0	0.0	$e^{(-0.5\Delta_i)}$	1.0	0.0	0.0
ER <sub>i</sub> (best/model i)	1.0	155791.1	76844.1	ER <sub>i</sub> (best/model i)	1.0	263377.1	151068.2
w <sub>i</sub>	1.0000	0.0000	0.00001	w <sub>i</sub>	1.0000	0.0000	0.00001
Rank <sub><math>\Delta_{aic}</math></sub>	1	Discard (3)	Discard (2)	Rank <sub><math>\Delta_{aic}</math></sub>	1	Discard (3)	Discard (2)

Table 4.19 Ranking of the RILEM B4, MC 2010 and WITS models for data Subset S2-02 (Dataset 1-HSC).

S2-02	ORIGINAL MODEL			S2-02	MODIFIED MODEL		
	RILEM B4	MC 2010	WITS		RILEM B4	MC 2010	WITS
RMSE	96.06	60.93	82.11	RMSE	41.35	42.40	26.15
Rank <sub>RMSE</sub>	3	1	2	Rank <sub>RMSE</sub>	2	3	1
R <sup>2</sup>	0.07	0.57	0.28	R <sup>2</sup>	0.80	0.82	0.94
R <sup>2</sup> <sub>adj</sub>	-0.03	0.46	0.09	R <sup>2</sup> <sub>adj</sub>	0.78	0.77	0.92
Rank <sub>R<sup>2</sup><sub>adj</sub></sub>	3	1	2	Rank <sub>R<sup>2</sup><sub>adj</sub></sub>	2	3	1
AIC <sub>c</sub>	103.34	97.34	104.03	AIC <sub>c</sub>	85.46	90.36	80.36
$\Delta_{aic}$	6.01	0.00	6.69	$\Delta_{aic}$	5.10	10.00	0.00
$e^{(-0.5\Delta_i)}$	0.05	1.00	0.04	$e^{(-0.5\Delta_i)}$	0.08	0.01	1.00
ER <sub>i</sub> (best/model i)	20.16	1.00	28.43	ER <sub>i</sub> (best/model i)	12.78	148.25	1.00
w <sub>i</sub>	0.0457	0.9219	0.0324	w <sub>i</sub>	0.0721	0.0062	0.9217
Rank <sub><math>\Delta_{aic}</math></sub>	2	1	3	Rank <sub><math>\Delta_{aic}</math></sub>	2	3	1

Table 4.20 Ranking of the RILEM B4, MC 2010 and WITS models for data Subset S2-08 (Dataset 1-HSC ).

S2-08	ORIGINAL MODEL			S2-08	PROPOSED & MODIFIED MODEL			
	RILEM B4	MC 2010	WITS		RILEM B4	MC 2010	WITS	NEW
RMSE	73.53	247.41	46.94	RMSE	20.82	22.87	20.39	13.24
Rank <sub>RMSE</sub>	2	3	1	Rank <sub>RMSE</sub>	3	4	2	1
R <sup>2</sup>	-7.41	-91.76	-2.40	R <sup>2</sup>	0.33	0.21	0.37	0.85
R <sup>2</sup> <sub>adj</sub>	-7.58	-95.71	-2.54	R <sup>2</sup> <sub>adj</sub>	0.31	0.17	0.34	0.85
Rank <sub>R<sup>2</sup><sub>adj</sub></sub>	2	3	1	Rank <sub>R<sup>2</sup><sub>adj</sub></sub>	3	4	2	1
AIC <sub>c</sub>	434.06	556.89	389.87	AIC <sub>c</sub>	307.99	318.74	307.24	269.03
$\Delta_{aic}$	44.18	167.02	0.00	$\Delta_{aic}$	38.96	49.71	38.21	0.00
$e^{(-0.5\Delta_i)}$	0.00	0.00	1.00	$e^{(-0.5\Delta_i)}$	0.00	0.00	0.00	1.00
ER <sub>i</sub> (best/model i)	3.93E+09	1.85E+36	1.00	ER <sub>i</sub> (best/model i)	2.88E+08	6.21E+10	1.98E+08	1.00000
w <sub>i</sub>	0.0000	0.0000	1.0000	w <sub>i</sub>	0.0000	0.0000	0.0000	1.0000
Rank <sub><math>\Delta_{aic}</math></sub>	Discard (2)	Discard (3)	1	Rank <sub><math>\Delta_{aic}</math></sub>	Discard (3)	Discard (4)	Discard (2)	1

#### 4.5.2 Model performances for time ranges 0 to 99, 100 to 199, 200 to 499 and 500 days or more (drying shrinkage).

Table 4.21, Table 4.22 and Table 4.23 give some example rankings, for drying shrinkage over the time ranges 0 to 99, 100 to 199, 200 to 499 and 500 days or more, of the original and modified RILEM B4, MC 2010 and WITS models for data Subsets S1-03 (without admixture), S2-02 (with mineral admixtures) and S2-08 (with chemical admixtures). Model rankings per shrinkage term for each data subset are given in Appendix II (CPUT Library Repository, 2020(b)).



Table 4.21 Ranking of the RILEM B4, MC 2010 and WITS models for data Subset S1-03 (Dataset 1-HSC) over the time range 0 to 99 days.

0-99 DAYS	S1-03			0-99 DAYS	S1-03		
	original RILEM B4	original MC 2010	original WITS		modified RILEM B4	modified MC 2010	modified WITS
RMSE	49.13	59.39	35.70	RMSE	42.99	38.22	31.33
Rank <sub>RMSE</sub>	2	3	1	Rank <sub>RMSE</sub>	3	2	1
R <sup>2</sup> <sub>adj</sub>	0.54	-0.13	0.61	R <sup>2</sup> <sub>adj</sub>	0.67	0.52	0.70
Rank <sub>R<sup>2</sup><sub>adj</sub></sub>	2	3	1	Rank <sub>R<sup>2</sup><sub>adj</sub></sub>	2	3	1
C.O.V	0.10	0.13	0.11	C.O.V	0.11	0.13	0.10
Rank <sub>C.O.V</sub>	1	3	2	Rank <sub>C.O.V</sub>	2	3	1

Table 4.22 Ranking of the RILEM B4, MC 2010 and WITS models for data Subset S2-02 (Dataset 1-HSC) over the time ranges 0 to 99, 100 to 199 and 200 to 499 days.

0-99 DAYS	S2-02			0-99 DAYS	S2-02		
	original RILEM B4	original MC 2010	original WITS		modified RILEM B4	modified MC 2010	modified WITS
RMSE	77.00	40.74	66.74	RMSE	41.71	37.31	23.89
Rank <sub>RMSE</sub>	3	1	2	Rank <sub>RMSE</sub>	3	2	1
R <sup>2</sup> <sub>adj</sub>	-0.37	0.32	-0.79	R <sup>2</sup> <sub>adj</sub>	0.46	0.44	0.82
Rank <sub>R<sup>2</sup><sub>adj</sub></sub>	2	1	3	Rank <sub>R<sup>2</sup><sub>adj</sub></sub>	2	3	1
C.O.V	0.34	0.18	0.30	C.O.V	0.19	0.17	0.11
Rank <sub>C.O.V</sub>	3	1	2	Rank <sub>C.O.V</sub>	3	2	1

100-199 DAYS	S2-02			100-199 DAYS	S2-02		
	original RILEM B4	original MC 2010	original WITS		modified RILEM B4	modified MC 2010	modified WITS
RMSE	123.84	83.39	104.26	RMSE	34.60	36.38	16.91
Rank <sub>RMSE</sub>	3	1	2	Rank <sub>RMSE</sub>	2	3	1
C.O.V	0.34	0.23	0.28	C.O.V	0.09	0.10	0.05
Rank <sub>C.O.V</sub>	3	1	2	Rank <sub>C.O.V</sub>	2	3	1

200-499 DAYS	S2-02			200-499 DAYS	S2-02		
	original RILEM B4	original MC 2010	original WITS		modified RILEM B4	modified MC 2010	modified WITS
RMSE	92.42	68.47	62.83	RMSE	18.29	26.02	20.66
Rank <sub>RMSE</sub>	3	2	1	Rank <sub>RMSE</sub>	1	3	2
R <sup>2</sup> <sub>adj</sub>	0.37	0.68	0.39	R <sup>2</sup> <sub>adj</sub>	0.93	0.80	0.95
Rank <sub>R<sup>2</sup><sub>adj</sub></sub>	3	1	2	Rank <sub>R<sup>2</sup><sub>adj</sub></sub>	2	3	1
C.O.V	0.22	0.16	0.15	C.O.V	0.04	0.06	0.05
Rank <sub>C.O.V</sub>	3	2	1	Rank <sub>C.O.V</sub>	1	3	2

Table 4.23 Ranking of the RILEM B4, MC 2010, WITS and composite models for data Subset S2-08 (Dataset 1-HSC) over the time ranges 0 to 99, 100 to 199 and 200 to 499 days and 500 days or more.

0-99 DAYS	S2-08			0-99 DAYS	S2-08			
	original RILEM B4	original MC 2010	original WITS		modified RILEM B4	modified MC 2010	modified WITS	NEW
RMSE	86.55	63.45	36.51	RMSE	29.66	35.85	27.17	19.00
Rank <sub>RMSE</sub>	3	2	1	Rank <sub>RMSE</sub>	3	4	2	1
R <sup>2</sup> <sub>adj</sub>	-2.56	-1.35	0.13	R <sup>2</sup> <sub>adj</sub>	0.59	0.25	0.57	0.90
Rank <sub>R2adj</sub>	3	2	1	Rank <sub>R2adj</sub>	2	4	3	1
C.O.V	0.39	0.29	0.16	C.O.V	0.13	0.16	0.12	0.09
Rank <sub>C.O.V</sub>	3	2	1	Rank <sub>C.O.V</sub>	3	4	2	1

100-199 DAYS	S2-08			100-199 DAYS	S2-08			
	original RILEM B4	original MC 2010	original WITS		modified RILEM B4	modified MC 2010	modified WITS	NEW
RMSE	29.57	163.25	26.78	RMSE	23.07	25.51	22.65	16.31
Rank <sub>RMSE</sub>	2	3	1	Rank <sub>RMSE</sub>	3	4	2	1
R <sup>2</sup> <sub>adj</sub>	-0.53	-52.17	-0.46	R <sup>2</sup> <sub>adj</sub>	0.05	-0.31	-0.05	0.73
Rank <sub>R2adj</sub>	2	3	1	Rank <sub>R2adj</sub>	2	4	3	1
C.O.V	0.117	0.649	0.106	C.O.V	0.092	0.101	0.090	0.065
Rank <sub>C.O.V</sub>	2	3	1	Rank <sub>C.O.V</sub>	3	4	2	1

200-499 DAYS	S2-08			200-499 DAYS	S2-08			
	original RILEM B4	original MC 2010	original WITS		modified RILEM B4	modified MC 2010	modified WITS	NEW
RMSE	43.11	232.42	39.54	RMSE	11.17	10.36	11.10	12.34
Rank <sub>RMSE</sub>	2	3	1	Rank <sub>RMSE</sub>	3	1	2	4
R <sup>2</sup> <sub>adj</sub>	-22.09	-948.48	-29.18	R <sup>2</sup> <sub>adj</sub>	-0.19	-0.52	-0.76	-0.64
Rank <sub>R2adj</sub>	1	3	2	Rank <sub>R2adj</sub>	1	2	4	3
C.O.V	0.18	0.98	0.17	C.O.V	0.05	0.04	0.05	0.05
Rank <sub>C.O.V</sub>	2	3	1	Rank <sub>C.O.V</sub>	3	1	2	4

≥ 500 DAYS	S2-08			≥ 500 DAYS	S2-08			
	original RILEM B4	original MC 2010	original WITS		modified RILEM B4	modified MC 2010	modified WITS	NEW
RMSE	82.13	287.36	53.07	RMSE	17.03	17.18	17.00	8.18
Rank <sub>RMSE</sub>	2	3	1	Rank <sub>RMSE</sub>	3	4	2	1
R <sup>2</sup> <sub>adj</sub>	-32.34	-426.26	-13.45	R <sup>2</sup> <sub>adj</sub>	-0.450	-0.517	-0.500	0.39
Rank <sub>R2adj</sub>	2	3	1	Rank <sub>R2adj</sub>	2	4	3	1
C.O.V	0.368	1.287	0.238	C.O.V	0.076	0.077	0.076	0.04
Rank <sub>C.O.V</sub>	2	3	1	Rank <sub>C.O.V</sub>	3	4	2	1

### 4.5.3 Model performance for autogenous shrinkage per subset

Table 4.24 and Table 4.25 give an idea of the relative performance of the RILEM B4 and MC 2010 models in predicting autogenous shrinkage for data Subsets S2-02a and S2-09a (with chemical admixtures). Model rankings for each data subset are given in Appendix JJ (CPUT Library Repository, 2020(b)).

Table 4.24 Ranking of the RILEM B4 and MC 2010 models for data Subset S2-02a (Dataset 2-HSC).

S2-02a	ORIGINAL MODEL		S2-02a	MODIFIED MODEL	
	RILEM B4	MC 2010		RILEM B4	MC 2010
RMSE	287.80	93.15	RMSE	27.266	25.706
Rank <sub>RMSE</sub>	2	1	Rank <sub>RMSE</sub>	2	1
R <sup>2</sup>	-19.12	-3.34	R <sup>2</sup>	0.76	0.75
R <sup>2</sup> <sub>adj</sub>	-20.78	-3.71	R <sup>2</sup> <sub>adj</sub>	0.74	0.73
Rank <sub>R2adj</sub>	2	1	Rank <sub>R2adj</sub>	1	2
AIC <sub>c</sub>	318.03	251.23	AIC <sub>c</sub>	185.14	181.08
Δ <sub>aic</sub>	66.79	0.00	Δ <sub>aic</sub>	4.06	0.00
e <sup>(-0.5Δ<sub>i</sub>)</sup>	0.00	1.00	e <sup>(-0.5Δ<sub>i</sub>)</sup>	0.13	1.00
ER <sub>i</sub> (best/model i)	3.19E+14	1.00E+00	ER <sub>i</sub> (best/model i)	7.61E+00	1.00E+00
w <sub>i</sub>	0.0000	1.0000	w <sub>i</sub>	0.1161	0.8839
Rank <sub>Δaic</sub>	Discard (2)	1	Rank <sub>Δaic</sub>	2	1

Table 4.25 Ranking of the RILEM B4 and MC 2010 models for data Subset S2-09a (Dataset 2-HSC).

S2-09a	ORIGINAL MODEL		S2-09a	MODIFIED MODEL	
	RILEM B4	MC 2010		original RILEM B4	modified MC 2010
RMSE	59.12	327.39	RMSE	59.12	61.95
Rank <sub>RMSE</sub>	1	2	Rank <sub>RMSE</sub>	1	2
R <sup>2</sup>	0.29	-29.79	R <sup>2</sup>	0.29	0.22
R <sup>2</sup> <sub>adj</sub>	0.17	-32.915	R <sup>2</sup> <sub>adj</sub>	0.17	0.072
Rank <sub>R2adj</sub>	1	2	Rank <sub>R2adj</sub>	1	2
AIC <sub>c</sub>	160.16	235.61	AIC <sub>c</sub>	160.16	158.73
Δ <sub>aic</sub>	0.00	75.45	Δ <sub>aic</sub>	1.43	0.00
e <sup>(-0.5Δ<sub>i</sub>)</sup>	1.00	0.00	e <sup>(-0.5Δ<sub>i</sub>)</sup>	0.49	1.00
ER <sub>i</sub> (best/model i)	1.00E+00	2.42E+16	ER <sub>i</sub> (best/model i)	2.05E+00	1.00E+00
w <sub>i</sub>	1.0000	0.0000	w <sub>i</sub>	0.3281	0.6719
Rank <sub>Δaic</sub>	1	Discard (2)	Rank <sub>Δaic</sub>	2	1

It was unnecessary to update the original RILEM B4 model parameters for Subset S2-09a as the original model already fitted these data optimally. In Table 4.25 it can be seen that the original RILEM B4 outperforms the modified MC 2010 for the statistical indicators RMSE and R<sup>2</sup><sub>adj</sub>.

#### 4.5.4 Model performances for time ranges 0 to 99, 100 to 199, 200 to 499 and 500 days or more (autogenous shrinkage).

Table 4.26, Table 4.27 and Table 4.28 give some example rankings, for autogenous shrinkage over the time ranges 0 to 99, 100 to 199 and 200 to 499 days, of the original and modified RILEM B4 and MC 2010 models for data Subsets S2-02a and S2-09a, both with chemical admixtures. Model rankings per shrinkage term for each data subset are given in Appendix KK (CPUT Library Repository, 2020(b)).

Table 4.26 Ranking of the RILEM B4 and MC 2010 models for data Subset S2-02a (Dataset 2-HSC) over the time ranges 0 to 99 and 100 to 199 days.

0-99 DAYS	S2-02a		0-99 DAYS	S2-02a	
	original RILEM B4	original MC 2010		modified RILEM B4	modified MC 2010
RMSE	247.93	98.15	RMSE	22.97	23.18
Rank <sub>RMSE</sub>	2	1	Rank <sub>RMSE</sub>	1	2
R <sup>2</sup> <sub>adj</sub>	-15.53	-2.86	R <sup>2</sup> <sub>adj</sub>	0.76	0.80
Rank <sub>R2adj</sub>	2	1	Rank <sub>R2adj</sub>	2	1
C.O.V	0.632	0.250	C.O.V	0.059	0.059
Rank <sub>C.o.v</sub>	2	1	Rank <sub>C.o.v</sub>	1	2

100-199 DAYS	S2-02a		100-199 DAYS	S2-02a	
	original RILEM B4	original MC 2010		modified RILEM B4	modified MC 2010
RMSE	337.74	106.50	RMSE	23.36	24.25
Rank <sub>RMSE</sub>	2	1	Rank <sub>RMSE</sub>	1	2
R <sup>2</sup> <sub>adj</sub>	-83.98	-3.33	R <sup>2</sup> <sub>adj</sub>	0.68	0.67
Rank <sub>R2adj</sub>	2	1	Rank <sub>R2adj</sub>	1	2
C.O.V	0.735	0.232	C.O.V	0.051	0.053
Rank <sub>C.o.v</sub>	2	1	Rank <sub>C.o.v</sub>	1	2

Table 4.27 Ranking of the RILEM B4 and MC 2010 models for data Subset S2-09a (Dataset 2-HSC) over the time ranges 0 to 99 days.

0-99 DAYS	S2-09a		0-99 DAYS	S2-09a	
	original RILEM B4	original MC 2010		original RILEM B4	modified MC 2010
RMSE	54.39	254.27	RMSE	54.39	60.08
Rank <sub>RMSE</sub>	1	2	Rank <sub>RMSE</sub>	1	2
R <sup>2</sup> <sub>adj</sub>	0.25	-17.33	R <sup>2</sup> <sub>adj</sub>	0.25	0.03
Rank <sub>R2adj</sub>	1	2	Rank <sub>R2adj</sub>	1	2
C.O.V	0.358	1.671	C.O.V	0.358	0.395
Rank <sub>C.o.v</sub>	1	2	Rank <sub>C.o.v</sub>	1	2

Table 4.28 Ranking of the RILEM B4 and MC 2010 models for data Subset S2-09a (Dataset 2-HSC) over the time ranges 100 to 199 and 200 to 499 days.

100-199 DAYS	S2-09a		100-199 DAYS	S2-09a	
	original RILEM B4	original MC 2010		original RILEM B4	modified MC 2010
RMSE	27.72	397.06	RMSE	27.72	34.17
Rank <sub>RMSE</sub>	1	2	Rank <sub>RMSE</sub>	1	2
R <sup>2</sup> <sub>adj</sub>	-1.46	-415.06	R <sup>2</sup> <sub>adj</sub>	-1.46	-1.13
Rank <sub>R<sup>2</sup><sub>adj</sub></sub>	1	2	Rank <sub>R<sup>2</sup><sub>adj</sub></sub>	2	1
C.O.V	0.171	1.841	C.O.V	0.171	0.158
Rank <sub>C.O.V</sub>	1	2	Rank <sub>C.O.V</sub>	2	1

200-499 DAYS	S2-09a		200-499 DAYS	S2-09a	
	original RILEM B4	original MC 2010		original RILEM B4	modified MC 2010
RMSE	33.10	420.55	RMSE	33.10	24.22
Rank <sub>RMSE</sub>	1	2	Rank <sub>RMSE</sub>	2	1
R <sup>2</sup> <sub>adj</sub>	-0.02	-94.81	R <sup>2</sup> <sub>adj</sub>	-0.02	0.82
Rank <sub>R<sup>2</sup><sub>adj</sub></sub>	1	2	Rank <sub>R<sup>2</sup><sub>adj</sub></sub>	2	1
C.O.V	0.142	1.808	C.O.V	0.142	0.104
Rank <sub>C.O.V</sub>	1	2	Rank <sub>C.O.V</sub>	2	1

As mentioned previously, it was not necessary to update the RILEM B4 model parameters for Subset S2-09a as the original model already fitted these data optimally. In Table 4.27 it can be seen that the original RILEM B4 out performs the modified MC 2010 for shrinkage time range 0 to 99 days only.

#### 4.6 Shrinkage prediction performance for the RILEM B4, MC 2010 and WITS models within their covariate limits.

As mentioned before, Datasets 3, 4 and 5 include data only from the experiments that are applicable to (i.e. that fall within the covariate ranges for which the models were developed) the RILEM B4, MC 2010 and WITS models, respectively. All the autogenous and drying shrinkage predictions for these datasets are given in Appendices CC to GG (CPUT Library Repository, 2020(b)). The experiments in each dataset were grouped according to the region where the experiment was conducted, the year in which the experimental data were published and the 28<sup>th</sup> day compressive strength ( $f_{cm28}$ ). RMSE and C.o.V values were calculated for each drying and autogenous shrinkage experiment over the entire duration and the C.o.V values were calculated per shrinkage time range. This data can be found tabulated in Appendix D.

All three models exhibited a considerably larger C.o.V for short-term shrinkage (0 to 99 days) compared to their values for the rest of the shrinkage time ranges, for both drying and autogenous shrinkage. The reasons for this are not obvious from the information available.

#### 4.6.1 RILEM B4 predictions for Dataset 3

Dataset 3 includes 69 drying and 31 autogenous shrinkage experiments. Figure 4.34 shows the mean C.o.V for drying and autogenous shrinkage for the data in each time range.

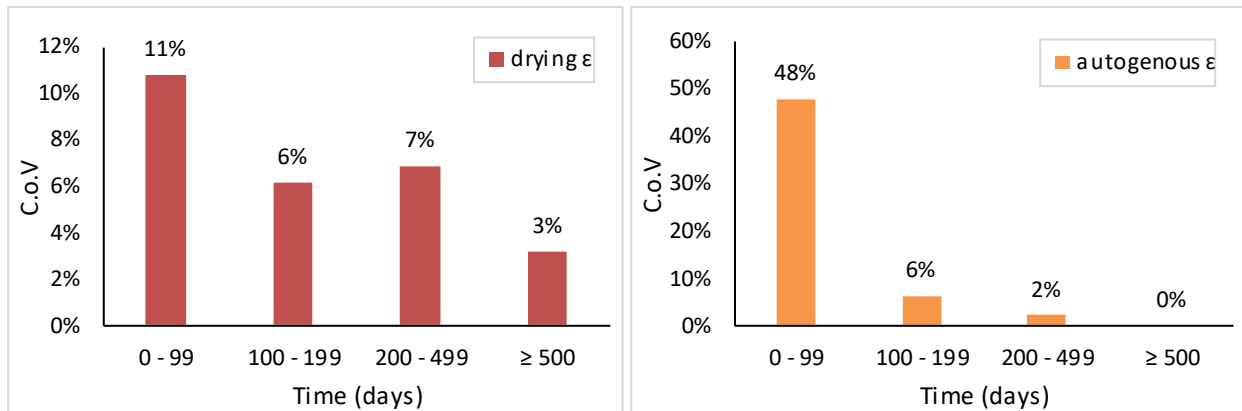


Figure 4.34 RILEM B4 overall mean C.o.V for drying (left) and autogenous (right) shrinkage - Dataset 3.

#### 4.6.2 MC 2010 predictions for Dataset 4

In doing predictions with the MC 2010 model, all known curing temperatures were taken as 'normal temperatures' as this is a requirement according to CEB-FIP (2012). Dataset 4 considers only CEM I, CEM II and CEM III with FA and SF. It does not include any data for CEM II type cement with pozzolanic additives. This dataset includes 85 drying and 152 autogenous shrinkage experiments. Figure 4.35 shows the mean C.o.V for the data in each drying and autogenous shrinkage time range.

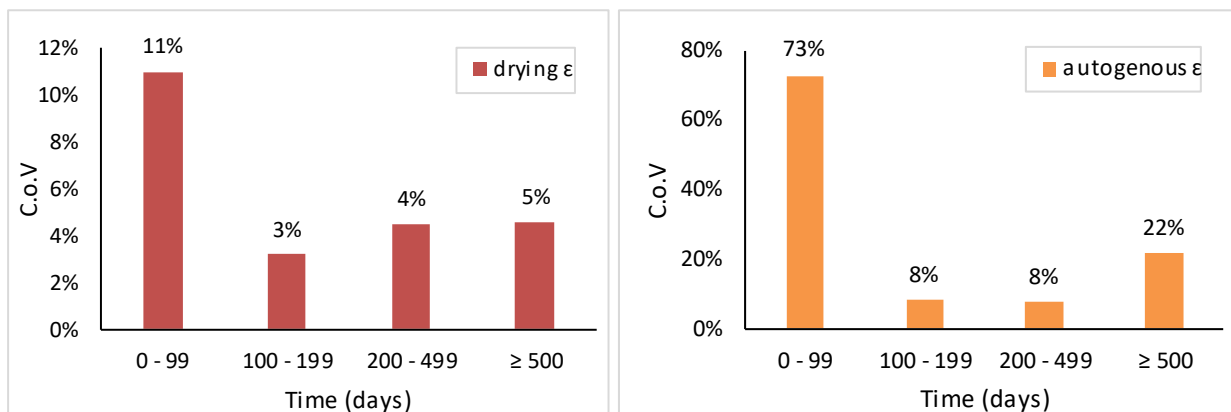


Figure 4.35 MC 2010 overall mean C.o.V for drying (left) and autogenous (right) shrinkage - Dataset 4.

#### 4.6.3 WITS model predictions for Dataset 5

Dataset 5 includes only 66 drying shrinkage experiments, all from the RSA database. Figure 4.36 shows the mean C.o.V for drying shrinkage for the data in each time range.

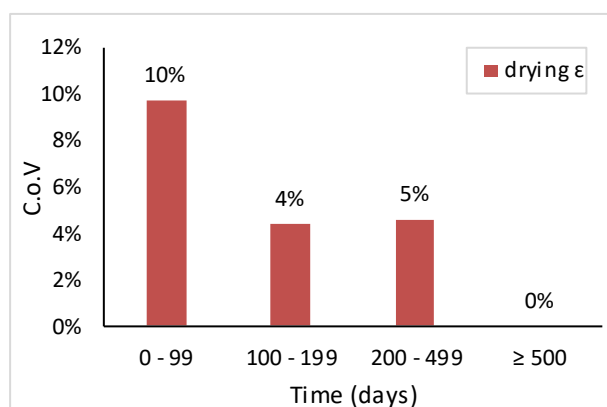


Figure 4.36 WITS model overall mean C.o.V for drying shrinkage - Dataset 5.

## 4.7 Results conclusion

Predictions using the original versions of the RILEM B4, MC 2010 and WITS models were made for the experiments included in Datasets 1-HSC, 2-HSC, 3, 4 and 5, which were extracted from the 2018 version NU database (Northwestern University, 2018), the technical report of Al-Manaseer and Fayyaz (2011) and the RSA database. Results from these predictions are given in this chapter.

Then, based on Dataset 1-HSC (drying shrinkage) and Dataset 2-HSC (autogenous shrinkage) these existing models were re-calibrated. The updated model parameters accounting for cement, aggregate and admixture types are presented for the derived data subsets, for both drying and autogenous shrinkage. Nineteen (19) data subsets were derived from Dataset 1-HSC and twelve (12) from Dataset 2-HSC. The modified models were validated against 10% of the experiments included in Dataset 1-HSC and Dataset 2-HSC, which were not used in modifying the models. The results for the all modified models for each “validation” experiment are also presented. For drying shrinkage (Dataset 1-HSC) Subsets S2-08, S2-09, S2-10 and S2-12, new composite models were proposed to simulate the early age shrinkage peak seen for these particular concrete compositions.

Predictions of the original and modified versions of the RILEM B4, MC 2010 and WITS models, as well as the composite models proposed in this study, for the experiments in the Datasets 1-HSC and 2-HSC, were compared. These comparisons were made for the entire shrinkage duration of each of the experiments using the statistical indicators RMSE,  $R^2_{adj}$  and AIC, and the models ranked accordingly (1 is best). Following this, the models were ranked by evaluating their performances over the specific time ranges (0 to 99 = short-term, 100 to 199 and 200 to 499 = medium-term and 500 days or more = long-term shrinkage), using the statistical indicators RMSE,  $R^2_{adj}$  and  $C.o.V_{all}$ . Sample rankings are presented, one each for the subset without admixtures, with mineral admixtures and with chemical admixtures.

Datasets 3, 4 and 5 were used to evaluate the RILEM B4, MC 2010 and WITS models against experiments for which the data were within the covariate ranges applicable to each model, respectively. The evaluation was done over the entire shrinkage duration of each experiment, using the statistical indicators RMSE and C.o.V. The C.o.V was used to evaluate the models over specific shrinkage time ranges (short, medium or long term shrinkage) as well. These results are both tabled and presented graphically. The applicability and performance of each model, with reference to (specimen) concrete origin, the year of the experiment or test period and the 28<sup>th</sup> day compressive strengths of the specimens are discussed next in chapter 5.

---

## Chapter 5 Discussion

This chapter evaluates the results presented in Chapter 4 and discusses how they compare with previous studies covered in Chapter 2. In discussing the results, they were grouped as follows:

- Analysis of original model predictions for Datasets 3, 4 and 5. The accuracies of the models (as determined by selected statistical indicators) were assessed for experiments from the same region and 28<sup>th</sup> day compressive strength range.
- Analysis of original and modified model predictions for Dataset 1-HSC and Dataset 2-HSC. The accuracies of the models were assessed via selected statistical indicators for data subsets without admixtures, with mineral admixtures and with both mineral and chemical admixtures. 10% of the data in each of Dataset 1-HSC and Dataset 2-HSC were used to validate the modified models. The shrinkage prediction results of the modified models for these validation experiments are compared and discussed.
- Analysis of proposed composite model predictions. The proposed composite model was assessed against the modified models for applicable data subsets for concrete specimens containing chemical admixtures.

### 5.1 Predictions for experiments falling within model applicable covariate range

The existing models, RILEM B4, MC 2010 and WITS, were each evaluated for a subset of data covering the covariate ranges for which the models were originally developed, namely Dataset 3, Dataset 4 and Dataset 5, respectively. These three data subsets were derived from the database (562 of the total of 2192 experiments in the compiled database) used in this study before any missing data analysis was conducted.

The lowest overall C.o.V<sub>all</sub> for the drying shrinkage component of the data subset applicable to each model was achieved by the WITS model, followed by the MC 2010 and then the RILEM B4 models. This might have been expected as much of the dataset used in this study to evaluate the WITS model was probably used to derive the model as well (Gaylard, 2011). For autogenous shrinkage, the lowest overall C.o.V<sub>all</sub> was achieved by the RILEM B4 model, which was expected as prediction of the autogenous shrinkage component was a major improvement incorporated into the B4 model. The RILEM B4 model was also developed using data from more modern concrete experiments included in the NU database (RILEM TC-242-MDC, 2015). Again, the data subset used in this study could well have been part of the data used to develop the RILEM B4 model. Both the RILEM B4 and MC 2010 models produced large C.o.V<sub>all</sub> values for autogenous shrinkage, about 13 to 28% greater than their C.o.V<sub>all</sub> values for drying shrinkage. This is a reflection of how much more conservative the models are for autogenous shrinkage than they are for drying shrinkage. Hubler *et al* (2015) indicated that the physical phenomena of autogenous shrinkage are not yet fully understood and so the autogenous shrinkage component of the RILEM B4 model is purely empirical. CEB-FIP (2012) suggests that for the MC 2010 model recalibration of the autogenous parameters, based on experiments analysing the internal RH and exposure to different environments, will increase its accuracy.

C.o.V<sub>all</sub> per geographical region (i.e. the country where the experiments were conducted) can be seen in Figure 5.1 and Figure 5.2 for drying and autogenous shrinkage, respectively. For drying shrinkage, the WITS model could only be used to predict for Southern African concretes, and achieved a C.o.V<sub>all</sub> less than 60%. Surprisingly the MC 2010 model achieved the lowest C.o.V<sub>all</sub> (< 40%) and the RILEM B4 the highest



C.o.V<sub>all</sub> (>100%) for the Southern African concretes. As suggested in the literature, the MC 2010 model predicted worse for North American than for European concretes. A possible reason for this could be the difference in cement classification and concrete composition, and that the European concrete shrinkage experiments used to optimise the MC 2010 model may contain a lower cement content (CEB-FIP, 2013; Gaylard *et al*, 2013). The RILEM B4 model also achieved a better C.o.V<sub>all</sub> for European and Australian concretes than for North American concretes, but performed better than the MC 2010 model in predicting drying shrinkage for the North American, European and East Asian concretes.

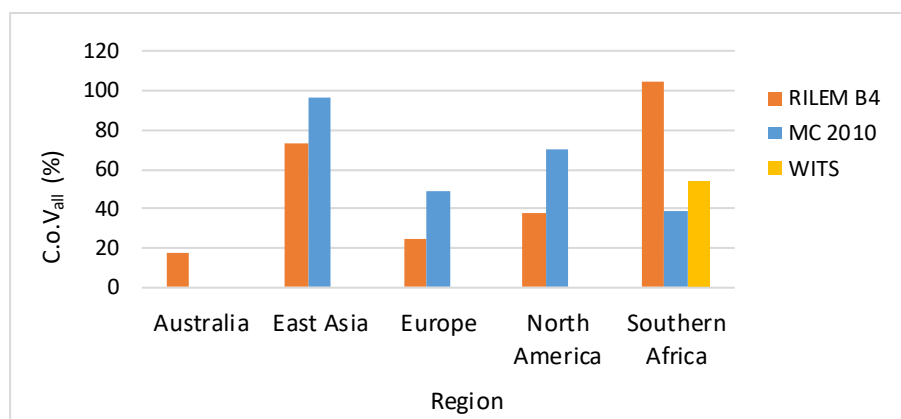


Figure 5.1 Drying shrinkage - overall C.o.V<sub>all</sub> values for the RILEM B4, MC 2010 and WITS models for experiments grouped by geographical region.

For autogenous shrinkage, the RILEM B4 model predictions were better than those of the MC 2010 model for all regions, achieving the lowest C.o.V<sub>all</sub> (<100%) for Middle Eastern concretes. The WITS model does not calculate autogenous shrinkage and is therefore not included in any autogenous shrinkage evaluations.

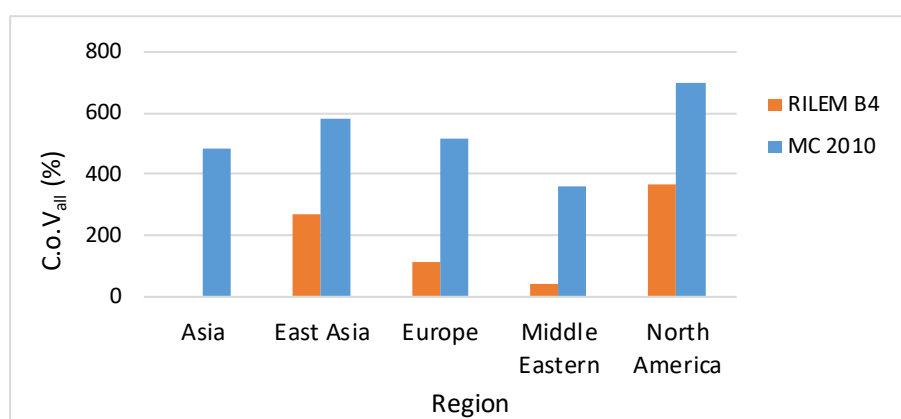


Figure 5.2 Autogenous shrinkage - overall C.o.V<sub>all</sub> values for the RILEM B4 and MC 2010 models for experiments grouped by geographical region.

The overall C.o.V<sub>all</sub> for NSC and HSC can be seen in Figure 5.3 and Figure 5.4 for drying and autogenous shrinkage, respectively. For drying shrinkage, the WITS model achieved the lowest C.o.V<sub>all</sub> for both NSC and HSC predictions. The RILEM B4 model performed the worst for HSC, achieving an overall C.o.V<sub>all</sub> >100%. This was not expected as the RILEM B4 model was developed (calibrated) using the largest and

latest published shrinkage database. According to CEB-FIP (2013) the MC 2010 model achieved a C.o.V<sub>all</sub> of 33 %, but in this study C.o.V for the MC 2010 model was greater than 33% for both NSC and HSC.

For autogenous shrinkage prediction the RILEM B4 model, once again, outperformed the MC 2010 model for both NSC and HSC. The RILEM B4 model also achieved better results for HSC predictions than for NSC predictions. According to CEB-FIP (2013) the MC 2010 model had a C.o.V<sub>all</sub> of 43.3 % for HSC and 29% for NSC. In this study the experimental data used to evaluate the MC 2010 model comes from concretes containing chemical admixtures, which explains the large discrepancy between the C.o.V<sub>all</sub> values of CEB-FIP (2013) and this study. Large scatter between the datasets used in the analyses to calculate the C.o.V values also contributes to these differences.

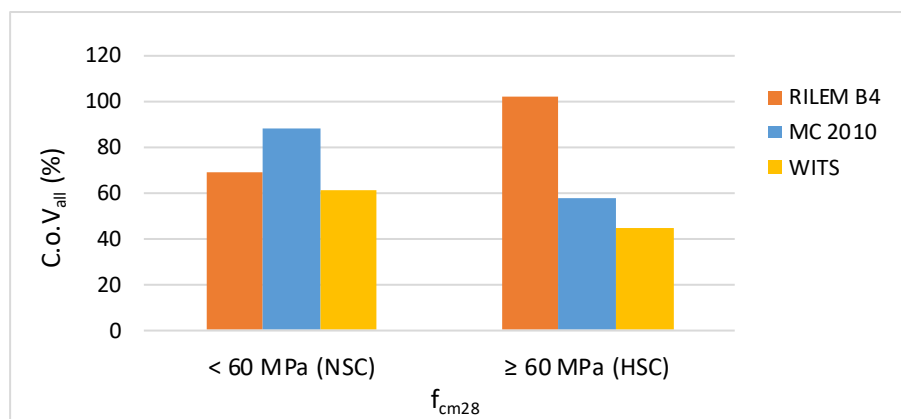


Figure 5.3 Drying shrinkage - overall C.o.V<sub>all</sub> values for the RILEM B4, MC 2010 and WITS models for NSC (< 60 MPa) and HSC (≥ 60 MPa) experiments.

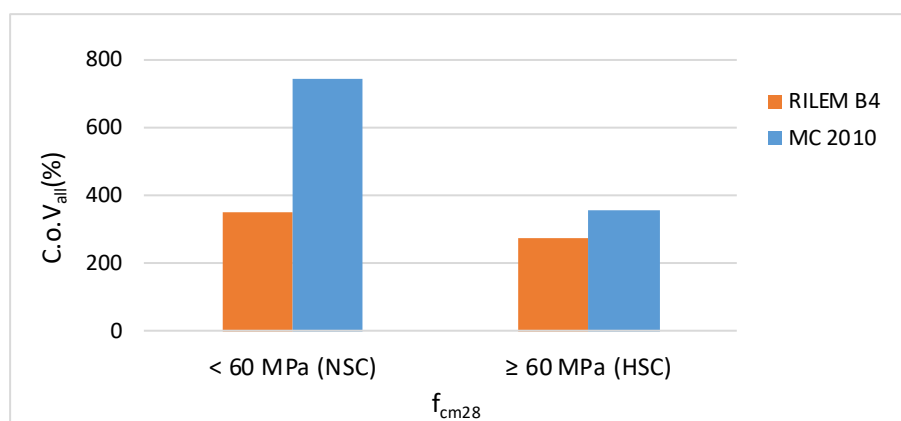


Figure 5.4 Autogenous shrinkage - overall C.o.V<sub>all</sub> values for the RILEM B4 and MC 2010 models for NSC (< 60 MPa) and HSC (≥ 60 MPa) experiments.

## 5.2 Original and modified model predictions for HSC without admixtures (drying $\epsilon$ )

Only Dataset 1-HSC (drying shrinkage) has data subsets without any admixtures, these being Subsets S1-01 to S1-05. These subsets share the same SANS 50197-1 (2013) cement classification of CEM I and a mean w/cm of 0.4, but each is for a different coarse aggregate type. The durations of all the experiments of these subsets did not exceed 500 days, therefore there is no discussion around long-term shrinkage.

For Subsets S1-01 to S1-05, the overall performances of the original RILEM B4 and WITS models ranked equally according to averaged values of the statistical indicators RMSE,  $R^2_{adj}$  and  $AIC_C$ , followed by the original MC 2010 model. After the model parameters were updated, the ranking order (from most to least accurate) were: the modified WITS, RILEM B4 and then MC 2010 model. Figure 5.5 is an example to show these rankings graphically, using data from experiment #0083.

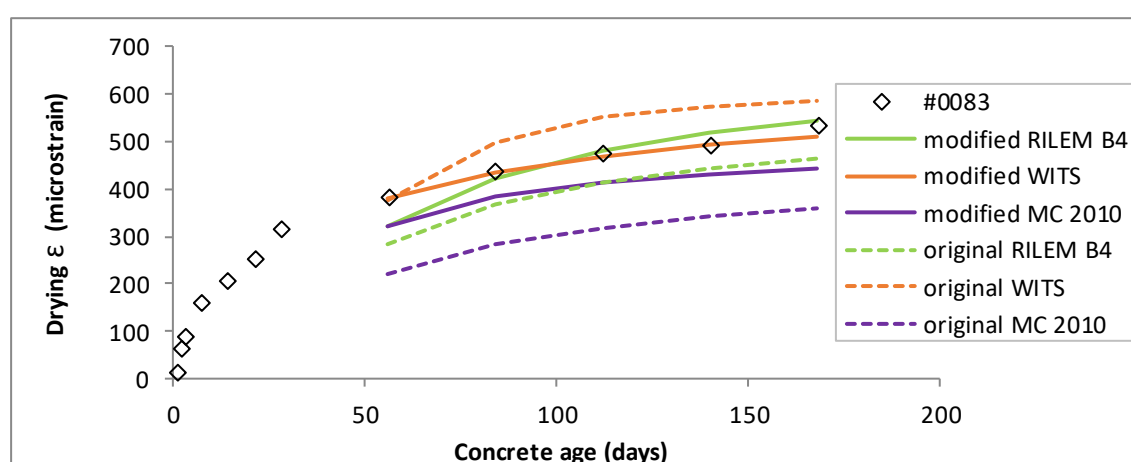


Figure 5.5 Graphical representation of overall ranking of original and modified model predictions for drying shrinkage data subsets without admixture.

When considering the original models' overall performances over each of the selected shrinkage time ranges 0 to 99, 100 to 199 and 200 to 499 days, averages of the statistical indicators RMSE,  $R^2_{adj}$  and  $C.o.V_{all}$  ranked the WITS model best, followed by the RILEM B4 and MC 2010 models for short-term shrinkage prediction, and the WITS model best, followed by the MC 2010 and RILEM B4 models for medium-term shrinkage prediction. After model parameters were updated, the modified RILEM B4 and WITS models ranked equally for short-term shrinkage prediction. For medium-term shrinkage prediction the WITS model was best, followed by the MC 2010 and RILEM B4 models.

For the data Subsets S1-01 to S1-05, for both short- and medium-term shrinkage periods, errors in all of the original model predictions are quite large. The original WITS model, however, predicted within an acceptable  $\pm 20\%$  error band over both time periods for Subset S1-05. After the model parameters were updated, for all applicable data subsets except S1-01 and S1-04, the modified models predicted shrinkage within an acceptable 20% error band. For S1-01, only the modified RILEM B4 produced deviations outside the  $\pm 20\%$  error band and for S1-04 all models performed badly, but showed improvement over the original results. This is due to the large variation seen in the actual shrinkage in S1-04. Table 5.1 indicates the error ranges for data subsets without admixtures.

Table 5.1 Subsets without admixtures: error ranges (%) of original and modified models for short- and medium-term drying shrinkage.

Models	Short term shrinkage 0-99 days		Medium-term shrinkage 100-499 days	
	Original model	Modified model	Original model	Modified model
RILEM B4	-52.5 % +64.2 %	- 52.6 % + 47.9 %	- 38.1 % + 48.8 %	-32.1 % +17.5 %
MC 2010	-5 % +65.2 %	- 42 % + 17.5 %	-4.5 % + 36.3 %	-15.2 % +21 %
WITS	-80.3 % +45.3 %	- 59.3 % + 20 %	- 94.6 % + 17.9 %	- 25 % + 15.9 %

### Model validation

Two experiments in the validation subset do not contain any admixtures, namely #0011 and #0105. Both of these experiments are from the South African database and were conducted in the years 2000 and 1983, respectively. Averaged ranking scores for the models for all the validation experiments showed the best performing model to be the modified RILEM B4 model, followed by the MC 2010 and WITS models, which ranked equally. For Experiment #0011, all model predictions were within a  $\pm 20\%$  error band, which is considered accurate enough (Gardner and Lockman, 2001). The modified RILEM B4 model predicted within a  $\pm 15\%$  error band which is considered excellent. For Experiment #0105, none of the models predicted within a  $\pm 20\%$  error band. This poor model calibration is likely due to the large variation seen in the actual shrinkage in S1-04. Figure 5.6 gives the distribution plot of the modified RILEM B4 model residuals for Experiment #0011, with a skewness of 1.24 and standard deviation of 16.89%.

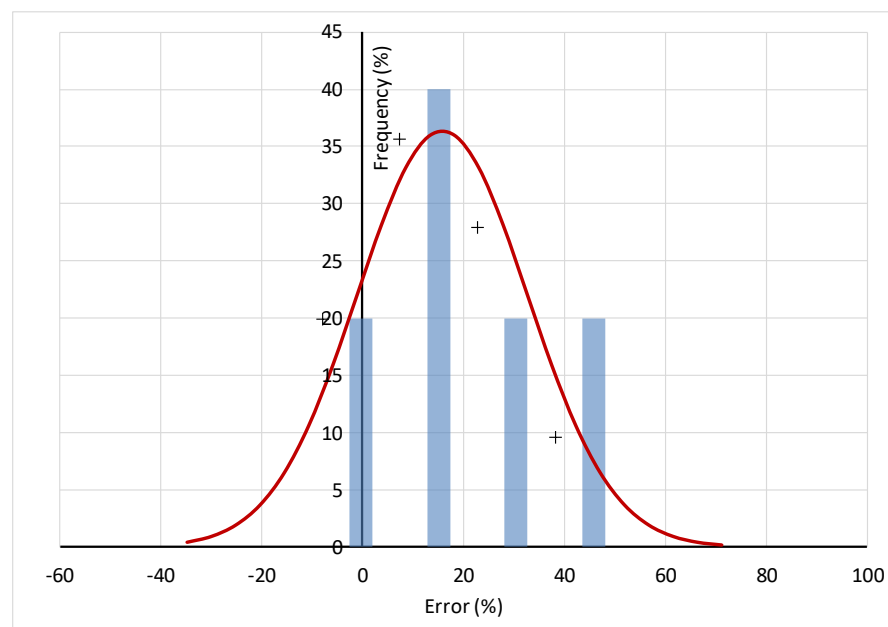


Figure 5.6 Modified RILEM B4 model: residual (error) distribution for Experiment #0011 (Dataset 1-HSC). (blue bars indicate residual distribution, + indicates scaled normal values for experimental bins, red line indicates scaled theoretical normal distribution -3 to 3 standard deviations).

### 5.3 Original and modified model predictions for HSC with mineral admixtures (drying $\epsilon$ )

Only Dataset 1-HSC (drying shrinkage) has data subsets with mineral admixtures and they are Subsets S2-01 to S2-03. These subsets share the same mean w/cm of 0.4 and Andesite coarse aggregate, but each differs in SANS 50197-1 (2013) cement classification. RH, T,  $t_{dry}$ , V/S and a/cm are constant between subsets.

For Subsets S2-01 to S2-03, the overall performance of the original MC 2010 was best, followed by the RILEM B4 and the WITS models, according to averaged values of the statistical indicators RMSE,  $R^2_{adj}$  and  $AIC_C$ . This seemed strange as all experiments in these subsets are from the South African database and were initially thought to have been part of data used in the development of the WITS model. On comparing the original model fits to each experiment of the applicable data subsets, it was seen that the WITS model predictions were the worst for the period 0 to 60 days. However, overall ranking of the models was obscured due to the relatively large number of data points between 0 and 60 days and few data points between day 60 and day 400. After updating the model parameters, the modified model rankings changed to (from most to least accurate): the modified WITS model, RILEM B4 model and then the MC 2010 model. Figure 5. is an example to show these rankings graphically, using data from Experiment #0249.

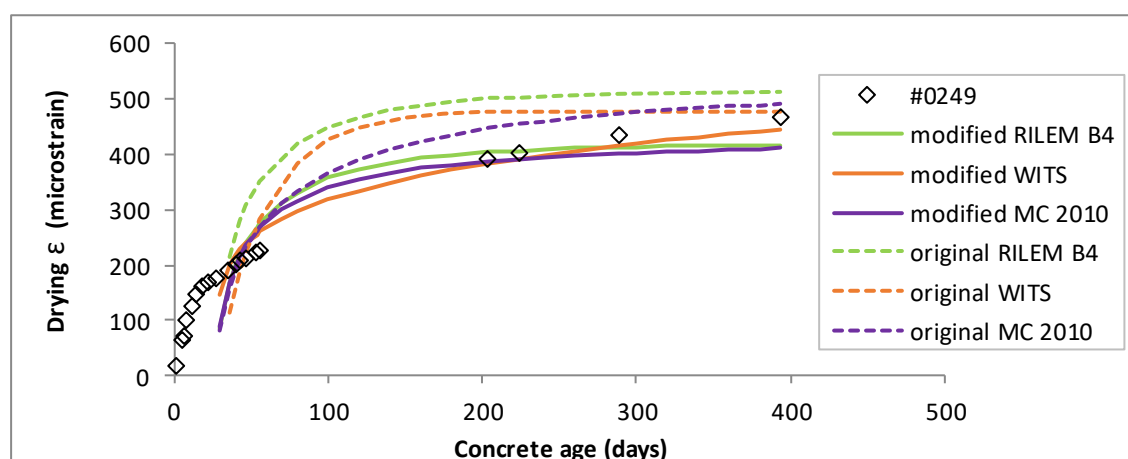


Figure 5.7 Graphical representation of overall ranking of original and modified model predictions for drying shrinkage - data subsets with mineral admixtures.

When considering the original models' overall performances over each of the selected shrinkage time ranges 0 to 99, 100 to 199 and 200 to 499 days, averages of the statistical indicators RMSE,  $R^2_{adj}$  and C.o.V<sub>all</sub> ranked the MC 2010 model best, followed by the RILEM B4 and WITS models for short-term shrinkage prediction, and the MC 2010 model best, followed by the WITS and RILEM B4 models for medium-term shrinkage prediction. After the model parameters were updated, the modified WITS model ranked best, followed by the MC 2010 and RILEM B4 models for short-term shrinkage prediction, and the RILEM B4 model best, followed by the WITS and MC 2010 models for medium-term shrinkage prediction.

For the data Subsets S2-01 to S2-03, the original models could not predict shrinkage for all the experiments within a  $\pm 20\%$  error band. For short-term shrinkage, the original WITS model gave the largest errors. After the model parameters were updated, the modified model predictions were still not within an acceptable  $\pm 20\%$  error band. Now though, the WITS model deviated the least from actual shrinkages,

with a maximum error of 23% over all shrinkage time ranges and all applicable data subsets. Table 5.2 gives the prediction error ranges for the short- and medium-term time intervals for data subsets with mineral admixtures. The large errors were expected due to the large variations in the actual shrinkage data of the applicable data subsets.

Table 5.2 Subsets with mineral admixtures: error ranges (%) of original and modified models for short- and medium-term drying shrinkage.

Models	Short term shrinkage 0-99 days		Medium-term shrinkage 100-499 days	
	Original model	Modified model	Original model	Modified model
RILEM B4	-54.2 % +40.7 %	-21.2 % +54.3 %	-60.2 % -0.5 %	-31.9 % +18.2 %
MC 2010	-18.1% +54.6 %	-22.1 % +50.8 %	-42 % +11.6 %	-35.3 % +20.5 %
WITS	-24.5 % +81.6 %	-22.1 % +22.4 %	-53.9 % +6.6 %	-21.4 % +14 %

### Model validation

One experiment of the validation data subset contains mineral admixtures, namely Experiment #0258. This experiment was conducted in South Africa in 2007. Ranking the models for this experiment indicated that the modified WITS model was the most accurate, followed by the RILEM B4 and MC 2010 models. Only the modified WITS model predicted shrinkages within a  $\pm 20\%$  error band (except for the first data point - underestimated by 29%). The modified RILEM B4 and MC 2010 model predictions are within a  $\pm 30\%$  error band for medium-term shrinkage. Figure 5. plots the distribution of the WITS model residuals for Experiment #0258, with a skewness of 1.9 and standard deviation of 41.4%.

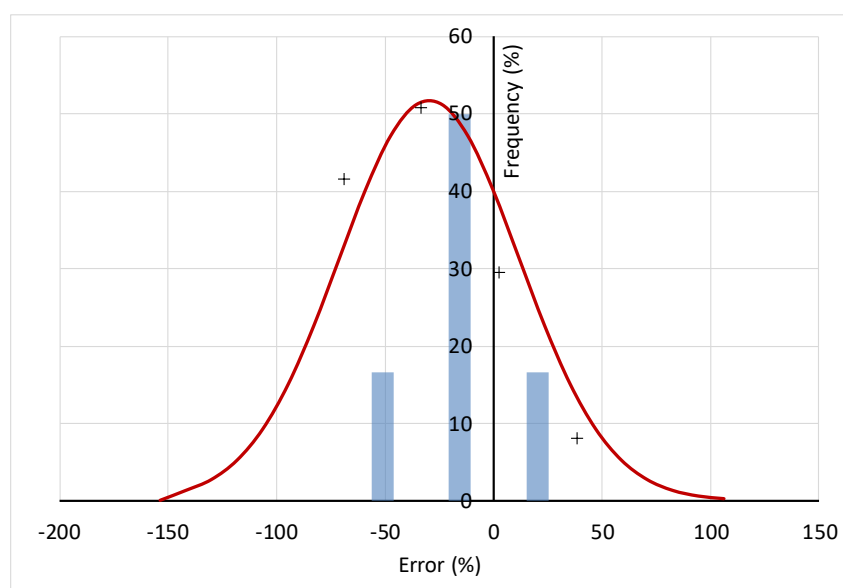


Figure 5.8 Modified WITS model: residual (error) distribution for Experiment #0258 (Dataset 1-HSC). (blue bars indicate residual distribution, + indicates scaled normal values for experimental bins, red line indicates scaled theoretical normal distribution -3 to 3 standard deviations).

## 5.4 Original and modified model predictions for HSC with mineral and chemical admixtures (drying $\epsilon$ )

The subsets from Dataset 1-HSC (drying shrinkage) with shrinkage data for concretes containing chemical admixtures are S2-04 to S2-14. The concrete specimens of all these subsets contain SP, but vary in admixture content and both mineral and chemical admixtures combinations. Only Subsets S2-08 to S2-14 share the same SANS 50197-1 (2013) cement classification, mean w/cm ratio of 0.33, granite coarse aggregate and covariates RH, T,  $t_{dry}$ , V/S and a/cm. Only Subsets S2-08 to S2-14 include experiments with long-term ( $\geq 500$  days) shrinkage data.

For Subsets S2-04 to S2-14, averaged values of the statistical indicators RMSE,  $R^2_{adj}$  and  $AIC_C$  ranked overall performance best for the original WITS model, followed by the RILEM B4 and MC 2010 models. After the model parameters were updated, the ranking order changed to (most to least accurate) the modified WITS model, then the MC 2010 model and the RILEM B4 model. Figure 5. shows these rankings graphically, using the data of Experiment 15.

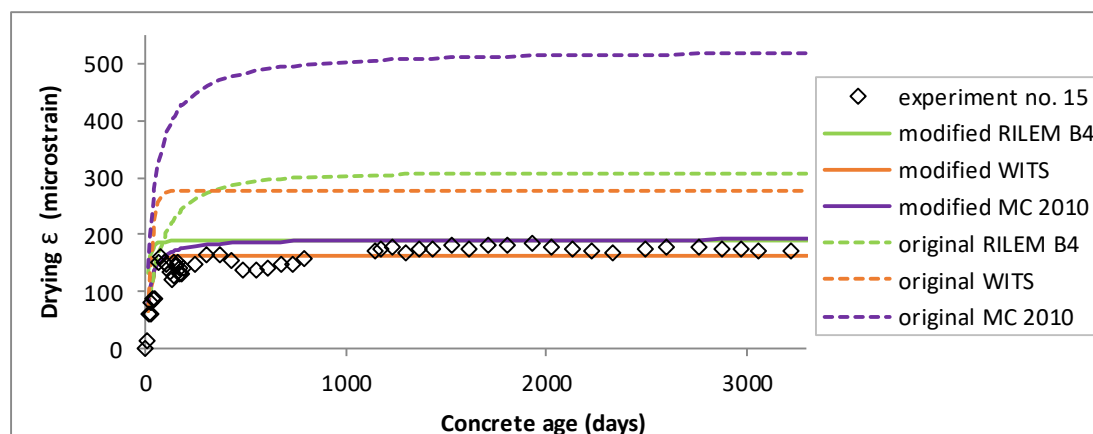


Figure 5.9 Graphical representation of overall ranking of original and modified model predictions and actual drying shrinkage – data subsets with mineral and chemical admixtures.

When considering the original models' overall performances for each of the selected shrinkage time ranges 0 to 99, 100 to 499 and  $\geq 500$  days, averages of the statistical indicators RMSE,  $R^2_{adj}$  and  $C.o.V_{all}$  ranked the WITS model best, followed by the RILEM B4 and MC 2010 models for short-, medium- and long-term shrinkage predictions. After updating the model parameters, the modified MC 2010 model gave the best predictions, followed by the WITS and RILEM B4 models for short-term shrinkage. The WITS model was best, followed by the MC 2010 and RILEM B4 models for medium- and long-term shrinkage.

For the data Subsets S2-04 to S2-14, the original models were unable to predict shrinkage for all the experiments within a  $\pm 20\%$  error band. The original RILEM B4 model deviated the least from the actual shrinkage values for the short- and medium-term periods, while the WITS model deviated the least from actual shrinkage in the long-term. After the model parameters were updated, the modified models predicted medium- and long-term shrinkage within an acceptable  $\pm 20\%$  error band. They were not, however, accurate in their short-term predictions, except for Subsets S2-06, S2-11 and S2-14. Errors in the WITS model predictions were within a  $\pm 20\%$  error band over all shrinkage time periods for data subset S2-08 only, due again to the large variations in the measured shrinkages in the applicable data subsets. Table 5.3 indicates the shrinkage prediction error ranges for data subsets for concretes with mineral and chemical admixtures.

Table 5.3 Subsets with mineral and chemical admixtures: error ranges (%) of original and modified models for short-, medium- and long-term drying shrinkage.

Models	Short term shrinkage 0-99 days		Medium-term shrinkage 100-499 days		Long term shrinkage ≥ 500 days	
	Original model	Modified model	Original model	Modified model	Original model	Modified model
RILEM B4	-68.7 % +89.1 %	-432.7 % +67.9 %	-113.1 % +64.9 %	-56.9 % +48.2 %	-115.4 % +28.8 %	-37.9 % +23.4 %
MC 2010	-234.9 % +95.6 %	-449 % +64 %	-253.5 % +73.7 %	-41.7 % +20.6 %	-256.6 % -16.4 %	-36.7 % +14.8 %
WITS	-157.9 % +99.6 %	-230.2 % +84.2 %	-130.2 % +38.5 %	-39 % +23.2 %	-102.5 % +34.5 %	-26.2 % +24.3 %

For Subsets S2-08, S2-09, S2-10 and S2-12, the overall performance of the proposed models was best, followed by the modified WITS, MC 2010 and RILEM B4 models, based on averaged values of the statistical indicators RMSE,  $R^2_{adj}$  and AICc. An example of these rankings is shown graphically in Figure 5. , using data from Experiment 6. When considering the proposed and modified models' overall performances for each of the selected shrinkage time ranges 0 to 99, 100 to 499 and ≥ 500 days, averages of the statistical indicators RMSE,  $R^2_{adj}$  and C.o.V<sub>all</sub> ranked the proposed composite models best, followed by the WITS model for short-, medium- and long-term shrinkage prediction. The early shrinkage peak seen in the data Subsets S2-08, S2-09, S2-10 and S2-12 was predicted by the proposed models, but not by the modified existing models. As can be seen in Figure 5.10 the modified WITS prediction reached the peak value, but then continued to over predict shrinkage for the rest of the experiment duration (medium- and long-term). The proposed model functions show more flexibility in predicting both the early shrinkage peaks and the final (medium- and long-term) shrinkage.

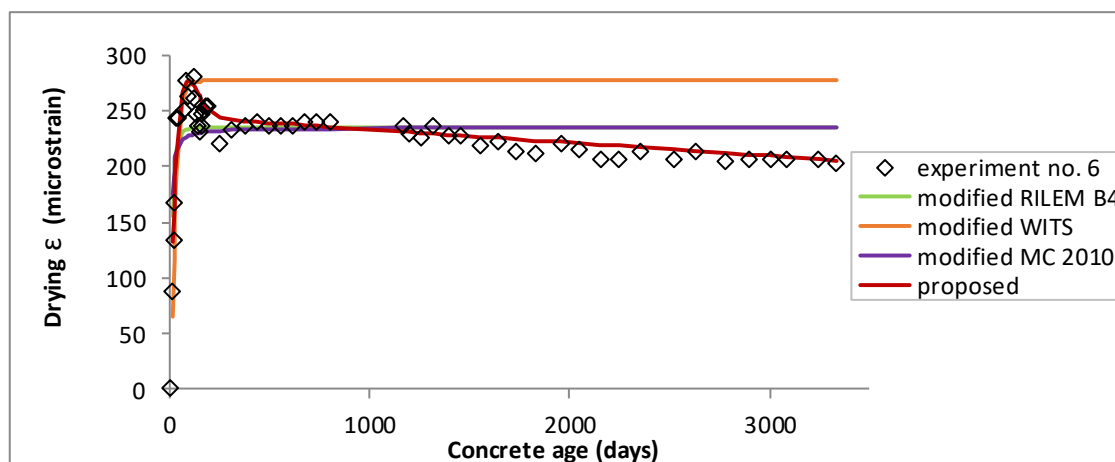


Figure 5.10 Graphical representation of overall ranking of proposed composite and modified model predictions for drying shrinkage - data subsets with mineral and chemical admixtures.

For the data Subsets S2-08, S2-09, S2-10 and S2-12, the modified models predicted drying shrinkage within a  $\pm 20\%$  error band for the medium- and long-term periods, for all the experiments. The proposed models' predictions deviated the least from the actual shrinkage measurements over all the time periods. Table 5.4 lists the error ranges achieved by all the models for the analyses for data Subsets S2-08, S2-09, S2-10 and S2-12.



Table 5.4 Subsets S2-08, S2-09, S2-10 and S2-12: error ranges (%) for modified and proposed composite shrinkage models for short-, medium and long-term periods - drying shrinkage.

Models	Short term shrinkage 0-99 days	Medium term shrinkage 100-499 days	Long term shrinkage ≥ 500 days
modified RILEM B4	-42.2 % +30.7 %	-10.7 % +16.1 %	-16.7 % +10.4 %
modified MC 2010	-42.8 % +18.3 %	-11.6 % +18.2 %	-16 % +9.3 %
modified WITS	-19.2 % +34.6 %	-7.2 % +15.8 %	-16.6 % +10.3 %
Proposed	-20.4 % +29.4 %	-14.2 % +7 %	-6.9 % +11.4 %

### Model validation

Three experiments included in the validation data subset were for concretes with chemical admixtures, namely #0258, 14 and 20. Experiment #0258 was conducted in South Africa during the 2007. Experiments 14 and 20 were done in the USA and their data published in 2011.

Averaged ranking scores for the models for all the validation experiments showed the best performing model to be the modified WITS model, followed by the MC 2010 and RILEM B4 models, which ranked equally. For Experiment 14, only the modified WITS model predicted within a 15% error band over all shrinkage terms, except for the first data point, which was underestimated by 49%. The modified MC 2010 predicted within a 20% error band for short- and medium-term shrinkage, except the for the first data point, and the RILEM B4 predicted within a 20% error band for medium- to long-term shrinkage. Figure 5.11 gives the distribution plot of the modified WITS model residuals for Experiment 14, with skewness of 0.138 and standard deviation of 15.28%.

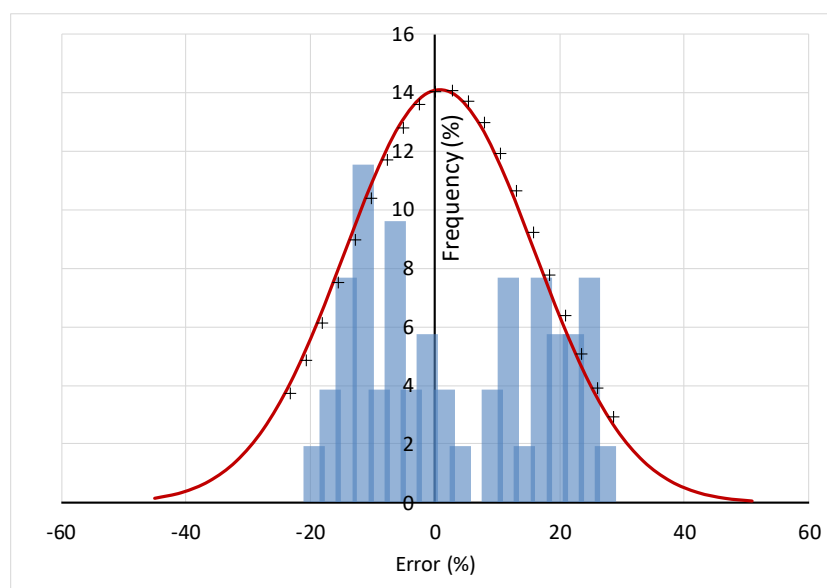


Figure 5.11 Modified WITS model: residual (error) distribution for Experiment 14 (Dataset 1-HSC). (blue bars indicate residual distribution, + indicates scaled normal values for experimental bins, red line indicates scaled theoretical normal distribution -3 to 3 standard deviations).

## 5.5 Original and modified model predictions for HSC with mineral and chemical admixtures (autogenous $\epsilon$ )

Only the RILEM B4 and MC 2010 models (of the models considered in this study) can predict autogenous shrinkage. The data subsets from Dataset 2-HSC (autogenous/basic shrinkage) that include data for concretes with chemical admixtures are S2-01a to S2-12a. All the specimens reported on in these data subsets contained SP or plasticiser, but all varied with regard to their covariate data. Each subset is considered individually. Some subsets include data from comparable experiments conducted by different authors in different geographical regions, but the majority of the derived subsets contain experiments that were conducted in the same laboratory. Only Subsets S2-03a, S2-06a to S2-11a include long-term ( $\geq 500$  days) shrinkage data.

For Subsets S2-01a to S2-12a, the overall performance of the original and modified RILEM B4 models ranked ahead of the MC 2010 models according to averaged values of the statistical indicators RMSE,  $R^2_{adj}$  and  $AIC_C$ , as seen graphically in Figure 5.12, which uses Experiment A\_086\_18 for example data.

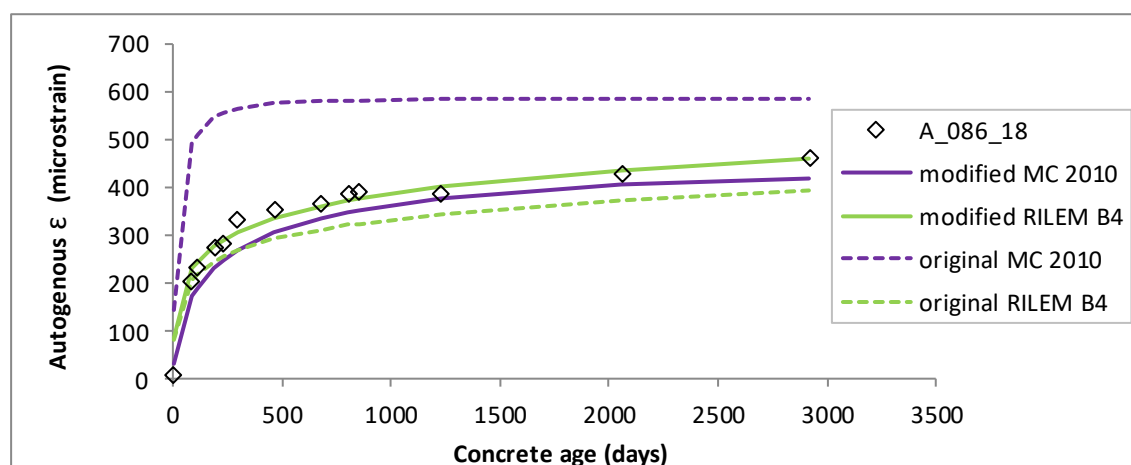


Figure 5.12 Graphical representation of overall ranking of original and modified model predictions for autogenous shrinkage of subsets – data subsets with mineral and chemical admixtures.

For the data Subsets S2-01a to S2-12a, the original models could not predict autogenous shrinkage within a  $\pm 20\%$  error band for all the experiments. The RILEM B4 model could do so for the experiments in S2-01a over the whole measurement time range, and for the experiments in S2-03a for long-term shrinkage only. After the model parameters were updated, autogenous shrinkage predictions were still outside the acceptable  $\pm 20\%$  error band over all the time intervals, except for the experiments included in data Subsets S2-01a and S2-02a. Maximum prediction errors occurred mostly in the short-term shrinkage period (0 to 99 days) for both models. Table 5.5 gives the calculated autogenous shrinkage prediction error ranges of each model for the experiments on concretes with mineral and chemical admixtures.

Table 5.5 Subsets S2-01a to S2-12a with mineral and chemical admixtures: error ranges (%) of original and modified models for short-, medium- and long-term periods - autogenous shrinkage.

Models	Short term shrinkage 0-99 days		Medium term shrinkage 100-499 days		Long term shrinkage ≥ 500 days	
	Original model	Modified model	Original model	Modified model	Original model	Modified model
RILEM B4	-2144.8 % +81 %	-381.2 % +99 %	-247.6 % +21 %	-98 % +14 %	-158.7 % +35.3 %	-80.8 % +29 %
MC 2010	-2943.3 % +59.3 %	-370 % +71.3 %	-320.5 % -5.20 %	-86.4 % +26.4 %	-289.2 % +15 %	-73.8 % +22.4 %

### Model validation

Four experiments of the validation data subset contain chemical admixtures, namely A\_068\_16, A\_086\_19, A\_086\_25 and A\_086\_35. A\_068\_16 was conducted in the USA in 1998 and the rest in Sweden during 2002. Averaged ranking scores for all the experiments suggested that the modified MC 2010 model performed better than the modified RILEM B4 model. For Experiment A\_068\_16, both the modified models predicted within a  $\pm 22\%$  error band over all shrinkage time periods, except for the first data point which was overestimated by  $> 39\%$  by both models. For Experiment A\_086\_19, both the modified models predicted shrinkage within a  $\pm 15\%$  error band over the whole time frame, again except for the first data point which was overestimated by  $> 55\%$ . For Experiments A\_86\_25 and A\_086\_35 neither model predicted within a  $\pm 20\%$  error band. As an example, Figure 5.13 gives the error distribution plot of the modified MC 2010 model residuals for Experiment A\_086\_19, which has a skewness of 0.135 and standard deviation of 28.43%.

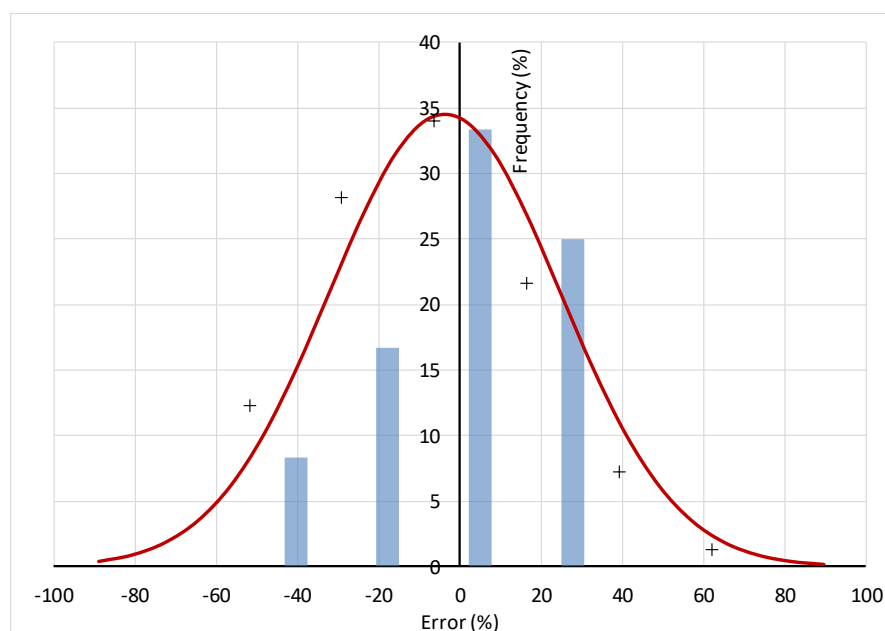


Figure 5.13 Modified MC 2010 model: residual ( error) distribution for validation Experiment A\_086\_19 (Dataset 2-HSC). (blue bars indicate residual distribution, + indicates scaled normal values for experimental bins, red line indicates scaled theoretical normal distribution -3 to 3 standard deviations).

## 5.6 Overall model performance - original and modified models

The actual vs. predicted (original and modified models) shrinkage plots presented in Figure 5.16 to Figure 5.18 give an overview of the errors (model performances) across all the data of all the selected subsets. The unity line (drawn continuous) represents predicted shrinkage exactly equalling actual shrinkage. The dotted lines indicate +20% and -20% deviations from the actual shrinkage. Data points falling below the unity line represent model underestimates and those above it model overestimates.

Considering Figure 5.16, Figure 5.14 and Figure 5.15, predictions of drying shrinkage for HSC (Dataset 1-HSC) show that the original WITS model (Figure 5.16) has a reasonably random distribution about the unity line, possibly underestimating shrinkages slightly. The original RILEM B4 model (Figure 5.14) tended to underestimate drying shrinkage whilst the original MC 2010 model (Figure 5.15) tended to overestimate it. Predictions of autogenous shrinkage for HSC (Dataset 2-HSC) were in most cases too high for both the original RILEM B4 model (Figure 5.17) and the MC 2010 model (Figure 5.18). For both drying and autogenous shrinkage the majority of the predictions of all the modified models fell within  $\pm 20\%$  of the actual shrinkages. For Dataset 1-HSC (drying shrinkage) predictions of the modified WITS and MC 2010 models had the least scatter and were random about the unity line. The modified RILEM B4 model predictions were also random about the unity line, but exhibited greater scatter than the other models. For Dataset 2-HSC (autogenous shrinkage) both the modified RILEM B4 model (Figure 5.17) and the modified MC 2010 model (Figure 5.18) predictions are random about the unity line, although the performance of the modified RILEM B4 model looks to be marginally better.

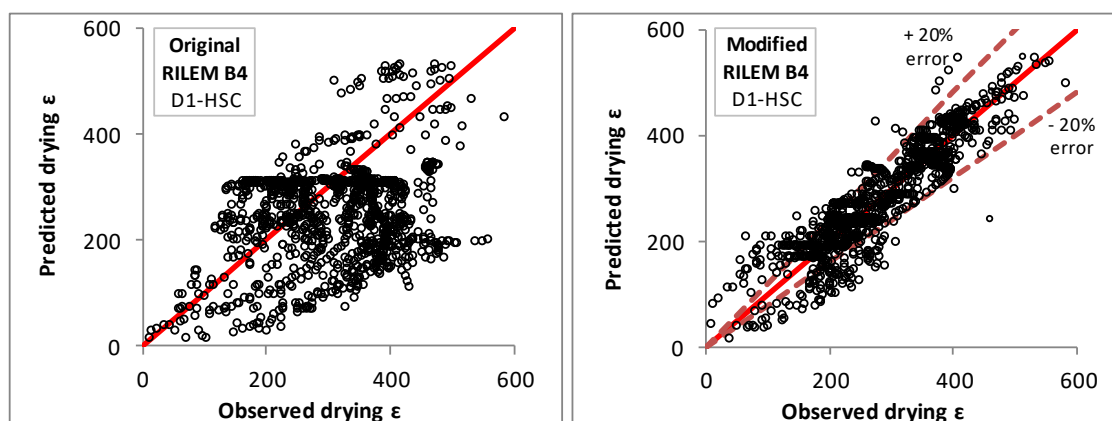


Figure 5.14 Original and modified RILEM B4 model: actual vs. predicted shrinkage for Dataset 1-HSC.

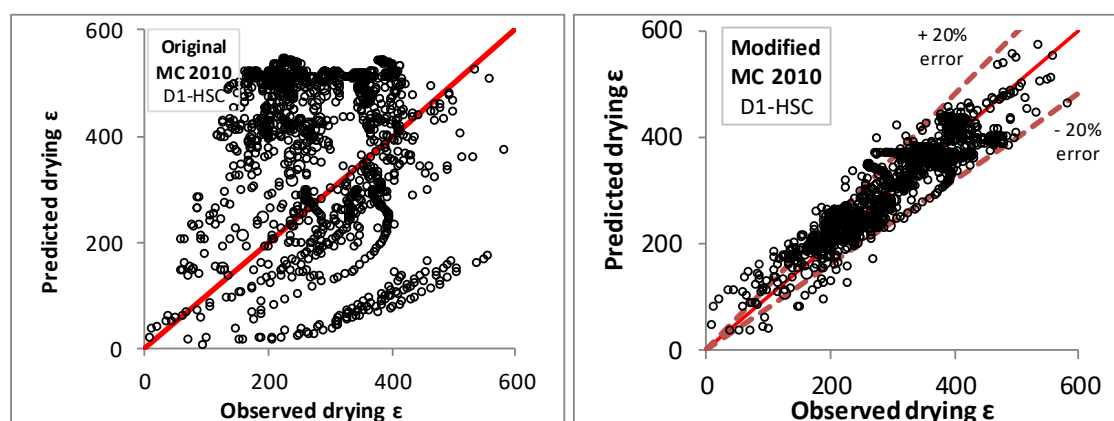


Figure 5.15 Original and modified MC 2010 model: actual vs. predicted shrinkage for Dataset 1-HSC.

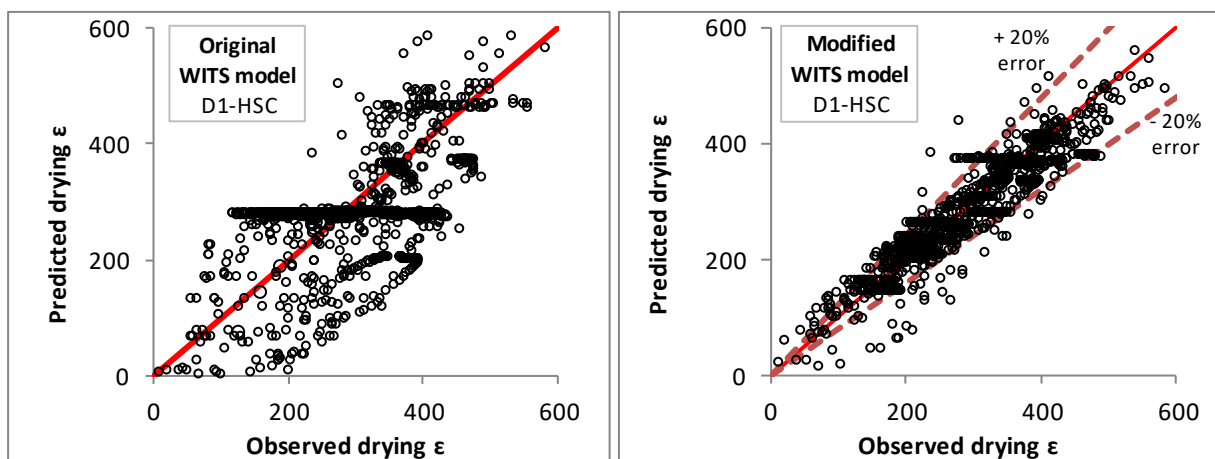


Figure 5.16 Original and modified WITS model: actual vs. predicted shrinkage for Dataset 1-HSC.

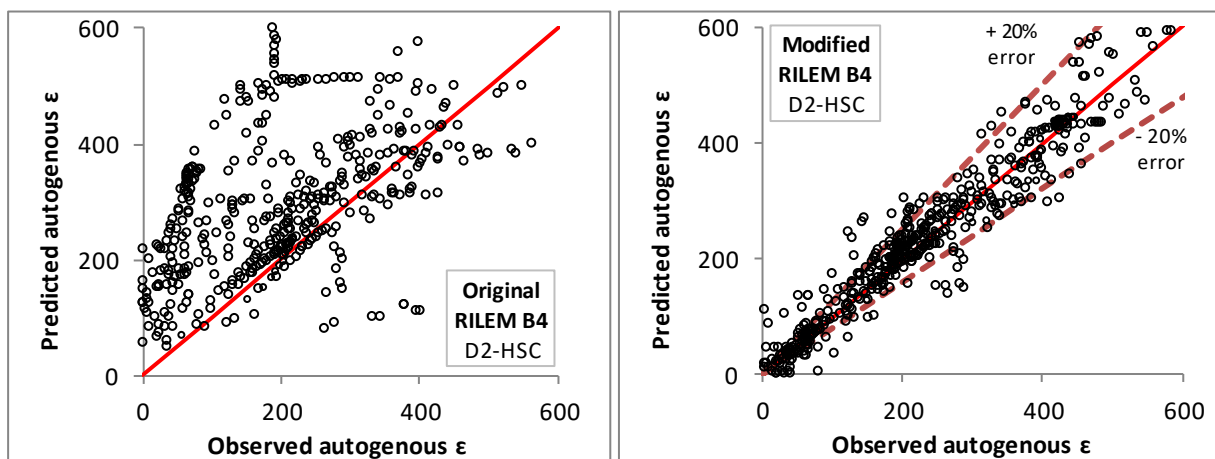


Figure 5.17 Original and modified RILEM B4 model: actual vs. predicted shrinkage for Dataset 2-HSC.

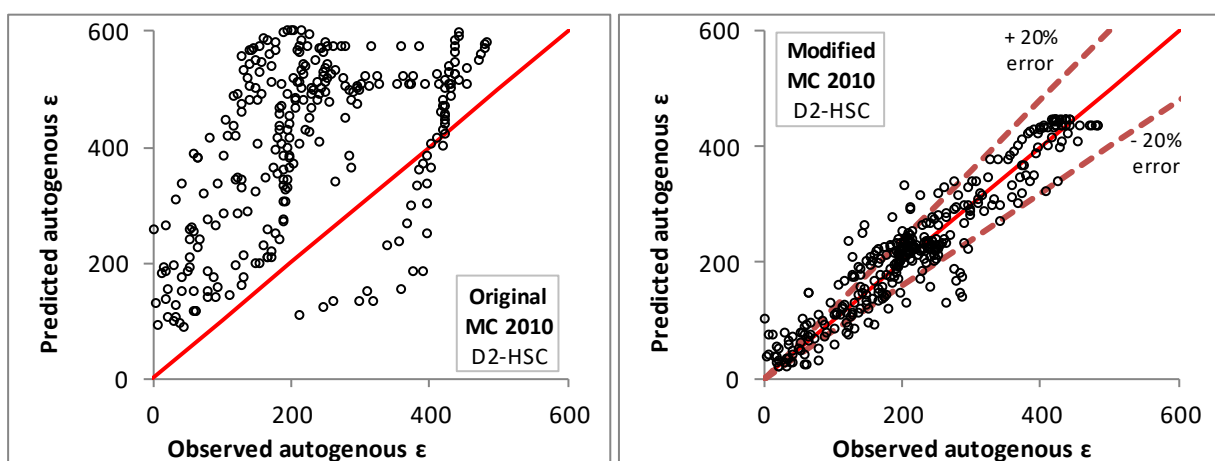


Figure 5.18 Original and modified MC 2010 model: actual vs. predicted shrinkage for Dataset 2-HSC.

The errors vs. time plots are shown in Figure 5.19 to Figure 5.23 and give an overall view of shrinkage prediction accuracies of the original and modified models over the entire Dataset 1-HSC (drying shrinkage) and Dataset 2-HSC (autogenous shrinkage), in both magnitude and distribution about zero. Negative errors (as a percentage) represent overestimation and positive errors (as a percentage) represent underestimation of actual shrinkage measurements.

For both Datasets 1-HSC and 2-HSC, all the original models largely overestimated shrinkage. The original MC 2010 model showed the greatest overestimation, up to an error of 257% above actual shrinkage, for Dataset 1-HSC. The original and modified models also showed the greatest errors in the short- and medium-term shrinkage periods (0 to 499 days) for both datasets. After model parameters were updated, the largest reduction in errors were seen in the medium- and long-term shrinkage measurement time periods.

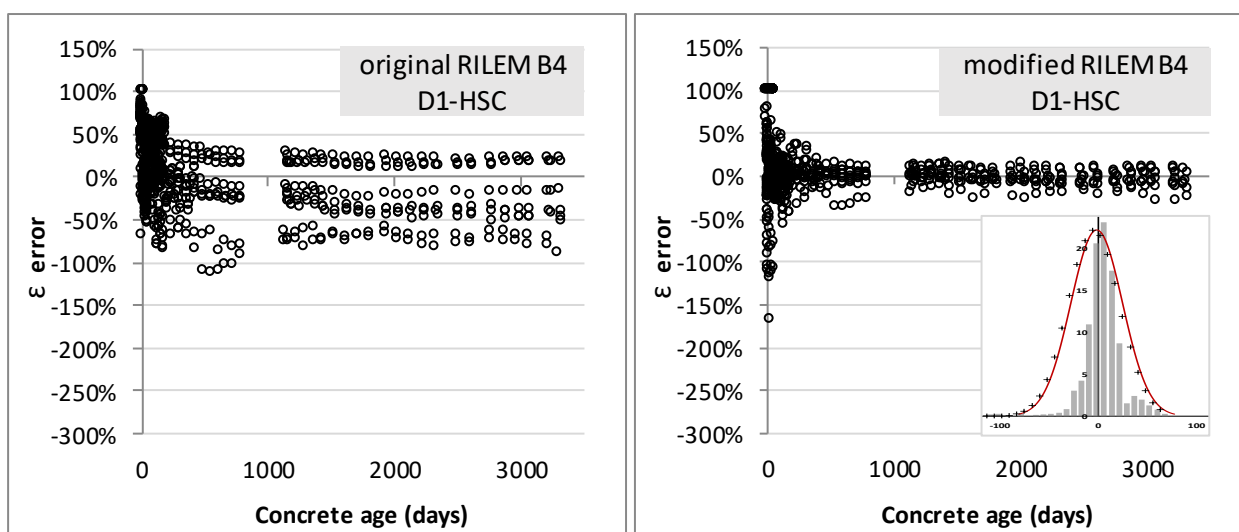


Figure 5.19 Original and modified RILEM B4 model error % over time for entire Dataset 1-HSC.

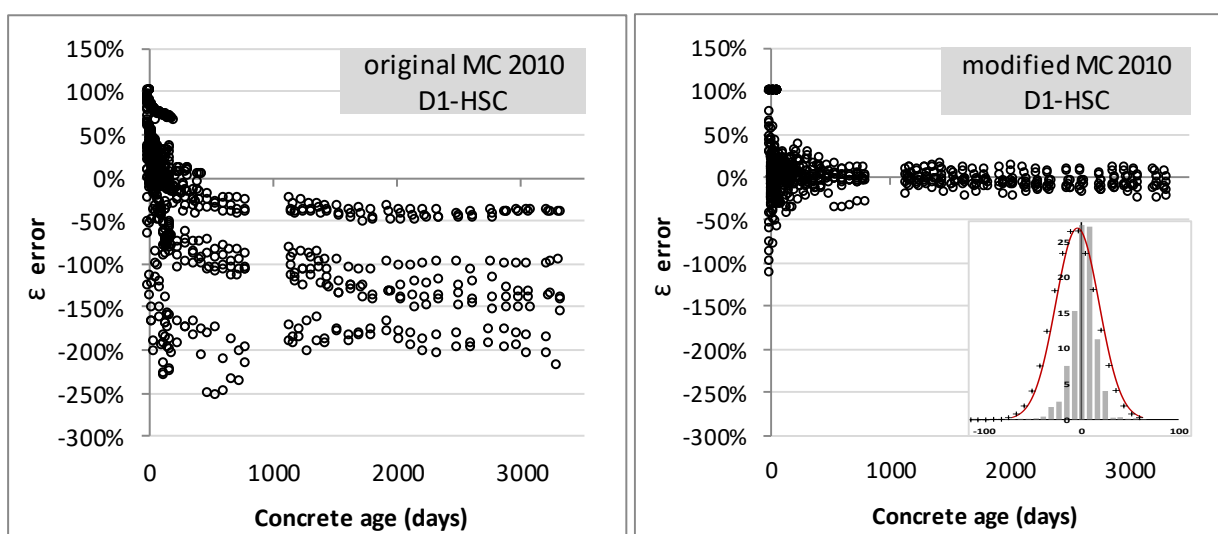


Figure 5.20 Original and modified MC 2010 model error % over time for entire Dataset 1-HSC.

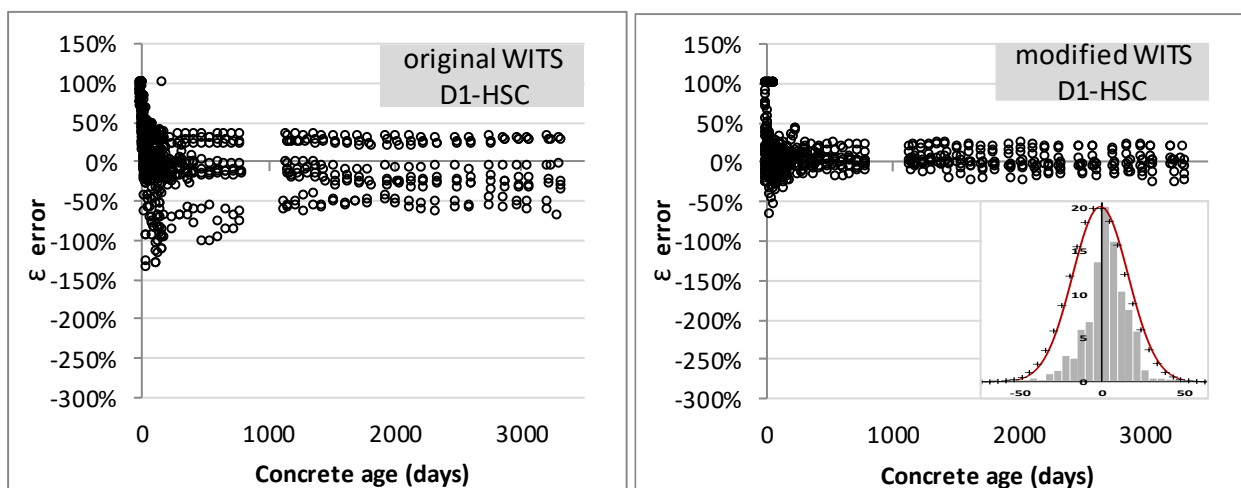


Figure 5.21 Original and modified WITS model error % over time for entire Dataset 1-HSC.

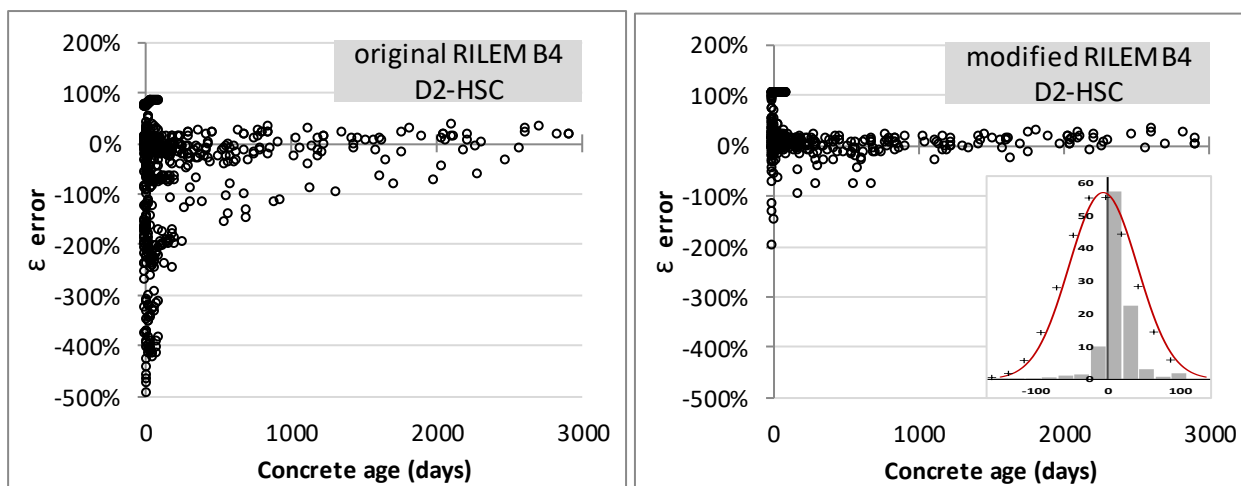


Figure 5.22 Original and modified RILEM B4 model error % over time for entire Dataset 2-HSC.

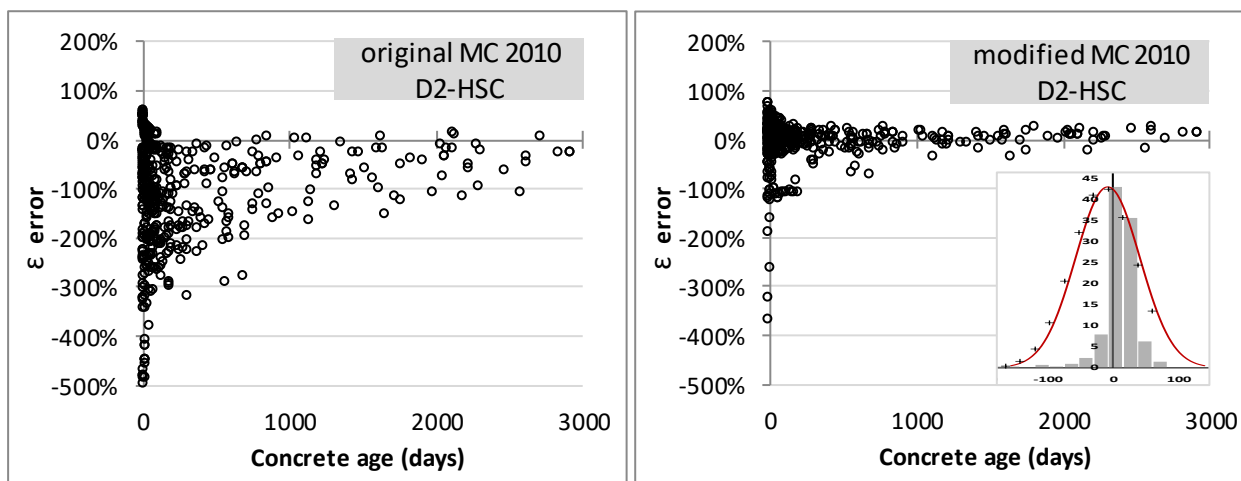


Figure 5.23 Original and modified MC 2010 model error % over time for entire Dataset 2-HSC.

To compare the performances of the models statistically, the dimensionless indicator  $C.o.V_{all}$  was used as it quantifies the scatter of the predictions about the mean value. The smaller  $C.o.V_{all}$  is, the closer the model prediction is to the actual shrinkage (Bazant & Li, 2008; Hubler *et al*, 2015).

All the modified model predictions achieved a  $C.o.V_{all}$  of less than 20% for the data subsets with and without admixtures, as seen in Figure 5.24 and Figure 5.25. The modified WITS model had the lowest  $C.o.V_{all}$  ( $\leq 13\%$ ) for all the drying shrinkage data subsets, suggesting this model to be superior to the modified RILEM B4 and MC 2010 models in predicting drying shrinkage for HSC. In this study the original RILEM B4 and MC 2010 models have a  $C.o.V_{all}$  of 39% and 38%, respectively for the data subsets without admixtures, which agrees well with Hubler *et al* (2015), who reported 32% and 41%, respectively.

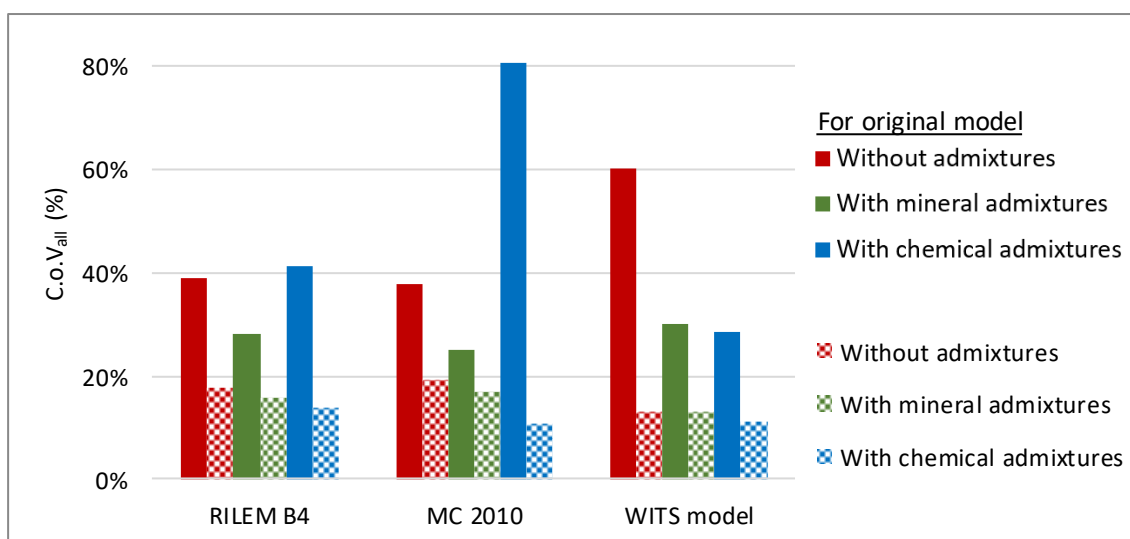


Figure 5.24 Original and modified model  $C.o.V_{all}$  for data subsets without admixtures, with mineral admixtures and with both mineral and chemical admixtures – drying shrinkage.

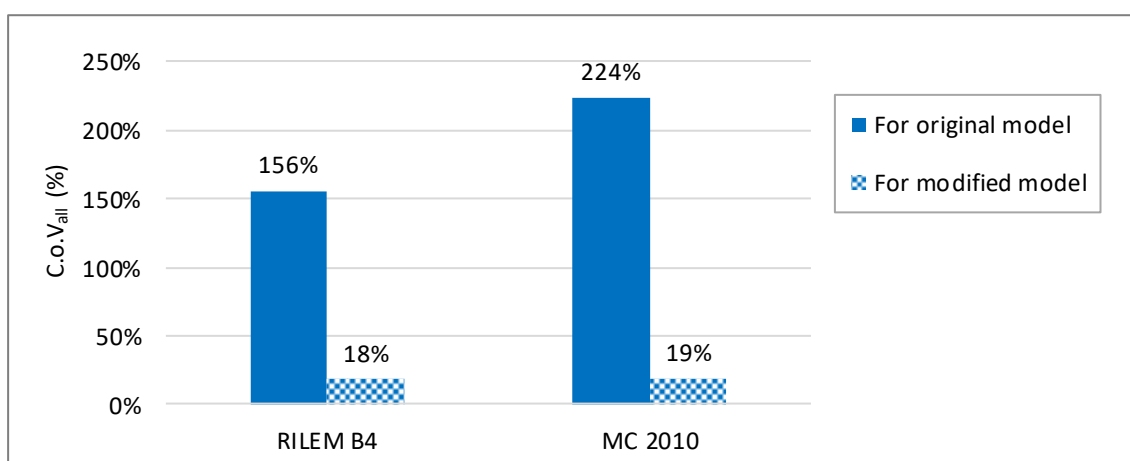


Figure 5.25 Original and modified model  $C.o.V_{all}$  for data subsets with mineral and chemical admixtures – autogenous shrinkage.



## 5.7 Original vs. modified model overall ranking

Averages of the statistical indicators RMSE,  $R^2_{adj}$ ,  $AIC_c$  and  $C.o.V_{all}$  obtained from the drying shrinkage predictions/analyses for HSC made using the original and modified versions of the RILEM B4, MC 2010 and WITS models for the entire Dataset 1-HSC (drying shrinkage), as well as for each of the time intervals considered (0 to 99, 100 to 199, 200 to 499 and  $\geq 500$  days), are shown in Table 5.6. Based on these statistical indicators, both the original and modified versions of the WITS model are the most accurate. Accuracy of the predictions of the modified RILEM B4 and MC 2010 models were close to each other and only a little worse than those of the modified WITS model, with the modified MC 2010 model being the better of the two.

Table 5.6 Summary of averaged statistical indicators RMSE,  $R^2_{adj}$ ,  $AIC_c$  and  $C.o.V_{all}$  for original and modified versions of the RILEM B4, MC 2010 and WITS models - Dataset 1-HSC.

Statistical indicators	original RILEM B4	original MC 2010	original WITS	Statistical indicators	modified RILEM B4	modified MC 2010	modified WITS
RMSE (overall)	89.94	166.77	93.88	RMSE (overall)	46.24	44.55	38.15
$R^2_{adj}$ (overall)	-10.41	-22.83	-7.92	$R^2_{adj}$ (overall)	-0.13	0.06	0.29
$AIC_c$ (overall)	458.10	355.76	296.83	$AIC_c$ (overall)	242.67	232.20	226.80
$C.o.V_{all}$ (overall)	0.39	0.65	0.40	$C.o.V_{all}$ (overall)	0.15	0.14	0.12
RMSE (0-99 days)	106.90	108.17	84.63	RMSE (0-99 days)	49.11	35.04	32.22
$R^2_{adj}$ (0-99 days)	-2.76	-2.89	-1.57	$R^2_{adj}$ (0-99 days)	0.48	0.64	0.68
$C.o.V_{all}$ (0-99 days)	0.39	0.58	0.38	$C.o.V_{all}$ (0-99 days)	0.25	0.15	0.15
RMSE (100-199 days)	112.80	134.04	84.86	RMSE (100-199 days)	39.80	34.40	25.78
$R^2_{adj}$ (100-199 days)	-36.37	-108.48	-23.30	$R^2_{adj}$ (100-199 days)	-9.36	-1.18	-1.11
$C.o.V_{all}$ (100-199 days)	0.36	0.70	0.36	$C.o.V_{all}$ (100-199 days)	0.18	0.12	0.10
RMSE (200-499 days)	99.13	141.78	62.10	RMSE (200-499 days)	30.27	26.86	21.17
$R^2_{adj}$ (200-499 days)	-79.50	-396.78	-82.85	$R^2_{adj}$ (200-499 days)	-4.25	-2.47	-2.18
$C.o.V_{all}$ (200-499 days)	0.34	2.30	0.27	$C.o.V_{all}$ (200-499 days)	0.11	0.22	0.08
RMSE ( $\geq 500$ days)	75.29	219.24	63.39	RMSE ( $\geq 500$ days)	24.25	20.24	18.84
$R^2_{adj}$ ( $\geq 500$ days)	-43.20	-238.82	-44.38	$R^2_{adj}$ ( $\geq 500$ days)	-3.15	-2.03	-1.07
$C.o.V_{all}$ ( $\geq 500$ days)	0.36	1.12	0.28	$C.o.V_{all}$ ( $\geq 500$ days)	0.10	0.09	0.09

For the data subsets without admixtures and with chemical admixtures, prediction accuracies of the original models follow this same ranking order: WITS model most accurate, followed by the RILEM B4 and MC 2010 models. However, for the subset of data for concretes with mineral admixtures the order of prediction accuracy (model ranking) was reversed, with the MC 2010 model now the most accurate, followed by the RILEM B4 model, then the WITS model.

In modifying the models and fitting them to the data in the various subsets considered here, the WITS model function showed better compatibility with the experimental shrinkage profiles than the RILEM B4 and MC 2010 models. The MC 2010 model was, however, the least complex to update and often showed the greatest improvements for this dataset. In all cases drying shrinkage predictions made for the HSC

experiments considered in this study were significantly better with the modified shrinkage models than with the original versions.

Averages of the statistical indicators RMSE,  $R^2_{adj}$ ,  $AIC_c$  and  $C.o.V_{all}$  obtained from the autogenous shrinkage predictions/analyses for HSC made using the original and modified versions of the RILEM B4 and MC 2010 models for the entire Dataset 2-HSC (autogenous shrinkage), as well as for each of the time intervals considered (0 to 99, 100 to 199, 200 to 499 and  $\geq 500$  days), are shown in Table 5.7. Based on these statistical indicators, the original and modified RILEM B4 model consistently outranked the MC 2010 model. This was to be expected as the RILEM B4 model includes admixture combination model parameters to account for cement hydration rate, which affects the magnitude of estimated autogenous shrinkages. However, the modified MC 2010 outranked the modified RILEM B4 for long term shrinkage ( $\geq 500$  days).

Table 5.7 Summary of averaged statistical indicators RMSE,  $R^2_{adj}$ ,  $AIC_c$  and  $C.o.V_{all}$  calculated for original and modified versions of the RILEM B4 and MC 2010 models - Dataset 2-HSC.

Statistical indicators	original RILEM B4	original MC 2010	Statistical indicators	modified RILEM B4	modified MC 2010
RMSE (overall)	167.97	246.20	RMSE (overall)	40.99	41.56
$R^2_{adj}$ (overall)	-15.65	-44.92	$R^2_{adj}$ (overall)	0.74	0.63
$AIC_c$ (overall)	191.04	209.90	$AIC_c$ (overall)	136.42	139.69
$C.o.V_{all}$ (overall)	1.56	2.24	$C.o.V_{all}$ (overall)	0.18	0.20
RMSE (0-99 days)	157.60	208.03	RMSE (0-99 days)	34.07	33.28
$R^2_{adj}$ (0-99 days)	-15.55	-42.87	$R^2_{adj}$ (0-99 days)	0.81	0.67
$C.o.V_{all}$ (0-99 days)	1.71	2.39	$C.o.V_{all}$ (0-99 days)	0.25	0.26
RMSE (100-199 days)	165.10	271.03	RMSE (100-199 days)	27.62	32.66
$R^2_{adj}$ (100-199 days)	950.01	1314.20	$R^2_{adj}$ (100-199 days)	2.59	3.63
$C.o.V_{all}$ (100-199 days)	1.04	1.47	$C.o.V_{all}$ (100-199 days)	0.14	0.16
RMSE (200-499 days)	103.22	287.79	RMSE (200-499 days)	40.54	39.47
$R^2_{adj}$ (200-499 days)	17.05	28.98	$R^2_{adj}$ (200-499 days)	3.42	3.53
$C.o.V_{all}$ (200-499 days)	0.62	1.32	$C.o.V_{all}$ (200-499 days)	0.164	0.156
RMSE ( $\geq 500$ days)	91.39	235.65	RMSE ( $\geq 500$ days)	50.52	44.28
$R^2_{adj}$ ( $\geq 500$ days)	-0.93	-5.20	$R^2_{adj}$ ( $\geq 500$ days)	0.759	0.761
$C.o.V_{all}$ ( $\geq 500$ days)	0.40	0.93	$C.o.V_{all}$ ( $\geq 500$ days)	0.16	0.13

## 5.8 Conclusions

The results of this study, recorded in Chapter 4, were discussed in detail. The performances of the shrinkage models considered, the RILEM B4, MC 2010 and WITS models, were analysed based on their applicability to NSC and HSC shrinkage experiments, the regions from which the experiments originated and their applicability to subsets with and without mineral and chemical admixtures. Graphical and statistical evaluations of the results corresponded.

Error percentage plots were used to assess the spread of over- and under-estimation (compared to actual or measured values) of shrinkage by each model, expected to be randomly distributed about zero for

---

suitable models. The modified models indeed showed random scatter about zero, a reasonably normal distribution of their residuals, and no trends, justifying the use of the least squares regression statistic RSS in the calculation of the AIC values. Tables indicating the overall maximum error percentages for each of the shrinkage time ranges considered (0 to 99, 100 to 499 and  $\geq 500$  days) for data subsets with and without chemical and mineral admixtures, were used to determine whether the models predicted within a  $\pm 20\%$  error band for all experiments for all data subsets.

About 10% of the data was not used to modify the models, but rather to validate them once updated. The validation analyses showed that the modified models could not predict within a  $\pm 20\%$  error band across all the experiments in the data subsets without admixtures. For the data subsets with mineral and chemical admixtures, the the modified models did not predict drying shrinkage within a  $\pm 20\%$  error band over the short-term (0 to 99 days), but could do so for the medium- and long-term shrinkage periods. The poorer calibration of the models over the short-term is attributed to there being too few drying shrinkage data points available (in all three of the model applicable data subsets) in this time range.

The statistical indicators used for overall (complete dataset) model ranking were RMSE,  $R^2_{adj}$  and AIC. For predictions over the separate shrinkage time ranges the indicators RMSE,  $R^2_{adj}$  and C.o.V<sub>all</sub> were used to rank the models. Aggregated results of the analyses for drying shrinkage prediction for the complete dataset (Dataset 1-HSC) showed the modified WITS model to be the best (most accurate), then the modified MC 2010 and modified RILEM B4 models. For the limited set of experiments that showed an early age peak in drying shrinkage, the proposed composite model gave the best results, as it was designed to model this peak, followed by the modified versions of the WITS, MC 2010 and RILEM B4 models. For autogenous shrinkage prediction, for both the complete dataset (Dataset 2-HSC) and for the time periods 0 to 99, 100 to 199, 200 to 499 and  $\geq 500$  days, predictions of the RILEM B4 model were better than those of the MC 2010 model. The modified RILEM B4 model also performed better than the modified MC 2010 model over the short- and medium-term periods, but did not predict long-term ( $\geq 500$  days) autogenous shrinkage as well as the modified MC 2010 model.

---

## Chapter 6 Conclusions and recommendations

This study considered the application of the RILEM B4, MC 2010 and WITS concrete shrinkage models in the prediction of drying and autogenous shrinkage of HSC. Initially a single database of concrete shrinkage results was compiled from the published 2018 version NU database (Northwestern University, 2018), Akthem Al-Manaseer and Abdullah Fayyaz's published experimental data (Al-Manaseer and Fayyaz, 2011) and the Concrete Institute of South Africa database, resulting in information and data on 2192 shrinkage experiments, covering drying, autogenous and total shrinkage. A reliable subset of data which included only drying and autogenous shrinkage experiments, with either rapid hardening or rapid development of early age strength cement type, a w/cm ratio  $\leq 0.42$  and  $f_{cm28} \geq 60$  MPa was extracted from the full dataset. This data subset was further divided into subsets with covariate data falling only in the ranges applicable (i.e. ranges for which the models were originally developed) to each of the RILEM B4, MC 2010 and WITS models.

These data subsets were used to test each model's performance (accuracy) in predicting shrinkage of both NSC and HSC. Where possible, missing data were imputed to increase the number of usable experiments for model predictions. The extracted experiments were then further divided into drying and autogenous shrinkage experiments after missing data were added. From these, subsets of data for HSC concrete (taken in this study as concretes with w/cm  $\leq 0.42$  and  $f_{cm28} \geq 60$  MPa) were derived and used to modify the existing shrinkage model parameters. A composite (empirical) model was proposed, derived using data from a limited number of subsets that showed a distinct peak in drying shrinkage between about 85 and 117 days. These data subsets are for concretes containing mineral and chemical admixtures such as SRA, SP and metakaolin, and the characteristic is seen only in a few experimental results.

Shrinkage predictions of the original and modified models were compared and used to rank the models for the complete HSC datasets, the data subsets and for individual shrinkage time periods (0 to 99, 100 to 199, 200 to 499 and  $\geq 500$  days) as appropriate, using the statistical indicators RMSE,  $R^2_{adj}$ , AIC and C.o.V<sub>all</sub>. Comparisons were also made across the different geographical regions from which the experiments originated, as different test specifications and cement classifications are used in these different regions.

### 6.1 Conclusions

Based on the datasets applicable to each model data range, the lowest overall C.o.V<sub>all</sub> across all the drying shrinkage data was achieved by the modified WITS model, followed by the modified MC 2010 and modified RILEM B4 models. For autogenous shrinkage, the lowest overall C.o.V<sub>all</sub> was achieved by the RILEM B4 model, which is expected as autogenous shrinkage was a major component incorporated in the improvement of the B3 model to the B4 model. Both the RILEM B4 and MC 2010 models had very large C.o.V values for autogenous shrinkage compared to their C.o.V values for drying shrinkage, reflecting how conservative the models are in autogenous shrinkage prediction compared to drying shrinkage prediction. (Hubler *et al*, 2015) indicated that the physical phenomena inherent in autogenous shrinkage are not yet fully understood and therefore the autogenous shrinkage component of the RILEM B4 model is purely empirical.

The MC 2010 model predicted shrinkage worse for North American concretes than for European concretes, possibly due to differences in cement classification and concrete composition, with the European concretes used to optimize the MC 2010 model having lower cement content (CEB-FIP, 2013;

Gaylard *et al*, 2013). The RILEM B4 model showed a similar trend, but performed better than the MC 2010 model for North American, European and East Asian concretes. Surprisingly the MC 2010 model achieved the lowest ( $< 40\%$  C.o.V<sub>all</sub>) for the Southern African concretes. Overall, for drying shrinkage, the WITS model achieved the lowest C.o.V<sub>all</sub> for both NSC and HSC, while for autogenous shrinkage the RILEM B4 model outperformed the MC 2010 model for both NSC and HSC.

Based on the HSC drying shrinkage experiments without admixtures, the overall performances of the original RILEM B4 and WITS models were equally good, followed by the MC 2010 model. According to Hubler *et al* (2015), for the NU database, the RILEM B4 model achieved a lower C.o.V<sub>all</sub> than the MC 2010 model over the short- and long-term shrinkage periods for experiments without admixtures. In this study, the C.o.V of the original MC 2010 model was lower by 4% and 3% than that of the RILEM B4 model for short- and long-term shrinkage, respectively. The original RILEM B4 and MC 2010 models had C.o.V<sub>all</sub> values of 39% and 38%, respectively for the data subsets without admixtures, which is close to what Hubler *et al* (2015) reported, namely 32% and 41%, respectively. The overall performance of the modified WITS model was best, followed by the RILEM B4 and MC 2010 models.

For experiments with mineral admixtures from the HSC drying shrinkage dataset, the overall performance of the original MC 2010 model was best, followed by the RILEM B4 and WITS models. This seemed strange as all experiments in these subsets are from the South African database and part of the data used in the development of the WITS model. The original WITS model was the least accurate for short-term shrinkage only. The overall performance was possibly influenced by the distribution of available data, in that many results are available for short-term shrinkage, but few for medium-term shrinkage. The overall performance of the modified WITS model was best, followed by the RILEM B4 and MC 2010 models. The modified WITS model predicted drying shrinkage within a  $\pm 20\%$  error band for the validating experiment data with mineral admixtures, while the RILEM B4 and MC 2010 models predicted within a  $\pm 30\%$  error band for the medium-term shrinkage period.

Based on data in the HSC drying shrinkage dataset from experiments with concretes containing mineral and chemical admixtures, the overall performance of the original WITS model was best, followed by the RILEM B4 and MC 2010 models. After model modification, the best overall performance was still achieved by the modified WITS model, but followed now by the MC 2010 and RILEM B4 models. The modified WITS model predicted drying shrinkages within a  $\pm 15\%$  error band for the validating experimental data with chemical admixtures (except for the first data point), and the RILEM B4 model agreed with the experimental data within  $\pm 20\%$  only for the medium- and long-term shrinkage periods. For the entire HSC dataset for drying shrinkage, as well as for each of the shrinkage time intervals considered (0 to 99, 100 to 199, 200 to 499 and  $\geq 500$  days) the original and modified WITS model agreed most closely with measured values.

For the limited number of concrete compositions whose data showed a peak over approximately the 85 to 117 day period, the proposed models outranked all the existing models overall (the complete dataset) and for each shrinkage time interval. They matched the early shrinkage peaks well and fitted better over the final (medium- and long-term) shrinkage time. This is to be expected though, as the mathematical form of the composite models is designed to match these experimental shrinkage profiles, something the mathematical forms of the RILEM B4, MC 2010 and WITS models can't do.

Based on the autogenous shrinkage experiments with mineral and chemical admixtures, the performances of both the original and modified RILEM B4 models were better than those of the MC 2010

---

models. This was so for the complete dataset and over each of the shrinkage time periods considered. For the majority of the experiments in the HSC autogenous shrinkage dataset, both modified models predicted values within a  $\pm 20\%$  error band, except for the first shrinkage data point, which was over- or underestimated significantly. When checked against the data of the validating experiments, both modified models predicted within a  $\pm 22\%$  error band, again except for the first autogenous shrinkage data point. A reason for this is not clear.

All the modified model predictions (for both drying and autogenous shrinkage) achieved an absolute C.o.V<sub>all</sub> of less than 20% for the data subsets with and without admixtures. The modified WITS model had the lowest C.o.V<sub>all</sub> ( $\leq 13\%$ ) for all the drying shrinkage data subsets, suggesting this model to be superior to the modified RILEM B4 and MC 2010 models in predicting drying shrinkage for HSC. The modified RILEM B4 model predicted autogenous shrinkage across all the HSC datasets used in this study about 10% more accurately than the MC 2010 model.

Based on the overall accuracies for the experiments considered in this study, namely concretes of cement types CEM I, CEM II (A-S), CEM II (B-S), CEM II (A-D), CEM II (A-Q), CEM II (B-M) and CEM III A; for w/cm ratio 0.28 to 0.4, for coarse aggregates with RD of 2.65 to 2.98 (Andesite, Dolerite, Granite, Sandstone, Quartzite) and for concretes with admixtures such as superplasticiser 0 to 3%, plasticiser 0 to 0.2 %, SRA 0 to 2.5%, SF 0 to 10%, FA 0 to 30%, GGBS 0 to 35%, GGCS 0 to 50%, GGFS 0 to 50% and metakaolin 0 to 13%, the WITS model is recommended for predicting drying shrinkage of both NSC and HSC, with or without admixtures. The MC 2010 model is less complex with fewer model parameters than both the WITS and RILEM B4 models, and easier to use. Therefore, it's recommended use is for preliminary design estimates of drying shrinkage. The RILEM B4 model is particularly advanced, and is more accurate in predicting autogenous shrinkage than the MC 2010 model, and so is to be recommended for autogenous shrinkage of NSC and HSC with the cement type CEM I and CEM II (A-D), for w/cm 0.23 to 0.25, for coarse aggregates Granite and Quartzite and for concretes with admixtures such as SP 0 to 3%, plasticiser 0 to 0.013%, RE 0 to 1%, AEA 0 to 0.005%, SF 0 to 10% and metakaolin 0 to 13%.

## 6.2 Recommendations

A combination of the existing models into one composite model, where the more accurate model predicts for certain time ranges. For example, the modified RILEM B4 predicts for the autogenous shrinkage time period 0 to 199 days and the modified MC 2010 model predicts from 200 days onwards for the HSCs considered in this study.

To better assess the overall accuracy and ranking of the prediction models, more statistical evaluation methods could be considered, such as the mean absolute deviation and Bažant's coefficient of variation with the weighting applied to each shrinkage time interval (on a logarithmic scale). The corrected CEB coefficient of variation and mean square error, presented in Gaylard (2011) could be used as well.

To further understand the relationship between drying and autogenous shrinkage in HSC specifically, simultaneous experimental tests of long durations ( $\geq 500$  days) should be conducted for both types of shrinkage using the same concrete compositions. Such tests should ensure that all the requirements of the test standards are met, and that all the relevant data is properly recorded. This type of data were not found in the published databases used in this study.

As the database for drying and autogenous shrinkage experiments for HSC with mineral and chemical admixtures grows, a more general model could be derived if the data suggests this is needed. Initially this could be an empirical composite model as suggested in this study, incorporating statistically derived scaling factors to enable better prediction of the early age shrinkage peaks (as seen in this study) and the final shrinkage. Additionally, the functions used for the early age and final shrinkage parts of the composite models suggested in this study could be replaced with any of the existing, established shrinkage models.

---

## References

Abdalmid, J.M., Ashour, A.F. & Sheehan, T. 2019. Long-term drying shrinkage of self-compacting concrete: Experimental and analytical investigations. *Construction and Building Materials*, 202: 825-837.

Abdel-Jawad, Y.A. 2006. The maturity method: Modifications to improve estimation of concrete strength at later ages. *Construction and Building Materials*, 20(10): 893-900, December.

Aictin, P. & Mindess, S. 2011. *Sustainability of concrete*. Oxon: Spon Press.

Alexander, M. & Beushausen, H. 2009. Deformation and volume change of hardened concrete. In Owens, G. (eds). *Fulton's concrete technology*. 9<sup>th</sup> rev. ed. Midrand: Cement & Concrete Institute: 111-154.

Al-Manaseer, A & Fayyaz, A. 2011. Creep and drying shrinkage of High Performance Concrete for the Skyway structures of the new San Francisco – Oakland Bay Bridge and Cement Paste (Technical Report No. CA 10-1131). Department of Civil Engineering, California.

Al-Manaseer, A.F. & Prado, A. 2015. Statistics comparisons of creep and shrinkage prediction models using RILEM and NU-ITI database. *ACI Materials Journal*, 112(1): 125-136.

American Concrete Institute Committee 363. 1997. *State-of-the-art report on high-strength concrete*. Detroit: ACI publications.

American Concrete Institute Committee 224. 2001. *Control of cracking in concrete structures*. Detroit: ACI publications

American Concrete Institute Committee 209. 2008. *Guide for modelling and calculating shrinkage and creep in hardened concrete*. Detroit: ACI publications.

ASTM C150. 2012. *Standard specification for Portland cement*. West Conshohocken: ASTM International.

ASTM C157. 2008. *Standard test method for length change of hardened hydraulic-cement mortar and concrete*. West Conshohocken: ASTM International.

ASTM C595. 2016. *Standard specification for blended hydraulic cements*. West Conshohocken: ASTM International.

Ballim, Y., Alexander, M. & Beushausen, H. 2009. In Owens, G. (eds). *Fulton's concrete technology*. 9<sup>th</sup> rev. ed. Midrand: Cement & Concrete Institute: 155-188.

Bažant, Z.P. & Baweja, S. 1995(a). Creep and shrinkage prediction models for analysis and design of concrete structures – Model B3. *Material and Structures*, 28: 357-365.

Bažant, Z.P. & Baweja, S. 1995(b). Justification and refinements of Model B3 for concrete creep and shrinkage – Statistics and sensitivity. *Material and Structures*, 28: 415-430.



- 
- Bažant, Z.P. & Baweja, S. 2000. Creep and shrinkage prediction models for analysis and design of concrete structures – Model B3. *The Adam Neville Symposium: Creep and shrinkage – structural design effects*, Akthem Al-Manasseer, ed., American Concrete Institute, Farmington Hills, 237-260.
- Bažant, Z.P. & Li, G-H. 2008. Unbiased statistical comparison of creep and shrinkage models. *ACI Materials Journal*, 105(6): 610-621.
- Beushausen, H. & Dehn, F. 2009. High-performance concrete. In Owens, G. (eds). *Fulton's concrete technology*. 9<sup>th</sup> rev. ed. Midrand: Cement & Concrete Institute: 297-304.
- Boshoff, W.P. & Combrink, R. 2013. Modelling the severity of plastic shrinkage cracking in concrete. *Cement and Concrete Research*, 48: 34-39.
- Bouziadi, F., Boulekbache, B. & Hamrat, M. 2016. The effects of fibre on the shrinkage of high-strength concrete under various curing temperatures. *Construction and Building Materials*, 114: 40-48.
- Bozdogan, H. 2000. Akaike's Information Criterion and recent developments in information complexity. *Journal of mathematical psychology*, 44:62-91.
- Buchwald, P. 2007. A general bilinear model to describe growth or decline time profiles. *Mathematical Biosciences*, 205: 108-136.
- Burnham, K.P. & Anderson, D.R. 2002. *Model Selection and Multimodel Inference. A Practical Information-Theoretic Approach*. 2nd ed. Springer Science + Business Media, LLC. New York. [ISBN 978-0-387-95364-9].
- Burnham, K.P., Anderson, D. R. & Huyvaert, K.P. 2011. AIC model selection and multimodal inference in behavioural ecology: some background, observations, and comparisons. *Behav Ecol Sociobiol*, 65:23-35.
- CEB-FIP. 2012. *Bulletin 65 CEB-FIP Model code 2010 Final Draft*. International Federation for Structural Concrete, Lausanne.
- CEB-FIP. 2013. *Bulletin 70 Code-type models for structural behaviour of concrete: Background of the constitutive relations and material models in the fib Model Code for structures 2010*. International Federation for Structural Concrete, Lausanne.
- Choi, S., Tareen, N., Kim, J., Park, S. & Park, I. 2018. Real-time strength monitoring for concrete structures using EMI technique incorporating with fuzzy logic. *Applied Science*, 8(75):1-13, January.
- Chu, I., Kwon, S.H., Amin, M.N. & Kim, J. 2012. Estimation of temperature effects on autogenous shrinkage of concrete by a new prediction model. *Construction and Building Materials*, 35: 171-182.
- Comité European du Béton. 1999. *Structural concrete – Textbook on behaviour, Design and performance, updated knowledge of the CEB/FIB model code 1990*. Fib Bulletin 2, vol 2, Federation Internationale du Béton, Lausanne, Switzerland, 37-52.
-

- 
- CPUT Library Respository. 2020(a). 213073838 R Noordien MEng CD Appendix AA, electronic dataset, Cape Peninsula University of Technology Library Respository, DOI: <https://doi.org/10.25381/cput.13194041.v2>
- CPUT Library Respository. 2020(b). 213073838 R Noordien MEng CD Appendix BB to KK, Cape Peninsula University of Technology Library Respository, DOI:
- Domone, P. 2010. Concrete. In Domone, P. Illston, J. (eds). *Construction Materials, their nature and behaviour*. Spon Press, OX: Abingdon: 83-208.
- Ebrahim, N. 2017. Using superabsorbent polymers in high performance concrete to mitigate autogenous and plastic shrinkage while observing the compressive strength. Msc Eng Thesis, Stellenbosch University, Stellenbosch.
- Fanourakis, G.C. 2017. Validation of the FIB 2010 and RILEM B4 models for predicting creep in concrete. *Architecture Civil Engineering Environment*, 3: 95-101.
- Frontline Systems. 2000-2020. Frontline solvers 2020 plug-in solver engines user guide. last viewed September 2020. <https://www.solver.com/developers#tab1>
- Fulton, F. S. 1986. *Fulton's concrete technology*. 6<sup>th</sup> rev. ed. Addis, B.J. & Davis, D.E (eds). Midrand: Portland Cement Institute.
- Gadagkar, S.R. & Call, G.B. 2015. Computational tools for fitting the Hill equation to dose-response curves. *Journal of Pharmacological and Toxicological Methods*, 71: 68-76.
- Gardner, N.J. & Lockman, M. J. 2001. Design provisions for drying shrinkage and creep of normal-strength concrete. *ACI Materials Journal*, 98(2): 159-167.
- Gardner, N.J. 2004. Comparison of prediction provisions for drying shrinkage and creep of normal strength concretes. *Canadian Journal of Civil Engineering*, February.
- Gaylard, P.C. 2011. Statistical modelling of the shrinkage behaviour of South African concretes. Unpublished MSc thesis, University of Witwatersrand, Johannesburg.
- Gaylard, P.C., Ballim, Y. & Fatti, L. P. 2013. A model for the drying shrinkage of South African concretes. *Journal of the South Africa Institute of Civil Engineering*, 55(1): 45-59, April.
- Goel, R., Kumar, R. & Paul, D. K. 2007. Comparative study of various creep and shrinkage prediction models for concrete. *Journal of materials in Civil Engineering*, 19(3): 249-260.
- Gonen, T. & Yazicioglu, S. 2006. The influence of mineral admixtures on the short and long-term performance of concrete. *Building and Environment*, 42: 3080-3085.
- Grieve, G. 2009. Cementitious materials. In Owens, G. (eds). *Fulton's concrete technology*. 9<sup>th</sup> rev. ed. Midrand: Cement & Concrete Institute: 1-16, 25-60.
-

- 
- Guðmundsson, J.G. 2013. Long-term creep and shrinkage in concrete using porous aggregate – the effects of elastic modulus. MSc thesis, Reykjavik University, Iceland.
- Gupta, S.M., Aggarwal, P. & Aggarwal, Y. 2006. Shrinkage of high strength concrete. *Asian journal of civil engineering (Building and housing)*, 7(2):183-194.
- Hassan, K.E., Cabrera, J.G. & Maliene, R.S. 2000. The effect of mineral admixture on the properties of high-performance concrete. *Cement and Concrete Research*, 22: 267-271.
- Hassoun, M.N. & Al-Manaseer, A.A. 2008. *Structural concrete: theory and design*. 4<sup>th</sup> rev. ed. New Jersey: Hoboken, N.J.: J. Wiley.
- Hill, A.V. 1910. The possible effects of aggregation of the molecules of haemoglobin on its dissociation curves. *Journal of Physiology*, 40: iv-vii.
- Holowaty, J. 2015. Conventional models for shrinkage of concrete. *American Journal of Materials Science and Application*, 3(6): 81-87.
- Hubler, M.H., Wedner, R. & Bažant, Z.P. 2015. Statistical justification of model B4 for drying and autogenous shrinkage of concrete and comparisons to other models. *Materials and Structures*, 48: 797-814.
- ISO 16311-1. 2014. Maintenance and repair of concrete structures – Part 1: General principles. Switzerland: ISO 2014.
- John, E.G. 1998. Simplified curve fitting using spreadsheet add-in. *International Journal Engineering Edition*, 14(5): 375-380.
- Kataoka, L.T., Machado, M.A.S. & Bittencourt, T.N. 2011. Short-term experimental data of drying shrinkage of granulated blast-furnace slag cement concrete. *Materials and Structures*, 44:671-679.
- Kim, J. & Lee, C. 1999. Moisture diffusion of concrete considering self-desiccation at early ages. *Cement and Concrete Research*, 29:1921-1927, August.
- Kochel, B. 2003. Logistic-exponential model for chemiluminescence kinetics. *Talanta*, 60: 377-393.
- Kovler, K. & Zhutovsky, S. 2006. Overview and future trends of shrinkage research. *Materials and Structure*, 39: 827-847.
- Labbé, S. & Lopez, M. 2020. Towards a more accurate shrinkage modeling of lightweight and infra-lightweight concrete. *Construction and Building Materials*, 246: 118369-118380.
- Lam, L., Wong, Y.L. & Poon, C.S. 1998. Effect of FA and SF on compressive and fracture behaviours of concrete. *Cement & Concrete*, 28(2): 271-283.
- Lee, J., Lim, K., Yoo, D. & Lim, N. 2017. Deformation characteristics of ultrahigh-strength concrete under unrestrained and restrained state. *Advances in Material Science and Engineering*, 2017: 1-8, July 5.
-

- 
- Mazloom, M. 2008. Estimating long-term creep and shrinkage of high-strength concrete. *Cement and Concrete Composites*, 30(4): 316-326.
- McArdle, B., Navakatikyan, M.A. & Davison, M. 2019. Application of Information Criteria to behavioral studies. <https://www.researchgate.net/publication/330337138>. DOI: 10.13140/RG.2.2.20378.90566
- Mehta, P.K. & Monteiro, P.J. M. 2006. *Concrete microstructure, properties and materials*. 3<sup>rd</sup> rev. ed. New York: The McGraw Hill Companies.
- Mucambe, E.S.D. 2010. Creep and shrinkage prediction models for concrete water retaining structures in South Africa. Unpublished MSc thesis, University of Stellenbosch, Stellenbosch.
- Myung, I.J. 2000. The Importance of Complexity in Model Selection. *Journal of Mathematical Psychology*, 44, 190-204.
- Northwestern University. 2018. *NU Database of Laboratory Creep and Shrinkage Data*, electronic dataset, Northwestern University, viewed April 2018, <http://www.civil.northwestern.edu/people/bazant/>
- Pan, Z. & Meng, S. 2016. Three-level experimental approach for creep and shrinkage of high-strength high-performance concrete. *Engineering Structures*, 120: 23-36.
- Pease, B.J. 2005. The role of shrinkage reducing admixtures on shrinkage, stress development and cracking. Unpublished MSc thesis, Purdue University, Lafayette.
- Pomeroy, C.D. & Marsh, B. (2014). Concrete. In Doran, D. & Cather, B. (eds). *Construction Materials Reference Book*. Routledge, OX: Abingdon: 141-153.
- Rajabipour, F., Sant, G. & Weiss, J. 2008. Interactions between shrinkage reducing admixtures (SRA) and cement paste's pore solution. *Cement and Concrete Research*, 38: 606-615.
- Rasoolinejad, M., Rahimi-Aghdam, S. & Bažant, Z.P. 2019. Prediction of autogenous shrinkage in concrete from material composition or strength calibrated by a large database, as update to model B4. *Materials and Structures*, 52(33): 1-17.
- RILEM TC-242-MDC. 2015. RILEM draft recommendation: TC-242-MDC multi-decade creep and shrinkage of concrete: material model and structural analysis. *Material and Structures*, 48: 753-770.
- Saliba, J., Rozière, E., Grondin, F. & Loukili, A. 2011. Influence of shrinkage-reducing admixtures on plastic and long-term shrinkage. *Cement & Concrete Composites*, 33: 209-217.
- Sagara, A. & Pane, I. 2015. A study on effects of creep and shrinkage in high strength concrete bridges. *Procedia Engineering*, 125: 1087-1093.
- SANS 50197-1. 2013. Cement: Part 1: Composition, specifications and conformity criteria for common cements. Pretoria: SABS Standards Division.
-

- 
- SANS 6085. 2006. Concrete tests – Initial drying shrinkage and wetting expansion of concrete. Pretoria: SABS Standards Division.
- SANS 10100-1. 2000. The structural use of concrete – Part 1: Design. Pretoria: SABS Standards Division.
- Seijo-Pardo, B., Alonso-Betanzos, A., Bennett, K.P., Bolón-Canedo, V., Josse, J., Saeed, M. & Guyon, I. 2019. Biases in feature selection with missing data. *Neurocomputing*, February 13.
- Setareh, M. & Darvas, R. 2007. *Concrete structures*. New Jersey: Pearson Education, Inc.
- Tam, C.M., Tam, W.Y. & Ng, K.M. 2012. Assessing drying shrinkage and water permeability of reactive powder concrete produced in Hong Kong. *Construction and Building Materials*, 26: 79-89.
- Van Schalkwyk, D.J. 2019-2020. Personal consultation. 19 September 2019 to 7 May 2020, Cape Town.
- Walraven, J.C. & Bigaj-van Vliet, A.J. 2011. The 2010 fib model code for structural concrete: a new approach to structural engineering. *Structural Concrete*, 12(3): 139-147.
- Walsh, S. & Diamond, D. 1994. Non-Linear curve fitting using Microsoft Excel Solver. *Elsevier Science Ltd*, 42(4): 561-572.
- Wedner, R., Hubler, M.H. & Bažant, Z.P. 2015(a). Comprehensive database for concrete creep and shrinkage: Analysis and recommendations for testing and recording. *ACI Materials Journal*, July-August.
- Wedner, R., Hubler, M.H. & Bažant, Z.P. 2015(b). Optimization method, choice of form and uncertainty quantification of model B4 using laboratory and multi-decade bridge databases. *Material and Structures*, January.
- Wedner, R., Hubler, M.H. & Bažant, Z.P. 2014. Model B4: Multi-decade creep and shrinkage prediction of traditional and modern concretes. Proceedings of Computational Modelling of Concrete Structures EURO-C 2014, 24 March 2014: 679-684. Austria.
- Wittmann, F.H. 1968. Surface tension, shrinkage and strength of hardened cement paste. *Materials and structures*, 1(6):547-552.
- Wittmann, F.H. 1982. *Creep and shrinkage mechanisms. Part II in Creep and shrinkage in concrete structures*, (ed) by Bažant, Z. P., Wittmann F. H., John Wiley & Sons, 129-163.

# Appendices

## Appendix A. MC 2010, RILEM B4 and WITS model formulae

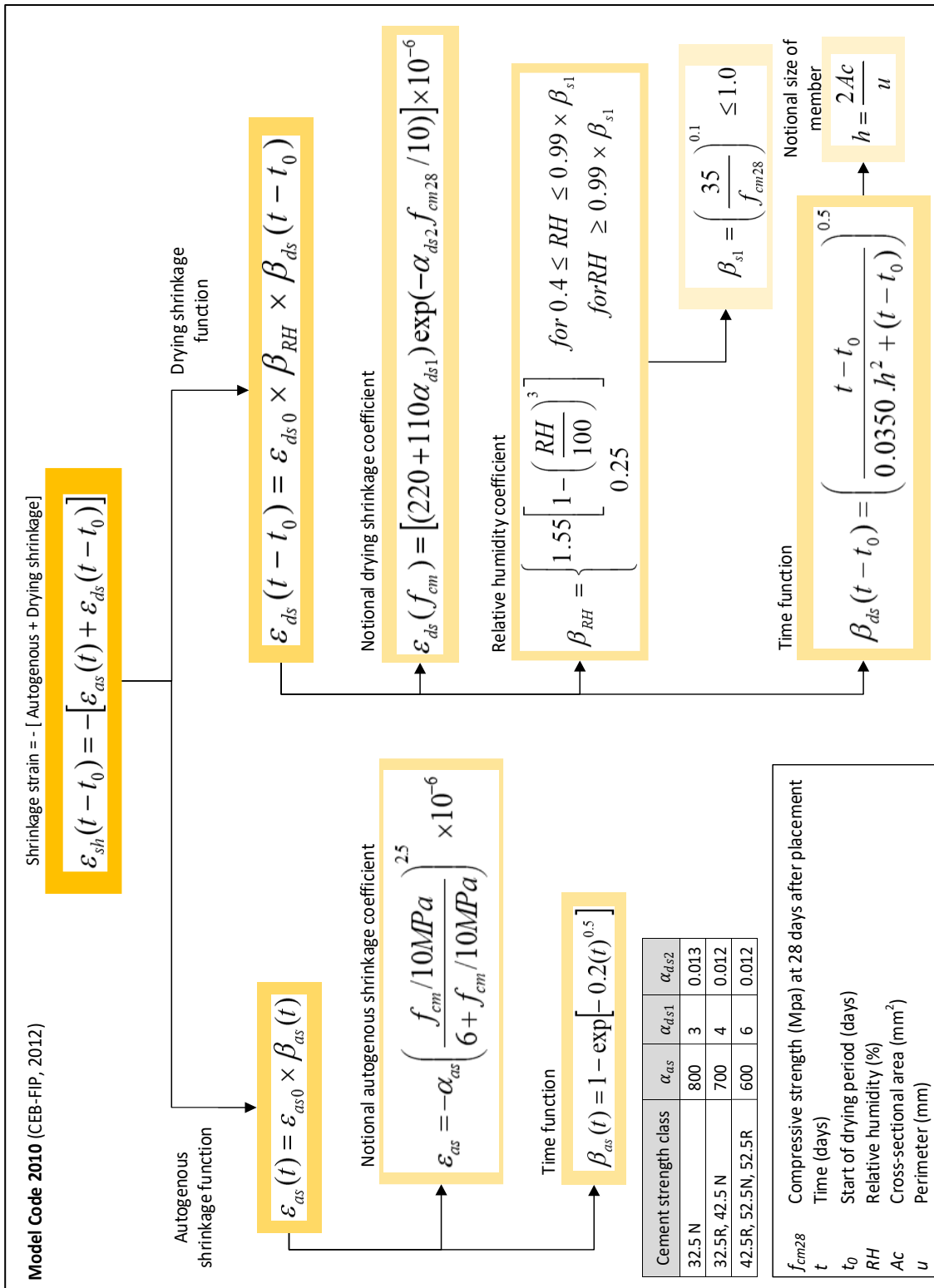


Figure A.1 Summary of the MC 2010 model formulae(CEB-FIP, 2012)

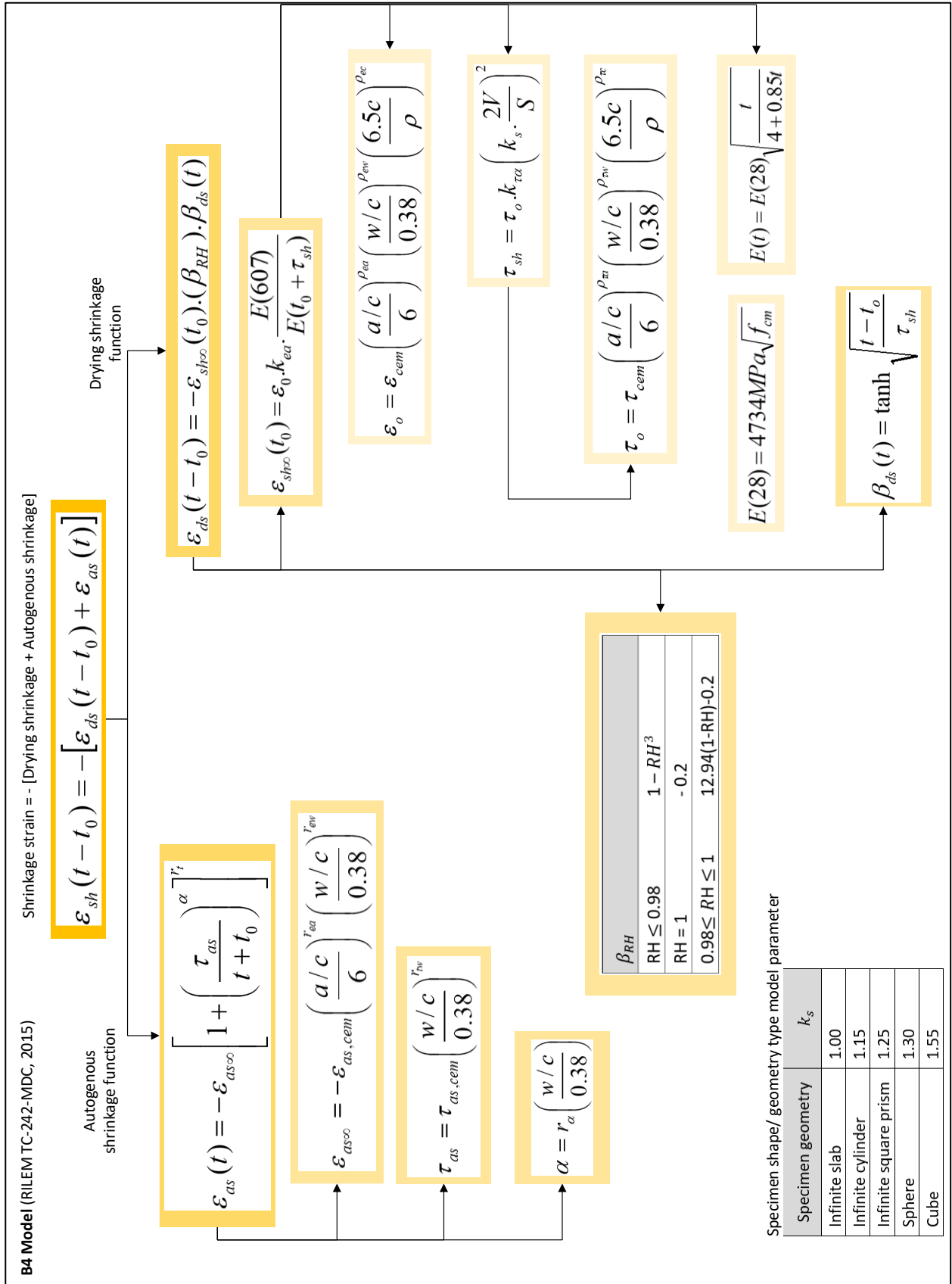


Figure A.2 Summary of the RILEM B4 model formulae (RILEM TC-242-MDC, 2015)

Table A.1 Cement type dependant RILEM B4 model parameters for drying shrinkage (RILEM TC-242-MDC, 2015).

Model parameters	R	RS	SL
$\tau_{cem}$	0.016	0.08	0.01
$P_{\tau a}$	-0.33	-0.33	-0.33
$P_{\tau w}$	-0.06	-2.4	3.55
$P_{\tau c}$	-0.1	-2.7	3.80
$\epsilon_{cem}$	$361 \times 10^{-6}$	$860 \times 10^{-6}$	$410 \times 10^{-6}$
$P_{\epsilon a}$	-0.8	-0.8	-0.8
$P_{\epsilon w}$	1.1	-0.27	1.00
$P_{\epsilon c}$	0.11	0.11	0.11

Table A.2 Cement type dependant RILEM B4 model parameters for autogenous shrinkage (RILEM TC-242-MDC, 2015).

Admixture class (% of c)	R	RS	SL
$\tau_{as,cem}$	1.00	41.0	1.00
$r_{\tau w}$	3.00	3.00	3.00
$r_t$	-4.5	-4.50	-4.50
$r_a$	1.00	1.40	1.00
$\epsilon_{as,cem}$	$210 \times 10^{-6}$	$-84.0 \times 10^{-6}$	$0.00 \times 10^{-6}$
$r_{\epsilon a}$	-0.75	-0.75	-0.75
$r_{\epsilon w}$	-3.50	-3.50	-3.50

Table A.3 Aggregate type dependant RILEM B4 model parameters for drying shrinkage (RILEM TC-242-MDC, 2015).

Aggregate type	$k_{\tau a}$	$k_{\epsilon a}$	Young's Modulus $E_{agg}$ (GPa)	Density $\rho_{agg}$ (g/cm <sup>3</sup> )
Diabase	0.06*	0.76*	70 – 90	2.8 – 3.0
Quartzite	0.59	0.71	50 – 90	2.5 – 2.8
Limestone	1.80	0.95	10 – 70	1.8 – 2.9
Sandstone	2.30	1.60	10 – 50	2.0 – 2.8
Granite	4.00	1.05	30 – 70	2.5 – 2.8
Quartz Diorite	15.0*	2.20*	50 – 100	2.7 – 3.1

\*denotes uncertain fitted parameters



Table A.4 Admixture combination type dependant RILEM B4 model parameters for drying and autogenous shrinkage (RILEM TC-242-MDC, 2015).

Model parameters	$\times \tau_{cem}$	$\times \epsilon_{as,cem}$	$\times r_{\epsilon w}$	$\times r_{\alpha}$
Re ( $\leq 0.5$ ), Fly ( $\leq 15$ )	6.00	0.58	0.50	2.60
Re ( $> 0.5, \leq 0.6$ ), Fly ( $\leq 15$ )	2.00	0.43	0.59	3.10
Re ( $> 0.5, \leq 0.6$ ), Fly ( $> 15, \leq 30$ )	2.10	0.72	0.88	3.40
Re ( $> 0.5, \leq 0.6$ ), Fly ( $> 30$ )	2.80	0.87	1.60	5.00
Re ( $> 0.6$ ), Fly ( $\leq 15$ )	2.00	0.26	0.22	0.95
Re ( $> 0.6$ ), Fly ( $> 15, \leq 30$ )	2.10	1.10	1.10	3.30
Re ( $> 0.6$ ), Fly ( $> 30$ )	2.10*	1.10	0.97	4.00
Fly ( $\leq 15$ ), Super ( $\leq 5$ )	0.32	0.71	0.55	1.71
Fly ( $\leq 15$ ), Super ( $> 5$ )	0.32*	0.55	0.92	2.30
Fly ( $> 15, \leq 30$ ), Super ( $\leq 5$ )	0.50	0.90	0.82	1.25
Fly ( $> 15, \leq 30$ ), Super ( $> 5$ )	0.50*	0.80	0.80	2.81
Fly ( $> 30$ ), Super ( $\leq 5$ )	0.63	1.38	0.00	1.20
Fly ( $> 30$ ), Super ( $> 5$ )	0.63*	0.95	0.76	3.11
Super ( $\leq 5$ ), Silica ( $\leq 8$ )	6.00	2.80	0.29	0.21
Super ( $\leq 5$ ), Silica ( $\geq 8$ )	3.00	0.96	0.26	0.71
Super ( $\geq 5$ ), Silica ( $\leq 8$ )	8.00	1.95	0.00	1.00
Silica ( $\leq 8$ )	1.90	0.47	0.00	1.20
Silica ( $> 8, \leq 18$ )	2.60	0.82	0.00	1.20
Silica ( $> 18$ )	1.00	1.50	5.00	1.00
AEA ( $\leq 0.05$ )	2.30	1.10	0.28	0.35
AEA ( $> 0.05$ )	0.44	4.28	0.00	0.36
WR ( $\leq 2$ )	0.50	0.38	0.00	1.90
WR ( $> 2, \leq 3$ )	6.00	0.45	1.51	0.30
WR ( $> 3$ )	2.40	0.40	0.68	1.40

\*assumed parameters – lacking data

WITS Model (Gaylard, 2011)

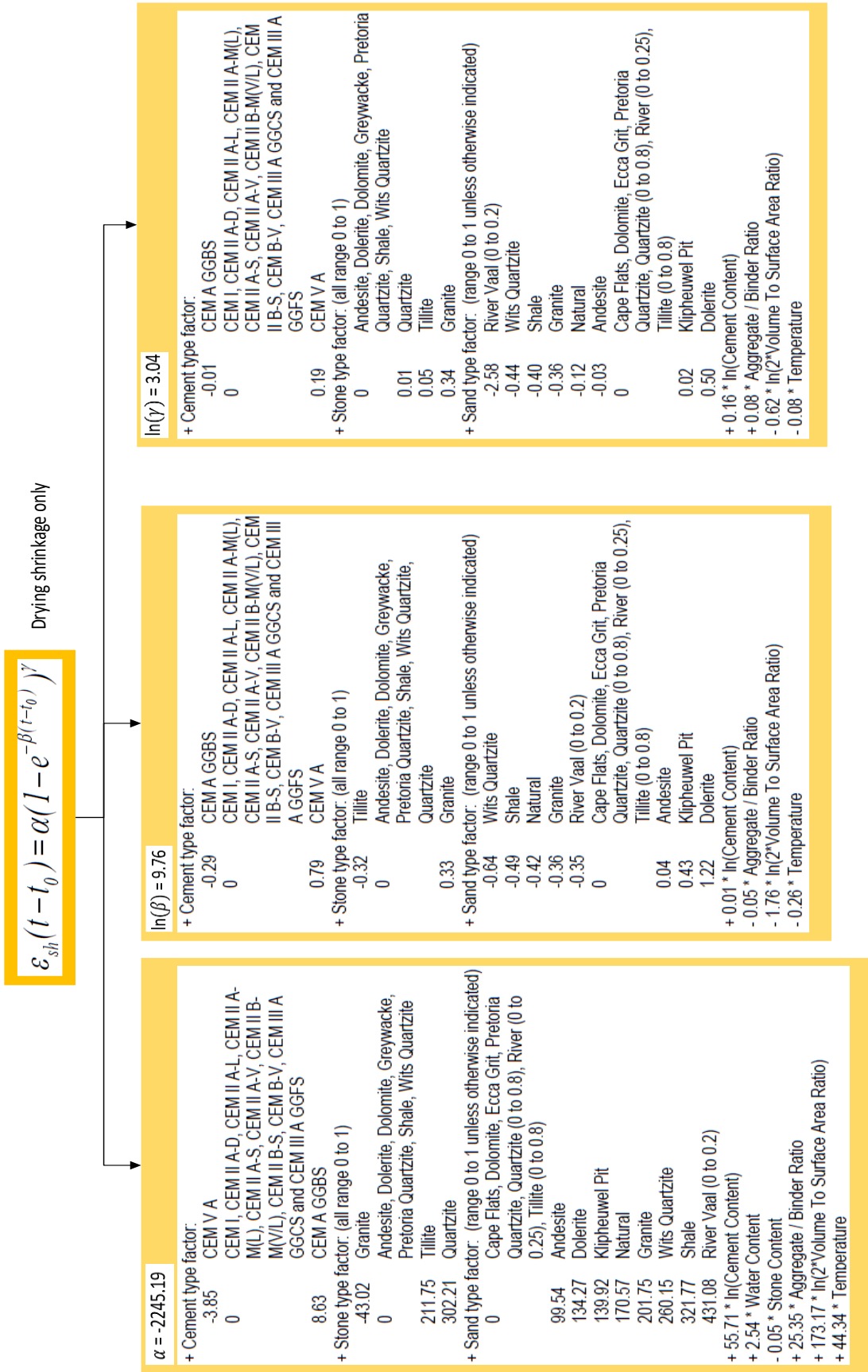


Figure A.3 Summary of the WITS model formulae (Gaylard, 2011)

Table A.5 Cement, stone and sand types considered by the WITS model (Gaylard, 2011; Gaylard *et al*, 2013).

Stone type	Cement type										
	CEM I	CEM II A - D	CEM II A - L	CEM II A - M(L)	CEM II A - S	CEM II A - V	CEM II B - M(V/L)	CEM II B - S	CEM II B - V	CEM III A	CEM VA
Andesite	✓		✓	✓	✓		✓	✓	✓	✓	✓
Dolerite	✓	✓	✓		✓	✓		✓	✓	✓	
Dolomite	✓							✓		✓	
Granite	✓							✓	✓	✓	
Greywacke	✓					✓			✓	✓	
Pretoria Quartzite	✓										
Quartzite	✓										
Shale										✓	
Tillite	✓							✓	✓	✓	
Wits Quartzite	✓									✓	
Sand type	Cement type										
	CEM I	CEM II A - D	CEM II A - L	CEM II A - M(L)	CEM II A - S	CEM II A - V	CEM II B - M(V/L)	CEM II B - S	CEM II B - V	CEM III A	CEM VA
Andesite	✓										
Cape Flats	✓					✓			✓		
Dolerite	✓	✓							✓	✓	
Dolomite	✓		✓		✓	✓		✓	✓	✓	
Ecca grit									✓		
Granite	✓		✓	✓			✓	✓	✓	✓	✓
Klipheuwel pit	✓									✓	
Natural	✓				✓			✓		✓	
Pretoria Quartzite	✓										
Quartzite (up to 80% *)	✓										
* Indicates maximum proportion of sand type in total sand content											

Table A.6 Cement and sand types considered by the WITS model continuation (Gaylard, 2011; Gaylard et al., 2013).

Sand type	Cement type										
	CEM I	CEM II A - D	CEM II A - L	CEM II A - M(L)	CEM II A - S	CEM II A - V	CEM II B - M(V/L)	CEM II B - S	CEM II B - V	CEM III A	CEM VA
River (up to 25% *)	✓									✓	
River Vaal (up to 20% *)	✓							✓	✓	✓	
Shale										✓	
Tillite (up to 80% *)	✓							✓	✓	✓	
Wits Quartzite	✓									✓	
* Indicates maximum proportion of sand type in total sand content											
Sand type	Stone type										
	Andesite	Dolerite	Dolomite	Granite	Grey-wacke	Pretoria Quartzite	Quartzite	Shale	Tillite	Wits Quartzite	
Andesite	✓										
Cape Flats					✓						
Dolerite		✓									
Dolomite		✓	✓								
Ecca grit		✓									
Granite	✓			✓							
Klipheuwel pit					✓						
Natural	✓	✓									
Pretoria Quartzite						✓					
Quartzite (up to 80% *)							✓				
River (up to 25% *)										✓	
River Vaal (up to 20% *)	✓		✓	✓	✓	✓	✓		✓	✓	
Shale											
Tillite (up to 80% *)									✓		
Wits Quartzite								✓		✓	

## Appendix B. Statistical results per data subset of Dataset 1-HSC & Dataset 2-HSC

Table B.1 Statistical indicator results of original model for data subsets without admixtures and with mineral admixtures of Dataset 1-HSC.

Subset No	CEM type - w/cm - Agg	Experiment No.	Original model											
			R <sup>2</sup> adj			RMSE			AICc			C.o.V		
			WITS	MC 2010	B4	WITS	MC 2010	B4	WITS	MC 2010	B4	WITS	MC 2010	B4
S1-01	CEM I - 0.41 - G	# 0158	-7.08	-27.2	-40.6	109.6	205.1	249.0	15.2	10.9	10.7	0.31	0.58	0.71
		# 0219												
		# 0108	-204.9	-5.7	-6.37	505.1	91.3	95.6	20.8	19.7	13.9	1.25	0.23	0.24
S1-02	CEM I - 0.41 - Q	# 0217												
		# 0261	0.61	0.49	0.004	74.5	84.7	118.6	94.8	96.2	72.3	0.19	0.22	0.31
		# 0264												
S1-03	CEM I - 0.41 - S	# 0079												
		# 0081												
		# 0083	-3.15	-12.6	-2.12	112.6	169.2	91.4	84.9	84.6	69.1	0.28	0.42	0.23
S1-04	CEM I - 0.41 - A	# 0221												
		# 0225												
		# 0015	-1.70	-6.24	-4.37	56.1	104.5	86.3	-	-	-	0.17	0.31	0.25
S1-05	CEM I - 0.41 - D	# 0031												
		# 0033												
		# 0228	-0.37	0.10	-0.30	99.7	78.1	91.1	96.9	91.4	88.1	0.30	0.24	0.27
S2-01	CEM II (A-S) - 0.40 - A	# 0237	0.09	0.46	-0.03	82.1	60.9	96.1	104.0	97.3	103.3	0.28	0.21	0.33
		# 0249												
		# 0234	-3.14	-2.82	-2.4	109.9	102.8	80.0	98.9	97.6	85.7	0.32	0.30	0.24
S2-02	CEM II (B-S) - 0.4 - A	# 0252												
		# 0234												
		# 0252												
S2-03	CEM III A - 0.4 - A	# 0234												
		# 0234												
		# 0252												
		Data subsets without admixtures												
		Data subsets with mineral admixtures												

Table B.2 Statistical indicator results of original model for data subsets without admixtures and with mineral admixtures of Dataset 1-HSC.

Subset No	CEM type - w/cm - Agg	Admixture class	Experiment No.	Original model											
				R <sup>2</sup> adj			RMSE			AICc			C.o.V		
				WITS	MC 2010	B4	WITS	MC 2010	B4	WITS	MC 2010	B4	WITS	MC 2010	B4
S2-04	CEM I - 0.28 - Q	>1 S	A_007_13 A_007_16	0.34	-10.19	-6.02	79.72	333.4	265.1	204.0	268.6	256.4	0.20	0.84	0.67
S2-05	CEM I - 0.40 - S	<1 S	# 0109 # 0255	0.37	-1.05	-0.17	58.19	99.62	87.86	92.43	98.5	68.9	0.17	0.30	0.26
S2-06	CEM II (A-D) - 0.36 - S	>1 S	A_070_34 A_070_38 A_070_39	-2.02	-0.64	-1.41	134.3	94.83	118.5	479.3	442.4	465.4	0.47	0.33	0.41
S2-07	CEM II (A-Q) - 0.29 - Q	>1 S	A_007_14 A_007_15	-0.85	-17.03	-7.92	97.72	296.0	207.9	222.9	273.9	255.4	0.28	0.85	0.60
S2-08	CEM II (B-M)-0.33 - G	<1 S, 25 FA <1 S, 30 FA	6 10	-2.54	-95.71	-7.58	46.94	247.4	73.53	389.9	556.9	434.1	0.20	1.07	0.32
S2-09	CEM II (B-M)-0.33 - G	<1 S, <0.5 P	31 33	-1.27	-11.46	-21.34	45.08	106.8	142.3	409.0	500.5	529.9	0.13	0.30	0.40
S2-10	CEM II (B-M)-0.33 - G	<1 S, 25 FA <1 S, 30 FA	5 9	-10.92	-16.82	-14.42	101.0	125.3	115.0	467.2	488.9	478.8	0.28	0.35	0.32
S2-11	CEM II (B-M)-0.33 - G	<1 S, 0.5 SRA <1 S, 1.0 SRA <1 S, 2.0 SRA <1 S, 2.5 SRA	7 13 15 16	-6.82	-73.46	-7.56	77.77	266.2	85.00	437.2	576.9	452.3	0.40	1.36	0.43
S2-12	CEM II (B-M)-0.33 - G	<1 S, <0.5 P	17 25	-28.86	-14.49	-34.09	140.6	103.0	151.7	505.3	473.2	511.7	0.35	0.26	0.38
S2-13	CEM II (B-M)-0.33 - G	<1 S, <0.5 P, 1.0 SRA <1 S, <0.5 P, 2.0 SRA <1 S, <0.5 P, 2.5 SRA	19 21 22	-1.67	-42.95	-1.92	58.05	236.0	61.3	425.7	572.6	432.0	0.25	1.02	0.26
S2-14	CEM II (B-M)-0.33 - G	<1 S, <0.5 P, 1.0 SRA <1 S, <0.5 P, 1.5 SRA <1 S, <0.5 P, 2.0 SRA <1 S, <0.5 P, 2.5 SRA	27 28 29 30	-1.94	-49.17	-2.25	51.89	242.6	58.3	404.7	581.3	427.2	0.23	1.10	0.26
Data subsets with mineral & chemical admixtures															

Table B.3 Statistical indicator results of modified models for data subsets without admixtures and with mineral admixtures of Dataset 1-HSC.

Subset No	CEM type - w/cm - Agg	Experiment No.	Modified models											
			R <sup>2</sup> <sub>adj</sub>			RMSE			AICc			C.o.V		
			B4	MC 2010	WITS	B4	MC 2010	WITS	B4	MC 2010	WITS	B4	MC 2010	WITS
S1-01	CEM I - 0.41 - G	# 0158	-4.46	-4.12	-0.01	90.17	87.33	38.73	8.20	11.53	7.63	0.26	0.25	0.11
		# 0219												
		# 0108	-0.67	-2.52	-0.51	45.43	66.08	43.25	11.15	7.47	6.43	0.11	0.16	0.11
S1-02	CEM I - 0.41 - Q	# 0217												
		# 0261	0.73	0.80	0.86	61.01	53.71	43.70	66.20	91.16	90.05	0.16	0.14	0.11
S1-03	CEM I - 0.41 - S	# 0264												
		# 0079												
S1-04	CEM I - 0.41 - A	# 0081												
		# 0083	-1.55	-1.34	-1.41	81.94	92.98	81.24	63.88	84.26	76.84	0.20	0.23	0.20
		# 0221												
		# 0225												
		# 0015	0.38	-0.40	0.34	34.34	50.79	33.72	-	-	-	0.10	0.15	0.10
S1-05	CEM I - 0.41 - D	# 0031												
		# 0033												
		# 0228	0.64	0.40	0.70	51.47	64.10	47.32	78.82	87.83	83.12	0.15	0.19	0.14
S2-01	CEM II (A-S) - 0.40 - A	# 0237												
		# 0246												
S2-02	CEM II (B-S) - 0.4 - A	# 0240	0.78	0.77	0.92	41.35	42.40	26.15	85.46	90.36	80.36	0.14	0.14	0.09
		# 0249												
S2-03	CEM III A - 0.4 - A	# 0234	0.01	-0.04	0.12	58.64	56.77	52.64	81.76	115.8	85.69	0.17	0.17	0.15
		# 0252												
		Data subsets without admixtures												
		Data subsets with mineral admixtures												

Table B.4 Statistical indicator results of modified models for data subsets with mineral and chemical admixtures of Dataset 1-HSC.

Subset No	CEM type - w/cm - Agg	Admixture class	Experiment No.	Modified models												
				R <sup>2</sup> adj			RMSE			AICc			C.o.V			
				B4	MC 2010	WITS NEW	B4	MC 2010	WITS NEW	B4	MC 2010	WITS NEW	B4	MC 2010	WITS NEW	
S2-04	CEM I - 0.28 - Q	>1 S	A_007_13	0.85	0.90	0.38	36.7	29.9	79.6	166	159	204	0.09	0.08	0.20	
			A_007_16													
S2-05	CEM I - 0.40 - S	<1 S	# 0109	0.57	0.53	0.87	51.6	54.9	28.7	63	92	84	0.15	0.16	0.09	
			# 0255													
S2-06	CEM II (A-D) - 0.36 - S	>1 S	A_070_34	0.57	0.53	0.58	48.0	50.0	46.6	377	382	373	0.17	0.17	0.16	
			A_070_38													
			A_070_39													
S2-07	CEM II (A-Q) - 0.29 - Q	>1 S	A_007_14	0.51	0.80	0.94	50.3	30.6	18.2	190	167	144	0.14	0.09	0.05	
			A_007_15													
S2-08	CEM II (B-M)-0.33 - G	<1 S, 25 FA <1 S, 30 FA	6	0.31	0.17	0.34	20.8	22.9	20.4	308	319	307	0.09	0.10	0.09	
			10													
S2-09	CEM II (B-M)-0.33 - G	<1 S, <0.5 P	31	0.19	0.53	0.78	27.2	20.7	14.0	353	327	286	0.08	0.06	0.04	
			33													
S2-10	CEM II (B-M)-0.33 - G	<1 S, 25 FA <1 S, 30 FA	5	0.54	0.46	0.67	20.1	21.8	16.9	304	314	289	0.06	0.06	0.05	
			9													
S2-11	CEM II (B-M)-0.33 - G	<1 S, 0.5 SRA <1 S, 1.0 SRA <1 S, 2.0 SRA <1 S, 2.5 SRA	7													
			13	-0.46	0.20	0.19	35.3	26.7	26.3	366	339	337	0.18	0.14	0.13	
			15													
			16													
S2-12	CEM II (B-M)-0.33 - G	<1 S, <0.5 P	17	-0.21	0.13	-0.01	28.0	24.5	25.8	341	322	334	0.07	0.06	0.06	
			25													
S2-13	CEM II (B-M)-0.33 - G	<1 S, <0.5 P, 1.0 SRA <1 S, <0.5 P, 2.0 SRA <1 S, <0.5 P, 2.5 SRA	19													
			21	0.52	0.68	0.74	24.5	19.2	17.9	337	308	305	0.11	0.08	0.08	
			22													
S2-14	CEM II (B-M)-0.33 - G	<1 S, <0.5 P, 1.0 SRA <1 S, <0.5 P, 1.5 SRA <1 S, <0.5 P, 2.0 SRA <1 S, <0.5 P, 2.5 SRA	27													
			28													
			29	-1.61	0.40	0.35	55.1	25.1	27.7	421	340	351	0.25	0.11	0.13	
			30													

Data subsets with mineral & chemical admixtures



Table B.5 Statistical indicator results of original models for data subsets with mineral and chemical admixtures of Dataset 2-HSC.

Subset No	CEM type - w/cm - Agg	Admixture class	Experiment No.	Original models							
				R <sup>2</sup> adj		RMSE		AICc		C.o.V	
				B4	MC 2010	B4	MC 2010	B4	MC 2010	B4	MC 2010
S2-01a	CEM I - 0.27 - G	1 S	A_072_04	0.84	-168.0	17.4	268.9	94.2	165.6	0.08	1.25
			A_072_05								
S2-02a	CEM I - 0.27 - Q	3 S	A_007_09	-20.8	-3.7	287.8	93.2	318.0	251.2	0.74	0.24
			A_007_12								
S2-03a	CEM I - 0.31 - G	1 S	A_072_06	0.75	-22.9	46.2	312.6	114.5	173.6	0.19	1.25
			A_086_18								
			A_086_20								
S2-04a	CEM I - 0.31 - G	<0.5 P	A_068_01	-8.91	-0.004	455.3	144.4	246.2	201.4	0.88	0.28
			A_068_19								
S2-05a	CEM I - 0.35 - G	3 S, 1RE	A_022_03	-136.7	-338.5	247.2	377.1	287.9	303.6	4.39	6.70
			A_022_05								
S2-06a	CEM II (A-D) - 0.23 - Q	2 S	A_086_41	0.56	0.5	95.7	99.7	134.8	135.4	0.32	0.33
			A_086_42								
S2-07a	CEM II (A-D) - 0.28 - G	2 S	A_086_36	0.37	-0.5	111.2	160.5	130.1	136.4	0.32	0.46
			A_086_37								
S2-08a	CEM II (A-D) - 0.28 - Q	1 S	A_086_26	0.23	-1.0	119.7	193.8	170.8	187.1	0.53	0.85
			A_086_30								
			A_086_31								
S2-09a	CEM II (A-D) - 0.34 - G		A_031_04								
			A_031_06	0.17	-32.9	59.1	327.4	160.2	235.6	0.31	1.73
			A_046_02								
			A_046_07								
S2-10a	CEM II (A-D) - 0.34 - Q	1 S	A_086_07	0.03	-7.6	95.9	298.5	169.2	209.2	0.54	1.67
			A_086_09								
			A_086_11								
S2-11a	CEM II (A-D) - 0.34 - Q	1 S (AE)	A_086_13	-10.6	-14.7	304.9	356.3	202.5	207.8	1.66	1.94
			A_086_14								
S2-12a	CEM III (A-D) - 0.29 - Q	3 S	A_007_06	-53.5	-13.3	404.9	207.8	354.4	316.0	2.24	1.15
			A_007_07								
Data subsets with mineral and chemical admixtures											

Table B.6 Statistical indicator results of modified models for data subsets with mineral and chemical admixtures of Dataset 2-HSC.

Subset No	CEM type - w/cm - Agg	Admixture class	Experiment No.	Modified models							
				R <sup>2</sup> adj		RMSE		AICc		C.o.V	
				B4	MC 2010	B4	MC 2010	B4	MC 2010	B4	MC 2010
S2-01a	CEM I - 0.27 - G	1 S	A_072_04	0.84	-0.15	17.41	23.87	94.20	97.88	0.08	0.11
			A_072_05								
S2-02a	CEM I - 0.27 - Q	3 S	A_007_09	0.74	0.73	27.27	25.71	185.1	181.1	0.07	0.07
			A_007_12								
S2-03a	CEM I - 0.31 - G	1 S	A_072_06	0.89	0.76	29.32	41.84	99.1	140.1	0.12	0.26
			A_086_18								
S2-04a	CEM I - 0.31 - G	<0.5 P	A_086_20								
			A_068_01	0.76	0.92	71.18	43.54	173.9	154.4	0.14	0.08
S2-05a	CEM I - 0.35 - G	3 S, 1RE	A_068_19								
			A_022_03	0.83	0.54	8.57	14.37	110.2	138.8	0.15	0.26
S2-06a	CEM II (A-D) - 0.23 - Q	2 S	A_022_05								
			A_086_41	0.88	0.86	50.91	55.47	118.8	121.4	0.17	0.18
S2-07a	CEM II (A-D) - 0.28 - G	2 S	A_086_42								
			A_086_36	0.77	0.78	59.94	58.55	110.0	109.5	0.17	0.17
S2-08a	CEM II (A-D) - 0.28 - Q	1 S	A_086_37								
			A_086_26	0.89	0.89	44.40	44.11	135.7	136.2	0.20	0.19
S2-09a	CEM II (A-D) - 0.34 - G		A_086_30								
			A_086_31								
			A_031_04	0.17	0.07	59.12	61.95	160.2	158.7	0.31	0.33
			A_046_02								
S2-10a	CEM II (A-D) - 0.34 - Q	1 S	A_046_07								
			A_086_07	0.69	0.74	58.18	52.41	151.4	147.9	0.33	0.29
S2-11a	CEM II (A-D) - 0.34 - Q	1 S (AE)	A_086_09								
			A_086_11	0.92	0.87	26.27	32.46	117.2	125.6	0.14	0.18
S2-12a	CEM II (A-D) - 0.29 - Q	3 S	A_086_13								
			A_086_14	0.91	0.83	16.69	22.88	169.0	188.0	0.09	0.13
Data subsets with mineral and chemical admixtures											

## Appendix C. Statistical results per shrinkage range of data subsets in Dataset 1-HSC & Dataset 2-HSC

Table C.1  $R^2_{adj}$  results of original models per shrinkage range for data subsets without and with mineral admixtures of Dataset 1-HSC.

Subset No	CEM type - w/cm - Agg	Experiment No.	Original models					
			$R^2_{adj}$ (0 - 99 days)			$R^2_{adj}$ (200 - 499 days)		
			B4	MC 2010	WITS	B4	MC 2010	WITS
S1-01	CEM I - 0.41 - G	# 0158	-	-	-	-	-	-
		# 0219	-	-	-	-	-	-
		# 0108	-	-	-	-	-	-
S1-02	CEM I - 0.41 - Q	# 0217	-	-	-	-	-	-
		# 0261	0.54	-0.13	0.61	-	-	-
S1-03	CEM I - 0.41 - S	# 0264	0.96	0.32	0.21	0.70	0.72	0.90
		# 0079						
S1-04	CEM I - 0.41 - A	# 0081						
		# 0083	0.96	0.32	0.21	0.70	0.72	0.90
		# 0221						
		# 0225						
S1-05	CEM I - 0.41 - D	# 0015	-	-	-	-	-	-
		# 0031	-	-	-	-	-	-
		# 0033	-	-	-	-	-	-
S2-01	CEM II (A-S) - 0.40 - A	# 0228	0.02	-0.54	-1.37	-0.03	0.37	0.03
		# 0237	0.02	-0.54	-1.37	-0.03	0.37	0.03
		# 0246	0.02	-0.54	-1.37	-0.03	0.37	0.03
S2-02	CEM II (B-S) - 0.4 - A	# 0240	-0.37	0.32	-0.79	0.37	0.68	0.39
		# 0249	-0.37	0.32	-0.79	0.37	0.68	0.39
S2-03	CEM III A - 0.4 - A	# 0234	0.02	-2.25	-4.88	0.89	0.85	0.86
		# 0252	0.02	-2.25	-4.88	0.89	0.85	0.86
		Data subsets without admixtures			Data subsets with mineral admixtures			

Table C.2  $R^2_{adj}$  results of original models per shrinkage range for data subsets with mineral and chemical admixtures of Dataset 1-HSC.

Subset No	CEM type - w/cm - Agg	Admixture class	Experiment No.	Original models											
				$R^2_{adj}$ (0 - 99 days)			$R^2_{adj}$ (100 - 199 days)			$R^2_{adj}$ (200 - 499 days)			$R^2_{adj}$ ( $\geq$ 500 days)		
				B4	MC 2010	WITS	B4	MC 2010	WITS	B4	MC 2010	WITS	B4	MC 2010	WITS
S2-04	CEM I - 0.28 - Q	>1 S	A_007_13	-5.37	-10.3	0.05	-10.7	-19.9	0.72	-	-	-	-	-	
			A_007_16												
S2-05	CEM I - 0.40 - S	<1 S	# 0109	0.56	-2.01	0.00	-	-	-	-	-	-	-		
			# 0255												
S2-06	CEM II (A-D) - 0.36 - S	>1 S	A_070_34	-1.41	-0.64	-2.02	-	-	-	-	-	-	-		
			A_070_38												
			A_070_39												
S2-07	CEM II (A-Q) - 0.29 - Q	>1 S	A_007_14	-7.79	-18.2	-1.70	-10.3	-25.3	0.53	-	-	-	-		
			A_007_15												
S2-08	CEM II (B-M)-0.33 - G	<1 S, 25 FA	6	-2.56	-1.35	0.13	-0.53	-52.2	-0.46	-22.1	-948	-29.2	-32.3		
		<1 S, 30 FA	10												
S2-09	CEM II (B-M)-0.33 - G	<1 S, <0.5 P	31	-11.7	-3.29	-2.22	-177	-27.7	-18.8	-292	-30.8	-58.6	-93.1		
			33												
S2-10	CEM II (B-M)-0.33 - G	<1 S, 25 FA	5	-7.17	-0.17	-3.76	-43.4	-2.68	-24.6	-101	-349	-160	-42.4		
		<1 S, 30 FA	9												
S2-11	CEM II (B-M)-0.33 - G	<1 S, 0.5 SRA	7												
		<1 S, 1.0 SRA	13	0.48	-5.49	-1.11	-14.6	-178	-37.9	-107	-1219	-153	-28.5		
		<1 S, 2.0 SRA	15												
		<1 S, 2.5 SRA	16												
S2-12	CEM II (B-M)-0.33 - G	<1 S, <0.5 P	17	-16.7	-2.55	-10.9	-122	-0.65	-74.6	-298	-118	-458	-122		
			25												
S2-13	CEM II (B-M)-0.33 - G	<1 S, <0.5 P, 1.0 SRA	19												
		<1 S, <0.5 P, 2.0 SRA	21	0.28	-2.50	0.06	-9.47	-221	-28.9	-26.5	-697	-37.0	-7.50		
		<1 S, <0.5 P, 2.5 SRA	22												
		<1 S, <0.5 P, 1.0 SRA	27												
S2-14	CEM II (B-M)-0.33 - G	<1 S, <0.5 P, 1.5 SRA	28												
		<1 S, <0.5 P, 2.0 SRA	29	0.74	-3.34	-0.03	-13.9	-426	-46.7	-10.8	-430	-15.0	-14.0		
		<1 S, <0.5 P, 2.5 SRA	30												
Data subsets with mineral & chemical admixtures															

Table C.3  $R^2_{adj}$  results of modified models per shrinkage range for data subsets without and with mineral admixtures of Dataset 1-HSC.

Subset No	CEM type - w/cm - Agg	Experiment No.	Modified models										
			$R^2_{adj}$ (0 - 99 days)				$R^2_{adj}$ - 499 days)						
			B4	MC 2010	WITS	B4	MC 2010	WITS	B4	WITS			
S1-01	CEM I - 0.41 - G	# 0158	-	-	-	-	-	-	-	-	-	-	-
		# 0219	-	-	-	-	-	-	-	-	-	-	-
		# 0108	-	-	-	-	-	-	-	-	-	-	-
		# 0217	-	-	-	-	-	-	-	-	-	-	-
		# 0261	0.67	0.52	0.70	-	-	-	-	-	-	-	-
		# 0264	0.67	0.52	0.70	-	-	-	-	-	-	-	-
S1-02	CEM I - 0.41 - Q	# 0079	-	-	-	-	-	-	-	-	-	-	-
		# 0081	-	-	-	-	-	-	-	-	-	-	-
		# 0083	0.94	0.67	0.76	0.91	0.07	0.87	-	-	-	-	-
		# 0221	0.94	0.67	0.76	0.91	0.07	0.87	-	-	-	-	-
		# 0225	0.94	0.67	0.76	0.91	0.07	0.87	-	-	-	-	-
		# 0015	0.94	0.67	0.76	0.91	0.07	0.87	-	-	-	-	-
S1-03	CEM I - 0.41 - S	# 0031	-	-	-	-	-	-	-	-	-	-	-
		# 0033	-	-	-	-	-	-	-	-	-	-	-
		# 0228	0.53	0.14	0.57	0.70	-0.04	0.43	-	-	-	-	-
		# 0237	0.53	0.14	0.57	0.70	-0.04	0.43	-	-	-	-	-
		# 0246	0.53	0.14	0.57	0.70	-0.04	0.43	-	-	-	-	-
		# 0240	0.53	0.14	0.57	0.70	-0.04	0.43	-	-	-	-	-
S1-04	CEM I - 0.41 - A	# 0249	0.46	0.44	0.82	0.93	0.80	0.95	-	-	-	-	-
		# 0234	0.46	0.44	0.82	0.93	0.80	0.95	-	-	-	-	-
		# 0252	0.28	0.47	0.65	0.21	0.26	-0.18	-	-	-	-	-
		# 0015	0.28	0.47	0.65	0.21	0.26	-0.18	-	-	-	-	-
		# 0031	0.28	0.47	0.65	0.21	0.26	-0.18	-	-	-	-	-
		# 0033	0.28	0.47	0.65	0.21	0.26	-0.18	-	-	-	-	-
S1-05	CEM I - 0.41 - D	# 0228	0.53	0.14	0.57	0.70	-0.04	0.43	-	-	-	-	-
		# 0237	0.53	0.14	0.57	0.70	-0.04	0.43	-	-	-	-	-
		# 0246	0.53	0.14	0.57	0.70	-0.04	0.43	-	-	-	-	-
		# 0240	0.53	0.14	0.57	0.70	-0.04	0.43	-	-	-	-	-
		# 0249	0.53	0.14	0.57	0.70	-0.04	0.43	-	-	-	-	-
		# 0234	0.53	0.14	0.57	0.70	-0.04	0.43	-	-	-	-	-
S2-01	CEM II (A-S) - 0.40 - A	# 0234	0.46	0.44	0.82	0.93	0.80	0.95	-	-	-	-	-
		# 0249	0.46	0.44	0.82	0.93	0.80	0.95	-	-	-	-	-
		# 0234	0.46	0.44	0.82	0.93	0.80	0.95	-	-	-	-	-
		# 0249	0.46	0.44	0.82	0.93	0.80	0.95	-	-	-	-	-
		# 0234	0.46	0.44	0.82	0.93	0.80	0.95	-	-	-	-	-
		# 0249	0.46	0.44	0.82	0.93	0.80	0.95	-	-	-	-	-
S2-02	CEM II (B-S) - 0.4 - A	# 0234	0.46	0.44	0.82	0.93	0.80	0.95	-	-	-	-	-
		# 0249	0.46	0.44	0.82	0.93	0.80	0.95	-	-	-	-	-
		# 0234	0.46	0.44	0.82	0.93	0.80	0.95	-	-	-	-	-
		# 0249	0.46	0.44	0.82	0.93	0.80	0.95	-	-	-	-	-
		# 0234	0.46	0.44	0.82	0.93	0.80	0.95	-	-	-	-	-
		# 0249	0.46	0.44	0.82	0.93	0.80	0.95	-	-	-	-	-
S2-03	CEM III A - 0.4 - A	# 0234	0.46	0.44	0.82	0.93	0.80	0.95	-	-	-	-	-
		# 0249	0.46	0.44	0.82	0.93	0.80	0.95	-	-	-	-	-
		# 0234	0.46	0.44	0.82	0.93	0.80	0.95	-	-	-	-	-
		# 0249	0.46	0.44	0.82	0.93	0.80	0.95	-	-	-	-	-
		# 0234	0.46	0.44	0.82	0.93	0.80	0.95	-	-	-	-	-
		# 0249	0.46	0.44	0.82	0.93	0.80	0.95	-	-	-	-	-
Data subsets without admixtures													
Data subsets with mineral admixtures													

Table C.4  $R^2_{adj}$  results of modified models per shrinkage range for data subsets with mineral and chemical admixtures of Dataset 1-HSC.

Subset No	CEM type - w/cm - Agg	Admixture class	Experiment No.	Modified models														
				$R^2_{adj}$ (0 - 99 days)			$R^2_{adj}$ (100 - 199 days)			$R^2_{adj}$ (200 - 499 days)			$R^2_{adj}$ ( $\geq$ 500 days)					
				B4	MC 2010	WITS	NEW	B4	MC 2010	WITS	NEW	B4	MC 2010	WITS	NEW	B4	MC 2010	WITS
S2-04	CEM I - 0.28 - Q	>1 S	A_007_13 A_007_16	0.77	0.87	0.06	-	0.98	0.93	0.89	-	-	-	-	-	-	-	-
				0.41	0.40	0.81	-	-	-	-	-	-	-	-	-	-	-	-
S2-05	CEM I - 0.40 - S	<1 S	#0109 #0255	0.57	0.53	0.58	-	-	-	-	-	-	-	-	-	-	-	-
				0.31	0.85	0.94	-	0.89	0.62	0.91	-	-	-	-	-	-	-	-
S2-06	CEM II (A-D) - 0.36 - S	>1 S	A_070_34 A_070_38 A_070_39	0.59	0.25	0.57	0.90	0.05	-0.31	-0.05	0.73	-0.19	-0.52	-0.76	-0.64	-0.45	-0.52	0.39
				0.77	0.83	0.91	0.82	-1.09	-1.06	0.08	0.65	-5.54	-3.33	-0.69	0.01	-9.63	-3.91	-1.03
S2-07	CEM II (A-Q) - 0.29 - Q	>1 S	A_007_14 A_007_15	0.69	0.54	0.81	0.96	-0.24	-0.38	0.10	0.53	-3.91	-6.86	-10.1	-0.47	-1.24	-0.83	-12.0
				0.0004	0.76	0.82	-	-2.73	-1.85	-1.56	-	-6.02	-5.98	-5.05	-	-2.80	-1.70	-2.16
S2-08	CEM II (B-M)-0.33 - G	<1 S, 25 FA <1 S, 30 FA	6 10	0.52	0.84	-0.32	0.92	-0.01	0.12	0.19	0.44	-9.91	-2.91	-1.45	-10.4	-8.43	-1.66	-2.16
				0.90	0.79	0.85	-	0.23	-0.59	-0.33	-	-1.19	-3.53	-0.82	-	-0.75	0.49	0.46
S2-09	CEM II (B-M)-0.33 - G	<1 S, <0.5 P	17 25	0.90	0.79	0.85	-	-	-	-	-	-	-	-	-	-	-	-
				0.90	0.79	0.85	-	0.23	-0.59	-0.33	-	-1.19	-3.53	-0.82	-	-0.75	0.49	0.46
S2-10	CEM II (B-M)-0.33 - G	<1 S, <0.5 P	19 21	0.90	0.79	0.85	-	-	-	-	-	-	-	-	-	-	-	-
				0.90	0.79	0.85	-	0.23	-0.59	-0.33	-	-1.19	-3.53	-0.82	-	-0.75	0.49	0.46
S2-11	CEM II (B-M)-0.33 - G	<1 S, <0.5 P, 1.0 SRA <1 S, <0.5 P, 2.0 SRA <1 S, <0.5 P, 2.5 SRA	22 27	0.90	0.79	0.85	-	-	-	-	-	-	-	-	-	-	-	-
				0.90	0.79	0.85	-	0.23	-0.59	-0.33	-	-1.19	-3.53	-0.82	-	-0.75	0.49	0.46
S2-12	CEM II (B-M)-0.33 - G	<1 S, <0.5 P, 1.0 SRA <1 S, <0.5 P, 1.5 SRA <1 S, <0.5 P, 2.0 SRA	28 29	0.90	0.79	0.85	-	-	-	-	-	-	-	-	-	-	-	-
				0.90	0.79	0.85	-	0.23	-0.59	-0.33	-	-1.19	-3.53	-0.82	-	-0.75	0.49	0.46
S2-13	CEM II (B-M)-0.33 - G	<1 S, <0.5 P, 2.5 SRA <1 S, <0.5 P, 2.5 SRA	30	0.90	0.79	0.85	-	-	-	-	-	-	-	-	-	-	-	-
				0.90	0.79	0.85	-	0.23	-0.59	-0.33	-	-1.19	-3.53	-0.82	-	-0.75	0.49	0.46
S2-14	CEM II (B-M)-0.33 - G	<1 S, <0.5 P, 2.5 SRA	30	0.90	0.79	0.85	-	-	-	-	-	-	-	-	-	-	-	-
				0.90	0.79	0.85	-	0.23	-0.59	-0.33	-	-1.19	-3.53	-0.82	-	-0.75	0.49	0.46
Data subsets with mineral & chemical admixtures																		

Table C.5 RMSE results of original models per shrinkage range for data subsets without and with mineral admixtures of Dataset 1-HSC.

Subset No	CEM type - w/cm - Agg	Experiment No.	Original models											
			RMSE (0 - 99 days)			RMSE (100 - 199 days)			RMSE (200 - 499 days)					
			B4	MC 2010	WITS	B4	MC 2010	WITS	B4	MC 2010	WITS			
S1-01	CEM I - 0.41 - G	# 0158	164.5	87.1	49.7	119.6	49.4	87.6	-	-	-	-	-	
		# 0219												
		# 0108	154.4	150.7	173.4	101.5	72.9	278.9	-	-	-	-	-	
		# 0217												
		# 0261	49.1	59.4	35.7	-	-	-	194.3	34.2	81.8			
		# 0264												
		# 0079												
		# 0081												
		# 0083	79.5	103.9	68.1	70.1	119.2	78.2	44.1	30.1	18.4			
S1-02	CEM I - 0.41 - Q	# 0221												
		# 0225												
		# 0015												
S1-03	CEM I - 0.41 - S	# 0031	77.4	92.0	62.0	44.8	55.5	55.5	-	-	-	-		
		# 0033												
		# 0228												
S1-04	CEM I - 0.41 - A	# 0237	61.2	57.5	76.8	186.7	115.4	167.0	91.8	58.7	62.1			
		# 0246												
		# 0240												
S1-05	CEM I - 0.41 - D	# 0249	77.0	40.7	66.7	123.8	83.4	104.3	92.4	68.5	62.8			
		# 0234												
		# 0252	44.6	73.3	92.6	149.2	110.8	131.7	83.5	77.6	65.9			
S2-01	CEM II (A-S) - 0.40 - A	# 0228												
		# 0237												
		# 0246												
		# 0240												
		# 0249												
		# 0234												
		# 0252												
		# 0015												
		# 0031												
S2-02	CEM II (B-S) - 0.4 - A	# 0033												
		# 0228												
		# 0237												
S2-03	CEM III A - 0.4 - A	# 0246												
		# 0240												
		# 0249												

Table C.6 RMSE results of original models per shrinkage range for data subsets with mineral and chemical admixtures of Dataset 1-HSC.

Subset No	CEM type - w/cm - Agg	Admixture class	Experiment No.	Original models											
				RMSE (0 - 99 days)			RMSE (100 - 199 days)			RMSE (200 - 499 days)			RMSE (≥ 500 days)		
				B4	MC 2010	WITS	B4	MC 2010	WITS	B4	MC 2010	WITS	B4	MC 2010	WITS
S2-04	CEM I - 0.28 - Q	>1 S	A_007_13 A_007_16	228.0	292.0	81.98	307.6	356.3	38.20	303.1	336.0	36.44	-	-	-
				30.17	69.54	44.23	82.07	72.95	29.38	218.7	69.84	1.57	-	-	-
S2-05	CEM I - 0.40 - S	<1 S	# 0109 # 0255												
S2-06	CEM II (A-D) - 0.36 - S	>1 S	A_070_34 A_070_38 A_070_39	116.1	91.94	130.2	-	-	-	-	-	-	-	-	
				187.2	266.2	103.2	226.4	300.8	40.84	-	-	-	-	-	
S2-07	CEM II (A-Q) - 0.29 - Q	>1 S	A_007_14 A_007_15	86.55	63.45	36.51	29.57	163.2	26.78	43.11	232.4	39.54	82.13	287.4	
				240.1	131.1	113.9	222.7	77.87	57.95	148.0	41.16	38.22	80.71	98.80	
S2-08	CEM II (B-M)-0.33 - G	<1 S, 25 FA <1 S, 30 FA	6 10	192.3	63.89	132.8	148.7	43.17	103.5	84.38	106.7	86.86	55.92	155.0	
				45.22	127.6	68.70	63.20	216.5	92.36	74.29	259.0	72.59	96.78	296.5	
S2-09	CEM II (B-M)-0.33 - G	<1 S, <0.5 P	31 33												
S2-10	CEM II (B-M)-0.33 - G	<1 S, 25 FA <1 S, 30 FA	5 9	232.4	91.59	171.0	188.8	20.16	141.2	129.9	71.38	132.6	95.44	123.1	
				43.44	112.7	62.23	47.18	194.4	62.13	55.90	232.3	55.37	60.58	265.3	
S2-11	CEM II (B-M)-0.33 - G	<1 S, <0.5 P, 1.0 SRA <1 S, <0.5 P, 2.0 SRA <1 S, <0.5 P, 2.5 SRA	17 25												
S2-12	CEM II (B-M)-0.33 - G	<1 S, <0.5 P, 1.0 SRA <1 S, <0.5 P, 2.0 SRA <1 S, <0.5 P, 2.5 SRA	19 21 22												
S2-13	CEM II (B-M)-0.33 - G	<1 S, <0.5 P, 1.0 SRA <1 S, <0.5 P, 1.5 SRA <1 S, <0.5 P, 2.0 SRA	27 28 29	29.58	127.9	57.81	33.08	191.8	56.55	49.01	239.4	46.19	66.65	276.0	
S2-14	CEM II (B-M)-0.33 - G	<1 S, <0.5 P, 2.5 SRA	30												

Data subsets with mineral & chemical admixtures



Table C.7 RMSE results of modified models per shrinkage range for data subsets without and with mineral admixtures of Dataset 1-HSC.

Subset No	CEM type - w/cm - Agg	Experiment No.	Modified models								
			RMSE (0 - 99 days)			RMSE (100 - 199 days)			RMSE (200 - 499 days)		
			B4	MC 2010	WITS	B4	MC 2010	WITS	B4	MC 2010	WITS
S1-01	CEM I - 0.41 - G	# 0158	80.73	44.84	21.12	76.24	50.89	26.24	-	-	-
		# 0219									
		# 0108	86.16	32.04	19.21	33.91	31.54	12.38	-	-	-
		# 0217									
		# 0261	42.99	38.22	31.33	-	-	-	68.99	21.08	18.25
		# 0264									
S1-02	CEM I - 0.41 - Q	# 0079									
		# 0081									
		# 0083	75.22	61.96	58.18	61.84	56.64	49.68	23.54	54.89	20.82
		# 0221									
		# 0225									
		# 0015									
S1-03	CEM I - 0.41 - S	# 0031	12.79	17.72	22.38	31.94	37.53	19.68	-	-	-
		# 0033									
		# 0228									
		# 0237	44.51	48.25	34.69	98.75	109.4	66.21	34.53	46.36	37.03
		# 0246									
		# 0240									
S1-04	CEM I - 0.41 - A	# 0249	41.71	37.31	23.89	34.60	36.38	16.91	18.29	26.02	20.66
		# 0234									
		# 0252	37.93	27.80	20.99	77.53	76.04	52.87	61.46	74.39	61.15
		# 0234									
		# 0252									
		# 0234									
S1-05	CEM I - 0.41 - D	# 0234									
		# 0252									
		# 0234									
		# 0252									
		# 0234									
		# 0252									
S2-01	CEM II (A-S) - 0.40 - A	# 0234									
		# 0252									
		# 0234									
		# 0252									
		# 0234									
		# 0252									
S2-02	CEM II (B-S) - 0.4 - A	# 0234									
		# 0252									
		# 0234									
		# 0252									
		# 0234									
		# 0252									
S2-03	CEM III A - 0.4 - A	# 0234									
		# 0252									
		# 0234									
		# 0252									
		# 0234									
		# 0252									
		Data subsets without admixtures									
		Data subsets with mineral admixtures									

Table C.8 RMSE results of modified models per shrinkage range for data subsets with mineral and chemical admixtures of Dataset 1-HSC.

Subset No	CEM type - w/cm - Agg	Admixture class	Experiment No.	Modified models														
				RMSE (0 - 99 days)			RMSE (100 - 199 days)			RMSE (200 - 499 days)			RMSE ( $\geq$ 500 days)					
				B4	MC 2010	WITS	NEW	B4	MC 2010	WITS	NEW	B4	MC 2010	WITS	NEW	B4	MC 2010	WITS
S2-04	CEM I - 0.28 - Q	>1 S	A_007_13 A_007_16	40.13	28.49	84.87	-	11.25	21.64	21.50	-	12.42	17.34	1.02	-	-	-	-
				44.83	38.40	20.97	-	28.10	42.14	18.70	-	20.15	37.12	13.84	-	-	-	-
S2-05	CEM I - 0.40 - S	<1 S	# 0109 # 0255	46.98	48.47	45.18	-	-	-	-	-	-	-	-	-	-	-	-
				54.28	24.81	15.97	-	22.21	30.19	17.27	-	-	-	-	-	-	-	-
S2-06	CEM II (A-D) - 0.36 - S	>1 S	A_070_34 A_070_38 A_070_39	29.66	35.85	27.17	19.00	23.07	25.51	22.65	16.31	11.17	10.36	11.10	12.34	17.03	17.18	17.00
				27.98	23.39	17.41	33.03	24.79	21.45	15.29	16.73	24.77	16.67	10.44	6.49	24.48	16.26	10.46
S2-07	CEM II (A-Q) - 0.29 - Q	>1 S	A_007_14 A_007_15	35.69	38.66	24.07	16.83	24.04	24.64	19.53	11.56	12.66	11.60	13.47	10.06	10.67	12.92	11.64
				5	9	7	13	15	16	17	25	19	21	22	27	28	29	30
S2-08	CEM II (B-M)-0.33 - G	<1 S, 25 FA <1 S, 30 FA	6 10	56.95	26.86	22.55	-	30.28	27.60	27.63	-	25.78	22.08	18.42	26.42	24.18	23.79	-
				31	33	5	9	7	13	15	16	17	25	19	21	22	27	28
S2-09	CEM II (B-M)-0.33 - G	<1 S, <0.5 P	31 33	27.98	23.39	17.41	33.03	24.79	21.45	15.29	16.73	24.77	16.67	10.44	6.49	24.48	16.26	10.46
				5	9	7	13	15	16	17	25	19	21	22	27	28	29	30
S2-10	CEM II (B-M)-0.33 - G	<1 S, 25 FA <1 S, 30 FA	5 9	35.69	38.66	24.07	16.83	24.04	24.64	19.53	11.56	12.66	11.60	13.47	10.06	10.67	12.92	11.64
				5	9	7	13	15	16	17	25	19	21	22	27	28	29	30
S2-11	CEM II (B-M)-0.33 - G	<1 S, 0.5 SRA <1 S, 1.0 SRA <1 S, 2.0 SRA <1 S, 2.5 SRA	7 13 15 16	56.95	26.86	22.55	-	30.28	27.60	27.63	-	25.78	22.08	18.42	26.42	24.18	23.79	-
				5	9	7	13	15	16	17	25	19	21	22	27	28	29	30
S2-12	CEM II (B-M)-0.33 - G	<1 S, <0.5 P	17 25	38.43	19.89	56.47	17.42	15.96	14.95	15.64	15.62	21.64	16.35	11.25	8.80	28.81	27.94	14.25
				5	9	7	13	15	16	17	25	19	21	22	27	28	29	30
S2-13	CEM II (B-M)-0.33 - G	<1 S, <0.5 P, 1.0 SRA <1 S, <0.5 P, 2.0 SRA <1 S, <0.5 P, 2.5 SRA	19 21 22	21.91	27.30	22.09	-	13.65	18.97	17.27	-	20.15	18.01	13.87	27.96	14.92	15.22	-
				5	9	7	13	15	16	17	25	19	21	22	27	28	29	30
S2-14	CEM II (B-M)-0.33 - G	<1 S, <0.5 P, 1.0 SRA <1 S, <0.5 P, 1.5 SRA <1 S, <0.5 P, 2.0 SRA <1 S, <0.5 P, 2.5 SRA	27 28 29 30	75.72	23.77	24.43	-	76.28	23.79	25.94	-	44.30	22.24	25.40	27.29	23.62	27.60	-
				5	9	7	13	15	16	17	25	19	21	22	27	28	29	30

Data subsets with mineral & chemical admixtures

Table C.9 C.o.V results of original models per shrinkage range for data subsets without and with mineral admixtures of Dataset 1-HSC.

Subset No	CEM type - w/cm - Agg	Experiment No.	Original models								
			C.o.V (0 - 99 days)			C.o.V (100 - 199 days)			C.o.V (200 - 499 days)		
			B4	MC 2010	WITS	B4	MC 2010	WITS	B4	MC 2010	WITS
S1-01	CEM I - 0.41 - G	# 0158	0.52	0.28	0.16	0.31	0.13	0.23	-	-	-
		# 0219									
S1-02	CEM I - 0.41 - Q	# 0108	0.41	0.40	0.47	0.24	0.17	0.65	-	-	-
		# 0217									
S1-03	CEM I - 0.41 - S	# 0261	0.14	0.17	0.10	-	-	-	0.35	0.06	0.15
		# 0264									
S1-04	CEM I - 0.41 - A	# 0079									
		# 0081									
		# 0083	0.24	0.31	0.20	0.16	0.27	0.18	0.09	0.06	0.04
		# 0221									
		# 0225									
S1-05	CEM I - 0.41 - D	# 0015	0.26	0.31	0.21	0.12	0.15	0.15	-	-	-
		# 0031									
		# 0033									
S2-01	CEM II (A-S) - 0.40 - A	# 0228	0.24	0.22	0.30	0.60	0.37	0.54	0.21	0.14	0.14
		# 0237									
		# 0246									
S2-02	CEM II (B-S) - 0.4 - A	# 0240	0.34	0.18	0.30	0.34	0.23	0.28	0.22	0.16	0.15
		# 0249									
S2-03	CEM III A - 0.4 - A	# 0234	0.16	0.28	0.32	0.46	0.34	0.41	0.20	0.19	0.16
		# 0252									
		Data subsets without admixtures			Data subsets with mineral admixtures						

Table C.10 C.o.V results of original models per shrinkage range for data subsets with mineral and chemical admixtures of Dataset 1-HSC.

Subset No	CEM type - w/cm - Agg	Admixture class	Experiment No.	Original models											
				C.o.V (0 - 99 days)			C.o.V (100 - 199 days)			C.o.V (200 - 499 days)			C.o.V (≥ 500 days)		
				B4	MC 2010	WITS	B4	MC 2010	WITS	B4	MC 2010	WITS	B4	MC 2010	WITS
S2-04	CEM I - 0.28 - Q	>1 S	A_007_13 A_007_16	0.64	0.82	0.23	0.62	0.71	0.08	0.61	0.67	0.07	-	-	-
				0.09	0.22	0.14	0.19	0.17	0.51	0.16	0.004	-	-	-	
S2-05	CEM I - 0.40 - S	<1 S	# 0109 # 0255	0.41	0.32	0.45	-	-	-	-	-	-	-	-	-
				0.58	0.83	0.32	0.53	0.71	0.10	-	-	-	-	-	
S2-06	CEM II (A-D) - 0.36 - S	>1 S	A_070_34 A_070_38 A_070_39	0.39	0.29	0.16	0.12	0.65	0.11	0.18	0.98	0.17	0.37	1.29	0.24
				0.73	0.40	0.35	0.60	0.21	0.40	0.11	0.10	0.20	0.27	0.43	0.22
S2-07	CEM II (A-Q) - 0.29 - Q	>1 S	A_007_14 A_007_15	0.57	0.19	0.39	0.39	0.11	0.27	0.24	0.30	0.24	0.16	0.43	0.22
				0.31	0.87	0.47	0.33	1.14	0.36	1.26	0.35	0.46	0.34	0.18	0.33
S2-08	CEM II (B-M)-0.33 - G	<1 S, 25 FA <1 S, 30 FA	6 10	0.62	0.24	0.46	0.45	0.05	0.34	0.32	0.18	0.33	0.24	0.31	0.31
				0.25	0.65	0.36	0.21	0.87	0.23	0.95	0.23	0.24	0.23	0.95	1.05
S2-09	CEM II (B-M)-0.33 - G	<1 S, <0.5 P	31 33	0.19	0.82	0.36	0.15	0.87	0.26	0.21	1.43	0.20	0.28	1.16	0.19
				0.19	0.82	0.36	0.15	0.87	0.26	0.21	1.43	0.20	0.28	1.16	0.19
S2-10	CEM II (B-M)-0.33 - G	<1 S, 25 FA <1 S, 30 FA	5 9	0.62	0.24	0.46	0.45	0.05	0.34	0.32	0.18	0.33	0.24	0.31	0.31
				0.25	0.65	0.36	0.21	0.87	0.23	0.95	0.23	0.24	0.23	0.95	1.05
S2-11	CEM II (B-M)-0.33 - G	<1 S, 0.5 SRA <1 S, 1.0 SRA <1 S, 2.0 SRA <1 S, 2.5 SRA	7 13 15 16	0.19	0.82	0.36	0.15	0.87	0.26	0.21	1.43	0.20	0.28	1.16	0.19
				0.19	0.82	0.36	0.15	0.87	0.26	0.21	1.43	0.20	0.28	1.16	0.19
S2-12	CEM II (B-M)-0.33 - G	<1 S, <0.5 P	17 25	0.62	0.24	0.46	0.45	0.05	0.34	0.32	0.18	0.33	0.24	0.31	0.31
				0.25	0.65	0.36	0.21	0.87	0.23	0.95	0.23	0.24	0.23	0.95	1.05
S2-13	CEM II (B-M)-0.33 - G	<1 S, <0.5 P, 1.0 SRA <1 S, <0.5 P, 2.0 SRA <1 S, <0.5 P, 2.5 SRA	19 21 22	0.19	0.82	0.36	0.15	0.87	0.26	0.21	1.43	0.20	0.28	1.16	0.19
				0.19	0.82	0.36	0.15	0.87	0.26	0.21	1.43	0.20	0.28	1.16	0.19
S2-14	CEM II (B-M)-0.33 - G	<1 S, <0.5 P, 1.0 SRA <1 S, <0.5 P, 1.5 SRA <1 S, <0.5 P, 2.0 SRA <1 S, <0.5 P, 2.5 SRA	27 28 29 30	0.19	0.82	0.36	0.15	0.87	0.26	0.21	1.43	0.20	0.28	1.16	0.19
				0.19	0.82	0.36	0.15	0.87	0.26	0.21	1.43	0.20	0.28	1.16	0.19

Data subsets with mineral & chemical admixtures

Table C.11 C.o.V results of modified models per shrinkage range for data subsets without and with mineral admixtures of Dataset 1-HSC.

Subset No	CEM type - w/cm - Agg	Experiment No.	Modified models											
			C.o.V (0 - 99 days)			C.o.V (100 - 199 days)			C.o.V - 499 days)			C.o.V (200 - 499 days)		
			B4	MC 2010	WITS	B4	MC 2010	WITS	B4	MC 2010	WITS	B4	MC 2010	WITS
S1-01	CEM I - 0.41 - G	# 0158	0.26	0.14	0.07	0.20	0.13	0.07	-	-	0.13	0.07	-	-
		# 0219												
		# 0108	0.23	0.09	0.05	0.08	0.07	0.03	-	-	0.07	0.03	-	-
		# 0217												
		# 0261	0.12	0.11	0.09	-	-	-	-	-	-	-	-	0.03
		# 0264												
S1-02	CEM I - 0.41 - Q	# 0079												
		# 0081												
		# 0083	0.22	0.18	0.17	0.14	0.13	0.11			0.13	0.11		0.04
		# 0221												
		# 0225												
		# 0015												
S1-03	CEM I - 0.41 - S	# 0031	0.04	0.06	0.07	0.09	0.10	0.05			0.10	0.05		-
		# 0033												
		# 0228												
		# 0237	0.17	0.19	0.13	0.32	0.35	0.21			0.35	0.21		0.09
		# 0246												
		# 0240	0.19	0.17	0.11	0.09	0.10	0.05			0.10	0.05		0.05
S1-04	CEM I - 0.41 - A	# 0249												
		# 0234	0.13	0.11	0.07	0.24	0.24	0.16			0.24	0.16		0.15
		# 0252												
		# 0015												
		# 0031												
		# 0033												
S1-05	CEM I - 0.41 - D	# 0228												
		# 0237	0.17	0.19	0.13	0.32	0.35	0.21			0.35	0.21		0.09
		# 0246												
		# 0240	0.19	0.17	0.11	0.09	0.10	0.05			0.10	0.05		0.05
		# 0249												
		# 0234	0.13	0.11	0.07	0.24	0.24	0.16			0.24	0.16		0.15
S2-01	CEM II (A-S) - 0.40 - A	# 0252												
		# 0015												
		# 0031												
		# 0033												
		# 0228												
		# 0237	0.17	0.19	0.13	0.32	0.35	0.21			0.35	0.21		0.09
S2-02	CEM II (B-S) - 0.4 - A	# 0246												
		# 0240	0.19	0.17	0.11	0.09	0.10	0.05			0.10	0.05		0.05
		# 0249												
		# 0234	0.13	0.11	0.07	0.24	0.24	0.16			0.24	0.16		0.15
		# 0252												
		# 0015												
S2-03	CEM III A - 0.4 - A	# 0031												
		# 0033												
		# 0228												
		# 0237	0.17	0.19	0.13	0.32	0.35	0.21			0.35	0.21		0.09
		# 0246												
		# 0240	0.19	0.17	0.11	0.09	0.10	0.05			0.10	0.05		0.05

Table C.12 C.o.V results of modified models per shrinkage range for data subsets with mineral and chemical admixtures of Dataset 1-HSC.

Subset No	CEM type - w/cm - Agg	Admixture class	Experiment No.	Modified models														
				C.o.V (0 - 99 days)			C.o.V (100 - 199 days)			C.o.V (200 - 499 days)			C.o.V (≥ 500 days)					
				B4	MC 2010	WITS	NEW	B4	MC 2010	WITS	NEW	B4	MC 2010	WITS	NEW	B4	MC 2010	WITS
S2-04	CEM I - 0.28 - Q	>1 S	A_007_13 A_007_16	0.11	0.08	0.24	-	0.02	0.04	0.04	0.04	0.03	0.00	-	-	-	-	-
S2-05	CEM I - 0.40 - S	<1 S	# 0109 # 0255	0.14	0.12	0.07	-	0.07	0.10	0.04	0.09	0.03	0.03	-	-	-	-	-
S2-06	CEM II (A-D) - 0.36 - S	>1 S	A_070_34 A_070_38 A_070_39	0.16	0.17	0.16	-	-	-	-	-	-	-	-	-	-	-	-
S2-07	CEM II (A-Q) - 0.29 - Q	>1 S	A_007_14 A_007_15	0.17	0.08	0.05	-	0.05	0.07	0.04	0.04	-	-	-	-	-	-	-
S2-08	CEM II (B-M)-0.33 - G	<1 S, 25 FA <1 S, 30 FA	6 10	0.13	0.16	0.12	0.09	0.09	0.10	0.09	0.10	0.04	0.05	0.04	0.05	0.08	0.08	0.04
S2-09	CEM II (B-M)-0.33 - G	<1 S, <0.5 P	31 33	0.09	0.07	0.05	0.10	0.07	0.06	0.04	0.04	0.05	0.03	0.02	0.07	0.05	0.03	0.02
S2-10	CEM II (B-M)-0.33 - G	<1 S, 25 FA <1 S, 30 FA	5 9	0.11	0.11	0.07	0.05	0.06	0.06	0.05	0.05	0.03	0.04	0.03	0.03	0.04	0.03	0.03
S2-11	CEM II (B-M)-0.33 - G	<1 S, 0.5 SRA <1 S, 1.0 SRA <1 S, 2.0 SRA <1 S, 2.5 SRA	7 13 15 16	0.39	0.18	0.15	-	0.16	0.14	0.15	-	0.12	0.09	-	0.13	0.12	0.11	-
S2-12	CEM II (B-M)-0.33 - G	<1 S, <0.5 P	17 25	0.10	0.05	0.15	0.05	0.04	0.04	0.04	0.04	0.04	0.03	0.02	0.07	0.07	0.04	0.02
S2-13	CEM II (B-M)-0.33 - G	<1 S, <0.5 P, 1.0 SRA <1 S, <0.5 P, 2.0 SRA <1 S, <0.5 P, 2.5 SRA	19 21 22	0.13	0.16	0.13	-	0.06	0.09	0.08	-	0.07	0.06	-	0.11	0.06	0.06	-
S2-14	CEM II (B-M)-0.33 - G	<1 S, <0.5 P, 1.0 SRA <1 S, <0.5 P, 1.5 SRA <1 S, <0.5 P, 2.0 SRA <1 S, <0.5 P, 2.5 SRA	27 28 29 30	0.48	0.15	0.15	-	0.34	0.11	0.12	-	0.13	0.11	-	0.11	0.10	0.12	-

Data subsets with mineral & chemical admixtures

Table C.13  $R^2_{adj}$  results of original models per shrinkage range for data subsets with mineral and chemical admixtures of Dataset 2-HSC.

Subset No	CEM type - w/cm - Agg	Admixture class	Experiment No.	Original model									
				$R^2_{adj}$ (0 - 99 days)		$R^2_{adj}$ (100 - 199 days)		$R^2_{adj}$ (200 - 499 days)		$R^2_{adj}$ ( $\geq$ 500 days)			
				B4	MC 2010	B4	MC 2010	B4	MC 2010	B4	MC 2010		
S2-01a	CEM I - 0.27 - G	1 S	A_072_04	0.84	-171.6	-	-	-	-	-	-	-	
			A_072_05										
S2-02a	CEM I - 0.27 - Q	3 S	A_007_09	-15.53	-2.86	-83.98	-3.33	-	-	-	-	-	
			A_007_12										
S2-03a	CEM I - 0.31 - G	1 S	A_072_06	1.07	-15.76	1.30	19.57	-	-	0.55	-6.32		
			A_086_18										
S2-04a	CEM I - 0.31 - G	<0.5 P	A_086_20										
			A_068_01	-8.91	0.00	-	-	-	-	-	-	-	
S2-05a	CEM I - 0.35 - G	3 S, 1RE	A_068_19	-136.6	-338.5	-	-	-	-	-	-	-	
			A_022_03										
S2-06a	CEM II (A-D) - 0.23 - Q	2 S	A_022_05	0.37	0.52	-	-	2.06	3.00	0.21	-0.02		
			A_086_41										
S2-07a	CEM II (A-D) - 0.28 - G	2 S	A_086_42	1.30	1.55	13.03	148.62	-1.53	28.52	-0.86	0.85		
			A_086_36										
S2-08a	CEM II (A-D) - 0.28 - Q	1 S	A_086_37	-0.08	-0.69	-	-	46.02	156.48	0.59	-0.91		
			A_086_26										
S2-09a	CEM II (A-D) - 0.34 - G	2 S	A_031_04	0.25	-17.33	-1.46	-415.1	-0.02	-94.81	-	-		
			A_031_06										
			A_046_02										
			A_046_07										
S2-10a	CEM II (A-D) - 0.34 - Q	1 S	A_086_07	-0.34	-6.42	-	-	-	-	0.30	-9.39		
			A_086_09										
S2-11a	CEM II (A-D) - 0.34 - Q	1 S (AE)	A_086_11	-12.07	-10.39	8752.6	12200	48.84	77.81	-9.65	-18.66		
			A_086_13										
S2-12a	CEM II (A-D) - 0.29 - Q	3 S	A_086_14	-47.92	-9.15	-128.5	-50.97	-	-	-	-		
			A_007_06										
			A_007_07										
Data subsets with mineral and chemical admixtures													

Table C.14  $R^2_{adj}$  results of modified models per shrinkage range for data subsets with mineral and chemical admixtures of Dataset 2-HSC.

Subset No	CEM type - w/cm - Agg	Admixture class	Experiment No.	Modified models											
				$R^2_{adj}$ (0 - 99 days)		$R^2_{adj}$ (100 - 199 days)		$R^2_{adj}$ (200 - 499 days)		$R^2_{adj}$ ( $\geq$ 500 days)					
				B4	MC 2010	B4	MC 2010	B4	MC 2010	B4	MC 2010				
S2-01a	CEM I - 0.27 - G	1 S	A_072_04	0.84	-0.15	-	-	-	-	-	-	-	-		
			A_072_05												
S2-02a	CEM I - 0.27 - Q	3 S	A_007_09	0.76	0.80	0.68	0.67	-	-	-	-	-	-		
			A_007_12												
S2-03a	CEM I - 0.31 - G	1 S	A_072_06	1.06	0.97	1.08	1.28	-	-	-	0.84	0.72	-		
			A_086_18												
S2-04a	CEM I - 0.31 - G	<0.5 P	A_086_20	0.76	0.92	-	-	-	-	-	-	-	-		
			A_068_01												
S2-05a	CEM I - 0.35 - G	3 S, 1RE	A_068_19	0.83	0.54	-	-	-	-	-	-	-	-		
			A_022_03												
S2-06a	CEM II (A-D) - 0.23 - Q	2 S	A_022_05	0.91	0.90	1.00	1.00	1.29	1.41	1.00	0.53	0.48	-		
			A_086_41												
S2-07a	CEM II (A-D) - 0.28 - G	2 S	A_086_42	1.12	1.07	2.77	3.78	5.20	4.77	0.89	0.90	-	-		
			A_086_36												
S2-08a	CEM II (A-D) - 0.28 - Q	1 S	A_086_37	0.96	0.91	1.00	1.00	10.15	10.07	0.83	0.91	-	-		
			A_086_26												
S2-09a	CEM II (A-D) - 0.34 - G	2 S	A_086_30	0.25	0.03	-1.46	-1.13	-0.02	0.82	1.00	1.00	1.00	-		
			A_031_04												
			A_031_06												
			A_046_02												
S2-10a	CEM II (A-D) - 0.34 - Q	1 S	A_046_07	0.81	0.82	1.00	1.00	1.00	1.00	0.50	0.57	-			
			A_086_07												
S2-11a	CEM II (A-D) - 0.34 - Q	1 S (AE)	A_086_09	0.93	0.87	17.36	25.69	1.22	1.21	0.88	0.82	-			
			A_086_11												
S2-12a	CEM II (A-D) - 0.29 - Q	3 S	A_086_13	0.92	0.82	0.74	0.80	-	-	-	-	-			
			A_007_06												
			A_007_07												

Data subsets with mineral and chemical admixtures



Table C.15 RMSE results of original models per shrinkage range for data subsets with mineral and chemical admixtures of Dataset 2-HSC.

Subset No	CEM type - w/cm - Agg	Admixture class	Experiment No.	Original model															
				RMSE (0 - 99 days)		RMSE (100 - 199 days)		RMSE (200 - 499 days)		RMSE (≥ 500 days)		RMSE (0 - 99 days)		RMSE (100 - 199 days)		RMSE (200 - 499 days)		RMSE (≥ 500 days)	
				B4	MC 2010	B4	MC 2010	B4	MC 2010	B4	MC 2010	B4	MC 2010	B4	MC 2010	B4	MC 2010	B4	MC 2010
Data subsets with mineral and chemical admixtures	S2-01a	CEM I - 0.27 - G	1 S	A_072_04	15.57	245.85	-	-	-	-	-	-	-	-	-	-	-	-	
				A_072_05															
	S2-02a	CEM I - 0.27 - Q	3 S	A_007_09	247.93	98.15	337.74	106.50	-	-	-	-	-	-	-	-	-	-	
				A_007_12															
	S2-03a	CEM I - 0.31 - G	1 S	A_072_06	48.59	289.93	38.53	310.97	58.91	297.23	49.74	212.99	-	-	-	-	-	-	
				A_086_18															
				A_086_20															
	S2-04a	CEM I - 0.31 - G	<0.5 P	A_068_01	418.81	132.81	-	-	-	-	-	-	-	-	-	-	-	-	
				A_068_19															
	S2-05a	CEM I - 0.35 - G	3 S, 1RE	A_022_03	230.94	353.68	-	-	-	-	-	-	-	-	-	-	-	-	
				A_022_05															
	S2-06a	CEM II (A-D) - 0.23 - Q	2 S	A_086_41	96.02	82.91	67.45	106.00	77.43	110.01	64.87	73.53	-	-	-	-	-	-	
				A_086_42															
	S2-07a	CEM II (A-D) - 0.28 - G	2 S	A_086_36	134.82	168.00	43.25	171.86	52.18	130.79	108.33	81.24	-	-	-	-	-	-	
				A_086_37															
	S2-08a	CEM II (A-D) - 0.28 - Q	1 S	A_086_26	121.39	151.80	140.39	250.01	127.65	240.16	72.54	160.09	-	-	-	-	-	-	
			A_086_30																
			A_086_31																
S2-09a	CEM II (A-D) - 0.34 - G	2 S 1 S 2 S 2 S	A_031_04	54.39	254.27	27.72	397.06	33.10	420.55	55.05	419.24	-	-	-	-	-	-		
			A_031_06																
			A_046_02																
			A_046_07																
S2-10a	CEM II (A-D) - 0.34 - Q	1 S	A_086_07	93.76	226.91	114.94	364.69	101.52	360.82	74.92	284.15	-	-	-	-	-	-		
			A_086_09																
			A_086_11																
S2-11a	CEM II (A-D) - 0.34 - Q	1 S (AE)	A_086_13	277.26	258.88	333.46	391.08	295.41	375.92	250.11	340.04	-	-	-	-	-	-		
			A_086_14																
S2-12a	CEM II (A-D) - 0.29 - Q	3 S	A_007_06	359.40	164.59	463.42	288.58	-	-	-	-	-	-	-	-	-	-		
			A_007_07																

Table C.16 RMSE results of modified models per shrinkage range for data subsets with mineral and chemical admixtures of Dataset 2-HSC.

Subset No	CEM type - w/cm - Agg	Admixture class	Experiment No.	Modified models							
				RMSE (0 - 99 days)		RMSE (100 - 199 days)		RMSE (200 - 499 days)		RMSE (≥ 500 days)	
				B4	MC 2010	B4	MC 2010	B4	MC 2010	B4	MC 2010
S2-01a	CEM I - 0.27 - G	1 S	A_072_04	15.57	21.16	-	-	-	-	-	-
				A_072_05	-	-	-	-	-	-	-
S2-02a	CEM I - 0.27 - Q	3 S	A_007_09	22.97	23.18	23.36	24.25	-	-	-	-
				A_007_12	-	-	-	-	-	-	-
S2-03a	CEM I - 0.31 - G	1 S	A_072_06	39.87	21.01	19.01	36.25	29.72	56.00	29.27	41.28
				A_086_18	-	-	-	-	-	-	-
S2-04a	CEM I - 0.31 - G	<0.5 P	A_068_01	65.48	40.06	-	-	-	-	-	-
				A_068_19	-	-	-	-	-	-	-
S2-05a	CEM I - 0.35 - G	3 S, 1RE	A_022_03	8.02	13.46	-	-	-	-	-	-
				A_022_05	-	-	-	-	-	-	-
S2-06a	CEM II (A-D) - 0.23 - Q	2 S	A_086_41	35.95	38.38	14.59	16.37	38.85	45.22	60.37	65.53
				A_086_42	60.38	47.30	14.86	21.81	53.13	56.77	56.98
S2-07a	CEM II (A-D) - 0.28 - G	2 S	A_086_36	22.92	32.00	55.75	72.52	43.58	37.27	48.19	35.39
				A_086_37	-	-	-	-	-	-	-
S2-08a	CEM II (A-D) - 0.28 - Q	1 S	A_086_26	22.92	32.00	55.75	72.52	43.58	37.27	48.19	35.39
				A_086_30	-	-	-	-	-	-	-
S2-09a	CEM II (A-D) - 0.34 - G	2 S	A_086_31	54.39	60.08	27.72	34.17	33.10	24.22	55.05	25.36
				A_031_04	-	-	-	-	-	-	-
S2-10a	CEM II (A-D) - 0.34 - Q	1 S	A_031_06	32.00	32.87	39.23	31.88	57.18	43.81	67.94	59.08
				A_046_02	20.47	28.07	19.19	20.35	22.10	19.60	32.83
S2-11a	CEM II (A-D) - 0.34 - Q	1 S (AE)	A_086_11	14.14	21.93	20.77	15.70	-	-	-	-
				A_086_13	-	-	-	-	-	-	-
S2-12a	CEM II (A-D) - 0.29 - Q	3 S	A_086_14	14.14	21.93	20.77	15.70	-	-	-	-
				A_007_06	-	-	-	-	-	-	-
				Data subsets with mineral and chemical admixtures							

Table C.17 C.o.V results of original models per shrinkage range for data subsets with mineral and chemical admixtures of Dataset 2-HSC.

Subset No	CEM type - w/cm - Agg	Admixture class	Experiment No.	Original model								
				C.o.V (0 - 99 days)		C.o.V (100 - 199 days)		C.o.V (200 - 499 days)		C.o.V (≥ 500 days)		
				B4	MC 2010	B4	MC 2010	B4	MC 2010	B4	MC 2010	
S2-01a	CEM I - 0.27 - G	1 S	A_072_04	0.08	1.14	-	-	-	-	-	-	-
			A_072_05									
S2-02a	CEM I - 0.27 - Q	3 S	A_007_09	0.63	0.25	0.74	0.23	-	-	-	-	-
			A_007_12									
S2-03a	CEM I - 0.31 - G	1 S	A_072_06	0.36	2.17	0.17	1.40	0.22	1.09	0.13	0.57	
			A_086_18									
			A_086_20									
S2-04a	CEM I - 0.31 - G	<0.5 P	A_068_01	0.81	0.26	-	-	-	-	-	-	
			A_068_19									
S2-05a	CEM I - 0.35 - G	3 S, 1RE	A_022_03	4.10	6.28	-	-	-	-	-	-	
			A_022_05									
S2-06a	CEM II (A-D) - 0.23 - Q	2 S	A_086_41	0.54	0.47	0.19	0.30	0.20	0.29	0.14	0.16	
			A_086_42									
S2-07a	CEM II (A-D) - 0.28 - G	2 S	A_086_36	0.90	1.12	0.14	0.57	0.14	0.35	0.23	0.17	
			A_086_37									
S2-08a	CEM II (A-D) - 0.28 - Q	1 S	A_086_26	1.25	1.56	0.62	1.10	0.49	0.93	0.20	0.44	
			A_086_30									
			A_086_31									
S2-09a	CEM II (A-D) - 0.34 - G	2 S	A_031_04									
			A_031_06	0.36	1.67	0.17	1.84	0.14	1.81	0.22	1.69	
			A_046_02									
			A_046_07									
S2-10a	CEM II (A-D) - 0.34 - Q	1 S	A_086_07	1.17	2.84	0.70	2.21	0.52	1.85	0.26	0.98	
			A_086_09									
			A_086_11									
S2-11a	CEM II (A-D) - 0.34 - Q	1 S (AE)	A_086_13	2.89	2.70	2.08	2.44	1.42	1.81	0.94	1.28	
			A_086_14									
S2-12a	CEM II (A-D) - 0.29 - Q	3 S	A_007_06	2.16	0.99	1.99	1.24	-	-	-	-	
			A_007_07									
Data subsets with mineral and chemical admixtures												

Table C.18 C.o.V results of modified models per shrinkage range for data subsets with mineral and chemical admixtures of Dataset 2-HSC.

Subset No	CEM type - w/cm - Agg	Admixture class	Experiment No.	Modified models									
				C.o.V (0 - 99 days)		C.o.V (100 - 199 days)		C.o.V (200 - 499 days)		C.o.V (≥ 500 days)			
				B4	MC 2010	B4	MC 2010	B4	MC 2010	B4	MC 2010		
S2-01a	CEM I - 0.27 - G	1 S	A_072_04	0.08	0.10	-	-	-	-	-	-	-	
			A_072_05										
S2-02a	CEM I - 0.27 - Q	3 S	A_007_09	0.06	0.06	0.05	0.05	-	-	-	-	-	
			A_007_12										
S2-03a	CEM I - 0.31 - G	1 S	A_072_06	0.30	0.16	0.08	0.16	0.11	0.21	0.08	0.11		
			A_086_18										
			A_086_20										
S2-04a	CEM I - 0.31 - G	<0.5 P	A_068_01	0.13	0.08	-	-	-	-	-	-	-	
			A_068_19										
S2-05a	CEM I - 0.35 - G	3 S, 1RE	A_022_03	0.14	0.24	-	-	-	-	-	-	-	
			A_022_05										
S2-06a	CEM II (A-D) - 0.23 - Q	2 S	A_086_41	0.20	0.22	0.04	0.05	0.10	0.12	0.13	0.14		
			A_086_42										
S2-07a	CEM II (A-D) - 0.28 - G	2 S	A_086_36	0.40	0.32	0.05	0.07	0.14	0.15	0.12	0.12		
			A_086_37										
S2-08a	CEM II (A-D) - 0.28 - Q	1 S	A_086_26	0.24	0.33	0.25	0.32	0.17	0.14	0.13	0.10		
			A_086_30										
			A_086_31										
S2-09a	CEM II (A-D) - 0.34 - G	2 S	A_031_04										
			A_031_06	0.36	0.39	0.17	0.16	0.14	0.10	0.22	0.10		
			A_046_02										
			A_046_07										
S2-10a	CEM II (A-D) - 0.34 - Q	1 S	A_086_07	0.40	0.41	0.24	0.19	0.29	0.22	0.23	0.20		
			A_086_09										
			A_086_11										
S2-11a	CEM II (A-D) - 0.34 - Q	1 S (AE)	A_086_13	0.21	0.29	0.12	0.13	0.11	0.09	0.10	0.12		
			A_086_14										
S2-12a	CEM II (A-D) - 0.29 - Q	3 S	A_007_06	0.08	0.13	0.09	0.07	-	-	-	-		
			A_007_07										

Data subsets with mineral and chemical admixtures

## Appendix D. Statistical results for each experiment in Dataset 3, 4 and 5.

Table D.1 RMSE and C.o.V values for each experiment and per shrinkage range for Dataset 3 (drying shrinkage) – RILEM B4 model.

File data reference	Region	< 60 MPa (NSC)	≥ 60 MPa (HSC)	RMSE	overall C.o.V	C.o.V (0-99 days)	C.o.V (100-199 days)	C.o.V (200-499 days)	C.o.V (≥ 500 days)
11	USA	✓		81.98	0.34	0.10	0.09	0.04	0.03
12	USA		✓	74.32	0.30	0.07	0.10	0.05	0.02
17	USA		✓	113.53	0.28	0.04	0.08	0.01	0.03
18	USA	✓		72.74	0.21	0.05	0.04	0.04	0.02
21	USA		✓	102.98	0.51	0.13	0.05	0.04	0.04
30	USA		✓	86.43	0.39	0.09	0.06	0.07	0.03
31	USA		✓	113.92	0.32	0.07	0.07	0.08	0.06
32	USA		✓	184.86	0.41	0.08	0.06	0.06	0.02
# 0013	RSA		✓	78.64	0.24	0.11	0.07	-	-
# 0016	RSA	✓		125.24	0.30	0.10	0.13	-	-
# 0019	RSA	✓		70.44	0.26	0.00	0.07	-	-
# 0021	RSA	✓		116.96	0.47	0.01	0.07	-	-
# 0023	RSA	✓		182.61	0.63	0.06	0.10	-	-
# 0025	RSA	✓		62.59	0.21	0.01	0.07	-	-
# 0027	RSA	✓		129.12	0.53	0.10	0.05	-	-
# 0029	RSA	✓		301.63	1.54	0.12	0.10	-	-
# 0032	RSA	✓		48.54	0.14	0.15	0.02	-	-
# 0033	RSA		✓	102.85	0.33	0.14	0.04	-	-
# 0035	RSA	✓		202.64	0.99	0.04	0.03	-	-
# 0037	RSA	✓		148.26	0.62	0.05	0.02	-	-
# 0039	RSA	✓		258.15	1.09	0.08	0.01	-	-
# 0041	RSA	✓		239.20	1.01	0.10	0.01	-	-
# 0043	RSA	✓		42.82	0.15	0.04	0.02	-	-
# 0045	RSA	✓		310.30	1.62	0.04	0.09	-	-
# 0047	RSA		✓	401.57	3.59	0.24	0.20	-	-
# 0049	RSA		✓	426.77	3.81	0.24	0.20	-	-
# 0051	RSA	✓		66.72	0.22	0.03	0.01	-	-
# 0053	RSA		✓	53.22	0.14	0.02	0.01	-	-
# 0108	RSA		✓	353.14	0.74	0.25	-	-	-
# 0109	RSA		✓	94.84	0.28	0.10	-	-	-
# 0110	RSA		✓	122.49	0.45	0.28	-	-	-
# 0111	RSA	✓		102.35	0.33	0.25	-	-	-
# 0150	RSA		✓	179.02	0.35	0.08	0.11	-	-
# 0158	RSA		✓	206.41	0.61	0.10	-	-	-
# 0217	RSA		✓	95.57	0.29	-	0.08	-	-
# 0219	RSA		✓	249.00	0.68	-	0.04	-	-
# 0255	RSA		✓	110.69	0.33	0.05	-	-	-
# 0258	RSA		✓	167.29	0.58	0.11	-	-	-
# 0261	RSA		✓	124.52	0.32	0.08	-	-	-
# 0264	RSA		✓	112.59	0.30	0.11	-	-	-
# 0267	RSA	✓		216.47	0.64	0.08	-	-	-
# 0270	RSA	✓		177.11	0.58	0.11	-	-	-
# 0276	RSA	✓		125.88	0.32	-	-	0.03	-
# 0280	RSA	✓		244.27	0.57	-	-	0.06	-
# 0283	RSA	✓		580.28	0.87	-	-	0.04	-

Table D.2 RMSE and C.o.V values for each experiment and per shrinkage range for Dataset 3 (drying shrinkage) – RILEM B4 model (continuation 1).

File data reference	Region	< 60 MPa (NSC)	≥ 60 MPa (HSC)	RMSE	overall C.o.V	C.o.V (0-99 days)	C.o.V (100-199 days)	C.o.V (200-499 days)	C.o.V (≥ 500 days)
# 0289	RSA	✓		128.67	0.41	0.07	-	-	-
A_003_01	Australia		✓	50.58	0.17	0.23	-	0.09	-
A_003_02	Australia		✓	57.56	0.17	0.14	-	0.08	-
A_003_03	Australia		✓	58.93	0.15	0.04	0.10	-	-
A_003_04	Australia		✓	81.54	0.20	0.03	0.08	-	-
A_033_03	Italy	✓		113.72	0.29	0.07	0.01	-	-
A_033_04	Italy	✓		64.05	0.18	0.06	0.02	-	-
A_068_02	USA		✓	212.48	0.44	0.20	-	-	-
A_068_21	USA		✓	199.08	0.43	0.21	-	-	-
A_068_24	USA		✓	210.23	0.42	0.16	-	-	-
A_068_25	USA	✓		58.16	0.31	0.14	-	-	-
A_068_26	USA	✓		217.96	0.43	0.22	-	-	-
A_068_27	USA	✓		79.95	0.33	0.08	-	-	-
A_070_23	China	✓		31.69	0.17	0.07	-	-	-
A_070_24	China	✓		46.59	0.37	0.27	-	-	-
A_070_28	China	✓		86.16	1.04	0.37	-	-	-
A_070_29	China	✓		114.21	1.95	0.84	-	-	-
S_053_01	JAP	✓		155.06	0.41	0.04	-	-	-
S_053_08	JAP	✓		22.51	0.09	0.04	-	-	-
S_053_22	JAP	✓		61.95	0.27	0.05	-	-	-
S_082_01	JAP	✓		108.28	0.29	0.11	0.03	0.18	-
S_082_13	JAP	✓		151.22	0.42	0.12	0.06	0.10	-
S_082_25	JAP	✓		191.82	0.57	0.14	0.07	0.16	-
S_082_37	JAP	✓		95.00	0.21	0.06	0.06	0.12	-

Table D.3 RMSE and C.o.V values for each experiment and per shrinkage range for Dataset 3 (autogenous shrinkage) – RILEM B4 model.

File data reference	Region	< 60 MPa (NSC)	≥ 60 MPa (HSC)	RMSE	overall C.o.V	C.o.V (0-99 days)	C.o.V (100-199 days)	C.o.V (200-499 days)
A_065_01	France	✓		41.61	0.46	0.86	-	-
A_065_05	France	✓		195.98	0.92	0.82	-	-
A_024_02	Korea	✓		93.99	1.14	0.79	-	-
A_033_01	Italy	✓		58.33	1.88	0.87	-	-
A_036_11	UK	✓		55.82	0.86	0.90	-	-
A_068_05	USA	✓		13.56	0.78	0.44	0.05	-
A_036_16	UK	✓		18.07	0.82	0.79	-	-
A_068_04	USA	✓		52.83	0.84	0.55	-	-
A_033_02	Italy	✓		77.96	2.01	0.16	0.02	0.036
A_068_09	USA	✓		265.59	13.01	0.12	0.05	0.013
A_068_20	USA	✓		521.02	2.36	0.22	0.05	0.017
A_009_08	US	✓		162.23	1.20	0.19	0.06	0.021
A_024_01	Korea	✓		401.08	1.88	1.97	0.16	-
A_009_04	US	✓		150.85	1.07	2.28	0.14	-
A_031_02	Iran	✓		83.17	0.59	0.63	-	-
A_009_06	US	✓		151.85	1.17	0.55	-	-
A_009_02	US		✓	160.00	1.18	1.64	-	-
A_068_01	USA		✓	445.36	0.89	0.10	-	-
A_068_08	USA		✓	197.59	1.14	0.10	0.03	-
A_068_12	USA		✓	198.59	1.14	0.12	-	-
A_068_16	USA		✓	449.08	0.89	0.04	0.05	-
A_068_19	USA		✓	465.33	0.87	0.31	-	-
A_072_03	Singapore		✓	355.32	9.28	0.43	-	-
A_009_10	US		✓	192.80	1.16	0.34	-	-
A_022_15	France		✓	127.22	1.10	0.73	-	-
A_053_08	Japan		✓	310.62	4.11	3.26	-	-
A_031_04	Iran		✓	69.80	0.43	0.72	-	-
A_031_06	Iran		✓	47.34	0.25	0.30	-	-
A_065_03	France		✓	23.77	0.16	0.22	-	-
A_065_07	France		✓	71.64	0.42	0.41	-	-
A_031_08	Iran		✓	45.67	0.23	2.30	-	-

Table D.4 RMSE and C.o.V values for each experiment and per shrinkage range for Dataset 4 (drying shrinkage) – MC 2010 model.

File data reference	Region	< 60 MPa (NSC)	≥ 60 MPa (HSC)	RMSE	overall C.o.V	C.o.V (0-99 days)	C.o.V (100-199 days)	C.o.V (200-499 days)	C.o.V (≥ 500 days)
12	USA		✓	224.37	0.91	0.06	0.11	0.06	0.03
17	USA		✓	113.60	0.28	0.07	0.05	0.01	0.05
18	USA	✓		206.65	0.58	0.12	0.05	0.06	0.03
21	USA		✓	277.97	1.37	0.30	0.06	0.05	0.06
30	USA		✓	255.24	1.16	0.35	0.44	-	-
# 0109	RSA		✓	299.63	0.89	-	-	-	-
# 0110	RSA		✓	68.35	0.25	0.11	-	-	-
# 0111	RSA	✓		262.74	0.84	0.02	-	-	-
# 0139	RSA		✓	-	-	0.14	-	-	-
# 0141	RSA		✓	-	-	0.16	-	-	-
# 0142	RSA		✓	-	-	0.15	-	-	-
# 0255	RSA		✓	70.95	0.21	0.10	-	-	-
# 0258	RSA		✓	75.77	0.26	0.08	-	-	-
# 0261	RSA		✓	91.22	0.23	0.14	-	-	-
# 0264	RSA		✓	78.28	0.21	0.13	-	-	-
# 0267	RSA	✓		119.82	0.35	0.17	-	-	-
# 0270	RSA	✓		61.87	0.20	0.05	-	-	-
# 0289	RSA	✓		-	-	0.05	-	-	-
A_007_13	UK		✓	322.14	0.84	0.13	0.01	-	-
A_007_16	UK		✓	344.63	0.85	0.18	0.02	-	-
A_033_04	Italy	✓		52.72	0.15	0.04	0.01	-	-
A_067_04	USA	✓		305.53	0.59	0.17	-	-	-
A_067_05	USA	✓		76.06	0.40	0.14	-	-	-
A_067_06	USA	✓		377.18	0.68	0.24	-	-	-
A_067_07	USA	✓		52.39	0.19	0.15	-	-	-
A_068_02	USA		✓	279.81	0.59	0.23	-	-	-
A_068_21	USA		✓	265.45	0.57	0.24	-	-	-
A_068_24	USA		✓	280.07	0.56	0.18	-	-	-
A_068_25	USA	✓		121.10	0.65	0.22	-	-	-
A_068_26	USA	✓		313.03	0.62	0.28	-	-	-
A_068_27	USA	✓		34.94	0.14	0.12	-	-	-
A_070_18	China	✓		133.64	0.34	0.07	-	-	-
A_070_19	China	✓		62.40	0.26	0.23	-	-	-
A_070_23	China	✓		105.83	0.56	0.20	-	-	-
A_070_24	China	✓		168.94	1.35	0.50	-	-	-
A_070_28	China	✓		218.51	2.63	0.72	-	-	-
A_070_29	China	✓		244.61	4.18	1.37	-	-	-
A_070_33	China		✓	236.26	0.56	0.11	-	-	-
A_070_34	China		✓	152.12	0.44	0.12	-	-	-



Table D.5 RMSE and C.o.V values for each experiment and per shrinkage range for Dataset 4 (drying shrinkage) – MC 2010 model (continuation 1).

File data reference	Region	< 60 MPa (NSC)	≥ 60 MPa (HSC)	RMSE	overall C.o.V	C.o.V (0-99 days)	C.o.V (100-199 days)	C.o.V (200-499 days)	C.o.V (≥ 500 days)
A_070_38	China		✓	80.24	0.29	0.11	-	-	-
A_070_39	China		✓	52.13	0.22	0.17	-	-	-
A_070_43	China		✓	39.59	0.21	0.13	-	-	-
A_070_44	China		✓	65.45	0.38	0.27	-	-	-
A_070_48	China		✓	239.13	0.64	0.13	-	-	-
A_070_49	China		✓	192.74	0.57	0.16	-	-	-
A_070_53	China		✓	139.18	0.49	0.15	-	-	-
A_070_54	China		✓	109.48	0.41	0.09	-	-	-
A_070_58	China		✓	60.09	0.27	0.11	-	-	-
A_070_59	China		✓	35.91	0.18	0.06	-	-	-
A_071_04	China		✓	427.29	0.81	0.08	-	-	-
A_071_05	China		✓	276.78	0.68	0.06	-	-	-
A_071_06	China		✓	157.95	0.54	0.04	-	-	-
A_071_07	China		✓	390.01	0.81	0.04	-	-	-
A_071_08	China		✓	257.65	0.69	0.02	-	-	-
A_071_09	China		✓	141.74	0.55	0.04	-	-	-
e_074_01	GB	✓		684.93	0.76	0.13	0.0039	0.01	0.04
e_074_02	GB	✓		331.79	0.39	0.04	0.0035	0.02	0.05
e_074_03	GB	✓		407.41	0.46	0.02	0.0044	0.02	0.03
e_074_04	GB	✓		237.66	0.34	0.04	0.0098	0.03	0.04
e_074_05	GB	✓		116.20	0.17	0.09	0.0042	0.03	0.03
e_074_06	GB	✓		1094.53	0.84	0.08	0.0197	0.02	0.04
e_074_07	GB	✓		652.15	0.55	0.03	0.0033	0.03	0.04
e_074_08	GB	✓		492.75	0.51	0.04	0.0055	0.04	0.03
e_074_09	GB	✓		353.32	0.43	0.03	0.0045	0.05	0.03
e_074_10	GB	✓		276.43	0.40	0.04	0.0102	0.04	0.05
e_074_11	GB	✓		97.83	0.19	0.05	0.0309	0.07	0.05
e_074_12	GB	✓		74.13	0.14	0.07	0.0095	0.06	0.07
e_074_13	GB	✓		93.80	0.20	0.12	0.0166	0.08	0.10
e_074_14	GB	✓		149.12	0.38	0.20	0.0128	0.09	0.14
e_074_15	GB	✓		568.64	0.50	0.05	0.0028	0.02	0.04
e_074_16	GB	✓		340.71	0.40	0.08	0.0154	0.04	0.05
e_074_17	GB	✓		331.92	0.42	0.15	-	0.04	0.05
e_074_18	GB	✓		135.68	0.23	0.16	0.04	0.09	0.04
S_053_01	JAP	✓		224.32	0.64	0.07	-	-	-
S_053_08	JAP	✓		30.38	0.12	0.04	-	-	-
S_053_15	JAP		✓	272.80	0.79	0.17	-	-	-
S_053_22	JAP	✓		88.51	0.44	0.27	-	-	-
S_053_29	JAP		✓	201.49	0.70	0.08	-	-	-

Table D.6 RMSE and C.o.V values for each experiment and per shrinkage range for Dataset 4 (drying shrinkage) – MC 2010 model (continuation 2).

File data reference	Region	< 60 MPa (NSC)	≥ 60 MPa (HSC)	RMSE	overall C.o.V	C.o.V (0-99 days)	C.o.V (100-199 days)	C.o.V (200-499 days)	C.o.V (≥ 500 days)
S_053_36	JAP		✓	89.68	0.36	0.02	-	-	-
S_053_43	JAP		✓	19.42	0.10	0.05	-	-	-
S_053_50	JAP		✓	33.20	0.19	0.09	-	-	-
S_082_01	JAP	✓		30.04	0.08	0.06	0.04	0.09	-
S_082_13	JAP	✓		46.26	0.13	0.03	0.07	0.05	-
S_082_25	JAP	✓		86.54	0.26	0.05	0.06	0.08	-
S_082_37	JAP	✓		46.49	0.10	0.04	0.07	0.06	-

Table D.7 RMSE and C.o.V values for each experiment and per shrinkage range for Dataset 4 (autogenous shrinkage) – MC 2010 model.

File data reference	Region	< 60 MPa (NSC)	≥ 60 MPa (HSC)	RMSE	overall C.o.V	C.o.V (0-99 days)	C.o.V (100-199 days)	C.o.V (200-499 days)	C.o.V (≥ 500 days)
A_001_01	Turkey	✓		67.75	0.23	0.05	-	-	-
A_001_04	Turkey	✓		36.55	0.15	0.13	-	-	-
A_001_07	Turkey	✓		51.79	0.25	0.13	-	-	-
A_001_10	Turkey	✓		103.36	0.53	0.33	-	-	-
A_001_13	Turkey	✓		129.49	0.69	0.27	-	-	-
A_007_01	UK		✓	99.46	0.62	0.16	-	-	-
A_007_04	UK		✓	171.59	0.75	0.19	-	-	-
A_007_05	UK		✓	237.41	1.24	0.50	0.03	-	-
A_007_08	UK		✓	335.27	3.12	1.29	0.12	-	-
A_007_09	UK		✓	84.17	0.22	0.21	0.02	-	-
A_007_12	UK		✓	128.11	0.32	0.28	0.04	-	-
A_022_01	France		✓	519.45	8.06	1.34	0.19	-	-
A_022_02	France		✓	374.15	2.30	0.48	0.03	-	-
A_022_03	France		✓	393.70	7.33	1.82		-	-
A_022_05	France		✓	353.73	6.27	1.94		-	-
A_022_07	France		✓	159.40	0.69	0.35	0.04	-	-
A_022_09	France		✓	294.72	1.80	0.56	0.06	-	-
A_022_11	France		✓	350.60	2.95	1.08	0.11	-	-
A_022_13	France		✓	340.31	2.83	1.00	0.10	-	-
A_022_15	France		✓	388.64	3.36	1.07	0.17	-	-
A_023_01	Korea	✓		534.31	14.05	5.24	0.31	-	-
A_023_02	Korea	✓		288.13	1.72	0.83	0.06	-	-
A_023_03	Korea	✓		259.24	1.09	0.47	0.04	-	-
A_023_04	Korea		✓	148.26	0.39	0.32	0.02	-	-
A_023_05	Korea	✓		581.37	22.28	7.98	0.38	-	-

Table D.8 RMSE and C.o.V values for each experiment and per shrinkage range for Dataset 4 (autogenous shrinkage) – MC 2010 model (Continuation 1).

File data reference	Region	< 60 MPa (NSC)	≥ 60 MPa (HSC)	RMSE	overall C.o.V	C.o.V (0-99 days)	C.o.V (100-199 days)	C.o.V (200-499 days)	C.o.V (≥ 500 days)
A_023_06	Korea	✓		368.70	2.58	1.17	0.08	-	-
A_023_07	Korea	✓		303.59	1.83	0.88	0.06	-	-
A_023_08	Korea		✓	180.15	0.62	0.42	0.04	-	-
A_023_09	Korea	✓		141.85	0.67	0.46	-	-	-
A_023_10	Korea	✓		163.00	0.86	0.53	-	-	-
A_023_11	Korea	✓		174.45	1.21	0.75	-	-	-
A_023_12	Korea	✓		185.59	1.64	0.99		-	-
A_023_13	Korea		✓	144.14	0.42	0.28	-	-	-
A_023_14	Korea		✓	119.30	0.37	0.26	-	-	-
A_023_15	Korea		✓	89.52	0.34	0.32	-	-	-
A_023_16	Korea	✓		118.56	0.70	0.40	-	-	-
A_024_01	Korea	✓		193.84	0.91	0.55	-	-	-
A_024_02	Korea	✓		365.48	4.42	1.78	-	-	-
A_024_03	Korea	✓		472.96	7.16	2.61	-	-	-
A_024_04	Korea	✓		415.55	8.23	2.83	-	-	-
A_031_02	Iran	✓		502.45	3.58	0.78	0.06	0.02	-
A_031_04	Iran		✓	445.25	2.65	0.82	0.02	0.03	-
A_031_06	Iran		✓	420.53	2.29	0.39	0.02	0.01	-
A_033_02	Italy	✓		334.08	8.63	8.58	0.04	-	-
A_036_11	UK	✓		432.28	6.67	1.75	-	-	-
A_036_16	UK	✓		462.78	20.95	3.97	-	-	-
A_038_10	Japan		✓	322.68	0.71	0.23	-	-	-
A_046_02	Sweden		✓	158.15	0.70	0.29	-	-	-
A_046_07	Sweden		✓	285.64	1.60	0.34	0.04	0.09	0.02
A_053_03	Japan		✓	256.49	7.29	3.09	-	-	-
A_053_06	Japan		✓	74.49	0.30	0.28	-	-	-
A_053_07	Japan		✓	74.91	0.35	0.32	-	-	-
A_053_08	Japan		✓	232.72	3.08	1.33	-	-	-
A_053_09	Japan		✓	172.39	1.64	0.87	-	-	-
A_061_01	Japan		✓	126.23	2.75	1.90	-	-	-
A_061_02	Japan		✓	234.11	0.81	0.33	-	-	-
A_061_03	Japan		✓	60.47	0.38	0.20	-	-	-
A_065_01	France	✓		795.87	8.71	0.96	-	-	-
A_065_03	France		✓	442.11	3.01	0.49	0.10	-	-
A_065_05	France	✓		628.75	2.96	0.40	-	-	-
A_065_07	France		✓	433.31	2.56	0.27	0.13	-	-
A_068_01	USA		✓	139.60	0.28	0.11	-	-	-
A_068_04	USA	✓		55.25	0.88	0.42	-	-	-
A_068_05	USA	✓		124.50	7.15	2.58	-	-	-
A_068_06	USA	✓		134.18	3.84	1.84	-	-	-

Table D.9 RMSE and C.o.V values for each experiment and per shrinkage range for Dataset 4 (autogenous shrinkage) – MC 2010 model (Continuation 2).

File data reference	Region	< 60 MPa (NSC)	≥ 60 MPa (HSC)	RMSE	overall C.o.V	C.o.V (0-99 days)	C.o.V (100-199 days)	C.o.V (200-499 days)	C.o.V (≥ 500 days)
A_068_07	USA	✓		150.85	16.84	6.78	-	-	-
A_068_08	USA		✓	147.91	0.85	0.56	-	-	-
A_068_09	USA	✓		106.08	5.20	2.30	-	-	-
A_068_12	USA		✓	149.10	0.86	0.56	-	-	-
A_068_16	USA		✓	142.94	0.28	0.08	-	-	-
A_068_19	USA		✓	149.21	0.28	0.06	-	-	-
A_068_20	USA	✓		191.90	0.86	0.22	-	-	-
A_070_01	China	✓		150.34	0.77	0.60	-	-	-
A_070_02	China		✓	211.15	1.88	1.16	-	-	-
A_070_03	China		✓	178.23	2.17	1.43	-	-	-
A_071_01	China		✓	72.53	0.26	0.17	-	-	-
A_071_02	China		✓	59.87	0.24	0.19	-	-	-
A_071_03	China		✓	129.10	0.82	0.39	-	-	-
A_072_01	Singapore		✓	333.55	2.04	0.36	-	-	-
A_072_02	Singapore		✓	381.19	2.69	0.82	-	-	-
A_072_03	Singapore		✓	519.99	13.58	3.87	-	-	-
A_072_04	Singapore		✓	238.93	1.08	0.42	-	-	-
A_072_05	Singapore		✓	293.72	1.55	0.56	-	-	-
A_072_06	Singapore		✓	358.03	2.22	0.60	-	-	-
A_072_07	Singapore		✓	206.10	0.81	0.22	-	-	-
A_072_08	Singapore		✓	214.98	0.90	0.35	-	-	-
A_072_09	Singapore		✓	301.83	1.53	0.47	-	-	-
A_074_01	Israel		✓	147.38	2.88	0.92	-	-	-
A_074_02	Israel		✓	189.90	9.60	4.34	-	-	-
A_074_03	Israel		✓	181.14	5.75	2.84	-	-	-
A_074_04	Israel		✓	137.87	1.90	1.14	-	-	-
A_074_05	Israel		✓	149.66	2.39	1.19	-	-	-
A_083_01	Korea	✓		513.73	13.75	5.18	0.30	-	-
A_083_02	Korea	✓		288.51	1.74	0.77	0.06	-	-
A_083_03	Korea	✓		215.20	1.01	0.56	0.04	-	-
A_083_04	Korea		✓	126.60	0.36	0.30	0.02	-	-
A_083_05	Korea	✓		146.03	0.88	0.57	-	-	-
A_083_06	Korea		✓	115.43	0.37	0.28	-	-	-
A_083_07	Korea	✓		571.69	21.36	6.74	0.35	-	-
A_083_08	Korea	✓		358.83	2.62	1.19	0.07	-	-
A_083_09	Korea	✓		302.61	1.74	0.78	0.06	-	-
A_083_10	Korea		✓	172.83	0.60	0.40	0.04	-	-
A_083_11	Korea	✓		185.55	1.69	0.98	-	-	-
A_083_12	Korea	✓		126.32	0.70	0.39	-	-	-
A_086_03	Sweden		✓	346.64	1.68	1.43	0.02	0.14	0.21

Table D.10 RMSE and C.o.V values for each experiment and per shrinkage range for Dataset 4 (autogenous shrinkage) – MC 2010 model (Continuation 3).

File data reference	Region	< 60 MPa (NSC)	≥ 60 MPa (HSC)	RMSE	overall C.o.V	C.o.V (0-99 days)	C.o.V (100-199 days)	C.o.V (200-499 days)	C.o.V (≥ 500 days)
A_086_07	Sweden		✓	265.28	1.33	1.45	-	0.17	0.14
A_086_09	Sweden		✓	344.15	2.74	1.63	-	-	0.24
A_086_11	Sweden		✓	285.99	1.35	0.74	-	-	0.22
A_086_13	Sweden		✓	347.02	1.95	1.06	0.09	-	0.15
A_086_14	Sweden		✓	365.63	1.93	1.47	0.11	0.17	0.24
A_086_18	Sweden		✓	250.18	0.79	1.02	0.02	0.09	0.08
A_086_19	Sweden		✓	304.79	1.10	0.04	0.06	0.03	0.14
A_086_25	Sweden		✓	235.87	1.21	0.93	-	0.01	0.17
A_086_26	Sweden		✓	223.17	1.16	0.76	-	0.07	0.22
A_086_30	Sweden		✓	184.70	0.79	0.55	-	0.02	0.16
A_086_31	Sweden		✓	173.56	0.67	0.32	-	0.09	0.16
A_086_35	Sweden		✓	146.25	0.50	0.03	-	0.04	0.12
A_086_36	Sweden		✓	191.64	0.63	0.13	0.03	0.07	0.17
A_086_41	Sweden		✓	68.21	0.21	0.08	-	0.08	0.09
A_086_42	Sweden		✓	131.14	0.48	0.18	-	0.02	0.12
e_015_10	USA	✓		494.68	4.07	1.81	-	-	-
e_015_11	USA	✓		576.05	9.57	7.04	-	-	-
e_015_12	USA	✓		549.33	6.87	3.74	-	-	-
e_015_16	USA	✓		602.48	13.79	5.91	-	-	-
e_074_19	GB	✓		166.13	1.29	0.49	-	0.07	0.31
e_074_20	GB	✓		583.24	5.83	2.32	0.44	0.10	0.26
e_074_21	GB	✓		738.61	13.54	14.53	-	0.37	0.51
e_074_22	GB	✓		689.89	5.78	3.94	-	0.01	0.26
e_074_23	GB	✓		740.85	8.63	6.39	0.50	0.24	0.27
e_074_24	GB	✓		70.45	1.06	0.70	0.44	0.24	0.51
e_074_25	GB	✓		588.06	4.56	3.10	0.17	0.19	0.26
e_074_26	GB	✓		702.99	8.36	4.09	0.53	0.12	0.35
e_074_27	GB	✓		691.15	7.22	6.79	0.13	0.06	0.35
e_074_28	GB	✓		692.23	6.26	3.33	0.13	0.14	0.20
e_074_29	GB	✓		248.16	1.48	0.66	0.13	0.38	0.44
e_074_30	GB	✓		605.34	3.49	2.42	0.12	0.06	0.31
e_074_31	GB	✓		633.49	4.01	8.94	0.25	0.09	0.36
e_074_32	GB	✓		598.45	4.43	9.03	0.11	0.05	0.24
e_074_33	GB	✓		105.41	1.41	0.63	-	0.13	0.45
e_074_34	GB	✓		701.74	7.52	8.60	-	0.10	0.45
e_074_35	GB	✓		664.48	4.79	4.62	0.17	0.11	0.27
e_074_36	GB	✓		668.83	4.66	5.68	0.08	0.10	0.22
e_076_01	D	✓		104.05	1.69	0.72	-	-	-
e_096_19	D		✓	526.01	9.11	4.03	0.36	0.08	-
e_096_20	D		✓	461.38	3.84	1.94	0.09	0.01	-
e_096_21	D		✓	416.16	3.29	1.64	0.15	0.05	-
e_096_22	D		✓	517.85	6.50	4.29	0.13	0.07	-
e_096_23	D		✓	458.61	4.16	1.79	0.12	0.03	-
e_096_24	D		✓	527.81	6.82	4.51	0.20	0.04	-
e_096_25	D		✓	440.42	3.44	1.59	0.10	0.004	-
e_096_26	D		✓	539.10	9.84	4.09	0.39	0.10	-
e_096_27	D		✓	540.48	8.75	3.99	0.29	0.07	-

Table D.11 RMSE and C.o.V values for each experiment and per shrinkage range for Dataset 5 – WITS model.

File data reference	Region	< 60 MPa (NSC)	≥ 60 MPa (HSC)	RMSE	overall C.o.V	C.o.V (0-99 days)	C.o.V (100-199 days)	C.o.V (200-499 days)
# 0013	RSA		✓	29.70	0.09	0.09	0.06	-
# 0015	RSA		✓	53.64	0.15	0.14	0.10	-
# 0016	RSA	✓		75.98	0.21	0.16	0.09	-
# 0017	RSA		✓	26.97	0.09	0.10	0.05	-
# 0019	RSA	✓		48.09	0.18	0.22	0.05	-
# 0021	RSA	✓		100.79	0.41	0.25	0.05	-
# 0023	RSA	✓		46.32	0.16	0.15	0.08	-
# 0025	RSA	✓		36.84	0.13	0.18	0.05	-
# 0027	RSA	✓		97.06	0.40	0.15	0.03	-
# 0029	RSA	✓		178.99	0.92	0.20	0.07	-
# 0031	RSA		✓	70.09	0.21	0.04	0.01	-
# 0032	RSA	✓		131.97	0.37	0.04	0.01	-
# 0033	RSA		✓	50.56	0.16	0.15	0.04	-
# 0035	RSA	✓		163.03	0.80	0.19	0.04	-
# 0037	RSA	✓		23.21	0.10	0.08	0.02	-
# 0039	RSA	✓		11.27	0.05	0.03	0.01	-
# 0041	RSA	✓		10.33	0.04	0.01	0.01	-
# 0043	RSA	✓		107.11	0.37	0.07	0.01	-
# 0045	RSA	✓		77.41	0.41	0.13	0.08	-
# 0047	RSA		✓	41.48	0.16	0.08	0.03	-
# 0049	RSA		✓	140.14	0.76	0.12	0.03	-
# 0051	RSA	✓		85.10	0.29	0.06	0.01	-
# 0053	RSA		✓	201.84	0.51	0.07	0.01	-
# 0077	RSA	✓		276.42	0.53	0.07	0.01	-
# 0078	RSA	✓		346.99	0.64	0.00	0.05	-
# 0079	RSA		✓	55.00	0.16	0.13	0.03	-
# 0080	RSA	✓		229.49	0.47	0.08	0.05	-
# 0081	RSA		✓	264.31	0.54	0.05	0.08	-
# 0083	RSA		✓	181.16	0.39	0.06	0.05	-
# 0085	RSA	✓		275.57	0.53	0.01	0.02	-
# 0087	RSA	✓		283.59	0.54	0.02	0.02	-
# 0091	RSA	✓		183.04	0.43	0.08	0.02	-
# 0093	RSA	✓		301.12	0.62	0.03	0.01	-
# 0095	RSA	✓		230.70	0.53	0.12	0.07	-
# 0097	RSA	✓		223.23	0.49	0.12	0.07	-
# 0109	RSA		✓	226.44	0.67	0.06	-	-
# 0110	RSA		✓	164.80	0.61	0.08	-	-
# 0111	RSA	✓		225.81	0.72	0.08	-	-
# 0123	RSA		✓	35.69	0.13	0.14	0.02	0.02

Table D.12 RMSE and C.o.V values for each experiment and per shrinkage range for Dataset 5 – WITS model (continuation).

File data reference	Region	< 60 MPa (NSC)	≥ 60 MPa (HSC)	RMSE	overall C.o.V	C.o.V (0-99 days)	C.o.V (100-199 days)	C.o.V (200-499 days)
# 0150	RSA		✓	277.99	0.54	0.06	0.04	-
# 0217	RSA		✓	79.18	0.24	-	0.07	-
# 0219	RSA		✓	190.09	0.52	-	0.02	-
# 0221	RSA		✓	193.51	0.57	-	0.04	-
# 0225	RSA		✓	170.58	0.44	0.09	-	0.03
# 0228	RSA		✓	194.66	0.50	0.11	-	0.03
# 0231	RSA		✓	142.10	0.42	0.15	-	0.04
# 0234	RSA		✓	202.43	0.53	0.14	-	0.04
# 0237	RSA		✓	100.60	0.33	0.17	-	0.14
# 0240	RSA		✓	117.78	0.40	0.21	0.12	0.02
# 0243	RSA	✓		126.68	0.43	0.19	0.12	0.07
# 0246	RSA		✓	96.10	0.31	0.13	-	0.03
# 0249	RSA		✓	107.23	0.36	0.17	-	0.08
# 0252	RSA		✓	110.63	0.37	0.13	-	0.01
# 0255	RSA		✓	231.64	0.70	0.09	-	-
# 0258	RSA		✓	160.89	0.56	0.07	-	-
# 0261	RSA		✓	276.51	0.71	0.12	-	-
# 0264	RSA		✓	243.04	0.65	-	-	-
# 0267	RSA	✓		163.90	0.48	0.10	-	-
# 0270	RSA	✓		105.40	0.34	0.10	-	-
# 0276	RSA	✓		190.53	0.48	-	-	0.04
# 0278	RSA	✓		411.00	0.82	-	-	0.03
# 0280	RSA	✓		428.19	0.99	-	-	0.07
# 0282	RSA	✓		372.04	0.98	-	-	0.03
# 0283	RSA	✓		880.15	1.32	-	-	0.04
# 0284	RSA	✓		464.77	1.10	-	-	0.04
# 0286	RSA	✓		410.24	1.01	-	-	0.07

**Appendix E. Original and modified shrinkage predictions of RILEM B4, MC 2010 and WITS model for Dataset 1-HSC**

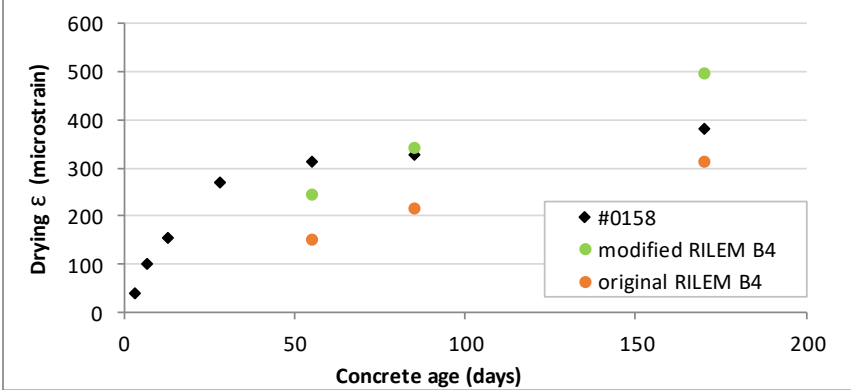


Figure E.1 RILEM B4 model predicted and actual drying shrinkage (microstrain) for Dataset 1-HSC, Subset S1-01, Experiment #0158

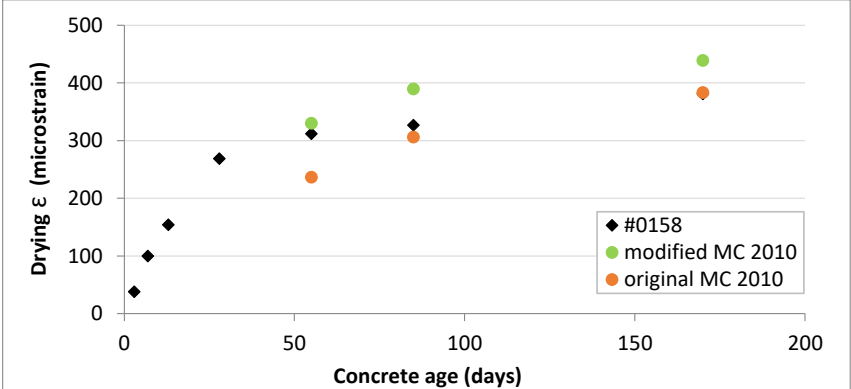


Figure E.2 MC 2010 model predicted and actual drying shrinkage (microstrain) for Dataset 1-HSC, Subset S1-01, Experiment #0158

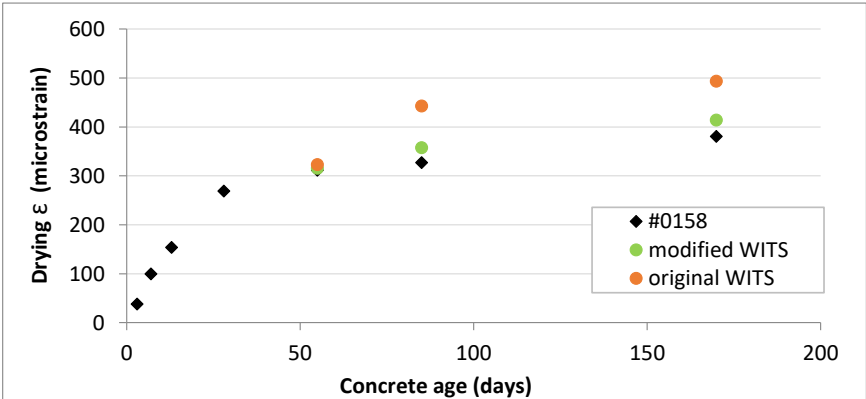


Figure E.3 WITS model predicted and actual drying shrinkage (microstrain) for Dataset 1-HSC, Subset S1-01, Experiment #0158



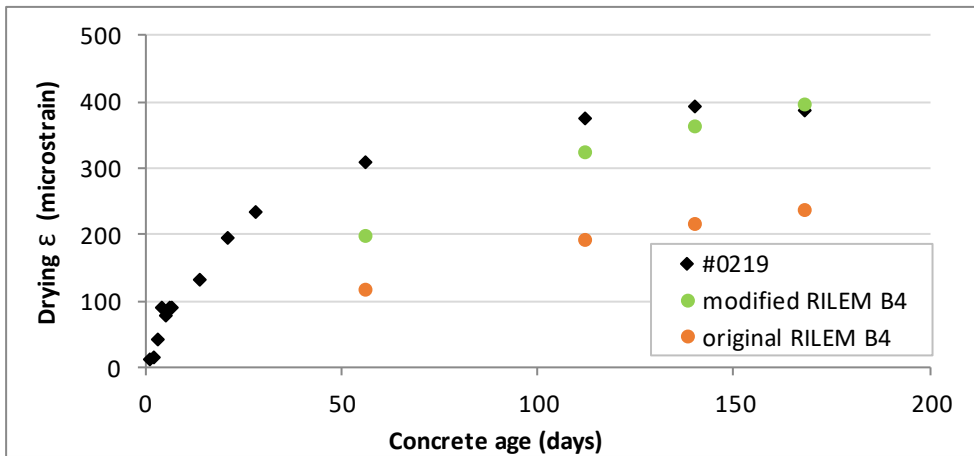


Figure E.4 RILEM B4 model predicted and actual drying shrinkage (microstrain) for Dataset 1-HSC, Subset S1-01, Experiment #0219

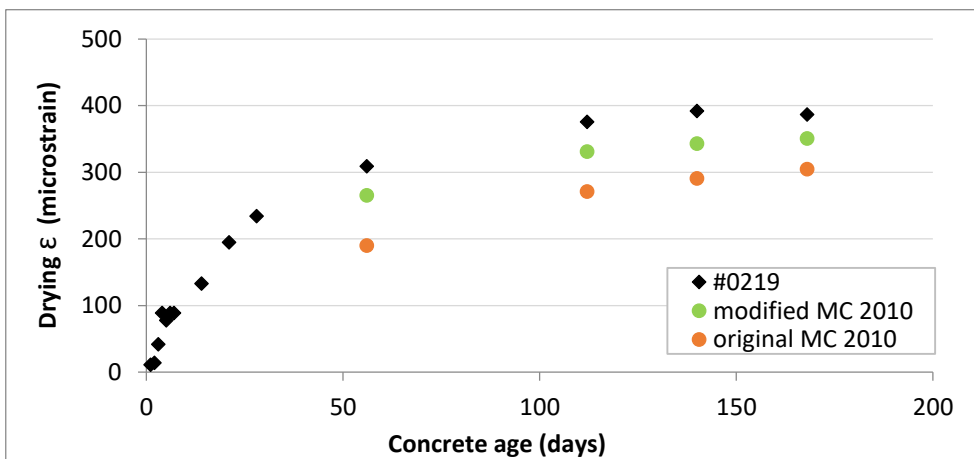


Figure E.5 MC 2010 model predicted and actual drying shrinkage (microstrain) for Dataset 1-HSC, Subset S1-01, Experiment #0219

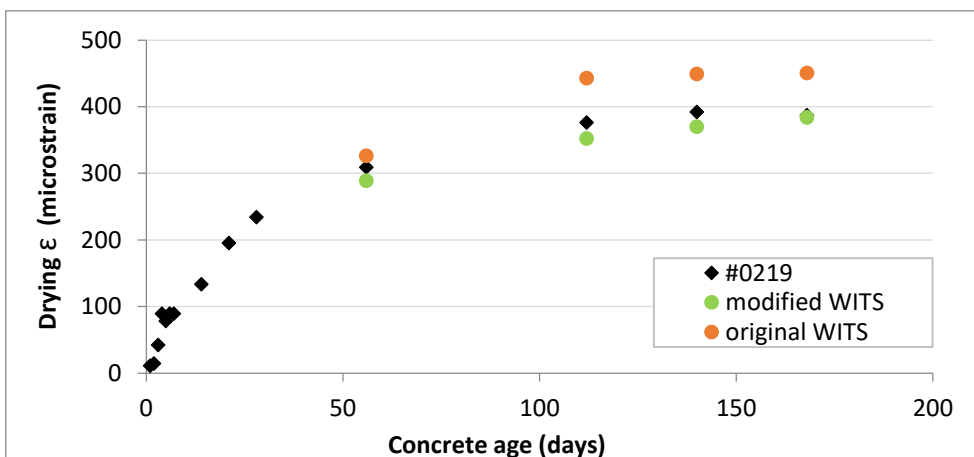


Figure E.6 WITS model predicted and actual drying shrinkage (microstrain) for Dataset 1-HSC, Subset S1-01, Experiment #0219

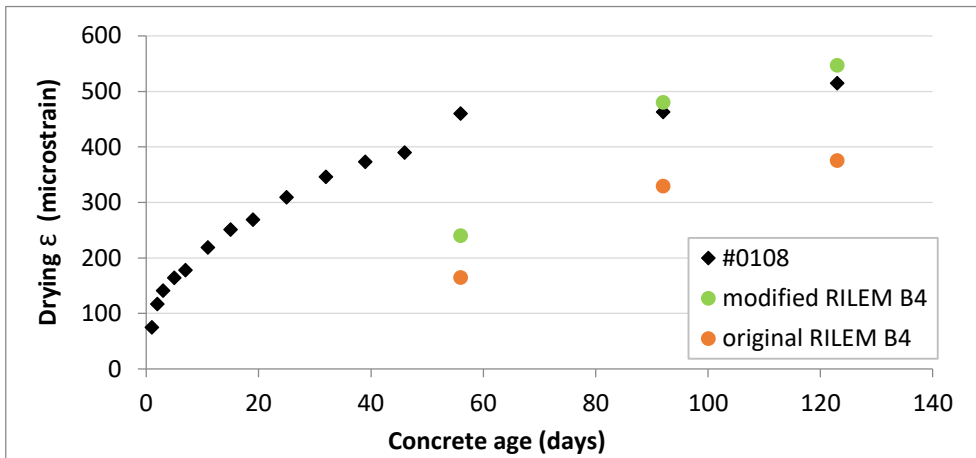


Figure E.7 RILEM B4 model predicted and actual drying shrinkage (microstrain) for Dataset 1-HSC, Subset S1-02, Experiment #0108

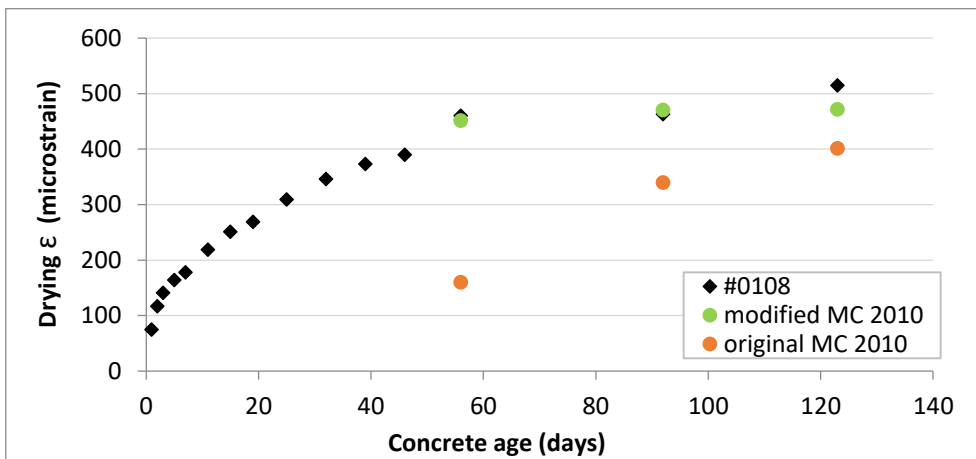


Figure E.8 MC 2010 model predicted and actual drying shrinkage (microstrain) for Dataset 1-HSC, Subset S1-02, Experiment #0108

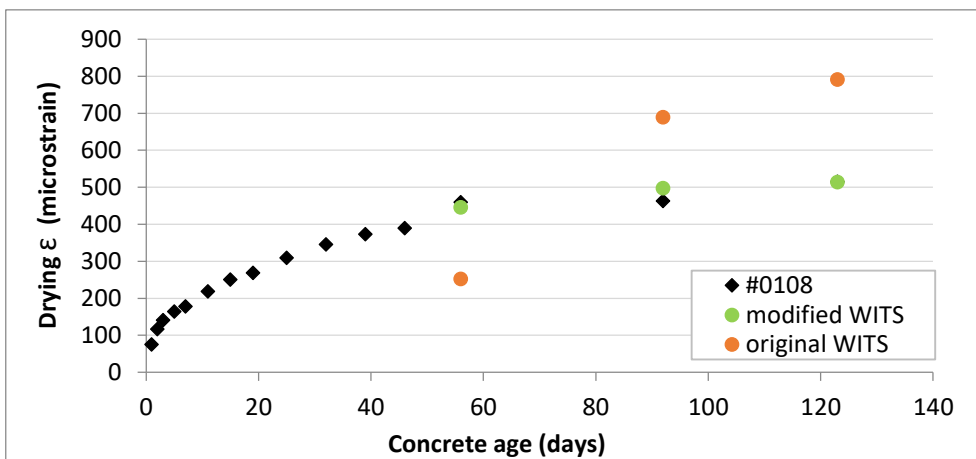


Figure E.9 WITS model predicted and actual drying shrinkage (microstrain) for Dataset 1-HSC, Subset S1-02, Experiment #0108

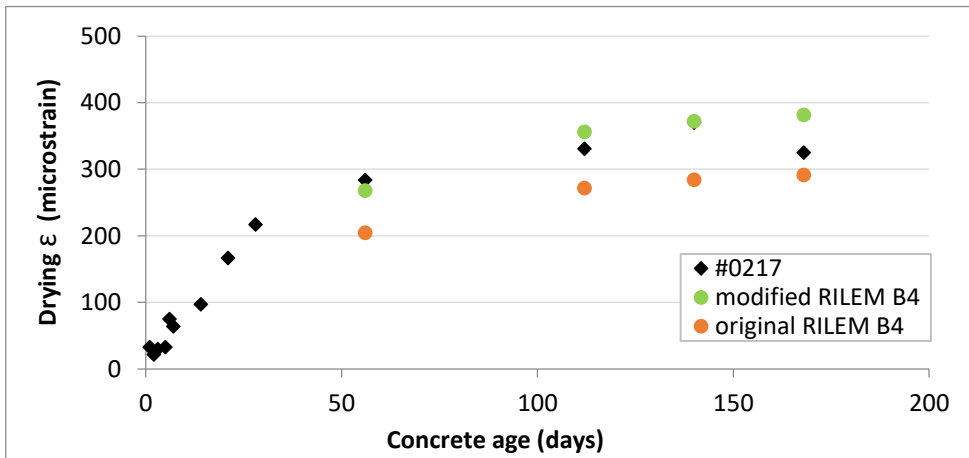


Figure E.10 RILEM B4 model predicted and actual drying shrinkage (microstrain) for Dataset 1-HSC, Subset S1-02, Experiment #0217

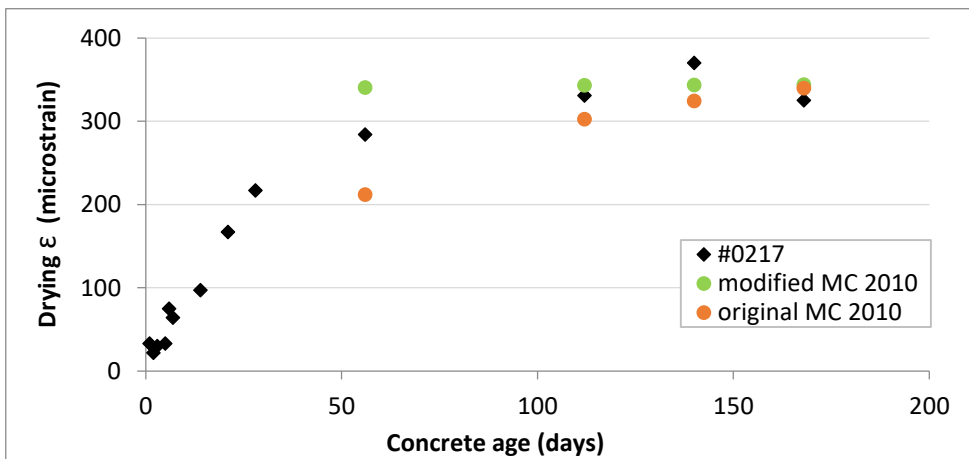


Figure E.11 MC 2010 model predicted and actual drying shrinkage (microstrain) for Dataset 1-HSC, Subset S1-02, Experiment #0217

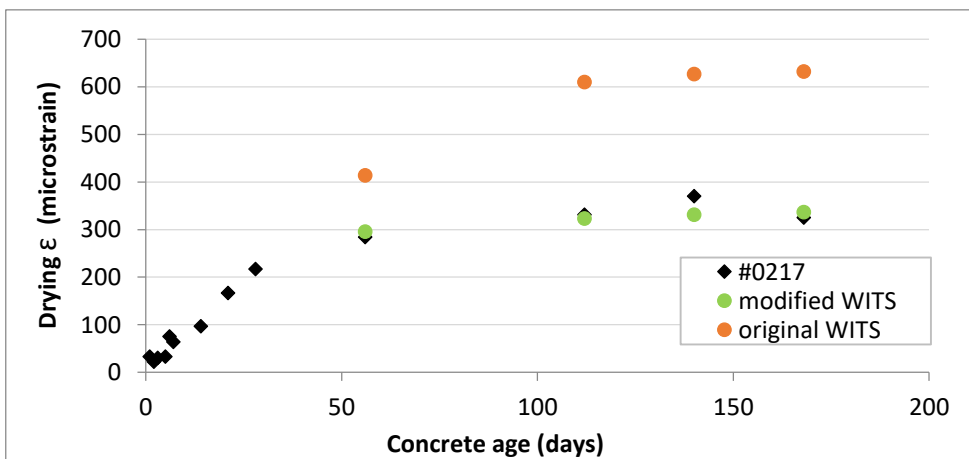


Figure E.12 WITS model predicted and actual drying shrinkage (microstrain) for Dataset 1-HSC, Subset S1-02, Experiment #0217

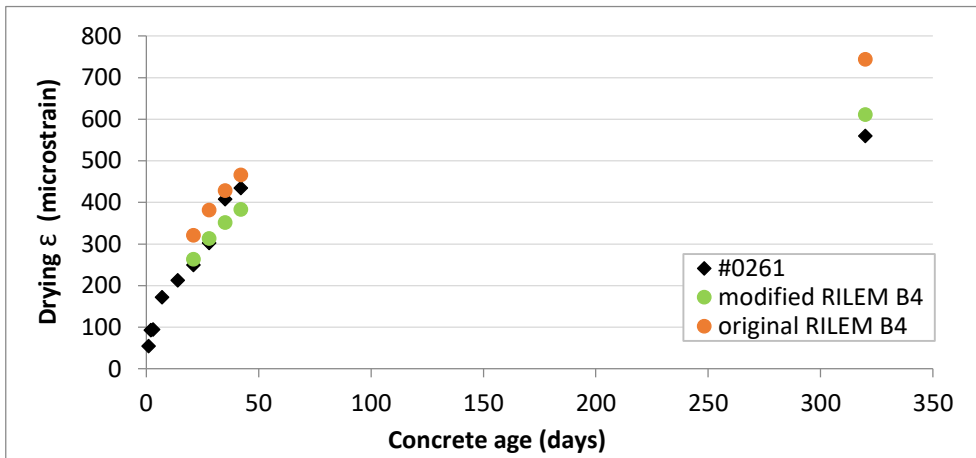


Figure E.13 RILEM B4 model predicted and actual drying shrinkage (microstrain) for Dataset 1-HSC, Subset S1-03, Experiment #0261

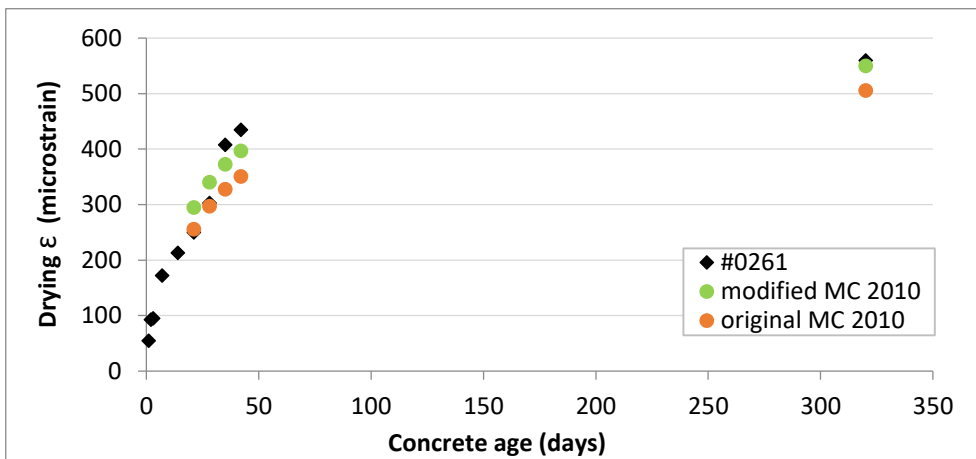


Figure E.14 MC 2010 model predicted and actual drying shrinkage (microstrain) for Dataset 1-HSC, Subset S1-03, Experiment #0261

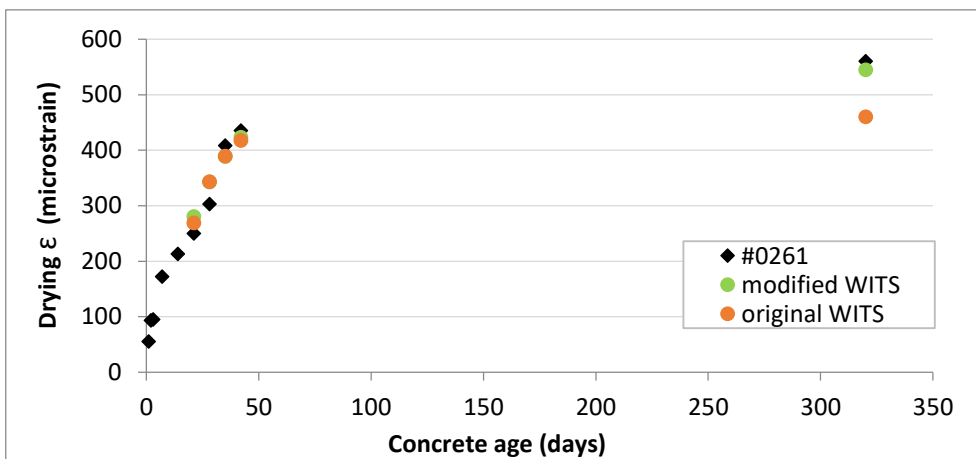


Figure E.15 WITS model predicted and actual drying shrinkage (microstrain) for Dataset 1-HSC, Subset S1-03, Experiment #0261

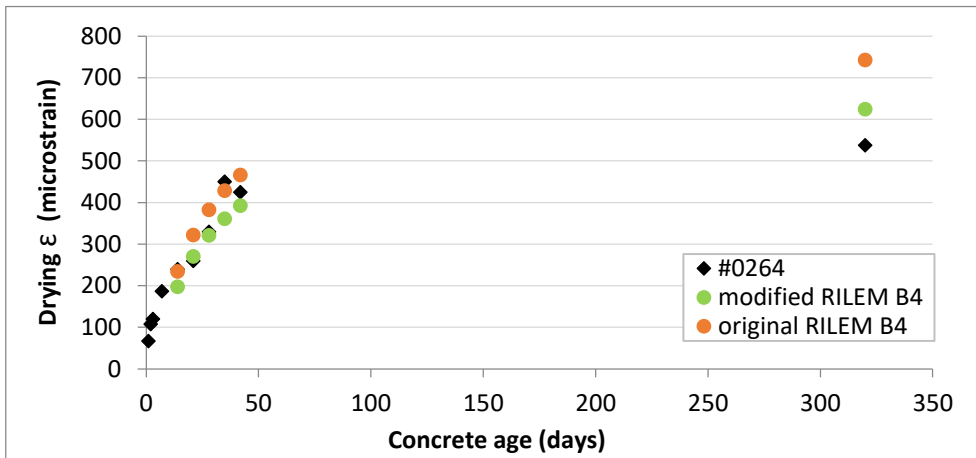


Figure E.16 RILEM B4 model predicted and actual drying shrinkage (microstrain) for Dataset 1-HSC, Subset S1-03, Experiment #0264

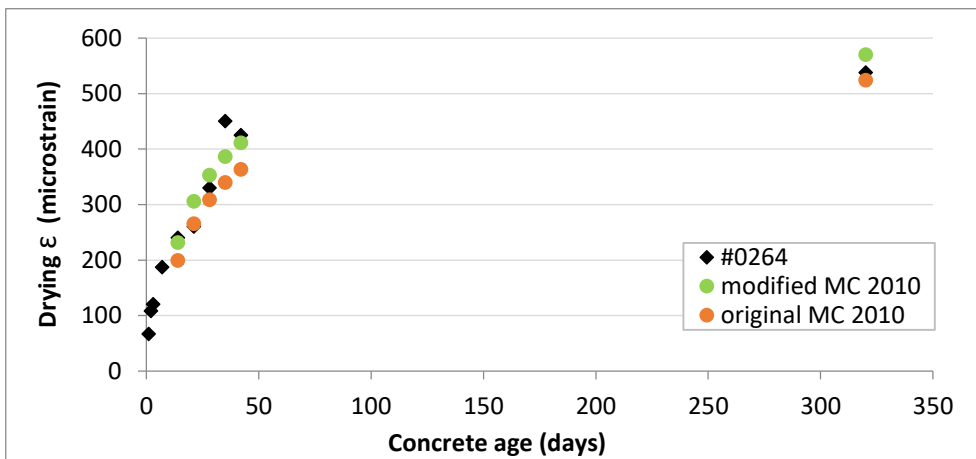


Figure E.17 MC 2010 model predicted and actual drying shrinkage (microstrain) for Dataset 1-HSC, Subset S1-03, Experiment #0264

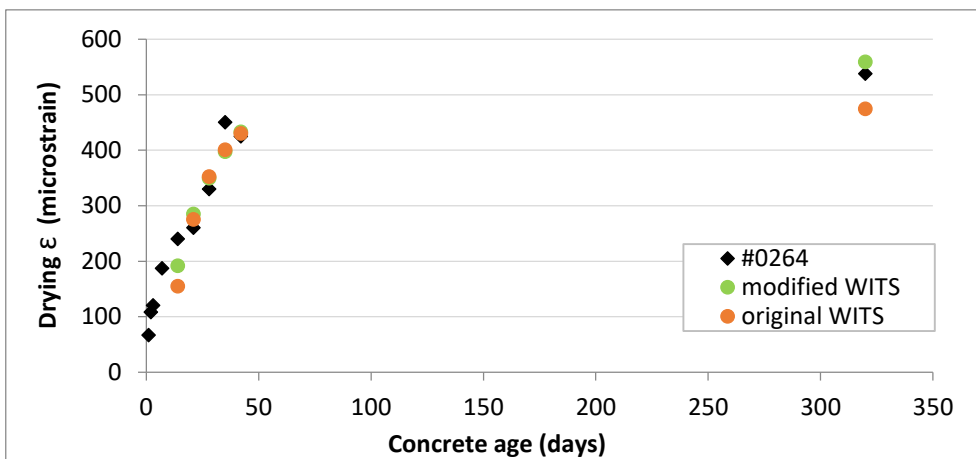


Figure E.18 WITS model predicted and actual drying shrinkage (microstrain) for Dataset 1-HSC, Subset S1-03, Experiment #0264

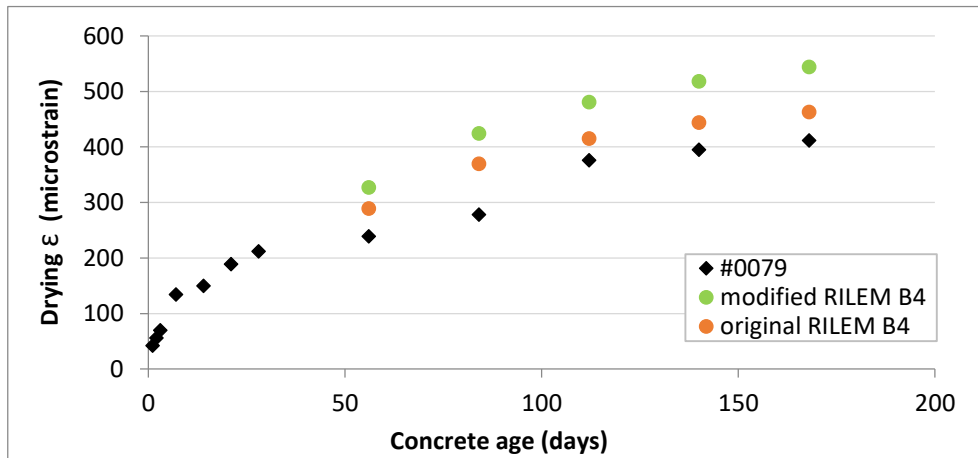


Figure E.19 RILEM B4 model predicted and actual drying shrinkage (microstrain) for Dataset 1-HSC, Subset S1-04, Experiment #0079

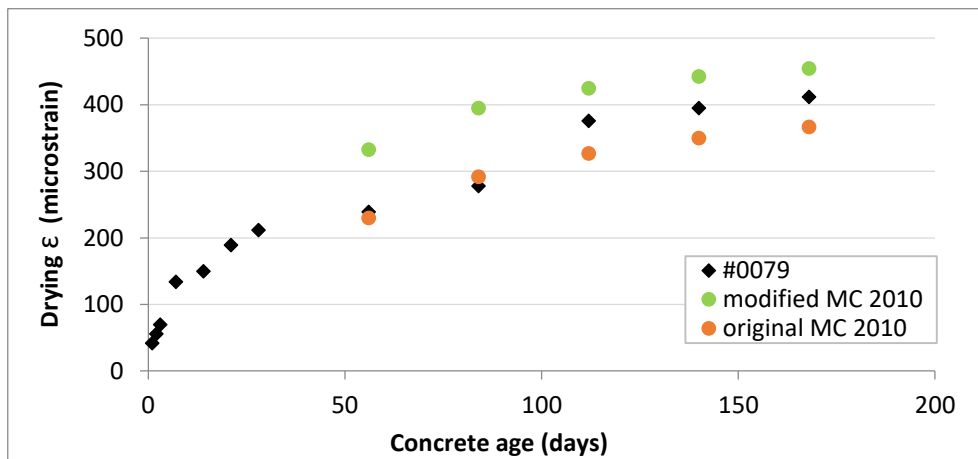


Figure E.20 MC 2010 model predicted and actual drying shrinkage (microstrain) for Dataset 1-HSC, Subset S1-04, Experiment #0079

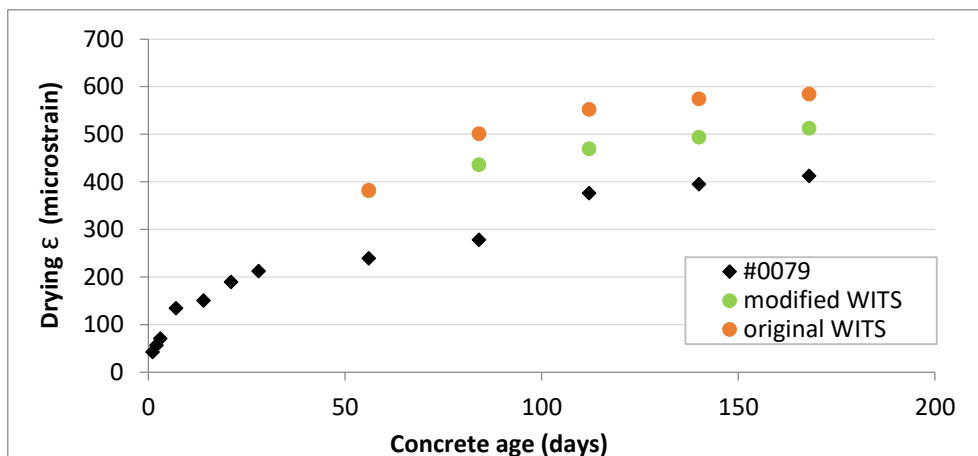


Figure E.21 WITS model predicted and actual drying shrinkage (microstrain) for Dataset 1-HSC, Subset S1-04, Experiment #0079

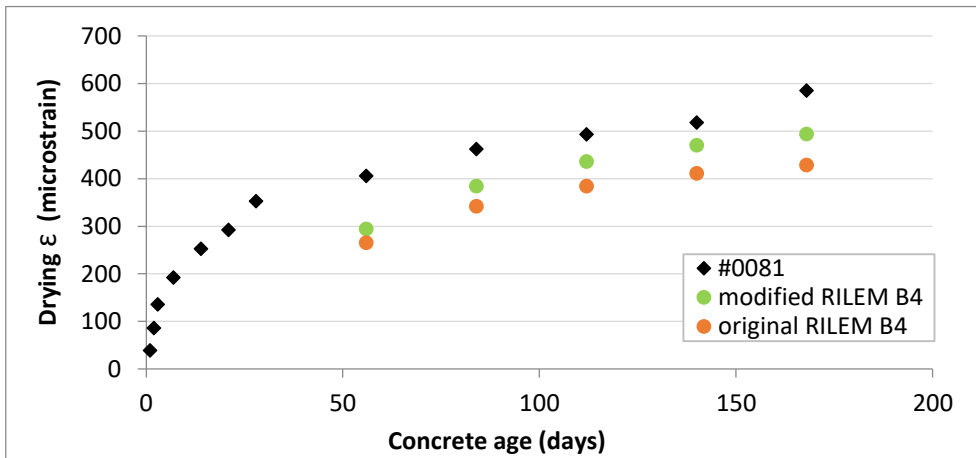


Figure E.22 RILEM B4 model predicted and actual drying shrinkage (microstrain) for Dataset 1-HSC, Subset S1-04, Experiment #0081

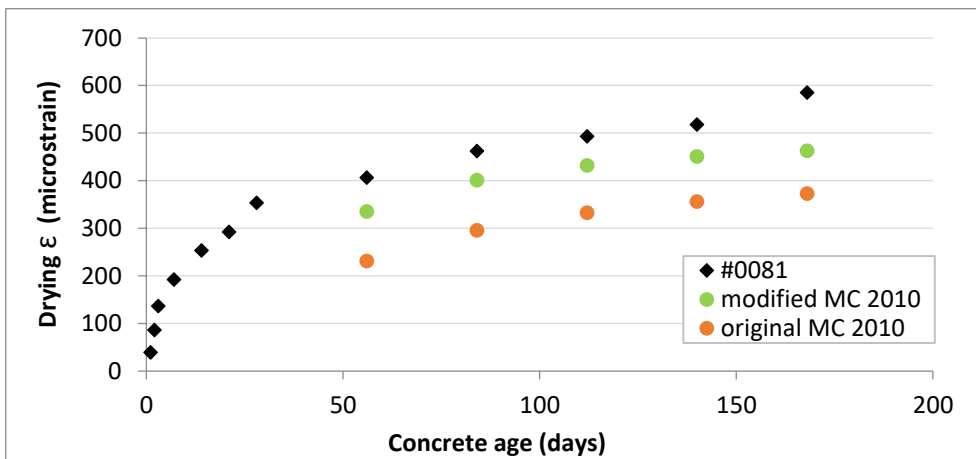


Figure E.23 MC 2010 model predicted and actual drying shrinkage (microstrain) for Dataset 1-HSC, Subset S1-04, Experiment #0081

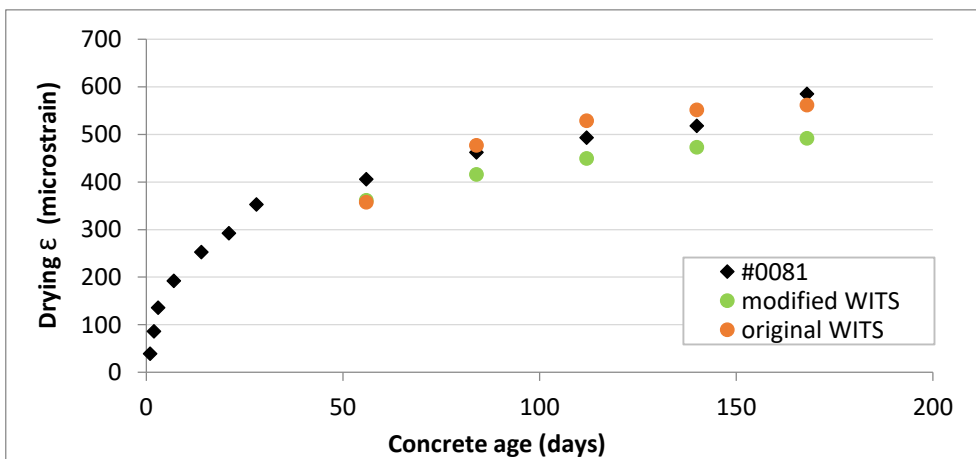


Figure E.24 WITS model predicted and actual drying shrinkage (microstrain) for Dataset 1-HSC, Subset S1-04, Experiment #0081

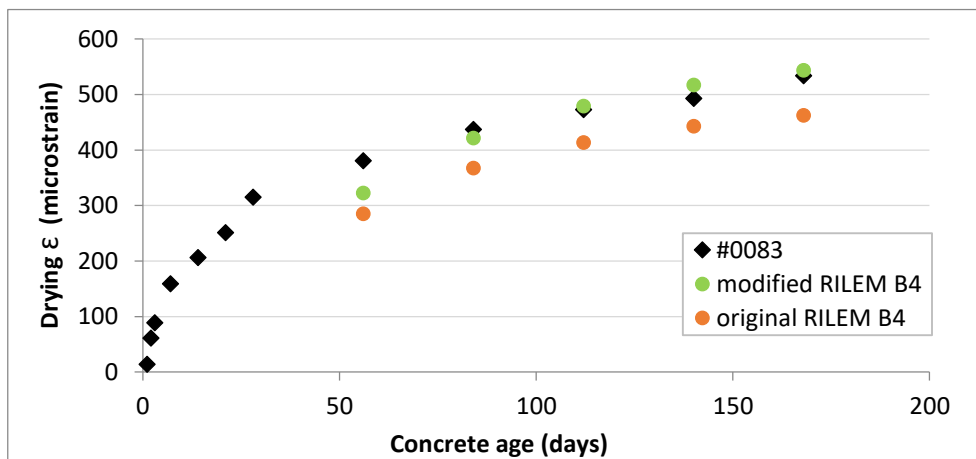


Figure E.25 RILEM B4 model predicted and actual drying shrinkage (microstrain) for Dataset 1-HSC, Subset S1-04, Experiment #0083

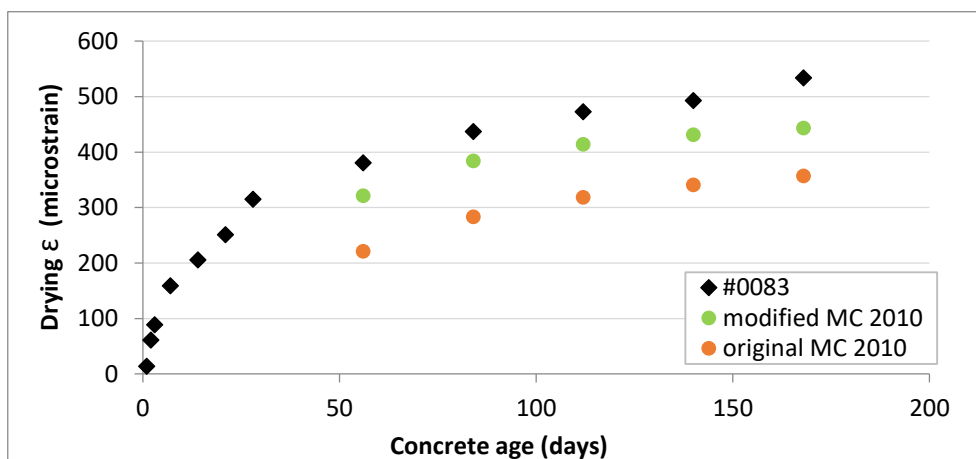


Figure E.26 MC 2010 model predicted and actual drying shrinkage (microstrain) for Dataset 1-HSC, Subset S1-04, Experiment #0083

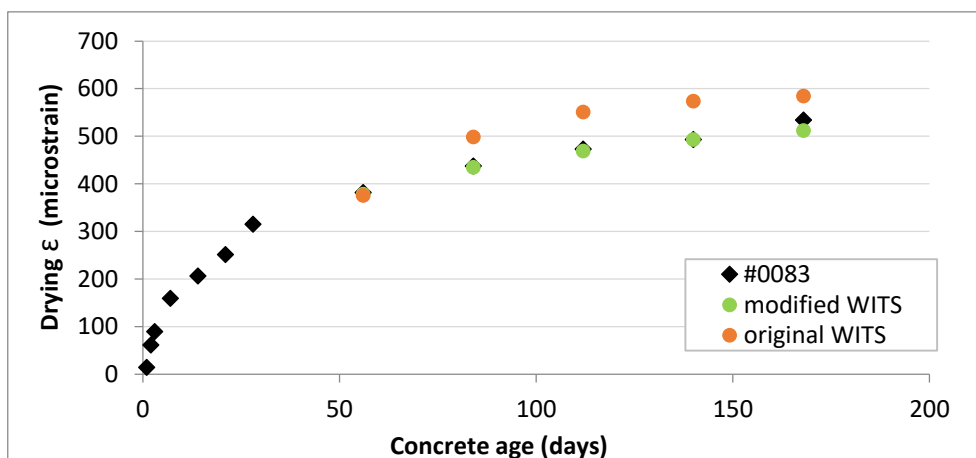


Figure E.27 WITS model predicted and actual drying shrinkage (microstrain) for Dataset 1-HSC, Subset S1-04, Experiment #0083



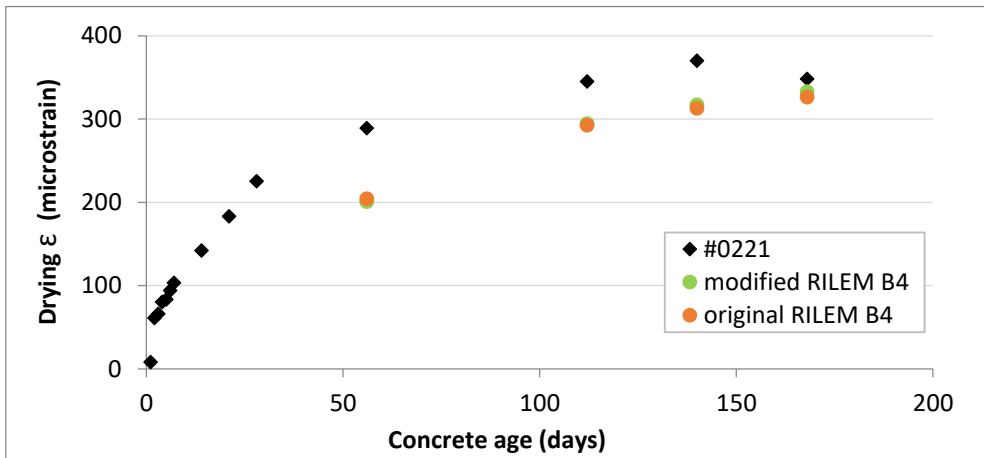


Figure E.28 RILEM B4 model predicted and actual drying shrinkage (microstrain) for Dataset 1-HSC, Subset S1-04, Experiment #0221

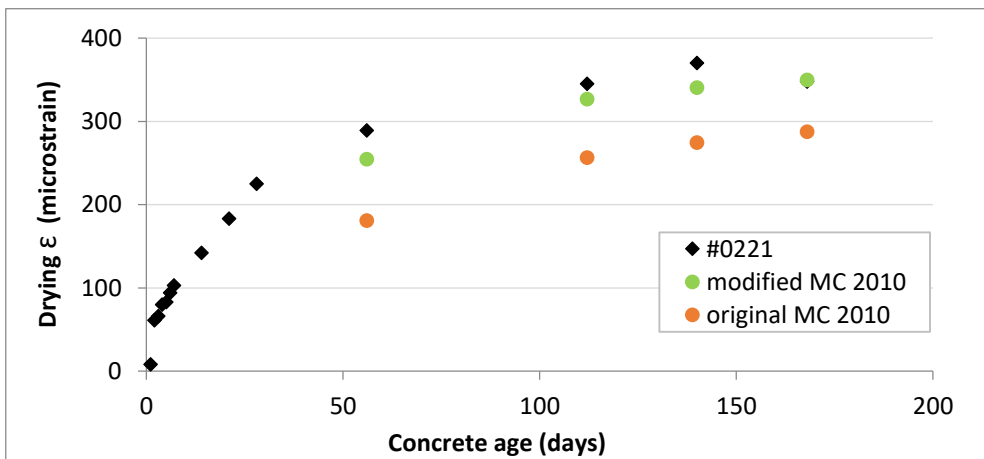


Figure E.29 MC 2010 model predicted and actual drying shrinkage (microstrain) for Dataset 1-HSC, Subset S1-04, Experiment #0221

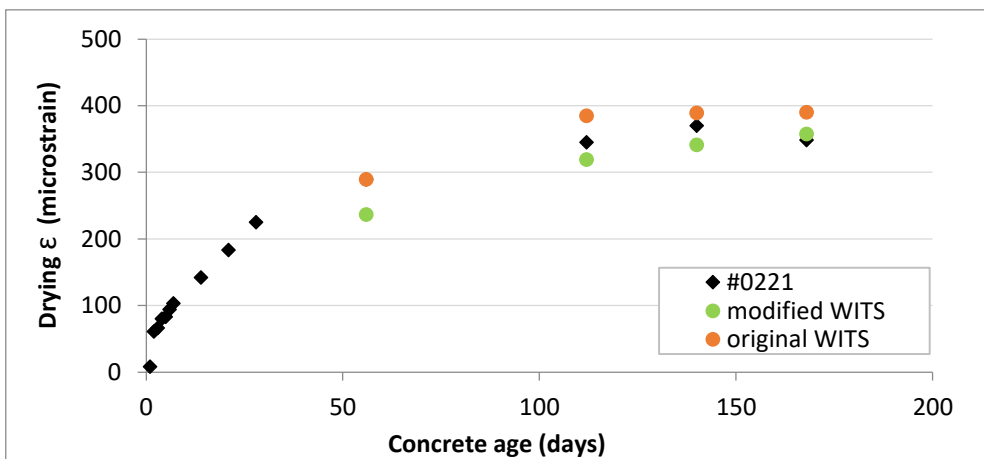


Figure E.30 WITS model predicted and actual drying shrinkage (microstrain) for Dataset 1-HSC, Subset S1-04, Experiment #0221

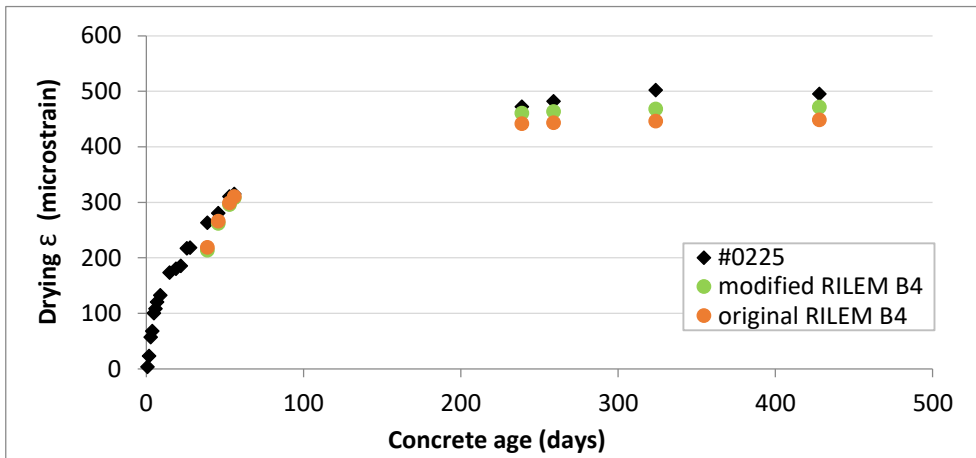


Figure E.31 RILEM B4 model predicted and actual drying shrinkage (microstrain) for Dataset 1-HSC, Subset S1-04, Experiment #0225

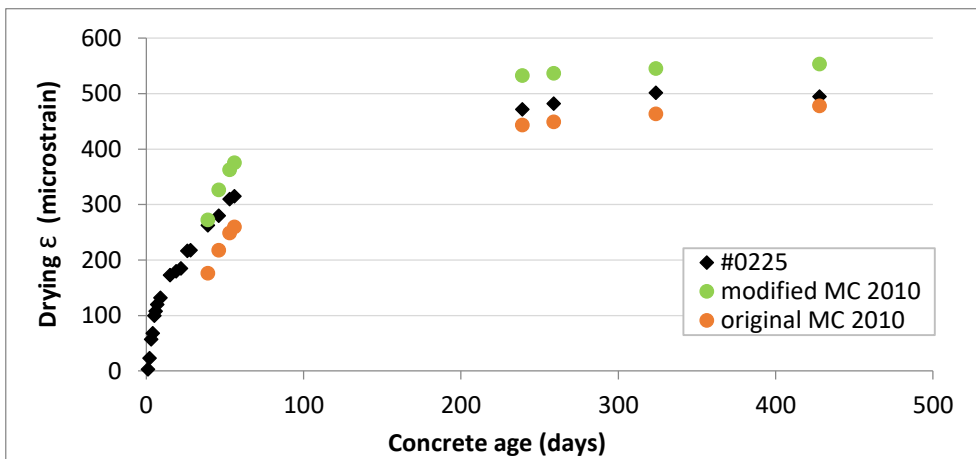


Figure E.32 MC 2010 model predicted and actual drying shrinkage (microstrain) for Dataset 1-HSC, Subset S1-04, Experiment #0225

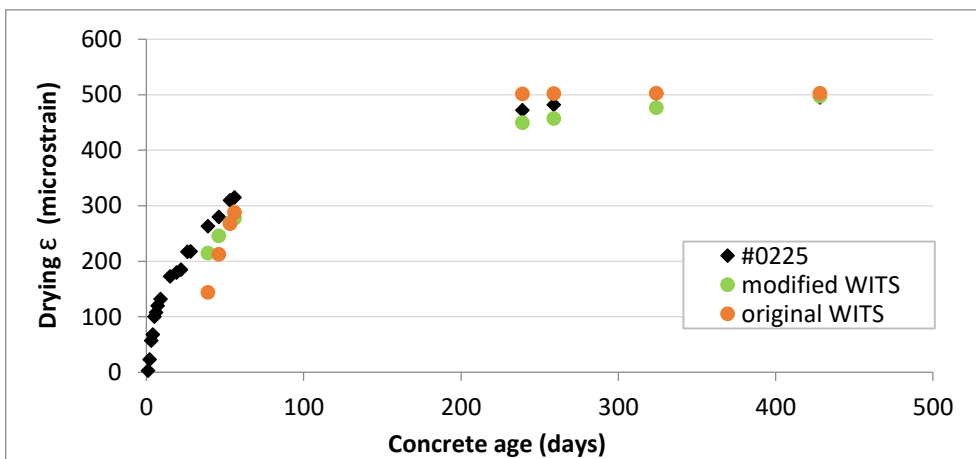


Figure E.33 WITS model predicted and actual drying shrinkage (microstrain) for Dataset 1-HSC, Subset S1-04, Experiment #0225

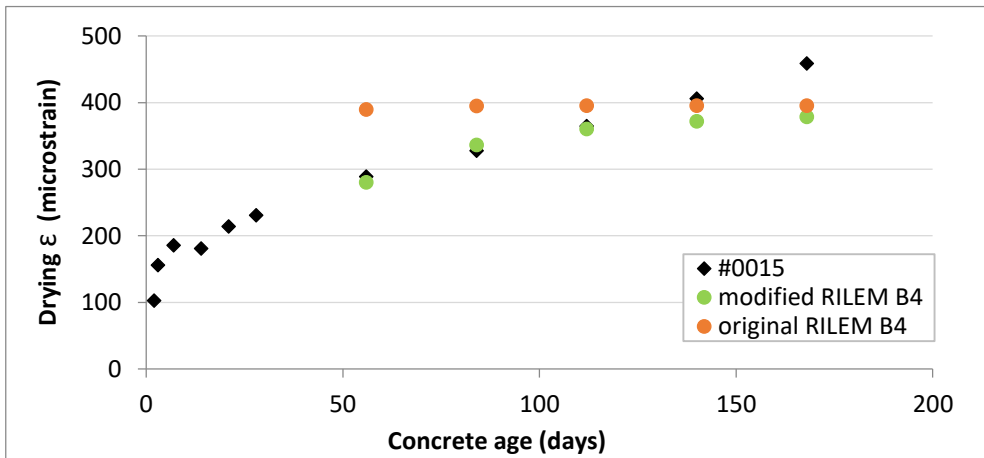


Figure E.34 RILEM B4 model predicted and actual drying shrinkage (microstrain) for Dataset 1-HSC, Subset S1-05, Experiment #0015

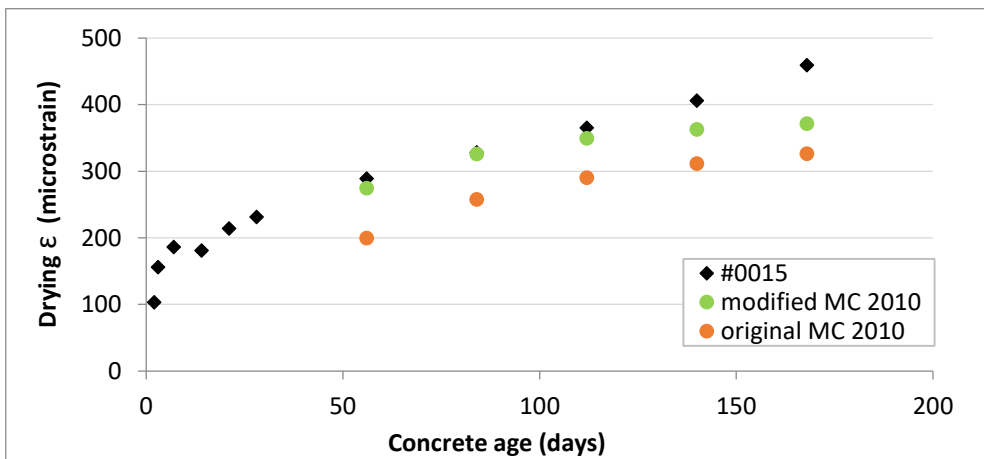


Figure E.35 MC 2010 model predicted and actual drying shrinkage (microstrain) for Dataset 1-HSC, Subset S1-05, Experiment #0015

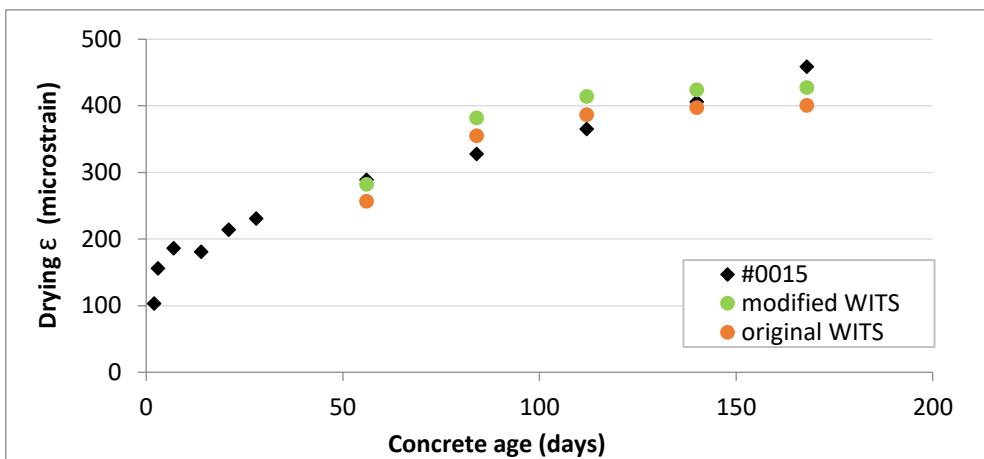


Figure E.36 WITS model predicted and actual drying shrinkage (microstrain) for Dataset 1-HSC, Subset S1-05, Experiment #0015

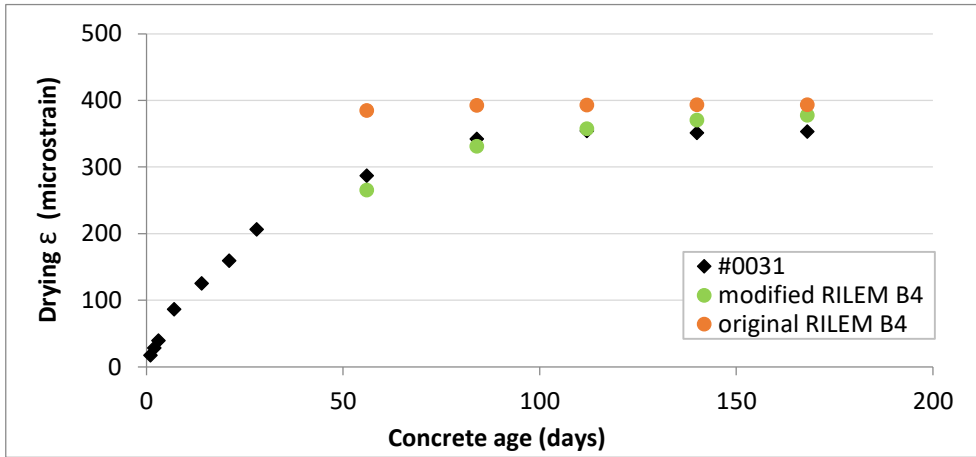


Figure E.37 RILEM B4 model predicted and actual drying shrinkage (microstrain) for Dataset 1-HSC, Subset S1-05, Experiment #0031

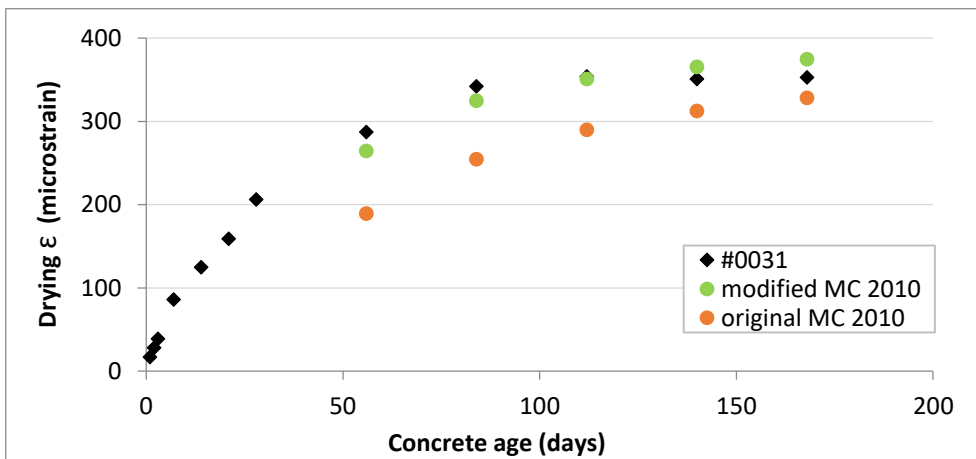


Figure E.38 MC 2010 model predicted and actual drying shrinkage (microstrain) for Dataset 1-HSC, Subset S1-05, Experiment #0031

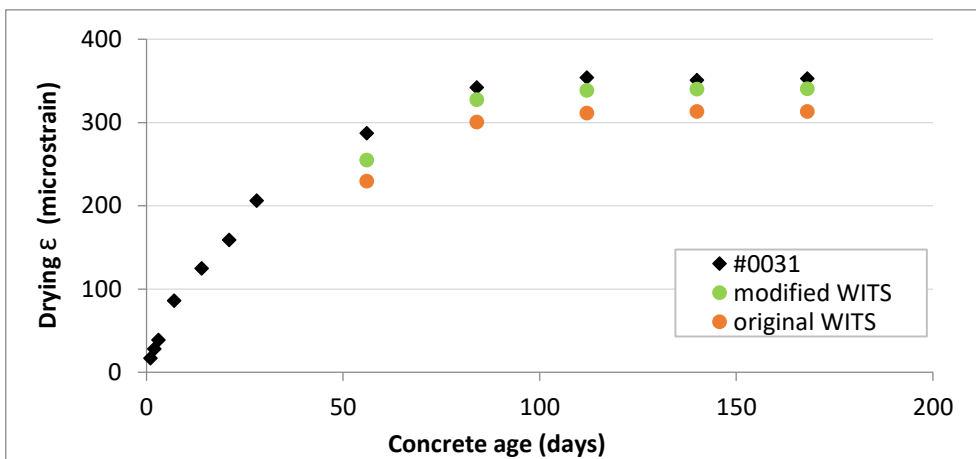


Figure E.39 WITS model predicted and actual drying shrinkage (microstrain) for Dataset 1-HSC, Subset S1-05, Experiment #0031

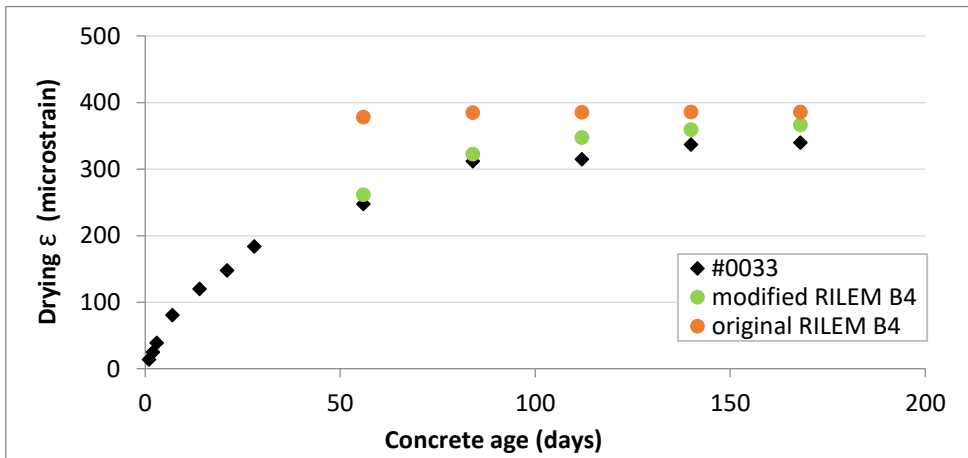


Figure E.40 RILEM B4 model predicted and actual drying shrinkage (microstrain) for Dataset 1-HSC, Subset S1-05, Experiment #0033

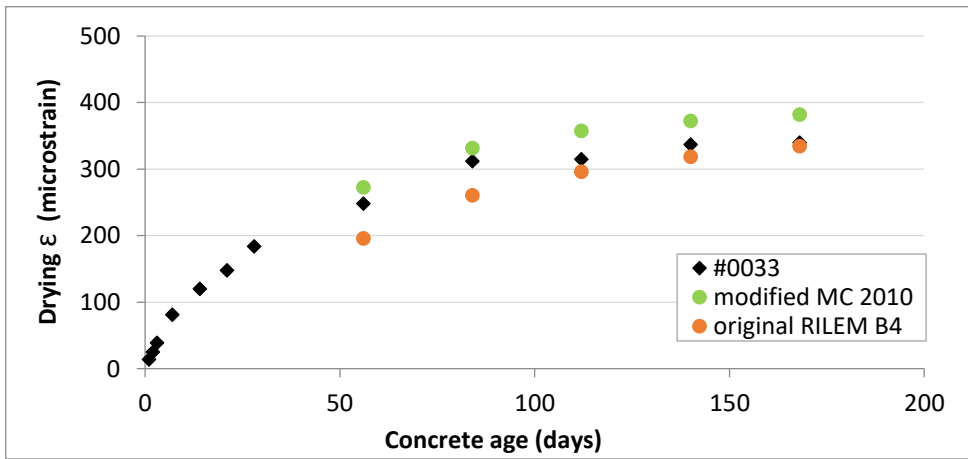


Figure E.41 MC 2010 model predicted and actual drying shrinkage (microstrain) for Dataset 1-HSC, Subset S1-05, Experiment #0033

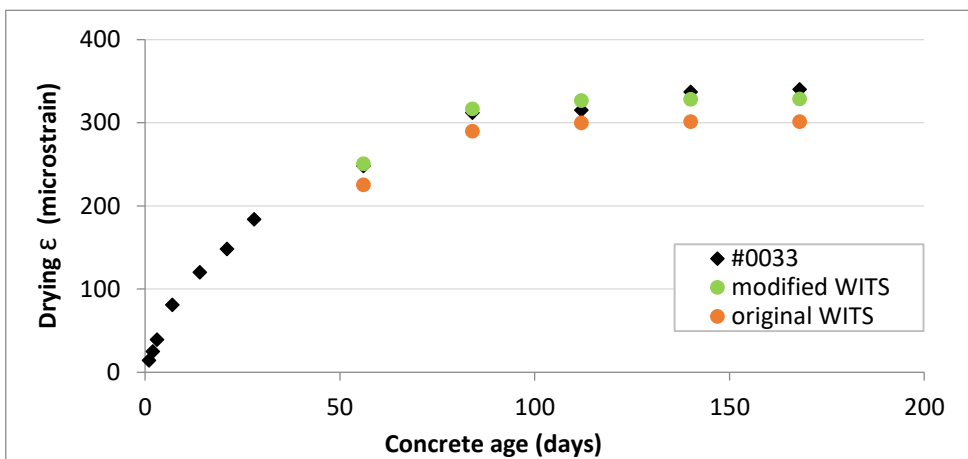


Figure E.42 WITS model predicted and actual drying shrinkage (microstrain) for Dataset 1-HSC, Subset S1-05, Experiment #0033

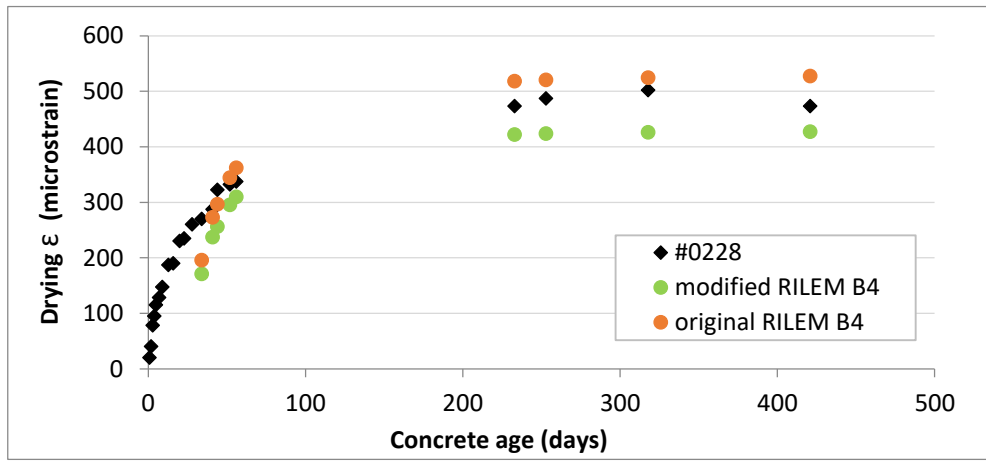


Figure E.43 RILEM B4 model predicted and actual drying shrinkage (microstrain) for Dataset 1-HSC, Subset S2-01, Experiment #0228

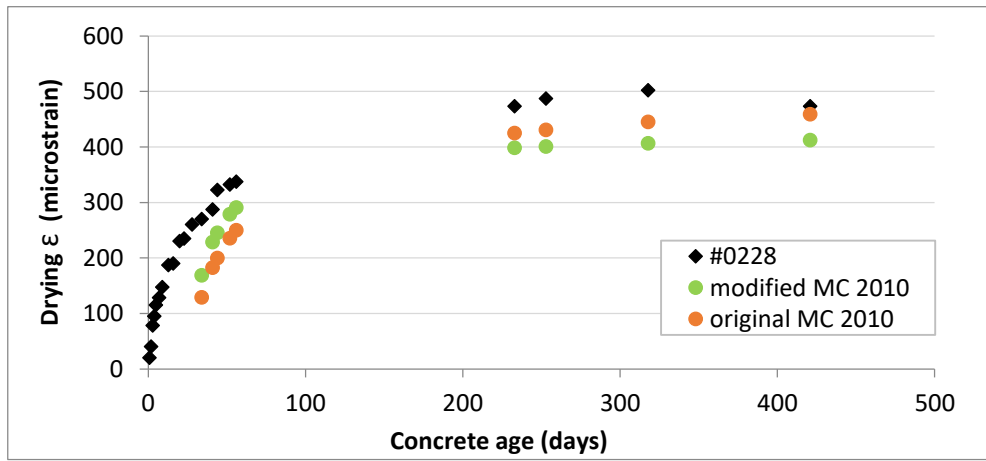


Figure E.44 MC 2010 model predicted and actual drying shrinkage (microstrain) for Dataset 1-HSC, Subset S2-01, Experiment #0228

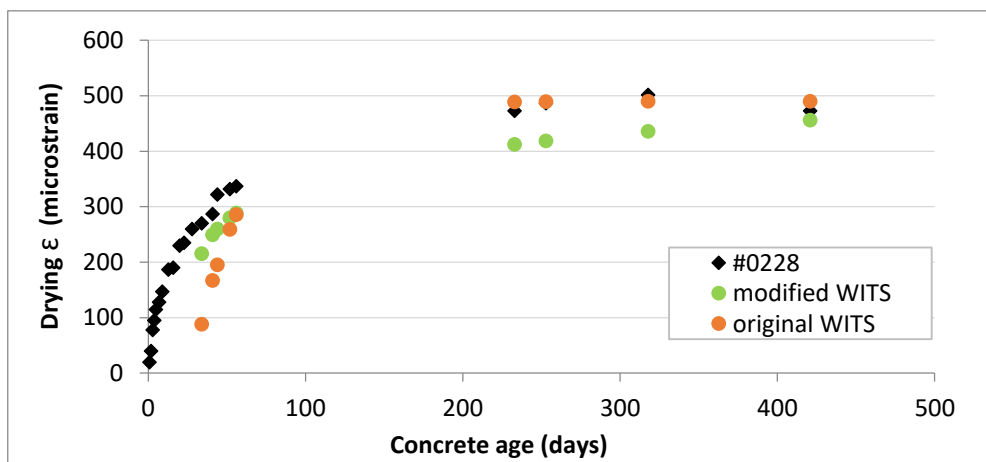


Figure E.45 WITS model predicted and actual drying shrinkage (microstrain) for Dataset 1-HSC, Subset S2-01, Experiment #0228

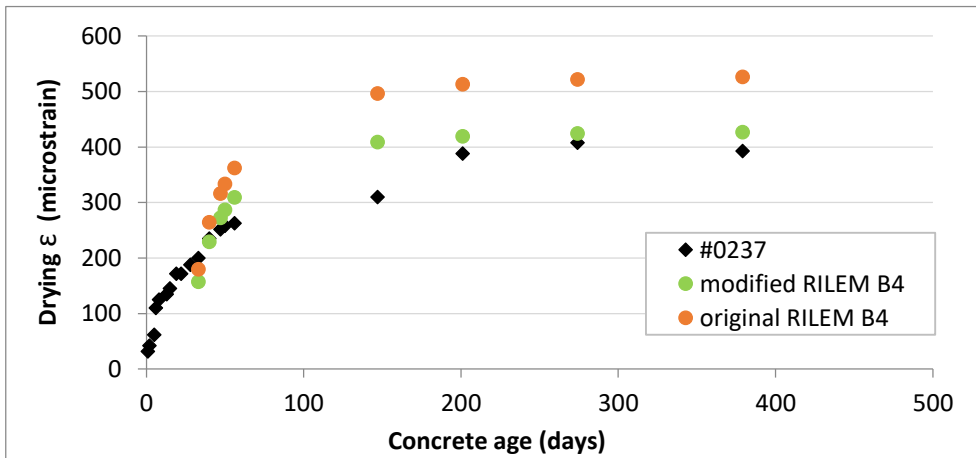


Figure E.46 RILEM B4 model predicted and actual drying shrinkage (microstrain) for Dataset 1-HSC, Subset S2-01, Experiment #0237

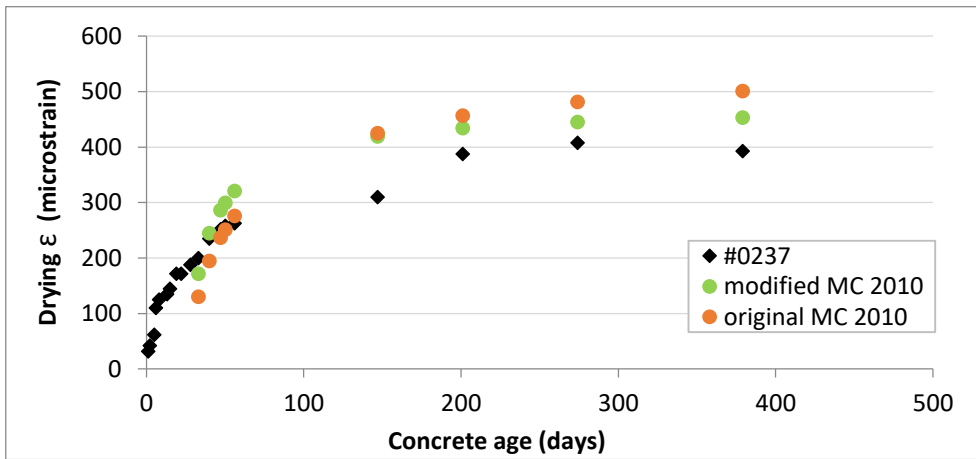


Figure E.47 MC 2010 model predicted and actual drying shrinkage (microstrain) for Dataset 1-HSC, Subset S2-01, Experiment #0237

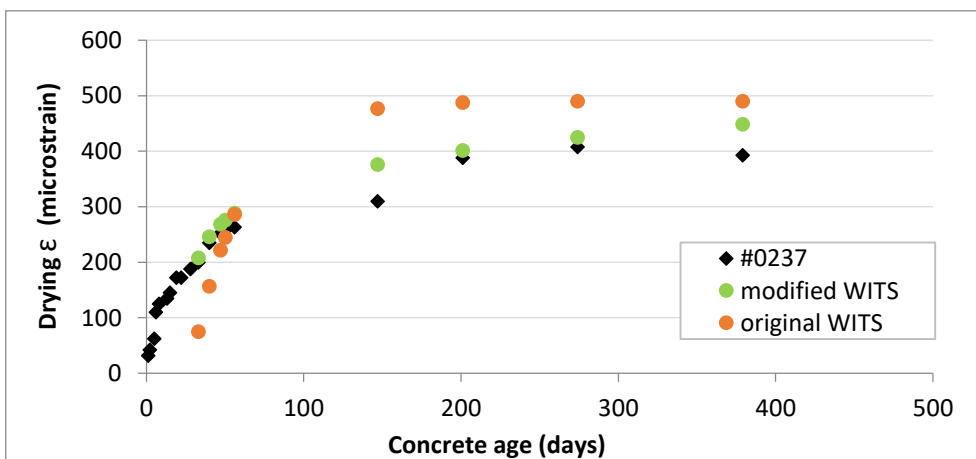


Figure E.48 WITS model predicted and actual drying shrinkage (microstrain) for Dataset 1-HSC, Subset S2-01, Experiment #0237

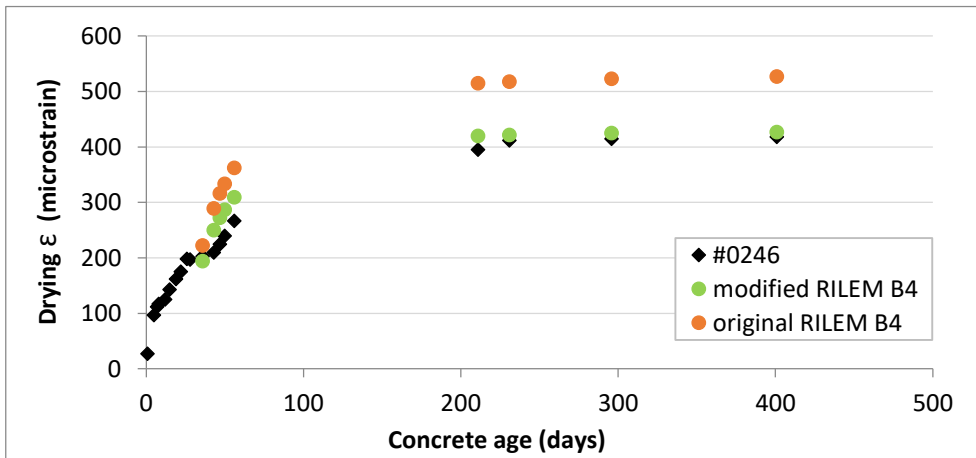


Figure E.49 RILEM B4 model predicted and actual drying shrinkage (microstrain) for Dataset 1-HSC, Subset S2-01, Experiment #0246

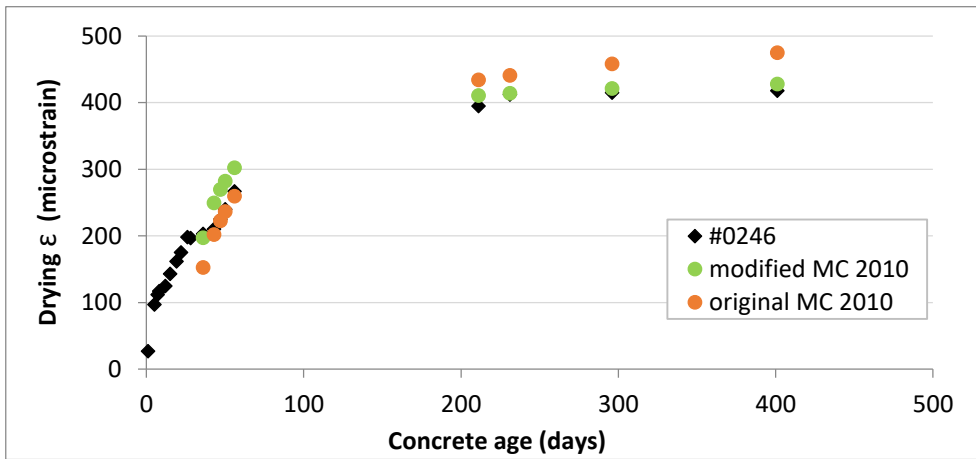


Figure E.50 MC 2010 model predicted and actual drying shrinkage (microstrain) for Dataset 1-HSC, Subset S2-01, Experiment #0246

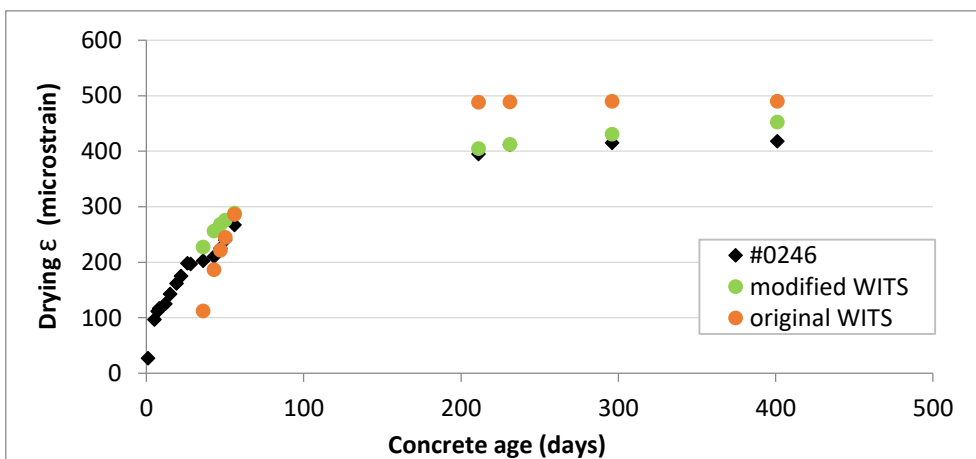


Figure E.51 WITS model predicted and actual drying shrinkage (microstrain) for Dataset 1-HSC, Subset S2-01, Experiment #0246



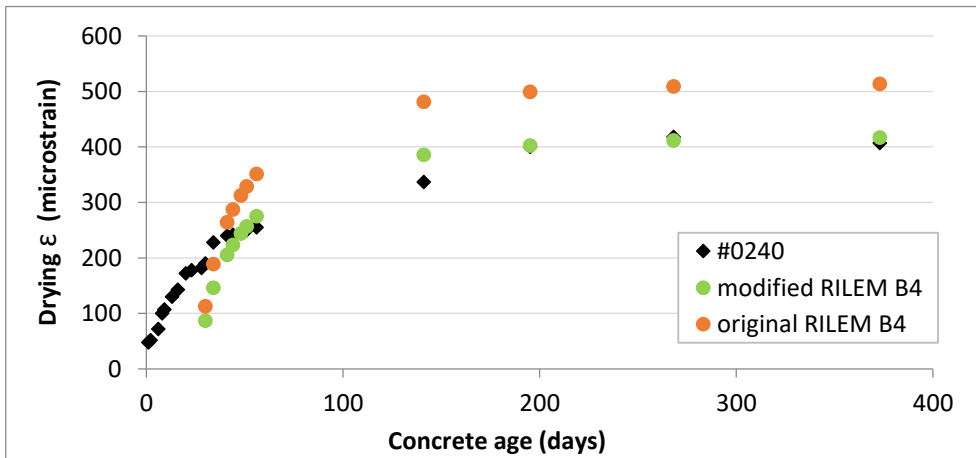


Figure E.52 RILEM B4 model predicted and actual drying shrinkage (microstrain) for Dataset 1-HSC, Subset S2-02, Experiment #0240

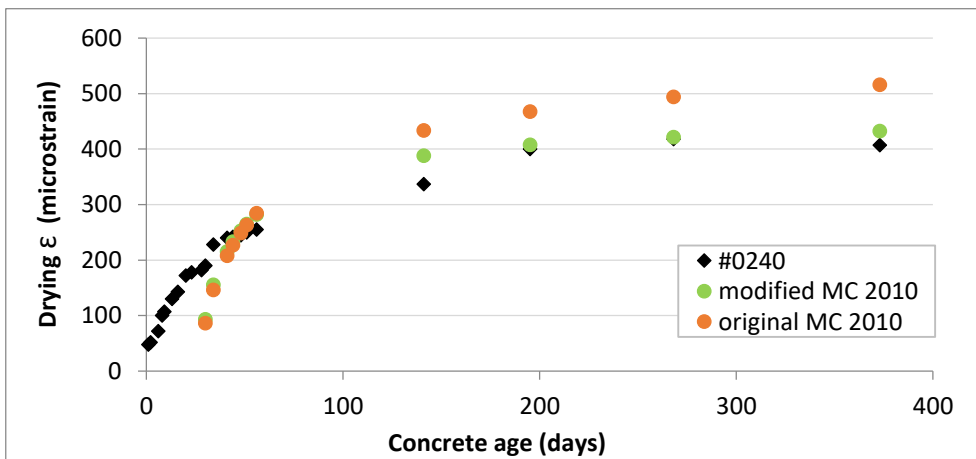


Figure E.53 MC 2010 model predicted and actual drying shrinkage (microstrain) for Dataset 1-HSC, Subset S2-02, Experiment #0240

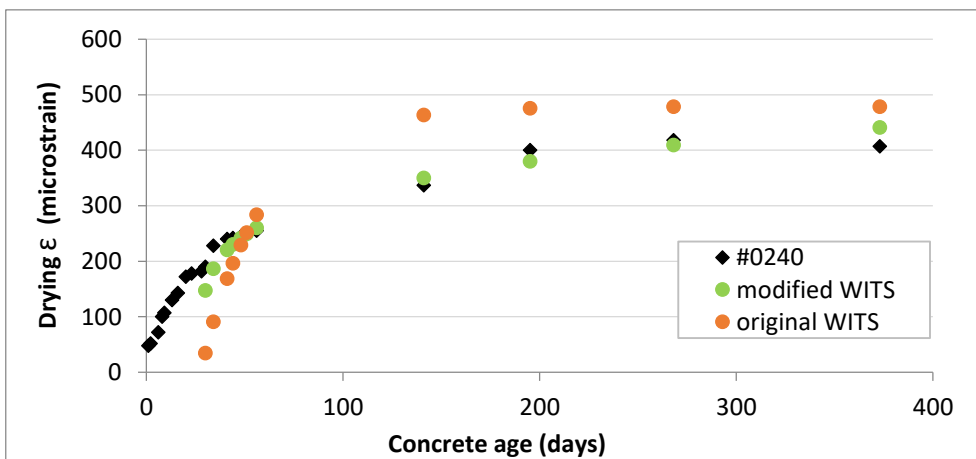


Figure E.54 WITS model predicted and actual drying shrinkage (microstrain) for Dataset 1-HSC, Subset S2-02, Experiment #0240

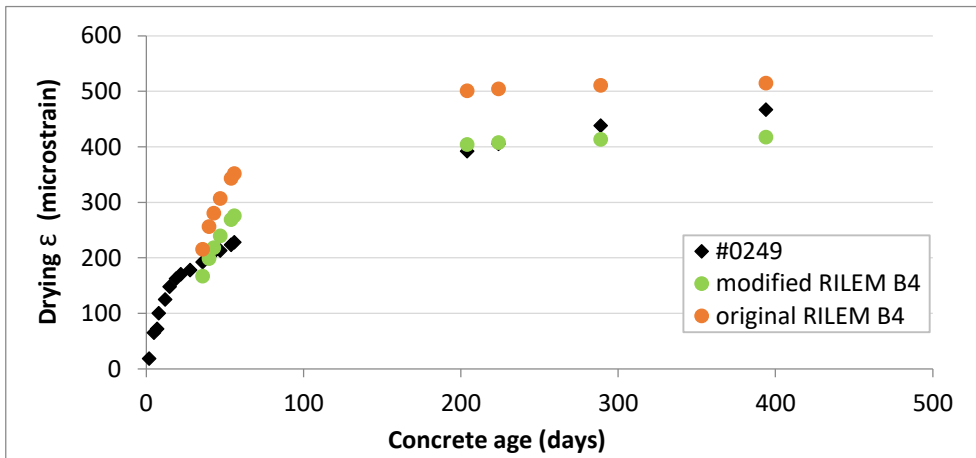


Figure E.55 RILEM B4 model predicted and actual drying shrinkage (microstrain) for Dataset 1-HSC, Subset S2-02, Experiment #0249

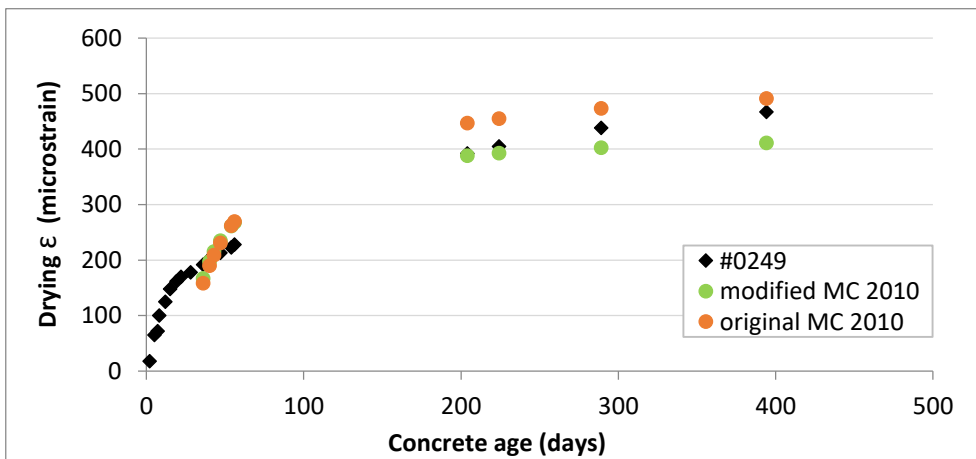


Figure E.56 MC 2010 model predicted and actual drying shrinkage (microstrain) for Dataset 1-HSC, Subset S2-02, Experiment #0249

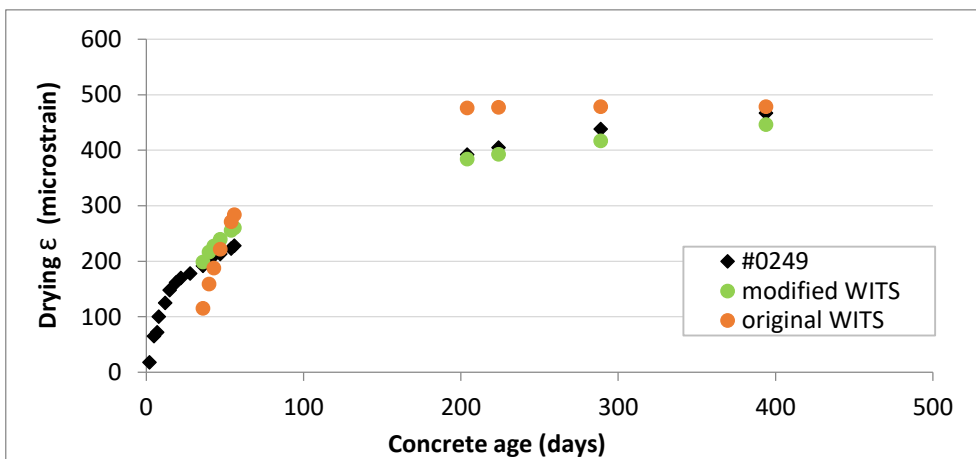


Figure E.57 WITS model predicted and actual drying shrinkage (microstrain) for Dataset 1-HSC, Subset S2-02, Experiment #0249

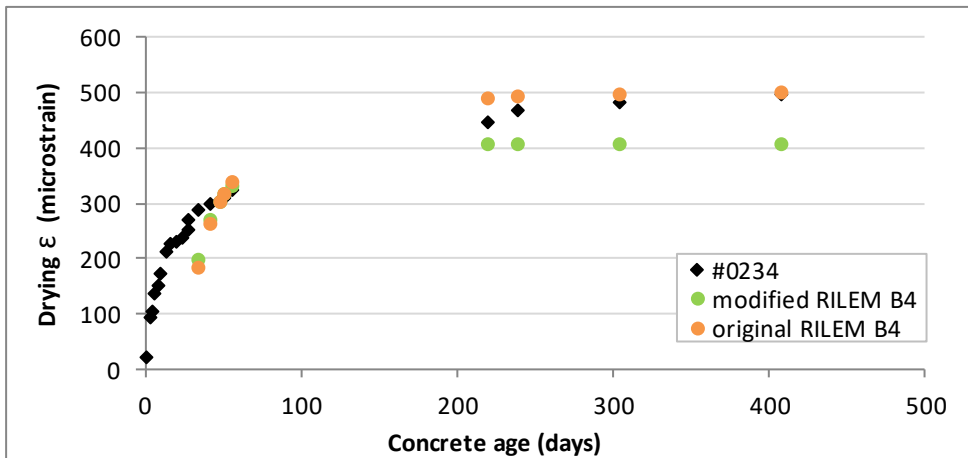


Figure E.58 RILEM B4 model predicted and actual drying shrinkage (microstrain) for Dataset 1-HSC, Subset S2-03, Experiment #0234

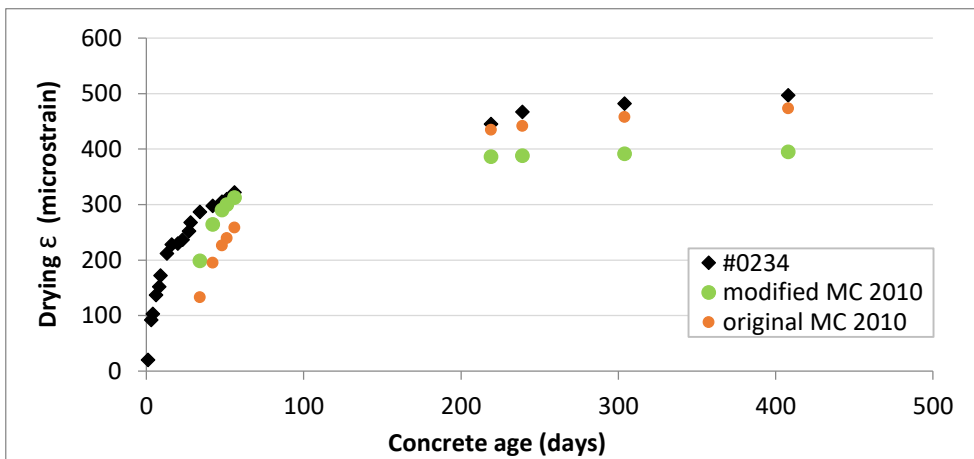


Figure E.59 MC 2010 model predicted and actual drying shrinkage (microstrain) for Dataset 1-HSC, Subset S2-03, Experiment #0234

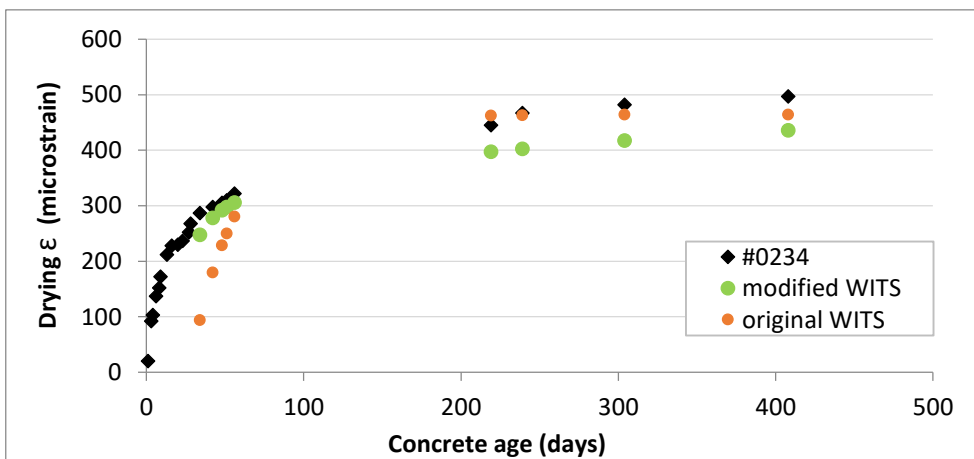


Figure E.60 WITS model predicted and actual drying shrinkage (microstrain) for Dataset 1-HSC, Subset S2-03, Experiment #0234

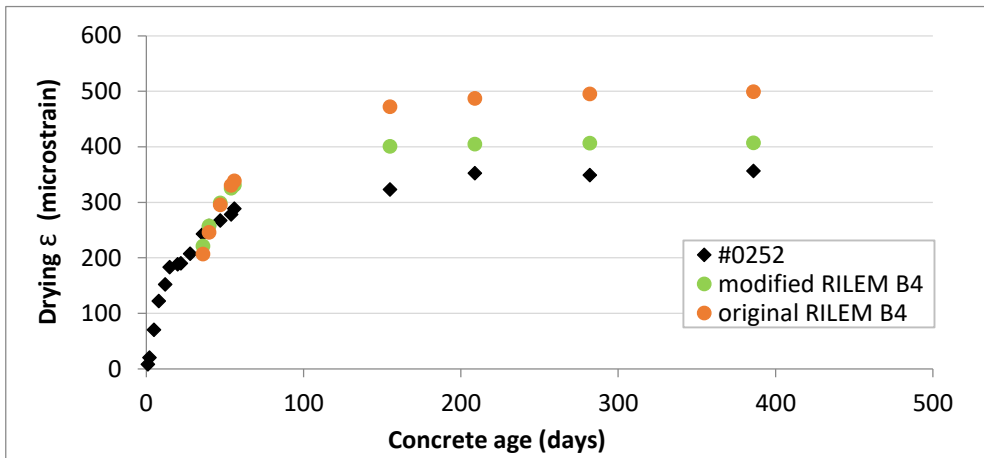


Figure E.61 RILEM B4 model predicted and actual drying shrinkage (microstrain) for Dataset 1-HSC, Subset S2-03, Experiment #0252

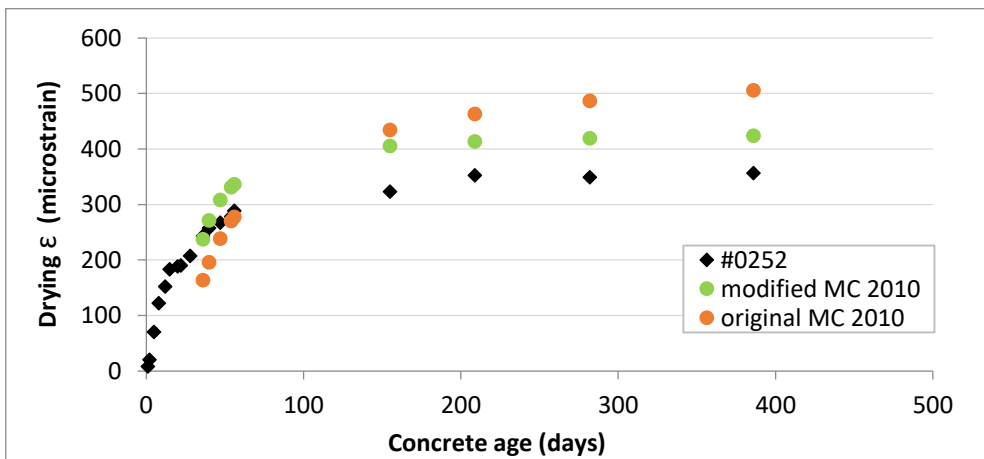


Figure E.62 MC 2010 model predicted and actual drying shrinkage (microstrain) for Dataset 1-HSC, Subset S2-03, Experiment #0252

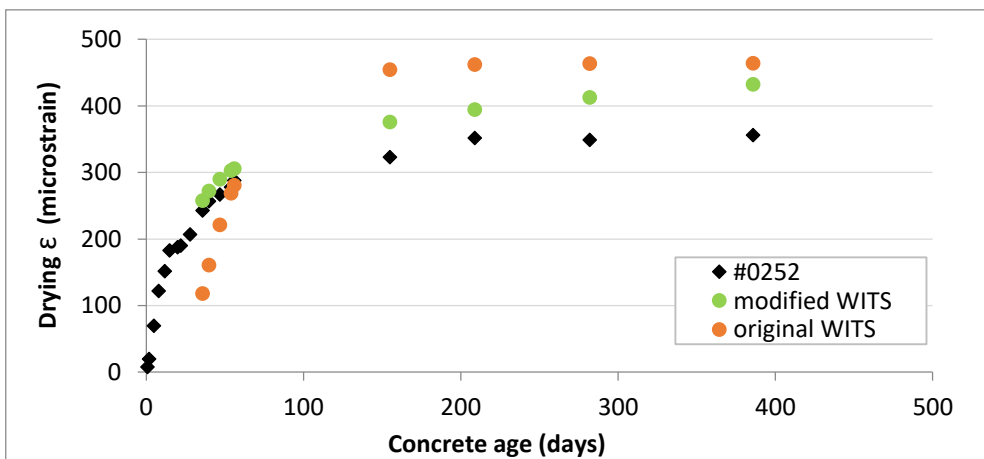


Figure E.63 WITS model predicted and actual drying shrinkage (microstrain) for Dataset 1-HSC, Subset S2-03, Experiment #0252

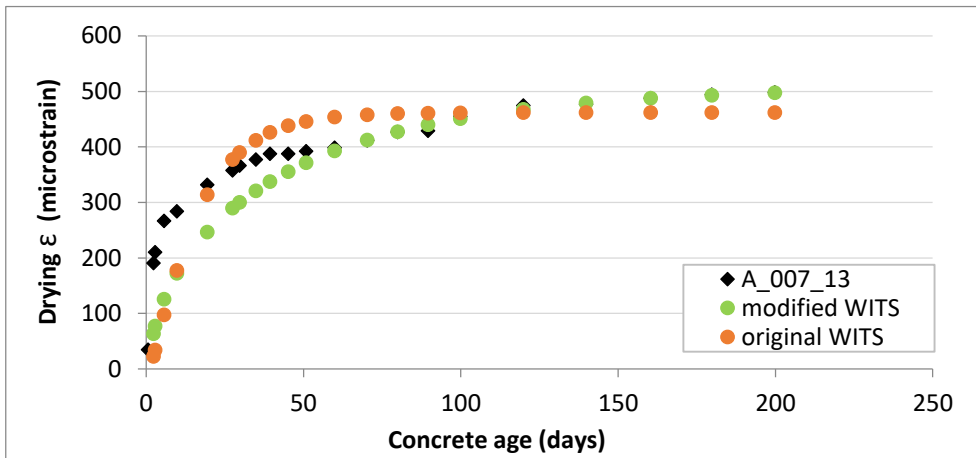


Figure E.64 RILEM B4 model predicted and actual drying shrinkage (microstrain) for Dataset 1-HSC, Subset S2-04, Experiment A\_007\_13

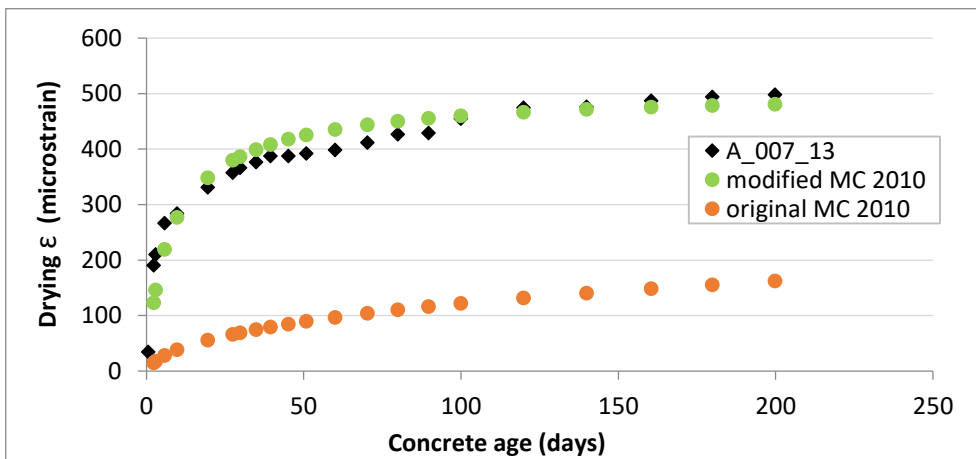


Figure E.65 MC 2010 model predicted and actual drying shrinkage (microstrain) for Dataset 1-HSC, Subset S2-04, Experiment A\_007\_13

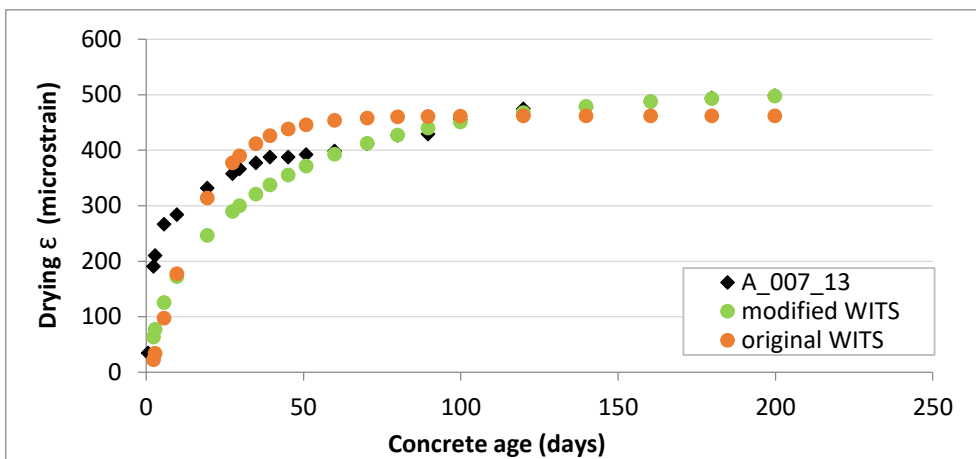


Figure E.66 WITS model predicted and actual drying shrinkage (microstrain) for Dataset 1-HSC, Subset S2-04, Experiment A\_007\_13

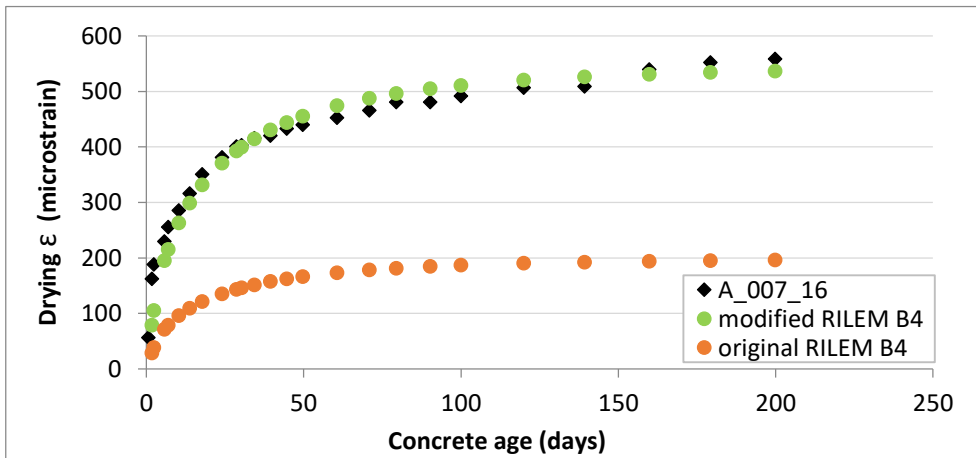


Figure E.67 RILEM B4 model predicted and actual drying shrinkage (microstrain) for Dataset 1-HSC, Subset S2-04, Experiment A\_007\_16

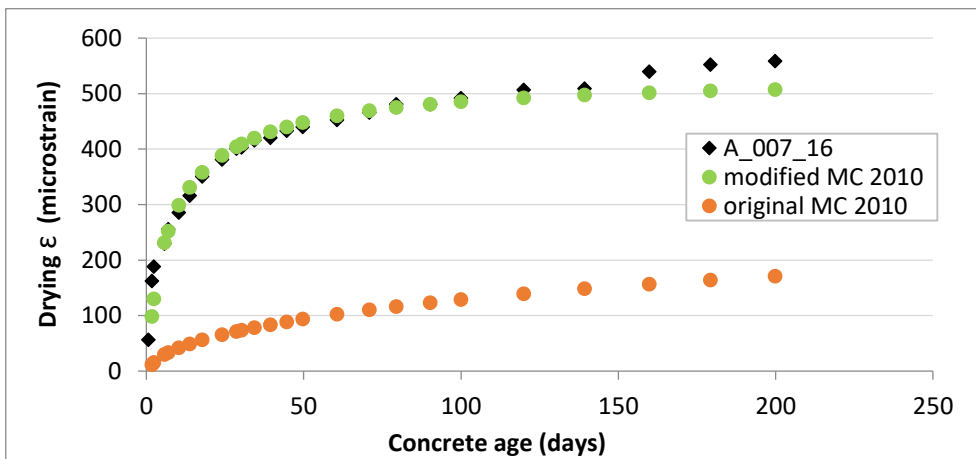


Figure E.68 MC 2010 model predicted and actual drying shrinkage (microstrain) for Dataset 1-HSC, Subset S2-04, Experiment A\_007\_16

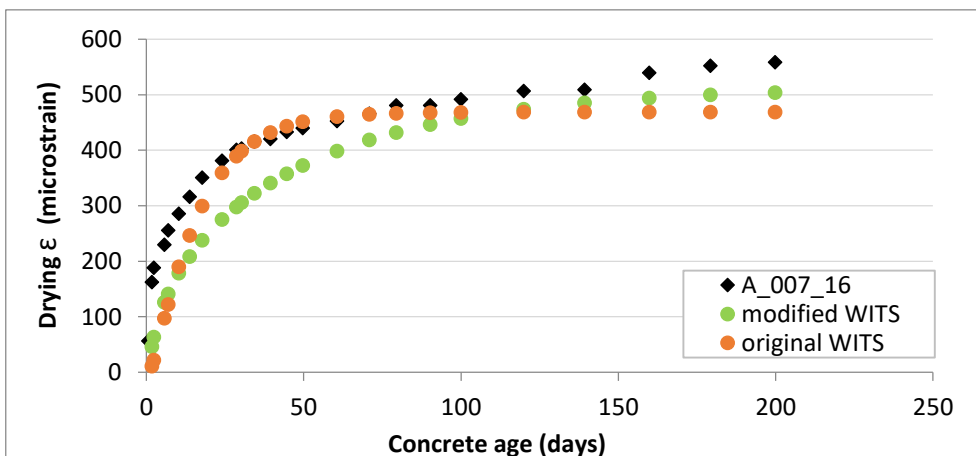


Figure E.69 WITS model predicted and actual drying shrinkage (microstrain) for Dataset 1-HSC, Subset S2-04, Experiment A\_007\_16

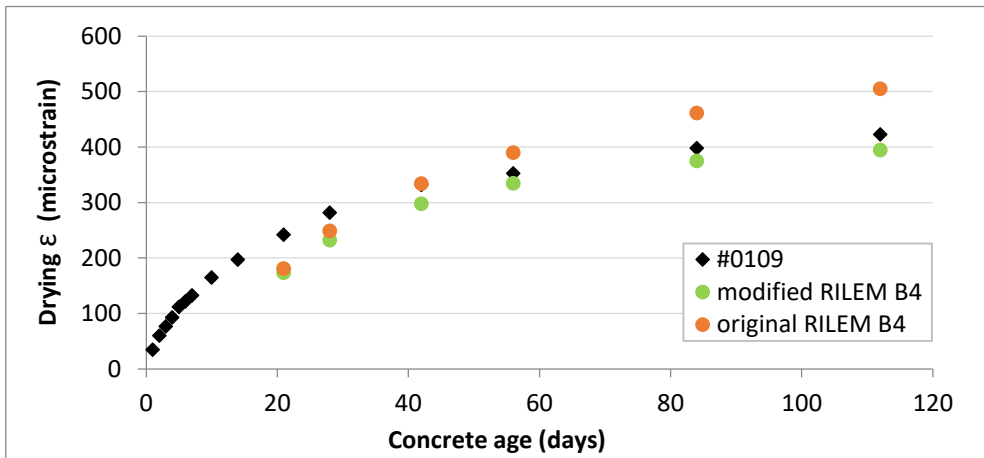


Figure E.70 RILEM B4 model predicted and actual drying shrinkage (microstrain) for Dataset 1-HSC, Subset S2-05, Experiment #0109

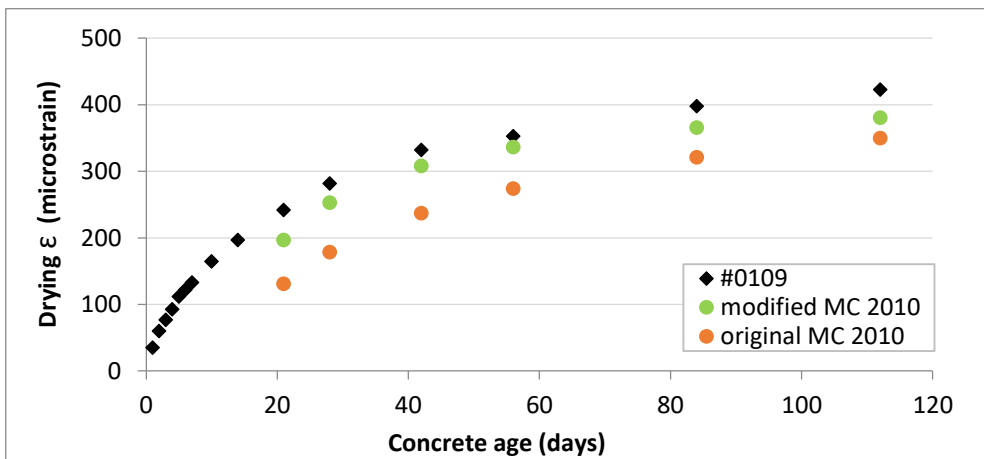


Figure E.71 MC 2010 model predicted and actual drying shrinkage (microstrain) for Dataset 1-HSC, Subset S2-05, Experiment #0109

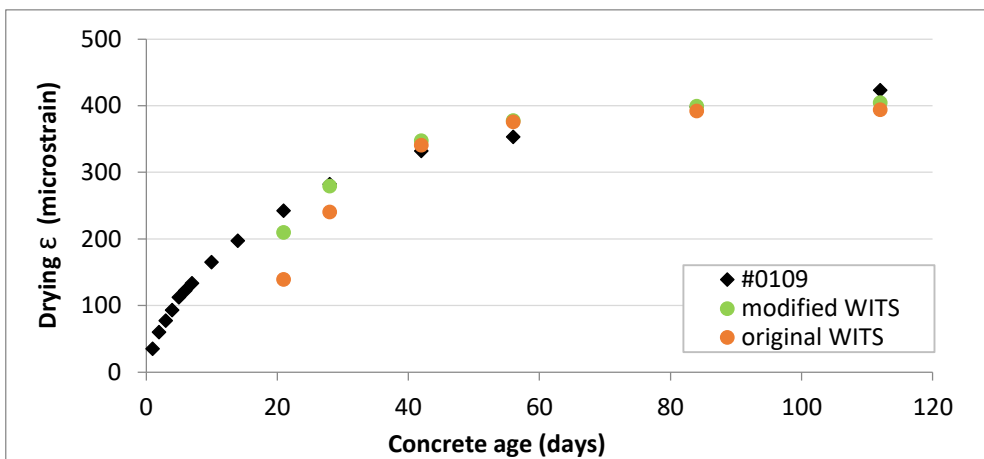


Figure E.72 WITS model predicted and actual drying shrinkage (microstrain) for Dataset 1-HSC, Subset S2-05, Experiment #0109

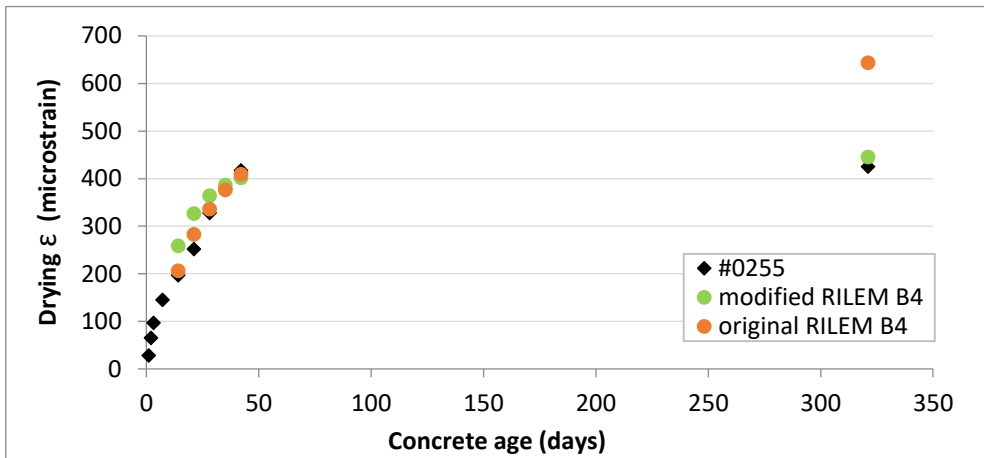


Figure E.73 RILEM B4 model predicted and actual drying shrinkage (microstrain) for Dataset 1-HSC, Subset S2-05, Experiment #0255

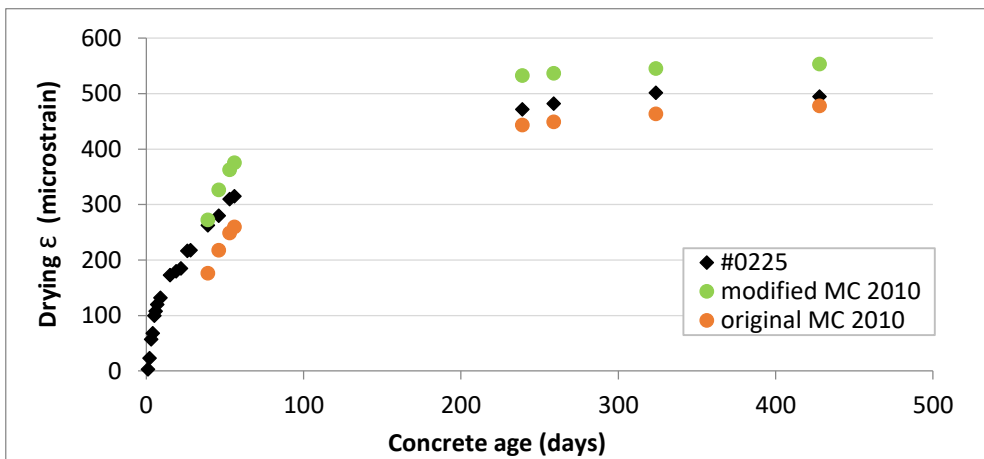


Figure E.74 MC 2010 model predicted and actual drying shrinkage (microstrain) for Dataset 1-HSC, Subset S2-05, Experiment #0255

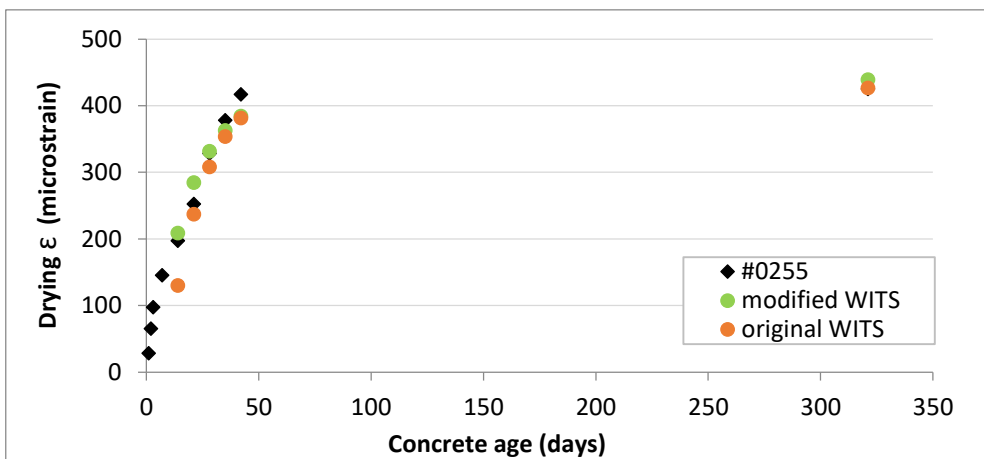


Figure E.75 WITS model predicted and actual drying shrinkage (microstrain) for Dataset 1-HSC, Subset S2-05, Experiment #0255



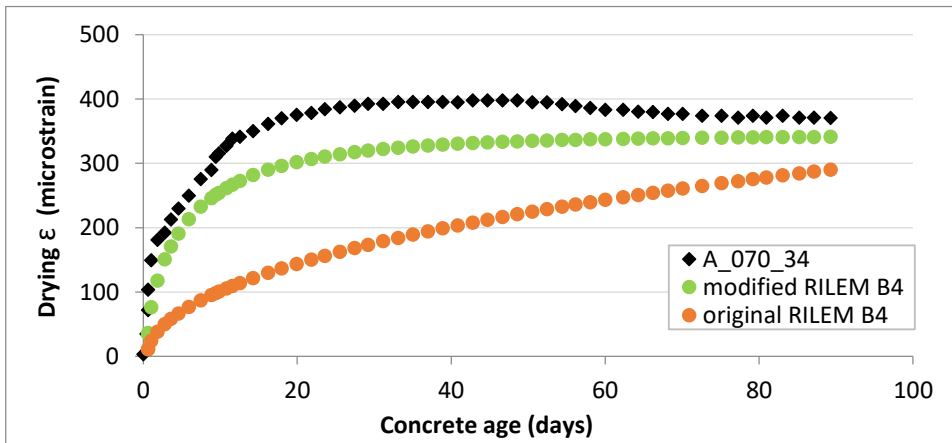


Figure E.76 RILEM B4 model predicted and actual drying shrinkage (microstrain) for Dataset 1-HSC, Subset S2-06, Experiment A\_070\_34

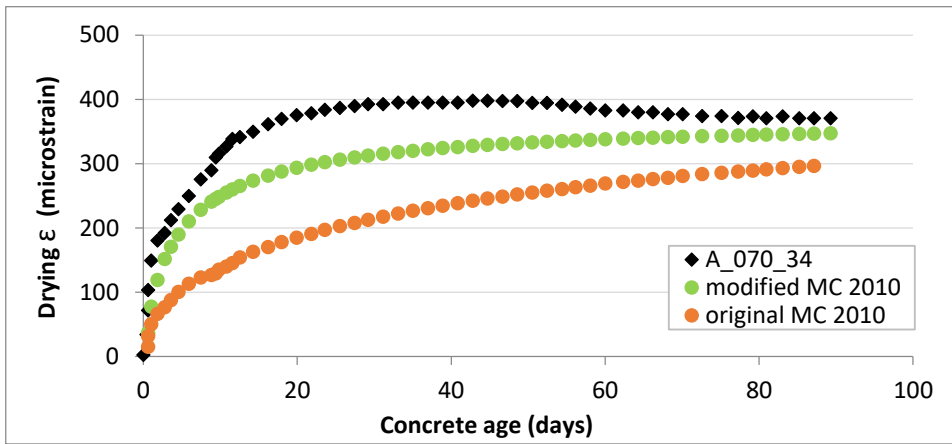


Figure E.77 MC 2010 model predicted and actual drying shrinkage (microstrain) for Dataset 1-HSC, Subset S2-06, Experiment A\_070\_34

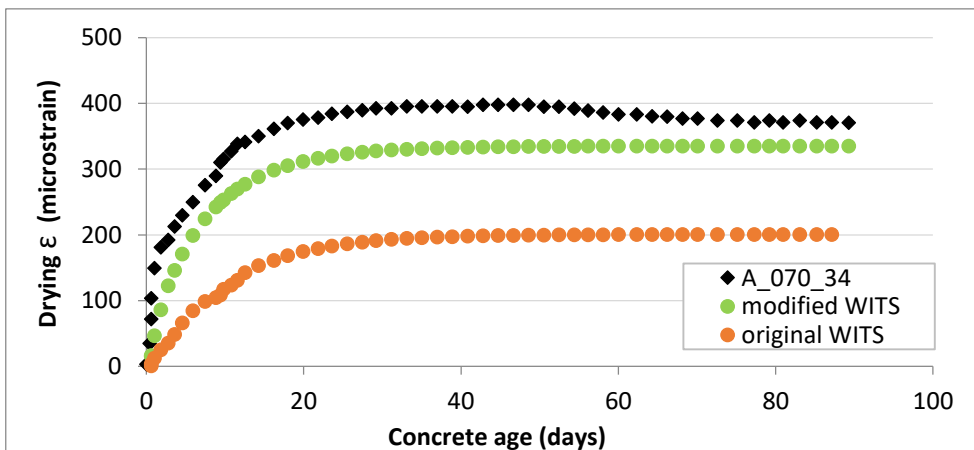


Figure E.78 WITS model predicted and actual drying shrinkage (microstrain) for Dataset 1-HSC, Subset S2-06, Experiment A\_070\_34

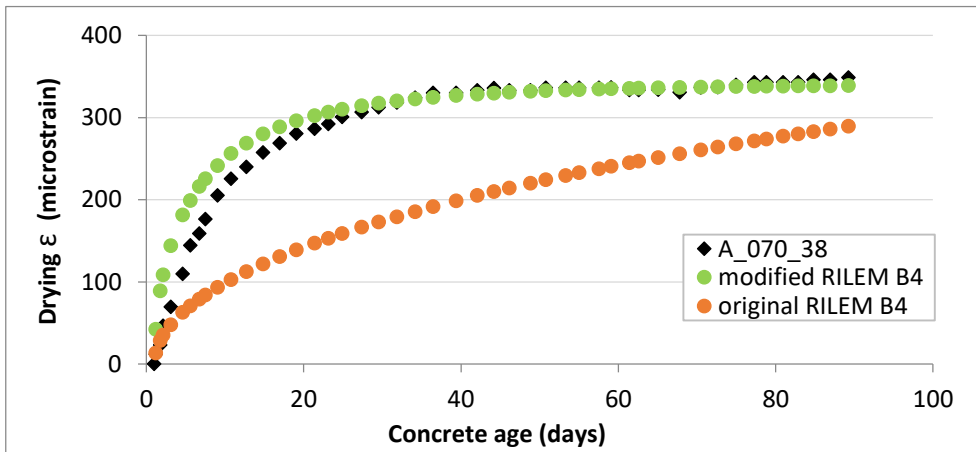


Figure E.79 RILEM B4 model predicted and actual drying shrinkage (microstrain) for Dataset 1-HSC, Subset S2-06, Experiment A\_070\_38

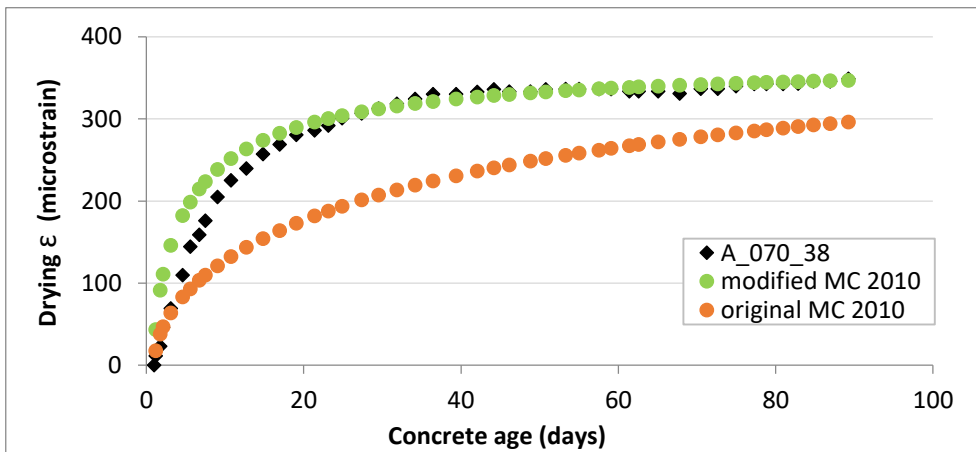


Figure E.80 MC 2010 model predicted and actual drying shrinkage (microstrain) for Dataset 1-HSC, Subset S2-06, Experiment A\_070\_38

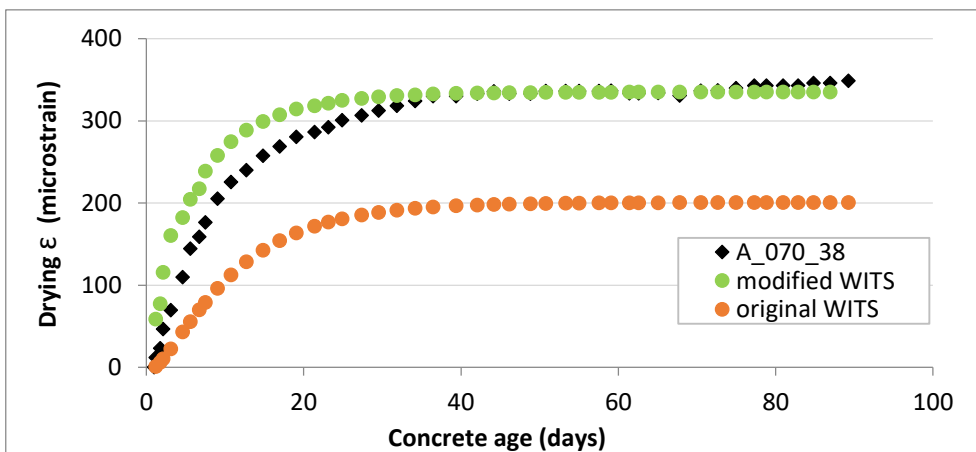


Figure E.81 WITS model predicted and actual drying shrinkage (microstrain) for Dataset 1-HSC, Subset S2-06, Experiment A\_070\_38

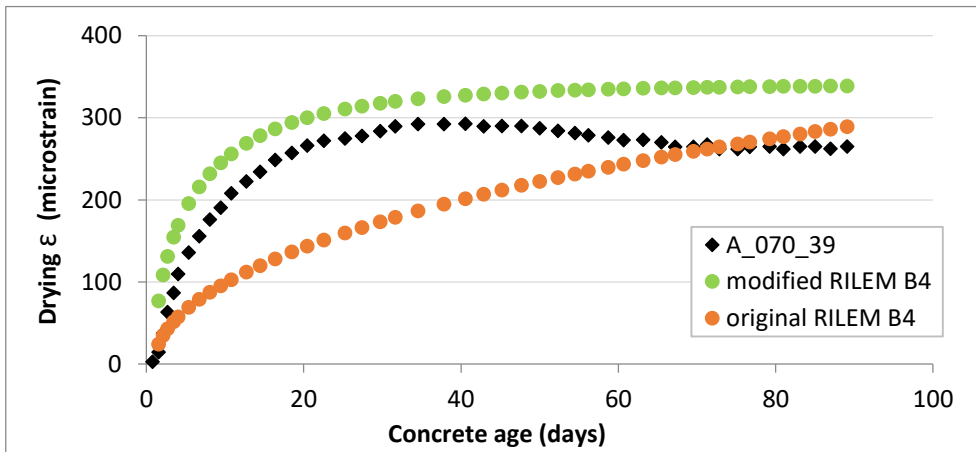


Figure E.82 RILEM B4 model predicted and actual drying shrinkage (microstrain) for Dataset 1-HSC, Subset S2-06, Experiment A\_070\_39

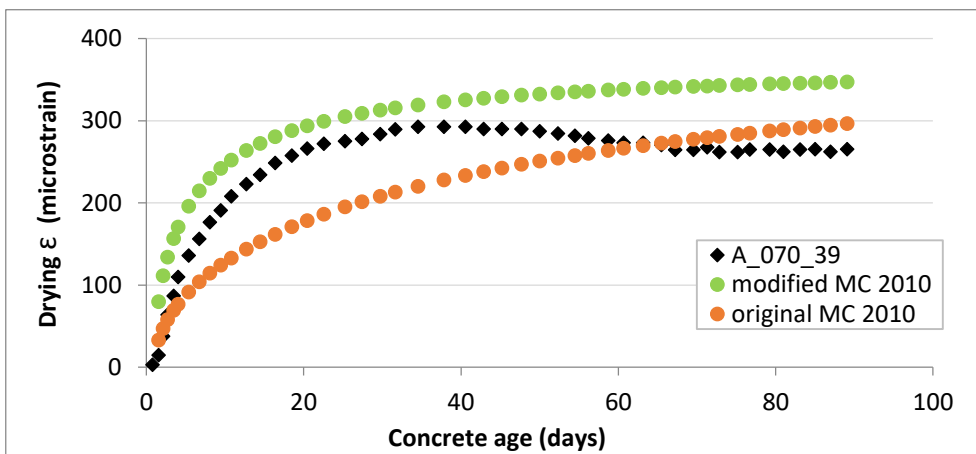


Figure E.83 MC 2010 model predicted and actual drying shrinkage (microstrain) for Dataset 1-HSC, Subset S2-06, Experiment A\_070\_39

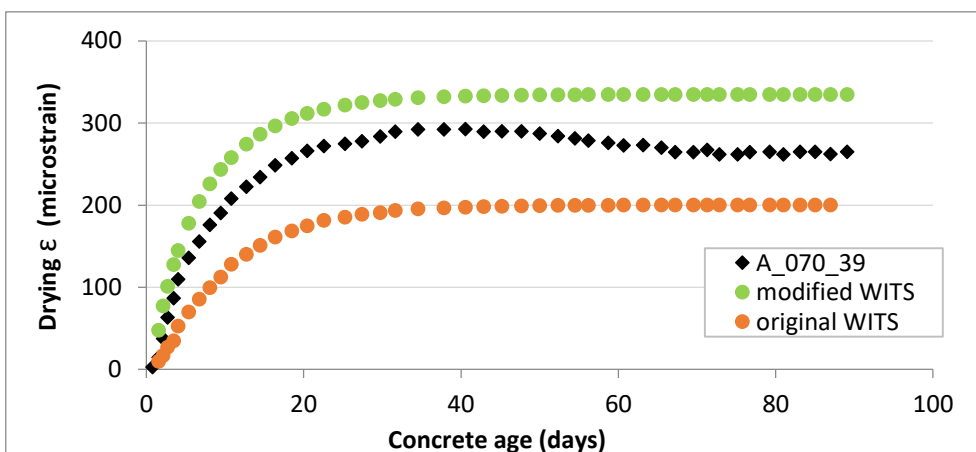


Figure E.84 WITS model predicted and actual drying shrinkage (microstrain) for Dataset 1-HSC, Subset S2-06, Experiment A\_070\_39

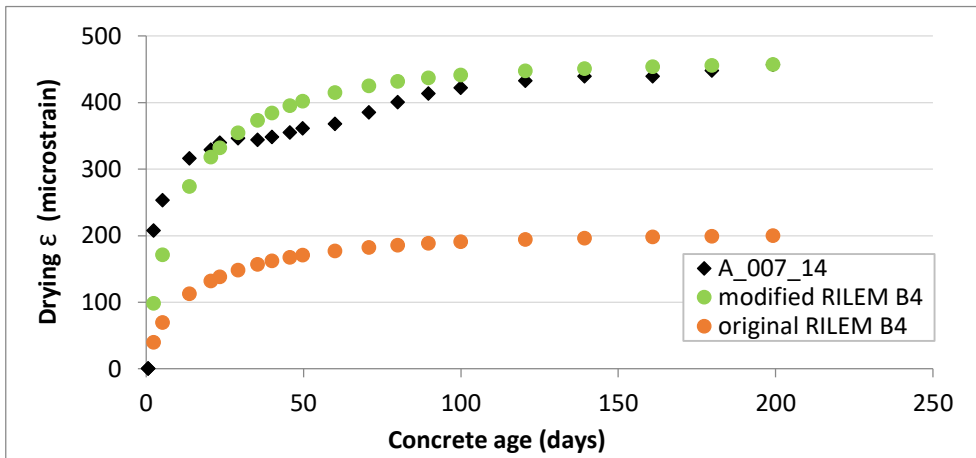


Figure E.85 RILEM B4 model predicted and actual drying shrinkage (microstrain) for Dataset 1-HSC, Subset S2-07, Experiment A\_007\_14

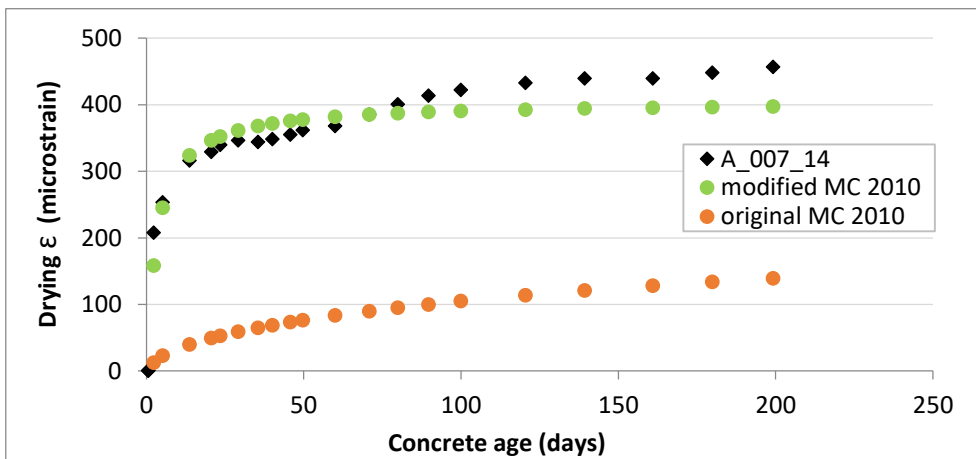


Figure E.86 MC 2010 model predicted and actual drying shrinkage (microstrain) for Dataset 1-HSC, Subset S2-07, Experiment A\_007\_14

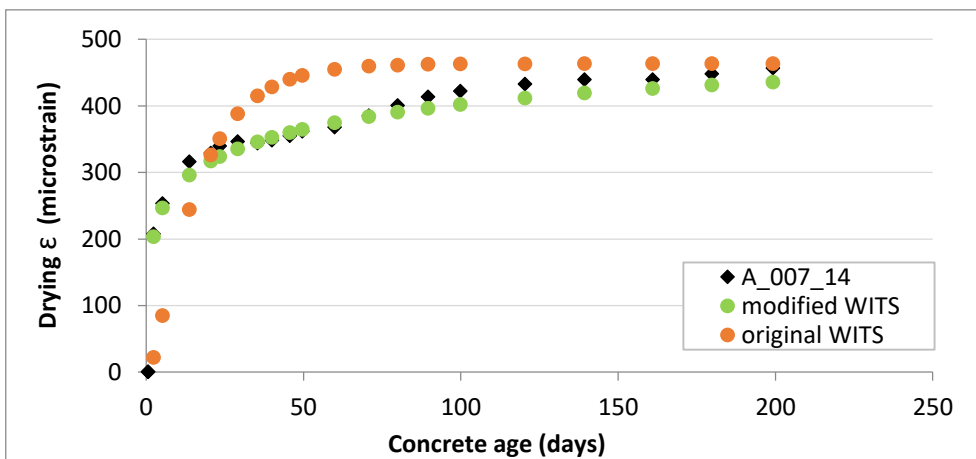


Figure E.87 WITS model predicted and actual drying shrinkage (microstrain) for Dataset 1-HSC, Subset S2-07, Experiment A\_007\_14

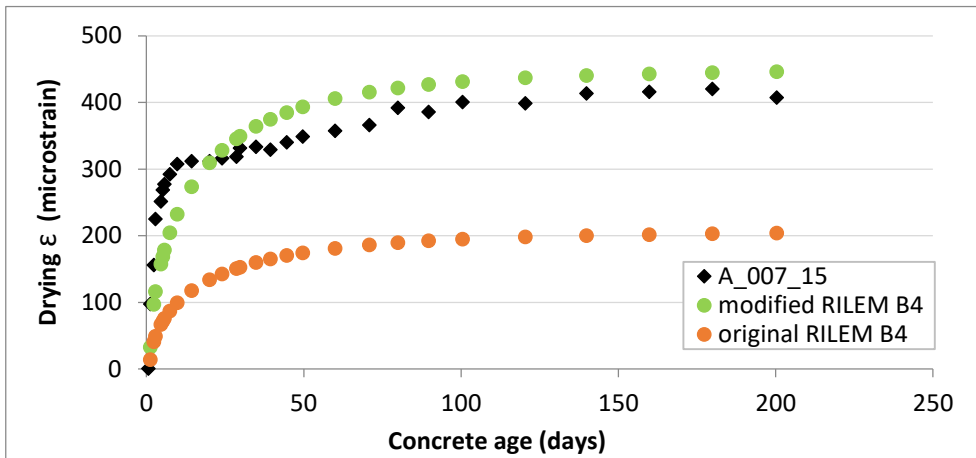


Figure E.88 RILEM B4 model predicted and actual drying shrinkage (microstrain) for Dataset 1-HSC, Subset S2-07, Experiment A\_007\_15

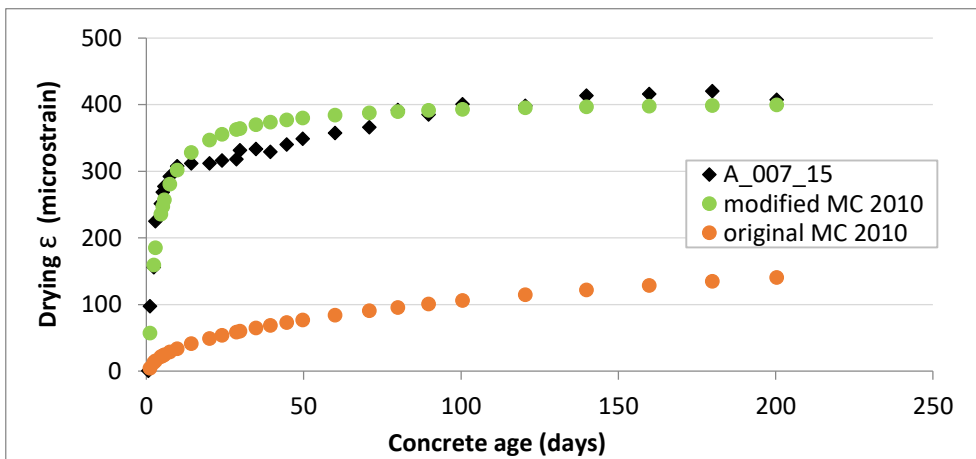


Figure E.89 MC 2010 model predicted and actual drying shrinkage (microstrain) for Dataset 1-HSC, Subset S2-07, Experiment A\_007\_15

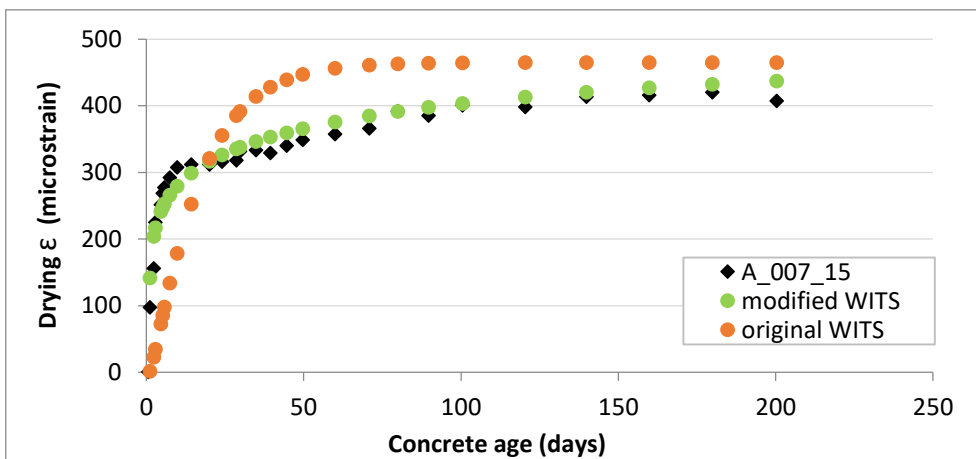


Figure E.90 WITS model predicted and actual drying shrinkage (microstrain) for Dataset 1-HSC, Subset S2-07, Experiment A\_007\_15

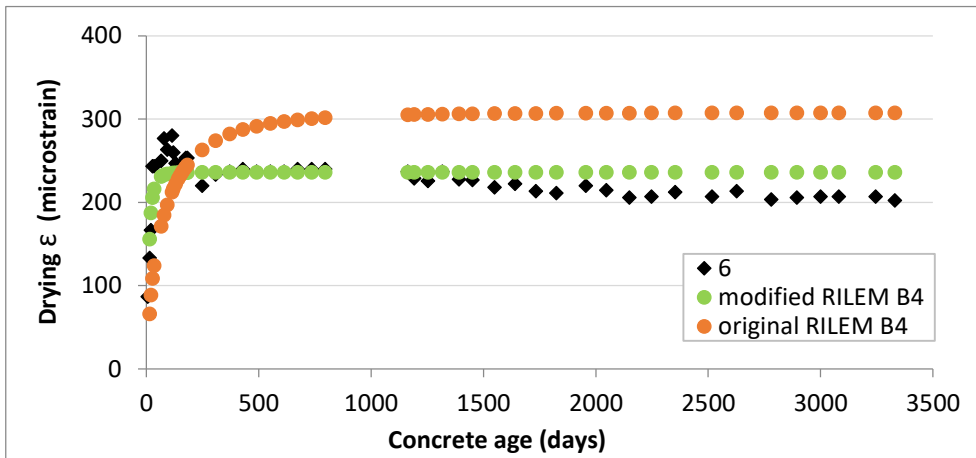


Figure E.91 RILEM B4 model predicted and actual drying shrinkage (microstrain) for Dataset 1-HSC, Subset S2-08, Experiment no. 6

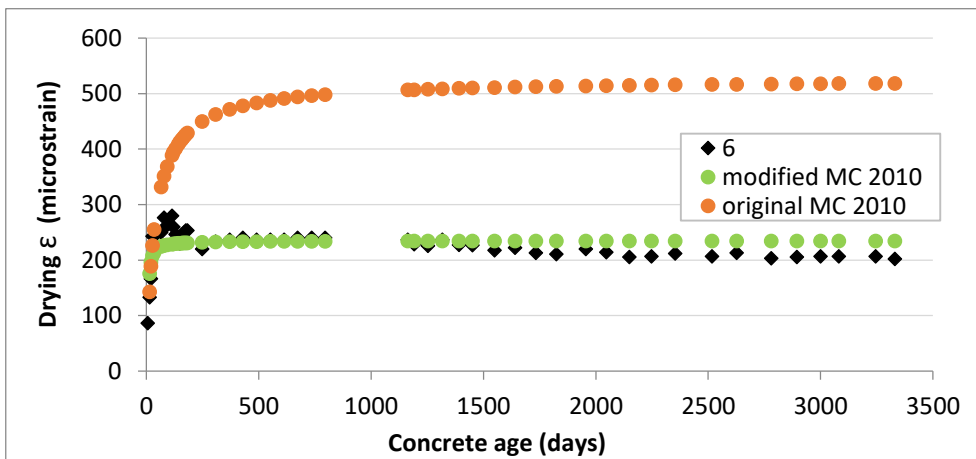


Figure E.92 MC 2010 model predicted and actual drying shrinkage (microstrain) for Dataset 1-HSC, Subset S2-08, Experiment no. 6

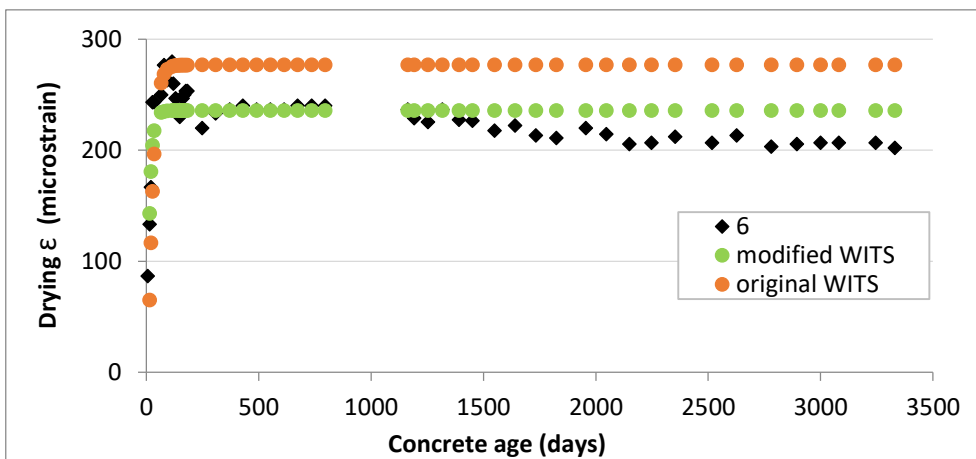


Figure E.93 WITS model predicted and actual drying shrinkage (microstrain) for Dataset 1-HSC, Subset S2-08, Experiment no. 6

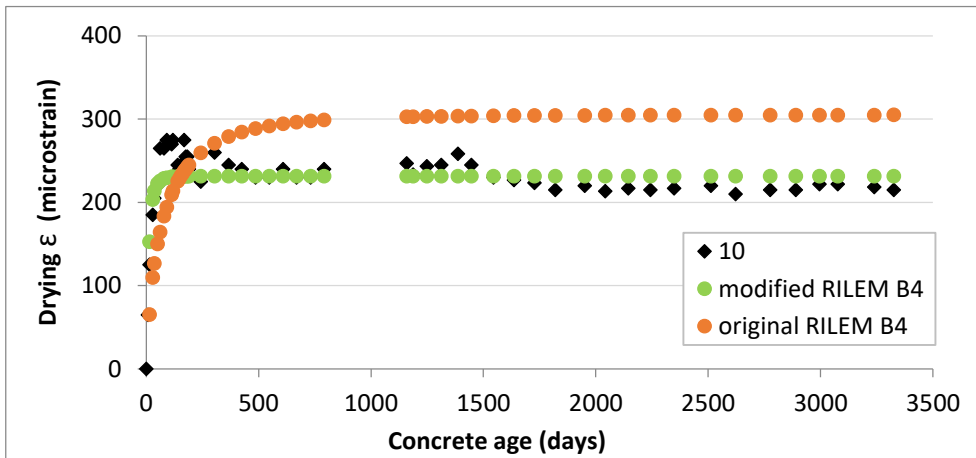


Figure E.94 RILEM B4 model predicted and actual drying shrinkage (microstrain) for Dataset 1-HSC, Subset S2-08, Experiment no. 10

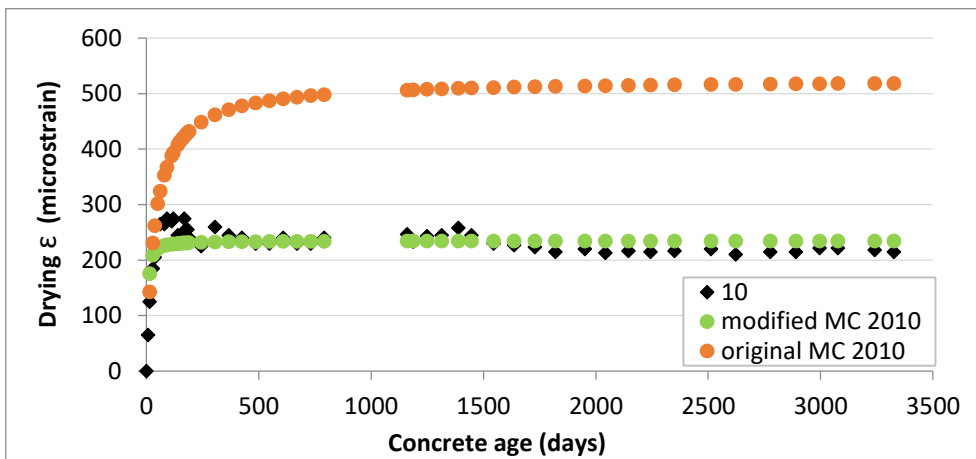


Figure E.95 MC 2010 model predicted and actual drying shrinkage (microstrain) for Dataset 1-HSC, Subset S2-08, Experiment no. 10

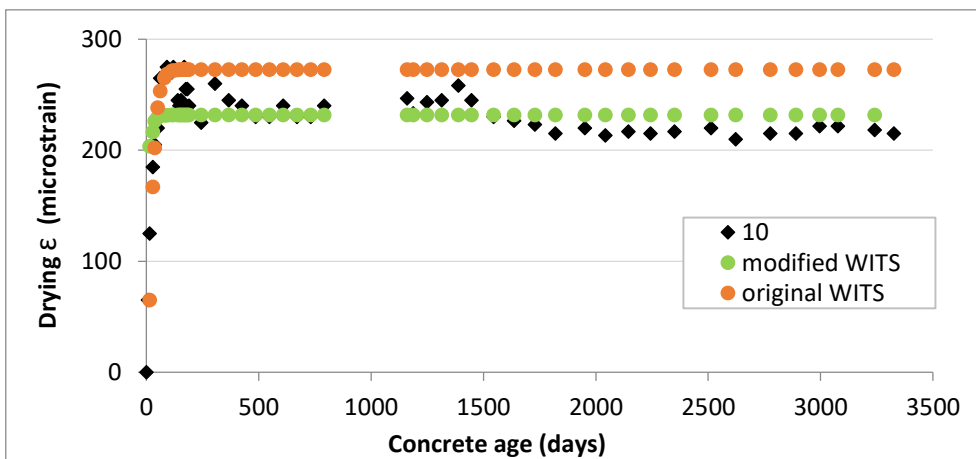


Figure E.96 WITS model predicted and actual drying shrinkage (microstrain) for Dataset 1-HSC, Subset S2-08, Experiment no. 10

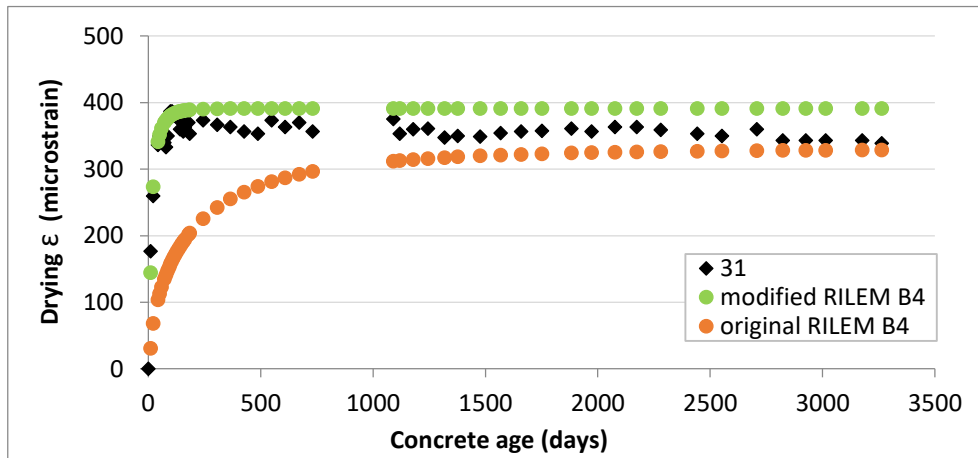


Figure E.97 RILEM B4 model predicted and actual drying shrinkage (microstrain) for Dataset 1-HSC, Subset S2-09, Experiment no. 31

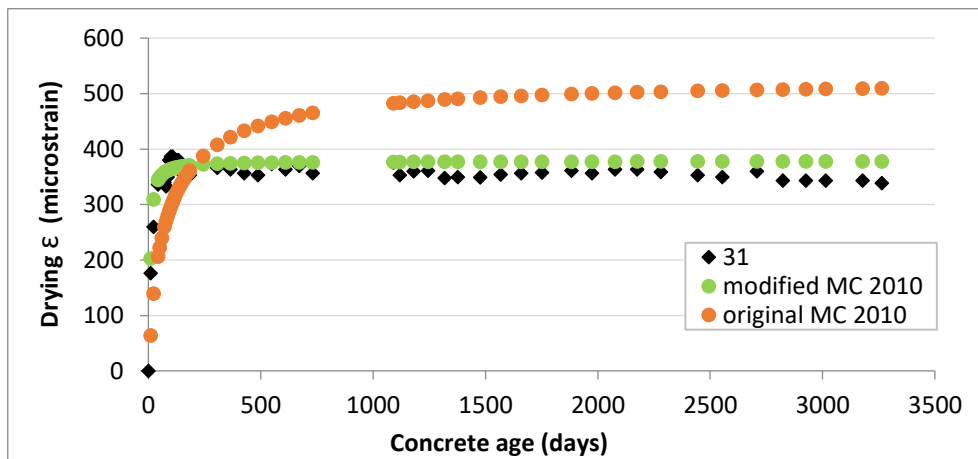


Figure E.98 MC 2010 model predicted and actual drying shrinkage (microstrain) for Dataset 1-HSC, Subset S2-09, Experiment no. 31

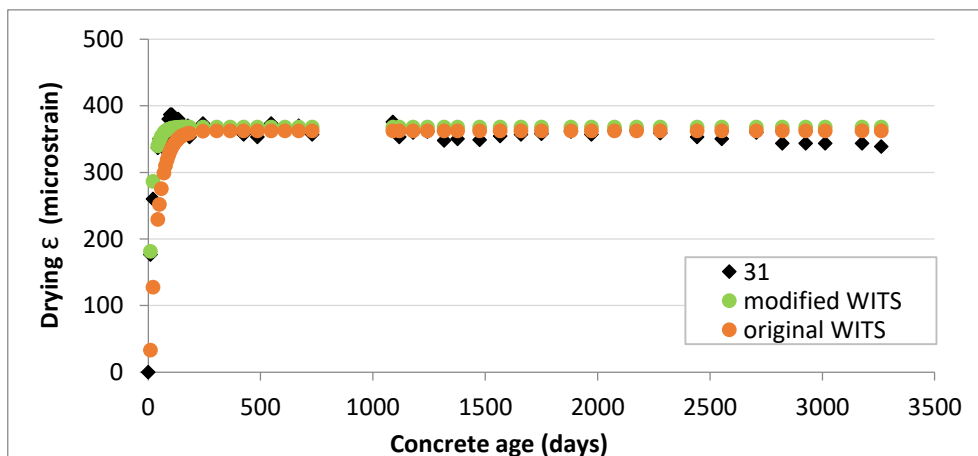


Figure E.99 WITS model predicted and actual drying shrinkage (microstrain) for Dataset 1-HSC, Subset S2-09, Experiment no. 31



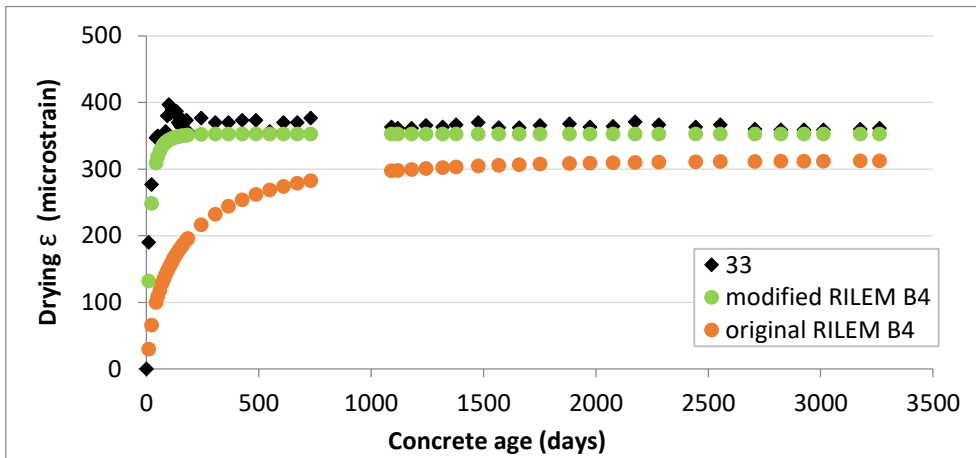


Figure E.100 RILEM B4 model predicted and actual drying shrinkage (microstrain) for Dataset 1-HSC, Subset S2-09, Experiment no. 33

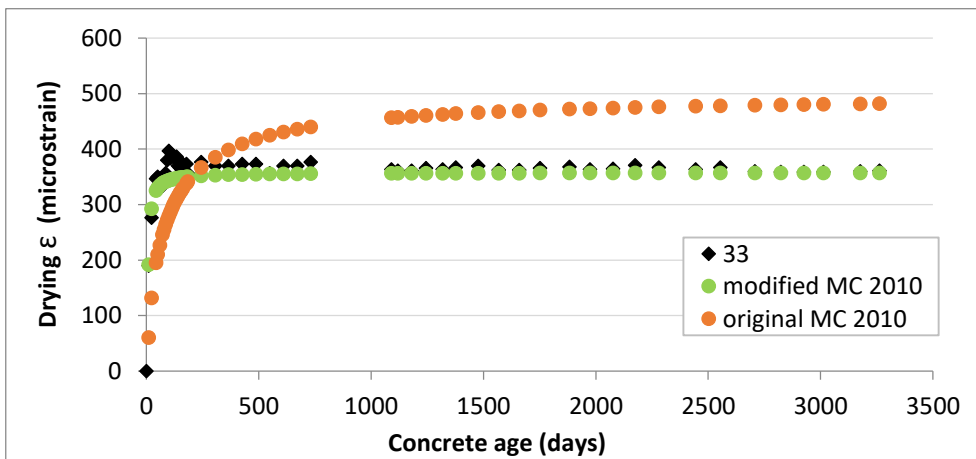


Figure E.101 MC 2010 model predicted and actual drying shrinkage (microstrain) for Dataset 1-HSC, Subset S2-09, Experiment no. 33

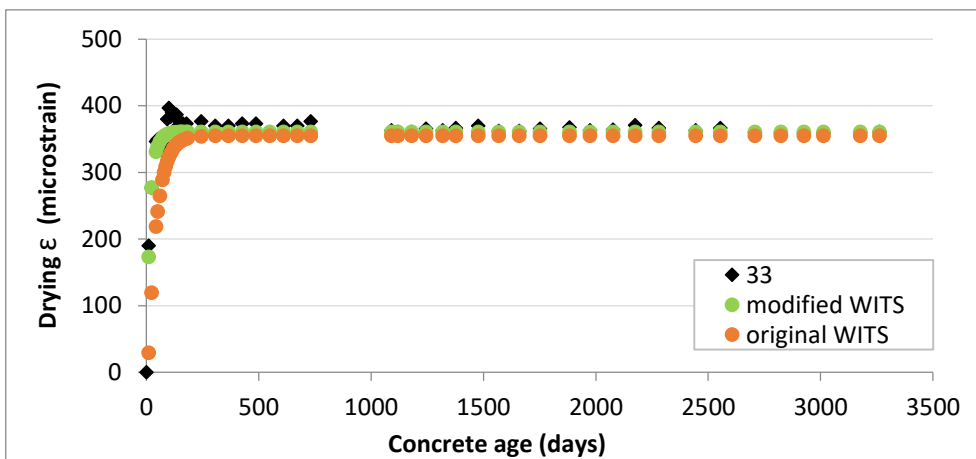


Figure E.102 WITS model predicted and actual drying shrinkage (microstrain) for Dataset 1-HSC, Subset S2-09, Experiment no. 33

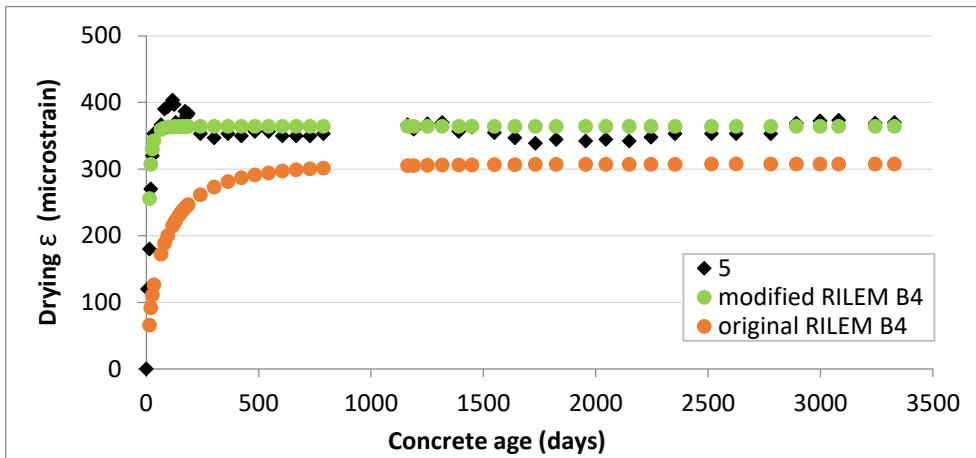


Figure E.103 RILEM B4 model predicted and actual drying shrinkage (microstrain) for Dataset 1-HSC, Subset S2-10, Experiment no. 5

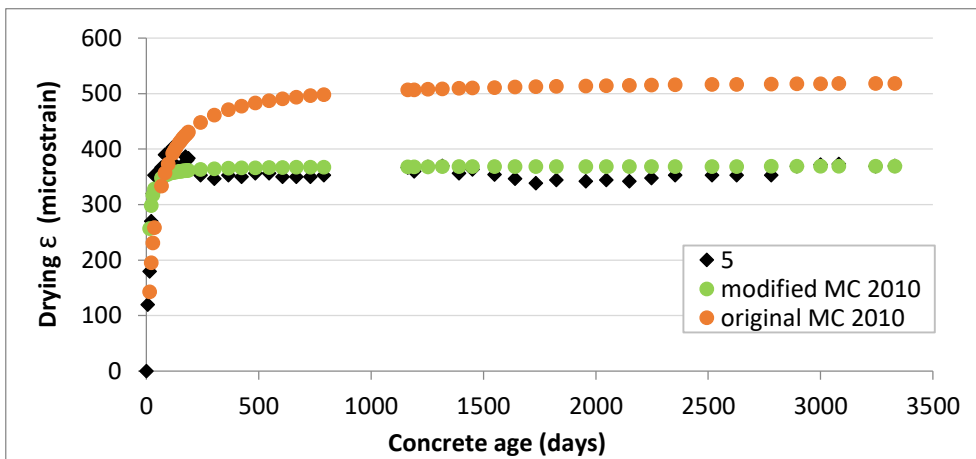


Figure E.104 MC 2010 model predicted and actual drying shrinkage (microstrain) for Dataset 1-HSC, Subset S2-10, Experiment no. 5

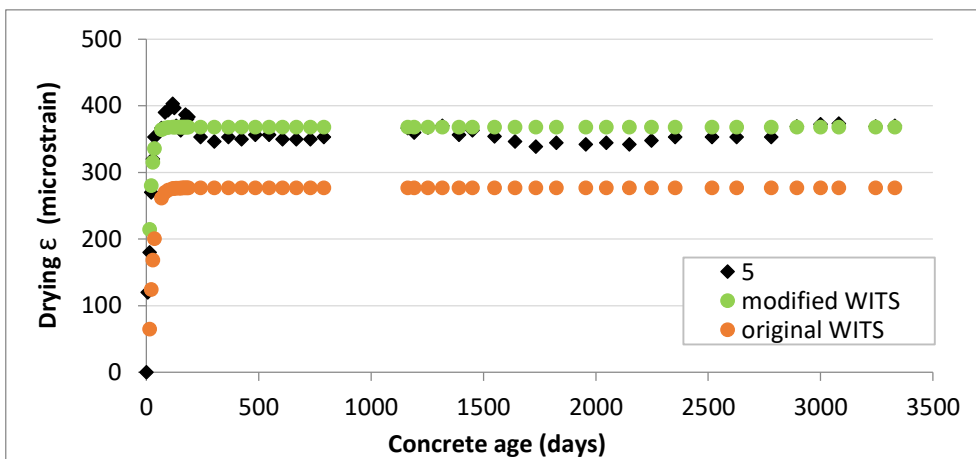


Figure E.105 WITS model predicted and actual drying shrinkage (microstrain) for Dataset 1-HSC, Subset S2-10, Experiment no. 5

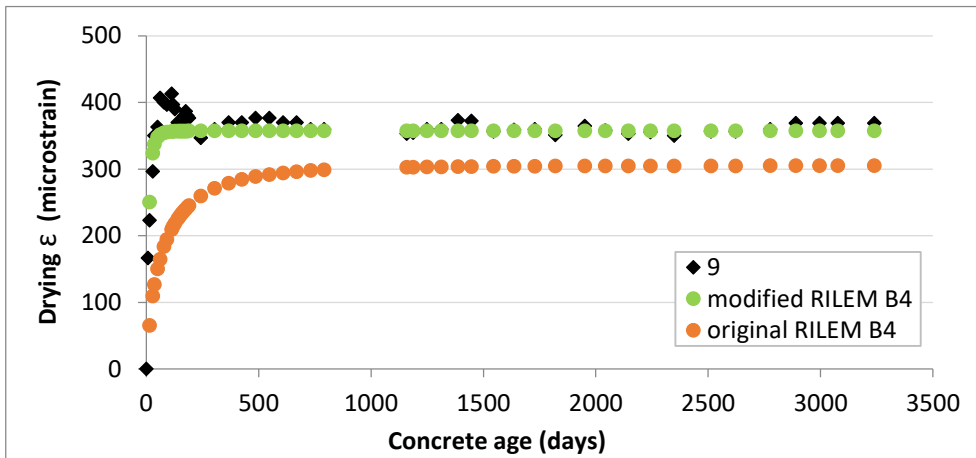


Figure E.106 RILEM B4 model predicted and actual drying shrinkage (microstrain) for Dataset 1-HSC, Subset S2-10, Experiment no. 9

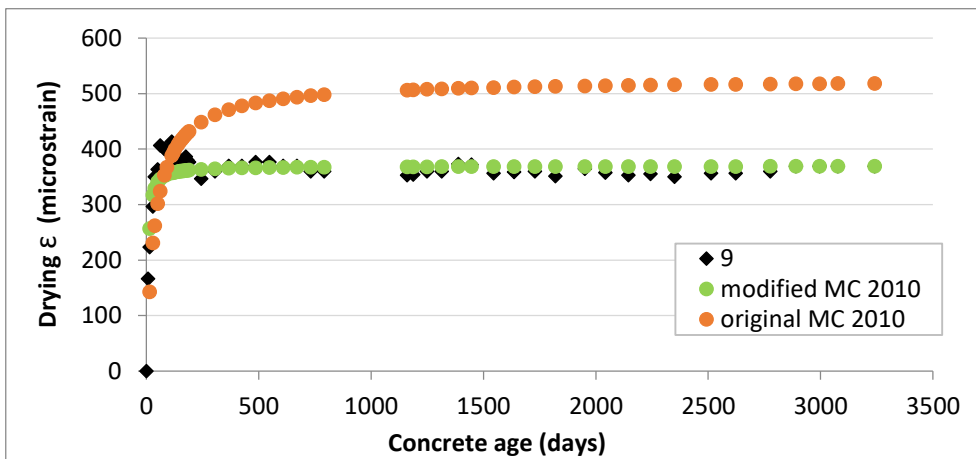


Figure E.107 MC 2010 model predicted and actual drying shrinkage (microstrain) for Dataset 1-HSC, Subset S2-10, Experiment no. 9

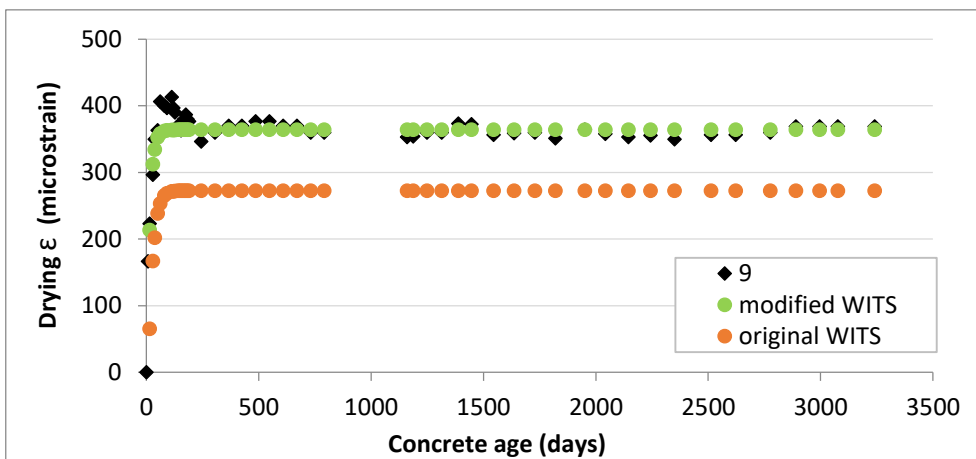


Figure E.108 WITS model predicted and actual drying shrinkage (microstrain) for Dataset 1-HSC, Subset S2-10, Experiment no. 9

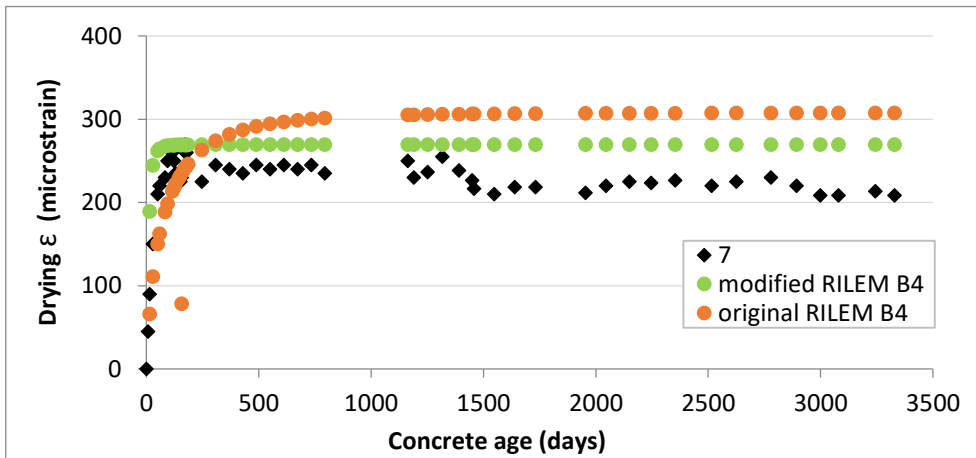


Figure E.109 RILEM B4 model predicted and actual drying shrinkage (microstrain) for Dataset 1-HSC, Subset S2-11, Experiment no. 7

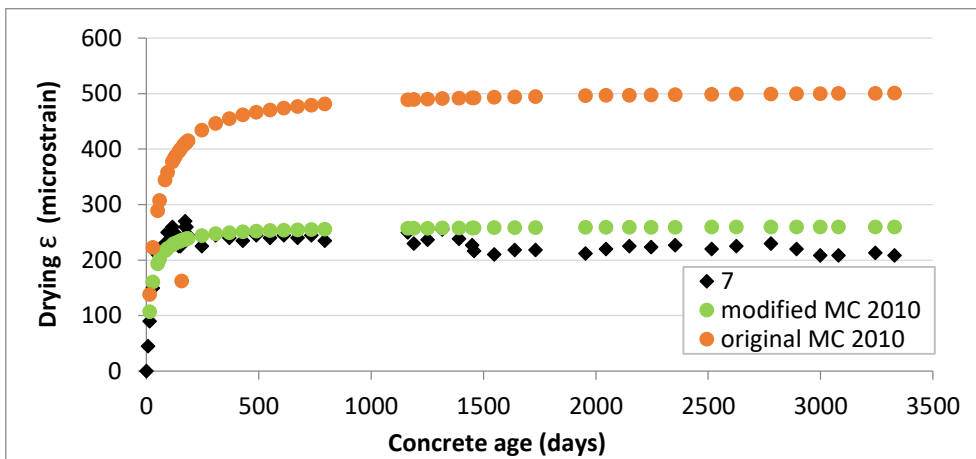


Figure E.110 MC 2010 model predicted and actual drying shrinkage (microstrain) for Dataset 1-HSC, Subset S2-11, Experiment no. 7

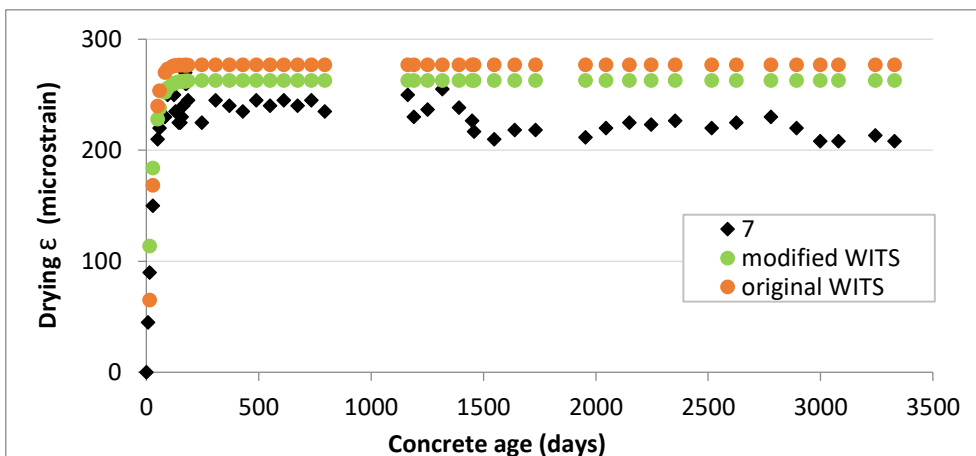


Figure E.111 WITS model predicted and actual drying shrinkage (microstrain) for Dataset 1-HSC, Subset S2-11, Experiment no. 7

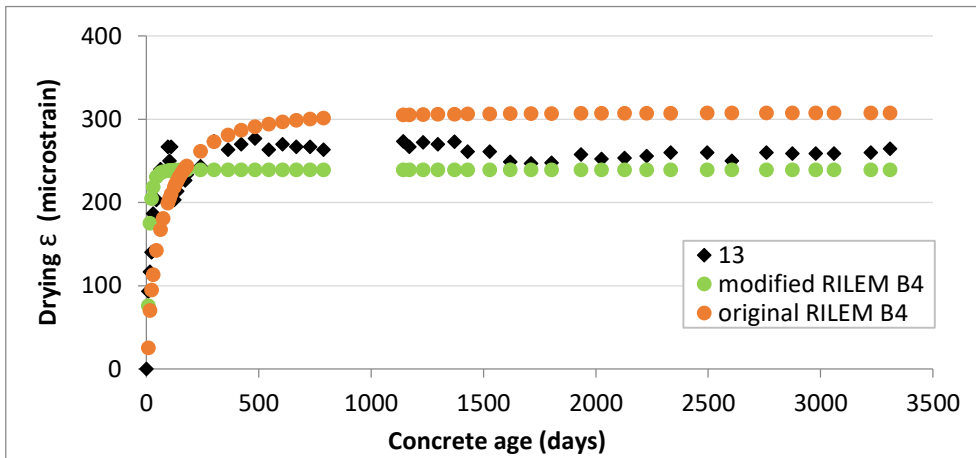


Figure E.112 RILEM B4 model predicted and actual drying shrinkage (microstrain) for Dataset 1-HSC, Subset S2-11, Experiment no. 13

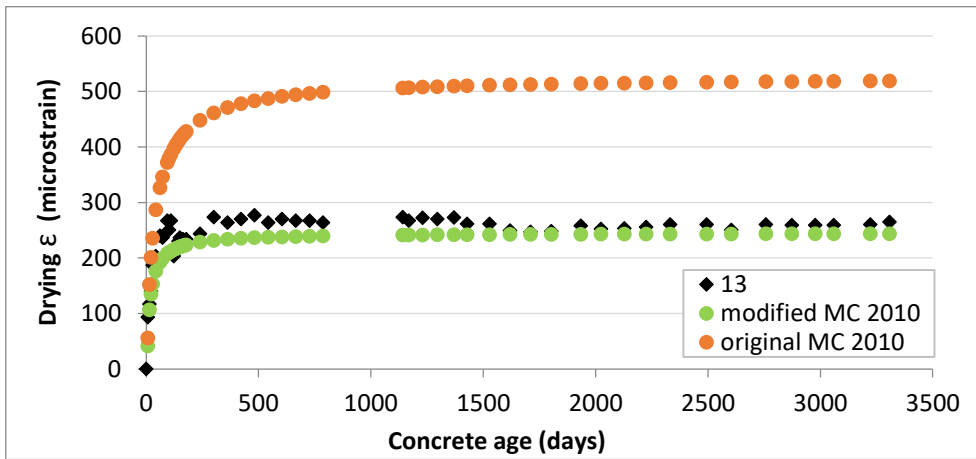


Figure E.113 MC 2010 model predicted and actual drying shrinkage (microstrain) for Dataset 1-HSC, Subset S2-11, Experiment no. 13

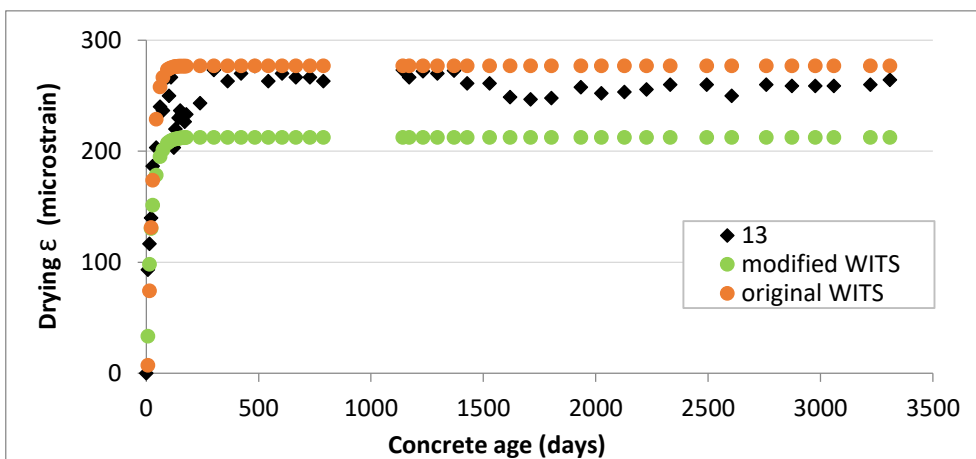


Figure E.114 WITS model predicted and actual drying shrinkage (microstrain) for Dataset 1-HSC, Subset S2-11, Experiment no. 13

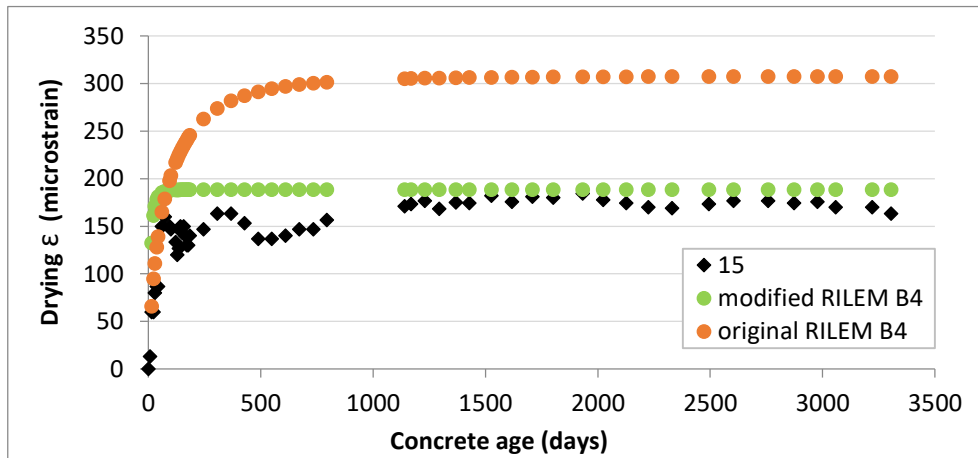


Figure E.115 RILEM B4 model predicted and actual drying shrinkage (microstrain) for Dataset 1-HSC, Subset S2-11, Experiment no. 15

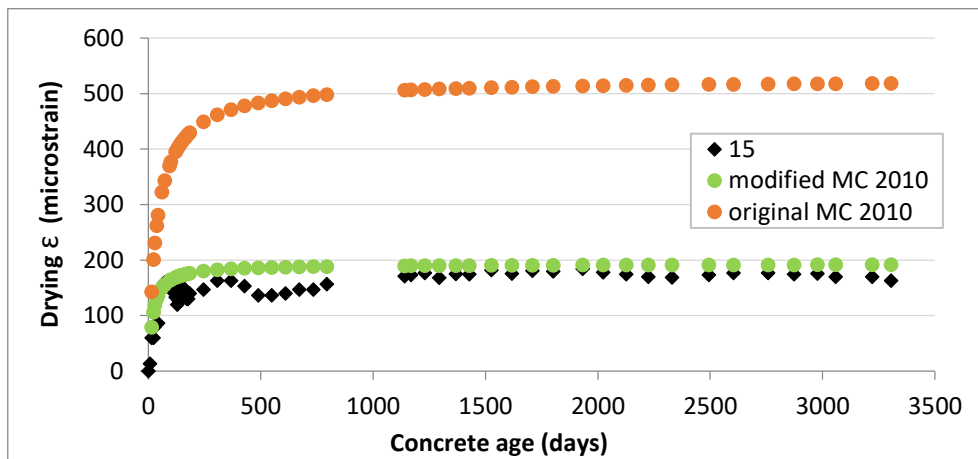


Figure E.116 MC 2010 model predicted and actual drying shrinkage (microstrain) for Dataset 1-HSC, Subset S2-11, Experiment no. 15

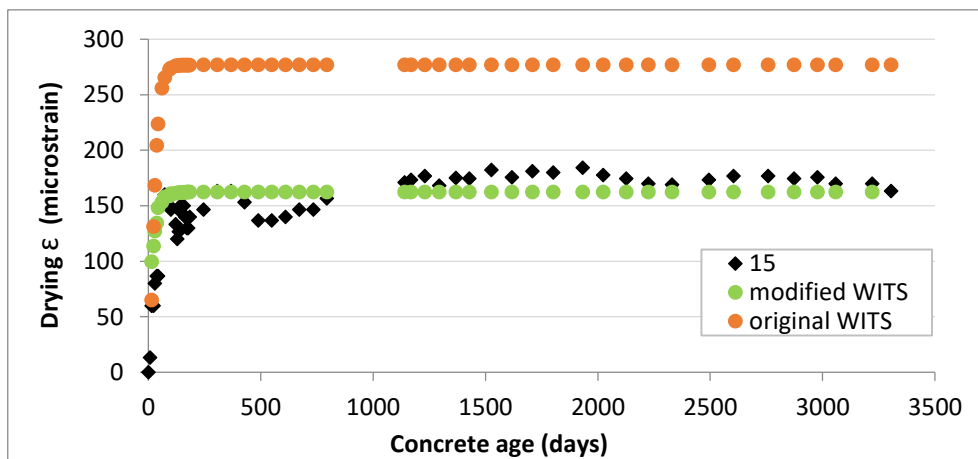


Figure E.117 WITS model predicted and actual drying shrinkage (microstrain) for Dataset 1-HSC, Subset S2-11, Experiment no. 15

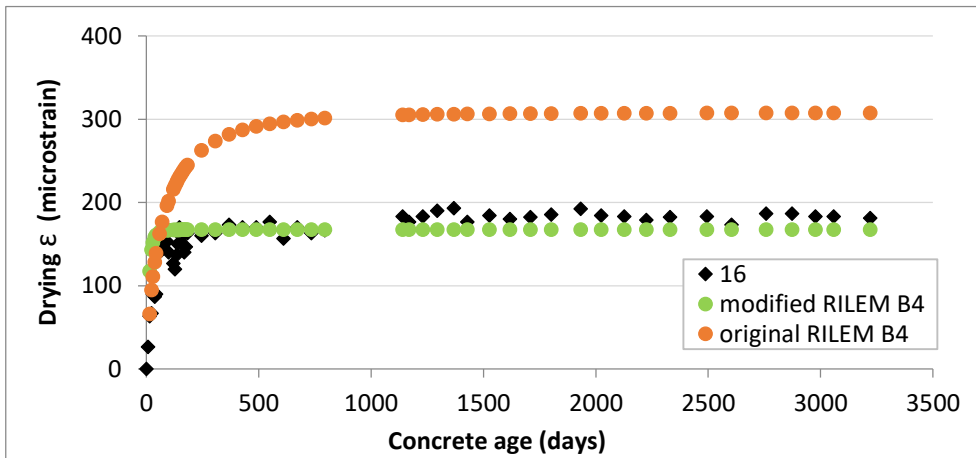


Figure E.118 RILEM B4 model predicted and actual drying shrinkage (microstrain) for Dataset 1-HSC, Subset S2-11, Experiment no. 16

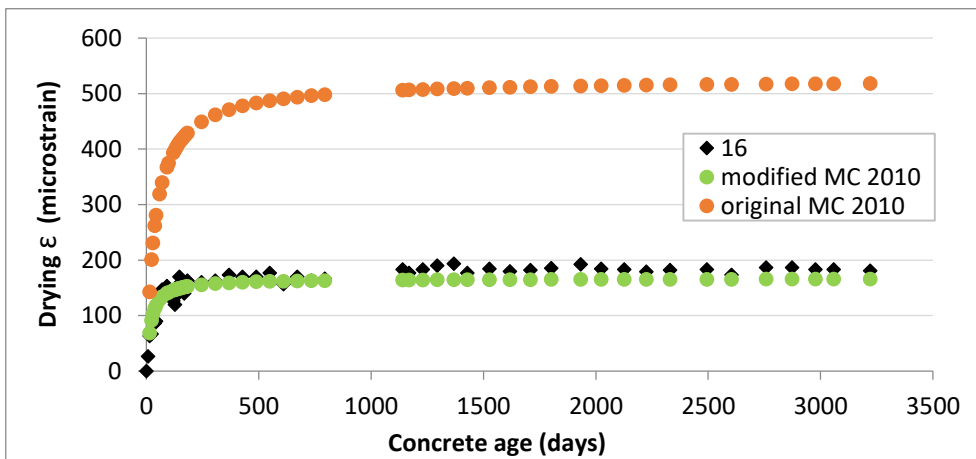


Figure E.119 MC 2010 model predicted and actual drying shrinkage (microstrain) for Dataset 1-HSC, Subset S2-11, Experiment no. 16

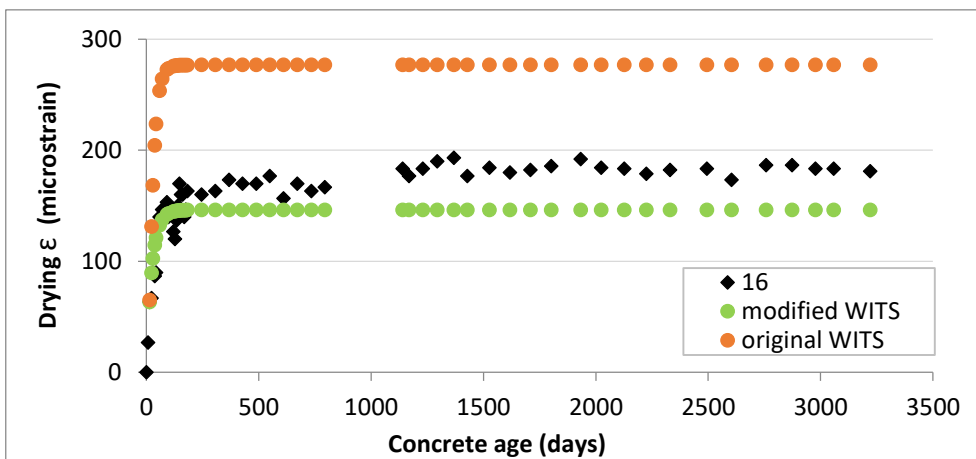


Figure E.120 WITS model predicted and actual drying shrinkage (microstrain) for Dataset 1-HSC, Subset S2-11, Experiment no. 16

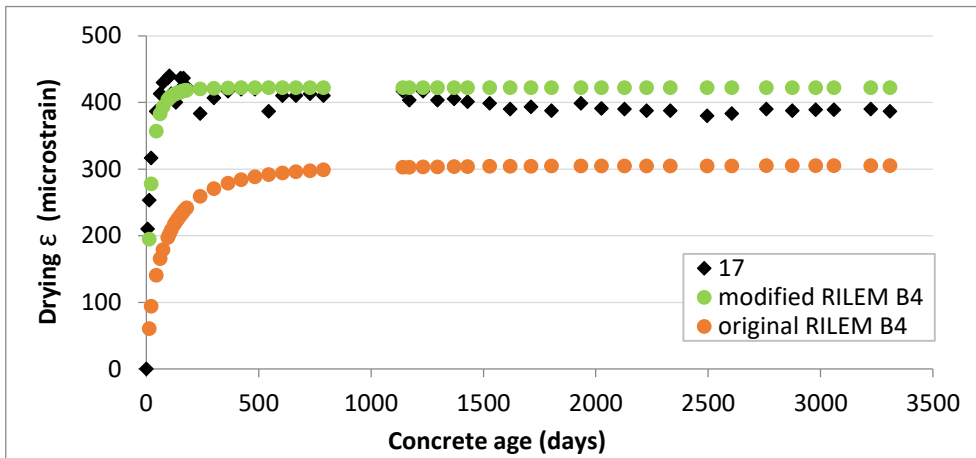


Figure E.121 RILEM B4 model predicted and actual drying shrinkage (microstrain) for Dataset 1-HSC, Subset S2-12, Experiment no. 17

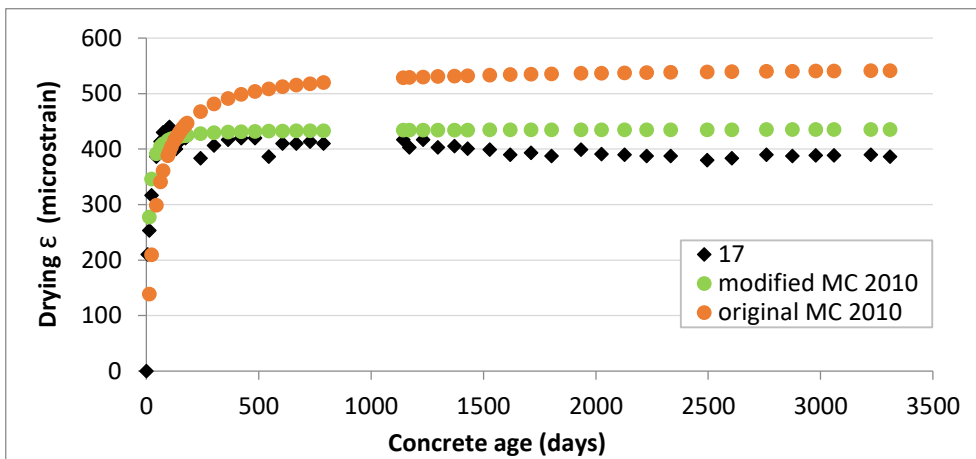


Figure E.122 MC 2010 model predicted and actual drying shrinkage (microstrain) for Dataset 1-HSC, Subset S2-12, Experiment no. 17

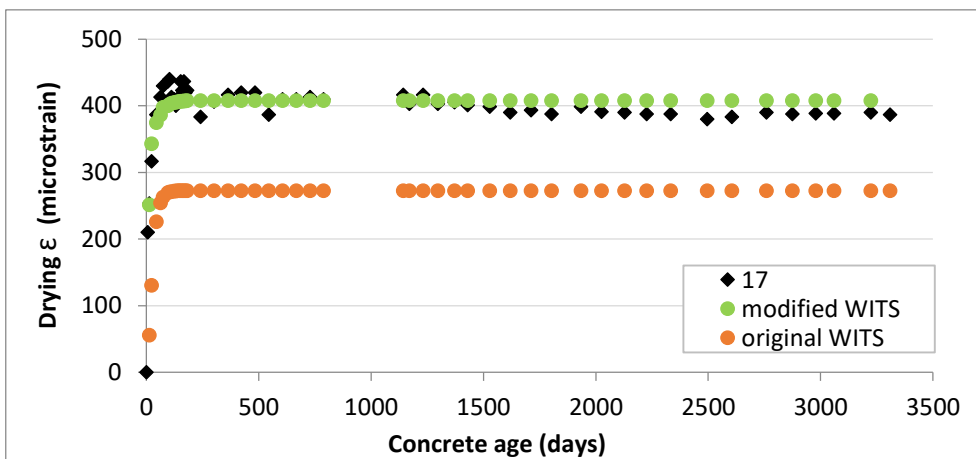


Figure E.123 WITS model predicted and actual drying shrinkage (microstrain) for Dataset 1-HSC, Subset S2-12, Experiment no. 17



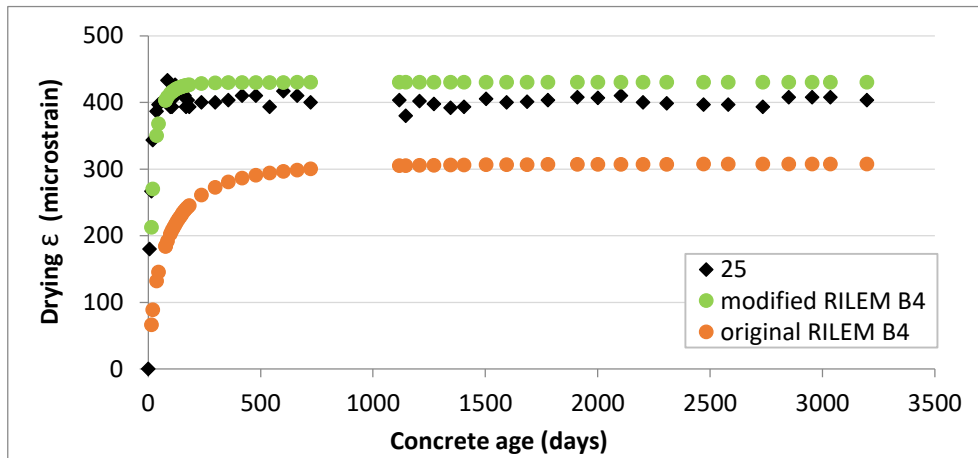


Figure E.124 RILEM B4 model predicted and actual drying shrinkage (microstrain) for Dataset 1-HSC, Subset S2-12, Experiment no. 25

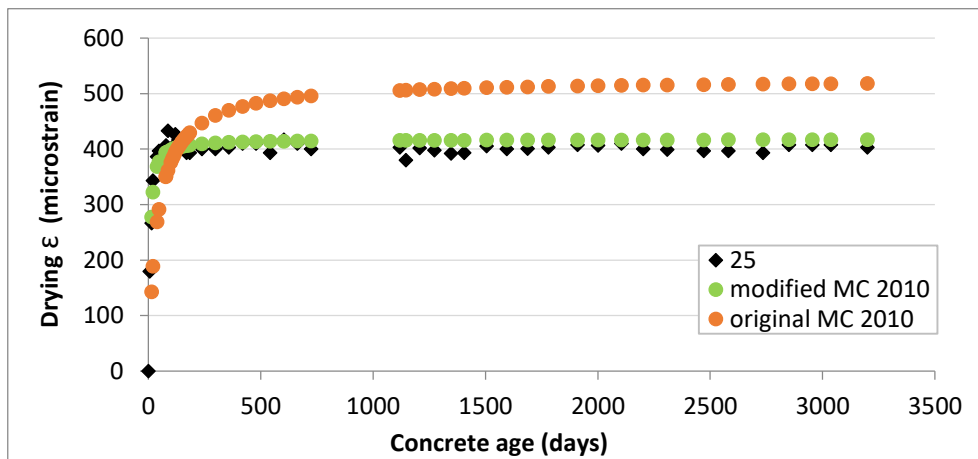


Figure E.125 MC 2010 model predicted and actual drying shrinkage (microstrain) for Dataset 1-HSC, Subset S2-12, Experiment no. 25

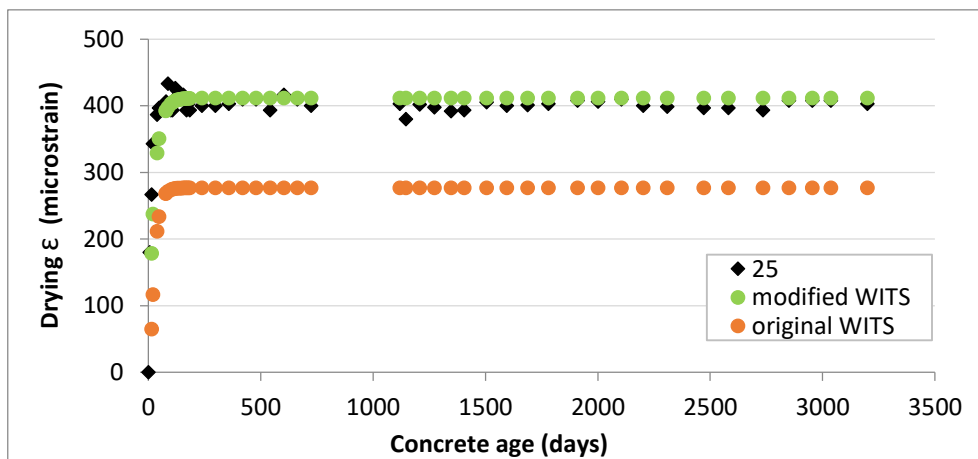


Figure E.126 WITS model predicted and actual drying shrinkage (microstrain) for Dataset 1-HSC, Subset S2-12, Experiment no. 25

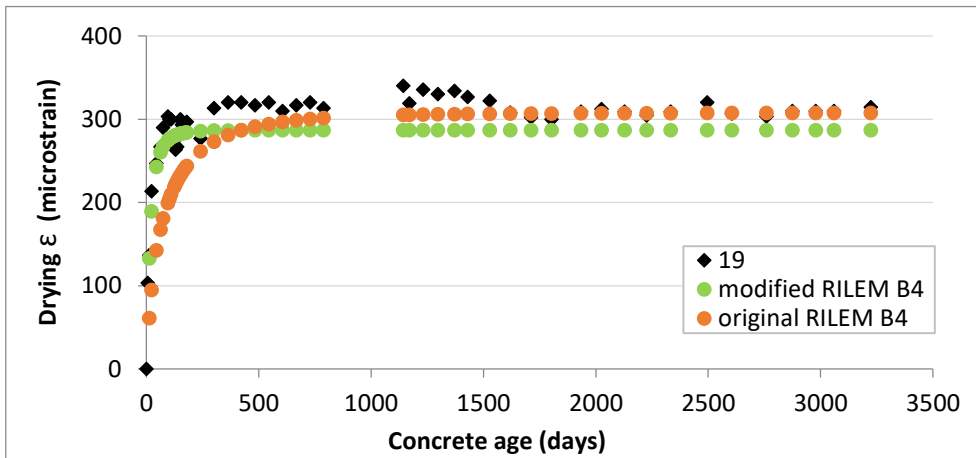


Figure E.127 RILEM B4 model predicted and actual drying shrinkage (microstrain) for Dataset 1-HSC, Subset S2-13, Experiment no. 19

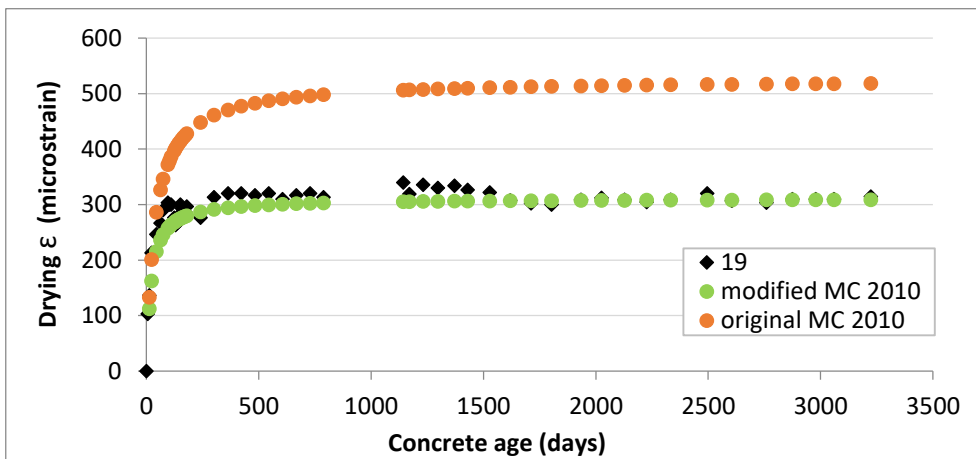


Figure E.128 MC 2010 model predicted and actual drying shrinkage (microstrain) for Dataset 1-HSC, Subset S2-13, Experiment no. 19

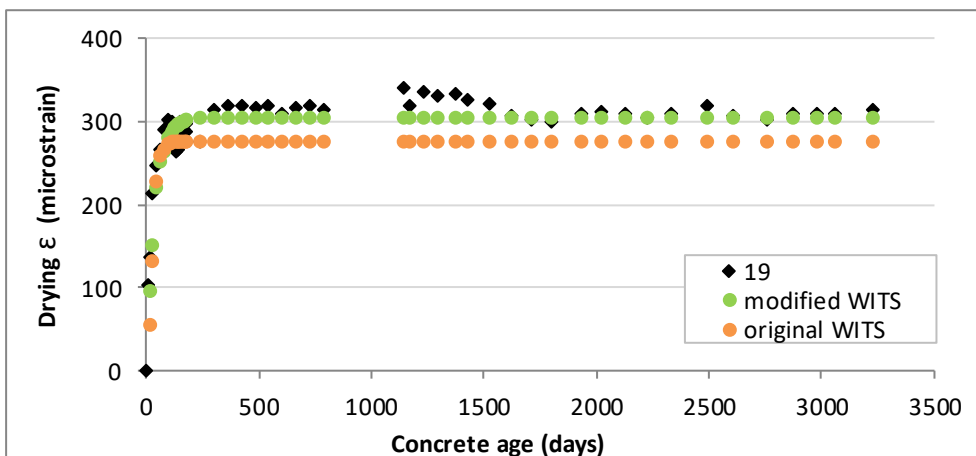


Figure E.129 WITS model predicted and actual drying shrinkage (microstrain) for Dataset 1-HSC, Subset S2-13, Experiment no. 19

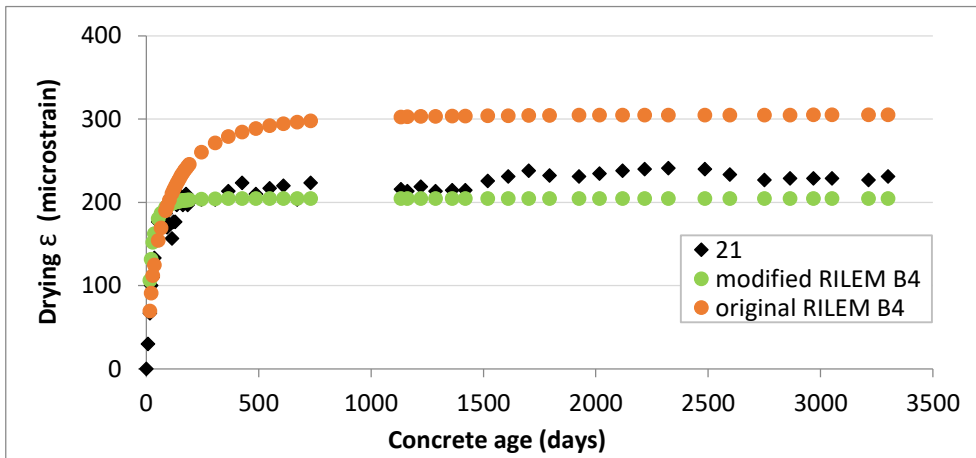


Figure E.130 RILEM B4 model predicted and actual drying shrinkage (microstrain) for Dataset 1-HSC, Subset S2-13, Experiment no. 21

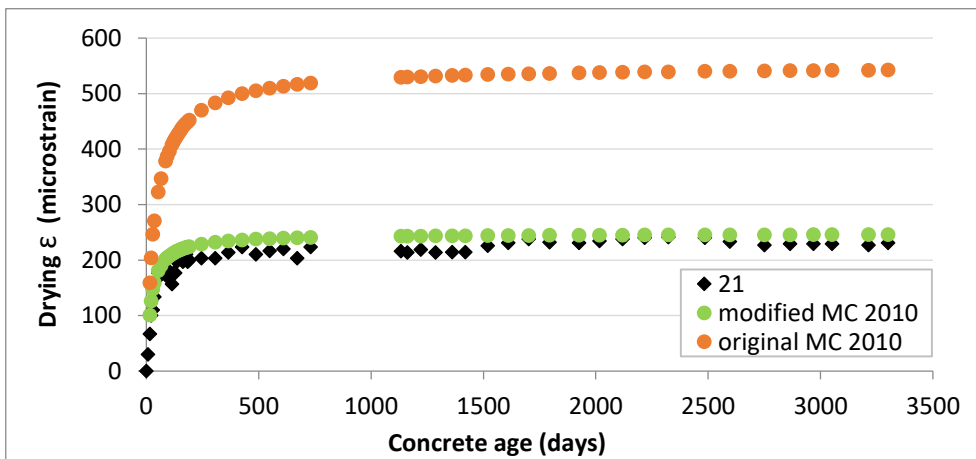


Figure E.131 MC 2010 model predicted and actual drying shrinkage (microstrain) for Dataset 1-HSC, Subset S2-13, Experiment no. 21

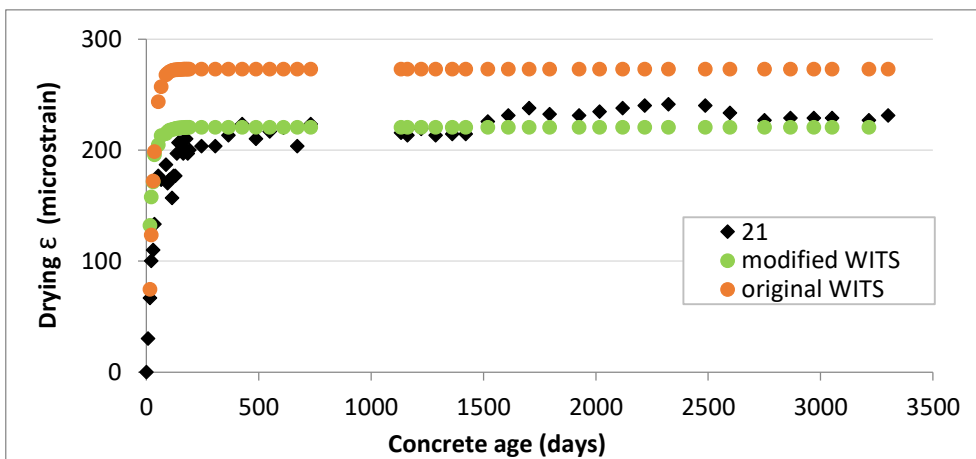


Figure E.132 WITS model predicted and actual drying shrinkage (microstrain) for Dataset 1-HSC, Subset S2-13, Experiment no. 21

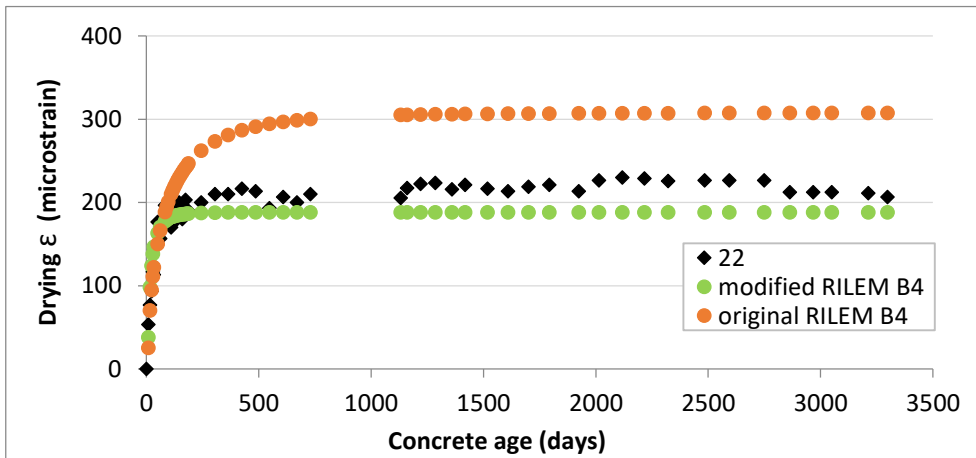


Figure E.133 RILEM B4 model predicted and actual drying shrinkage (microstrain) for Dataset 1-HSC, Subset S2-13, Experiment no. 22

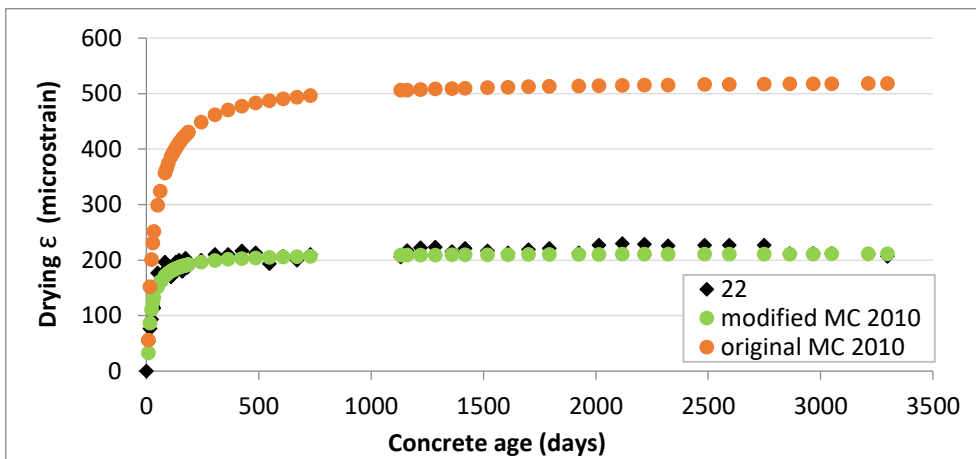


Figure E.134 MC 2010 model predicted and actual drying shrinkage (microstrain) for Dataset 1-HSC, Subset S2-13, Experiment no. 22

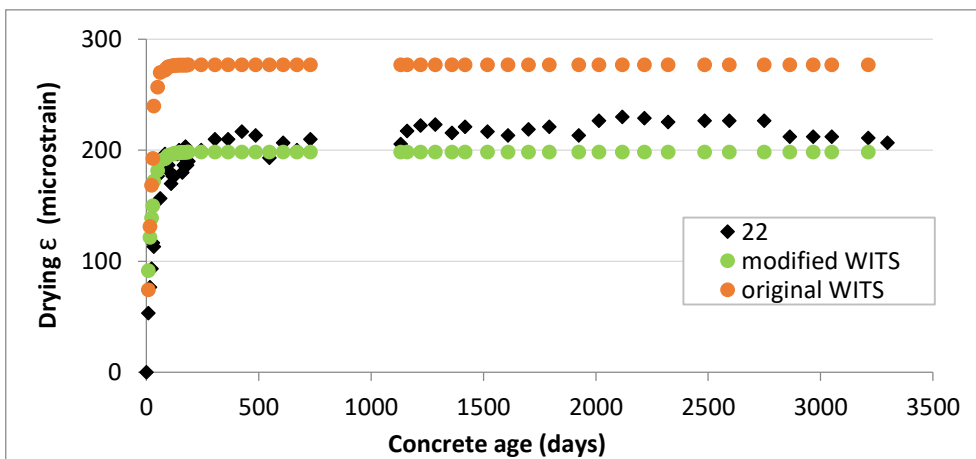


Figure E.135 WITS model predicted and actual drying shrinkage (microstrain) for Dataset 1-HSC, Subset S2-13, Experiment no. 22

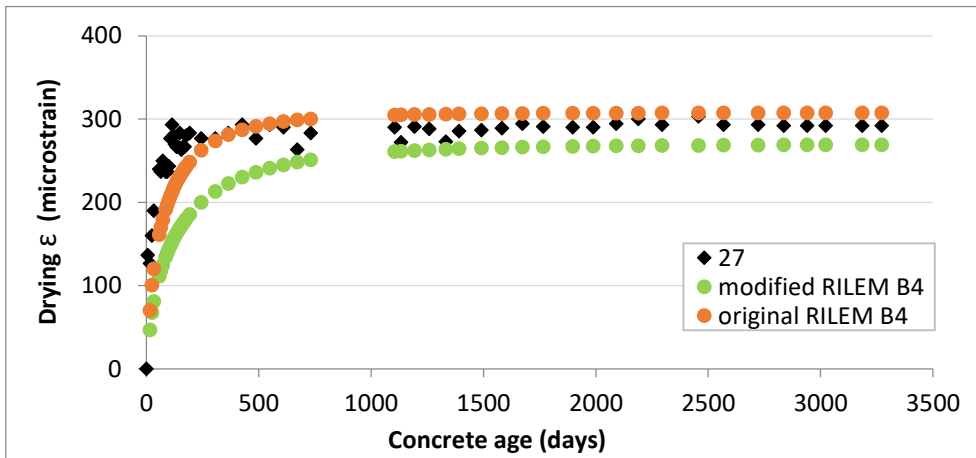


Figure E.136 RILEM B4 model predicted and actual drying shrinkage (microstrain) for Dataset 1-HSC, Subset S2-14, Experiment no. 27

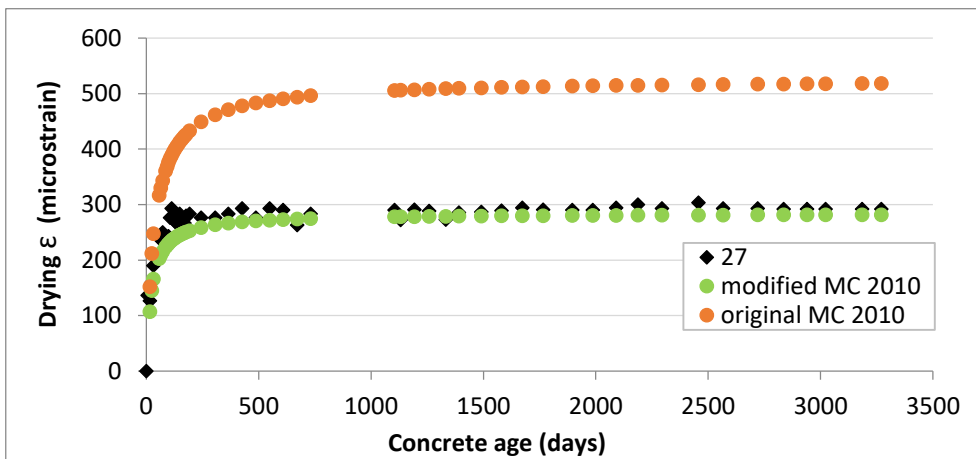


Figure E.137 MC 2010 model predicted and actual drying shrinkage (microstrain) for Dataset 1-HSC, Subset S2-14, Experiment no. 27

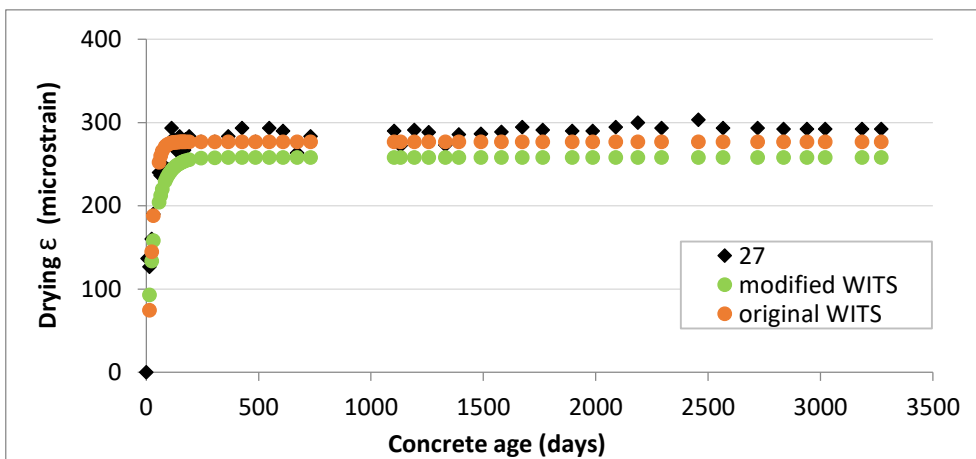


Figure E.138 WITS model predicted and actual drying shrinkage (microstrain) for Dataset 1-HSC, Subset S2-14, Experiment no. 27

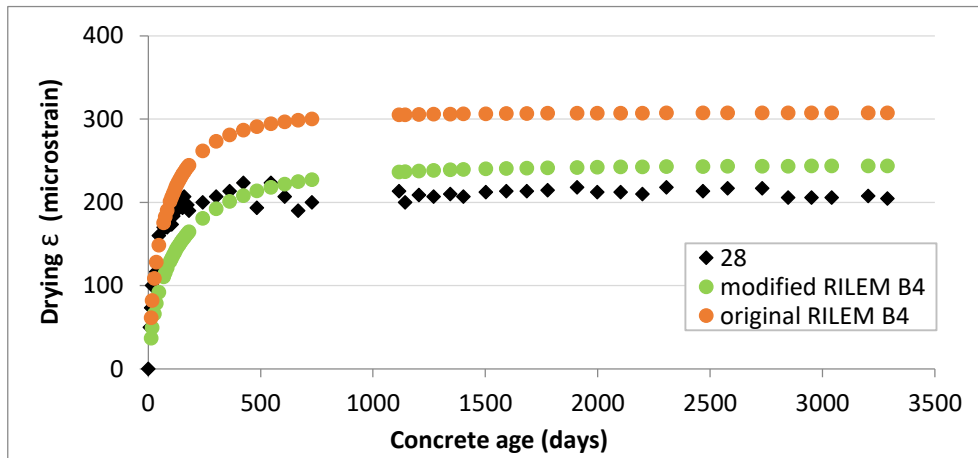


Figure E.139 RILEM B4 model predicted and actual drying shrinkage (microstrain) for Dataset 1-HSC, Subset S2-14, Experiment no. 28

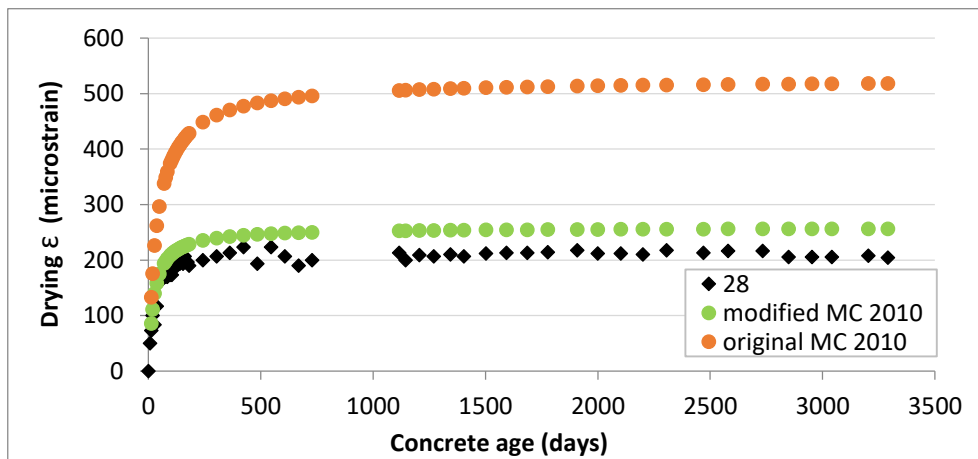


Figure E.140 MC 2010 model predicted and actual drying shrinkage (microstrain) for Dataset 1-HSC, Subset S2-14, Experiment no. 28

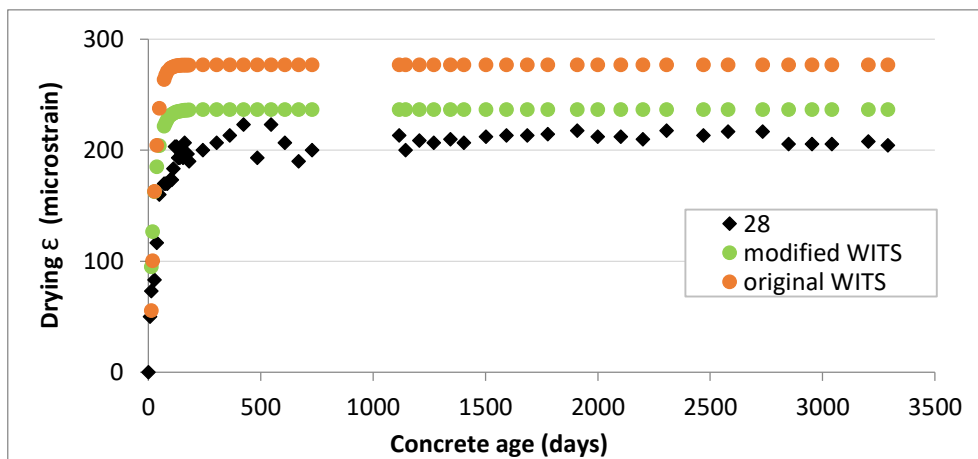


Figure E.141 WITS model predicted and actual drying shrinkage (microstrain) for Dataset 1-HSC, Subset S2-14, Experiment no. 28

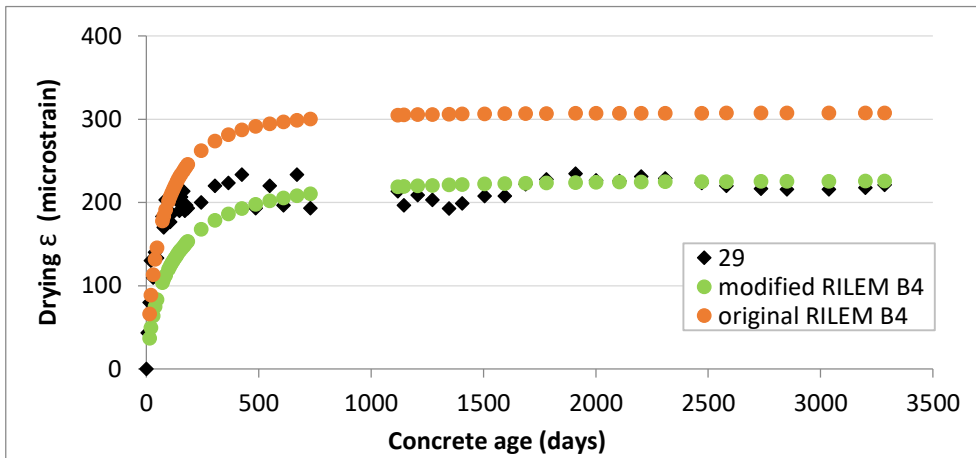


Figure E.142 RILEM B4 model predicted and actual drying shrinkage (microstrain) for Dataset 1-HSC, Subset S2-14, Experiment no. 29

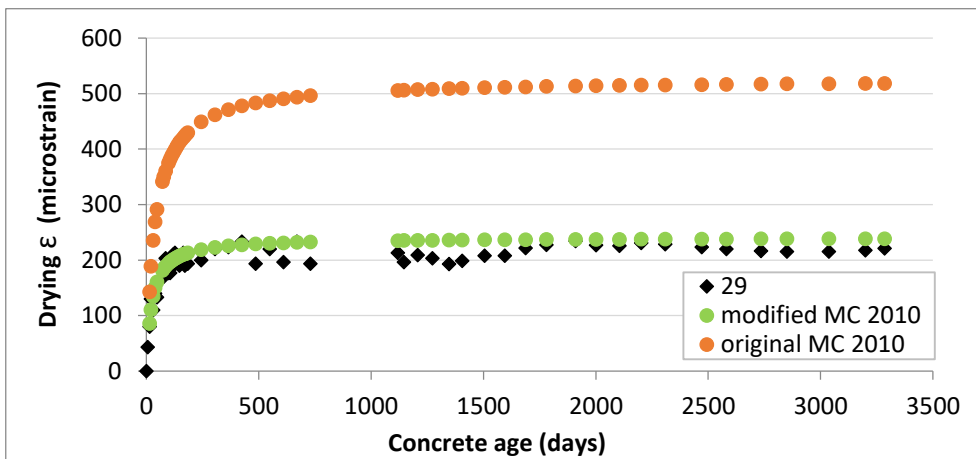


Figure E.143 MC 2010 model predicted and actual drying shrinkage (microstrain) for Dataset 1-HSC, Subset S2-14, Experiment no. 29

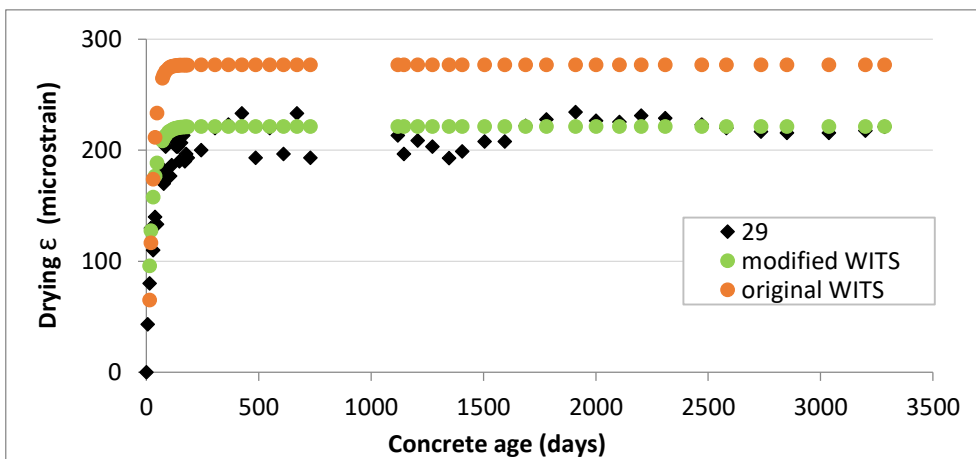


Figure E.144 WITS model predicted and actual drying shrinkage (microstrain) for Dataset 1-HSC, Subset S2-14, Experiment no. 29

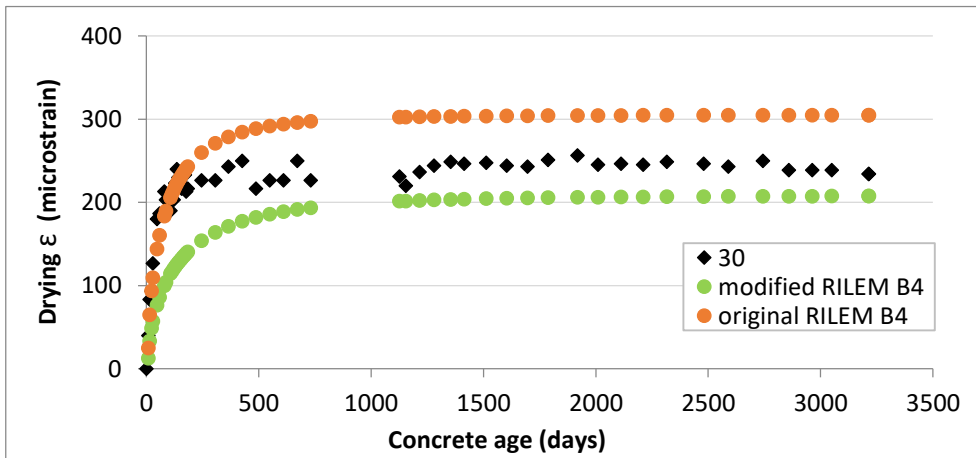


Figure E.145 RILEM B4 model predicted and actual drying shrinkage (microstrain) for Dataset 1-HSC, Subset S2-14, Experiment no. 30

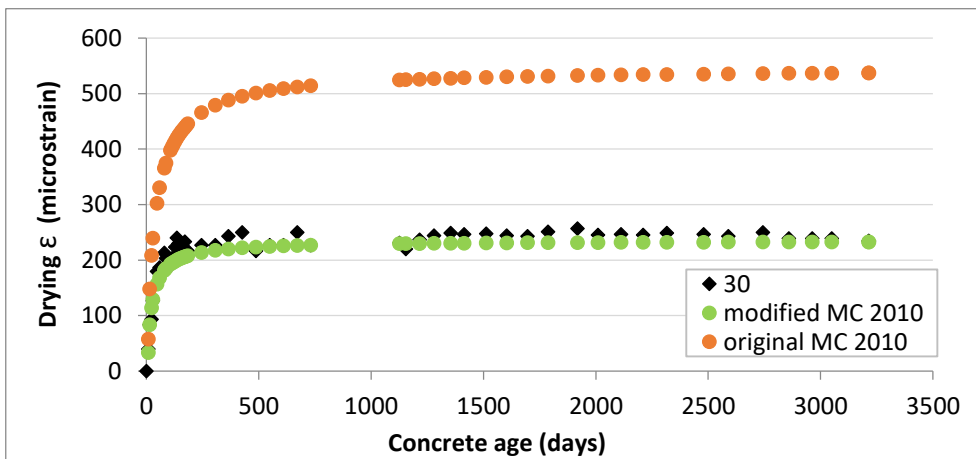


Figure E.146 MC 2010 model predicted and actual drying shrinkage (microstrain) for Dataset 1-HSC, Subset S2-14, Experiment no. 30

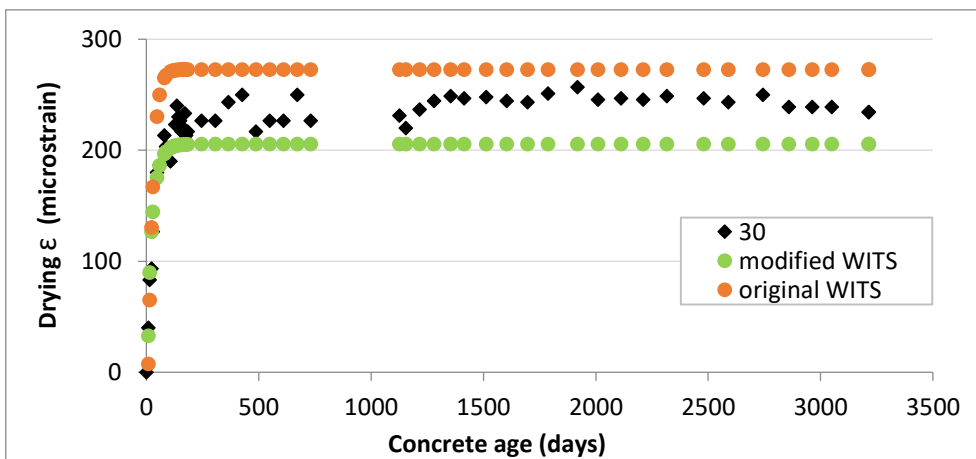


Figure E.147 WITS model predicted and actual drying shrinkage (microstrain) for Dataset 1-HSC, Subset S2-14, Experiment no. 30



**Appendix F. Original and modified shrinkage predictions of RILEM B4 and MC 2010 for Dataset 2-HSC**

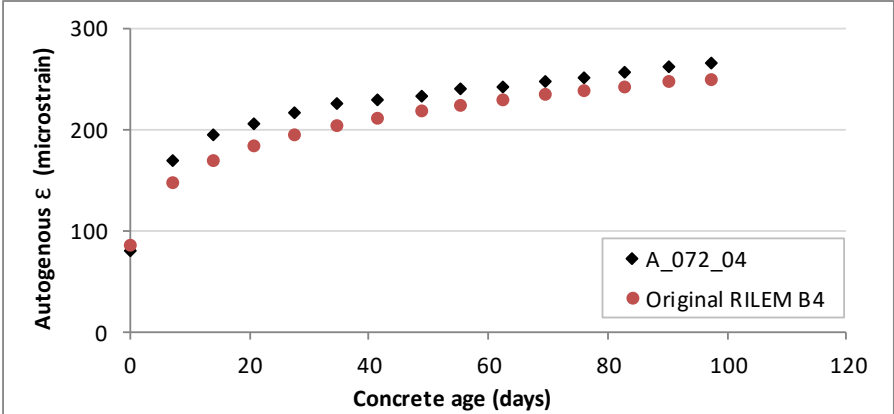


Figure F.1 RILEM B4 model predicted and actual drying shrinkage (microstrain) for Dataset 2-HSC, Subset S2-01a, Experiment A\_072\_04

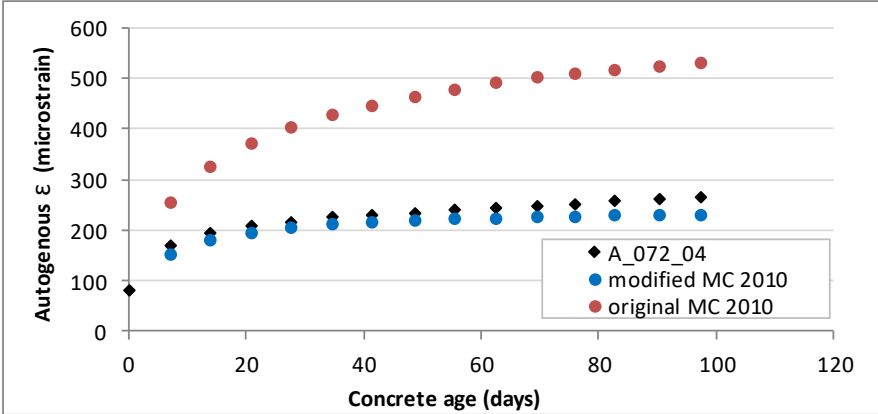


Figure F.2 MC 2010 model predicted and actual drying shrinkage (microstrain) for Dataset 2-HSC, Subset S2-01a, Experiment A\_072\_04

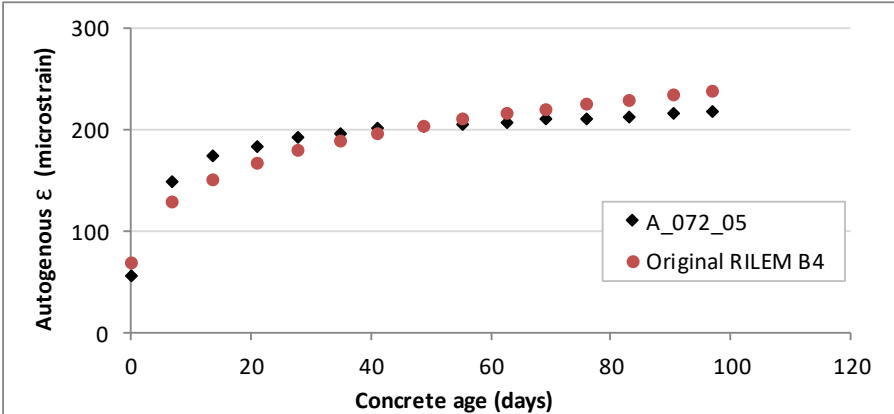


Figure F.3 RILEM B4 model predicted and actual drying shrinkage (microstrain) for Dataset 2-HSC, Subset S2-01a, Experiment A\_072\_05

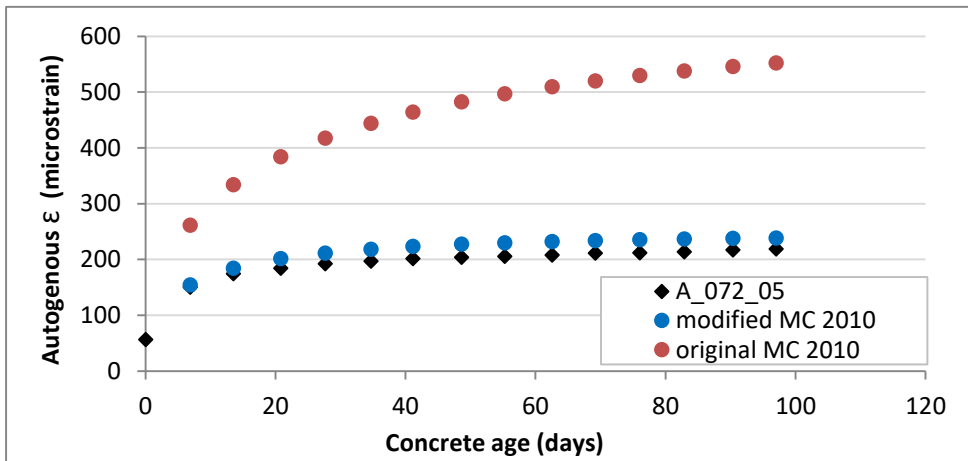


Figure F.4 MC 2010 model predicted and actual drying shrinkage (microstrain) for Dataset 2-HSC, Subset S2-01a, Experiment A\_072\_05

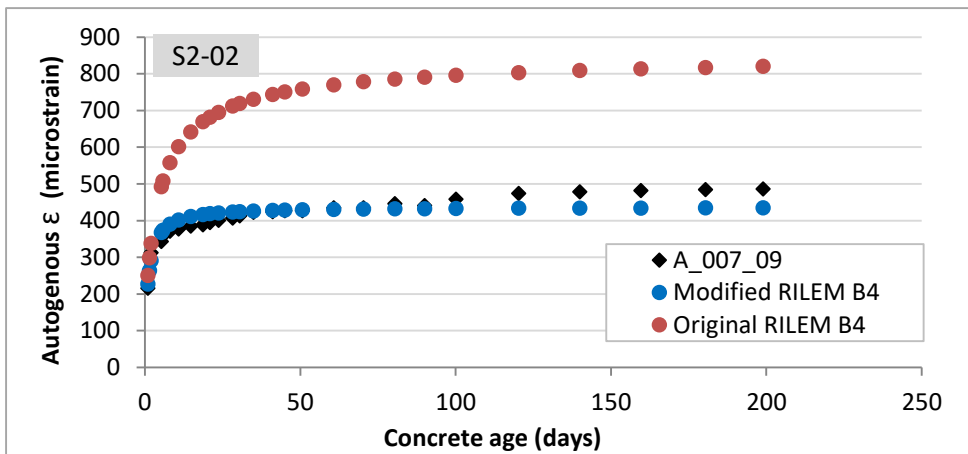


Figure F.5 RILEM B4 model predicted and actual drying shrinkage (microstrain) for Dataset 2-HSC, Subset S2-02a, Experiment A\_007\_09

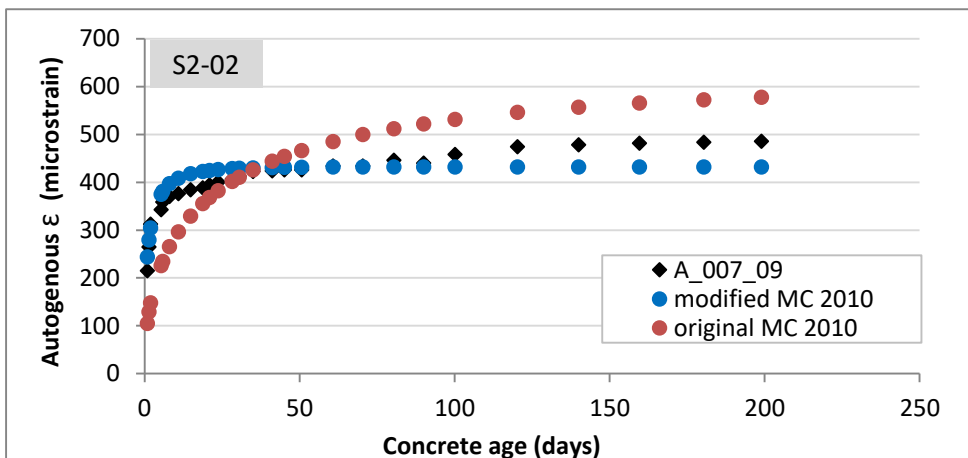


Figure F.6 MC 2010 model predicted and actual drying shrinkage (microstrain) for Dataset 2-HSC, Subset S2-02a, Experiment A\_007\_09

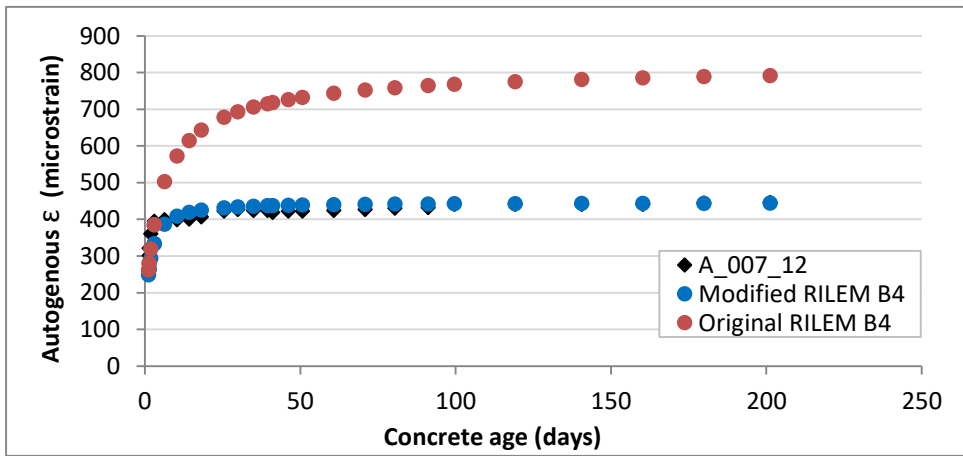


Figure F.7 RILEM B4 model predicted and actual drying shrinkage (microstrain) for Dataset 2-HSC, Subset S2-02a, Experiment A\_007\_12

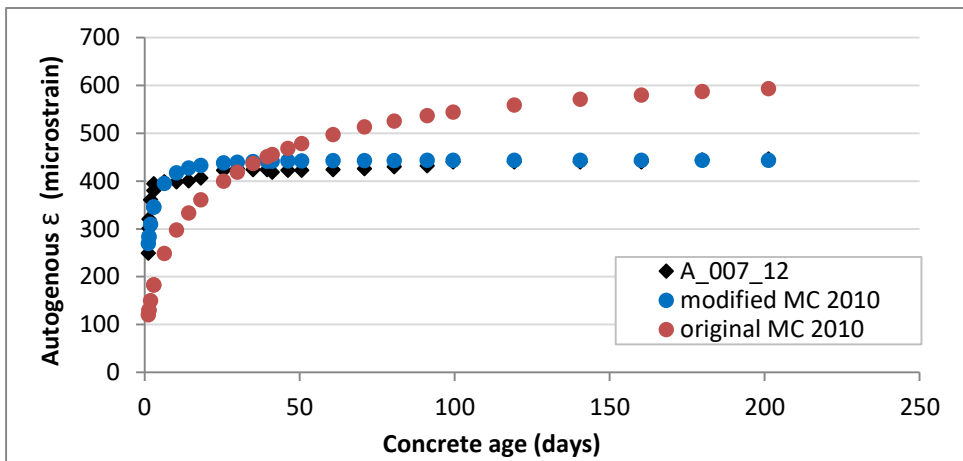


Figure F.8 MC 2010 model predicted and actual drying shrinkage (microstrain) for Dataset 2-HSC, Subset S2-02a, Experiment A\_007\_12

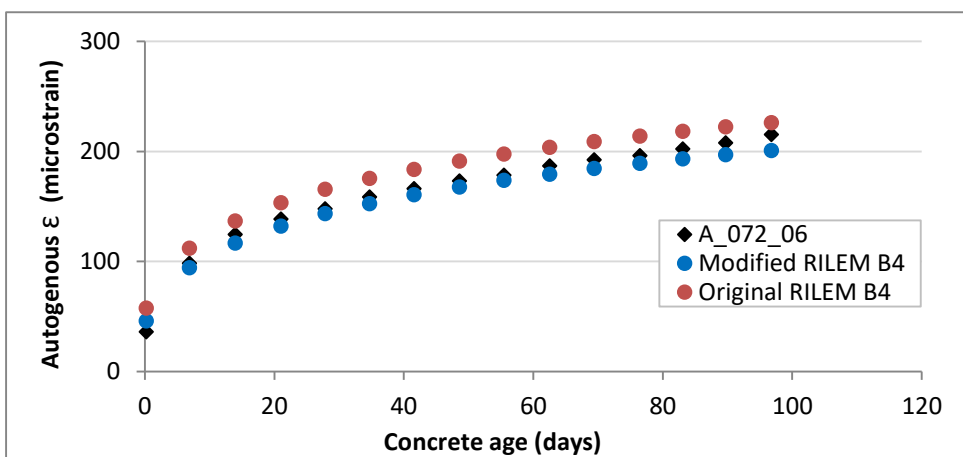


Figure F.9 RILEM B4 model predicted and actual drying shrinkage (microstrain) for Dataset 2-HSC, Subset S2-03a, Experiment A\_072\_06

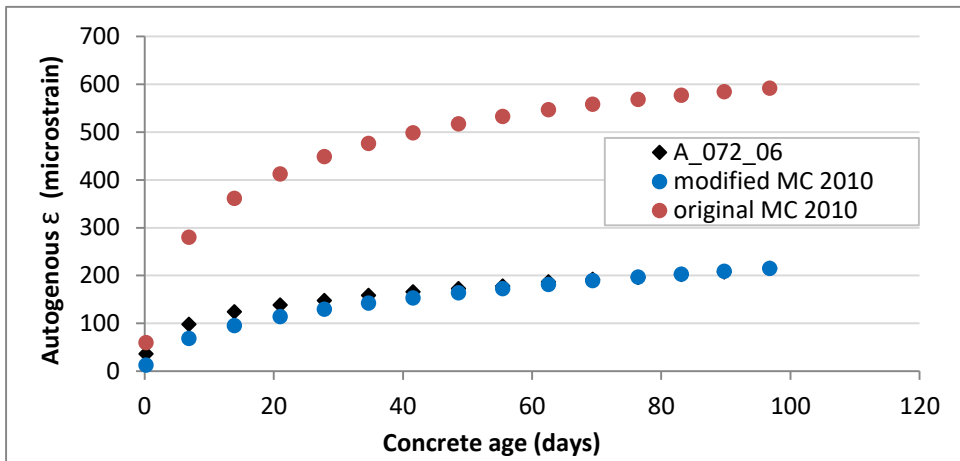


Figure F.10 MC 2010 model predicted and actual drying shrinkage (microstrain) for Dataset 2-HSC, Subset S2-03a, Experiment A\_072\_06

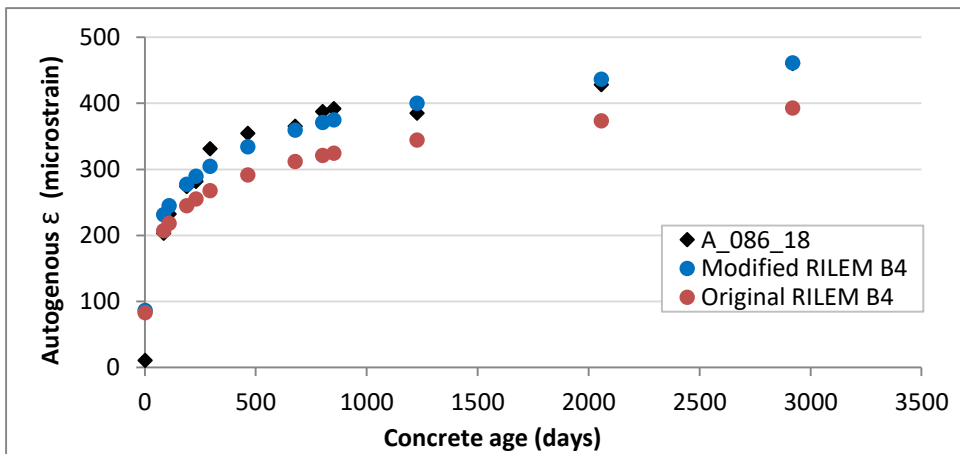


Figure F.11 RILEM B4 model predicted and actual drying shrinkage (microstrain) for Dataset 2-HSC, Subset S2-03a, Experiment A\_086\_18

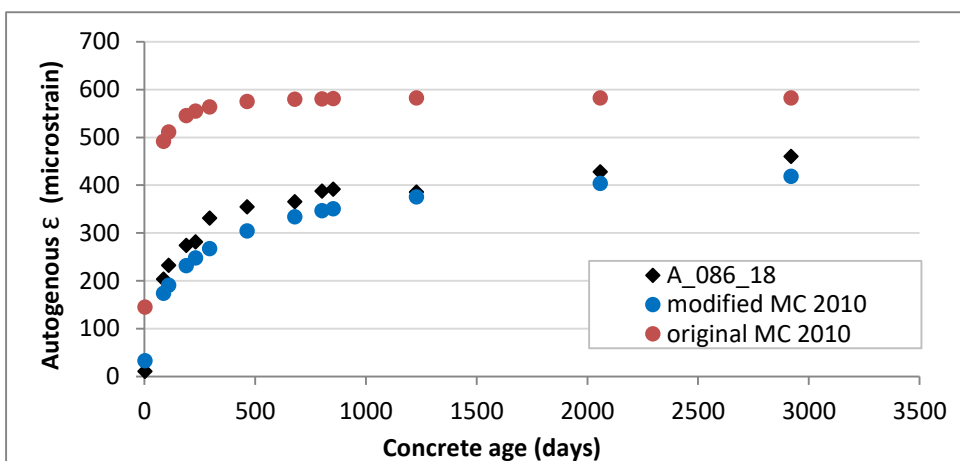


Figure F.12 MC 2010 model predicted and actual drying shrinkage (microstrain) for Dataset 2-HSC, Subset S2-03a, Experiment A\_086\_18

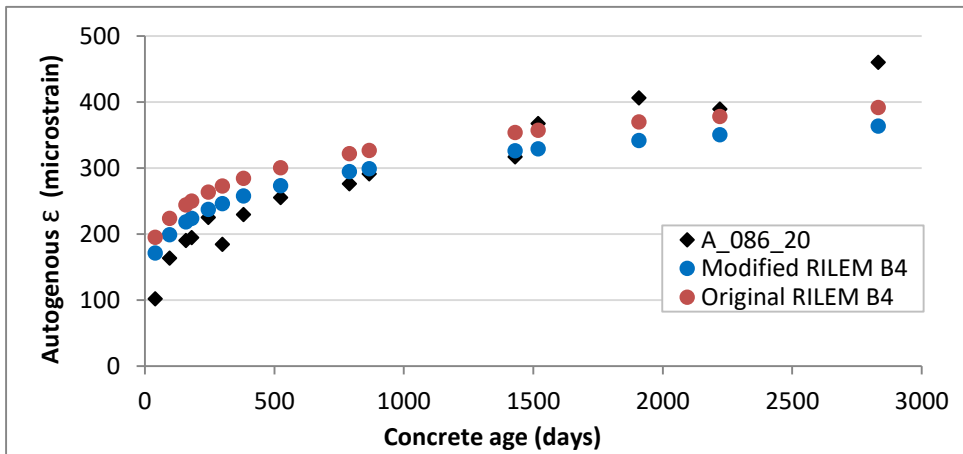


Figure F.13 RILEM B4 model predicted and actual drying shrinkage (microstrain) for Dataset 2-HSC, Subset S2-03a, Experiment A\_086\_20

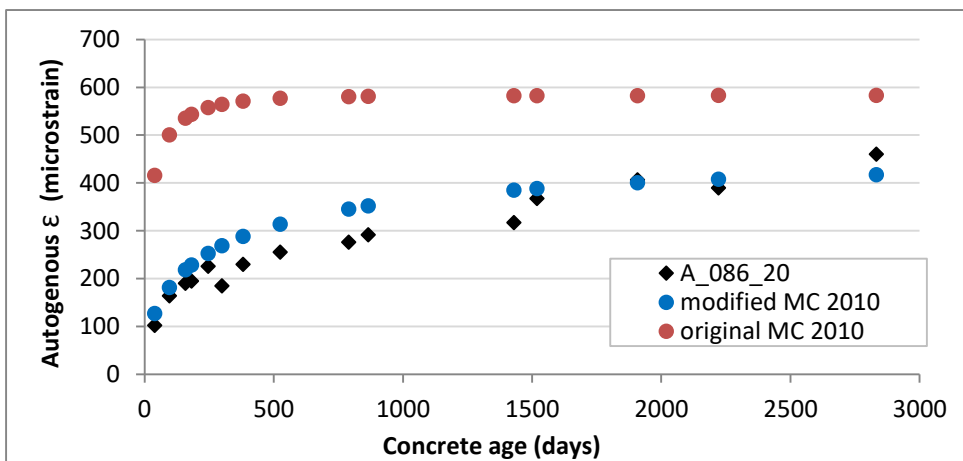


Figure F.14 MC 2010 model predicted and actual drying shrinkage (microstrain) for Dataset 2-HSC, Subset S2-03a, Experiment A\_086\_20

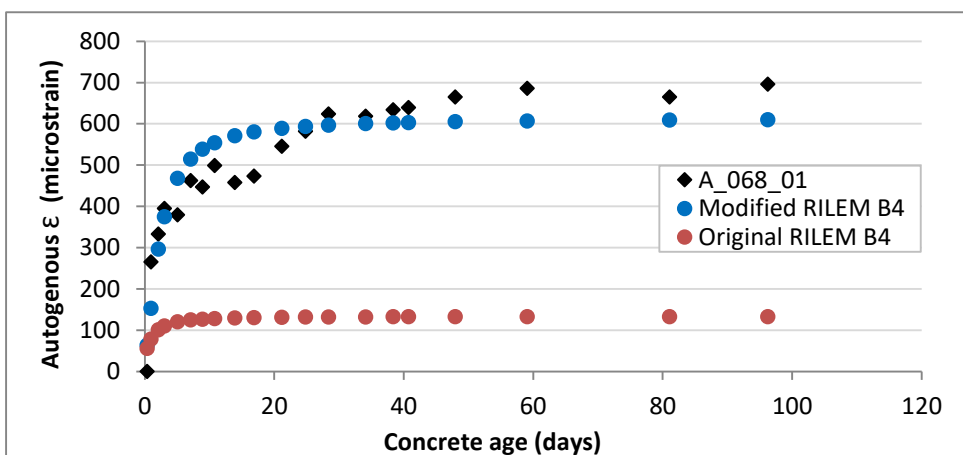


Figure F.15 RILEM B4 model predicted and actual drying shrinkage (microstrain) for Dataset 2-HSC, Subset S2-04a, Experiment A\_068\_01

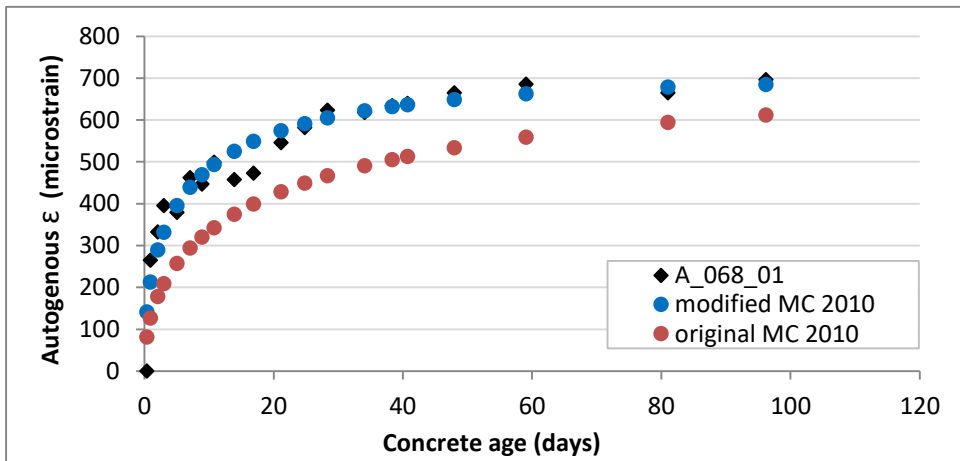


Figure F.16 MC 2010 model predicted and actual drying shrinkage (microstrain) for Dataset 2-HSC, Subset S2-04a, Experiment A\_068\_01

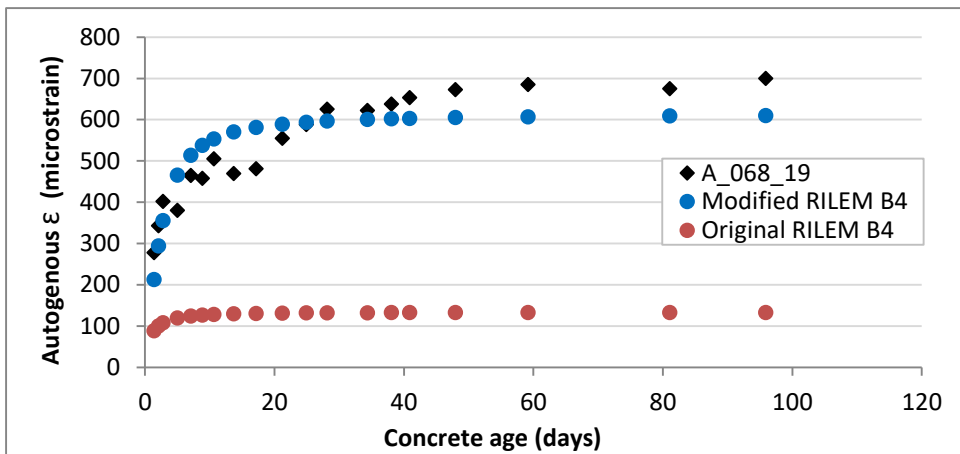


Figure F.17 RILEM B4 model predicted and actual drying shrinkage (microstrain) for Dataset 2-HSC, Subset S2-04a, Experiment A\_068\_19

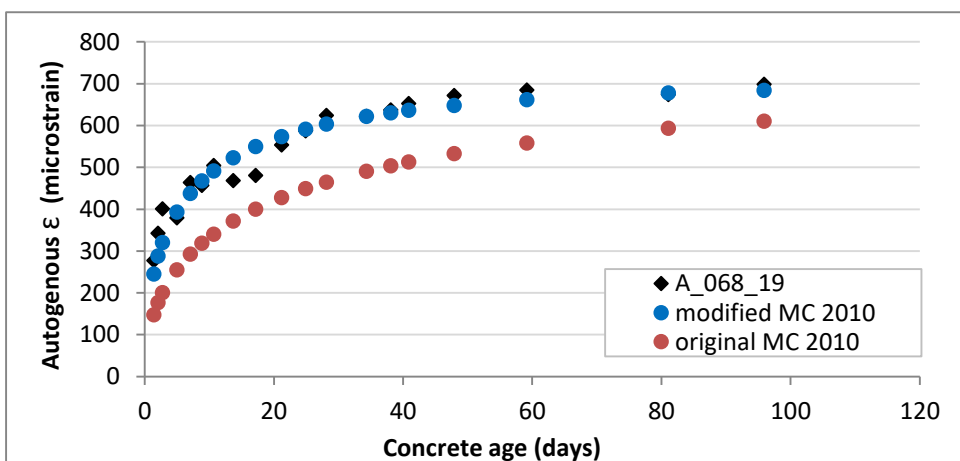


Figure F.18 MC 2010 model predicted and actual drying shrinkage (microstrain) for Dataset 2-HSC, Subset S2-04a, Experiment A\_068\_19

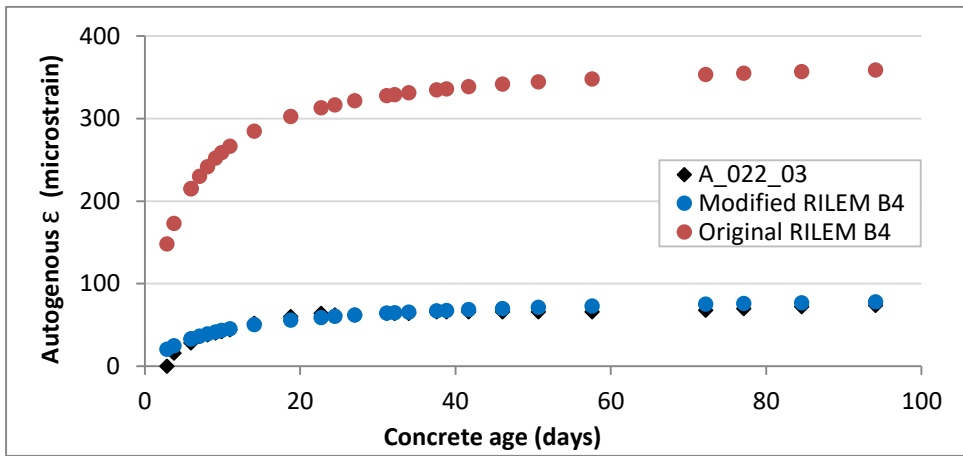


Figure F.19 RILEM B4 model predicted and actual drying shrinkage (microstrain) for Dataset 2-HSC, Subset S2-05a, Experiment A\_022\_03

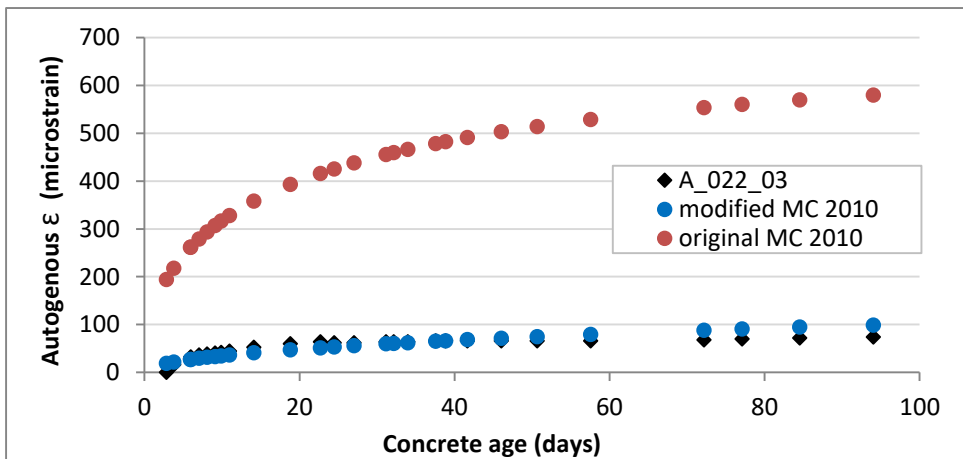


Figure F.20 MC 2010 model predicted and actual drying shrinkage (microstrain) for Dataset 2-HSC, Subset S2-05a, Experiment A\_022\_03

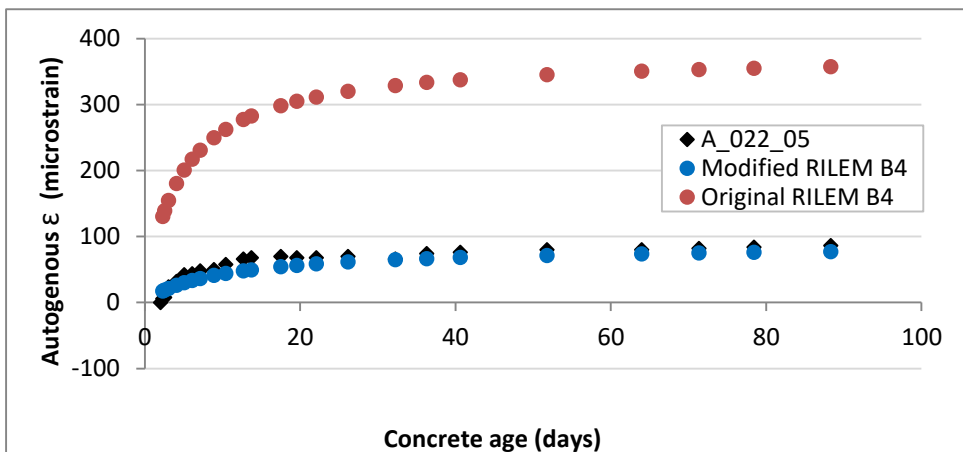


Figure F.21 RILEM B4 model predicted and actual drying shrinkage (microstrain) for Dataset 2-HSC, Subset S2-05a, Experiment A\_022\_05

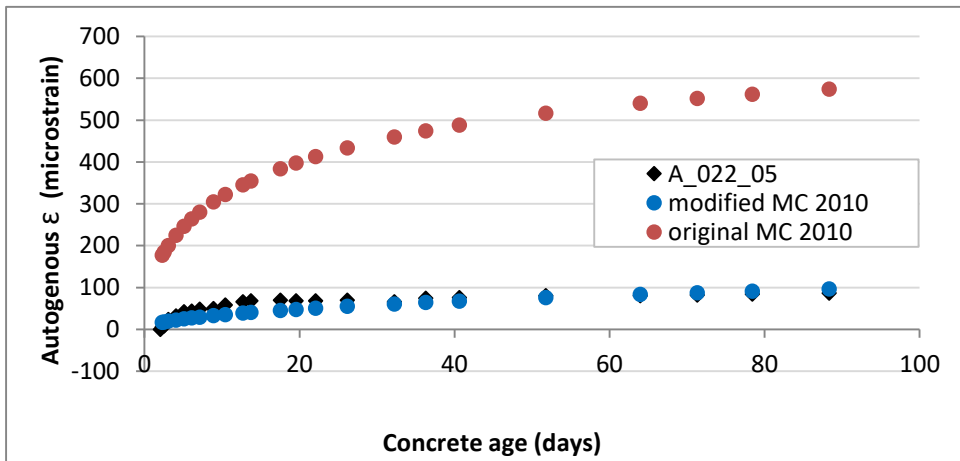


Figure F.22 MC 2010 model predicted and actual drying shrinkage (microstrain) for Dataset 2-HSC, Subset S2-05a, Experiment A\_022\_05

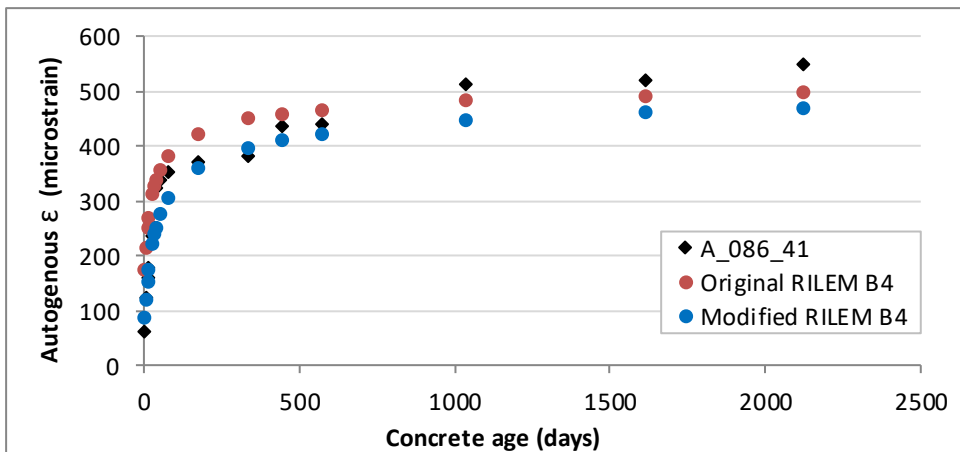


Figure F.23 RILEM B4 model predicted and actual drying shrinkage (microstrain) for Dataset 2-HSC, Subset S2-06a, Experiment A\_086\_41

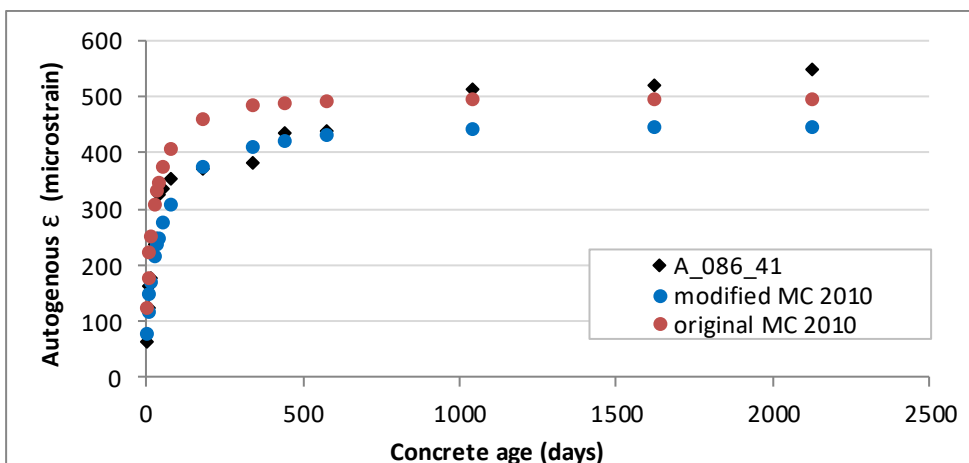


Figure F.24 MC 2010 model predicted and actual drying shrinkage (microstrain) for Dataset 2-HSC, Subset S2-06a, Experiment A\_086\_41



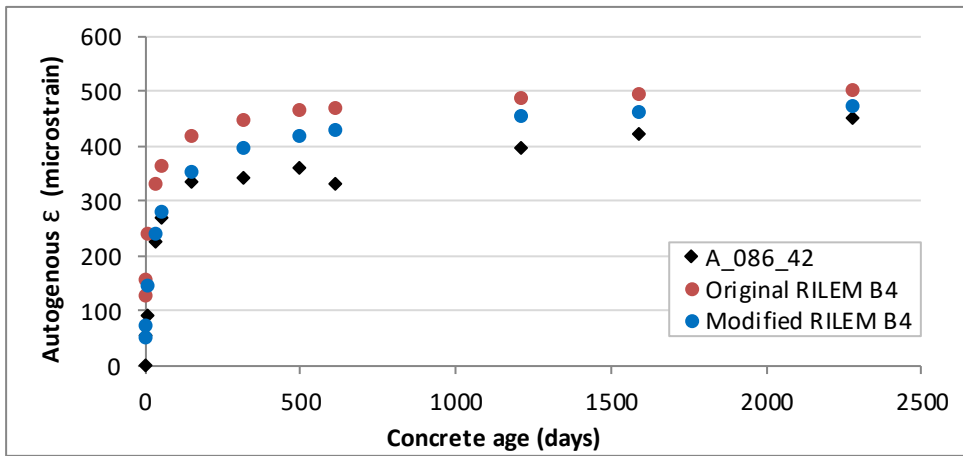


Figure F.25 RILEM B4 model predicted and actual drying shrinkage (microstrain) for Dataset 2-HSC, Subset S2-06a, Experiment A\_086\_42

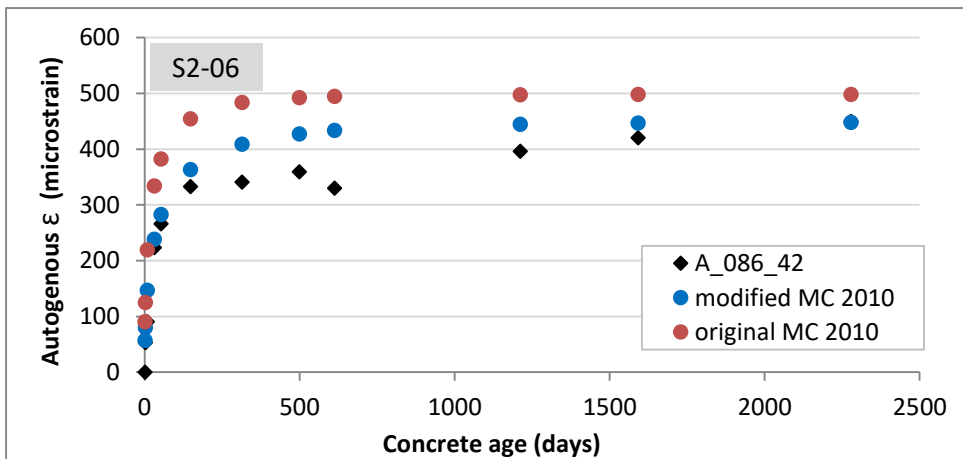


Figure F.26 MC 2010 model predicted and actual drying shrinkage (microstrain) for Dataset 2-HSC, Subset S2-06a, Experiment A\_086\_42

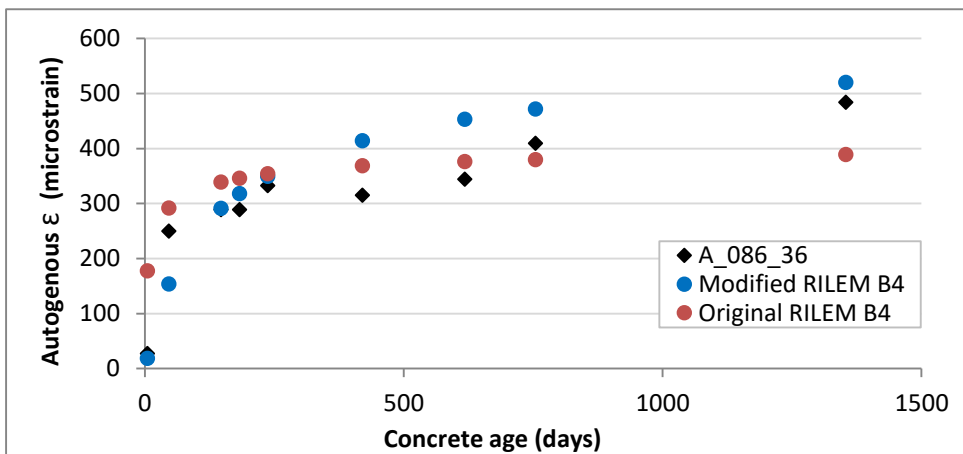


Figure F.27 RILEM B4 model predicted and actual drying shrinkage (microstrain) for Dataset 2-HSC, Subset S2-07a, Experiment A\_086\_36

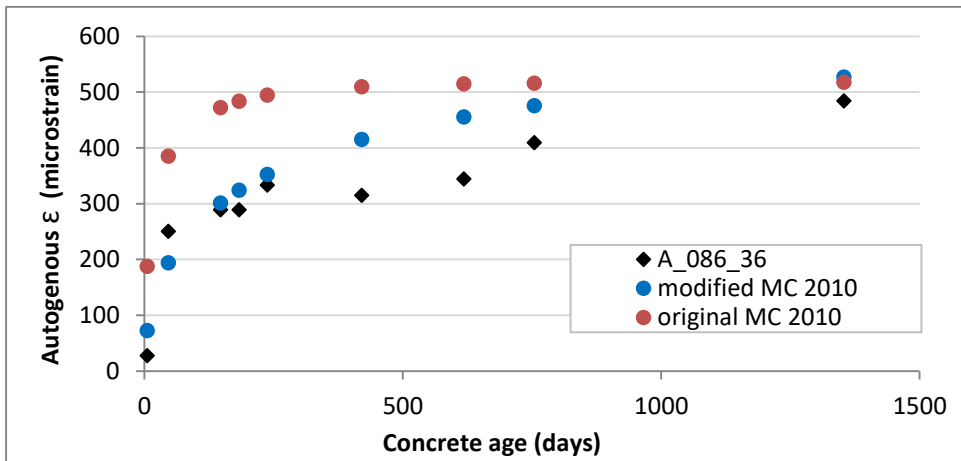


Figure F.28 MC 2010 model predicted and actual drying shrinkage (microstrain) for Dataset 2-HSC, Subset S2-07a, Experiment A\_086\_36

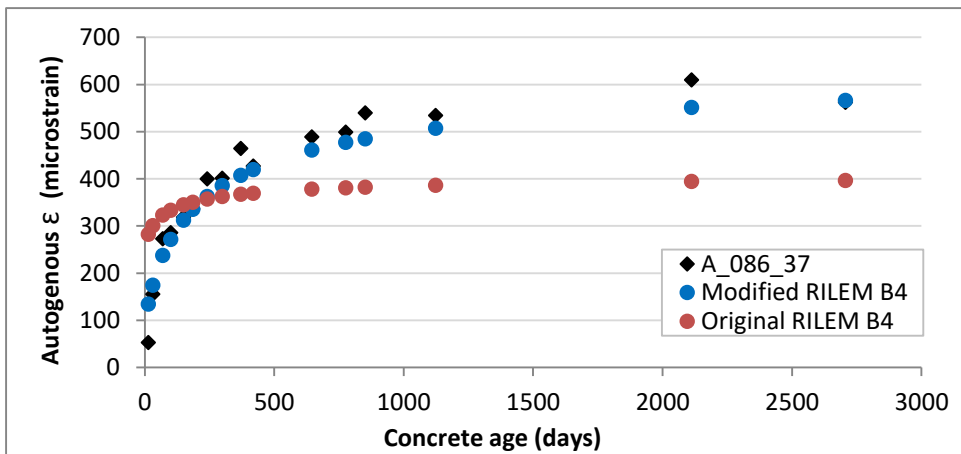


Figure F.29 RILEM B4 model predicted and actual drying shrinkage (microstrain) for Dataset 2-HSC, Subset S2-07a, Experiment A\_086\_37

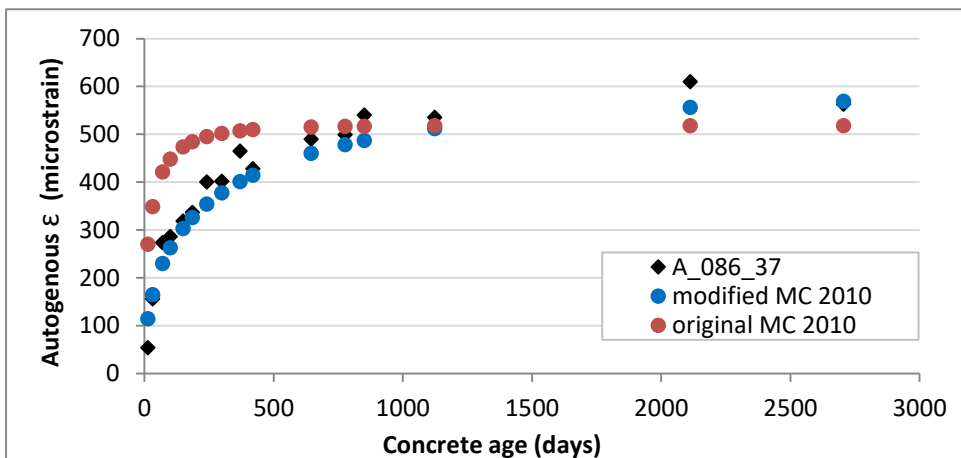


Figure F.30 MC 2010 model predicted and actual drying shrinkage (microstrain) for Dataset 2-HSC, Subset S2-07a, Experiment A\_086\_37

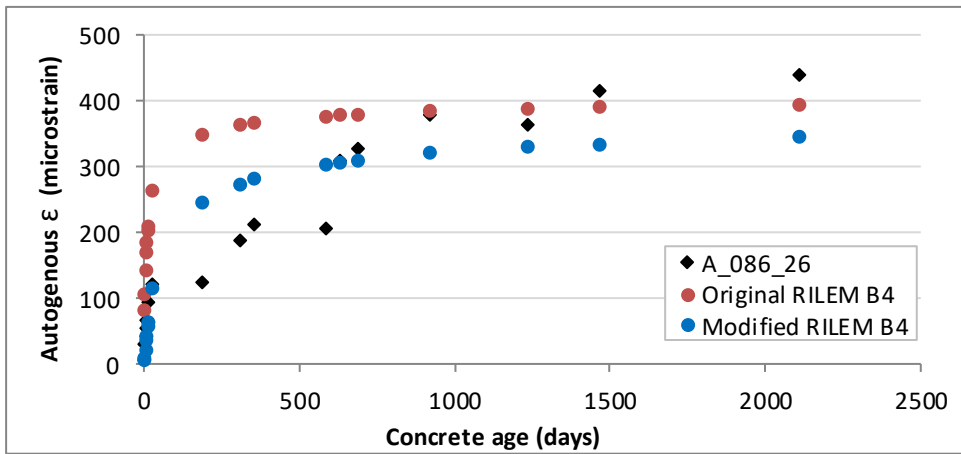


Figure F.31 RILEM B4 model predicted and actual drying shrinkage (microstrain) for Dataset 2-HSC, Subset S2-08a, Experiment A\_086\_26

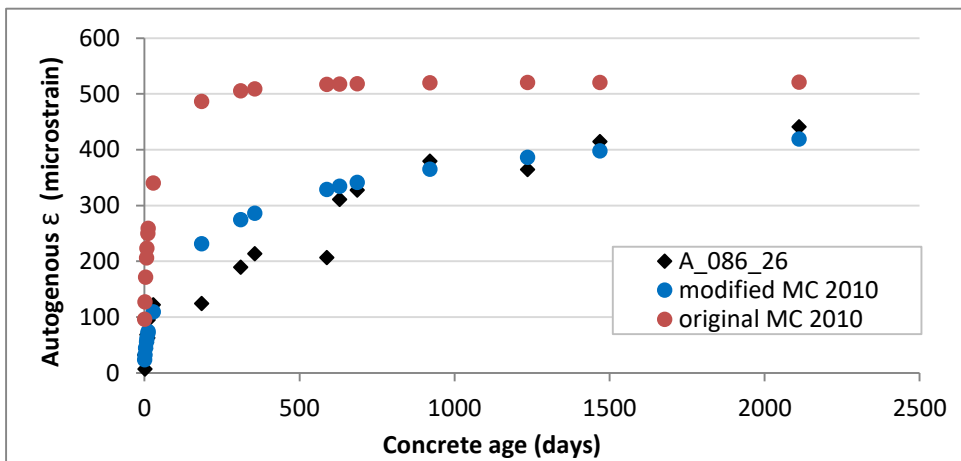


Figure F.32 MC 2010 model predicted and actual drying shrinkage (microstrain) for Dataset 2-HSC, Subset S2-08a, Experiment A\_086\_26

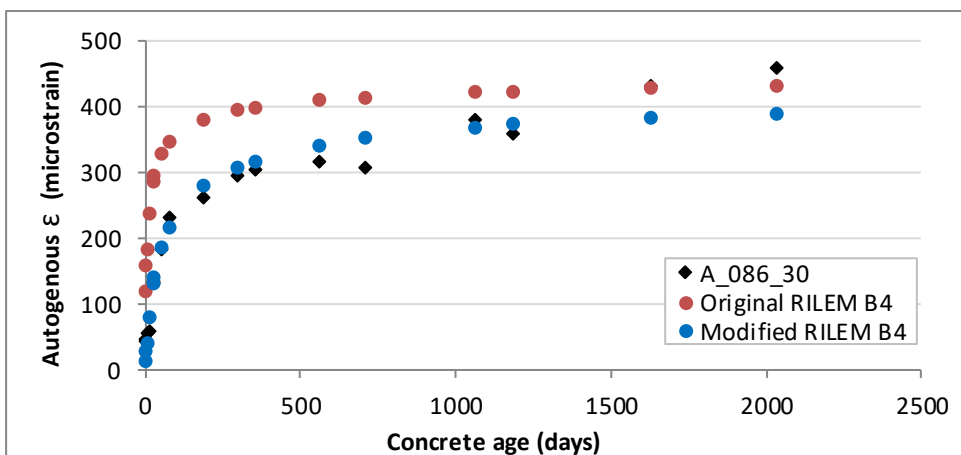


Figure F.33 RILEM B4 model predicted and actual drying shrinkage (microstrain) for Dataset 2-HSC, Subset S2-08a, Experiment A\_086\_30

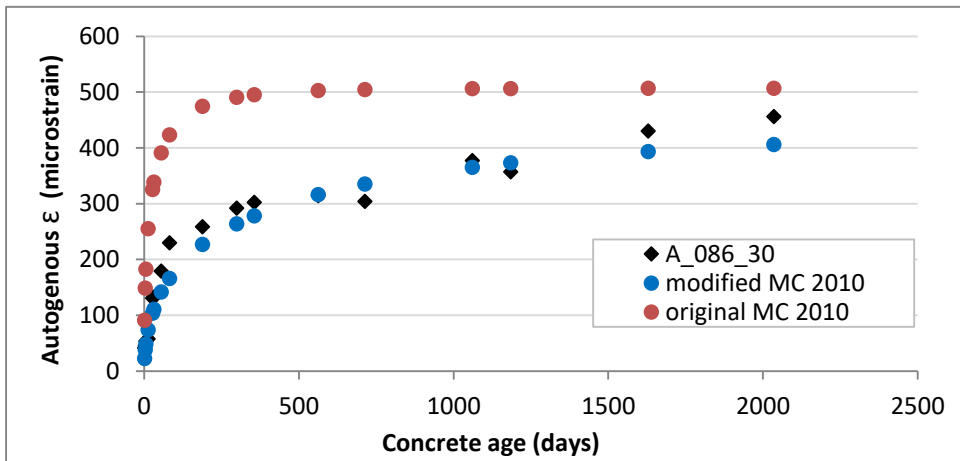


Figure F.34 MC 2010 model predicted and actual drying shrinkage (microstrain) for Dataset 2-HSC, Subset S2-08a, Experiment A\_086\_30

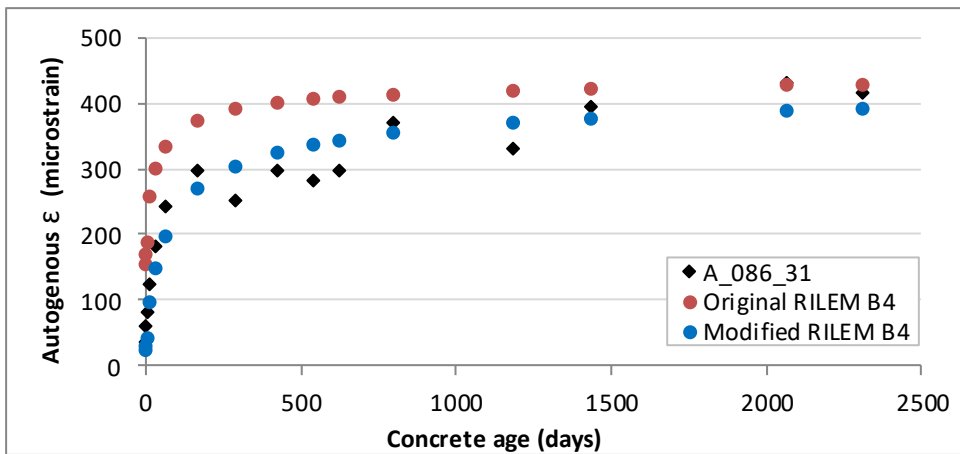


Figure F.35 RILEM B4 model predicted and actual drying shrinkage (microstrain) for Dataset 2-HSC, Subset S2-08a, Experiment A\_086\_31

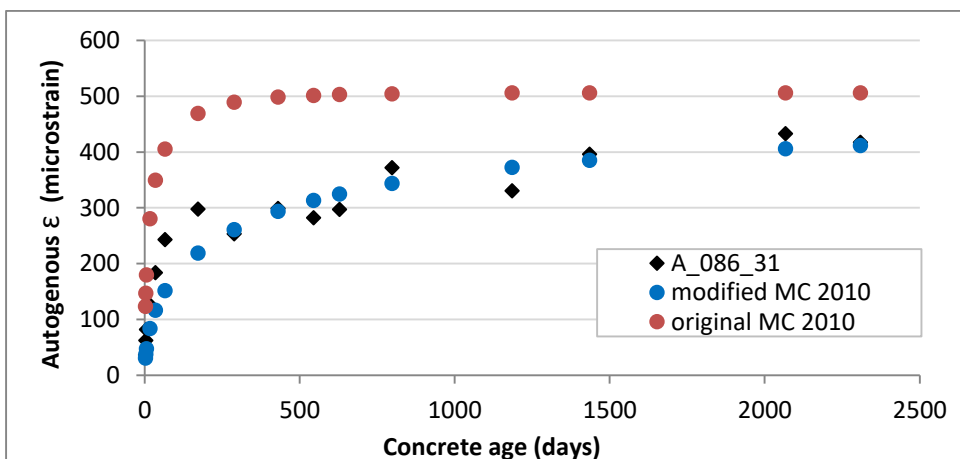


Figure F.36 MC 2010 model predicted and actual drying shrinkage (microstrain) for Dataset 2-HSC, Subset S2-08a, Experiment A\_086\_31

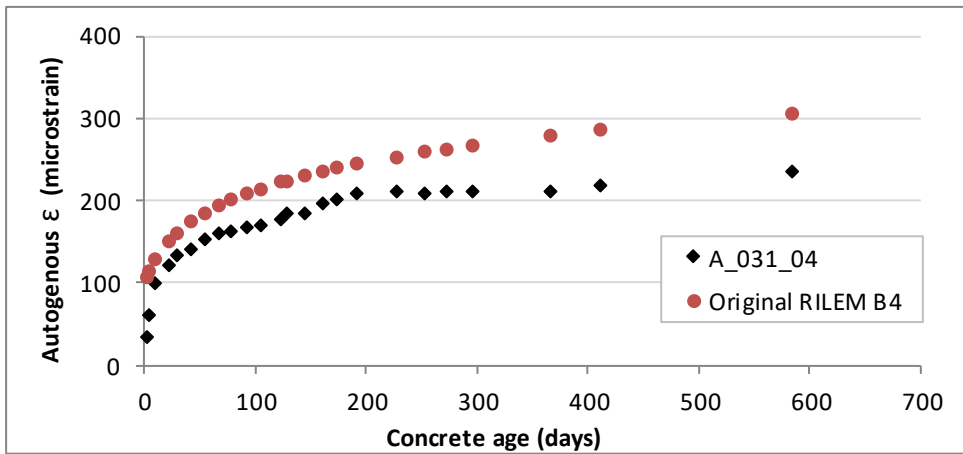


Figure F.37 RILEM B4 model predicted and actual drying shrinkage (microstrain) for Dataset 2-HSC, Subset S2-09a, Experiment A\_031\_04

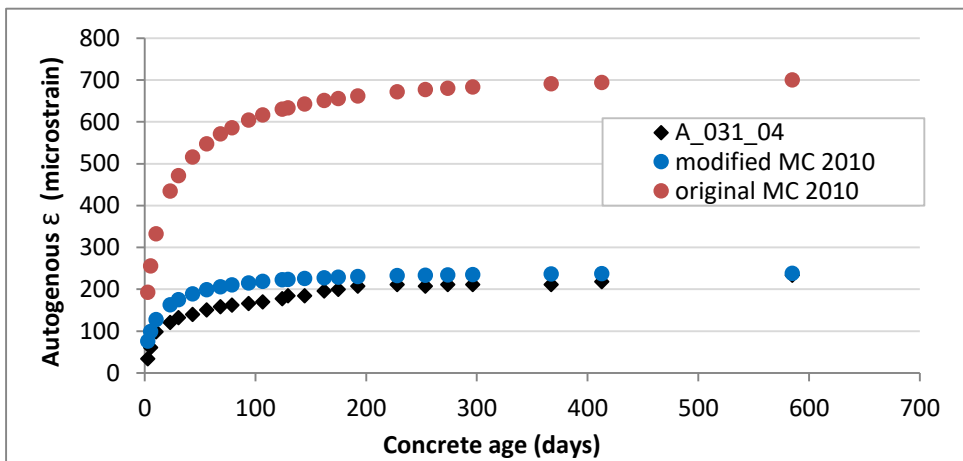


Figure F.38 MC 2010 model predicted and actual drying shrinkage (microstrain) for Dataset 2-HSC, Subset S2-09a, Experiment A\_031\_04

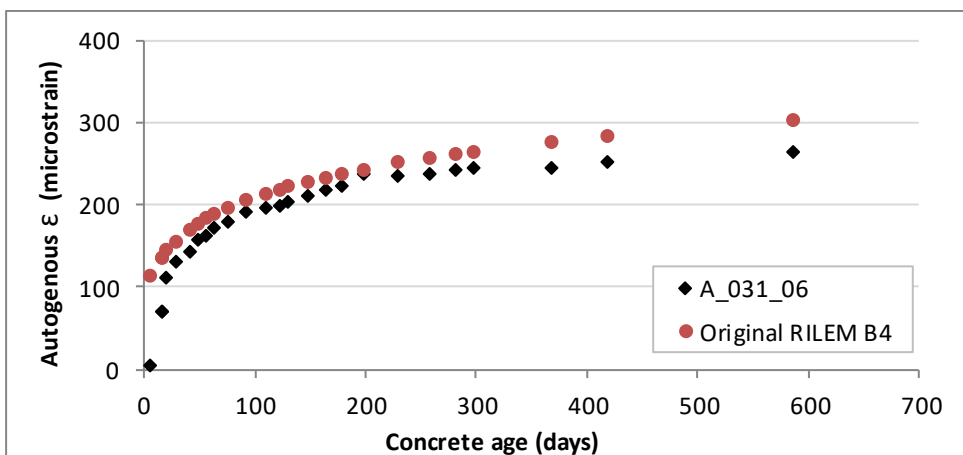


Figure F.39 RILEM B4 model predicted and actual drying shrinkage (microstrain) for Dataset 2-HSC, Subset S2-09a, Experiment A\_031\_06

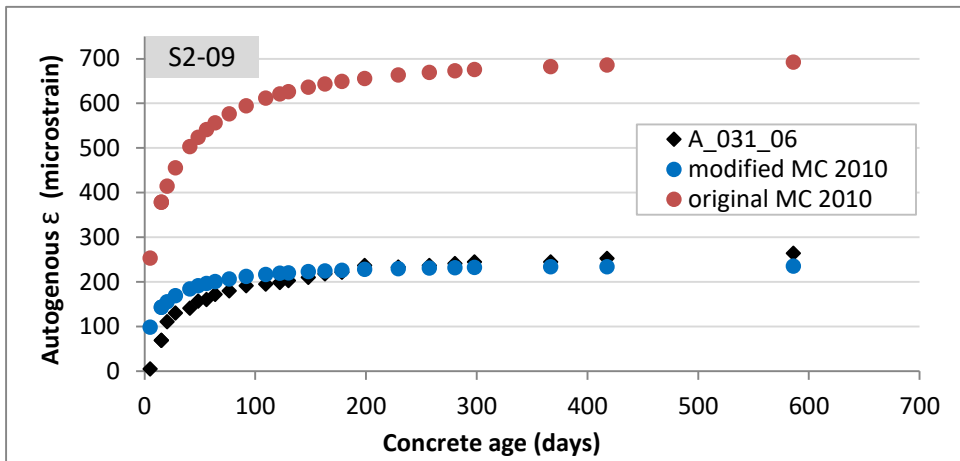


Figure F.40 MC 2010 model predicted and actual drying shrinkage (microstrain) for Dataset 2-HSC, Subset S2-09a, Experiment A\_031\_06

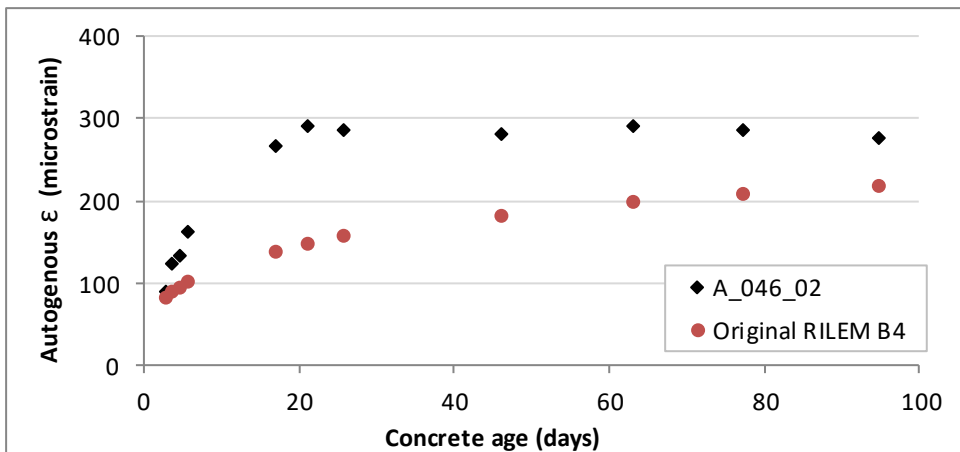


Figure F.41 RILEM B4 model predicted and actual drying shrinkage (microstrain) for Dataset 2-HSC, Subset S2-09a, Experiment A\_046\_02

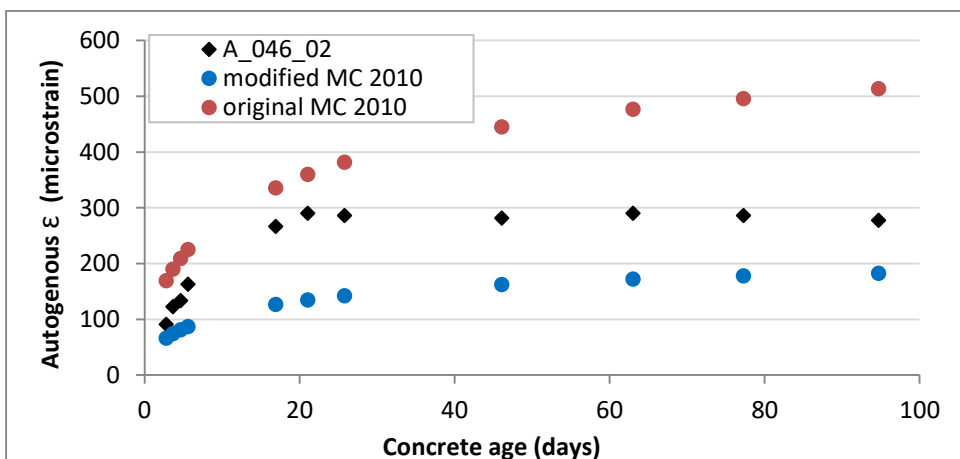


Figure F.42 MC 2010 model predicted and actual drying shrinkage (microstrain) for Dataset 2-HSC, Subset S2-09a, Experiment A\_046\_02

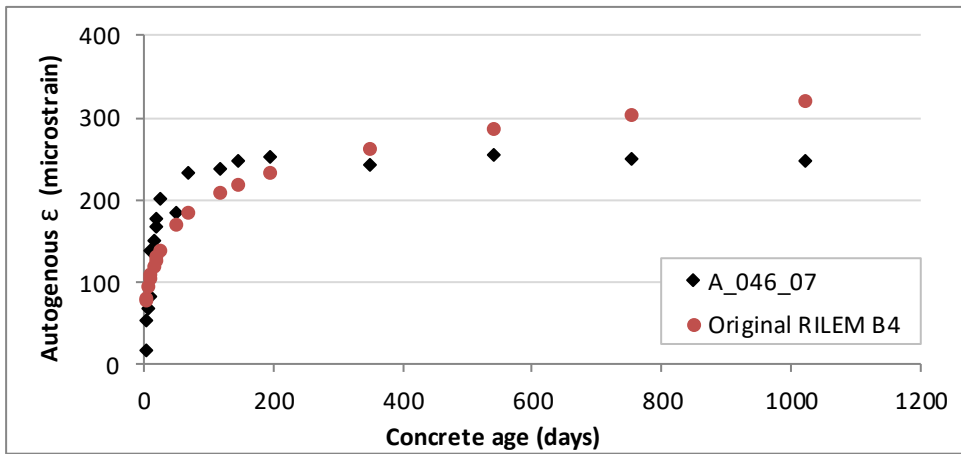


Figure F.43 RILEM B4 model predicted and actual drying shrinkage (microstrain) for Dataset 2-HSC, Subset S2-09a, Experiment A\_046\_07

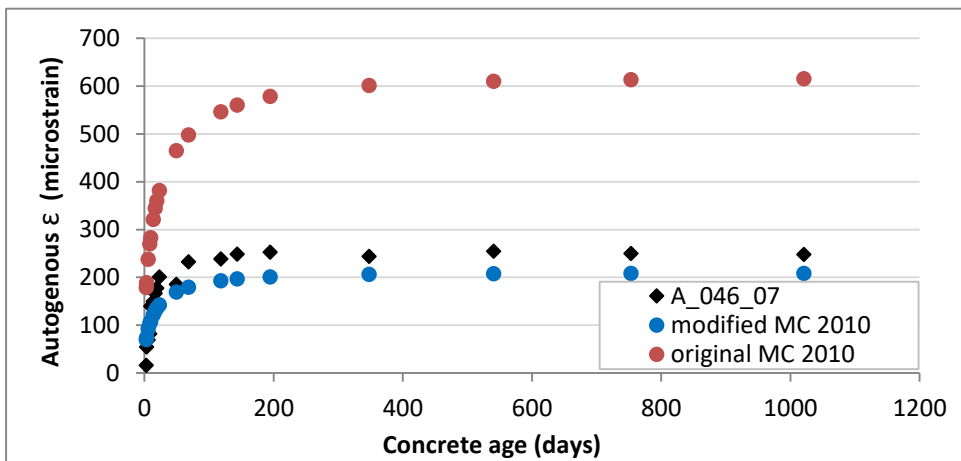


Figure F.44 MC 2010 model predicted and actual drying shrinkage (microstrain) for Dataset 2-HSC, Subset S2-09a, Experiment A\_046\_07

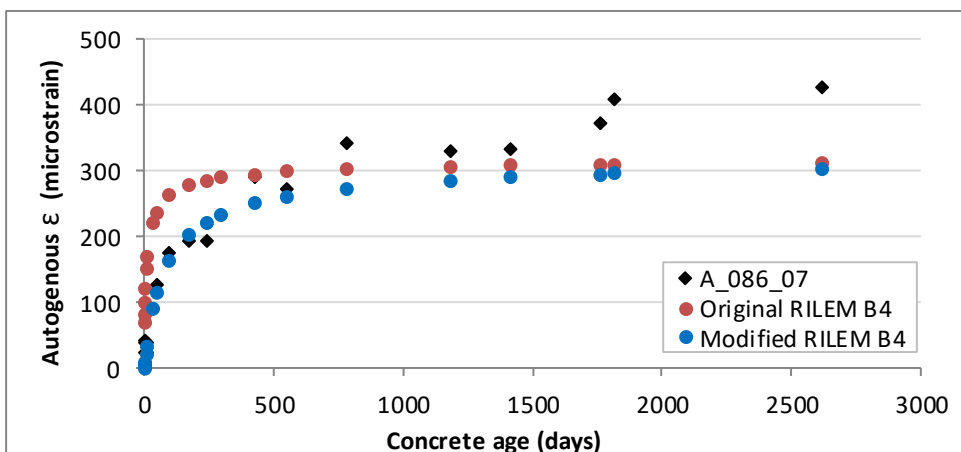


Figure F.45 RILEM B4 model predicted and actual drying shrinkage (microstrain) for Dataset 2-HSC, Subset S2-10a, Experiment A\_086\_07

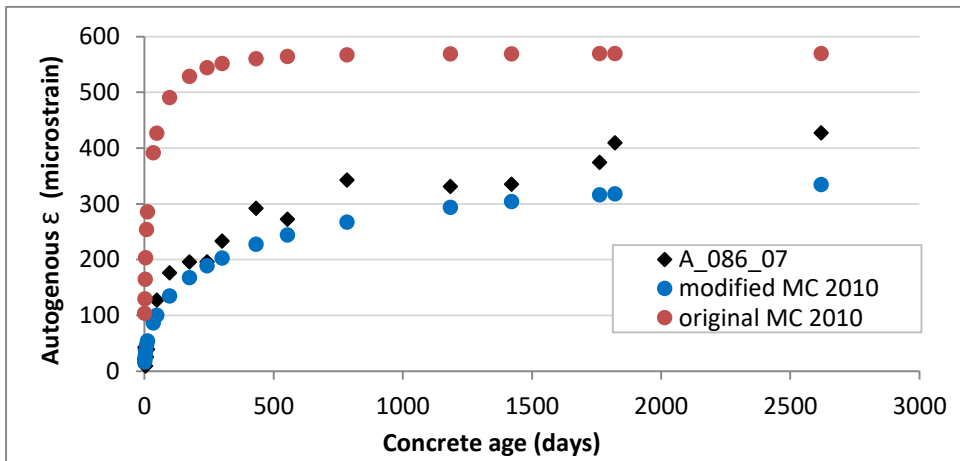


Figure F.46 MC 2010 model predicted and actual drying shrinkage (microstrain) for Dataset 2-HSC, Subset S2-10a, Experiment A\_086\_07

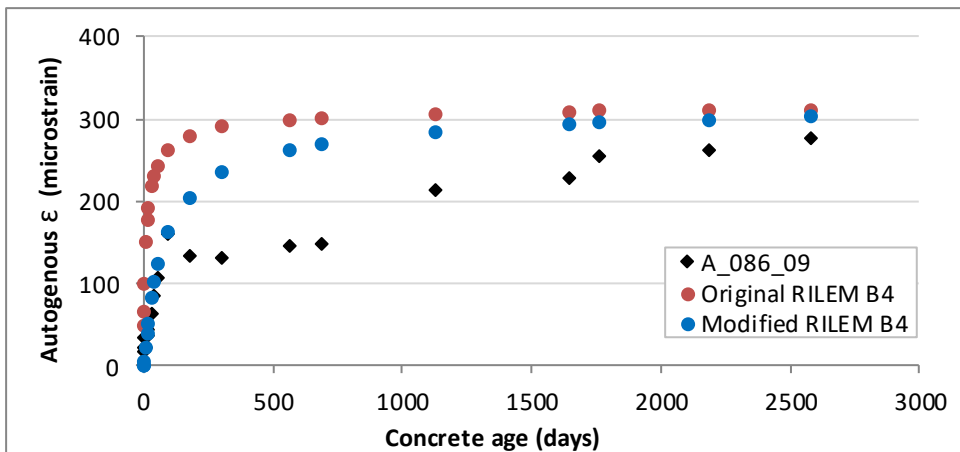


Figure F.47 RILEM B4 model predicted and actual drying shrinkage (microstrain) for Dataset 2-HSC, Subset S2-10a, Experiment A\_086\_09

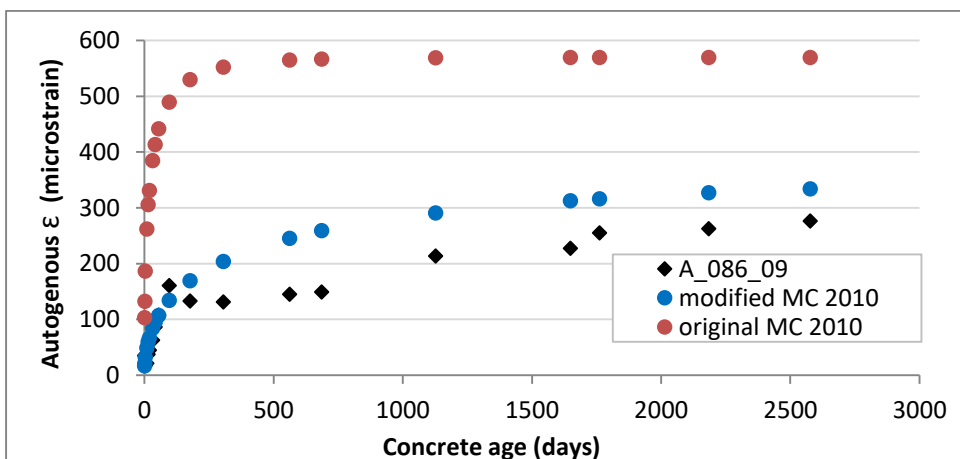


Figure F.48 MC 2010 model predicted and actual drying shrinkage (microstrain) for Dataset 2-HSC, Subset S2-10a, Experiment A\_086\_09



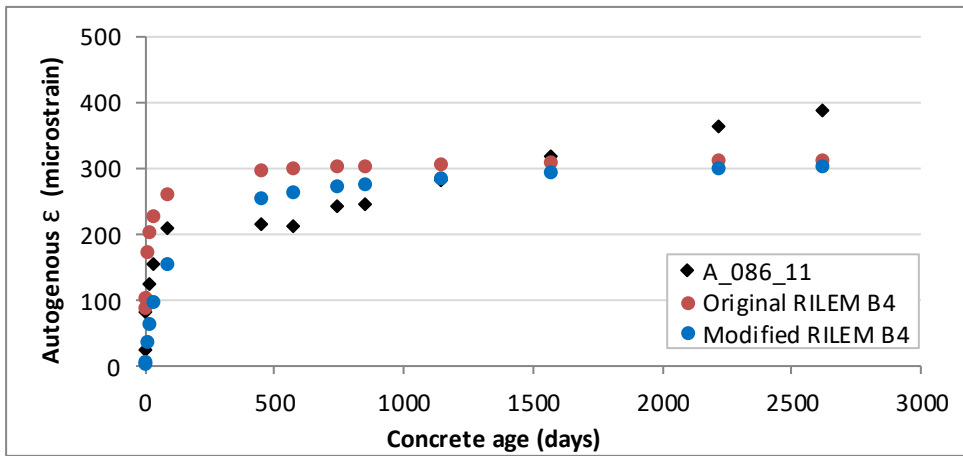


Figure F.49 RILEM B4 model predicted and actual drying shrinkage (microstrain) for Dataset 2-HSC, Subset S2-10a, Experiment A\_086\_11

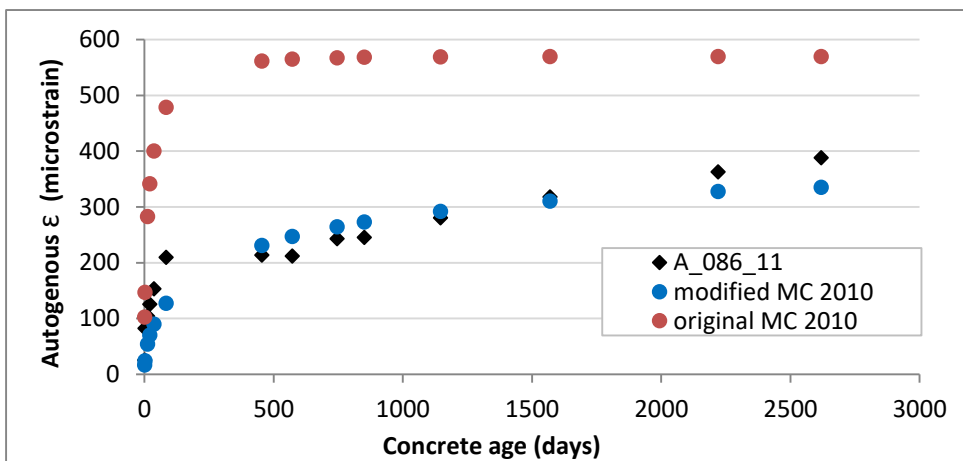


Figure F.50 MC 2010 model predicted and actual drying shrinkage (microstrain) for Dataset 2-HSC, Subset S2-10a, Experiment A\_086\_11

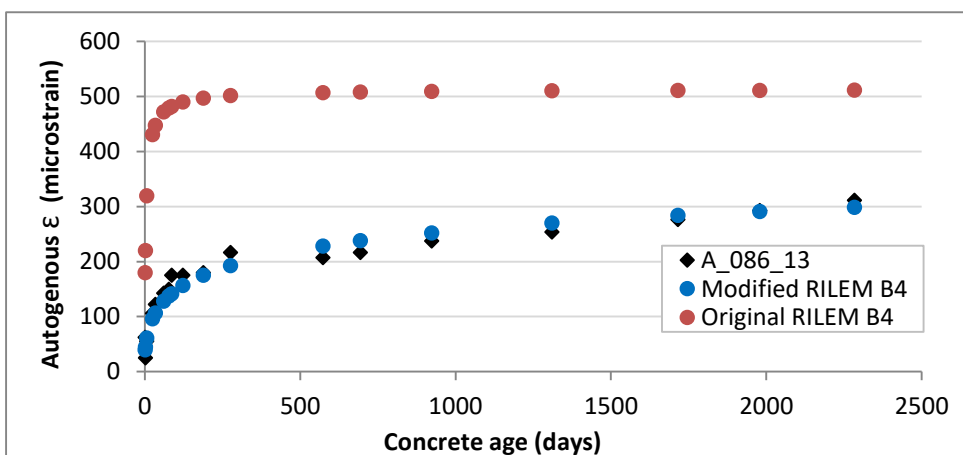


Figure F.51 RILEM B4 model predicted and actual drying shrinkage (microstrain) for Dataset 2-HSC, Subset S2-11a, Experiment A\_086\_13

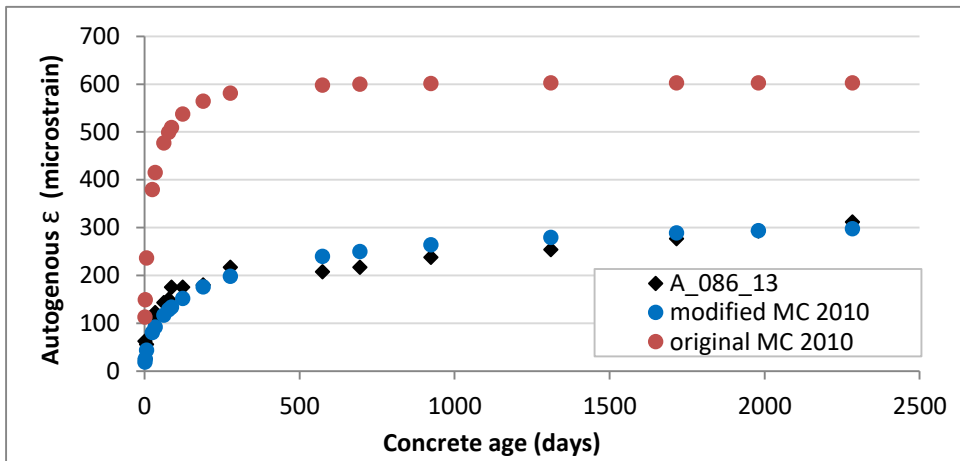


Figure F.52 MC 2010 model predicted and actual drying shrinkage (microstrain) for Dataset 2-HSC, Subset S2-11a, Experiment A\_086\_13

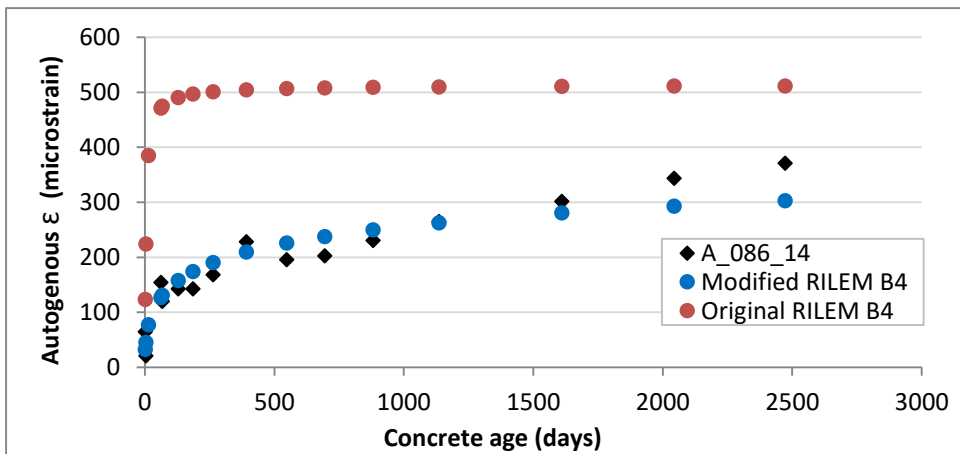


Figure F.53 RILEM B4 model predicted and actual drying shrinkage (microstrain) for Dataset 2-HSC, Subset S2-11a, Experiment A\_086\_14

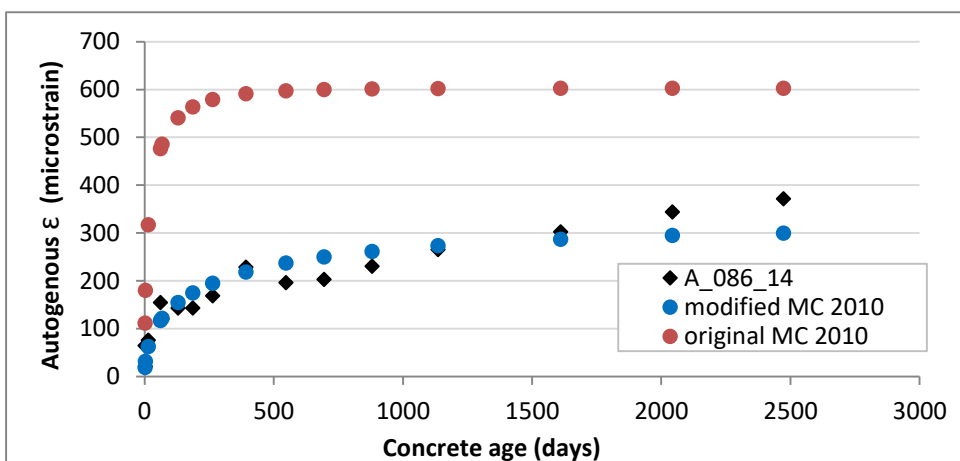


Figure F.54 MC 2010 model predicted and actual drying shrinkage (microstrain) for Dataset 2-HSC, Subset S2-11a, Experiment A\_086\_14

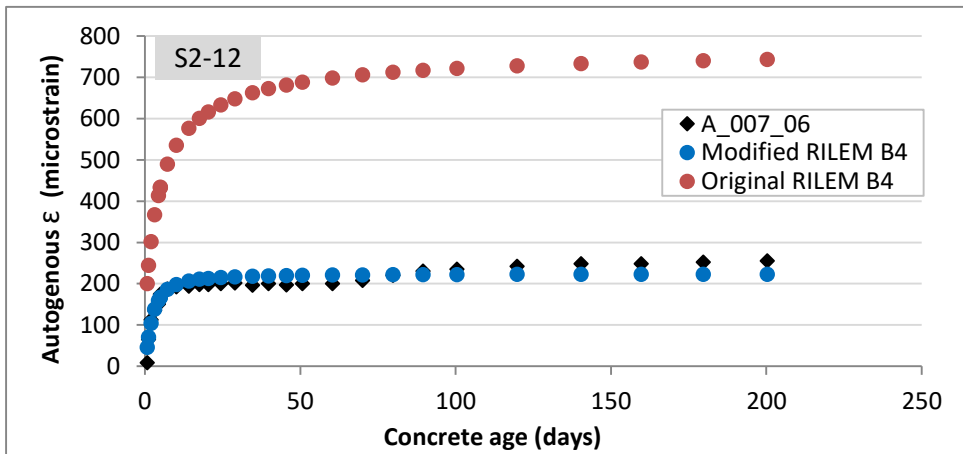


Figure F.55 RILEM B4 model predicted and actual drying shrinkage (microstrain) for Dataset 2-HSC, Subset S2-12a, Experiment A\_007\_06

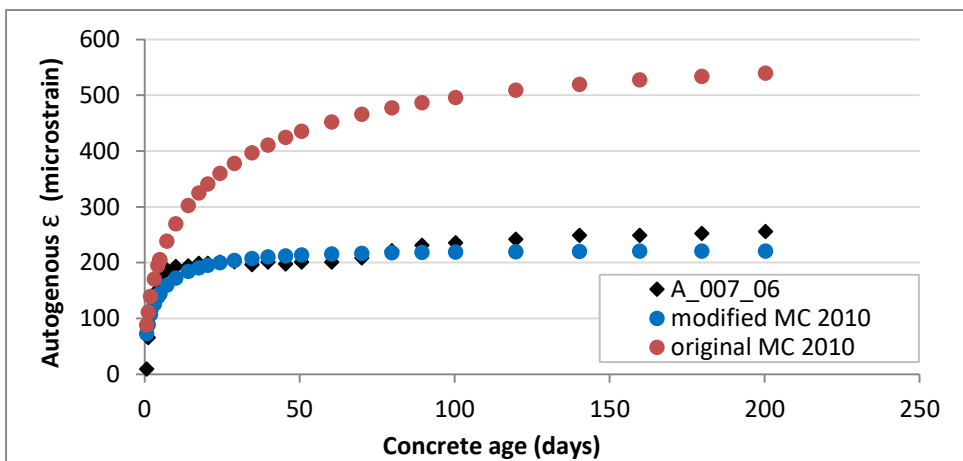


Figure F.56 MC 2010 model predicted and actual drying shrinkage (microstrain) for Dataset 2-HSC, Subset S2-12a, Experiment A\_007\_06

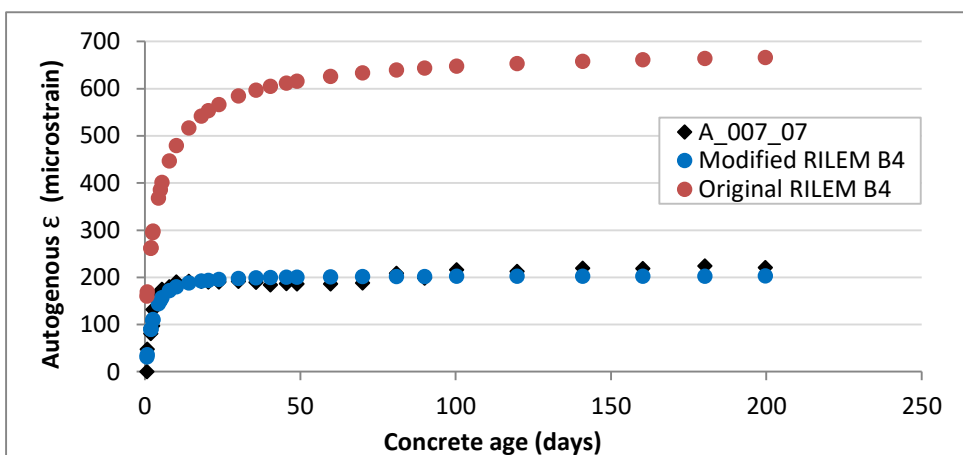


Figure F.57 RILEM B4 model predicted and actual drying shrinkage (microstrain) for Dataset 2-HSC, Subset S2-12a, Experiment A\_007\_07

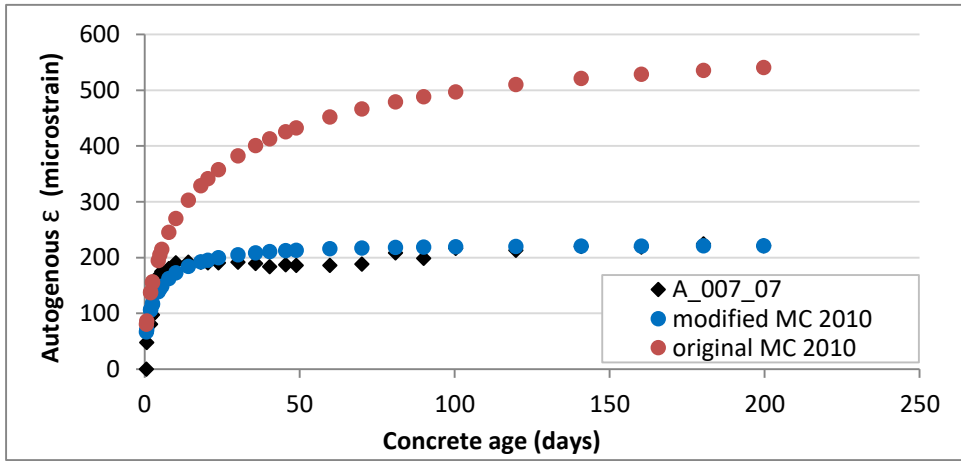


Figure F.58 MC 2010 model predicted and actual drying shrinkage (microstrain) for Dataset 2-HSC, Subset S2-12a, Experiment A\_007\_07